DYNAMIC BIOMARKERS OF RESPONSE TO ANTI-IMMUNE CHECKPOINT INHIBITORS IN CANCER

EDITED BY: Said Dermime, Maysaloun Merhi and Taha Merghoub
PUBLISHED IN: Frontiers in Immunology and Frontiers in Oncology

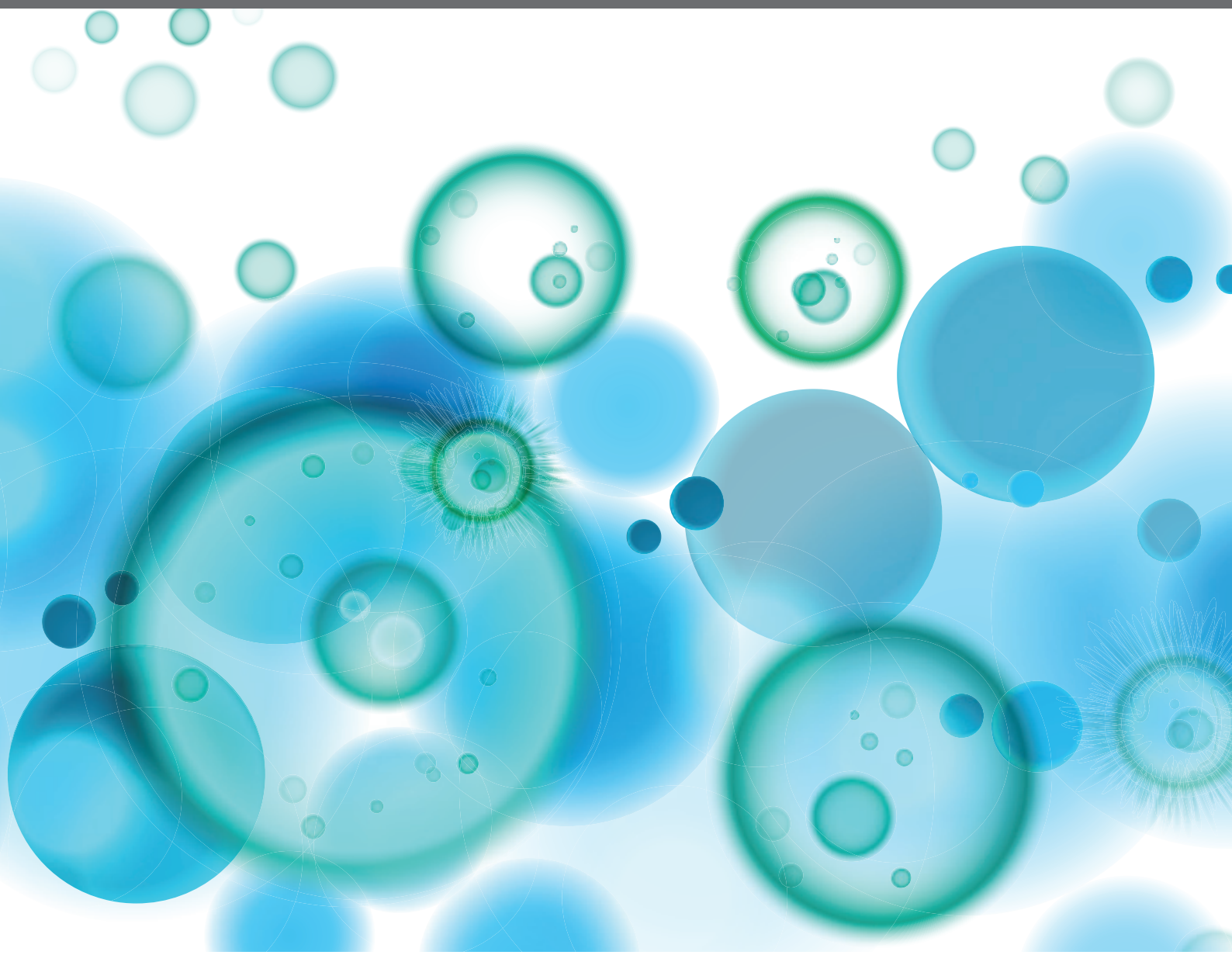

frontiers Research Topics

frontiers

ISSN 1664-8714
ISBN 978-2-88971-863-4
DOI 10.3389/978-2-88971-863-4

About Frontiers

Frontiers is more than just an open-access publisher of scholarly articles: it is a pioneering approach to the world of academia, radically improving the way scholarly research is managed. The grand vision of Frontiers is a world where all people have an equal opportunity to seek, share and generate knowledge. Frontiers provides immediate and permanent online open access to all its publications, but this alone is not enough to realize our grand goals.

Frontiers Journal Series

The Frontiers Journal Series is a multi-tier and interdisciplinary set of open-access, online journals, promising a paradigm shift from the current review, selection and dissemination processes in academic publishing. All Frontiers journals are driven by researchers for researchers; therefore, they constitute a service to the scholarly community. At the same time, the Frontiers Journal Series operates on a revolutionary invention, the tiered publishing system, initially addressing specific communities of scholars, and gradually climbing up to broader public understanding, thus serving the interests of the lay society, too.

Dedication to Quality

Each Frontiers article is a landmark of the highest quality, thanks to genuinely collaborative interactions between authors and review editors, who include some of the world's best academicians. Research must be certified by peers before entering a stream of knowledge that may eventually reach the public - and shape society; therefore, Frontiers only applies the most rigorous and unbiased reviews.
Frontiers revolutionizes research publishing by freely delivering the most outstanding research, evaluated with no bias from both the academic and social point of view. By applying the most advanced information technologies, Frontiers is catapulting scholarly publishing into a new generation.

What are Frontiers Research Topics?

Frontiers Research Topics are very popular trademarks of the Frontiers Journals Series: they are collections of at least ten articles, all centered on a particular subject. With their unique mix of varied contributions from Original Research to Review Articles, Frontiers Research Topics unify the most influential researchers, the latest key findings and historical advances in a hot research area! Find out more on how to host your own Frontiers Research Topic or contribute to one as an author by contacting the Frontiers Editorial Office: frontiersin.org/about/contact

DYNAMIC BIOMARKERS OF RESPONSE TO ANTI-IMMUNE CHECKPOINT INHIBITORS IN CANCER

Topic Editors:
Said Dermime, National Center for Cancer Care and Research, Qatar
Maysaloun Merhi, Hamad Medical Corporation, Qatar
Taha Merghoub, Memorial Sloan Kettering Cancer Center, United States

Topic Editor Dr. Merghou is co-founder of and has equity in Imvaq therapeutics. Dr. Merghou reports grants from Bristol-Myers Squibb, Surface Oncology, Kyn Therapeutics, Infinity Pharmaceuticals, Peregrine Pharmeceuticals, Adaptive Biotechnologies, Leap Therapeutics, Aprea. The other Topic Editors declare no conflict of interest with regard to the Research Topic theme.

Citation: Dermime, S., Merhi, M., Merghoub, T., eds. (2021). Dynamic Biomarkers of Response to Anti-Immune Checkpoint Inhibitors in Cancer. Lausanne: Frontiers Media SA. doi: 10.3389/978-2-88971-863-4

Table of Contents

frontiers in Immunology

EDITORIAL
published: 21 October 2021
doi: 10.3389/fimmu.2021.781872

Editorial: Dynamic Biomarkers of Response to Anti-Immune Checkpoint Inhibitors in Cancer

Said Dermime[1,2,3]*, *Maysaloun Merhi*[1,2] *and Taha Merghoub*[4,5,6,7]

[1] National Center for Cancer Care and Research, Hamad Medical Corporation, Doha, Qatar, [2] Translational Cancer Research Facility, Translational Research Institute, Hamad Medical Corporation, Doha, Qatar, [3] College of Health and Life Sciences, Hamad Bin Khalifa University, Doha, Qatar, [4] Ludwig Collaborative, Swim Across America Laboratory, Memorial Sloan Kettering Cancer Center (MSK), New York, NY, United States, [5] Parker Institute for Cancer Immunotherapy, Memorial Sloan Kettering Cancer Center (MSK), New York, NY, United States, [6] Human Oncology and Pathogenesis Program, Department of Medicine, Memorial Sloan Kettering Cancer Center (MSK), New York, NY, United States, [7] Department of Medicine, Weill Cornell Medicine, New York, NY, United States

Keywords: immune checkpoint inhibitors (ICI), programmed cell death protein 1 (PD1), programmed cell death ligand 1 (PD-L1), dynamic biomarkers, irAEs

Editorial on the Research Topic

Dynamic Biomarkers of Response to Anti-Immune Checkpoint Inhibitors in Cancer

OPEN ACCESS

Edited and reviewed by:
Catherine Sautes-Fridman, INSERM U1138 Centre de Recherche des Cordeliers (CRC), France

***Correspondence:**
Said Dermime
Sdermime@hamad.qa

Specialty section:
This article was submitted to Cancer Immunity and Immunotherapy, a section of the journal Frontiers in Immunology

Received: *23 September 2021*
Accepted: *05 October 2021*
Published: *21 October 2021*

Citation:
Dermime S, Merhi M and Merghoub T (2021) Editorial: Dynamic Biomarkers of Response to Anti-Immune Checkpoint Inhibitors in Cancer. Front. Immunol. 12:781872. doi: 10.3389/fimmu.2021.781872

Immune checkpoint blockade (ICB) has been approved as first- or second-line therapy options in a broadening range of metastatic cancer and is increasingly explored in the treatment of early stage tumors. However, clinical responses are limited to a small group of patients and potentially long-lasting responses were observed in 10% to 40% of cancer patients, depending on the malignancy subtype (1, 2). Considerable efforts have been made to identify predictive factors of response to ICB with the aim to use this therapy in patients with a high probability of response and to avoid exposing non-responder subjects to their potential side effects. Whilst a range of biomarkers have been investigated, their predictive potential remains unsatisfactory. In current clinical practice only PD-L1 expression in tumor tissues is used as predictive biomarker of response to PD-1 immune checkpoint blockade. However, a small proportion of patients with absent PD-L1 tumor expression may still respond to PD-1 blockade, making it difficult to restrict prescription of these therapies solely based on this biomarker. Hence, the search for novel biomarkers of response to checkpoint inhibitors remains an unmet need. One promising emerging approach is to focus on dynamic biomarkers, which would allow, when tested in the patient early after exposition to the therapeutic agents, to identify those patients presenting an immune response failure. The study of the dynamics of the immune system and of the tumor under immune checkpoint blockade shed light on their mechanisms of activity. Indeed, some immune pathways induced by ICB therapy may affect anti-tumor activity, whilst others may correlate with immune related adverse events (irAE) rather than with response. Moreover, tumor-intrinsic mechanisms of immune escape may develop following ICB and will consequently affect treatment outcome. We have recently summarized the dynamics of the immune system and of the tumor under immune checkpoint blockade. We emphasized the importance of studying mechanisms influencing response to ICB and focused on the multitude of immune cells subsets (including effector and immunosuppressive T cells and B cells subsets) that were shown to be impacted by CTLA-4 and PD-1/PD-L1 blockade monotherapy (3). In this Research Topic, we

compiled reviews and original research articles reflecting the current advances in the study of dynamic biomarkers as predictors of the response to checkpoint inhibitors therapies in cancer. Four complimentary areas are addressed in this topic.

MONITORING SPECIFIC ANTI-TUMOR IMMUNE RESPONSES TO TUMOR ASSOCIATED ANTIGENS AND/OR NEOANTIGENS BEFORE AND DURING IMMUNE CHECKPOINT INHIBITORS TREATMENT

It has been demonstrated that Tumor Mutational Burden (TMB) is a useful biomarker to predict the response to immunotherapy in cancer patients. Usuda et al. indicated that high TMB and high PD-L1 expression can predict a favorable outcome of ICB therapy in lung cancer patients. Nie et al. reported that an increased TMB profile in elderly melanoma patients may restore the age-related immune dysfunction leading to favorable immune response to anti-PD-1/anti-PD-L1 therapy comparable between patients younger or older than 75 years old. An integrative analysis by Mo et al. showed that the gene mutation CTNNB1 (catenin beta-1), which is associated with a better prognosis in multiple tumors, would help in improving the clinical outcome of immunotherapy in patients with hepatocellular carcinoma (HCC). Interestingly, this study has reported a significant increase in tumor infiltrated NK cells in the HCC mutation group compared to wild-type group. Moreover, CTNNB1 mutation was associated with a downregulation of 4 immunoinhibitory genes including the NK cells immune checkpoint receptor CD96. Chen et al. showed that cyclin D1 (CCND1) amplification triggered multiple immunosuppressive hallmarks and may be useful to predict immune response to ICB. Bioinformatic and biostatistical analysis tools have been shown useful to predict gene signatures associated with clinical benefit of immune checkpoint blockade therapy. Indeed, the group of Chen R. L. have established an immune-related risk signature in squamous-cell lung cancer (SQLC) by identifying 8 immune-related genes that correlated with immune cells infiltration and clinical outcome in SQLC patients. Moreover, Chen S. et al. have developed an immunotherapy-responsive model including 10 prognostic genes that might be helpful to predict response to ICB in patients with metastatic urothelial carcinoma. Xue et al. have established and validated a signature profile including 23 immune related gene pairs (IRGP) associated with higher overall survival in cutaneous melanoma (CM) patients. This study showed that low 23-IRGP value with increased expression of PD-1/PD-L1 were associated with a better prognosis and suggested that the 23-IRGP could be a useful predictive biomarker of response to ICB therapy in CM patients. These findings indicate that immune related genes can be explored as promising biomarkers for predicting immunotherapy clinical outcomes. However, Wu S. et al. reported that mismatch repair deficiency and microsatellite instability are not sensitive predictive biomarkers in triple negative breast cancer and that the investigation of concomitant expression of immune checkpoints such as PD-L1 and LAG-3 in tumor tissue will be more helpful for establishing a successful ICB treatment *via* dual blockade antibodies therapy. Wu D. et al. identified highly immunogenic clonal neoantigen (in an epidermal growth factor receptor (EGFR)-mutated NSCLC patient benefitting from anti-PD-1 blockade after acquiring resistance to EGFR-Tyrosine kinase inhibitor (TKI) therapy. This study validated 4 clonal neoantigens, including 2 derived from EGFR 19del, 1 from Tumor protein P53 A161T (TP53 A161T) and 1 from DENN domain containing D6B R398Q (DENND6B R398Q) and emphasized the urgent need of robust approaches to explore specific clonal neoantigens derived from driver mutations to predict clinical benefit of ICB in EGFR-TKI resistant NSCLC patients. Zhang et al. showed a 20% decrease of 4 serum tumor biomarkers; carcinoembryonic antigen (CEA), cancer antigen 125 (CA125), cytokeratin 19 fragment (CYFRA21-1) and squamous cell carcinoma related antigen (SCC-Ag) at 6 weeks after anti-PD-1/PD-L1 therapy compared to baseline and this was associated with an improved prognosis of late-stage NSCLC patients. The group of Yao Chen stressed the need of predictive biomarkers to properly select those patients resistant to standard therapies but might benefit from a novel combination involving ICB. This group showed that high circulating-free DNA (cfDNA), high circulating tumor DNA (ct-DNA) and specific mutations (such as MIKI67 and hyper-progressive disease-related gene mutations) are associated with poor outcome in late-stage NSCLC patient treated with combination of ICB and anti-angiogenic therapy. The NY-ESO-1 cancer testis antigen has been shown to be expressed in several tumors. It is a highly immunogenic tumor-specific antigen inducing both humoral and T cell responses and it is considered as an attractive target for immunotherapy. In fact, NY-ESO-1 can be considered as a dynamic biomarker and a potential target of immunotherapy (4). Indeed, it has been demonstrated that melanoma patients treated with ipilimumab had an increased rate of NY-ESO-1-specific immunity that was associated with improved clinical benefit of the treatment, especially in patients developing both NY-ESO-1-specific antibody and specific CD8+ T cells (5). We have shown that immunological monitoring of NY-ESO-1-specific T cells response is a useful biomarker of response to anti-PD-1 treatment. We have characterized the expression of immunological markers before and after anti-PD-1 treatment in a patient with recurrent Head and neck Squamous cell carcinoma (HNSCC) who showed a transient regression and stability of the tumor after ICB for over 7 months. We observed that clinical responsiveness to anti-PD-1 treatment correlated with immunity to NY-ESO-1. Our results showed that NY-ESO-1-specific T cells response was increased after the fifth cycles of treatment (stable disease) but had a significant decline at progression, and that PD-1+ T cells population was markedly reduced after anti-PD-1 treatment (6). Recently, we have characterized a dynamic NY-ESO-1- specific T cells population that was significantly increased at treatment response in a patient with a metastatic gastric cancer who displayed a long-lasting response to combined radio-immunotherapy (4).

IDENTIFICATION OF PHENOTYPIC MARKERS IN IMMUNE CELLS BEFORE AND DURING IMMUNE CHECKPOINT INHIBITORS TREATMENT

Several studies have demonstrated that phenotypic characteristics of immune cells play an important role in predicting the prognosis of cancer patients and their response to different anti-cancer therapies, specifically ICB. Indeed, in a patient with metastatic gastric cancer who responded to combined radio-immunotherapy, we have identified a peripheral CD107+ cytotoxic T cells subset within a specific CD8/HLA-A2-NY-ESO-1 T cell population that was low at disease progression (2.5%), markedly increased at disease resolution (12.9%) and significantly decreased again at disease re-progression (3.6%) (4). In a retrospective study including 79 cancer patients who received anti-PD-1 therapy, Yuan et al. observed that responders had lower number of peripheral B cells compared to patients who developed post-treatment progressive disease. These findings suggest that blood B cells might be a potential biomarker for anti-PD-1 therapeutic outcome. Interestingly, Araujo B. de Lima et al. suggested that patients responding to ICB present a pre-existing immune cells signature qualified as "favorable immune periphery" useful to predict individuals who will benefit from ICB therapy. This group characterized peripheral immune cells phenotypic profile at baseline, 6 then 20 weeks after starting ICB in 33 patients with solid tumors. The results showed that high levels of circulating CD8+ PD-1+ T cells, of effector-memory CD8+ T cells, abundance of dendritic cells (DCs) and low levels of myeloid-derived suppressor cells and monocytes at baseline correlated with good prognosis and response to ICB treatment. Zielinski et al. discussed novel technologies that have the potential to accelerate the characterization of functional phenotype of immune cells before and during anti-cancer therapies to evaluate patients' response and to predict their prognosis. This study suggests high throughput approaches including multi-omics, single cells sequencing, flow cytometry, mass cytometry and bioinformatics for the exploration of immune cells dynamics and discovery of novel cancer biomarkers. Kidman et al. also pointed out the application of sequencing and single-cells analysis in characterizing dynamic changes in the T cell receptor (TCR) repertoire during ICB therapy to evaluate treatment outcome and stratify patients according to predicted beneficial response. Briefly, this study reported that anti-CTLA-4 treatment increases TCR diversity and clonal expansion of the peripheral and tumor-infiltrating lymphocytes. Moreover, this study suggested that the expression of PD-1+ blood T cells and the expansion of intra-tumoral TCR clonotypes could be predictive biomarkers of response to PD1/PD-L1 blockade. The same group has identified in murine model a subset of antigen specific CD8+ T cells correlating with a successful response to ICB (Principe et al.). Hence, this study suggested that increased effector memory antigen-specific CD8+ cytotoxic T cells in the presence of reduced regulatory T cells (Tregs) within tumors is predictive of response to anti-PD-L1 and anti-CTLA-4 treatment. Hübbe et al. discussed strategies described to stimulate endogenous DCs for improved anti-tumor immune response to ICB. Accordingly, the presence of adequately activated DCs could be considered as a biomarker for response to ICB since engagement of stimulated DCs will have an impact on the expansion, proliferation and priming of antigen-specific anti-tumor T cells. Finally, the expression levels of the inhibitory proteins PD-1 and CTLA-4 by T cells can be a useful prognostic biomarker associated with cancer immunity. Indeed, based on pan-cancer analysis of large cancer datasets, Liu et al. showed that a differential expression profiles of these immune cells inhibitory receptors are observed by cancer type and are associated with several parameters that play a key role in response to immunotherapy including tumor cell infiltration and TMB.

IDENTIFICATION OF CYTOKINES/CHEMOKINES SPECIFICALLY GENERATED BEFORE AND DURING IMMUNE CHECKPOINT INHIBITORS TREATMENT

Cytokines and chemokines are biomarkers that play a pivotal role in immune cells activity. It has been shown that differential expression levels of these biomarkers were observed during ICB and can be helpful in monitoring the clinical outcome. We have shown that several cytokines/chemokines involved in immune activation were upregulated after ICB (nivolumab) treatment of HNSCC patient; 2 biomarkers were reduced at progression [interleukin (IL)-10: ****$p < 0.0001$ and CX3CL1: ****$p < 0.0001$] (6). On the other hand, some cytokines/chemokines contributing to immune inhibition were downregulated after nivolumab treatment; 2 biomarkers were increased at progression (IL-6: ****$p < 0.0001$ and IL-8: ****$p < 0.0001$) (6). We have also shown that downregulation of IFN-γ, tumor necrosis factor-α (TNF-α) and few interleukins (IL-2, IL-5 and IL-6) concomitant with an upregulation of perforin, soluble FAS, macrophage inflammatory protein-3α (MIP-3α) and C-X-C motif chemokine 11/Interferon–inducible T Cell Alpha Chemoattractant) correlated with disease resolution in a metastatic gastric patient treated with combined radioimmunotherapy (4).

BIOMARKERS ASSOCIATED WITH TREATMENT RELATED TOXICITY AFTER TREATMENT WITH IMMUNE CHECKPOINT INHIBITORS

As a consequence of their activity as modulators of the immune response, ICB can exert immune-related adverse events (irAEs) potentially leading to severe outcome and discontinuation of therapy. In addition to most common side effects including dermatological (reticular, erythematous rash), gastrointestinal (diarrhea, colitis), and endocrine (thyroid, adrenal, pituitary glands) effect, rarely described hematological irAEs associated

with ICB therapy (thrombocytopenia, aplastic anemia, etc.) are emphasized in a systematic review of 49 case report articles which also summarized the current approaches used to manage this toxicity (Omar et al.). The pattern and the onset of irAEs differ by ICB treatment and by cancer type resulting in a highly variable clinical presentation considered as a complicated challenge for oncologists. Therefore, the identification of biomarkers for early recognition and appropriate management of ICB-iRAEs is critical for clinical practice. Indeed, several studies have urged the need of accurate irAEs biomarkers and highlighted the difficulty to distinguish them from regular toxicities. Pringle et al. reported an infiltration of CD4+ and CD8+ T cells and an increased expression of proliferative (ki67+) and senescent (p16+) epithelial cells in the salivary gland tissue of a NSCLC patient who was suffering from post-durvalumab (anti-PD-L1) hyposalivation. The review article by Hommes et al. presents a combination of biomarkers that can be useful to predict ICB toxicity, including blood-based (neutrophil-to-lymphocyte ratio, absolute lymphocyte count, lymphocytes, autoantibodies and various serum cytokines/chemokines), immunogenetic (single nucleotide polymorphisms, human leucocyte antigen subtypes) and microbial biomarkers (microbiome composition). However, this study highlights the limitations related to the specificity and accuracy of these biomarkers. Rose L. M. et al. evaluated the association between tumor type, pre-treatment clinical parameters and the occurrence of irAEs in cancer patients treated with ICB as a monotherapy or in combination. This retrospective study suggests that demographic parameters (female, obesity) and preexisting clinical factors, such as high eosinophils or white blood cells counts and pre-existing autoimmune disease, could help identify cancer patients at higher risk of developing irAEs (Rose L. M. et al.). An interesting review by Xu et al.). summarized the key potential biomarkers from the tumor microenvironment, peripheral blood, targeted organs, host-related demographic parameters and treatment history, associated with an increased incidence of ICB-related toxicities. However, with the modification of the tumor status, tumor microenvironment, immune response and potential concomitant therapies, dynamic monitoring would be required for several biomarkers to manage the toxic outcome accurately and adequately. In conclusion, the identification of specific biomarkers for ICB-related toxicities is still at exploratory research stage and needs further and larger investigations. In an attempt to overcome the side effects of ICIs monoclonal antibodies, researchers are trying to target checkpoint inhibitors such as PD-L1 using novel immunotherapeutic approaches. In a phase I clinical trial, Jørgensen et al. showed that subcutaneous vaccination with IO103 peptide against PD-L1 induced significantly high immunogenicity with low-grade and reversible toxicity in multiple myeloma patients.

CONCLUSION

The study of the dynamics of the immune system and tumor microenvironment during ICB is crucial to predict favorable response and to manage undesirable adverse events. Dynamic predictive biomarkers of ICB identified so far are still at exploration phase and have limited reliability on a patient basis. The development of models combining multiple variables dynamics and using novel system approaches such as multi-omics, single cells analysis and rigorous biostatistics and bioinformatics tools is key in the identification of reliable predictive dynamic biomarkers to pave the way towards a more personalized, beneficial and safer ICB therapy.

AUTHOR CONTRIBUTIONS

SD, TM, and MM developed and designed the topic, selected authors, and reviewers, reviewed submitted articles and supported their publication. MM, TM, and SD wrote the editorial. All authors revised the manuscript and approved the submitted version.

FUNDING

SD and MM are supported by the Medical Research Center at Hamad Medical Corporation under the approved grant MRC-01-19-300. TM is supported by the Ludwig Institute for Cancer Research, NIH/NCI Cancer Center Support Grant P30 CA008748, the Parker Institute for Cancer Immunotherapy and Swim Across America.

REFERENCES

1. Robert C, Schachter J, Long GV, Arance A, Grob JJ, Mortier L, et al. Pembrolizumab *Versus* Ipilimumab in Advanced Melanoma. *N Engl J Med* (2015) 372(26):2521–32. doi: 10.1056/NEJMoa1503093
2. Wolchok JD, Chiarion-Sileni V, Gonzalez R, Rutkowski P, Grob JJ, Cowey CL, et al. Overall Survival With Combined Nivolumab and Ipilimumab in Advanced Melanoma. *N Engl J Med* (2017) 377(14):1345–56. doi: 10.1056/NEJMoa1709684
3. Relecom A, Merhi M, Inchakalody V, Uddin S, Rinchai D, Bedognetti D, et al. Emerging Dynamics Pathways of Response and Resistance to PD-1 and CTLA-4 Blockade: Tackling Uncertainty by Confronting Complexity. *J Exp Clin Cancer Res* (2021) 40(1):74. doi: 10.1186/s13046-021-01872-3
4. Merhi M, Raza A, Inchakalody VP, Siveen KS, Kumar D, Sahir F, et al. Persistent Anti-NY-ESO-1-Specific T Cells and Expression of Differential Biomarkers in a Patient With Metastatic Gastric Cancer Benefiting From Combined Radioimmunotherapy Treatment: A Case Report. *J Immunother Cancer* (2020) 8(2). doi: 10.1136/jitc-2020-001278
5. Yuan J, Adamow M, Ginsberg BA, Rasalan TS, Ritter E, Gallardo HF, et al. Integrated NY-ESO-1 Antibody and CD8+ T-Cell Responses Correlate With Clinical Benefit in Advanced Melanoma Patients Treated With Ipilimumab. *Proc Natl Acad Sci USA* (2011) 108(40):16723–8. doi: 10.1073/pnas.1110814108
6. Merhi M, Raza A, Inchakalody VP, Nashwan AJJ, Allahverdi N, Krishnankutty R, et al. Squamous Cell Carcinomas of the Head and Neck Cancer Response to Programmed Cell Death Protein-1 Targeting and Differential Expression of Immunological Markers: A Case Report. *Front Immunol* (2018) 9:1769. doi: 10.3389/fimmu.2018.01769

Conflict of Interest: TM has acted as a consultant for Immunogenesis, Immunos Therapeutics and Pfizer, has received research support from Adaptive Biotechnologies, Aprea, Bristol Myers Squibb, Infinity Pharmaceuticals, Kyn Therapeutics, Leap Therapeutics, Peregrine Pharmaceuticals and Surface Oncology, is listed as a co-inventor on patents relating to the use of oncolytic viral therapy, alphavirus-based vaccines, antibodies targeting CD40, GITR, OX40, PD-1 and CTLA-4 and neo-antigen modelling, and is a cofounder of and holds an equity in IMVAQ Therapeutics.

The remaining authors declare that the research was conducted in the absence of any commercial or financial relationships that could be construed as a potential conflict of interest.

Publisher's Note: All claims expressed in this article are solely those of the authors and do not necessarily represent those of their affiliated organizations, or those of the publisher, the editors and the reviewers. Any product that may be evaluated in this article, or claim that may be made by its manufacturer, is not guaranteed or endorsed by the publisher.

frontiers in Oncology

CASE REPORT
published: 02 April 2020
doi: 10.3389/fonc.2020.00420

Lack of Conventional Acinar Cells in Parotid Salivary Gland of Patient Taking an Anti-PD-L1 Immune Checkpoint Inhibitor

Sarah Pringle[1], Bert van der Vegt[2], Xiaoyan Wang[1], Nico van Bakelen[3], T. Jeroen N. Hiltermann[4], Fred K. L. Spijkervet[3], Arjan Vissink[3], Frans G. M. Kroese[1] and Hendrika Bootsma[1]*

[1] Department of Rheumatology and Clinical Immunology, University of Groningen, University Medical Center Groningen, Groningen, Netherlands, [2] Department of Pathology and Medical Biology, University of Groningen, University Medical Center Groningen, Groningen, Netherlands, [3] Department of Oral and Maxillofacial Surgery, University of Groningen, University Medical Center Groningen, Groningen, Netherlands, [4] Department of Pulmonary Disease, University of Groningen, University Medical Center Groningen, Groningen, Netherlands

OPEN ACCESS

Edited by:
Maysaloun Merhi, Hamad Medical Corporation, Qatar

Reviewed by:
Alan Baer, Johns Hopkins University, United States
Karl Albert Brokstad, University of Bergen, Norway

***Correspondence:**
Sarah Pringle
s.a.pringle@umcg.nl

Specialty section:
This article was submitted to Cancer Immunity and Immunotherapy, a section of the journal Frontiers in Oncology

Received: *15 January 2020*
Accepted: *10 March 2020*
Published: *02 April 2020*

Citation:
Pringle S, van der Vegt B, Wang X, van Bakelen N, Hiltermann TJN, Spijkervet FKL, Vissink A, Kroese FGM and Bootsma H (2020) Lack of Conventional Acinar Cells in Parotid Salivary Gland of Patient Taking an Anti-PD-L1 Immune Checkpoint Inhibitor. Front. Oncol. 10:420. doi: 10.3389/fonc.2020.00420

Background: Salivary glands (SGs) can be damaged by immune checkpoint inhibitor (ICI) therapy. In patients with ICI-induced SG dysfunction, 60% progress to fulfill classification criteria for primary Sjögren's syndrome (pSS), owing to immune foci in SGs and/or anti-SSA autoantibody positivity. We report the SG tissue analysis of a patient with SG dysfunction after treatment with a programmed death ligand-1 (PD-L1) inhibitor, compared to that of a dry mouth ("sicca") control and pSS patient.

Case presentation: The patient received the PD-L1 inhibitor durvalumab (10 mg/kg, every 2 weeks by intravenous infusion) as adjuvant treatment for stage 3 non-small cell lung carcinoma, following concurrent chemo radiotherapy. At 43 weeks after 21 cycles of Durvalumab, the patient was not capable of producing unstimulated or stimulated parotid gland saliva, and a biopsy was taken. Immunohistochemical analysis showed no classical $AQP5^+$ $CK7^-$ acinar cell clusters (CK7 marks intercalated ducts, IDs). In contrast, the parenchyma was dominated by hybrid epithelial "structures" with ID-like morphology, containing a mixture of $AQP5^+CK7^-$, $AQP5^-CK7^+$, and $AQP5^+CK7^+$ cells (30 structures/mm^2). These structures were present at lower frequencies in sicca control (2/mm^2) and pSS (10/mm^2) tissue. Hybrid structures contained proliferating ($Ki67^+$) cells and senescent ($p16^+$) cells. Striated ducts showed no abnormal morphology post PD-L1 treatment, in contrast to pSS tissue. PD-L1 expression was detected in the SG parenchyma following anti-PD-L1 therapy. The SG post-PD-L1 therapy further demonstrated focal lymphocytic sialadentitis, harboring disperse, and focal $CD4^+$ T cell-rich infiltrates. $CD8^+$ T cells were also present. In this patient, these $CD4^+$ and $CD8^+$ T cells were observed in-between and inside hybrid structures. $CD20^+$ B-cells were infrequently detected following PD-L1 blockade, in contrast to their preponderance in pSS SG tissue.

Conclusion: This patient lacked conventional SG acinar cells following anti-PD-L1 therapy and demonstrated presence of hybrid intercalated duct-like structures.

Understanding which mechanisms and dynamics underpinning this aberrant parenchyma may be crucial to understand how SG dysfunction post ICI therapy, and potentially other affected organs. Furthermore, although the patient treated with anti-PD-L1 antibody examined here fulfills the criteria for pSS and demonstrated focal lymphocytic sialadentitis, the further histopathological characteristics do not resemble pSS.

Keywords: checkpoint inhibitors, anti PD-L1 therapy, salivary gland dysfunction, immune related adverse event, cancer treatment, sicca syndrome, hyposalivation

BACKGROUND

Immune checkpoint inhibitor (ICI) therapy is the engagement of the immune system to kill tumor cells via the blockade of immune system inhibitory checkpoints, mostly employing cytotoxic T-lymphocyte associated protein 4 (CTLA-4), programmed cell death protein-1 (PD-1) and programmed death ligand-1 (PD-L1). ICIs are efficacious in melanoma, lung cancer and head and neck cancer treatment (1). In up to 60% of patients taking ICIs, however, inflammatory diseases such as colitis, pneumonitis, arthritis, inflammatory myopathy, vasculitis, nephritis and sialadentitis, resembling primary Sjögren's syndrome [pSS, including salivary gland (SG) hypofunction] are observed (1–4). "Sicca" syndrome arising from SG hypofunction, including dry mouth, are reported at frequencies of 5% of all patients taking ICIs (1–5).

In a healthy scenario, SG acinar cells produce and secrete saliva, channeled through ducts into the mouth. The vast majority of saliva is produced by the major (parotid, submandibular, and sublingual) SGs, with small contributions from the minor SGs located in the lips and oral cavity. SGs are thought to be maintained by the proliferation and differentiation of tissue resident progenitor cells, largely located in the intercalated and striated ducts (6–9). The observation that ICI-induced hyposalivation cannot be rescued by corticosteroid treatment to dampen inflammation suggests that inflammation is not causing SG hypofunction (3, 10, 11). The SG epithelium is endowed with an ability to receive and transduce inflammatory signals, and actively participate in inflammatory processes, suggesting that a closer examination of the processes following ICI use is crucial to our comprehension of this side-effect (12).

In the case presented here, we compare a parotid SG following prolonged anti-PD-L1 therapy with a sicca control parotid SG, and with a parotid SG from a patient with pSS, to compare the effect of ICI treatment on the SG parenchyma. pSS is an autoimmune disease characterized partly by SG dysfunction, including lymphocytic infiltration, and the presence of anti-SSA autoantibodies, resulting in hyposalivation and oral dryness. SG lymphocytic infiltration in later stages of pSS is predominantly B-cell based, and can also include presence of germinal centers and lymphoepithelial lesions (LELs) (13, 14). An increase in IgG plasma cells in the glands, resulting in <70% IgA plasma cells, further characterizes pSS. Presence of anti-SSA antibodies in blood, and/or a positive focus score (a read-out of SG lymphocytic infiltration extent) plus reduced saliva output leads to classification of our patient as suffering from pSS [ACR-EULAR 2016 criteria (15)]. Studies have suggested that ∼60% of patients treated with ICIs and experiencing dry mouth complaints also demonstrate presence of SSA antibodies and/or a positive focus score, designating them technically as suffering from pSS (3, 5, 10, 11). The nature of the lymphocytic infiltration following ICI therapy has been suggested to be $CD4^+$ T cell dominated in the minor SGs (3, 5). That of the major SGs and indeed the pathology of the parenchyma, responsible for the majority of saliva production and secretion, has not been documented.

CASE PRESENTATION

The patient (male, 52 years old) received the PD-L1 checkpoint inhibitor durvalumab as an adjuvant treatment for stage 3b non-small cell lung carcinoma of the right upper lobe, following chemo-radiotherapy. Durvalumab was administered intravenously every 2 weeks at a dose of 10 mg/kg, as previously published (16). The patient had a history of psoriasis. The patient completed 1 year, 26 cycles of durvalumab. At cycle 11, he presented clinically with a subjective sensation of dry mouth, "*sicca*" complaints, and was not able to produce any unstimulated or stimulated parotid saliva Additional clinical data is presented in **Table 1**. Ultrasonography revealed moderate change in SG topography (HOCEVAR score of 14/48), but remained under the threshold score of 15/48 for a positive result (17–19). The Schirmer's test for ocular dryness was positive (4 mm tear fluid /5 min), as opposed to the ocular staining score (OSS), which was negative (0). In order to examine the pathology of the SG, a parotid SG biopsy was performed following our previously published protocol (20).

For comparison, parotid SG tissue from a sicca control pSS patient were also analyzed. The sicca control patient demonstrated reduced saliva production, negative HOCEVAR score of 9/48, negative ocular dryness scores and no signs of pSS development (**Table 1**). The patient with pSS was not capable of producing unstimulated parotid saliva, produced reduced volumes of stimulated parotid saliva (**Table 1**). The patient with pSS also demonstrated SSA autoantibody positivity, a positive ultrasound score (26/48), and positive test results for ocular dryness (**Table 1**). All parotid salivary gland biopsies were immunostained as previously reported, with CD45, CD20, CD3, CD4, CD8, Ki67, IgA, IgG, Bcl6, high molecular

TABLE 1 | Clinical characteristics of patients.

Characteristics		Sicca control	pSS	Anti-PD-L1
Sex		Female	Female	Male
Age		68	47	52
Unstimulated whole saliva (ml/min)		ND	0.05	0
Stimulated whole saliva (ml/min)		1.35	0.37	0
Unstimulated parotid saliva (ml/min)	Left	0	0	0
	Right	0	0	0
Stimulated parotid saliva (ml/min)	Left	0	0.09	0
	Right	0.06	0.05	0
Unstimulated submandibular/sublingual saliva (ml/min)	Left + Right	0.02	0.05	0
Stimulated submandibular/sublingual saliva (ml/min)	Left + Right	0.14	0.23	0
Focus score (foci/4mm^2)		0	2.5	1.0
Lymphoepithelial lesions (LELs)		No	Yes	No
Germinal Center		No	Yes	No
IgG plasma cells		No	No	No
Ultrasound score		–(9/48)	+(26/48)	–(14/48)
Ocular staining score (OSS)		0	3	0
Schirmer's test (mm/5min)		6	0	4
ANA titre		Neg	1:640	1:160
SSA		–	+	+

ND, no data; ANA, anti-nuclear antibody; HC, healthy control. Ultrasound was scored using the Hocevar et al. scoring system, as validated in Mossel et al., Annals Rheumatic Diseases, 2017 (17). Ocular staining score (OSS) is considered positive for ocular dryness with a score of >3 in at least one eye. Schirmer's test is considered suggestive of ocular dryness with <5 mm tear fluid/5 min in at least one eye. Serum levels of anti-SSA antibodies were assessed with ELISA tests and scored as positive according to standard procedures if more than 10 IU/mL.

weight cytokeratins, p16 and PD-L1 (all Ventana) (21). Biopsies were additionally double immunostained for AQP5 and CK7, following antigen retrieval with EDTA buffer (pH = 8) for 15 min. A double staining kit containing secondary antibodies from Thermofisher was used (TL-012-MARH). Primary antibodies of AQP5 (Abcam, clone EPR3747, 1:200) and CK7 (Sigma-Aldrich, clone RCK105, 1:100) were diluted in PBS.

Lack of Conventional Acinar Cells and Skewing of the Epithelial Compartment Toward Hybrid Intercalated Duct-Like Structures

In order to examine the effect of anti-PD-L1 therapy on the SG, we examined the striated ducts (SDs), intercalated ducts (IDs) and acinar cells. The SDs of the SG in pSS can undergo invasion by B cells, become proliferative and lead to formation of LELs. The SDs of the sicca control patient demonstrated minimal presence of Ki67$^+$ proliferative cells (**Figure 1a**). Proliferative epithelial cells, defined by immunostaining for Ki67 and high molecular weight cytokeratins (hmwCK) in serial sections, were detected in the pSS tissue (**Figures 1b–d**). No effect of anti-PD-L1 therapy was apparent on SDs, which displayed a phenotype similar to the sicca control and minimal proliferative cells, marked by Ki67$^+$ (**Figures 1a,e**).

In order to probe how durvalumab effects the acinar and ID cell compartments, we immunostained tissue with AQP5 to mark acinar cells and CK7 to denote IDs. In healthy conventional acinar cells, AQP5 is expressed at the apical cell membrane, and CK7 is not heavily expressed. In sicca control and pSS biopsies, clusters of AQP5$^+$CK7$^-$ acinar cells with large cytoplasm:nucleus ratios and are easily identifiable (280/mm^2 sicca control; 170/mm^2 pSS; **Figures 1f,g**). AQP5 is localized apically in healthy acinar cell clusters (**Figure 1f**, inset). In pSS tissue, these conventional acini demonstrated some dysregulation of AQP5 localization, in line with other studies of the minor SGs, but maintained their large cytoplasm:nucleus ratio (22). Acinar clusters in pSS tissue also contained occasional CK7$^+$ cells. (**Figure 1g** inset). In tissue following PD-L1 blockade, AQP5$^+$CK7$^-$ acinar clusters with large cytoplasm:nucleus ratio and apically located AQP5 were not detectable (**Figure 1h**). The parenchyma post-PD-L1 blockade was instead dominated by mixture of AQP5$^+$CK7$^-$, AQP5$^-$CK7$^+$, and AQP5$^+$CK7$^+$ cell clusters, whereby AQP5 localization was homogenous throughout the cells and cells maintained a low cytoplasm:nucleus ratio (**Figures 1h,i**). Interestingly, "hybrid" epithelial structures comprising a mixture of AQP5$^+$ and CK7$^+$ cells comprised 70% of total epithelial cell clusters (33 structures /mm^2; **Figures 1h,j**). Such hybrid epithelial structures were also present in sicca control and pSS tissue, but at much lower frequencies (sicca control 2% of total IDs, 2 IDs/mm^2; pSS 12%, 10/mm^2; **Figures 1j,k**). In sicca control and pSS tissue, CD4$^+$ and CD8$^+$ T cells were detected sporadically in SG parenchyma (acinar cells plus IDs; **Figures 1l,m,o,p**). Both T cell subsets were present dispersed at visibly higher frequencies, both in-between and inside epithelial structures following anti-PD-L1 therapy (**Figures 1n,q**).

Intercalated Duct-Like Structures Cells Are Proliferative and Potentially Senescent and Following Anti-PD-L1 Therapy

In order to probe parenchymal cell dynamics, we immunostained for the senescence marker p16, and Ki67. In the sicca control and pSS parotid SGs, Ki67$^+$ proliferating cells were detected at a total frequency of 6/mm^2 and 24/mm^2, respectively (**Figures 2a,b**). Ninety percent of Ki67$^+$ cells (equal to 5 cells/mm^2) were located in the epithelium (SDs, IDs, and acini) in sicca control tissue, and 66% (equal to 16 cells/mm^2) in pSS tissue (**Figure 2d**). In tissue following anti PD-L1 therapy, 275 Ki67$^+$ cells/mm^2 were detected, of which 85% (equal to 230 cells /mm^2) were located within the ID-like epithelial structures (**Figures 2c,d**). The remaining Ki67$^+$ cells were located in SDs (**Figures 2c,d**).

p16 can be used to denote senescent cells. p16$^+$ cells were present at frequencies of 31/mm^2 in sicca control tissue (**Figures 2e,h**), and were mostly stromal/non epithelial in nature. We have previously shown that the epithelium of parotid SGs in the autoimmune disease pSS is likely to contain

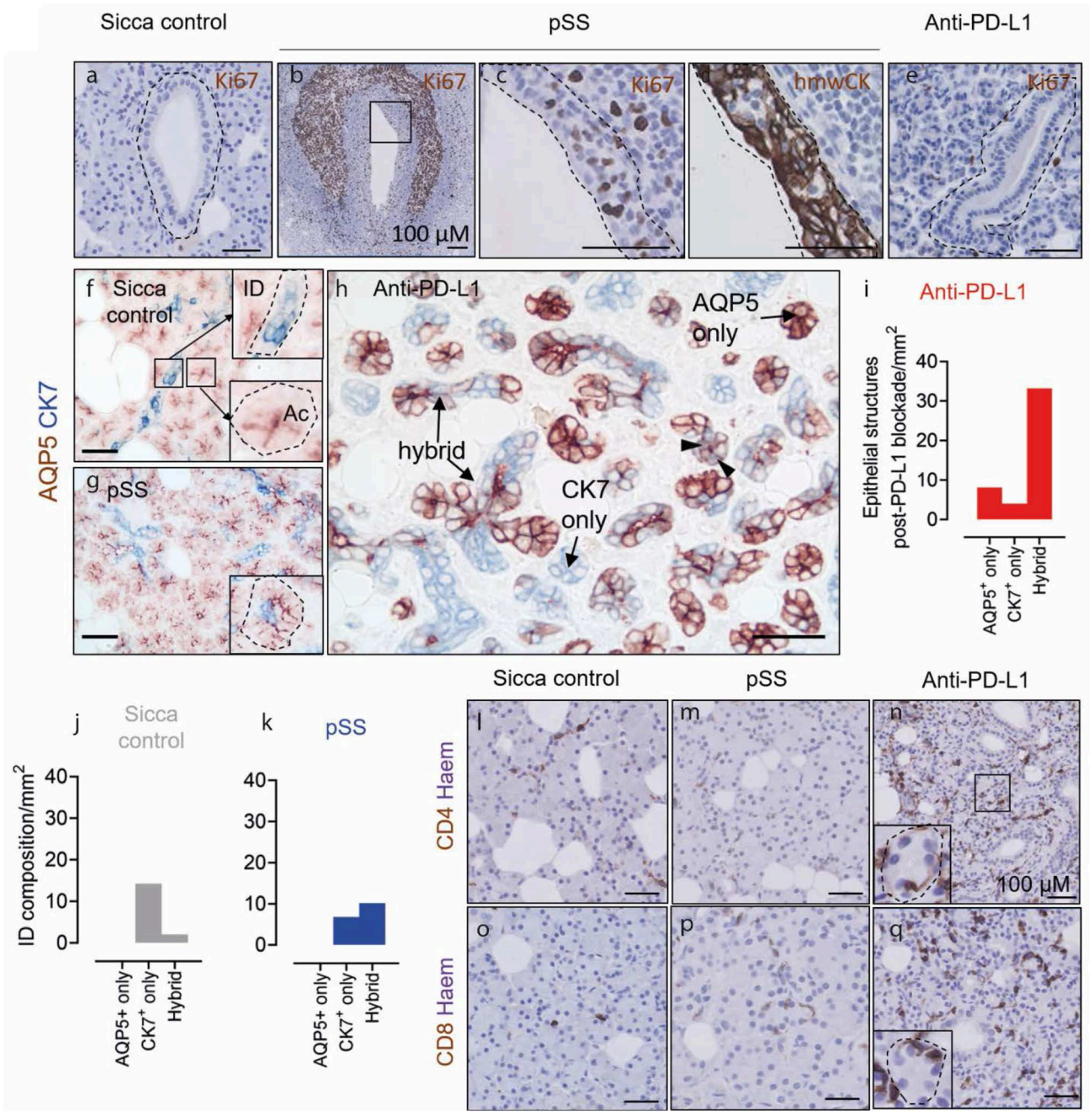

FIGURE 1 | Lack of acinar cells and presence of AQP5$^+$ CK7$^+$ hybrid epithelial structures in the parotid salivary gland following anti-PD-L1 therapy. **(a,b,c,e)** Ki67 staining in striated ducts of sicca control, pSS and post-anti-PD-L1 therapy tissue. Panels **(c,d)** (immunostained for high molecular weight cytokeratins (hmwCK) to mark SD cells, outlined in dashed line) show high resolution of area in inset in **(b)**. **(f–h)** AQP5 and K7 double immunostaining of sicca control, pSS and post-anti-PD-L1 therapy tissue. Insets in **(f)** shows normal K7 and apical AQP5 staining patterns of intercalated ducts and acinar cell, respectively. Inset in **(g)** show acinar cell clusters in pSS with occasional CK7$^+$ cell presence. Block arrows in **(h)** denote AQP5-K7 double-positive cells. **(i)** Quantification of AQP5 and CK7 cell content of epithelial cell structures following anti-PD-L1 blockade. **(j)** Quantification of composition of intercalated duct in sicca control tissue. **(k)** Quantification of composition of intercalated ducts in pSS tissue. **(l,m)** CD4 immunostaining. **(o–q)** CD8 immunostaining. All scale bars represent 50 μm, unless otherwise stated.

elevated numbers of p16$^+$ senescent cells (8). Indeed, p16$^+$ cells were detected in pSS tissue at a total frequency of 37/mm^2 (**Figures 2f,h**). In pSS tissue, p16$^+$ cells were mostly located in striated ducts, in line with our previous studies (13/mm^2 in SDs, 8/mm^2 IDs, 9/mm^2 acinar cells; **Figures 2f,h**). p16$^+$ cells were present in SG tissue following anti-PD-L1 therapy at a frequency of 51/mm^2, higher than both sicca control and pSS, of which 95% (equal to 48 cells/mm^2) were located in the ID-like epithelial structures described in **Figures 1, 2g,h**.

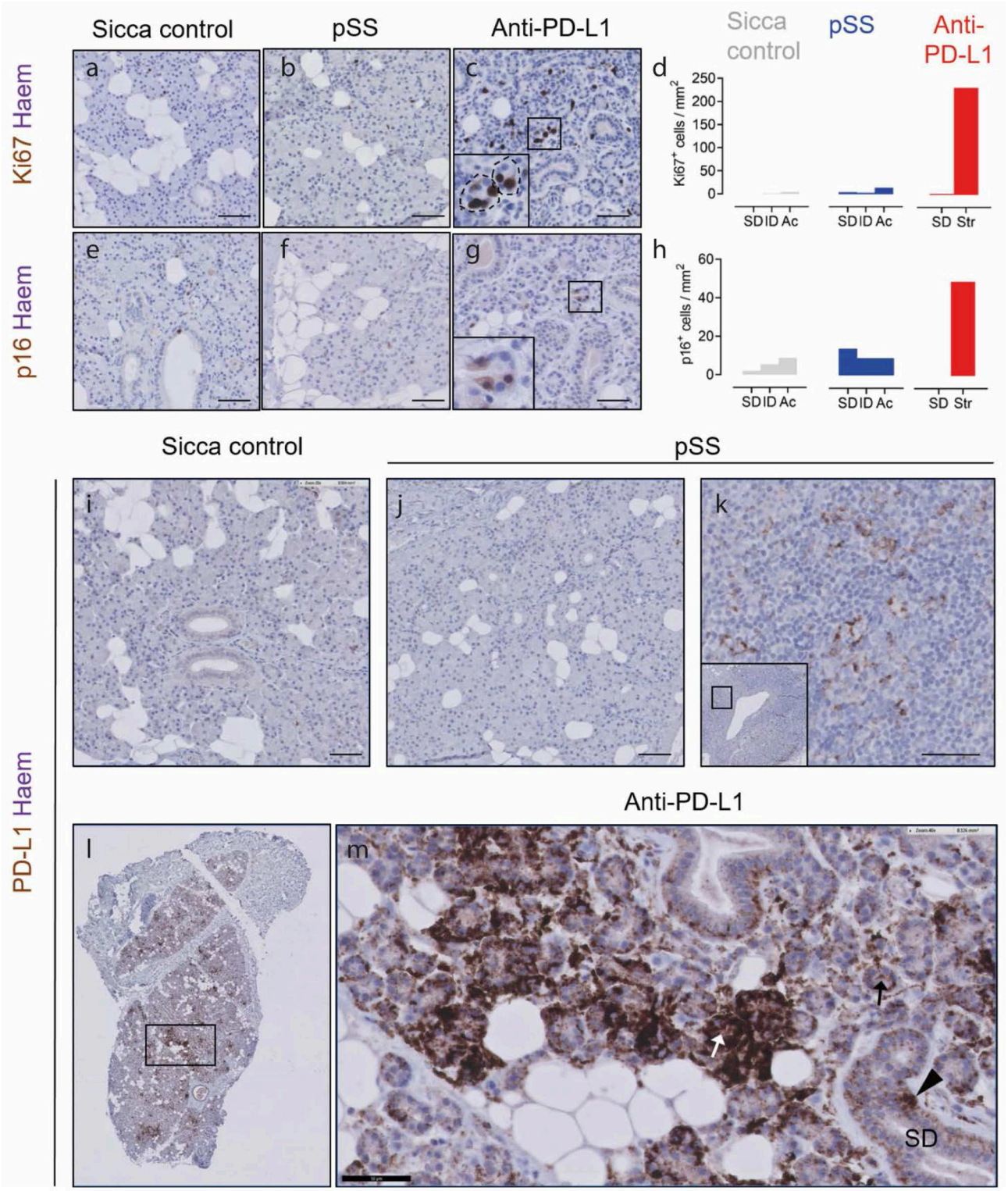

FIGURE 2 | Hybrid epithelial structures following PD-L1 therapy are proliferative, potentially senescent and express PD-L1. **(a–c)** Ki67 immunostaining of sicca control, pSS and post PD-L1 therapy SG tissue. Inset in **(c)** shows high resolution image of boxed area in main panel. **(d)** Quantification of Ki67$^+$ epithelial cell types (sicca control and pSS tissue) or hybrid epithelial structures (str; anti-PD-L1 blockade). **(e–g)** Immunostaining of sicca control, pSS and post-PD-L1 blockade tissue for p16. **(h)** Quantification of frequency of p16$^+$ cells in epithelial cell types (sicca control and pSS tissue), and hybrid epithelial structures (str; anti-PD-L1 tissue). SDs,

(Continued)

FIGURE 2 | striated ducts; ID, intercalated ducts; Ac, acini clusters. **(i)** PD-L1 immunostaining in sicca control. **(j)** PD-L1 immunostaining in pSS tissue. **(k)** PD-L1 immunostaining in germinal center of pSS SG tissue, showing PD-L1$^+$ lymphocytes. **(l)** Low resolution microscopy of PD-L1 immunostaining in patient taking durvalumab. **(m)** High resolution image of patient taking durvalumab, showing intensely PD-L1$^+$ epithelial structures (white arrow), lightly positive epithelial structures (black arrow) and positive striated duct cells (block arrow). All scale bars represent 50 μM.

Intercalated Duct-Like Structures and Striated Ducts Express PD-L1 Following Anti-PD-L1 Therapy

In order to establish if anti-PD-L1 therapy may exert a direct effect on the SG epithelium, we performed immunostaining for PD-L1. In sicca control and pSS tissue, no PD-L1$^+$ cells were present in the SG parenchyma (**Figures 2i,j**). PD-L1$^+$ presumptive dendritic cells were detected in the germinal center of pSS tissue (**Figure 2k**). In tissue following PD-L1 blockade, unconventional epithelial structures were either lightly or intensely PD-L1$^+$ (**Figures 2l,m**). Striated ducts also demonstrated some PD-L1 positivity (**Figure 2m**).

Patient Parotid SG Following Prolonged PD-L1 Inhibitor Use Contains Mostly CD4$^+$ T Cell Infiltrate and Does Not Resemble pSS Parotid SG Gross Pathology

In order to compare SG histopathological findings (i.e., nature of sialadentitis, presence of LELs, IgG plasma cells, and germinal centers) in a patient with sicca following PD-L1 blockade to that observed in pSS, we performed immunohistochemical staining for infiltrating lymphoid cells. Sicca control parotid SGs show dispersed, scarce CD45$^+$ cell presence, no focal CD45$^+$ cell presence, no focal lymphocytic sialadentitis, no LELs, germinal centers or IgG plasma cell presence (**Figure 3a**). These features were all present in the parotid biopsy of the pSS patient examined (**Figures 3b–g**; clinical details in **Table 1**). CD45$^+$ leukocytes were present throughout the biopsy post PD-L1 blockade, both periductally and dispersed between the epithelial cells of the parenchyma (**Figure 3h**). The infiltrate was composed of a majority of CD4$^+$ T cells, in addition to considerable presence of CD8$^+$ T cells, and a minor contribution to total infiltrate from CD20$^+$ B cells (**Figures 3i–o**). CD4$^+$ and CD8$^+$ lymphocytes present were both diffusely dispersed through the tissue and focally clustered around the striated ducts, in a similar manner to pSS ("focal sialadentitis"; **Figures 3k,l,n,o**). No LELs, germinal centers or IgG secreting plasma cells were observed in this biopsy (**Figures 1p**, **3**, **Table 1**). A focus score of 1.0 was calculated for the anti-PD-L1 treated patient (the focus score of the pSS patient was 2.5). Together with the lack of saliva production, this focus score would lead to classification of this patient post-PD-L1 therapy as suffering from pSS.

DISCUSSION AND CONCLUSIONS

In this case study, we examine parotid SG morphology of a patient with sicca complaints following anti-PD-L1 therapy, with particular attention for the epithelium. The most striking observation was the lack of cells responsible for producing saliva, namely conventional acinar cell clusters with apically located AQP5 expression and high cytoplasm:nucleus ratio. Intercalated duct-like epithelial structures composed of a mixture of AQP5$^+$CK7$^-$, AQP5$^-$CK7$^+$, and AQP5$^+$CK7$^+$ cells dominated the parenchyma instead, whereby AQP5 was mislocalized. Considering the lack of parotid SG function by this patient, these structures are presumably not capable of saliva production. This appears to be in contrast with the phenotype of the minor SGs observed post-ICI use, whereby conventional acinar cells are still present, suggesting striking differences in the reactionary abilities between major and minor SGs (3, 5). The phenotype is also dissimilar to parotid SG dysfunction induced by radiation, where saliva production is lost immediately following radiation (as opposed to around 70 days post ICI commencement), and where tissue will demonstrate both fibrosis and acinar cell cluster loss (23).

A predominance of CD4$^+$ T cell lymphocytic infiltration in the parotid SG post-PD-L1 therapy was observed, although CD8$^+$ T cell presence was also considerable. CD20$^+$ B-cells were nearly absent. This is in agreement with literature examining minor SGs, where mostly CD4$^+$ infiltrate was observed (3, 5). CD4$^+$ and CD8$^+$ T cells were found both focally around but not inside SDs, in addition to dispersed throughout the tissue. Both CD4$^+$ and CD8$^+$ T cells also infiltrated the ID-like epithelial structures post PD-L1 blockade. Interestingly, CD8$^+$ T cells and CD4$^+$ T cells were also found sporadically in acinar cell clusters of SG tissue from sicca control and pSS patients, albeit at lower frequency. These data may suggest that CD8$^+$ cell presence in the SG parenchyma is detrimental to SG/acinar function, considering neither sicca control or pSS patient produced normal amounts of saliva (24).

The phenotype of the SG described in the current case study raises questions about the sequence of events occurring in the SG following anti-PD-L1 therapy, and their effect on acinar cells. PD-L1 expression was greater in the SG parenchyma after anti-PD-L1 blockade, compared to sicca and pSS control tissues. Which stimuli originally triggers this increased PD-L1 expression, and any effect thereafter on SG function of epithelial PD-L1 interaction with PD-L1 blocking therapeutics such as durvalumab remains to be clarified. Existing studies have documented a relationship between PD-L1 expression and interferon-γ levels (IFNγ), whereby IFNγ has been shown to increase PD-L1 expression, and PD-L1 expression to be protective against interferon-γ induced toxicity (25, 26). CD4$^+$ and CD8$^+$ T cells recruited to the SG may be responsible for the gross alterations in parotid SG dynamics observed, although which particular CD4$^+$ or CD8$^+$ subsets are responsible will require phenotyping of the infiltrate. Proliferative (Ki67$^+$) and potentially senescent (p16$^+$) epithelial cells were detected in this SG post PD-L1 therapy. The ability to proliferate implies that a

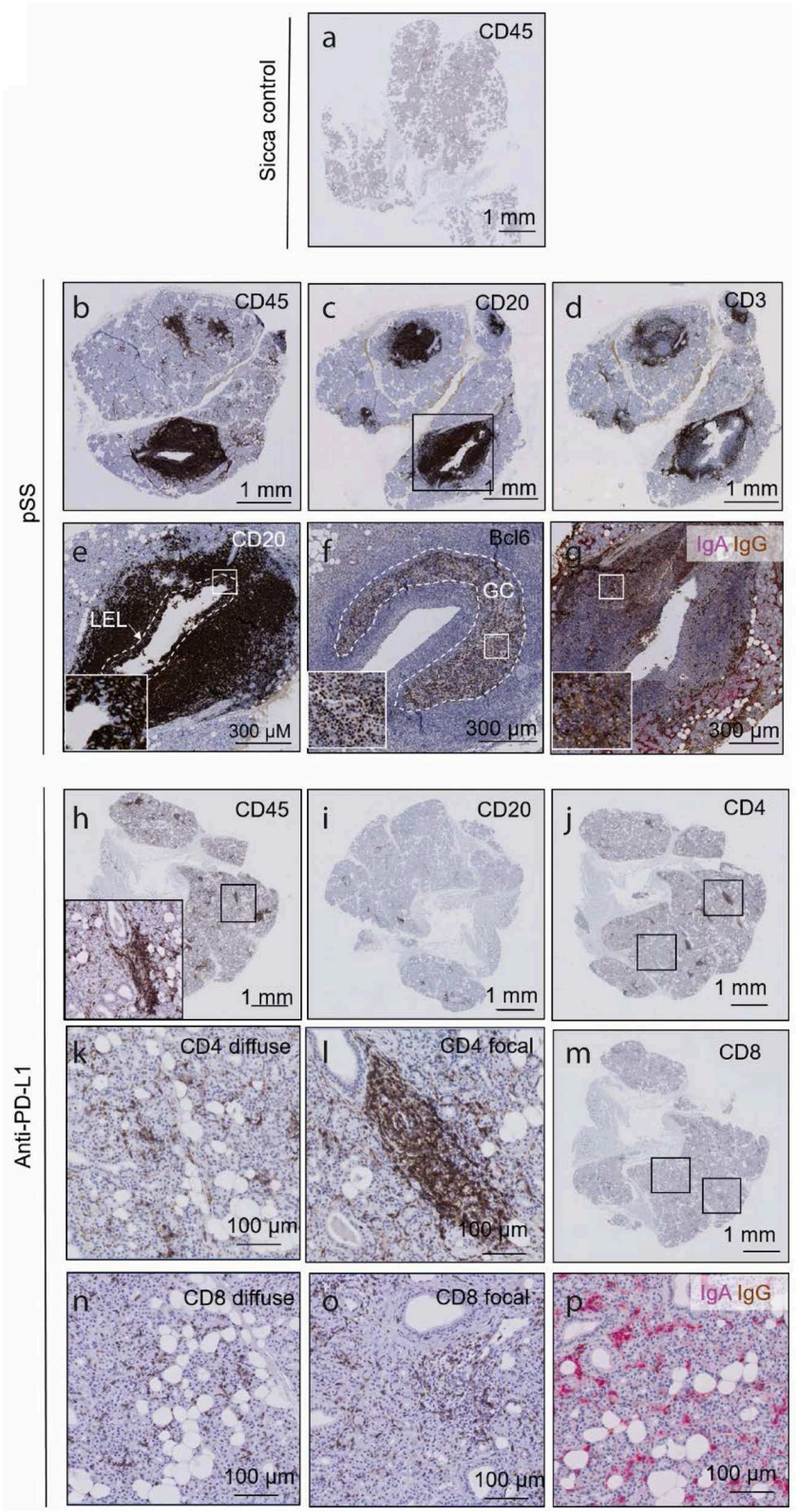

FIGURE 3 | The histology of a parotid salivary gland following prolonged anti PD-L1 therapy contains focal lymphocytic sialadentitis, but does not resemble the parotid gland in pSS. **(a)** CD45 immunohistochemical of sicca control. **(b–d)** CD45, CD20 and CD3 immunohistochemical staining of a parotid salivary gland from a

(Continued)

FIGURE 3 | pSS patient. **(e)** High resolution images of a lymphoepithelial lesion, whereby B cells are seen to invade striated ducts. Through as yet unclear mechanisms, both B cells and epithelial cells proliferate, and may represent a precursor stadium to MALT lymphomas. White dashed line demarcates boundaries of original striated duct. Inset box shows $CD20^+$ B cells in between $CD20^-$ epithelial cells. **(f)** High resolution image of a germinal center, indicated by Bcl-6 positivity. Bcl-6 positive B cells are characteristic of germinal centers. Dashed white line outlines boundaries of germinal center. Inset shows Bcl-6-positive nuclei of B cells. **(g)** Double immunohistochemical staining for IgA and IgG classes of antibodies. IgA represents the isotype normally found in mucosal tissues such as the SG (red label). Where >80% of labeled cells are IgG positive (brown), class switching is assumed to have occurred, such as the present example. **(h–n)** CD45, CD20, CD8, and CD4 immunohistochemical staining of a parotid salivary gland from patient following prolonged anti-PD-L1 therapy. Insets in **(h)** shows high resolution of boxed area. **(k)** High resolution image of diffuse CD8 immunostaining. **(l)** High resolution image of focally organized CD8 immunostaining. **(n)** High resolution image of focally organized CD4 immunostaining. **(o)** High resolution image of focal CD8 immunostaining. **(p)** IgA IgG double immunostaining following prolonged anti-PD-L1 therapy, showing majority of pink, IgA class antibodies.

SG resident progenitor cell population may have been affected by anti-PD-L1 therapy, directly or indirectly. The observed skewing toward unconventional epithelial structures may represent an attempt by progenitor cells to restore acinar cell balance, which may have not reached completion.

Sixty percent of patients experiencing lack of saliva production following checkpoint inhibitor use will progress to fulfill classification criteria for pSS. Recent studies suggest that small proportion (7 or 15%, in recent reports) of these patients display anti-SSA positivity, with the remaining fulfilling classification criteria owing to positive focus scores (3, 5). SGs affected by pSS, at least in its advanced stages, are notable for their preponderance of $CD20^+$ B cells, in addition to germinal center, LELs, and IgG producing plasma cell presence. These features were not present in the SG examined here following anti-PD-L1 therapy, in line with recent reports examining the minor SGs. Thus although foci are present, the nature of the infiltrate and the pathology observed are not consistent with the classical SG of a pSS patient (3, 5). The parotid SG examined in this case does not resemble that in pSS, histopathologically, despite the presence of anti-SSA in the serum.

In conclusion, our observations suggest that epithelial tissues such as the SG can react dramatically to anti-PD-L1 therapy. Our data supports a recent observation by Warner et al., who reported that hyposalivation following ICI therapy cannot be resolved with anti-inflammatory corticosteroid use. These data imply that the presence of infiltration is not the reason for lack of SG function observed. According to our data, the SG epithelium may be grossly dysregulated following PD-L1 blockade (3). Whether ICI therapy targeting other receptors (anti-CTLA4; anti-PD-1) also results in loss of acinar structures remains to be shown. Exhaustive additional studies will be necessary to comprehend fully the mechanisms behind PD-L1 blockade induced SG dysfunction, to understand how to affect tumor cell removal using ICIs with minimal epithelial organ dysfunction.

ETHICS STATEMENT

Salivary gland biopsy was performed as part of a diagnostic work up procedure for primary Sjögren's syndrome, under Institutional Review Board approval numbers METc2013.066, METc 2018-558. Patients gave informed consent for tissue use. Written informed consent was obtained from the individuals for the publication of any potentially identifiable images or data included in this article.

AUTHOR CONTRIBUTIONS

SP: conception, design, analysis, and interpretation. BV and NB: acquisition and interpretation. XW and TH: acquisition. FS: interpretation. AV and HB: interpretation and draft writing. FK: interpretation, draft writing, and design. All authors read and approved the final manuscript.

FUNDING

This research was funded by Dutch Arthritis Foundation Translational Research Grant (T015-052) and a Dutch Arthritis Foundation Long Term Project Grant (LLP-29). Grants were awarded for investigation of salivary gland pathologies in and involved with primary Sjogren's syndrome. Grants include consideration of fees for open access publishing.

REFERENCES

1. Michot JM, Bigenwald C, Champiat S, Collins M, Carbonnel F, Postel-Vinay S, et al. Immune-related adverse events with immune checkpoint blockade: a comprehensive review. *Eur J Cancer*. (2016) 54:139–48. doi: 10.1016/j.ejca.2015.11.016
2. Cappelli LC, Gutierrez AK, Baer AN, Albayda J, Manno RL, Haque U, et al. Inflammatory arthritis and sicca syndrome induced by nivolumab and ipilimumab. *Ann Rheum Dis*. (2017) 76:43–50. doi: 10.1136/annrheumdis-2016-209595
3. Warner BM, Baer AN, Lipson EJ, Allen C, Hinrichs C, Rajan A, et al. Sicca syndrome associated with immune checkpoint inhibitor therapy. *Oncologist*. (2019) 24:1259–69. doi: 10.1634/theoncologist.2018-0823
4. Tocut M, Brenner R, Zandman-Goddard G. Autoimmune phenomena and disease in cancer patients treated with immune checkpoint inhibitors. *Autoimmun Rev*. (2018) 17:610–6. doi: 10.1016/j.autrev.2018.01.010
5. Ortiz Brugués A, Sibaud V, Herbault-Barrés B, Betrian S, Korakis I, De Bataille C, et al. Sicca syndrome induced by immune checkpoint inhibitor therapy: optimal management still pending. *Oncologist*. (2020) 25:e391–5. doi: 10.1634/theoncologist.2019-0467
6. Aure MH, Konieczny SF, Ovitt CE. Salivary gland homeostasis is maintained through acinar cell self-duplication. *Dev Cell*. (2015) 33:231–7. doi: 10.1016/j.devcel.2015.02.013
7. May AJ, Cruz-Pacheco N, Emmerson E, Gaylord EA, Seidel K, Nathan S, et al. Diverse progenitor cells preserve salivary gland ductal architecture after radiation induced damage. *Development*. (2018) 145:166363. doi: 10.1242/dev.166363

8. Pringle S, Wang X, Verstappen GMPJ, Terpstra JH, Zhang CK, He A, et al. Salivary gland stem cells age prematurely in primary Sjögren's syndrome. *Arthritis Rheumatol.* (2019) 71:133–42. doi: 10.1002/art.40659
9. Weng P-L, Aure MH, Maruyama T, Ovitt CE. Limited regeneration of adult salivary glands after severe injury involves cellular plasticity. *Cell Rep.* (2018) 24:1464–70.e3. doi: 10.1016/j.celrep.2018.07.016
10. Gibney GT, Kudchadkar RR, DeConti RC, Thebeau MS, Czupryn MP, Tetteh L, et al. Safety, correlative markers, and clinical results of adjuvant nivolumab in combination with vaccine in resected high-risk metastatic melanoma. *Clin Cancer Res.* (2015) 21:712–20. doi: 10.1158/1078-0432.CCR-14-2468
11. Ramos-Casals M, Maria A, Suárez-Almazor ME, Lambotte O, Fisher BA, Hernández-Molina G, et al. Sicca/Sjögren's syndrome triggered by PD-1/PD-L1 checkpoint inhibitors. Data from the International ImmunoCancer Registry (ICIR). *Clin Exp Rheumatol.* (2019) 37(Suppl. 1):114–22.
12. Pringle S, Wang X, Bootsma H, Spijkervet FKL, Vissink A, Kroese FGM. Small-molecule inhibitors and the salivary gland epithelium in Sjögren's syndrome. *Expert Opin Investig Drugs*. (2019) 28:605–16. doi: 10.1080/13543784.2019.1631796
13. Kroese FG, Abdulahad WH, Haacke E, Bos NA, Vissink A, Bootsma H. B-cell hyperactivity in primary Sjögren's syndrome. *Expert Rev Clin Immunol.* (2014) 10:483–99. doi: 10.1586/1744666X.2014.891439
14. van Ginkel MS, Haacke EA, Bootsma H, Arends S, van Nimwegen JF, Verstappen GM, et al. Presence of intraepithelial B-lymphocytes is associated with the formation of lymphoepithelial lesions in salivary glands of primary Sjögren's syndrome patients. *Clin Exp Rheumatol.* (2019) 118:42–8.
15. Shiboski CH, Shiboski SC, Seror R, Criswell LA, Labetoulle M, Lietman TM, et al. 2016 American College of Rheumatology/European League Against Rheumatism classification criteria for primary Sjögren's syndrome: a consensus and data-driven methodology involving three international patient cohorts. *Ann Rheum Dis.* (2017) 76:9–16. doi: 10.1136/annrheumdis-2016-210571
16. Antonia SJ, Villegas A, Daniel D, Vicente D, Murakami S, Hui R, et al. Durvalumab after chemoradiotherapy in stage III non–small-cell lung cancer. *N Engl J Med*. (2017) 377:1919–29. doi: 10.1056/NEJMoa1709937
17. Mossel E, Delli K, van Nimwegen JF, Stel AJ, Haacke EA, Kroese FGM, et al. The parotid gland connection: ultrasound and biopsies in primary Sjögren's syndrome. *Ann Rheum Dis.* (2017) 77:e38. doi: 10.1136/annrheumdis-2017-212331
18. Mossel E, Delli K, van Nimwegen JF, Stel AJ, Kroese FGM, Spijkervet FKL, et al. Ultrasonography of major salivary glands compared with parotid and labial gland biopsy and classification criteria in patients with clinically suspected primary Sjögren's syndrome. *Ann Rheum Dis.* (2017) 76:1883–9. doi: 10.1136/annrheumdis-2017-211250
19. van Nimwegen JF, Mossel E, Delli K, van Ginkel MS, Stel AJ, Kroese FGM, et al. Incorporation of salivary gland ultrasonography into the ACR-EULAR criteria for primary Sjögren's syndrome. *Arthritis Care Res*. (2019). doi: 10.1002/acr.24017
20. Spijkervet FKL, Haacke E, Kroese FGM, Bootsma H, Vissink A. Parotid gland biopsy, the alternative way to diagnose Sjögren syndrome. *Rheum Dis Clin North Am.* (2016) 42:485–99. doi: 10.1016/j.rdc.2016.03.007
21. Haacke EA, van der Vegt B, Vissink A, Spijkervet FKL, Bootsma H, Kroese FGM. Standardisation of the detection of germinal centres in salivary gland biopsies of patients with primary Sjögren's syndrome is needed to assess their clinical relevance. *Ann Rheum Dis.* (2017) 22:212164. doi: 10.1136/annrheumdis-2017-212164
22. Yoshimura S, Nakamura H, Horai Y, Nakajima H, Shiraishi H, Hayashi T, et al. Abnormal distribution of AQP5 in labial salivary glands is associated with poor saliva secretion in patients with Sjögren's syndrome including neuromyelitis optica complicated patients. *Mod Rheumatol.* (2016) 26:384–90. doi: 10.3109/14397595.2015.1083146
23. Stramandinoli-Zanicotti RT, Sassi LM, Schussel JL, Torres MF, Funchal M, Smaniotto GH, et al. Effect of fractionated radiotherapy on the parotid gland: an experimental study in Brazilian minipigs. *Int Arch Otorhinolaryngol.* (2013) 17:163–7. doi: 10.7162/S1809-97772013000200008
24. Molina C, Alliende C, Aguilera S, Kwon Y-J, Leyton L, Martínez B, et al. Basal lamina disorganisation of the acini and ducts of labial salivary glands from patients with Sjögren's syndrome: association with mononuclear cell infiltration. *Ann Rheum Dis.* (2006) 65:178–83. doi: 10.1136/ard.2004.033837
25. Jalali S, Price-Troska T, Bothun C, Villasboas J, Kim H-J, Yang Z-Z, et al. Reverse signaling via PD-L1 supports malignant cell growth and survival in classical Hodgkin lymphoma. *Blood Cancer J.* (2019) 9:22. doi: 10.1038/s41408-019-0185-9
26. Lecis D, Sangaletti S, Colombo MP, Chiodoni C. Immune checkpoint ligand reverse signaling: looking back to go forward in cancer therapy. *Cancers*. (2019) 11:624–36. doi: 10.3390/cancers11050624

Conflict of Interest: The authors declare that the research was conducted in the absence of any commercial or financial relationships that could be construed as a potential conflict of interest.

frontiers in Oncology

CASE REPORT
published: 02 June 2020
doi: 10.3389/fonc.2020.00689

Higher Tumor Mutation Burden and Higher PD-L1 Activity Predicts the Efficacy of Immune Checkpoint Inhibitor Treatment in a Patient With Four Lung Cancers. A Case Report

Katsuo Usuda[1], Yo Niida[2,3], Shun Iwai[1], Aika Funasaki[1], Atsushi Sekimura[1], Nozomu Motono[1], Sohsuke Yamada[4] and Hidetaka Uramoto[1]*

[1] Department of Thoracic Surgery, Kanazawa Medical University, Ishikawa, Japan, [2] Center for Clinical Genomics, Kanazawa Medical University, Ishikawa, Japan, [3] Division of Genomic Medicine, Kanazawa Medical University, Ishikawa, Japan, [4] Department of Pathology and Laboratory Medicine, Kanazawa Medical University, Ishikawa, Japan

We experienced a patient who had four lung cancers with different pathological features, with the most advanced being diagnosed as pStage IIA. A month after the resection, the original lung cancer had metastasized to the lung and to the liver. Of the original lung cancers that were resected, the biggest adenocarcinoma of S3 showed 50 × 31 × 17 mm (invasion 50 mm) and pT2bN0M0 (pStage IIA) with epidermal growth factor receptor (EGFR) mutation (–) and anaplastic lymphoma kinase (ALK) translocation (–), but expression of programmed death ligand 1 (PD-L1) (+) tumor proportion score (TPS) 80%. The pleomorphic carcinoma showed 23 × 20 × 17 mm (invasion 23 mm) and pT1cN0M0 (pStage Ic) with EGFR (–), ALK (–), PD-L1 (+), TPS 95%. Tumor mutation burden (TMB), microsatellite instability (MSI), and structural chromosome aberration analysis by DNA microarray were performed. One hundred somatic mutations in the adenocarcinoma and 75 somatic mutations in the pleomorphic carcinoma were identified, which showed an extremely high mutation rate, although only 16 somatic mutations were common between the two cancers. Chromosomal structural aberrations differed greatly between the two cancers, but common aberrations were found in chromosomes 8 and 10 and partially common aberration in chromosomes 4, 14, 17, and X. These results indicated that each lung cancer originated from a common ancestor clone and developed on an individual molecular evolution. The patient received a single injection of pembrolizumab and 13 injections of atezolizumab. Immune checkpoint inhibitor treatment made metastatic pulmonary and liver lesions reduce in size and show as Partial response (PR). Multiple lung cancers with high PD-L1 activity tend to be TMB-high, reflecting rapid molecular evolution and relevance to the patient's response to immune checkpoint inhibitors. Genomic examination could help determine what had happened in multiple cancers on progression and provide useful data to patient treatment. Each lung cancer originated from a common ancestor clone and developed on an individual molecular evolution.

Keywords: lung cancer, immune checkpoint inhibitor (ICI), programmed death ligand 1 (PD-L1), tumor mutation burden (TMB), microsatellite instability (MSI)

OPEN ACCESS

Edited by:
Said Dermime,
National Center for Cancer Care and Research, Qatar

Reviewed by:
Luca Mologni,
University of Milano-Bicocca, Italy
Eyad Elkord,
University of Salford, United Kingdom

****Correspondence:***
Katsuo Usuda
usuda@kanazawa-med.ac.jp

Specialty section:
This article was submitted to Cancer Immunity and Immunotherapy, a section of the journal Frontiers in Oncology

Received: *24 January 2020*
Accepted: *14 April 2020*
Published: *02 June 2020*

Citation:
Usuda K, Niida Y, Iwai S, Funasaki A, Sekimura A, Motono N, Yamada S and Uramoto H (2020) Higher Tumor Mutation Burden and Higher PD-L1 Activity Predicts the Efficacy of Immune Checkpoint Inhibitor Treatment in a Patient With Four Lung Cancers. A Case Report. Front. Oncol. 10:689. doi: 10.3389/fonc.2020.00689

INTRODUCTION

Clinically valuable prognostic and predictive biomarkers that can reliably determine the patients most likely to benefit from adjuvant chemotherapy are still in the developmental stages. The recent progress of antibodies that target the programmed death 1 (PD-1) as well as programmed death ligand 1 (PD-L1) pathways plays critical in the management of advanced non–small cell lung cancer (NSCLC). Similar to the PD-L1 expression, tumor mutation burden (TMB) and microsatellite instability (MSI) are being used for the first time as predictive biomarkers for identifying patients likely to positively react to immune checkpoint inhibitors (1–5). However, the overlap between the PD-L1, TMB, and MSI differs among cancer types, and only 0.6% of cases were positive for all the three markers in malignant tumors (3).

We herein report a patient with four lung cancers who had a remarkable response to immune checkpoint inhibitors for NSCLC. The TMBs of the lung cancers were identified to be 105.9 mutations per megabase (mut/Mbp) in adenocarcinoma and 79.4 mut/Mbp in pleomorphic carcinoma by next-generation sequencing analysis of cancer gene panel test, SureSelect NCC Oncopanel (Agilent) National Cancer Center Hospital in Japan, Tokyo, Japan.

CASE PRESENTATION

A CT scan showed that an 87-year-old man had three nodules in his right upper lobe of the lung (**Figure 1**). These nodules were highly suspected to be cancerous (cT2bN0M0, cStage IIA), and he underwent a right upper lobectomy and lymphadenectomy of ND1 for lung cancer under a complete video-assisted thoracoscopic surgery procedure. A pathological examination revealed that out of the four lung cancers one was a pleomorphic carcinoma, and three were adenocarcinomas. The biggest adenocarcinoma of S3 showed 50 × 31 × 17mm (invasion 50 mm) and pT2bN0M0 (pStage IIA) with epidermal growth factor receptor in real-time polymerase chain reaction (PCR) (EGFR) (–), anaplastic lymphoma kinase (ALK) (–), and expression of PD-L1 (+) tumor proportion score (TPS) 80%. The pleomorphic carcinoma showed 23 × 20 × 17 mm (invasion 23 mm) and pT1cN0M0 (pStage Ic) with EGFR (–), ALK (–), and PD-L1 (+) TPS 95%. One month after resection, there were multiple metastases to lung and liver that had developed quickly. The liver metastasis was diagnosed pathologically as a metastasis of the pleomorphic carcinoma by percutaneous liver biopsy.

The TMB and MSI were analyzed under SureSelect NCC Oncopanel (Agilent) and Bethesda panel assay in the patient's lung cancer samples. Also, OncoScan CNV (Affymetrix) Thermo Fisher Scientific, Tokyo, Japan was performed to analyze chromosomal aberrations (**Figures 2**, **3**). A pleomorphic carcinoma had a uniform carcinoma which cancer cells had occupied more than 80% of the central tumor area (**Figure 2**). The biggest adenocarcinoma had a un-uniform adenocarcinoma with stroma and lymphocytic infiltration which cancer cells had occupied 20 to 30% of the central tumor area. The second adenocarcinoma showed an arrangement of islands. The third adenocarcinoma showed adenocarcinoma *in situ* and

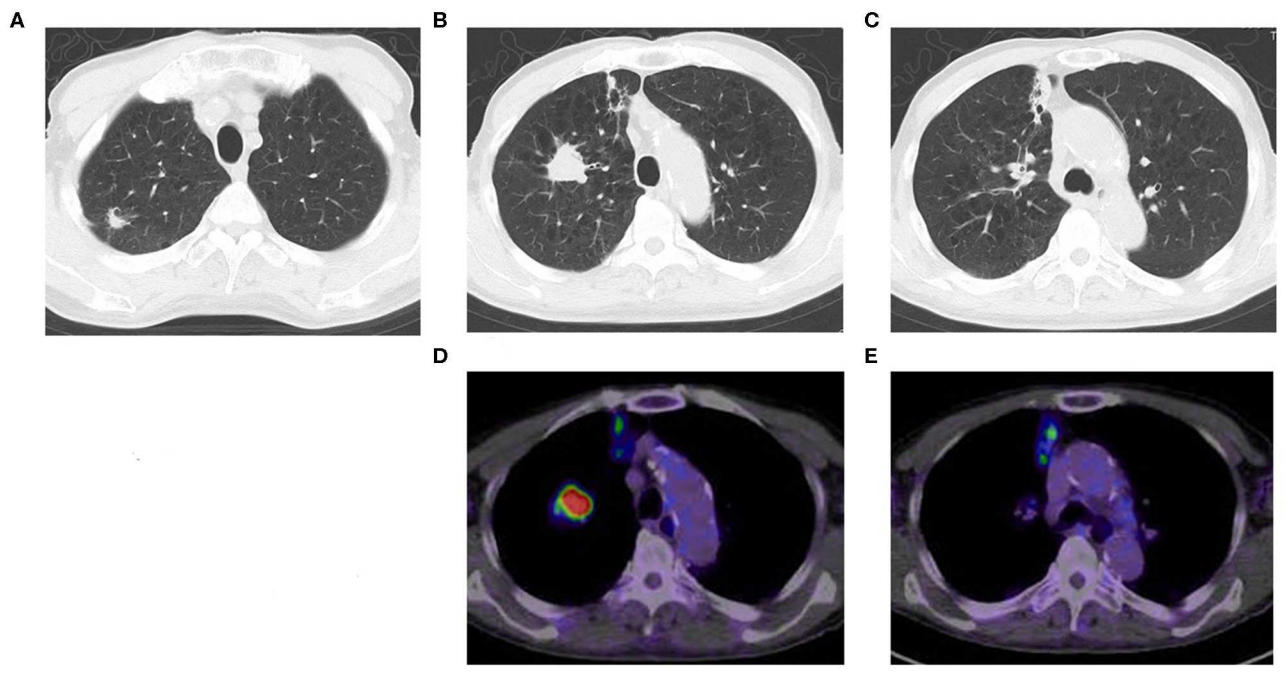

FIGURE 1 | Chest CT shows multiple lung cancers. **(A)** Adenocarcinoma, **(B)** pleomorphic carcinoma, **(C)** adenocarcinoma, **(D)** positron emission tomography computed tomography (PET-CT) of pleomorphic carcinoma **(B)**, **(E)** PET-CT of adenocarcinoma **(C)**.

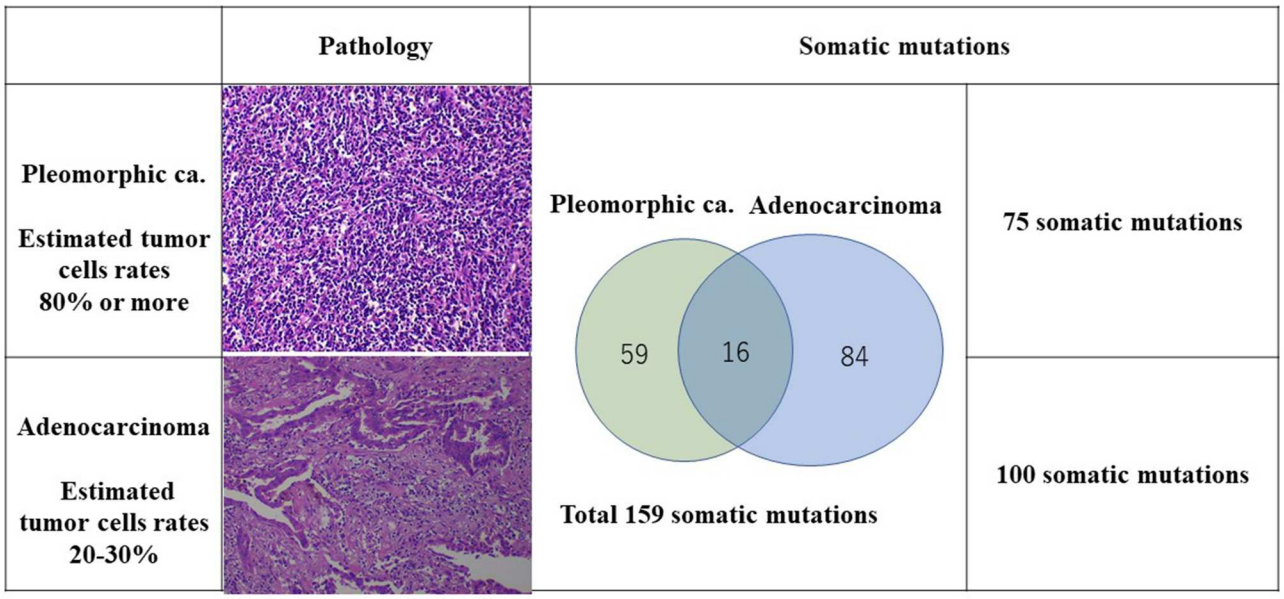

FIGURE 2 | Relationship between pathology and somatic mutations.

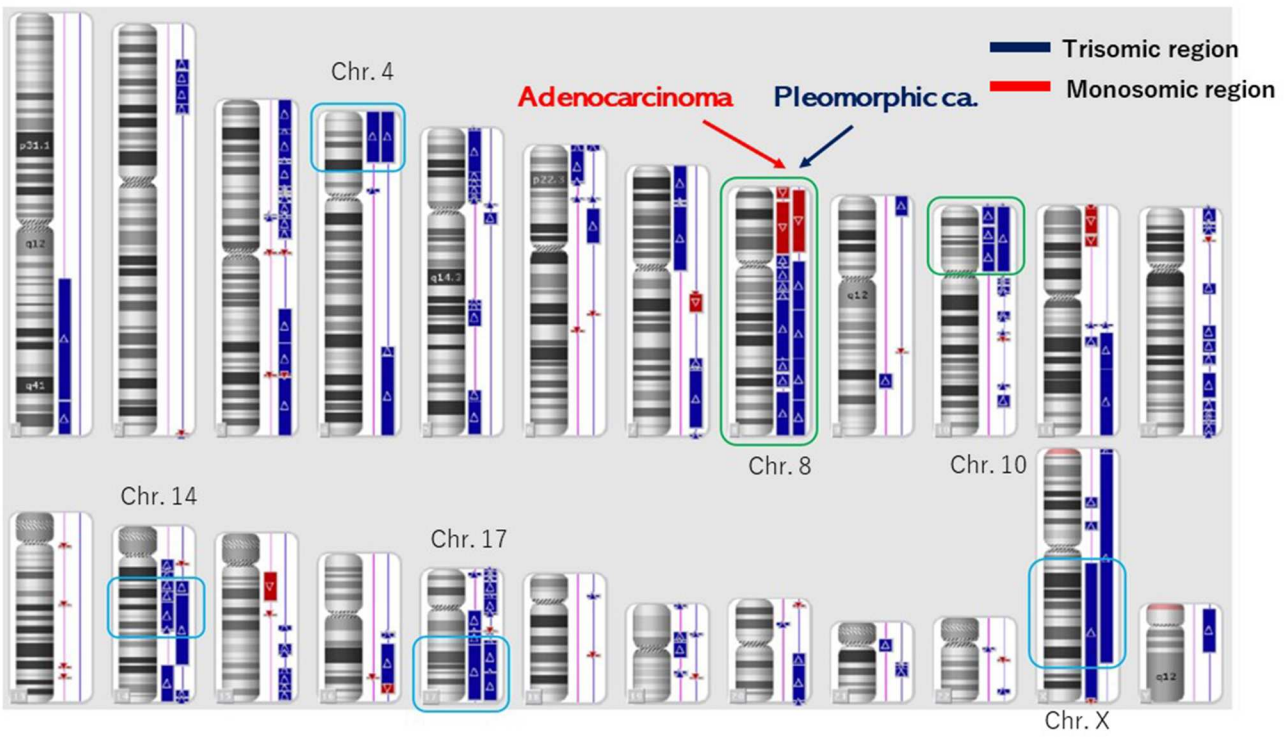

FIGURE 3 | Structural chromosome aberration analysis by OncoScan CNV. Common chromosomal aberrations were found in chromosomes 8 and 10, and the process that piled up independent chromosomal aberrations was inquired of these tumors having a common origin.

normal tissue. The second and third adenocarcinomas were not trimmed for carcinoma tissue for DNA analysis. Finally, DNA was extracted from the formalin-fixed paraffin-embedded tissues of the pleomorphic carcinoma and the biggest adenocarcinoma. DNA from the normal tissue was used as the normal control.

The number of target bases of NCC Oncopanel was 944,153 bp (0.944 Mb). Therefore, when TMB was defined as the total number of somatic mutations per 1-Mb read, the TMB was identified to be 79.4 mut/Mbp in the pleomorphic carcinoma and 105.9 mut/Mbp in the adenocarcinoma. Finally, 75 somatic mutations were identified in the pleomorphic carcinoma and 100 somatic mutations in the adenocarcinoma, which showed an extremely high hypermutation rate, although only 16 somatic mutations were common between the two cancers. There were no instabilities of the microsatellite in both the adenocarcinoma and the pleomorphic carcinoma, and it was judged as microsatellite stable (MSS). The adenocarcinoma had a driver mutation of L858R of EGFR assumed to be homozygous; variant allele frequency is 0.278, with tumor content of the sample being 20 to 30%, and other somatic mutations' allele frequencies were divided into two groups, with average 0.124 ($n = 58$) and 0.308 ($n = 42$), which seemed to represent heterozygous and homozygous mutations, respectively. These results indicate that this adenocarcinoma has uniform genetic characteristics. On the other hand, although the pleomorphic carcinoma presented a uniform pathologic finding, no specific driver mutation was found, and average allele frequencies of somatic mutations are divided to 0.98 ($n = 1$), 0.28 ($n = 42$), and 0.121 ($n = 32$). Because tumor content of the sample is ∼80%, the former two represent homozygous and heterozygous mutations, respectively, but the last one indicates that only a part of the tumor has these mutations. Therefore, it is assumed that this pleomorphic carcinoma is heterogeneous at the molecular level. Structural chromosome aberration analysis by DNA microarray showed great difference between two tumors, but also common chromosomal aberration in chromosomes 8 and 10 and partially common chromosomal aberration in chromosomes 4, 14, 17, and X (**Figure 3**). Higher TMB and higher PD-L1 activity predicted a positive response to the immune checkpoint inhibitor in this patient.

One hour after pembrolizumab (200 mg) had been given to the patient intravenously, he had right abdominal pain, appetite loss, chills, and a fever of 38.7°C. White blood cell count increased to 12,790/mm^3 on day 1 and decreased until it finally stabilized on day 2. C-reactive protein was 3.99 on day 1 and increased to 10.23 mg/dL by day 3 until finally stabilizing. The episode was judged as an infusion-related reaction of grade 3. The patient received acetaminophen (400 mg) and hydration (1,000 mL), which led to the amelioration of symptoms. One month after pembrolizumab injection, multiple metastatic pulmonary and liver tumors were reduced in size and judged as PR (**Figure 4**).

Because of the pembrolizumab infusion-related reaction, pembrolizumab was discontinued, and atezolizumab was selected for the immune checkpoint inhibitor treatment. The patient received acetaminophen (400 mg) and fexofenadine hydrochloride (60 mg) 1 h before atezolizumab injection to prevent infusion-related reactions. The patient tolerated atezolizumab (1,200 mg) without any subsequent infusion-related reactions. Atezolizumab was given to the patient intravenously every 3 weeks for 13 courses. Multiple metastatic pulmonary lesions were reduced in size and almost disappeared, and multiple metastatic liver tumors were reduced in size. Overall response evaluation of immune checkpoint inhibitors at 12 months after the treatment was judged as PR (**Figure 4**).

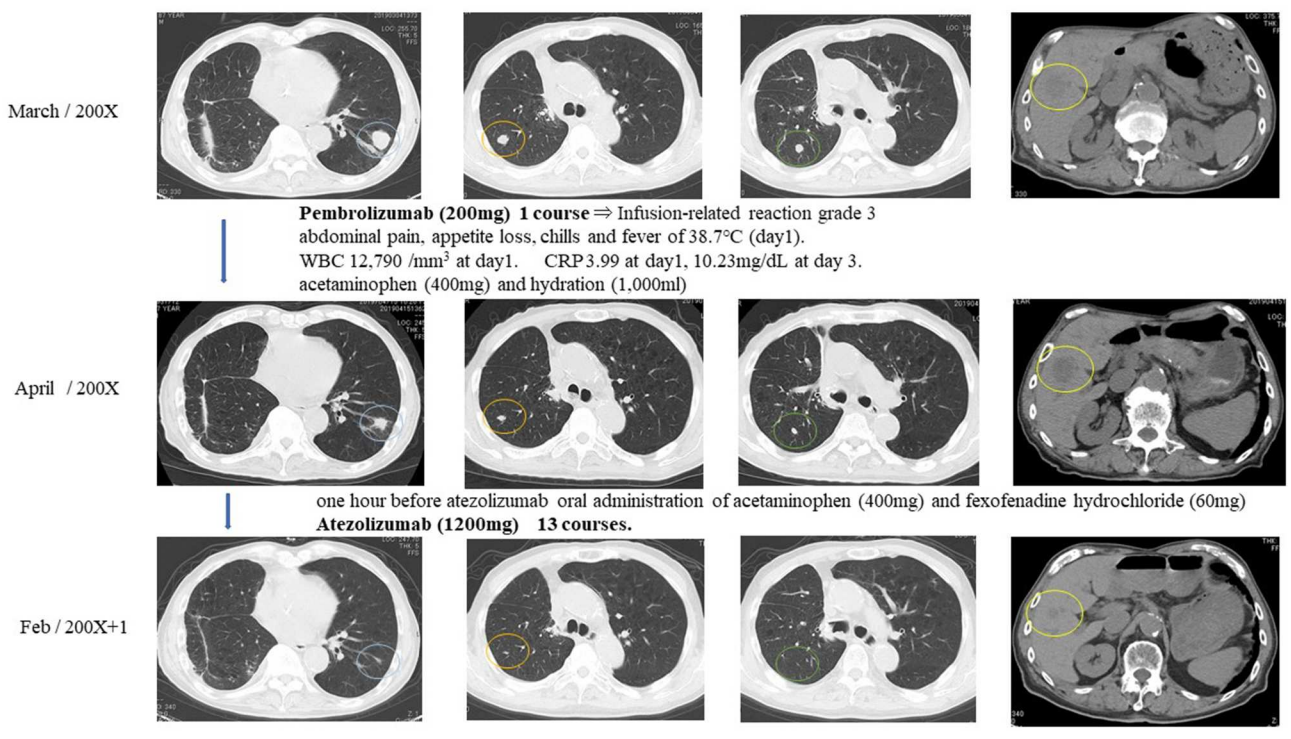

FIGURE 4 | Response evaluation was shown as PR after intravenous injection of immune checkpoint inhibitors.

DISCUSSION

Programmed death 1 (PD-1) and programmed death ligand 1 (PD-L1) inhibitors in the treatment of advanced NSCLC are currently available and have demonstrated antitumor activity (6–8). PD-1 and PD-L1 inhibitors significantly improved the overall survival (OS), progression-free survival, and objective response rate in patients with advanced NSCLC with PD-L1 expression. Furthermore, a high PD-L1 expression was likely to be associated with increased benefits.

The TMB is defined as the total number of somatic mutations of the genomic coding area and associated with the emergence of neoantigens that trigger antitumor immunity (9). The TMB was recently confirmed to be a biomarker of the efficacy of PD-1 and PD-L1 inhibitors (1, 5). Although objective cutoff points for the TMB are not universally established, the cutoff points have been set at around 10 mut/Mbp in previous studies. Therefore, our case, whose TMBs were 105.9 mut/Mbp in adenocarcinoma and 79.4 mut/Mbp in pleomorphic carcinoma, was defined as TMB-high. High nonsynonymous TMB (>8 mut/Mb) was prognostic for favorable outcomes in patients with resected NSCLC (10). High nonsynonymous TMB was shown to have a better prognosis in patients with resected NSCLC (10). Multivariate analysis demonstrated clonal mutation burden as a promising independent prognostic factor for OS in SCLC patients (11). High TMB (> 21 mut/Mb) was a good prognostic factor in OS (21.7 vs. 10.4 months, $P = 0.012$) (12). Multivariate analysis presented that high TMB was an independent prognostic factor (12).

However, other chromosomal aberrations were greatly different between the pleomorphic carcinoma and the adenocarcinoma, and the process of independent chromosomal aberration was assumed, although these tumors had a common origin. The pleomorphic carcinoma presented a uniform pathologic finding, but suspected to have various subclones genomically. Although the pleomorphic carcinoma did not have a specific driver mutation, it could become a good target of immune checkpoint inhibitors reflecting high somatic mutation rate. The adenocarcinoma would have a driver mutation of L858R of EGFR in homozygous and be relatively uniform genomically in NCC Oncopanel. There is an apparent discrepancy between negative EGFR (Cycleave methods) expression in real-time PCR and a putative EGFR driver mutation (L858R) in NCC Oncopanel in the adenocarcinoma. The discrepancy was thought to be based on the methods of EGFR examinations. In our experience, pleomorphic carcinomas rarely express an EGFR expression. In this case, the pleomorphic carcinoma with no specific driver mutation of EGFR had metastases to the liver and the lungs. Epidermal growth factor receptor–tyrosine kinase inhibitor (EGFR-TKI) was not used because of the negative expression of EGFR. When the adenocarcinoma relapsed, EGFR-TKI was used based on the NCC Oncopanel.

Microsatellite instability is also considered an independent predictive biomarker of immune checkpoint inhibitors (2, 3). Microsatellite instability is the situation of genetic hypermutability and represents the phenotypic results of mismatch repair (MMR) deficiency. Cancers with instability at two or more of these loci are defined as MSI-high (MSI-H), whereas those with instability at a single locus are defined as MSI-low (MSI-L), and those with no instability at any of these loci are defined as MSS. Whereas the examination for MSI is MSS, the frequent occurrence of the mutation would not mean the failure of the MMR mechanism. In addition to the PD-L1 expression, MSI would be a different biomarker from TMB, and TMB and MSI are considered independent predictive biomarkers for selecting patients likely to benefit from immune checkpoint inhibitor treatment.

The overall rates of PD-L1 positivity, MSI-H, and TMB-high of cancers were 3.0, 7.7, and 25.4%, respectively (3). Only 0.6% of the cancer cases were positive for all three markers (3). The overlap rates between PD-L1, TMB, and MSI were reportedly low in NSCLC (3): TMB-high and MSI-H were found in 0.5%, TMB-high and PD-L1 positivity in 7.7%, MSI-H and PD-L1 positivity in 0.4%, and positivity in all three markers in 0.3% of NSCLC cases (3). This reported case was classified as TMB-high, PD-L1 positivity, and MSS. These data present several different mechanisms in this case. This discrepancy may be attributed to other biomarkers associated with the efficacy of PD-l and PD-L1 inhibitors. Programmed death ligand 1 expressions and TMB were independent variables, and a composite of PD-L1 plus TMB further supported the efficacy of immune checkpoint inhibitor treatment (13). Higher PD-L1 TPS scores as well as higher TMB of both lung cancers indicated strongly immune checkpoint inhibitors for the therapy. Higher PD-L1 TPS scores of this different lung cancers showed to have a common origin, which was supported by the 16 common somatic mutations. In these lung cancers, common chromosomal aberrations were found in chromosomes 8 and 10, which showed two different lung cancers originated from the same origin and then differentiated independently. These lung cancers had the same gene abnormality of PD-L1 positivity, TMB-high, MSS, and common chromosomal aberration, which presented the same origin instead of different cell types.

The patient had multiple lung cancers of different histologic types, which showed a postoperative immediate relapse. The lung cancer was TMB-high, so the immune checkpoint inhibitor proved to be successful in treating the relapse. The cancer genome analysis showed the lung cancers had different genetic backgrounds. One of which was an adenocarcinoma, and the other, a pleomorphic carcinoma, but both would have developed from a common ancestor. They share some similar molecular evolution that differs from their common ancestor but eventually followed independent evolutionary lines. We think this was a rare case that had simultaneous examinations of gene panel test and microarrays. The speed of the mutation in the gene was high, so it contributed to the simultaneous cancer developments, and therefore TMB was super high, and the immunity checkpoint inhibitors were good indicators. Whereas the chromosomal aberration looks remarkable, but it is only MSS. There is no homologous recombination deficiency, showing no mutation of the DNA MMR gene.

Infusion-related reactions in immune checkpoint inhibitor treatment occur in ∼3% of patients, and recognition of infusion-related reactions induced by pembrolizumab is

an important aspect of its usage (14, 15). Corticosteroid, antihistamine, and antipyretic analgesics were reported to be useful for prevention of infusion-related reactions (14).

One limitation of this study was the lack of genomic data of metastatic lesions. There was not enough carcinoma tissue of the metastatic liver tumor to extract DNA. When two or more lung cancers are detected or other malignancies are detected at the condition of PD-L1 (+), there will be the possibility of a common genomic abnormality of TMB-high. One of the strengths of this study was the existence of the pathologically and genomically sufficient data of multiple simultaneous lung cancers and the outcome for immune checkpoint inhibitors.

CONCLUSION

Multiple lung cancers with high PD-L1 activity tended to be TMB-high reflecting rapid molecular evolution and relevance to the patient's response to immune checkpoint inhibitors. Genomic examination could help determine what will happen in multiple cancers on progression and provide useful data for patient treatment. Each lung cancer originated from a common ancestor clone and developed on an individual molecular evolution.

ETHICS STATEMENT

Written informed consent was obtained from the patient for the publication of any potentially identifiable images or data included in this article.

AUTHOR CONTRIBUTIONS

KU performed the research, wrote the paper. SI, AF, AS, and NM were performed therapy to a patient. YN contributed to analyze the genetic status of this patient. SY performed pathological examination of lung cancers. HU contributed to supervision of this study and revision of the manuscript.

FUNDING

This study was supported partly by a Grant-in-Aid for Scientific Research from the Ministry of Education, Culture, Sports, Science and Technology, Japan (Grant number: 20 K 09172).

ACKNOWLEDGMENTS

We thank Mr. Dustin Keeling, who helped us revise the paper in English.

REFERENCES

1. Hellmann MD, Ciuleanu TE, Pluzanski A, Lee JS, Otterson GA, Audigier-Valette C, et al. Nivolumab plus ipilimumab in lung cancer with a high tumor mutational burden. *N Engl J Med.* (2018) 378:2093–104. doi: 10.1056/NEJMoa1801946
2. Overman M, Kopetz S, McDermott R, Leach J, Lonardi S, Lenz H, et al. Nivolumab ± ipilimumab in treatment of patients with metastatic colorectal cancer with and without high microsatellite instability (MSI-H): CheckMate-142 interim results. *J Clin Oncol.* (2016) 34:3501. doi: 10.1200/JCO.2016.34.15_suppl.3501
3. Vanderwalde A, Spetzler D, Xiao N, Gatalica Z, Marshall J. Microsatellite instability status determined by next-generation sequencing and compared with PD-L1 and tumor mutational burden in 11,348 patients. *Cancer Med.* (2018) 7:746–56. doi: 10.1002/cam4.1372
4. de la Chapelle A, Hampel H. Clinical relevance of microsatellite instability in colorectal cancer. *J Clin Oncol.* (2010) 28:d3380–7. doi: 10.1200/JCO.2009.27.0652
5. Schrock A, Sharma N, Peled N, Bufill J, Srkalovic G, Spigel D, et al. Updated dataset assessing tumor mutation burden (TMB) as a biomarker for response to PD-1/PD-L1 targeted therapies in lung cancer (LC). *J Thorac Oncol.* (2017) 12:S422. doi: 10.1016/j.jtho.2016.11.487
6. Fehrenbacher L, Spira A, Ballinger M, Kowanetz M, Vansteenkiste J, Mazieres J, et al. Atezolizumab versus docetaxel for patients with previously treated non-small-cell lung cancer (POPLAR): a multicentre, open-label, phase 2 randomised controlled trial. *Lancet.* (2016) 387:1837–46. doi: 10.1016/S0140-6736(16)00587-0
7. Borghaei H, Paz-Ares L, Horn L, Spigel DR, Steins M, Ready E, et al. Nivolumab versus docetaxel in advanced nonsquamous no-small-cell lung cancer. *N Engl J Med.* (2015) 373:1627–39. doi: 10.1056/NEJMoa1507643
8. Hendricks LE, Rouleau E, Besse B. Clinical utility of tumor mutational burden in patients with non-small cell lung cancer treated with immunotherapy. *Transl Lung Cancer Res.* (2018) 7:647–60. doi: 10.21037/tlcr.2018.09.22
9. Rizvi NA, Hellmann MD, Snyder A, Kvistborg P, Makarov V, Havel JJ, et al. Cancer immunology. Mutation landscape determines sensitivity to PD-1 blockade in non-small cell lung cancer. *Science.* (2015) 348:124–8. doi: 10.1126/science.aaa1348
10. Devarakonda S, Rotolo F, Tsao MS, Lanc I, Brambilla E, Masood A, et al. Tumor mutation burden as a biomarker in resected non-small-cell ung cancer. *J Clin Oncol.* (2018) 36:2995–3006. doi: 10.1200/JCO.2018.78.1963
11. Wang Y, Han X, Wang X, Sheng W, Chen Z, Shu W, et al. Genomic based analyses reveal unique mutational profiling and identify prognostic biomarker for overall survival in Chinese small-cell lung cancer. *Jpn J Clin Oncol.* (2019) 49:1143–50. doi: 10.1093/jjco/hyz131
12. Zhou M, Fan J, Li Z, Li P, Sun Y, Yang Y, et al. Prognostic impact of tumor mutation burden and the mutation in KIAA1211 in small cell lung cancer. *Respir Res.* (2019) 20:248. doi: 10.1186/s12931-019-1205-9
13. Rizvi H, Sanchez-Vega F, La K, Chatila W, Jonsson P, Halpenny D, et al. Molecular determinants of response to anti-programmed cell death (PD)-1 and anti-programmed death-ligand 1 (PD-L1) blockade in patients with non-small-cell lung cancer profiled with targeted next-generation sequencing. *J Clin Oncol.* (2018) 36:633–41. doi: 10.1200/JCO.2017.75.3384
14. Choi B, McBride A, Scott AJ. Treatment with pembrolizumab after hypersensitivity reaction to nivolumab in a patient with hepatocellular carcinoma. *Am J Health Syst Pharm.* (2019) 76:1749–52. doi: 10.1093/ajhp/zxz189
15. Almutairi AR, McBride A, Slack M, Erstad BL, Abraham I. Potential immune-related adverse events associated with monotherapy and combination therapy of ipilimumab, nivolumab, and pembrolizumab for advanced melanoma: a systematic review and meta-analysis. *Front Oncol.* (2020) 10:91. doi: 10.3389/fonc.2020.00091

Conflict of Interest: The authors declare that the research was conducted in the absence of any commercial or financial relationships that could be construed as a potential conflict of interest.

frontiers in Immunology

ORIGINAL RESEARCH
published: 10 June 2020
doi: 10.3389/fimmu.2020.01173

Dynamics of Serum Tumor Markers Can Serve as a Prognostic Biomarker for Chinese Advanced Non-small Cell Lung Cancer Patients Treated With Immune Checkpoint Inhibitors

Zhibo Zhang[1,2,3†], Fang Yuan[1†], Runzhe Chen[4†], Ye Li[5], Junxun Ma[1], Xiang Yan[1], Lijie Wang[1], Fan Zhang[1], Haitao Tao[1], Dong Guo[6], Zhiyue Huang[6], Sujie Zhang[1], Xiaoyan Li[1], Xiaoyu Zhi[1,2], Xiangwei Ge[1,2], Yi Hu[1] and Jinliang Wang[1*]*

[1] Department of Oncology, The First Medical Center of Chinese PLA General Hospital, Beijing, China, [2] Medical School of Chinese PLA, Beijing, China, [3] The 78th Group Army Hospital of Chinese PLA, Mudanjiang, China, [4] Departments of Thoracic/Head and Neck Medical Oncology and Genomic Medicine, The University of Texas MD Anderson Cancer Center, Houston, TX, United States, [5] Department of Radiotherapy, The First Medical Center of Chinese PLA General Hospital, Beijing, China, [6] BeiGene (Shanghai) Co., Ltd., Shanghai, China

Background: Serum tumor markers carcinoembryonic antigen (CEA), cancer antigen 125 (CA125), cytokeratin 19 fragment (CYFRA21-1) and squamous-cell carcinoma-related antigen (SCC-Ag) are routinely used for monitoring the response to chemotherapy or targeted therapy in advanced-stage non-small cell lung cancer (NSCLC), however their role in immunotherapy remains unclear. The aim of this study was to investigate whether dynamics of these serum markers were associated with the efficacy and prognosis of Chinese late-stage NSCLC patients treated with programmed cell death-1/programmed cell death ligand-1 (PD-1/PD-L1) inhibitors.

Methods: We initiated a longitudinal prospective study on advanced NSCLC patients treated with PD-1/PD-L1 inhibitors in Chinese PLA general hospital (Beijing, China). Blood samples of baseline and after 6 weeks' treatment were collected. CT scan were used by all patients to evaluate treatment efficacy according to RECIST 1.1. Serum tumor markers levels were measured with an electrochemical luminescence for SCC-Ag and with a chemiluminescent microparticle immunoassay for serum CEA, CA125, and CYFRA21-1. At least 20% decreases of the biomarkers from baseline were considered as meaningful improvements after 6 weeks of treatment with immune checkpoint inhibitors (ICIs). Optimization-based method was used to balance baseline covariates between different groups. Associations between serum tumor biomarker improvements and objective response rate (ORR), progression-free survival (PFS), and overall survival (OS) were analyzed.

Results: A total of 308 Chinese patients with advanced NSCLC were enrolled in the study. After balancing baseline covariates, patients with meaningful improvements in <2 out of 4 biomarkers (CEA, CA125, CYFRA21-1, and SCC-Ag) was ended up with lower ORR (0.08 vs. 0.35, $p < 0.001$), shorten PFS (median: 5.4 vs. 12.5 months, $p < 0.001$), and OS (median: 11.7 vs. 25.6 months, $p < 0.001$) in the total

OPEN ACCESS

Edited by:
Maysaloun Merhi, Hamad Medical Corporation, Qatar

Reviewed by:
Ying Ma, University of Texas MD Anderson Cancer Center, United States
Pierre Busson, Centre National de la Recherche Scientifique (CNRS), France
Tiancai Liu, Southern Medical University, China

***Correspondence:**
Yi Hu
huyi0401@aliyun.com
Jinliang Wang
wangjinliang301@163.com

† These authors have contributed equally to this work

Specialty section:
This article was submitted to Cancer Immunity and Immunotherapy, a section of the journal Frontiers in Immunology

Received: *12 March 2020*
Accepted: *12 May 2020*
Published: *10 June 2020*

Citation:
Zhang Z, Yuan F, Chen R, Li Y, Ma J, Yan X, Wang L, Zhang F, Tao H, Guo D, Huang Z, Zhang S, Li X, Zhi X, Ge X, Hu Y and Wang J (2020) Dynamics of Serum Tumor Markers Can Serve as a Prognostic Biomarker for Chinese Advanced Non-small Cell Lung Cancer Patients Treated With Immune Checkpoint Inhibitors. Front. Immunol. 11:1173. doi: 10.3389/fimmu.2020.01173

population. Subgroup analysis of patients with adenocarcinoma revealed that patients with meaningful improvements in <2 out of 4 biomarkers had significant lower ORR (0.06 vs. 0.36, $p < 0.001$), shorten PFS (median: 4.1 vs. 11.9 months, $p < 0.001$), and OS (median: 11.9 vs. 24.2 months, $p < 0.001$). So as in patients with squamous cell carcinoma, meaningful improvements in at least 2 out of 4 biomarkers were linked to better ORR (0.42 vs. 0.08, $p = 0.014$), longer PFS (median: 13.1 vs. 5.6 months, $p = 0.001$), and OS (median: 25.6 vs. 10.9 months, $p = 0.06$).

Conclusions: The dynamic change of CEA, CA125, CYFRA21-1, and SCC-Ag from baseline have prognostic value for late-stage NSCLC patients treated with PD-1/PD-L1 inhibitors. Decrease of associated biomarkers serum levels were associated with favorable clinical outcomes.

Keywords: non-small cell lung cancer, serum tumor markers, Chinese patients, immune checkpoint inhibitors, prognostic biomarker

INTRODUCTION

Lung cancer is the leading cause of cancer-related deaths worldwide (1, 2). As the most common subtype of lung cancer, non-small cell lung cancer (NSCLC) accounts for 80–85% of the total cases. Over 60% of the NSCLC patients present with locally advanced or metastatic diseases at the time of diagnosis, and surgical resection may not be a treatment option (3). For these patients, although chemotherapy or targeted therapy has improved clinical outcomes in certain subtypes of lung cancer, up to 90% of patients inevitably relapse with the 5-year survival rate below 20% (4–6).

The emergence of immune checkpoint blockade (ICB) therapy targeting programmed cell death-1/programmed cell death ligand-1 (PD-1/PD-L1) have revolutionized the treatment of NSCLC, with large number of clinical trials demonstrating their increased effectiveness (7–10). Unfortunately, response rate is only ∼20% for advanced NSCLC in unselected populations, thus biomarker development remains critical to avoid ineffective treatments (11). PD-L1 expression and tumor mutation burden (TMB) are the most studied and validated predictors of clinical benefit in NSCLC patients with ICB therapy (12–15), while their roles are still controversial (7, 16–19). Moreover, detecting these biomarkers usually requires and invasive procedures followed by pathological assessment or even complicated and expensive methodologies such as the next generation sequencing (NGS). Therefore, non-invasive method and convenient biomarkers with relatively low cost are urgently needed.

Abbreviations: NSCLC, non-small cell lung cancer; ADC, adenocarcinoma; SCC, squamous cell carcinoma; CA125, cancer antigen 125; CEA, carcinoembryonic antigen; CYFRA21-1, cytokeratin 19 fragment; SCC-Ag, squamous-cell carcinoma-related antigen; ICB, immune checkpoint blockade; ICIs, immune checkpoint inhibitors; CR, complete response; PR, partial response; SD, stable disease; PD, progressive disease; ORR, objective response rate; PFS, progression-free survival; OS, overall survival; PD-1/PD-L1, programmed cell death-1/programmed cell death ligand-1; RECIST, Response Evaluation Criteria in Solid Tumors; TMB, tumor mutation burden.

Serum carcinoembryonic antigen (CEA), cancer antigen 125 (CA125), cytokeratin 19 fragment (CYFRA21-1), and squamous-cell carcinoma-related antigen (SCC-Ag) might be relevant for the prognosis of patients and have been widely used as biomarkers predicting the efficacy of chemotherapy or targeted therapy in NSCLC patients (20–27). However, their roles and post-treatment changes from baseline in advanced NSCLC treated by immune checkpoint inhibitors (ICIs) remains unclear. The aim of this study was to investigate whether dynamics of serum tumor markers were associated with the efficacy and prognosis of Chinese late-stage NSCLC patients treated with ICIs.

METHODS

Study Design

This observational study was performed in a real-life clinical practice setting. A total of 308 consecutive NSCLC patients from stage IIIB to IV receiving PD-1/PD-L1 checkpoint inhibitors were prospectively enrolled in Chinese PLA general hospital (Beijing, China) from January 2015 to January 2019. ICIs were treated for at least 6 weeks, and serum biomarkers (CEA, CA125 CYFRA21-1, and SCC-Ag) were measured at ICIs treatment initiation and after 6 weeks. During treatment, response was evaluated at least once.

The efficacy of immunotherapy was assessed according to Response Evaluation Criteria in Solid Tumors (RECIST) version 1.1 (28), including complete response (CR), partial response (PR), stable disease (SD), and progressive disease (PD). ORR was defined as the percentage of patients who have ever achieved a CR or PR since the first ICIs treatment. The time interval between date of commencement of PD-1/PD-L1 inhibitors treatment and date of disease progression or death (PFS) or death alone (OS) was calculated for each patient. The data cut-off date was Oct 6, 2019.

The baseline covariates including age, gender, histological type, clinical stage, smoking history, Eastern Cooperative Oncology Group Performance Status (ECOG PS), metastatic sites (lung, liver, and brain), radiotherapy, treatment (monotherapy

TABLE 1 | Characteristics of patients at baseline.

Characteristics	No. of patients (n = 308)	Percentage (%)
Age, median (range)	61 (33–91)	
Gender		
Male	236	76.6
Female	72	23.4
Histological type		
Adenocarcinoma	173	56.2
Squamous	113	36.7
Others	22	7.1
Clinical stage		
IIIB	53	17.2
IIIC	13	4.2
IV	242	78.6
Smoking history		
Never smoker	116	37.7
Smoker or ex-smoker	192	62.3
Treatment type		
Monotherapy	149	48.4
Combination therapy	159	51.6
ECOG PS		
0–1	276	89.6
≥2	32	14.4
Prior lines of therapy		
1 line	100	32.5
2 lines	109	35.4
≥3 lines	99	32.1
Radiation history		
Yes	201	65.3
No	107	34.7
Metastasis sites		
Liver	33	10.7
Lung	102	33.1
Brain	53	17.2
Drug		
Pembrolizumab	162	52.6
Nivolumab	125	40.6
Atelizumab	8	2.6
Duvalumab	13	4.2
CEA (ng/ml)		
Median (range)	6.2 (0.5–5207.0)	
Normal (≤5.0)	139	45.1
High (>5.0)	169	54.9
CA125 (ng/ml)		
Median (range)	36.0 (3.2–2002.0)	
Normal (≤35.0)	149	48.4
High (>35.0)	159	51.6
CYFRA21-1 (ng/ml)		
Median (range)	5.1 (1.4–345.6)	
Normal (≤4.0)	122	39.6
High (>4.0)	186	60.4
SCC-Ag (ng/ml)		
Median (range)	1.2 (0.2–70.0)	
Normal (≤1.8)	217	70.5
High (>1.8)	91	29.5

ECOG PS, Eastern Cooperative Oncology Group Performance Status; CEA, Carcinoembryonic antigen; CA125, Cancer antigen125; CYFRA21-1, Cytokeratin 19 fragment; SCC-Ag, Squamous-cell carcinoma-related antigen.

TABLE 2 | ORR in the whole weighted sample by groups.

	Group	Actual size	Effective size	Estimated ORR	95% CI	*P*-value
ORR	1	185	157	0.07	0.04–0.12	<0.001
	2	123	82	0.36	0.25–0.45	

Group 1, meaningful improvements in <2 out of 4 biomarkers (CEA, CA125, CYFRA21-1, and SCC-Ag); Group 2, meaningful improvements in ≥2 out of 4 biomarkers (CEA, CA125, CYFRA21-1, and SCC-Ag). ORR, objective response ratio.

or combination therapy), and prior lines of therapy (one line, two lines, and at least three lines) were collected. Lab test results including hemoglobin, white blood count, neutrophil, lymphocyte, monocyte, lactate dehydrogenase, platelet, and albumin were also routinely recorded.

Specimen Collection and Tumor Markers Assay

Blood samples were collected before the first ICIs treatment and after 6 weeks. Serum levels of CEA, CA125, and CYFRA21-1 were detected with electrochemical luminescence (CEA assay kit, CA125 quantitative determination kit and Non-small cell lung cancer associated antigen 21-1 detection kit; Roche), whereas SCC-Ag was measured with chemiluminescent microparticle immunoassay (Architect SCC reagent kit; Abbott). According to instructions of manufacturers, the reference range was 0–5.0 ng/ml for CEA, 0.1–35.0 ng/ml for CA125, 0.1–4.0 ng/ml for CYFRA21-1, and 0–1.8 ng/ml for SCC-Ag. Lab test results and levels of serum tumor markers were categorized by low, normal, and high based on the reference range, respectively (**Supplementary Table 1**). PD-L1 expression was evaluated by immunohistochemistry and tumor proportion score using PD-L1 antibody (Dako 22C3) before ICIs treatment.

The study protocol was approved by the Ethics Committee of Chinese PLA General Hospital. The study was conducted in accordance with the principles of the Declaration of Helsinki and Good Clinical Practice guidelines defined by the International Conference on Harmonization. Written informed consent was collected from all patients before enrollment.

Statistical Analysis

A post-treatment decline in serum marker level ≥20% from baseline was considered as meaningful improvement. Two groups were subsequently divided based on whether meaningful improvements of at least two serum biomarkers or not. Optimization-based methods were utilized to balance the baseline covariates between different groups (29). A weight under the following criteria was assigned to each patient: (1) Absolute value of standardized mean difference no more than 0.15; (2) Variance ratio between 0.67 (1/1.5) and 1.5. The effective sample sizes in the weighted sample were calculated by Kish's approximate formula. Group difference in ORR was calculated by Chi-square test. Median PFS and OS were estimated by Kaplan-Meier method and their 95% confidence intervals (CIs) were constructed by Brookmeyer and Crowley method, group

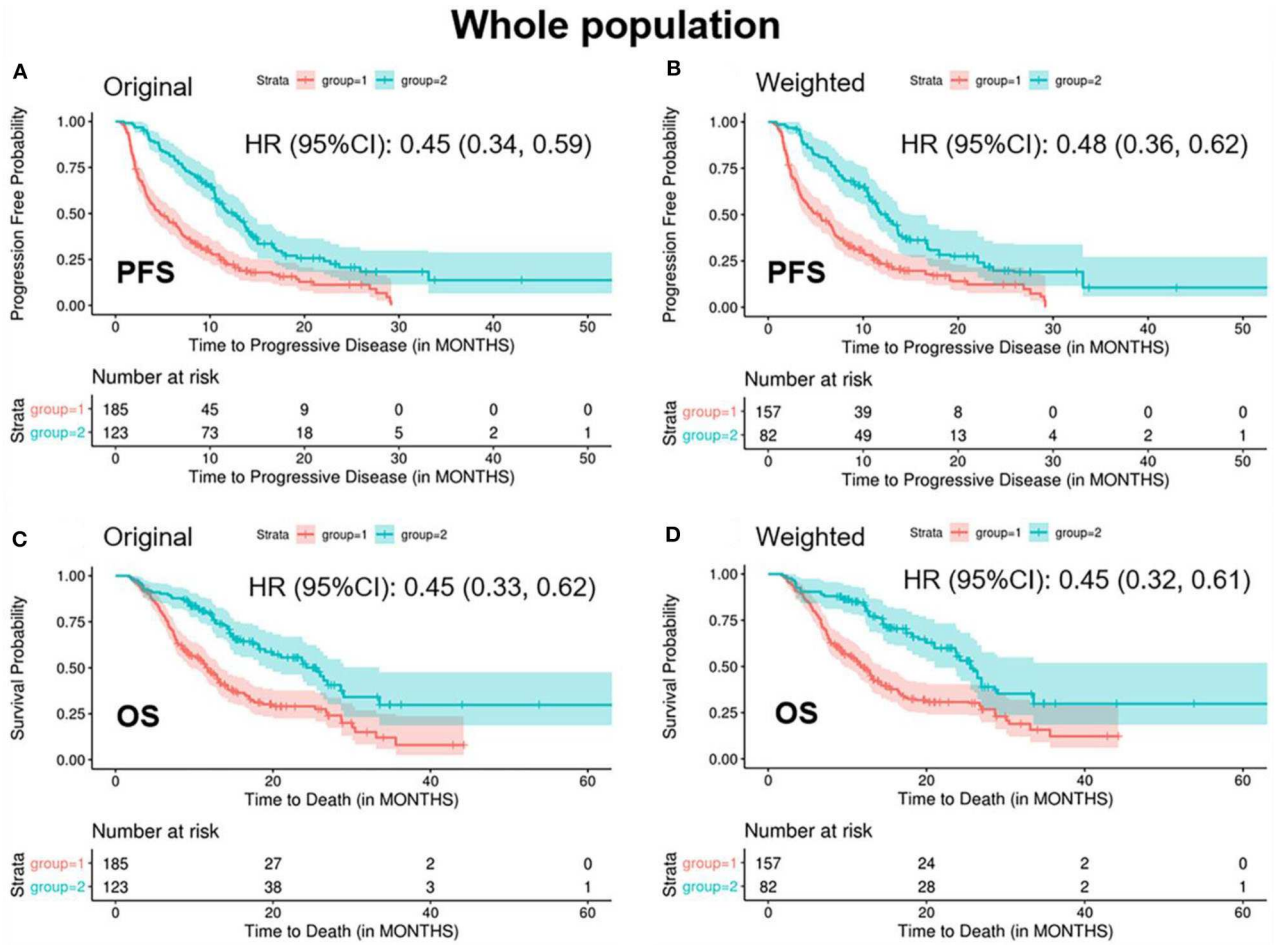

FIGURE 1 | Kaplan-Meier curves of PFS/OS in the original and weighted sample of whole population. group 1: meaningful improvements in <2 out of 4 biomarkers (CEA, CA125, CYFRA21-1, and SCC-Ag); group 2: meaningful improvements in ≥2 out of 4 biomarkers (CEA, CA125, CYFRA21-1, and SCC-Ag). Kaplan-Meier curves of **(A,C)** were based on the original sample; Kaplan-Meier curves of **(B,D)** were based on the weighted sample.

difference was assessed by Log-rank test. Hazard ratio (HR) with its 95% CI were calculated using Cox proportional hazards models. All statistical tests were bilateral with significance level 0.05. All analyses were performed in R, with the R packages *WeightIt* version 0.5.1 (*https://cran.r-project.org/web/packages/WeightIt/index.html)* for optimization-based methods and *survey* version 3.36 (*https://cran.r-project.org/web/packages/survey/index.html)* in the weighted sample.

RESULTS

Baseline Patient Characteristics

The main clinical characteristics of all the participants at baseline were presented in **Table 1**. Among 308 included patients, 56.2% were adenocarcinoma (ADC), 36.7% were squamous cell carcinoma (SCC) and the rest 7.1% belong to other subtypes. According to the eighth edition TNM staging of International Lung Cancer Research Association (30), 17.2% were stage IIIB, 4.2% were stage IIIC, and 78.6% were stage IV. 52.6% of patients used the drug of Pembrolizumab, 40.6% used Nivolumab, and the remaining patients used Atelizumab or Duvalumab. The median level of serum markers at baseline was 6.2 ng/ml for CEA (range 0.5–5207.0), 36.0 ng/ml for CA125 (range 3.2–2002.0), 5.1 ng/ml for CYFRA21-1 (range 1.4–345.6), and 1.2 ng/ml for SCC-Ag

TABLE 3 | ORR in sub-populations of ADC and SCC by groups.

Histological type	Group	Actual size	Effective size	Estimated ORR	95% CI	*P*-value
ADC	1	104	81	0.06	0.01–0.12	<0.001
	2	69	43	0.36	0.22–0.50	
SCC	1	68	47	0.08	0.01–0.16	0.014
	2	45	14	0.42	0.16–0.68	

Group 1, meaningful improvements in <2 out of 4 biomarkers (CEA, CA125, CYFRA21-1, and SCC-Ag); Group 2, meaningful improvements in ≥2 out of 4 biomarkers (CEA, CA125, CYFRA21-1, and SCC-Ag). ADC, adenocarcinoma; SCC, squamous cell carcinoma; ORR, objective response ratio.

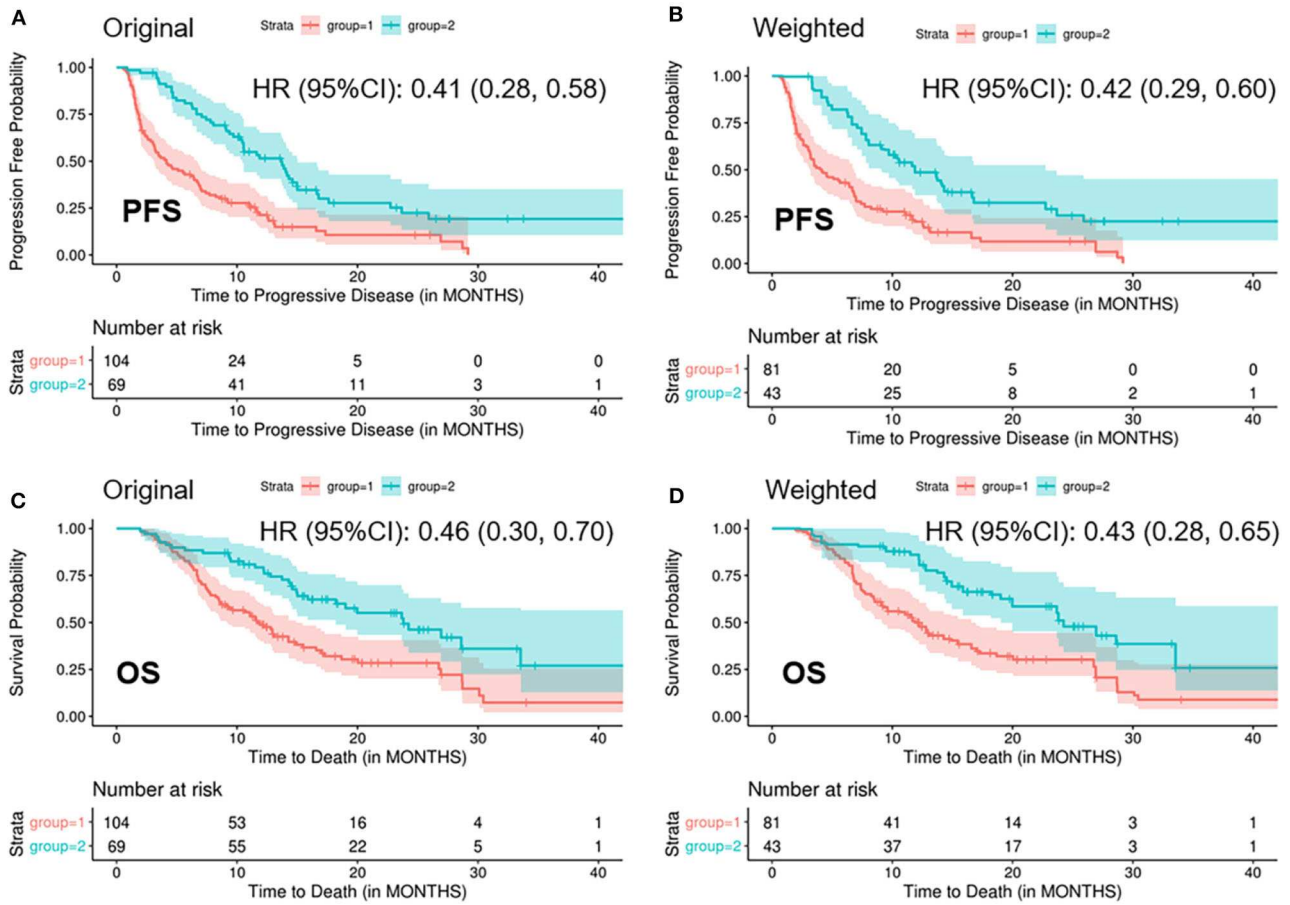

FIGURE 2 | Kaplan-Meier curves of PFS/OS in the original and weighted sample of adenocarcinoma. group 1: meaningful improvements in <2 out of 4 biomarkers (CEA, CA125, CYFRA21-1, and SCC-Ag); group 2: meaningful improvements in ≥2 out of 4 biomarkers (CEA, CA125, CYFRA21-1, and SCC-Ag). Kaplan-Meier curves of **(A,C)** were based on the original sample; Kaplan-Meier curves of **(B,D)** were based on the weighted sample.

(range 0.2–70.0). Proportion of patients with elevated levels of CEA, CA125, CYFRA21-1, and SCC-Ag were 54.9, 51.6, 60.4, and 29.5%, respectively.

Association Between Dynamics of Tumor Markers and Clinical Outcomes

The Total Population

The total population was divided into two groups by meaningful improvements in <2 out of 4 biomarkers (CEA, CA125, CYFRA21-1, and SCC-Ag) ("<2/4 biomarkers improvement group") and at least 2 out of 4 biomarkers ("≥2/4 biomarkers improvement group"). Standardized mean difference values of treatment type (combination therapy) and prior lines of therapy (one line, two lines) before balancing was 0.25, 0.24, and 0.18, respectively, followed by optimization-based weighting procedure to balance all baseline covariates between the two groups (**Supplementary Table 2**).

In the weighted samples, the ORR in the "<2/4 biomarker improvement group" was significantly lower than the "≥2/4 biomarkers improvement group" (0.08 vs. 0.35, $p < 0.001$) (**Table 2**). The patients in the "<2/4 biomarker improvement group" also had significantly shorten PFS (median: 5.4 vs. 12.5 months, $p < 0.001$) and OS (median: 11.7 vs. 25.6 months, $p < 0.001$) compared with the "≥2/4 biomarkers improvement group." The Kaplan-Meier curves of PFS and OS in both original and weighted sample were presented in **Figure 1**.

Subgroup Analysis of ADC

In patients with ADC, standardized mean difference of treatment type (combination therapy), prior lines of therapy (one line), and platelets (high level) was 0.25, 0.21, and 0.16, respectively, between the two groups before balancing (**Supplementary Table 3**). After balancing by the optimization-based method, patients in the "<2/4 biomarkers improvement group" were less likely to respond to treatment (ORR: 0.06 vs. 0.36, $p < 0.001$), more likely to progress (median PFS: 4.1 vs. 11.9 months, $p < 0.001$) and decease (median OS: 11.9 vs. 24.2 months, $p < 0.001$) (**Table 3** and **Figure 2**).

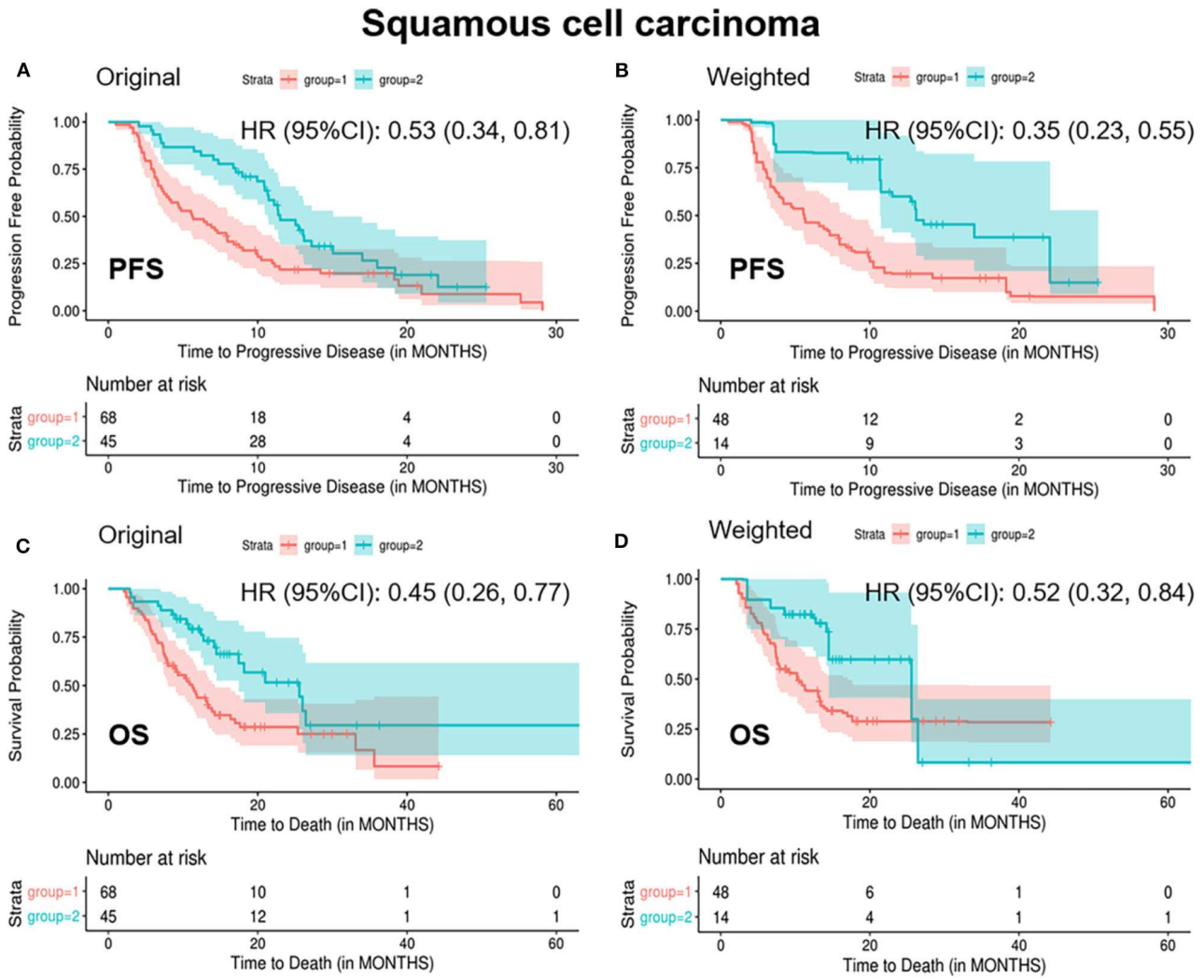

FIGURE 3 | Kaplan-Meier curves of PFS/OS in the original and weighted sample of squamous cell carcinoma. group 1: meaningful improvements in <2 out of 4 biomarkers (CEA, CA125, CYFRA21-1, and SCC-Ag); group 2: meaningful improvements in ≥2 out of 4 biomarkers (CEA, CA125, CYFRA21-1, and SCC-Ag). Kaplan-Meier curves of **(A,C)** were based on the original sample; Kaplan-Meier curves of **(B,D)** were based on the weighted sample.

Subgroup Analysis of SCC

In patients with SCC, standardized mean difference of the baseline covariates stage (IV), treatment type (combination therapy), prior lines of therapy (one line, two lines), and radiation history (yes) before balancing was 0.16, 0.26, 0.29, 0.34, and 0.19, respectively (**Supplementary Table 4**). After balancing by the optimization-based method, patients in the "<2/4 biomarkers improvement group" were less likely to respond to treatment (ORR: 0.08 vs. 0.42, $p = 0.014$), more likely to progress (median PFS: 5.6 vs. 13.1 months, $p = 0.001$) and decease (median OS: 10.2 vs. 25.6 months, $p = 0.06$) (**Table 3** and **Figure 3**).

Association Between Dynamics of Tumor Markers and PD-L1 Expression

PD-L1 expression was measured before ICIs treatment in 70 patients, of which 44 (62.8%) were diagnosed with ADC and 26 (37.2%) were SCC. Overall, there were 12 (17.1%) patients with PD-L1 expression negative, 25 (35.7%) patients with PD-L1 expression 1–50%, and 33 (47.1%) patients with PD-L1 expression >50%. However surprisingly, our analysis showed no correlations of PD-L1 expression with dynamics of tumor markers, either in the whole group or any subgroups.

DISCUSSION

Recently, immune checkpoint inhibitors such as PD-1/PD-L1 inhibitors, have been widely used for advanced-stage cancer treatment. Despite of enormous success in treatment of NSCLC (31), not all patients could get long-term benefit from the treatment of ICIs (11). PD-L1 expression and TMB have been widely used as predictive markers, but their roles are still controversial (32). Reliable markers remain to be

detected to identify patients who would get benefit from ICIs treatment.

In this study, we evaluated the baseline levels as well as post-treatment changes of routinely measured serum tumor markers in clinical practice to explore their associations with response to ICB therapy in patients with late-stage NSCLC. We demonstrated that dynamic changes of CEA, CA125, CYFRA21-1, and SCC-Ag were associated with the efficacy and prognosis of late-stage NSCLC patients treated with PD-1/PD-L1 inhibitors. Similar results were also observed in the subsequent subgroup analysis on ADC and SCC. Therefore, monitoring the changes in levels of serum tumor markers could be a promising prognostic factor for advanced NSCLC patients with ICIs treatment.

The approach of monitoring dynamic changes of serum tumor markers is more convenient and affordable compared to the most adopted PD-L1 expression or TMB. In contrast to other non-invasive biomarkers like lactate dehydrogenase (LDH) and neutrophil-to-lymphocyte ratio (NLR) (33–36), dynamics of serum tumor markers were also found to be more remarkably associated with response and survival according to our results, and this could also be supported by two recent studies (37, 38). Overall, as far as we know, this is the first and largest cohort study evaluating the relationship of routinely measured serum tumors markers with the efficacy and prognosis of patients receiving ICB therapy.

Optimization-based methods were used in our study. It considered the balance of baseline covariates between two groups compared to inverse propensity score weighting methods, in which only the balance of propensity score was considered in the algorithm. After balancing baseline covariates, possible confounding effects from clinical characteristics could be avoided and the collinearity in baseline covariates could also be controlled. Of noted, this is the first application of this novel statistical method in the clinical observational study.

Although we balanced all measurable baseline variates to avoid bias, there were still some limitations in our study. Firstly, the results may be influenced by the method used for choosing the cut-off point. Twenty percent was selected as a threshold to identify meaningful change in biomarkers according to previous reports, and meaningful improvement in at least two biomarkers was considered as a prognostic factor which was not data-driven. Secondly, only patients receiving more than 6 weeks of ICB treatment were enrolled in this study with baseline and post-treatment serum markers been measured, which may increase selective bias. Thirdly, dynamic change of baseline and after 6 weeks' tumor levels were used for our analysis, whether a shorter interval time is better need further investigation. Fourthly, this observational study was based on the single institution which may cause selection bias. Fifthly, we used the methods of electrochemical luminescence and chemiluminescent microparticle immunoassay for testing tumor markers, some new methods with high sensitivity and specificity may be more helpful for early detection of tumor markers (39, 40). Last but not least, though weighting method were used to balance all measurable baseline covariates, some unrecorded baseline covariates such as TMB could be potential confounders.

CONCLUSIONS

In summary, we proposed a new strategy of monitoring dynamics of serum tumor markers and highlight their importance as a potential prognostic biomarker of advanced NSCLC treated with ICIs. Decrease of associated biomarkers serum levels were associated with favorable clinical outcomes. Further investigations will be required to evaluate the roles of these serum markers with different cut-off values as well as earlier dynamic changes from baseline in larger multi-center patient populations.

DATA AVAILABILITY STATEMENT

All datasets generated for this study are included in the article/**Supplementary Material**.

ETHICS STATEMENT

The studies involving human participants were reviewed and approved by People's Liberation Army General Hospital. The patients/participants provided their written informed consent to participate in this study.

AUTHOR CONTRIBUTIONS

ZZ, FY, RC, YL, JM, XY, LW, FZ, HT, DG, ZH, SZ, XL, XZ, XG, YH, and JW contributed to the study design. YH and JW were responsible for interpretation of the results. DG and ZH contributed to statistical analysis. ZZ, FY, and RC were prepared for the manuscript. All authors contributed to data analysis.

ACKNOWLEDGMENTS

We thank all the participants who made the study possible.

SUPPLEMENTARY MATERIAL

The Supplementary Material for this article can be found online at: https://www.frontiersin.org/articles/10.3389/fimmu.2020.01173/full#supplementary-material

REFERENCES

1. Siegel RL, Miller KD, Jemal A. Cancer statistics (2019). *CA Cancer J Clin*. (2019) 69:7–34. doi: 10.3322/caac.21551
2. Tan WL, Jain A, Takano A, Newell EW, Iyer NG, Lim WT, et al. Novel therapeutic targets on the horizon for lung cancer. *Lancet Oncol*. (2016) 17:e347–e62. doi: 10.1016/S1470-2045(16)30123-1
3. Osmani L, Askin F, Gabrielson E, Li QK. Current WHO guidelines and the critical role of immunohistochemical markers in the subclassification of non-small cell lung carcinoma (NSCLC): moving from targeted therapy to immunotherapy. *Semin Cancer Biol*. (2018) 52:103–9. doi: 10.1016/j.semcancer.2017.11.019
4. Siegel RL, Miller KD, Jemal A. Cancer statistics (2017). *CA Cancer J Clin*. (2017) 67:7–30. doi: 10.3322/caac.21387
5. Travis WD, Brambilla E, Burke AP, Marx A, Nicholson AG. Introduction to the 2015. World Health Organization classification of tumors of the lung, pleura, thymus, and heart. *J Thorac Oncol*. (2015) 10:1240–42. doi: 10.1097/JTO.0000000000000663
6. Ke B, Wei T, Huang Y, Gong Y, Shi L. Interleukin-7 resensitizes non-small-cell lung cancer to cisplatin via inhibition of ABCG2. *Mediat Inflamm*. (2019) 2019:7241418. doi: 10.1155/2019/7241418
7. Brahmer J, Reckamp KL, Baas P, Crino L, Eberhardt WE, Poddubskaya E, et al. Nivolumab versus docetaxel in advanced squamous-cell non-small-cell lung cancer. *N Engl J Med*. (2015) 373:123–35. doi: 10.1056/NEJMoa1504627
8. Borghaei H, Paz-Ares L, Horn L, Spigel DR, Steins M, Ready NE, et al. Nivolumab versus docetaxel in advanced nonsquamous non-small-cell lung cancer. *N Engl J Med*. (2015) 373:1627–39. doi: 10.1056/NEJMoa1507643
9. Herbst RS, Baas P, Kim DW, Felip E, Perez-Gracia JL, Han JY, et al. Pembrolizumab versus docetaxel for previously treated, PD-L1-positive, advanced non-small-cell lung cancer (KEYNOTE-010): a randomised controlled trial. *Lancet*. (2016) 387:1540–50. doi: 10.1016/S0140-6736(15)01281-7
10. Rittmeyer A, Barlesi F, Waterkamp D, Park K, Ciardiello F, von Pawel J, et al. Atezolizumab versus docetaxel in patients with previously treated non-small-cell lung cancer (OAK): a phase 3, open-label, multicentre randomised controlled trial. *Lancet*. (2017) 389:255–65. doi: 10.1016/S0140-6736(16)32517-X
11. Barbee MS, Ogunniyi A, Horvat TZ, Dang TO. Current status and future directions of the immune checkpoint inhibitors ipilimumab, pembrolizumab, and nivolumab in oncology. *Ann Pharmacother*. (2015) 49:907–37. doi: 10.1177/1060028015586218
12. Aguiar PN Jr, Santoro IL, Tadokoro H, de Lima Lopes G, Filardi BA, Oliveira P, et al. A pooled analysis of nivolumab for the treatment of advanced non-small-cell lung cancer and the role of PD-L1 as a predictive biomarker. *Immunotherapy*. (2016) 8:1011–9. doi: 10.2217/imt-2016-0032
13. Wang Z, Duan J, Cai S, Han M, Dong H, Zhao J, et al. Assessment of blood tumor mutational burden as a potential biomarker for immunotherapy in patients with non-small cell lung cancer with use of a next-generation sequencing cancer gene panel. *JAMA Oncol*. (2019) 5:696–702. doi: 10.1001/jamaoncol.2018.7098
14. Ready N, Hellmann MD, Awad MM, Otterson GA, Gutierrez M, Gainor JF, et al. First-Line nivolumab plus ipilimumab in advanced non-small-cell lung cancer (checkmate 568): outcomes by programmed death ligand 1 and tumor mutational burden as biomarkers. *J Clin Oncol*. (2019) 37:992–1000. doi: 10.1200/JCO.18.01042
15. Gandara DR, Paul SM, Kowanetz M, Schleifman E, Zou W, Li Y, et al. Blood-based tumor mutational burden as a predictor of clinical benefit in non-small-cell lung cancer patients treated with atezolizumab. *Nat Med*. (2018) 24:1441–8. doi: 10.1038/s41591-018-0134-3
16. Bhaijee F, Anders RA. PD-L1 expression as a predictive biomarker: is absence of proof the same as proof of absence? *JAMA Oncol*. (2016) 2:54–5. doi: 10.1001/jamaoncol.2015.3782
17. Cristescu R, Mogg R, Ayers M, Albright A, Murphy E, Yearley J, et al. Pan-tumor genomic biomarkers for PD-1 checkpoint blockade-based immunotherapy. *Science*. (2018) 362:eaar3593. doi: 10.1126/science.aar3593
18. Buttner R, Gosney JR, Skov BG, Adam J, Motoi N, Bloom KJ, et al. Programmed death-ligand 1 immunohistochemistry testing: a review of analytical assays and clinical implementation in non-small-cell lung cancer. *J Clin Oncol*. (2017) 35:3867–76. doi: 10.1200/JCO.2017.74.7642
19. Ilie M, Long-Mira E, Bence C, Butori C, Lassalle S, Bouhlel L, et al. Comparative study of the PD-L1 status between surgically resected specimens and matched biopsies of NSCLC patients reveal major discordances: a potential issue for anti-PD-L1 therapeutic strategies. *Ann Oncol*. (2016) 27:147–53. doi: 10.1093/annonc/mdv489
20. Zhang ZH, Han YW, Liang H, Wang LM. Prognostic value of serum CYFRA21-1 and CEA for non-small-cell lung cancer. *Cancer Med*. (2015) 4:1633–8. doi: 10.1002/cam4.493
21. Yang Q, Zhang P, Wu R, Lu K, Zhou H. Identifying the best marker combination in CEA, CA125, CY211, NSE, and SCC for lung cancer screening by combining roc curve and logistic regression analyses: is it feasible? *Dis Markers*. (2018) 2018:2082840. doi: 10.1155/2018/2082840
22. Masaki T, Takanori A, Eiichi C, Kunihide N. Postoperative serum CEA level is a more significant prognostic factor than post/preoperative serum CEA ratio in non-small cell cancer patients. *Asian Pac J Cancer Prev*. (2015) 16:7809–12. doi: 10.7314/APJCP.2015.16.17.7809
23. Susana C, Isaac NE, Marina L, Pablo M, Eva C, Davis T, et al. Serum tumor markers CEA, CYFRA21-1, and CA-125 are associated with worse prognosis in advanced non-small-cell lung cancer (NSCLC). *Clin Lung Cancer*. (2011) 12:172–9. doi: 10.1016/j.cllc.2011.03.019
24. Jiang ZF, Wang M, Xu JL. Thymidine kinase 1 combined with CEA, CYFRA21-1 and NSE improved its diagnostic value for lung cancer. *Life Sci*. (2018) 194:1–6. doi: 10.1016/j.lfs.2017.12.020
25. Yoshimura A, Uchino J, Hasegawa K, Tsuji T, Shiotsu S, Yuba T, et al. Carcinoembryonic antigen and CYFRA 21-1 responses as prognostic factors in advanced non-small cell lung cancer. *Transl Lung Cancer Res*. (2019) 8:227–34. doi: 10.21037/tlcr.2019.06.08
26. Holdenrieder S, Wehnl B, Hettwer K, Simon K, Uhlig S, Dayyani F. Carcinoembryonic antigen and cytokeratin-19 fragments for assessment of therapy response in non-small cell lung cancer: a systematic review and meta-analysis. *Br J Cancer*. (2017) 116:1037–45. doi: 10.1038/bjc.2017.45
27. Ma R, Xu H, Wu J, Sharma A, Bai S, Dun B, et al. Identification of serum proteins and multivariate models for diagnosis and therapeutic monitoring of lung cancer. *Oncotarget*. (2017) 8:18901–13. doi: 10.18632/oncotarget.14782
28. Eisenhauer EA, Therasse P, Bogaerts J, Schwartz LH, Sargent D, Ford R, et al. New response evaluation criteria in solid tumours: revised RECIST guideline (version 1.1). *Eur J Cancer*. (2009) 45:228–47. doi: 10.1016/j.ejca.2008.10.026
29. Zubizarreta JR. Stable weights that balance covariates for estimation with incomplete outcome data. *J Am Stat Assoc*. (2015) 110:910–22. doi: 10.1080/01621459.2015.1023805
30. Nicholson AG, Chansky K, Crowley J, Beyruti R, Kubota K, Turrisi A, et al. The international association for the study of lung cancer lung cancer staging project: proposals for the revision of the clinical and pathologic staging of small cell lung cancer in the forthcoming eighth edition of the TNM classification for lung cancer. *J Thorac Oncol*. (2016) 11:300–11. doi: 10.1016/j.jtho.2015.10.008
31. Nishino M, Ramaiya NH, Hatabu H, Hodi FS. Monitoring immune-checkpoint blockade: response evaluation and biomarker development. *Nat Rev Clin Oncol*. (2017) 14:655–68. doi: 10.1038/nrclinonc.2017.88
32. Dal Bello MG, Alama A, Coco S, Vanni I, Grossi F. Understanding the checkpoint blockade in lung cancer immunotherapy. *Drug Discov Today*. (2017) 22:1266–73. doi: 10.1016/j.drudis.2017.05.016
33. Zhang Z, Li Y, Yan X, Song Q, Wang G, Hu Y, et al. Pretreatment lactate dehydrogenase may predict outcome of advanced non-small-cell lung cancer patients treated with immune checkpoint inhibitors: a meta-analysis. *Cancer Med*. (2019) 8:1467–73. doi: 10.1002/cam4.2024
34. Jiang T, Qiao M, Zhao C, Li X, Gao G, Su C, et al. Pretreatment neutrophil-to-lymphocyte ratio is associated with outcome of advanced-stage cancer patients treated with immunotherapy: a meta-analysis. *Cancer Immunol Immunother*. (2018) 67:713–27. doi: 10.1007/s00262-018-2126-z
35. Jiang T, Bai Y, Zhou F, Li W, Gao G, Su C, et al. Clinical value of neutrophil-to-lymphocyte ratio in patients with non-small cell lung cancer treated with PD-1/PD-L1 inhibitors. *Lung Cancer*. (2019) 130:76–83. doi: 10.1016/j.lungcan.2019.02.009
36. Sacdalan DB, Lucero JA, Sacdalan DL. Prognostic utility of baseline neutrophil-to-lymphocyte ratio in patients receiving immune checkpoint inhibitors: a review and meta-analysis. *Oncol Targets Ther*. (2018) 11:955–65. doi: 10.2147/OTT.S153290
37. Dal Bello MG, Filiberti RA, Alama A, Orengo AM, Mussap M, Coco S, et al. The role of CEA, CYFRA21-1 and NSE in monitoring tumor response to

nivolumab in advanced non-small cell lung cancer (NSCLC) patients. *J Transl Med*. (2019) 17:74. doi: 10.1186/s12967-019-1828-0
38. Lang D, Horner A, Brehm E, Akbari K, Hergan B, Langer K, et al. Early serum tumor marker dynamics predict progression-free and overall survival in single PD-1/PD-L1 inhibitor treated advanced NSCLC-A retrospective cohort study. *Lung Cancer*. (2019) 134:59–65. doi: 10.1016/j.lungcan.2019.05.033
39. Wang H, Zhai X, Liu T, Liang J, Bian L, Lin L, et al. Development of a novel immunoassay for the simple and fast quantitation of neutrophil gelatinase-associated lipocalin using europium(III) chelate microparticles and magnetic beads. *J Immunol Methods*. (2019) 470:15–9. doi: 10.1016/j.jim.2019.04.004
40. Zhao H, Lin G, Liu T, Liang J, Ren Z, Liang R, et al. Rapid quantitation of human epididymis protein 4 in human serum by amplified luminescent proximity homogeneous immunoassay (AlphaLISA). *J Immunol Methods*. (2016) 437:64–9. doi: 10.1016/j.jim.2016.08.006

Conflict of Interest: The authors declare that the research was conducted in the absence of any commercial or financial relationships that could be construed as a potential conflict of interest.

The reviewer YM declared a shared affiliation, with no collaboration, with one of the authors, RC, to the handling editor at the time of review.

frontiers in Oncology

ORIGINAL RESEARCH
published: 12 June 2020
doi: 10.3389/fonc.2020.00853

An Integrative Analysis Reveals the Underlying Association Between CTNNB1 Mutation and Immunotherapy in Hepatocellular Carcinoma

*Zhuomao Mo†, Yongdan Wang†, Zhirui Cao, Pan Li and Shijun Zhang**

Department of Traditional Chinese Medicine, The First Affiliated Hospital, Sun Yat-sen University, Guangzhou, China

OPEN ACCESS

Edited by:
Said Dermime, National Center for Cancer Care and Research, Qatar

Reviewed by:
Abdelali Agouni, Qatar University, Qatar
Mona Omar Mohsen, University of Oxford, United Kingdom

***Correspondence:**
Shijun Zhang
2806973376@qq.com

†*These authors have contributed equally to this work*

Specialty section:
This article was submitted to Cancer Immunity and Immunotherapy, a section of the journal Frontiers in Oncology

Received: *08 April 2020*
Accepted: *29 April 2020*
Published: *12 June 2020*

Citation:
Mo Z, Wang Y, Cao Z, Li P and Zhang S (2020) An Integrative Analysis Reveals the Underlying Association Between CTNNB1 Mutation and Immunotherapy in Hepatocellular Carcinoma. Front. Oncol. 10:853. doi: 10.3389/fonc.2020.00853

Background: Tumor mutational burden (TMB) was verified to be closely associated with immune checkpoint inhibitors, but it is unclear whether gene mutation has an effect on immunotherapy of hepatocellular carcinoma (HCC). This research aimed to investigate the underlying correlation between gene mutation and immunotherapy in HCC.

Methods: The somatic gene mutation data and gene expression data were retrieved from International Cancer Genome Consortium database and The Cancer Genome Atlas (TCGA) database. The mutational genes were selected by the intersection of three cohorts and further identified using survival analysis and TMB correlation analysis. After the identification of key mutational gene, we explored the correlation between gene mutation and both the immune cell infiltration and immune inhibitors. The signaling pathways associated with gene mutation were confirmed through gene set enrichment analysis. Furthermore, the survival analysis and mutational analysis based on TCGA cohort were performed for the validation of included gene.

Results: As one of the frequently mutational genes in HCC, *CTNNB1* was finally included in our research, for which it showed the significant result in survival analysis and the positive association with TMB of the three cohorts. Meanwhile, the validation of TCGA showed the significant results. Furthermore, natural killer (NK) cells and neutrophil were found to significantly infiltrate *CTNNB1* mutation group from two cohorts. Besides, further analysis demonstrated that four types of immune inhibitors (*CD96*, *HAVCR2*, *LGALS9*, and *TGFB1*) were downregulated in *CTNNB1* mutation group.

Conclusion: Our research firstly revealed the underlying association between *CTNNB1* mutation and immunotherapy, and we speculated that *CTNNB1* mutation may modulate NK cells by affecting CD96. However, more functional experiments should be performed for verification.

Keywords: hepatocellular carcinoma, CTNNB1, gene mutation, immunotherapy, immune inhibitor

INTRODUCTION

Globally, liver cancer is a highly malignant tumor with high prevalence and poor outcomes, which results in ∼850,000 new cases per year (1). As the major subtype of liver cancer, hepatocellular carcinoma (HCC) accounts for 85–90% of all liver cancer cases (1) and has become the second leading cause of cancer-associated deaths (2). It has been reported that the 5-year survival rate is 30.5% in patients with local HCC while <5% in patients with distant metastasis (3). At present, partial hepatectomy and liver transplantation are still the main treatments for early-stage patients, but a significant proportion of patients are not eligible for these treatments. Furthermore, the postoperative recurrence or distant metastasis is prevalent in patients after surgery (4). Although the systemic therapy with sorafenib is regarded as a first-line chemotherapeutic therapy in patients with advanced HCC, the high resistance rate has significantly limited the benefit of sorafenib therapy (5). Therefore, there is an urgent need to find a novel and effective therapy to improve the clinical outcomes of HCC patients.

The initiation, development, metastasis, and recurrence of HCC are closely related to the immune system (6). It has been reported that dysregulation of the immune system including alteration in the number or function of immune cells (7) and the release of chemokine and cytokine (8) result in the progression of HCC. Accordingly, immunotherapy has attracted increasing attention in HCC. As an important breakthrough in the field of immunotherapy, immune checkpoint inhibitors target three main molecules: cytotoxic T-lymphocyte-associated molecule-4 (*CTLA-4*), programmed cell death receptor-1 (*PD-1*), and programmed cell death ligand-1 (*PD-L1*) (9). It has been reported that camrelizumab showed antitumor activity and manageable

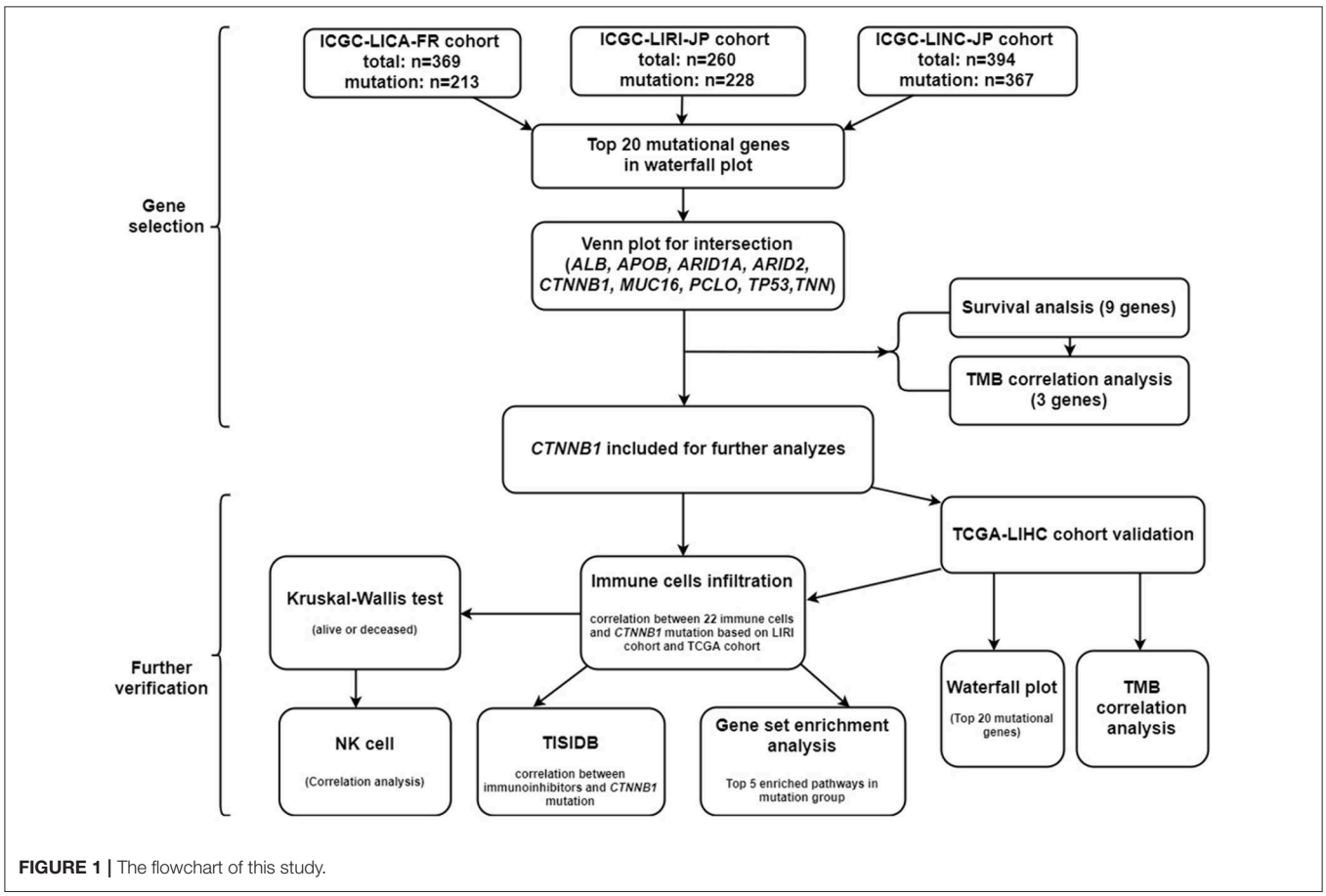

FIGURE 1 | The flowchart of this study.

toxicities in advanced HCC patients by blocking the interaction between *PD-1* and its ligands (10). Another clinical trial (11) also indicated that tremelimumab (*CTLA-4* blockade) showed antitumor and antiviral activities in advanced HCC patients. Nevertheless, only a minority of patients can respond to these immunotherapies, and fewer still achieve a lasting response (12). Consequently, it is one of the critical challenges to explore the molecular mechanism of immunotherapeutic responsiveness in HCC.

Tumor mutational burden (TMB) was defined as the total number of errors in somatic gene coding, base substitution, gene insertion, or deletion detected in every million base. Accumulation of somatic mutation contributes to the occurrence of tumor and the expression of neoantigens (13). Meanwhile, it has been reported that TMB can be used to predict the efficacy of immune checkpoint blockade and become a useful biomarker in some cancers for identification of patients who will benefit from immunotherapy (14). However, the potential association between gene mutation and immunotherapy in HCC is still unclear.

In this research, we firstly identified that *CTNNB1* was one of the frequently mutated genes in HCC and highly associated with survival and TMB. Next, we explored the relationship between *CTNNB1* mutation and immune cell infiltration and found that natural killer (NK) cells significantly infiltrated the *CTNNB1* mutation group. Therefore, we further investigated the correlation between *CTNNB1* mutation and immune inhibitors. We finally found that *CD96* was negatively associated with CTNNB1 mutation and speculated that *CTNNB1* may modulate NK cells by affecting *CD96*. Our research proposed a new underlying association between *CTNNB1* mutation and immunotherapy in HCC, which may help in improving the efficacy of immunotherapy in HCC patients.

MATERIALS AND METHODS

Data Collection

The somatic gene mutation data, gene expression data, and clinical messages were retrieved from International Cancer Genome Consortium (ICGC) database (https://dcc.icgc.org/) and The Cancer Genome Atlas (TCGA) database (https://portal.gdc.cancer.gov/). Three independent cohorts (LIRI-JP, LICA-FR, and LINC-JP) in ICGC database were employed in our research. All the three cohorts were used for mutational gene selection, and the LIRI-JP cohort was employed for further analyses (owing to gene expression data and more known clinical parameters). In addition, the TCGA-LIHC cohort was used for further validation.

Selection of Key Mutational Genes

Based on the "GenVisR" package under the R studio software, the details of mutation from the three cohorts were visualized in waterfall plot. After that, we employed the intersection of the three cohorts for further analyses and used the Venn plot to visualize. To investigate the time-dependent prognostic value of included genes, the survival analysis was performed using the "survival" package. Moreover, we explored the association between included genes and TMB. To calculate the TMB of each case, the total number of mutations counted was divided by the exome size (38 Mb was utilized as the exome size). The mutational genes were eligible for further analyses if they were significantly different in both the survival analysis and TMB correlation analysis. A P-value < 0.05 was considered a significant difference in this section. Besides, the mutational analysis and TMB correlation analysis were performed again based on the TCGA-LIHC cohort for validation.

TABLE 1 | Baseline patient characteristic in three cohorts.

Clinical characteristics		Number	Percent
LICA-FR (n = 369)			
Survival status	Survival	92	25
	Death	115	31
	Not reported	162	44
Age	≤65 years	205	56
	>65 years	164	44
Gender	Female	76	21
	Male	293	79
T classification	T1	54	14.6
	T2	65	17.6
	T3	40	10.8
	T4	1	0.3
	Not reported	209	56.7
N classification	N0	160	43
	N1	0	0
	Not reported	209	57
M classification	M0	159	43
	M1	1	0.3
	Not reported	209	56.7
LINC-JP (n = 394)			
Survival status	Survival	269	68
	Death	79	20
	Not reported	46	12
Age	≤65 years	175	45
	>65 years	206	52
	Not reported	13	3
Gender	Female	95	24
	Male	299	76
Stage	I	16	4.1
	II	69	17.5
	III	67	17
	IV	43	10.9
	Not reported	199	50.5
LIRI-JP (n = 260)			
Survival status	Survival	214	82.4
	Death	46	17.6
Age	≤65 years	98	37.7
	>65 years	162	62.3
Stage	I	40	15.4
	II	117	45
	III	80	30.8
	IV	23	8.8

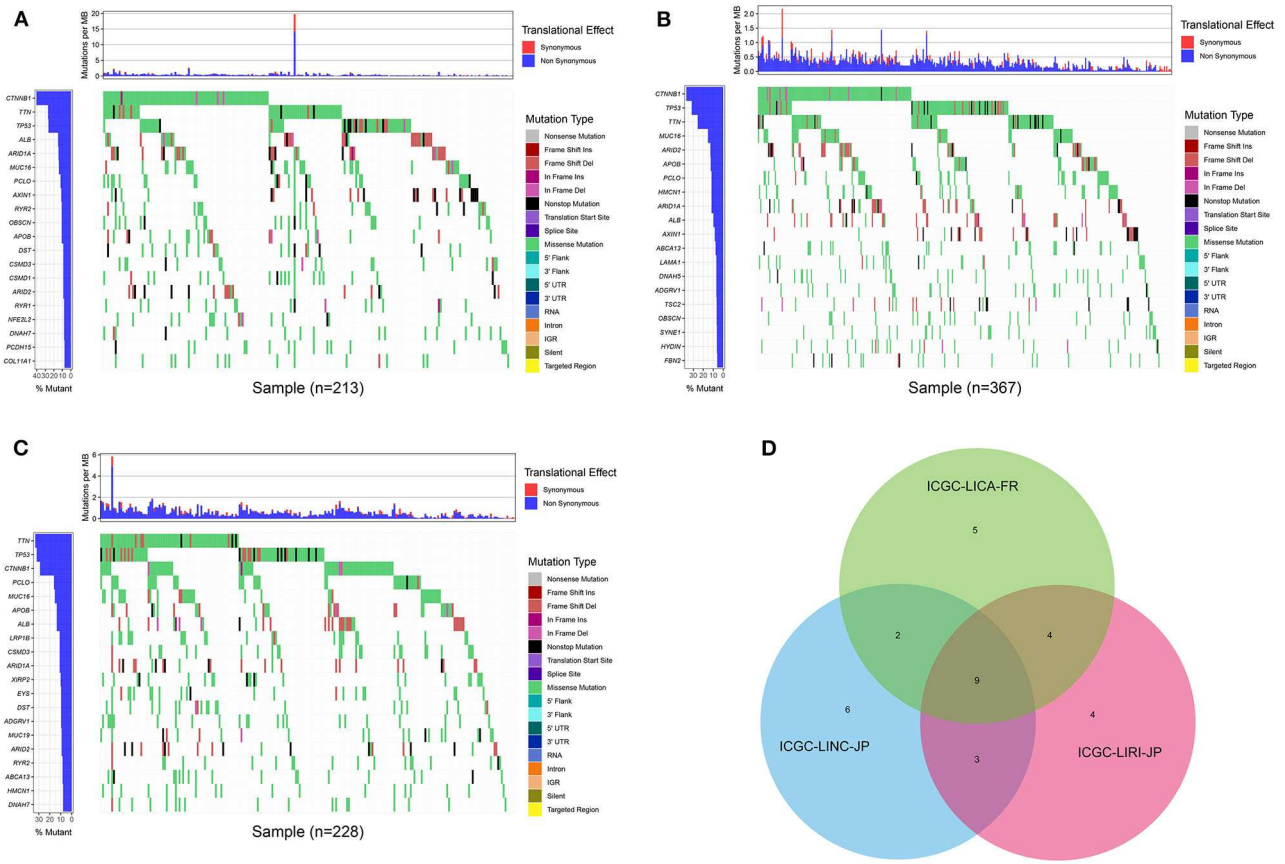

FIGURE 2 | Waterfall plot with the details of gene mutation from three cohorts. **(A)** The waterfall plot of LICA-FR. **(B)** The waterfall plot of LINC-JP. **(C)** The waterfall plot of LIRI-JP. **(D)** The Venn plot of three cohorts.

Immune Cell Infiltration and Immune Inhibitors

To explore the underlying mechanism between mutational gene and immune cells, we estimated the abundance of immune cell infiltration with different mutational status in the cases of the LIRI-JP cohort on the basis of the CIBERSORT algorithm. CIBERSORT is a deconvolution algorithm that evaluates the proportions of 22 tumor-infiltrating lymphocyte subsets. The number of permutations was set to 1,000, and the sample in the cohort was eligible for further validation if a P-value $<$ 0.05. Meanwhile, the results of immune cell infiltration were verified in TIMER website (http://timer.cistrome.org/) on the basis of the TCGA-LIHC cohort. Besides, we investigated the correlation between 22 types of immune cells and survival. In addition, we evaluated the correlation between gene mutation and the expression of immunoinhibitory genes from TISIDB website (http://cis.hku.hk/TISIDB/index.php) (15). Both $P <$ 0.05 and mean difference of median-value > 0.6 were considered significant association in TISIDB website.

Gene Set Enrichment Analysis

Gene set enrichment analysis (GSEA) is a computational method that identifies whether a prior defined set of genes shows statistically significant differences between two biological states (16). In this research, we performed the GSEA to identify statistically different pathways from Gene Ontology (GO) and Kyoto Encyclopedia of Genes and Genomes (KEGG) databases between the mutation group and wild-type group. The normalized enrichment score was used to evaluate the pathways, and the top 5 significant pathways in two groups were visualized using the "ggplot" package.

RESULTS

Identification of Key Mutational Genes

First of all, we summarized the flowchart, as shown in **Figure 1**. The clinical details of the ICGC cohorts are shown in **Table 1**. As illustrated in **Figure 2**, the details of the top 20 most frequently mutated genes are demonstrated in waterfall plots. Interestingly, we observed that some genes frequently mutated in all the three cohorts. So we executed a comparative analysis of the 20 most frequently mutated genes among the three cohorts. The Venn plot in **Figure 2D** shows that nine genes (*ALB*, *APOB*, *ARID1A*, *ARID2*, *CTNNB1*, *MUC16*, *PCLO*, *TP53*, and *TTN*) were included in the intersection of the three cohorts. After that, we performed a survival analysis to evaluate nine

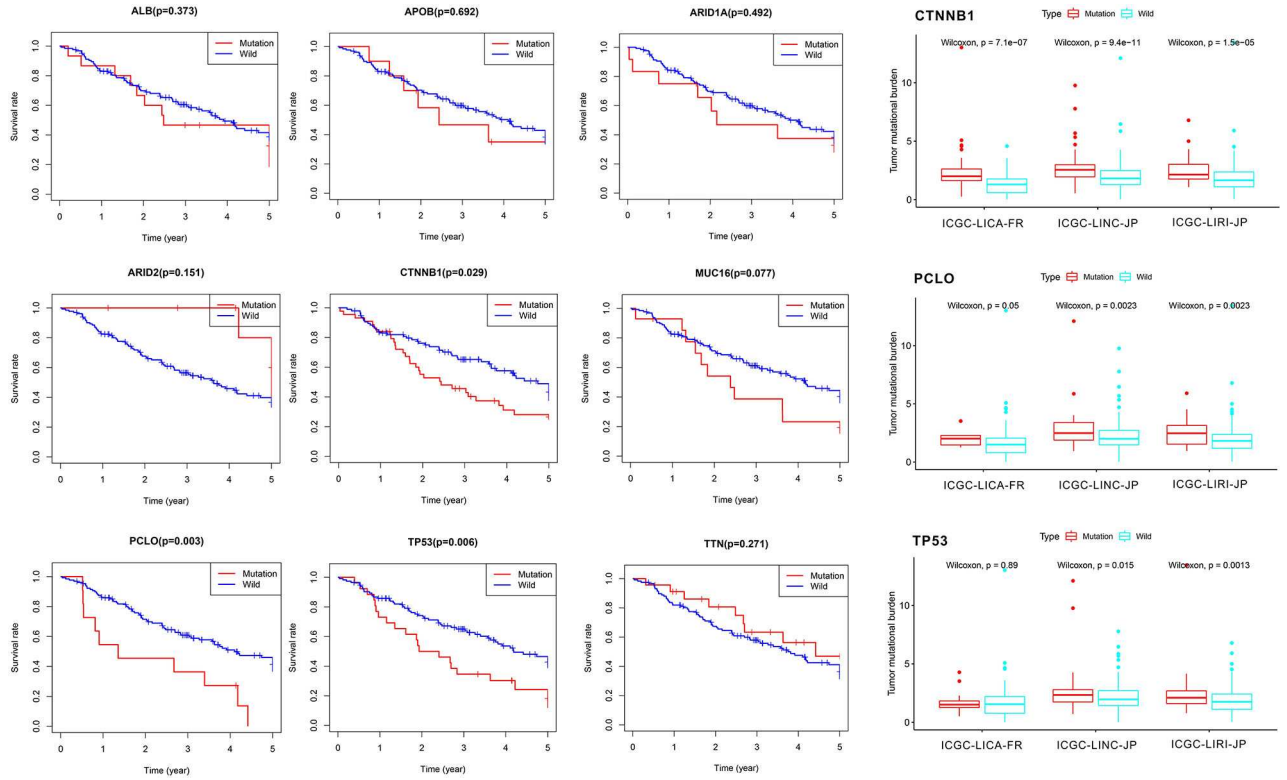

FIGURE 3 | Survival analysis and tumor mutational burden (TMB) correlation analysis.

genes. The results of the survival analysis in **Figure 3** indicated that a significant difference was found between the mutation group and wild-type group in the three genes (*CTNNB1*, *PCLO*, and *TP53*). Furthermore, we evaluated the correlation between the three genes and TMB, and the results indicated that only *CTNNB1* mutation was statistically significant with TMB in the three cohorts. Therefore, we focused on *CTNNB1* mutation in subsequent analyses. In addition, the validation of the TCGA-LIHC cohort demonstrated that *CTNNB1* was one of the frequently mutated genes (**Figure 4A**) and positively related to TMB in HCC (**Figure 4B**).

Immune Cell Infiltration and Immune Inhibitors

As shown in **Figure 5**, the relative percent of 22 immune cell infiltration was visualized based on the LIRI-JP cohort. Between the mutation group and wild-type group, significant differences were found ($P < 0.05$) in five types of immune cells (CD8 T cells, regulatory T cells, gamma delta T cells, activated NK cells, and neutrophils) on the basis of the LIRI-JP cohort (**Figure 5**). In the TCGA-LIHC cohort, significant differences were found (**Figure 5**) in six types of immune cells (mast cell activated, monocyte, neutrophil, NK cell activated, T cell $CD4^+$ memory resting, and T cell $CD4^+$ naive). Both NK cell activated and neutrophil were significantly infiltrated the mutation group of two cohorts. In addition, the results of **Figure 6** show that CTNNB1 mutation was negatively associated with *CD96*, *HAVCR2*, *LGALS9*, and *TGFB1*. And the expression difference of median between the two groups was −0.965 (*CD96*), −0.679 (*HAVCR2*), −0.733 (*LGALS9*), and −0.951 (*TGFB1*). Moreover, **Figure 7A** demonstrates that a significant difference was found between the live group and deceased group in dendritic cell activated and NK cell activated. Consequently, we focused on NK cells and further explored the correlation between NK cells and clinical parameters. The results from **Figure 7B** show that a significantly positive correlation was found between stage and NK cell infiltration in HCC. The verification from **Figures 7C–F** also indicates that the expression and methylation of CTNNB1 were significantly associated with CD96 expression and NK cell abundance.

Underlying Pathways Associated With CTNNB1 Mutation

To investigate underlying pathways of GO and KEGG, we used GSEA to find significantly enriched terms by comparing the mutation and wild-type groups. We selected the 10 most relevant pathways according to the normalized enrichment score (five pathways in the mutation group and five in the wild-type group). As illustrated in **Figure 8**, 10 relevant pathways (oxidoreductase activity acting on the aldehyde or oxo group of donors, sulfur amino acid metabolic process, C4 dicarboxylate transport, organic acid catabolic process, and xenobiotic metabolic process

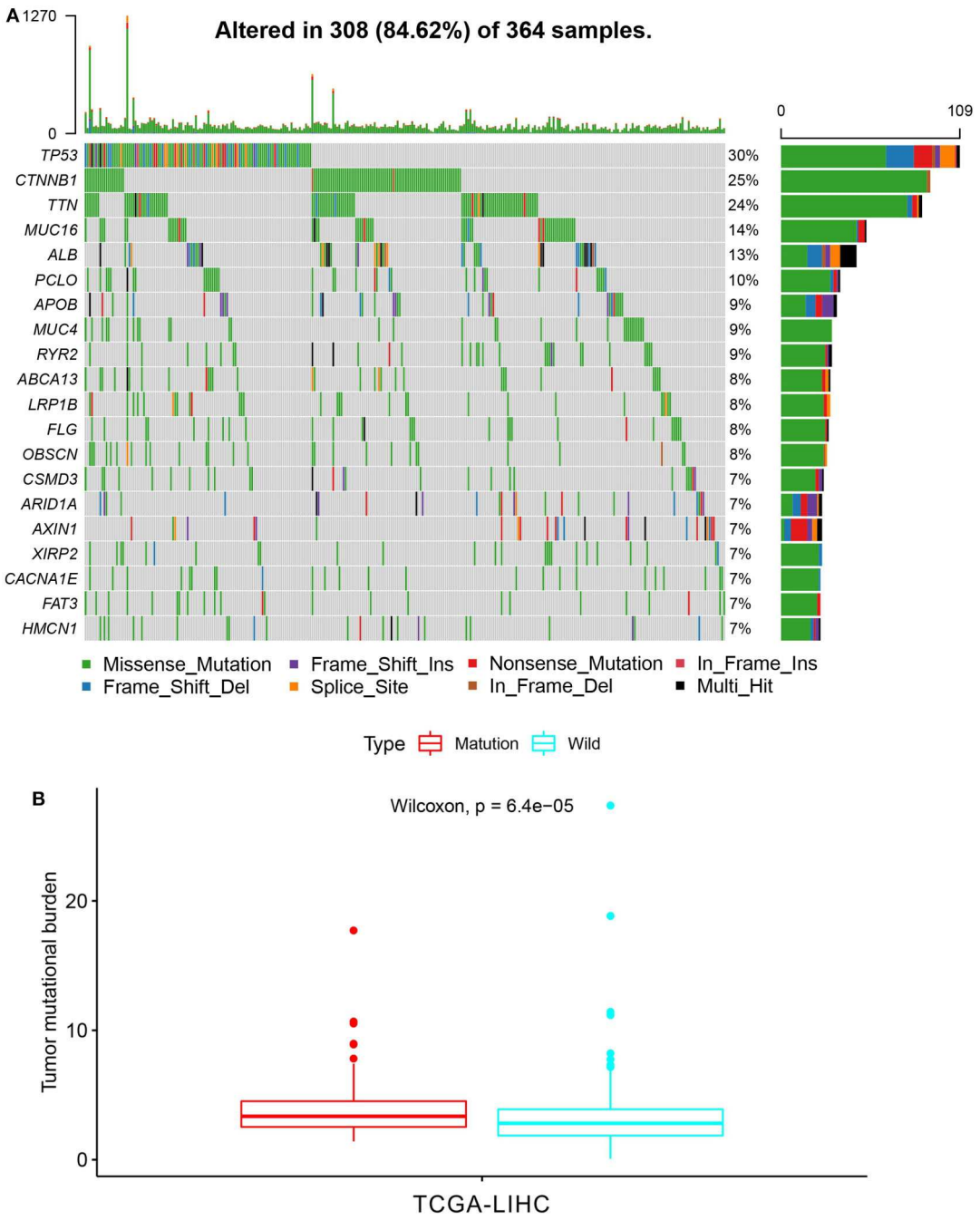

FIGURE 4 | Validation based on TCGA-LIHC cohort. **(A)** The waterfall plot of TCGA-LIHC. **(B)** Tumor mutational burden (TMB) correlation analysis.

in GO; tyrosine metabolism, fatty acid metabolism, butanoate metabolism, metabolism of xenobiotics by cytochrome P450, and primary bile acid biosynthesis in KEGG) are enriched in the mutation group, whereas other 10 pathways (negative regulation of axon extension, positive regulation of astrocyte differentiation, plasma membrane phospholipid scrambling, plasma membrane organization, and cellular component maintenance in GO; renal cell carcinoma, regulation of actin cytoskeleton, bladder cancer, notch signaling pathway, and focal adhesion in KEGG) enriched in the wild-type group.

DISCUSSION

With the increasing exploration of the immune system, immunotherapy was considered to have a crucial role in treatment of cancer. It has been verified that TMB was

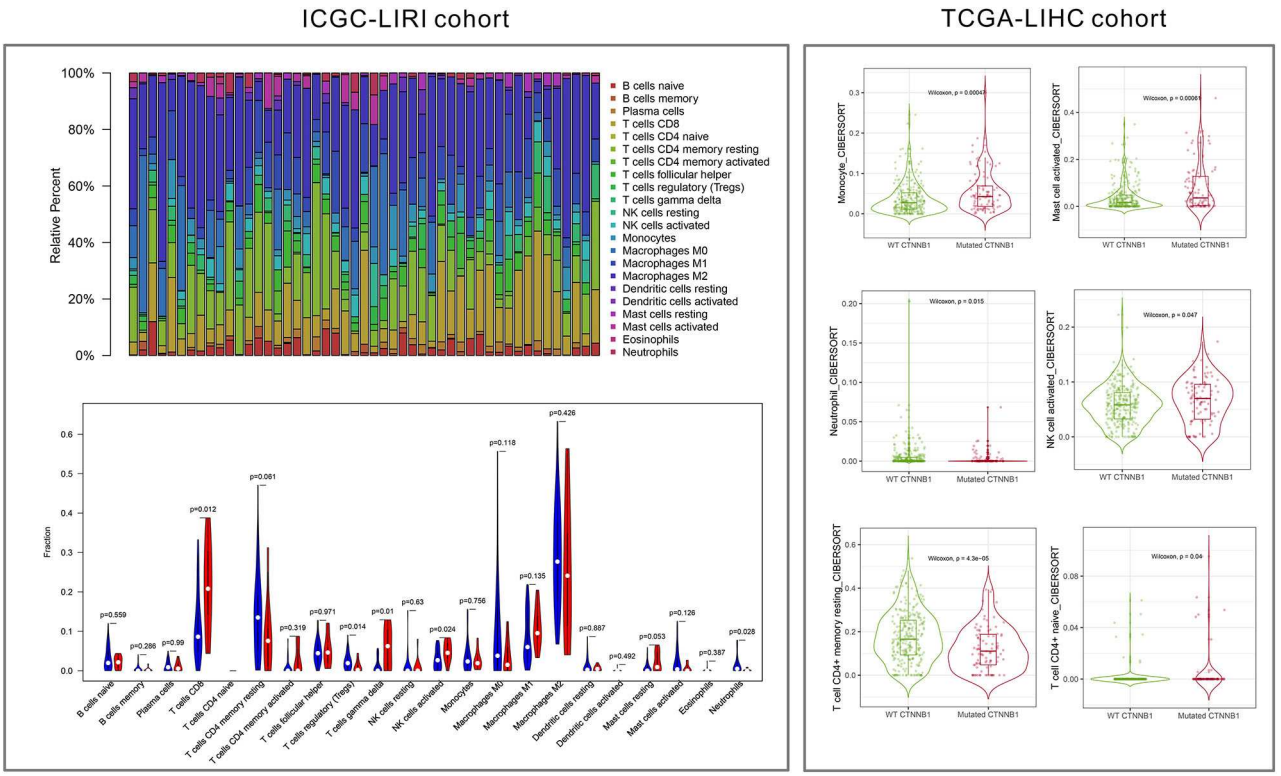

FIGURE 5 | Immune cell infiltration from LIRI cohort and LIHC cohort.

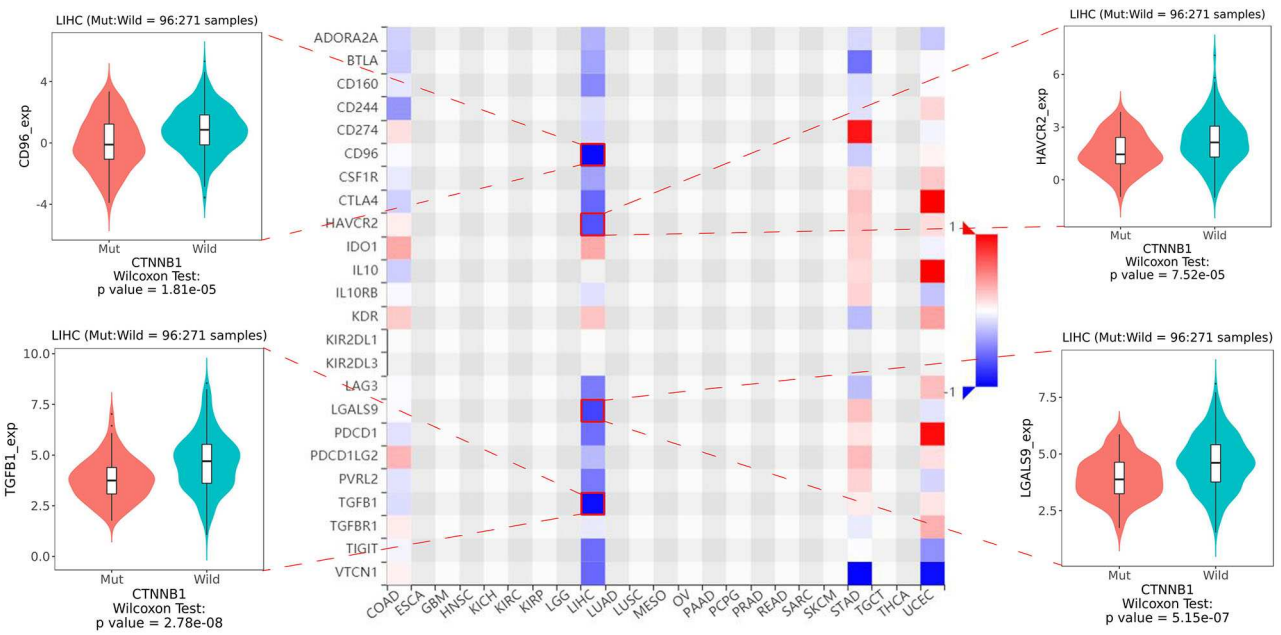

FIGURE 6 | The heatmap of 24 types of immune inhibitors and significant results from correlation analysis.

closely related to immune checkpoint inhibitors. However, the mechanism between gene mutation and immunotherapy in HCC was still unclear. Consequently, in our research, we firstly analyzed the details of gene mutation from the three cohorts. Then we performed a comparative analysis to find the intersection of the three cohorts, and we found

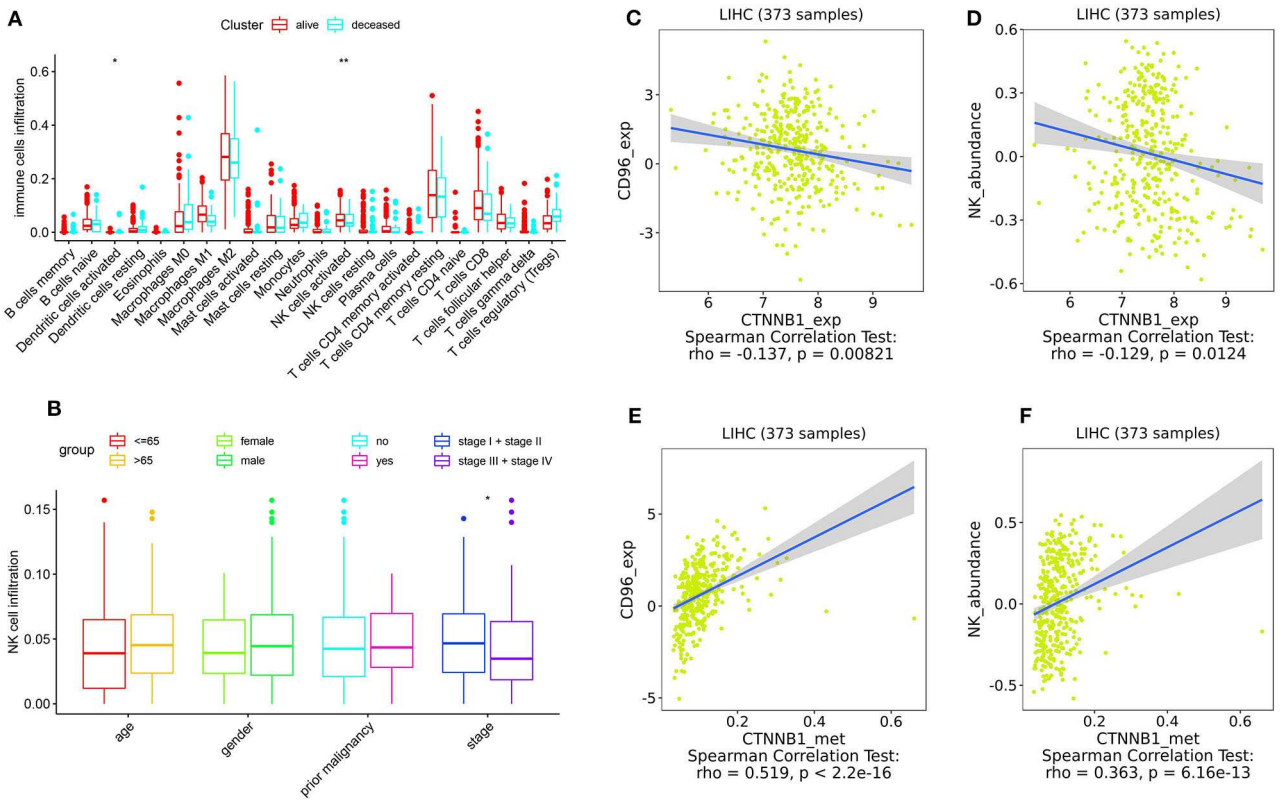

FIGURE 7 | Correlation analysis. **(A)** The correlation between 22 types of immune cells and survival. **(B)** The correlation between NK cells and clinical parameters. **(C,D)** The correlation between CTNNB1 expression and CD96, and NK cells, respectively. **(E,F)** The correlation between CTNNB1 methylation and CD96, and NK cells, respectively. Notes: "*" in the plots means $P < 0.05$, "**" means $P < 0.01$.

that only three mutational genes were significantly associated with overall survival. Among the three genes, only *CTNNB1* was significantly associated with TMB in all three cohorts. Therefore, *CTNNB1* was selected for further investigation. *CTNNB1* (catenin beta-1) is a key regulatory molecule of canonical Wnt signaling pathway. An activating mutation in exon 3 of *CTNNB1* results in accumulation of β-catenin in the nucleus and activates the transcription of downstream target gene such as lymphoid enhancer-binding factor 1 (*LEF1*) (17), and *LEF1* is a transcription factor that has been implicated in the pathogenesis of multiple tumors (18). It has been reported that *CTNNB1* mutation was highly associated with many kinds of human tumors, such as biliary tract cancer (19), lung adenocarcinoma (20), and endometrioid ovarian carcinoma (21). In our research, *CTNNB1* mutation was significantly associated with a better prognosis and a higher TMB. A higher TMB leads to the exposure of more neoantigens, which may cause a T cell-dependent immune response (22). Meanwhile, previous studies (23, 24) indicated that *CTNNB1* significantly mutated in immune subtypes of HCC. As a result, *CTNNB1* mutation may have an effect on immunotherapy. To further explore the mechanism between *CTNNB1* mutation and immunotherapy, we compared the difference of immune cell infiltration between the mutation group and wild-type group. Interestingly, we found that NK cells significantly positively infiltrated the mutation group. Meanwhile, the results indicated that more NK cells significantly infiltrated the survival group. Accordingly, we focused on NK cells in subsequent analyses.

NK cell is an important part of the innate immune system, which can secrete cytokines and cytolytic activity against target cells. It has been verified that NK cells can efficiently eradicate heterogeneous tumor cells after a long-term treatment (25). Concerning HCC, the lack of NK cell number and the defects of NK cell function facilitated the escape of tumor cells from immune surveillance (26). In patients with advanced-stage HCC, NK cells were significantly decreased in number with impaired tumor necrosis factor alpha (TNF-α) and interferon-gamma (IFN-γ) production (27). Our results also showed the positive correlation between NK cell infiltration and stage. However, no significant correlation was found between NK cell infiltration and other clinical parameters like age and gender, which may attribute to the small sample size. Based on the implication of CTNNB1 mutation and NK cells in HCC, we speculated that *CTNNB1* mutation may enhance the effect of immunotherapy by NK cells.

Furthermore, we investigated the correlation between *CTNNB1* mutation and immunoinhibitory genes. In our research, we found that *CTNNB1* mutation was negatively

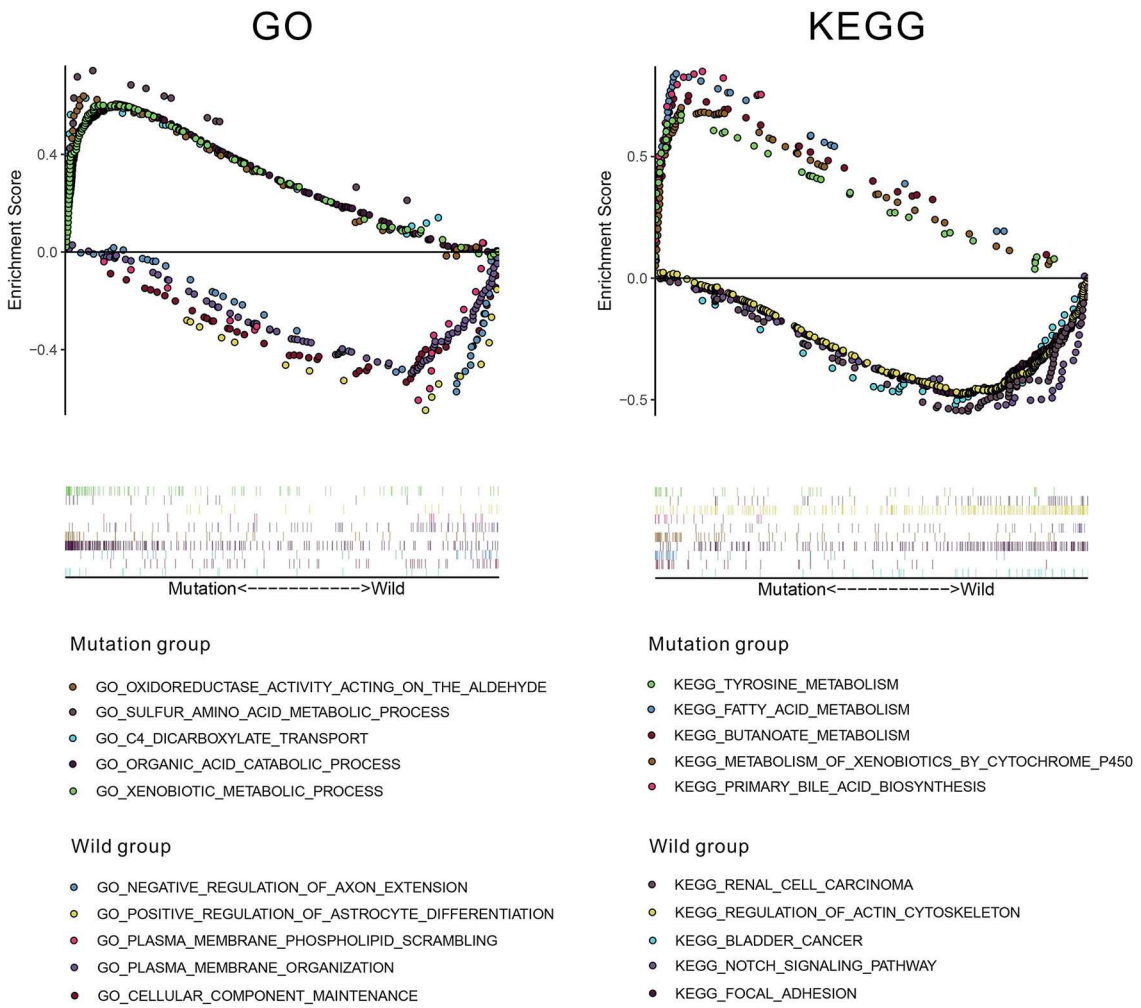

FIGURE 8 | The results of gene set enrichment analysis (GSEA) based on Gene Ontology (GO) and Kyoto Encyclopedia of Genes and Genomes (KEGG) databases.

associated with four immunoinhibitory genes. Among them, *CD96* is the novel immune checkpoint receptor in NK cells (28). Accumulating data support the targeting of *CD96* for improving antitumor immune response (29). Galectin-9 (*LGALS9*) is the most relevant ligand that interacts with Tim-3 (*HAVCR2*) (30). Binding of Tim-3 (*HAVCR2*) to galectin-9 (*LGALS9*) leads to Th1 cell death by apoptosis (30). Meanwhile, Tim-3 (*HAVCR2*) is an inducible human NK cell receptor that enhances IFN-γ production in response to galectin-9 (*LGALS9*) (31). In terms of *TGFB1*, it has been reported that *TGFB1* suppresses the function of NK cells by inducing miRNA23a (32). Four types of immune inhibitors showed the close association with NK cells, which verified the relationship between *CTNNB1* mutation and NK cells. On the one hand, our result indicated that *CD96* was most negatively correlated with CTNNB1 mutation. On the other hand, not only the mutation but also the expression and methylation of *CTNNB1* significantly related to *CD96* and NK cells. Consequently, we speculated that there is an underlying interactive association among CTNNB1, CD96, and NK cells. Considering the signaling pathways associated with *CTNNB1* mutation, we employed GSEA to find the significantly enriched pathways in the mutation group. Although we did not find any pathways related to immune response, five pathways involved metabolism were observed. Immune activation is now understood to be fundamentally linked to intrinsic and/or extrinsic metabolic process. It has been reported that carbohydrate and amino acid metabolism are hallmarks for the innate immune cell activation and function (33). Meanwhile, immune cells exhibit various responses against different types of microbes, which seems to be associated with changes in energy metabolism (34). But it is uncertain whether *CTNNB1* mutation affects the immunotherapy through metabolic pathways.

To our knowledge, it is the first research that focused on the gene mutation and immunotherapy in HCC. Our research revealed the implication of *CTNNB1* mutation in the immunotherapy of HCC. Furthermore, because *CTNNB1* mutation positively associated with immune inhibitors, *CTNNB1* mutation may serve as the novel biomarker in identifying the

patients who will benefit from immune checkpoint blockade treatment. Nevertheless, some limitations in our research have to be pointed out. First, NK cells can be divided into subsets based on the expression of CD56 and CD16. It is necessary to investigate the mechanism among different NK cell subsets, CTNNB1 and CD96 in HCC. Second, the results of GSEA were preliminary; the current evidences of pathways still need to be validated in clinical trials and functional experiments.

CONCLUSION

Our research firstly revealed the underlying association between *CTNNB1* mutation and immunotherapy, and we speculated that *CTNNB1* mutation may modulate NK cells by affecting CD96. However, more functional experiments should be performed for verification.

DATA AVAILABILITY STATEMENT

Publicly available datasets were analyzed in this study. This data can be found here: TCGA database (https://portal.gdc.cancer.gov/) and ICGC database (https://dcc.icgc.org/).

AUTHOR CONTRIBUTIONS

ZM and SZ designed the manuscript. ZM and YW wrote and completed the manuscript. ZC and PL completed the data download and analysis. All the authors approved the final manuscript.

FUNDING

This study was funded by the National Natural Science Foundation of China (No. 81873248 and No. 81673903).

REFERENCES

1. Llovet JM, Zucman-Rossi J, Pikarsky E, Sangro B, Schwartz M, Sherman M, et al. Hepatocellular carcinoma. *Nat Rev Dis Primers*. (2016) 2:16018. doi: 10.1038/nrdp.2016.18
2. Ferlay J, Soerjomataram I, Dikshit R, Eser S, Mathers C, Rebelo M, et al. Cancer incidence and mortality worldwide: sources, methods and major patterns in GLOBOCAN 2012. *Int J Cancer*. (2015) 136:E359–86. doi: 10.1002/ijc.29210
3. Oweira H, Petrausch U, Helbling D, Schmidt J, Mehrabi A, Schöb O, et al. Prognostic value of site-specific extra-hepatic disease in hepatocellular carcinoma: a SEER database analysis. *Expert Rev Gastroenterol Hepatol*. (2017) 11:695–701. doi: 10.1080/17474124.2017.1294485
4. Bruix J, Gores GJ, Mazzaferro V. Hepatocellular carcinoma: clinical frontiers and perspectives. *Gut*. (2014) 63:844–55. doi: 10.1136/gutjnl-2013-306627
5. Niu L, Liu L, Yang S, Ren J, Lai PBS, Chen GG. New insights into sorafenib resistance in hepatocellular carcinoma: responsible mechanisms and promising strategies. *Biochim Biophys Acta Rev Cancer*. (2017) 1868:564–70. doi: 10.1016/j.bbcan.2017.10.002
6. Shi Y, Men X, Li X, Yang Z, Wen H. Research progress and clinical prospect of immunocytotherapy for the treatment of hepatocellular carcinoma. *Int Immunopharmacol*. (2020) 82:106351. doi: 10.1016/j.intimp.2020.106351
7. Ma C, Kesarwala AH, Eggert T, Medina-Echeverz J, Kleiner DE, Jin P, et al. NAFLD causes selective CD4(+) T lymphocyte loss and promotes hepatocarcinogenesis. *Nature*. (2016) 531:253–7. doi: 10.1038/nature16969
8. Ma HY, Yamamoto G, Xu J, Liu X, Karin D, Kim JY, et al. IL-17 signaling in steatotic hepatocytes and macrophages promotes hepatocellular carcinoma in alcohol-related liver disease. *J Hepatol*. (2019) 72:946–59. doi: 10.1016/j.jhep.2019.12.016
9. Peeraphatdit TB, Wang J, Odenwald MA, Hu S, Hart J, Charlton MR. Hepatotoxicity from immune checkpoint inhibitors: a systematic review and management recommendation. *Hepatology*. (2020). doi: 10.1002/hep.31227. [Epub ahead of print].
10. Qin S, Ren Z, Meng Z, Chen Z, Chai X, Xiong J, et al. Camrelizumab in patients with previously treated advanced hepatocellular carcinoma: a multicentre, open-label, parallel-group, randomised, phase 2 trial. *Lancet Oncol*. (2020) 21:571–80. doi: 10.1016/S1470-2045(20)30011-5
11. Sangro B, Gomez-Martin C, De La Mata M, Inarrairaegui M, Garralda E, Barrera P, et al. A clinical trial of CTLA-4 blockade with tremelimumab in patients with hepatocellular carcinoma and chronic hepatitis C. *J Hepatol*. (2013) 59:81–8. doi: 10.1016/j.jhep.2013.02.022
12. Braun DA, Burke KP, Van Allen EM. Genomic approaches to understanding response and resistance to immunotherapy. *Clin Cancer*. (2016) 22:5642–50. doi: 10.1158/1078-0432.CCR-16-0066
13. Gubin MM, Artyomov MN, Mardis ER, Schreiber RD. Tumor neoantigens: building a framework for personalized cancer immunotherapy. *J Clin Invest*. (2015) 125:3413–21. doi: 10.1172/JCI80008
14. Chan TA, Yarchoan M, Jaffee E, Swanton C, Quezada SA, Stenzinger A, et al. Development of tumor mutation burden as an immunotherapy biomarker: utility for the oncology clinic. *Ann Oncol*. (2019) 30:44–56. doi: 10.1093/annonc/mdy495
15. Ru B, Wong CN, Tong Y, Zhong JY, Zhong SSW, Wu WC, et al. TISIDB: an integrated repository portal for tumor-immune system interactions. *Bioinformatics*. (2019) 35:4200–2. doi: 10.1093/bioinformatics/btz210
16. Subramanian A, Tamayo P, Mootha VK, Mukherjee S, Ebert BL, Gillette MA, et al. Gene set enrichment analysis: a knowledge-based approach for interpreting genome-wide expression profiles. *Proc Natl Acad Sci USA*. (2005) 102:15545–50. doi: 10.1073/pnas.0506580102
17. Taketo MM. Shutting down Wnt signal-activated cancer. *Nat Genet*. (2004) 36:320–2. doi: 10.1038/ng0404-320
18. Suzuki Y, Ichihara S, Kawasaki T, Yanai H, Kitagawa S, Shimoyama Y, et al. β-catenin (CTNNB1) mutation and LEF1 expression in sinonasal glomangiopericytoma (sinonasal-type hemangiopericytoma). *Virchows Arch*. (2018) 473:235–9. doi: 10.1007/s00428-018-2370-9
19. Hogdall D, Larsen OF, Linnemann D, Svenstrup Poulsen T, Hogdall EV. Exome sequencing of 22 genes using tissue from patients with biliary tract cancer. *APMIS*. (2020) 128:3–9. doi: 10.1111/apm.13003
20. Zhou C, Li W, Shao J, Zhao J, Chen C. Analysis of the clinicopathologic characteristics of lung adenocarcinoma with mutation. *Front Genet*. (2019) 10:1367. doi: 10.3389/fgene.2019.01367
21. Pierson WE, Peters PN, Chang MT, Chen LM, Quigley DA, Ashworth A, et al. An integrated molecular profile of endometrioid ovarian cancer. *Gynecol Oncol*. (2020) 157:55–61. doi: 10.1016/j.ygyno.2020.02.011
22. Mcgranahan N, Furness AJS, Rosenthal R, Ramskov S, Lyngaa R, Saini SK, et al. Clonal neoantigens elicit T cell immunoreactivity and sensitivity to immune checkpoint blockade. *Science*. (2016) 351:1463–9. doi: 10.1126/science.aaf1490
23. Li W, Wang H, Ma Z, Zhang J, Ou-Yang W, Qi Y, et al. Multi-omics analysis of microenvironment characteristics and immune escape mechanisms of hepatocellular carcinoma. *Front Oncol*. (2019) 9:1019. doi: 10.3389/fonc.2019.01019
24. Wei L, Delin Z, Kefei Y, Hong W, Jiwei H, Yange Z. A classification based on tumor budding and immune score for patients with hepatocellular carcinoma. *Oncoimmunology*. (2020) 9:1672495. doi: 10.1080/2162402X.2019.1672495
25. Dianat-Moghadam H, Rokni M, Marofi F, Panahi Y, Yousefi M. Natural killer cell-based immunotherapy: from transplantation toward targeting cancer stem cells. *J Cell Physiol*. (2018) 234:259–73. doi: 10.1002/jcp.26878

26. Liu P, Chen L, Zhang, H. Natural killer cells in liver disease and hepatocellular carcinoma and the NK cell-based immunotherapy. *J Immunol Res*. (2018) 2018:1206737. doi: 10.1155/2018/1206737
27. Wu Y, Kuang DM, Pan WD, Wan YL, Lao XM, Li XF. Monocyte/marcrophage-elicited natural killer cell dysfunction in hepatocellular carcinoma is mediated by CD48/2B4 interactions. *Hepatology*. (2013) 57:1107–16. doi: 10.1002/hep.26192
28. Kim N, Kim HS. Targeting checkpoint receptors and molecules for therapeutic modulation of natural killer cells. *Front Immunol*. (2018) 9:2041. doi: 10.3389/fimmu.2018.02041
29. Dougall WC, Kurtulus S, Smyth MJ, Anderson AC. TIGIT and CD96: new checkpoint receptor targets for cancer immunotherapy. *Immunol Rev*. (2017) 276:112–20. doi: 10.1111/imr.12518
30. Zhu C, Anderson AC, Schubart A, Xiong H, Imitola J, Khoury SJ, et al. The Tim-3 ligand galectin-9 negatively regulates T helper type 1 immunity. *Nat Immunol*. (2005) 6:1245–52. doi: 10.1038/ni1271
31. Gleason MK, Lenvik TR, Mccullar V, Felices M, O'brien MS, Cooley SA, et al. Tim-3 is an inducible human natural killer cell receptor that enhances interferon gamma production in response to galectin-9. *Blood*. (2012) 119:3064–72. doi: 10.1182/blood-2011-06-360321
32. Berchem G, Noman MZ, Bosseler M, Paggetti J, Baconnais S, Le Cam E, et al. Hypoxic tumor-derived microvesicles negatively regulate NK cell function by a mechanism involving TGF-β and miR23a transfer. *Oncoimmunology*. (2016) 5:e1062968. doi: 10.1080/2162402X.2015.1062968
33. Zhao H, Raines LN, Huang SC-C. Carbohydrate and amino acid metabolism as hallmarks for innate immune cell activation and function. *Cells*. (2020) 9:E562. doi: 10.3390/cells9030562
34. Hosomi K, Kunisawa J. Diversity of energy metabolism in immune responses regulated by microorganisms and dietary nutrition. *Int Immunol*. (2020). doi: 10.1093/intimm/dxaa020. [Epub ahead of print].

Conflict of Interest: The authors declare that the research was conducted in the absence of any commercial or financial relationships that could be construed as a potential conflict of interest.

frontiers in Immunology

CASE REPORT
published: 23 July 2020
doi: 10.3389/fimmu.2020.01366

Identification of Clonal Neoantigens Derived From Driver Mutations in an *EGFR*-Mutated Lung Cancer Patient Benefitting From Anti-PD-1

Di Wu[1†], Yangyang Liu[1†], Xiaoting Li[2], Yiying Liu[2], Qifan Yang[1], Yuting Liu[1], Jingjing Wu[1], Chen Tian[1], Yulan Zeng[1], Zhikun Zhao[2], Yajie Xiao[2], Feifei Gu[1], Kai Zhang[1], Yue Hu[1] and Li Liu[1*]*

[1] Cancer Center, Union Hospital, Tongji Medical College, Huazhong University of Science and Technology, Wuhan, China, [2] YuceBio Technology Co., Ltd., Shenzhen, China

OPEN ACCESS

Edited by:
Maysaloun Merhi,
Hamad Medical Corporation, Qatar

Reviewed by:
Xuyao Zhang,
University of Pennsylvania, United States
Shaofei Wang,
Fudan University, China

***Correspondence:**
Yue Hu
huyue_cmu@126.com
Li Liu
liulist2013@163.com

[†] These authors have contributed equally to this work

Specialty section:
This article was submitted to Cancer Immunity and Immunotherapy, a section of the journal Frontiers in Immunology

Received: 03 March 2020
Accepted: 28 May 2020
Published: 23 July 2020

Citation:
Wu D, Liu Y, Li X, Liu Y, Yang Q, Liu Y, Wu J, Tian C, Zeng Y, Zhao Z, Xiao Y, Gu F, Zhang K, Hu Y and Liu L (2020) Identification of Clonal Neoantigens Derived From Driver Mutations in an EGFR-Mutated Lung Cancer Patient Benefitting From Anti-PD-1. Front. Immunol. 11:1366. doi: 10.3389/fimmu.2020.01366

Epidermal growth factor receptor (*EGFR*) tyrosine kinase inhibitors (TKIs) have been recommended as the first-line therapy for non-small cell lung cancer (NSCLC) patients harboring *EGFR* mutations. However, acquired resistance to EGFR-TKIs is inevitable. Although immune checkpoint blockades (ICBs) targeting the programmed cell death 1 (PD-1)/PD-ligand (L)1 axis have achieved clinical success for many cancer types, the clinical efficacy of anti-PD-1/PD-L1 blockades in *EGFR* mutated NSCLC patients has been demonstrated to be lower than those without *EGFR* mutations. Here, we reported an advanced NSCLC patient with *EGFR* driver mutations benefitting from anti-PD-1 blockade therapy after acquiring resistance to EGFR-TKI. We characterized the mutational landscape of the patient with next-generation sequencing (NGS) and successfully identified specific T-cell responses to clonal neoantigens encoded by *EGFR* exon 19 deletion, *TP53 A116T* and *DENND6B R398Q* mutations. Our findings support the potential application of immune checkpoint blockades in NSCLC patients with acquired resistance to EGFR-TKIs in the context of specific clonal neoantigens with high immunogenicity. Personalized immunomodulatory therapy targeting these neoantigens should be explored for better clinical outcomes in *EGFR* mutated NSCLC patients.

Keywords: neoantigens, cancer immunotherapy, immune checkpoint blockade, epidermal growth factor receptor, tyrosine kinase inhibitor

INTRODUCTION

Lung cancer, in which about 80% of cases are identified as non-small cell lung cancer (NSCLC), is regarded as the leading cause of cancer-related death in the world (1). Alterations associated with specific genes, such as epidermal growth factor receptor (*EGFR*) or anaplastic lymphoma kinase (*ALK*), contribute to the development and progression of lung cancer. Relevant targeted therapies directing against these driver gene mutations have achieved successful clinical outcomes (2, 3). The *EGFR* driver mutations are known to be prevalent among Asian NSCLC patients (4). Although *EGFR* tyrosine kinase inhibitors (TKIs) could improve the objective response rate (ORR) and progression-free survival (PFS) of *EGFR* mutated patients, acquired resistance is inevitable and often occurs after 9–14 months of therapy (5). Although the administration of third-generation

EGFR-TKIs targeting the *EGFR T790M* mutation, such as Osimertinib, has shown promising outcomes (6), acquired resistance still exists (7). Thus, novel effective treatment strategies remain urgently needed.

Recently, immune checkpoint blockades (ICBs), including anti-programmed cell death-1 (PD-1) and programmed cell death-ligand 1 (PD-L1) blockades, have been demonstrated to robustly enhance anti-tumor immunity in patients with a wide range of cancers, especially with NSCLC (8, 9). Despite the sustained response of ICBs in NSCLC, the clinical efficacy of anti-PD-1/PD-L1 blockades in *EGFR* mutated NSCLC patients has been reported to be moderate compared with those without *EGFR* mutations (10, 11). Moreover, results from several clinical trials indicated that the combination therapy of EGFR-TKIs and ICBs led to a high incidence of treatment-related adverse effects (12). As a result, immune checkpoint blockades have been excluded from daily clinical applications for NSCLC patients with *EGFR* driver mutations. Nevertheless, some *EGFR* mutated lung cancer patients enrolled in clinical trials could still respond to ICB therapy. Therefore, it is necessary to characterize the underlying mechanism and identify prognostic biomarkers for predicting clinical benefits with anti-PD-1/PD-L1 blockade therapy in this specific NSCLC subpopulation.

Unlike tumor-associated antigens (TAA), which are found both in tumor cells and normal tissues, tumor neoantigens are exclusively processed by tumor cells and presented by major histocompatibility complex (MHC) molecules. Individual MHC:peptide complex can be recognized by T-cell receptor with high specificity (13, 14). This mechanism provides promising targets for personalized immunomodulatory therapy such as cancer vaccine and adoptive T-cell transfer therapy (15, 16). Interestingly, previous reports suggested that neoantigens can be served as the targets of highly specific and durable anti-tumor immunity (17, 18), and neoantigen-specific T-cell response can be identified in patients benefitting from ICBs. Neoantigens derived from *EGFR* mutations have been reported in preclinical study (19), but it remains confusing whether *EGFR* driver mutations could generate true neoantigens in suppressive tumor microenvironment (TME).

With the development of next-generation sequencing (NGS) technologies and bioinformatics algorithms, neoantigen can be successfully identified *in silico* in many solid tumors (20). Monitoring neoantigen-specific T-cell response to anti-PD-1/PD-L1 blockades in peripheral blood has become a feasible way to predict the prognosis of cancer patients (13, 21). Nevertheless, only a small amount of neoantigens were identified to be truly immunogenic, and clinical applications based on neoantigens are still in its infancy stage (17). Given the current limiting treatment options for NSCLC patients after EGFR-TKI resistance, novel personalized therapeutic strategies based on T-cell immunity to neoantigens could improve clinical outcomes when candidate neoantigens are available.

Here, we reported an advanced NSCLC patient with *EGFR* driver mutations achieved durable clinical benefits from Nivolumab monotherapy. By conducting whole-exome sequencing (WES), RNA sequencing (RNA-seq), and TCR sequencing, we were able to depict a comprehensive landscape of genomic alterations and predict candidate neoantigens from tumor tissue obtained before the initiation of Nivolumab. We also successfully validated anti-tumor immunity to some high-quality neoantigens *in vitro*, including two derived from *EGFR* driver mutation. These results displayed that immune checkpoint blockades could elicit robust endogenous T-cell response to clonal neoantigens generated from driver mutations. Our findings may provide clinical evidences that ICBs should not be completely excluded from therapy options for NSCLC patients after the failure of EGFR-TKIs. Furthermore, personalized immunomodulatory therapy targeting specific clonal neoantigens should be developed for clinical practice in the future.

RESULT

Case Presentation

A 34-year-old male patient suffered from chest and back pain in January 2017. Radiological examinations revealed a 65-mm nodule in the middle lobe of the right lung, several metastatic pulmonary nodules in both lungs, and multiple bone lesions. The patient underwent a bronchoscopy biopsy, and pathological examination revealed lung adenocarcinoma with *EGFR* exon 19 deletion (*EGFR 19del*). His clinical stage was T4N2M1b stage IV (**Figure 1A**). The patient was initially treated with Icotinib from February 2017 until progression occurred in July 2017. Additionally, intensity-modulated radiation therapy (IMRT) targeting bone metastases in the lumbar spine, pelvic cavity, and left femur were given with a total dose of 36 Gy in 12 fractions. After that, he was administered with Pemetrexed plus Nedaplatin for four cycles and Pemetrexed for another one cycle until progression occurred in November 2017. After systemic chemotherapy, he turned to traditional Chinese medicine treatment, until the onset of brain metastases in the right frontal lobe and left basal ganglia in June 2018 (**Figures 1B,C**).

The patient was, thereafter, enrolled in a phase 3 clinical trial for Nivolumab monotherapy (NCT03195491). Regardless of PD-L1 and tumor mutational burden (TMB) status, this trial enrolled advanced lung cancer patients who failed previous systemic therapies. Biopsy of tumor sample obtained before Nivolumab initiation indicated *EGFR T790M* mutation. The patient presented with dizziness after two cycles of Nivolumab administration in August 2018, and magnetic resonance imaging (MRI) scans showed an increased lesion size and edema of the left basal ganglia, as well as multiple brain metastases (**Figure 1C**). After dehydration therapy with Mannitol, Nivolumab was reinitiated for another two cycles. According to RECIST 1.1 Criteria, he achieved partial response (PR) with decreased tumor size of lung and brain metastases in September 2018. After 10 cycles of Nivolumab treatment, the patient experienced hypothyroidism with elevated levels of TSH and decreased levels of both FT3 and FT4, and treatment with Levothyroxine was applied to relieve the symptoms. Generally, Nivolumab was well-tolerated. Currently, the patient receives an intravenous infusion

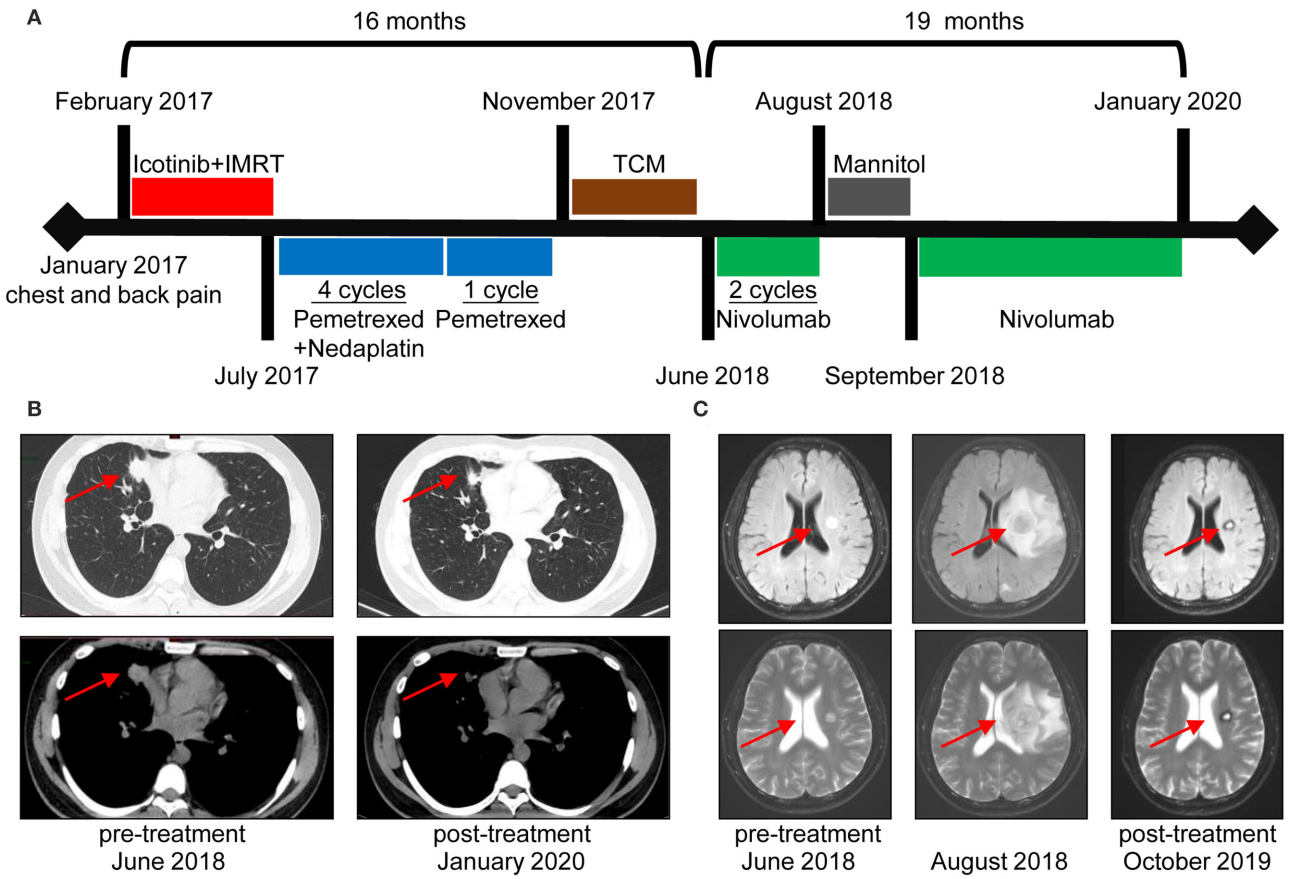

FIGURE 1 | Durable clinical response to Nivolumab in a non-small cell lung cancer (NSCLC) patient with epidermal growth factor receptor (*EGFR*) driver mutations. **(A)** Clinical timeline of patient, with major treatment indicated. The patient has been benefitting from immunotherapy for more than 19 months. **(B)** Chest computed tomography (CT) of the metastatic lung tumors before Nivolumab initiation (June 2018) and last time follow-up (January 2020). **(C)** Magnetic resonance imaging (MRI) before and after Nivolumab treatment. Images in the middle revealed an increased size of the left basal ganglia lesion accompanied by edema and multiple brain nodule metastases. A rapid decrease in lesions was noted in the following radiological evaluations.

of Nivolumab at 240 mg every 2 weeks. Based on the follow-up examinations, the patient has achieved PR for more than 1 year.

Comprehensive Analysis of Genome and Immune Landscape

Of the tumor analyzed, a PD-L1 tumor proportion score (TPS) of ≥50% was revealed (**Figure 2A**). Based on sequence data, tumor mutational burden (TMB) was 6.00 muts/Mb, and tumor neoantigen burden (TNB) was 2.67 neos/Mb. Peripheral blood mononuclear cells (PBMCs) collected before Nivolumab initiation and thereafter every 2 months were investigated by TCR sequencing. We selected T-cell clones with a frequency of $\geq 10^{-3}$ to investigate the dynamic TCR changes. The maintenance of most high-frequency clones was detected (**Figures 2B,C**). Only one high-frequency clone decreased sharply after 2 months of Nivolumab therapy. This may partly explain the pseudoprogression after four cycles of Nivolumab treatment in August 2018 and durable clinical response throughout the whole study.

Prediction and Validation of Immunogenic Neoantigens

To evaluate potential factors contributing to the durable response of the patient, we followed a restricted pipeline integrating NGS technology and validation experiment aiming at identifying true neoantigens. According to WES results of lung tumor samples, 84 somatic non-synonymous mutations were identified, and 28 of them were likely to bind to the corresponding HLA alleles with high affinity (IC50 < 500 nmol/L) (**Supplementary Table 1**). A total of six genes were found to be truly expressed at the transcript level, including *EGFR*, *TP53*, *POLA2*, *AP2AM1*, *DENND6B*, and *TTC37*. Ultimately, 13 HLA-A*11:01-restricted candidate neoantigen peptides generated from these six genes were selected for further analysis. Furthermore, clonal neoantigens can be derived from *EGFR*, *TP53*, and *DENND6B* mutations, whereas *POLA2*, *AP2AM1*, and *TTC37* mutations could only generate subclonal neoantigens (**Table 1**). Then, both mutant and wild-type peptides were synthesized and tested by IFN-γ ELISPOT assay to validate the immunogenicity of these neoantigens. As a result, 4 out of 13 mutant peptides could elicit a strong response,

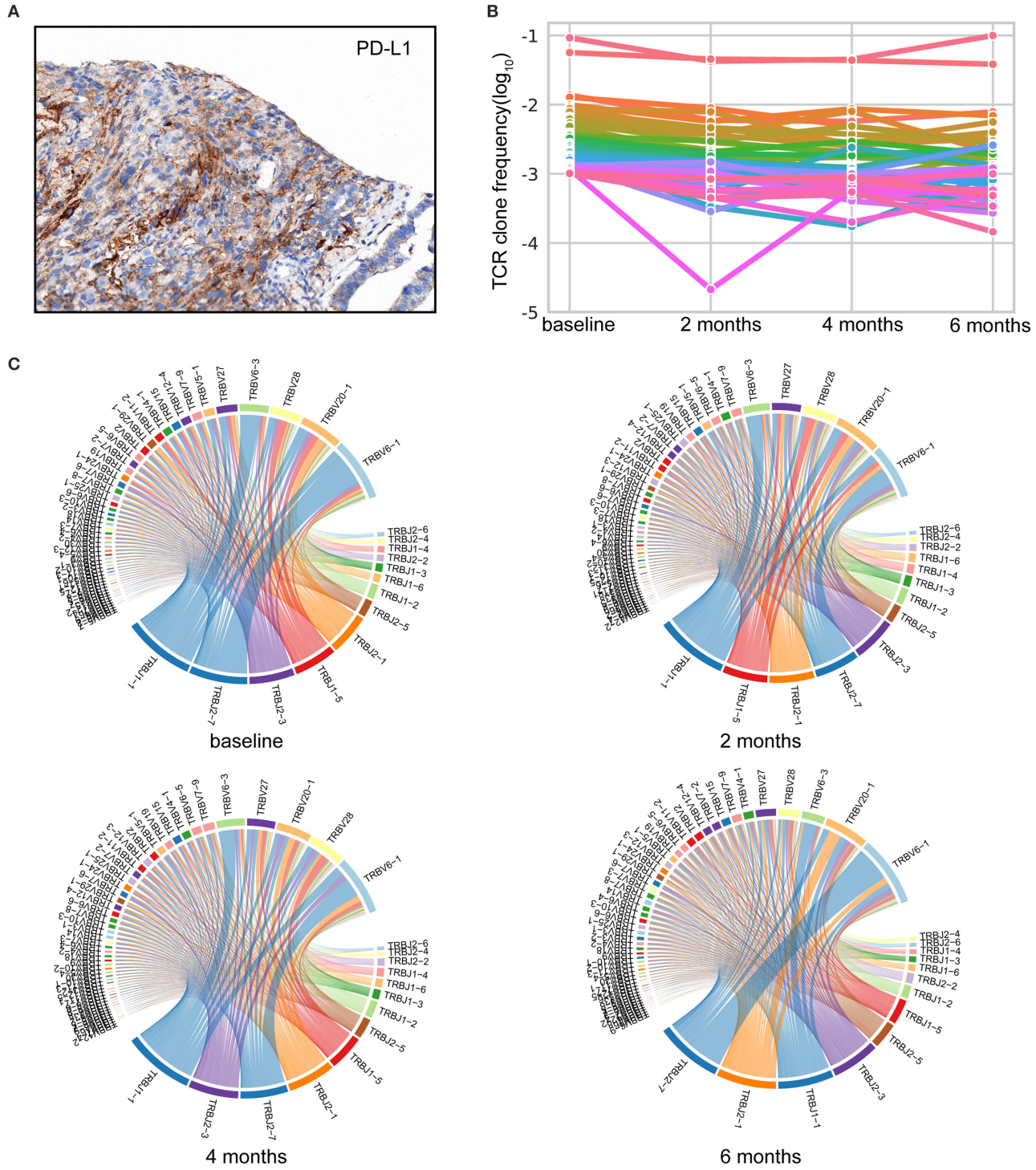

FIGURE 2 | Comprehensive analysis of the immune landscape. **(A)** Immunohistochemistry (IHC) image with anti-programmed cell death-ligand 1 (PD-L1) antibody (Dako IHC 22C3 platform). Microscope magnification 400×. A PD-L1 tumor proportion score (TPS) of ≥50% was detected. **(B)** Maintenance of the high-frequency T-cell clones throughout Nivolumab treatment. TCR-seq was conducted on PBMCs collected pre and post Nivolumab treatment. T-cell clones with a frequency of $\geq 10^{-3}$ in the baseline are shown. Each line represents one clone. **(C)** Representative TRBV–TRBJ junction circos plots. Bands represent different V and J gene segments. Ribbons imply V/J pairings. The width of the band is proportional to the usage frequency.

TABLE 1 | HLA-A*11:01 restricted candidate neoantigens validated in IFN-γ ELISPOT assay.

				Mutant peptide		Wild-type peptide	
	Number	**Gene**	**Mutation**	**Sequence**	**IC50 (nM)***	**Sequence**	**IC50 (nM)***
Clonal neoantigens	C1	EGFR	E746_A750del	IPVAIKTSPK	131.9	IPVAIKELRE	28,185.9
	C2	EGFR	E746_A750del	AIKTSPKANK	404.4	AIKELREATS	37,251.5
	C3	TP53	A161T	RVRAMTIYKQ	288.6	RVRAMAIYKQ	486.1
	C4	TP53	A161T	GTRVRAMTIYK	165.5	GTRVRAMAIYK	251.6
	C5	TP53	A161T	TRVRAMTIYK	30.7	TRVRAMAIYK	44
	C6	TP53	A161T	RVRAMTIYK	16.1	RVRAMAIYK	20.9
	C7	DENND6B	R398Q	QLLKGVQKK	498.5	RLLKGVQKK	165.1
	C8	DENND6B	R398Q	KALLKQLLK	54.8	KALLKRLLK	71.5
	C9	DENND6B	R398Q	KQLLKGVQK	420.6	KRLLKGVQK	17,851.5
Subclonal neoantigens	S1	AP2M1	V377M	KASENAIMWK	51.6	KASENAIVWK	91.8
	S2	AP2M1	V377M	ASENAIMWK	41.6	ASENAIVWK	68
	S3	POLA2	E448K	FSYSDLSRK	47.3	FSYSDLSRE	15,881.9
	S4	TTC37	D95A	KDALPGVYQK	171.6	KDDLPGVYQK	7,311.9

**HLA-binding affinities for peptides, predicted by NetMHCpan v3.0. Peptides with an IC50 < 500 nM can be regarded as major histocompatibility complex (MHC) binders.*

whereas the wild-type counterpart generated no significant response. Besides, there were no notable T-cell responses to subclonal neoantigens (**Figure 3**).

The Dynamic Change of TCR Repertoire After Neoantigen Stimulation

Although IFN-γ ELISPOT assay could reveal the reactivity between immunogenic neoantigens and autologous T cells, we utilized TCR sequencing to further confirm whether T cell responded to neoantigens. Owing to the limited amounts of PBMCs, we only validated the above 4 out of 13 neoantigens generated from *EGFR 19del*, *TP53 A161T*, and *DENND6B R398Q* mutations.

After stimulating PBMCs with neoantigens, the frequency of some T-cell clones stimulated by mutant peptides was much higher than those clones stimulated by corresponding wild-type peptides. These clones were defined as significant clones, which may specifically recognize neoantigens (**Supplementary Table 2**). Matching significant clones to those found in blood samples, 18 clones remained at high frequency during this study, and 7 clones could only be detected after the initiation of Nivolumab (**Supplementary Figure 1**).

DISCUSSION

Owing to the limited therapeutic strategies for NSCLC patients acquired resistance to EGFR-TKIs, it may be tempting to begin immune checkpoint blockades therapy for its well tolerance and low toxicity. Some retrospective studies suggest that *EGFR* mutated NSCLC cannot benefit from anti-PD-1/PD-L1 blockade therapies (10, 11). However, long-term follow-up of these clinical trials and some case reports showed that a group of *EGFR* mutated NSCLC patients sustained a durable response. Most studies focused on elucidating the underlying mechanism of the negative clinical outcomes (22–25). Little efforts have been made to stratify a small group of patients with *EGFR* driver mutation, who are likely to benefit from immunotherapy. To our knowledge, this is the first report on assessing the predictive biomarker from the perspective of neoantigens in an *EGFR* mutated NSCLC patient receiving Nivolumab. Our results may provide clinical evidences for the potential application of immune checkpoint blockades in NSCLC patients with acquired resistance to EGFR-TKIs.

PD-L1 expression is employed as a general biomarker for immune checkpoint blockade treatment (26). Previous studies demonstrated that EGFR signaling pathway could intrinsically upregulate tumor PD-L1 expression and contribute to the immune escape of *EGFR* mutated NSCLC (10). Conversely, real-world studies showed a higher expression level of PD-L1 in *EGFR* wild-type NSCLC (27, 28). A recent study manifested that the proportion of PD-L1-positive tumors in patients receiving EGFR-TKIs tended to be increased after EGFR-TKI therapy (29). As a result, these contradictory results cannot fully explain the relationship between EGFR signaling pathway and PD-L1 expression. Our patient had a PD-L1 tumor proportion score (TPS) of ≥50%, which may contribute to his durable response to ICBs. For both *EGFR* mutated and wild-type NSCLC in the ATLANTIC trial, patients with higher tumor PD-L1 expression can achieve a better objective response from Durvalumab treatment (29). However, some patients with high PD-L1 expression failed with immunotherapy unexpectedly (30). The opposite results revealed that PD-L1 expression may not be a reliable predictive biomarker for NSCLC with *EGFR* driver mutations receiving immunotherapy, and new effective biomarkers are still needed.

Currently, tumor mutational burden (TMB) is considered as a positive prognostic factor for ICBs (31). Patients with high TMB could have better objective responses to anti-PD-1/PD-L1 blockades compared with those with low TMB (14). Similarly, tumor neoantigen burden (TNB) describes those mutations at the transcript level or protein level and is supposed as the surrogate of TMB. However, some researches showed that

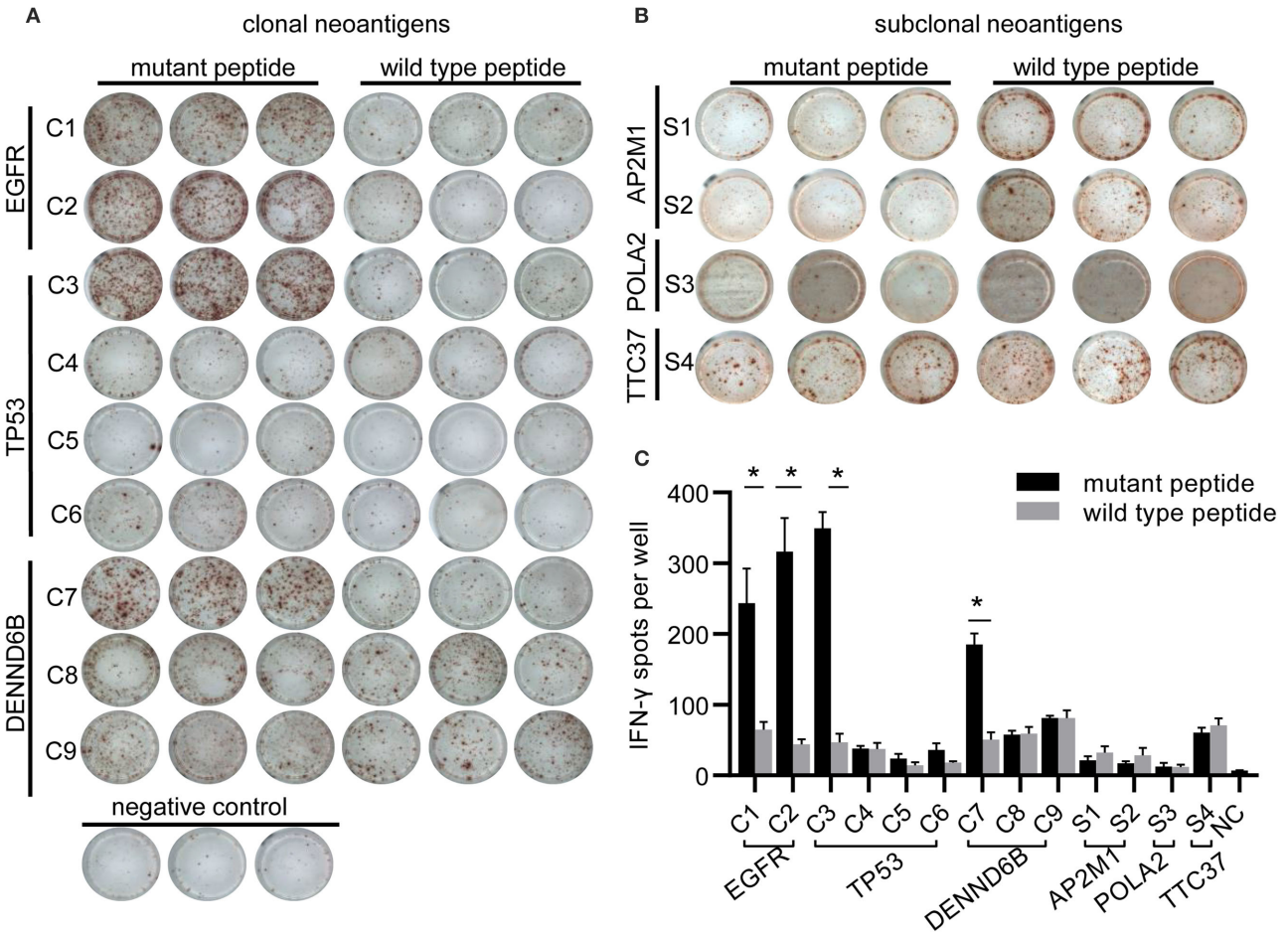

FIGURE 3 | Immunogenicity of candidate neoantigens. **(A,B)** Representative images from IFN-γ ELISPOT assay. Peripheral blood mononuclear cells (PBMCs; 2×10^5 per well) from the patient were stimulated for 10 days with individual peptides in the presence of cytokines (IL-2, IL-7, and IL-15) and were stimulated again on day 10. T-cell reactivity was assessed by IFN-γ ELISPOT assay. **(C)** Bar graph showing IFN-γ ELISPOT assay data. PBMCs stimulated with no peptide were regarded as negative controls (NC). At least two independent experiments were done in triplicate. $^*p < 0.05$.

patients with high TNB may still be resistant to ICBs (32). On this account, identifying high-quality neoantigens could optimize the prediction of pre-existing immunity to tumors and boost the effect of ICBs for proper immunosurveillance (33).

We presented a pipeline combining *in silico* and *in vitro* approaches to identify true neoantigens. Neoantigens expressed by a large proportion of tumor cells were defined as clonal neoantigens (34). In contrast, subclonal neoantigens may be generated during tumor evolution, which mediated immune escape and facilitated tumor invasion (35). In this study, we only successfully detected T-cell response to clonal neoantigens in IFN-γ ELISPOT assay, which could partly be explained by the loss of subclonal neoantigens after Nivolumab treatment (36). Here, a total of four clonal neoantigens, including two arising from *EGFR 19del*, 1 from *TP53 A161T*, and 1 from *DENND6B R398Q*, respectively, were validated in this case. Although immunotherapy targeting *EGFR* mutations have been widely discussed (34), there was no research on identifying neoantigens generated from *EGFR* mutations in NSCLC patients. Neoantigens derived from hotspot mutations of *TP53*, the most frequently altered gene across solid tumors, have already been screened for novel therapeutic approaches (35). *TP53 A161T*, which is present in approximate 0.06% of cancer patients (37), remained uncharacterized, and future exploration is warranted. Additionally, the role of *DENND6B* in tumors is largely unknown. Based on our results, we speculated that neoantigens derived from driver mutations facilitated clinical benefit in patients treated with immune checkpoint blockades. Therefore, *EGFR* mutated NSCLC patients could be recommended to choose anti-PD-1/PD-L1 blockades in the presence of clonal neoantigens derived from driver mutations with high immunogenicity.

Previous studies had shown that memory T cells from peripheral blood could respond to neoantigens in tumor tissue (38), and $CD8^+PD\text{-}1^{+/high}$ T-cell subsets were preferentially enriched upon neoantigen stimulation (39, 40). Analyzing

features of $CD8^+$ T cells seemed to be an alternative choice for monitoring immune response. Our former research had already identified the peripheral blood TCR repertoire of NSCLC patients as a useful prognostic biomarker (41). In this study, we investigated the dynamic change in TCR frequencies and found that the maintenance of high-frequency T-cell clones might be associated with a durable response to Nivolumab. By comparing each T-cell clone after neoantigen peptide stimulation, we identified some neoantigen-specific T-cell clones, which are likely responsible for the recognition of MHC:peptide complex. A recent study has raised the hypothesis of clonal replacement after immunotherapy, and researchers founded that expanded T-cell clones were recruited from blood rather than continuously presented in tumors (42). Consistent with the hypothesis, we observed that some significant clones only expanded after the initiation of Nivolumab. Further research should be conducted to characterize the anti-tumor immunity of these T-cell clones.

Besides tumor-intrinsic factors, tumor microenvironment (TME) will also affect the efficacy of immunotherapy. A newly published research focused on TME found that *EGFR* driver gene alterations, despite its inescapable role in tumor growth, contributed directly to a non-inflamed phenotype, with high regulatory T-cell (Treg) infiltration and low $CD8^+$ T-cell infiltration (27). For our patient, Nivolumab was initiated only after multiline therapies, including EGFR-TKIs, chemotherapy, and radiotherapy. Thus, we presumed an enhanced suppressive activity of TME, and we did not conduct a comprehensive analysis on TME.

The clinical implications of our research were profound. A previous study showed that the anti-EGFR antibody titer was characterized as highest in NSCLC patients with *EGFR* exon 19 deletion, suggesting that this mutation is immunogenic and can be expressed at protein level (43). We may infer that the peptide sequences derived from *EGFR* exon 19 deletion (IPVAIKTSPK, AIKTSPKANK) may be a potential therapeutic target of cancer vaccine for NSCLC. Moreover, HLA-A*11:01 was the most frequent HLA-A allele in Asians (44). *EGFR 19del* is the most common mutation in *EGFR* mutated NSCLC patients, accounting for ∼45% of all cases (43). Consequently, it is reasonable that our results can provide important clinical data for a subgroup of NSCLC patients with both *EGFR* mutations and HLA-A*11:01 allele.

There are some expected limitations of our study. At first, TCR profiling was only performed on peripheral blood and cultured PBMCs due to a lack of tumor tissue. A mapping of TCR in tumor and metastatic sites will make the results more convincing. Second, recent research has highlighted the important role of MHC class II-restricted neoantigens in the anti-tumor response (45). In this study, we only focused on MHC-I-restricted neoantigens. Investigations of MHC class II-restricted neoantigens may be carried out in the future with more advanced technologies.

Overall, our data suggested that high-quality neoantigen can be generated from *EGFR* driver mutation. ICBs can be used for advanced NSCLC with acquired resistance to EGFR-TKIs in the context of specific clonal neoantigens with high immunogenicity. Monitoring of neoantigen-specific T-cell response might be beneficial for improving the survival rate of NSCLC patients. Personalized immunomodulatory therapy targeting these neoantigens should be explored for better clinical outcomes. We hope our findings may help pave the way for future researches on *EGFR* mutated NSCLC.

MATERIALS AND METHODS

Patient Samples

Peripheral blood was obtained from the patient before the initiation of Nivolumab and every 2 months after treatment. PBMCs were isolated by Ficoll-Hypaque density centrifugation and were analyzed immediately after isolation. Lung cancer tissue sample was obtained by computed tomography (CT)-guided lung biopsy before Nivolumab treatment.

This study was approved by the Institutional Review Board of Tongji Medical College of Huazhong University of Science and Technology. The patient gave his written informed consent for the collection of blood and tissue samples in accordance with the Declaration of Helsinki.

Immunohistochemistry

The Dako PD-L1 IHC 22C3 pharmDx assay was used to detect PD-L1 protein expression in formalin-fixed paraffin-embedded (FFPE) tumor tissue slides. A four-tiered grading system was applied to evaluate the proportion of PD-L1 expression in tumor cells: TC0 for negative expression, TC1 for 1–5%, TC2 for 5–50%; TC3 for more than 50%.

Whole-Exome Sequencing and RNA Sequencing

Whole-exome sequencing was carried out on the FFPE tumor tissue and matched normal samples. Peripheral blood was served as normal sample. Genomic DNAs were from tumor tissue, and blood was, respectively, extracted using the Qiagen DNA FFPE and Qiagen DNA blood mini kit (Qiagen). RNA was extracted from FFPE tumor tissue slides using RNeasy FFPE Kit (Qiagen). Sequencing libraries were constructed using Agilent SureSelect Human All Exon V6 kit (Agilent Technologies, USA), and sequencing procedures were performed on an Illumina HiSeq X-Ten platform with 150-bp paired-end reads. Raw reads were filtered using SOAPnuke (v1.5.6) to remove low-quality reads with unknown bases "N" more than 10%. Clean reads were aligned to the human reference genome (UCSCGRCh37/hg19) with the BWA (v0.7.12) for WES and RSEM (v1.3.0) for RNA sequencing. Somatic single-nucleotide variants (SNVs) and indels were identified using VarScan (v2.4.1) and subsequently filtered by an in-house approach to remove the possible false-positive variants (46). Aligned RNA reads were then analyzed using RSEM (v1.3.0). Tumor purity was evaluated computationally in paired samples using AscatNGS (v3.1.0) (47). Tumor mutational burden (TMB) was determined as the number of non-silent somatic mutations per megabase of exome examined. High and low TMB was determined according to a cut-off value of 10 and 2.5 muts/Mb, respectively. The expression of neoantigens was calculated according to both the variant allele frequency of corresponding mutations and the expression level

of genes involved. Tumor neoantigen burden (TNB) was defined as the number of neoantigens per megabase of exome examined, and high TNB was determined according to a cut-off value of 4.5 neos/Mb.

HLA Typing and Neoantigen Prediction

HLA typing of tumor samples and paired normal samples was assessed from WES results using POLYSOLVER (v1.0) and Bwakit (v0.7.11) (48), and were further used for neoantigen prediction. By using in-house software, all the non-silent mutations were translated into 21-mer peptide sequence centered on mutated amino acid. Then, the 21-mer peptide was used to create 9- to 11-mer peptide via a sliding window approach for predicting the binding affinity of major histocompatibility complex class I (MHC I) proteins and their peptide ligands. NetMHCpan (v3.0) was used to determine the binding strength of mutant peptides to patient-specific HLA alleles (49). The predicted peptides were scored according to the following indexes: strong binding affinity, mutation type, variant allele frequency, proteasomal C terminal cleavage, transporter associated with antigen processing, transporting efficiency, and gene expression. Peptides of score higher than 0 were selected. If selected peptides were generated from the same mutation, it can be only counted as one neoantigen.

In vitro PBMC Expansion

PBMCs were rested according to previous studies (16, 50). Autologous PBMCs (2×10^5 cells per well) were co-cultured with separate peptides derived from candidate neoantigens (10 μg/ml) with RPMI-1640 supplemented with 10% fetal bovine serum, 10 U/ml of penicillin–streptomycin, 2 mmol/L L-glutamine, and 1× non-essential amino acid. Cell culture was conducted for 10 days at 37°C in a 5% CO_2 atmosphere, and half of the culture media was replaced by fresh culture media containing 100 IU/ml IL-2, 50 ng/ml IL-7, and 50 ng/ml IL-15 on days 3, 5, and 7. Half of the culture media was replaced with fresh media without cytokines on day 9.

IFN-γ ELISPOT Assay

The frequency of neoantigen-specific T cells after 10 days of coculture was determined by IFN-γ ELISPOT kit (Dakewei, China) (51). Briefly, PBMCs (2×10^5 per well) and peptides (10 μg/ml) were added to triplicate wells. PBMCs cultured without peptides were regarded as the negative controls. Plates were scanned by Elispot Reader System (Cell Technology Inc., Columbia, MD), and the results were analyzed with Elispot software (AID, Strassberg, Germany).

TCR Sequencing

DNA extracted from PBMCs was prepared for TCR β-chain amplification using Short Read iR-Profile Reagent System HTBI-vc and sequenced using the NextSeq system. V-D-J gene segments in CDR3 sequences were identified by MiXCR (v2.1.10). Basic quantification of clonotypes was assessed with VDJ tools (v1.1.10). High-frequency clones were defined as T-cell clones with a frequency of $\geq 10^{-3}$. TCRs from simulated PBMCs were further analyzed by comparing the frequency of each T-cell clone being stimulated by the mutant peptide with the same clone being stimulated by the wild-type peptide. Neoantigen-specific T-cell clones were identified with an odd ratio higher than 10 and a value of $p < 0.01$.

Statistics

All the statistical analyses were conducted by GraphPad Prism version 8.0 (GraphPad Software, USA). TCR sequencing was compared using a one-sided Fisher's exact test. Other values were compared using an unpaired two-tailed Student's *t*-test. A value of $p < 0.05$ was considered statistically significant.

DATA AVAILABILITY STATEMENT

The data in this study is available on the GEO - GSE150972. Other raw data supporting the conclusions of this article will be made available by the authors, without undue reservation, to any qualified researcher.

ETHICS STATEMENT

This study was approved by the Institutional Review Board of Tongji Medical College of Huazhong University of Science and Technology. The patient gave his written informed consent for the collection of blood and tissue samples in accordance with the Declaration of Helsinki. Written informed consent was obtained from the patient for the publication of any potentially identifiable images or data included in this article.

AUTHOR CONTRIBUTIONS

DW and YaL designed and performed the experiments. YiL, QY, and JW performed and analyzed the sequencing data. CT, ZZ, YX, YZ, and XL performed data analysis and statistical oversight. FG, YuL, and KZ provided technical assistance. LL and YH were responsible for the provision of study resources, materials, and patient access. DW wrote the manuscript. All authors read and approved the final manuscript.

FUNDING

This study was funded by the National Key R&D Program of China (No. 2016YFC13038) and the National Natural Science Foundation of China (No. 81773056 and No. 81902934).

ACKNOWLEDGMENTS

We would like to thank the patient and his family as well as YuceBio Technology Company for their assistance with the study.

SUPPLEMENTARY MATERIAL

The Supplementary Material for this article can be found online at: https://www.frontiersin.org/articles/10.3389/fimmu.2020.01366/full#supplementary-material

REFERENCES

1. Siegel RL, Miller KD, Jemal A. Cancer statistics, 2019. *CA Cancer J Clin.* (2019) 69:7–34. doi: 10.3322/caac.21551
2. Mok TS, Wu Y-L, Thongprasert S, Yang C-H, Chu D-T, Saijo N, et al. Gefitinib or carboplatin–paclitaxel in pulmonary adenocarcinoma. *N Engl J Med.* (2009) 361:947–57. doi: 10.1056/NEJMoa0810699
3. Kwak EL, Bang Y-J, Camidge DR, Shaw AT, Solomon B, Maki RG, et al. Anaplastic lymphoma kinase inhibition in non–small-cell lung cancer. *N Engl J Med.* (2010) 363:1693–703. doi: 10.1056/NEJMoa1006448
4. Yatabe Y, Kerr KM, Utomo A, Rajadurai P, Du X, Chou T-Y, et al. EGFR mutation testing practices within the Asia Pacific region: results of a multicenter diagnostic survey. *J Thorac Oncol.* (2015) 10:438–45. doi: 10.1097/JTO.0000000000000422
5. Tan CS, Gilligan D, Pacey S. Treatment approaches for EGFR-inhibitor-resistant patients with non-small-cell lung cancer. *Lancet Oncol.* (2015) 16:e447–59. doi: 10.1016/S1470-2045(15)00246-6
6. Sullivan I, Planchard D. Osimertinib in the treatment of patients with epidermal growth factor receptor T790M mutation-positive metastatic non-small cell lung cancer: clinical trial evidence and experience. *Ther Adv Respir Dis.* (2016) 10:549–65. doi: 10.1177/1753465816670498
7. Yang Z, Yang N, Ou Q, Xiang Y, Jiang T, Wu X, et al. Investigating novel resistance mechanisms to third-generation EGFR tyrosine kinase inhibitor osimertinib in non–small cell lung cancer patients. *Clin Cancer Res.* (2018) 24:3097–107. doi: 10.1158/1078-0432.CCR-17-2310
8. Borghaei H, Paz-Ares L, Horn L, Spigel DR, Steins M, Ready NE, et al. Nivolumab versus docetaxel in advanced nonsquamous non–small-cell lung cancer. *N Engl J Med.* (2015) 373:1627–39. doi: 10.1056/NEJMoa1507643
9. Reck M, Rodríguez-Abreu D, Robinson AG, Hui R, Csoszi T, Fülöp A, et al. Pembrolizumab versus chemotherapy for PD-L1–positive non–small-cell lung cancer. *N Engl J Med.* (2016) 375:1823–33. doi: 10.1056/NEJMoa1606774
10. Gainor JF, Shaw AT, Sequist LV, Fu X, Azzoli CG, Piotrowska Z, et al. EGFR mutations and ALK rearrangements are associated with low response rates to PD-1 pathway blockade in non–small cell lung cancer: a retrospective analysis. *Clin Cancer Res.* (2016) 22:4585–93. doi: 10.1158/1078-0432.CCR-15-3101
11. Lee CK, Man J, Lord S, Links M, Gebski V, Mok T, et al. Checkpoint inhibitors in metastatic EGFR-mutated non–small cell lung cancer—a meta-analysis. *J Thorac Oncol.* (2017) 12:403–7. doi: 10.1016/j.jtho.2016.10.007
12. Kotake M, Murakami H, Kenmotsu H, Naito T, Takahashi T. High incidence of interstitial lung disease following practical use of osimertinib in patients who had undergone immediate prior nivolumab therapy. *Ann Oncol.* (2017) 28:669–70. doi: 10.1093/annonc/mdw647
13. Schumacher TN, Schreiber RD. Neoantigens in cancer immunotherapy. *Science.* (2015) 348:69–74. doi: 10.1126/science.aaa4971
14. Rizvi NA, Hellmann MD, Snyder A, Kvistborg P, Makarov V, Havel JJ, et al. Mutational landscape determines sensitivity to PD-1 blockade in non–small cell lung cancer. *Science.* (2015) 348:124–8. doi: 10.1126/science.aaa1348
15. Ott PA, Dotti G, Yee C, Goff SL. An update on adoptive T-cell therapy and neoantigen vaccines. *Am Soc Clin Oncol Educ Book.* (2019) 39:e70–8. doi: 10.1200/EDBK_238001
16. Keskin DB, Anandappa AJ, Sun J, Tirosh I, Mathewson ND, Li S, et al. Neoantigen vaccine generates intratumoral T cell responses in phase Ib glioblastoma trial. *Nature.* (2019) 565:234–9. doi: 10.1038/s41586-018-0792-9
17. Jiang T, Shi T, Zhang H, Hu J, Song Y, Wei J, et al. Tumor neoantigens: from basic research to clinical applications. *J Hematol Oncol.* (2019) 12:93. doi: 10.1186/s13045-019-0787-5
18. Yi M, Qin S, Zhao W, Yu S, Chu Q, Wu K. The role of neoantigen in immune checkpoint blockade therapy. *Exp Hematol Oncol.* (2018) 7:28. doi: 10.1186/s40164-018-0120-y
19. Ofuji K, Tada Y, Yoshikawa T, Shimomura M, Yoshimura M, Saito K, et al. A peptide antigen derived from EGFR T790M is immunogenic in non-small cell lung cancer. *Int J Oncol.* (2015) 46:497–504. doi: 10.3892/ijo.2014.2787
20. Roudko V, Greenbaum B, Bhardwaj N. Computational prediction and validation of tumor-associated neoantigens. *Front Immunol.* (2020) 11:27. doi: 10.3389/fimmu.2020.00027
21. McGranahan N, Furness AJ, Rosenthal R, Ramskov S, Lyngaa R, Saini SK, et al. Clonal neoantigens elicit T cell immunoreactivity and sensitivity to immune checkpoint blockade. *Science.* (2016) 351:1463–9. doi: 10.1126/science.aaf1490
22. Yu S, Sha H, Qin X, Chen Y, Li X, Shi M, et al. EGFR E746-A750 deletion in lung cancer represses antitumor immunity through the exosome-mediated inhibition of dendritic cells. *Oncogene.* (2020) 39:2643–57. doi: 10.1038/s41388-020-1182-y
23. Jia Y, Li X, Jiang T, Zhao S, Zhao C, Zhang L, et al. EGFR-targeted therapy alters the tumor microenvironment in EGFR-driven lung tumors: implications for combination therapies. *Int J Cancer.* (2019) 145:1432–44. doi: 10.1002/ijc.32191
24. Jia Y, Zhao S, Jiang T, Li X, Zhao C, Liu Y, et al. Impact of EGFR-TKIs combined with PD-L1 antibody on the lung tissue of EGFR-driven tumor-bearing mice. *Lung Cancer.* (2019) 137:85–93. doi: 10.1016/j.lungcan.2019.09.016
25. Peng S, Wang R, Zhang X, Ma Y, Zhong L, Li K, et al. EGFR-TKI resistance promotes immune escape in lung cancer via increased PD-L1 expression. *Mol Cancer.* (2019) 18:165. doi: 10.1186/s12943-019-1073-4
26. Melosky B, Chu Q, Juergens RA, Leighl N, Ionescu D, Tsao MS, et al. Breaking the biomarker code: PD-L1 expression and checkpoint inhibition in advanced NSCLC. *Cancer Treat Rev.* (2018) 65:65–77. doi: 10.1016/j.ctrv.2018.02.005
27. Sugiyama E, Togashi Y, Takeuchi Y, Shinya S, Tada Y, Kataoka K, et al. Blockade of EGFR improves responsiveness to PD-1 blockade in EGFR-mutated non–small cell lung cancer. *Sci Immunol.* (2020) 5:aav3937. doi: 10.1126/sciimmunol.aav3937
28. Ji M, Liu Y, Li Q, Li X, Ning Z, Zhao W, et al. PD-1/PD-L1 expression in non-small-cell lung cancer and its correlation with EGFR/KRAS mutations. *Cancer Biol Ther.* (2016) 17:407–13. doi: 10.1080/15384047.2016.1156256
29. Garassino MC, Cho B-C, Kim J-H, Mazières J, Vansteenkiste J, Lena H, et al. Durvalumab as third-line or later treatment for advanced non-small-cell lung cancer (ATLANTIC): an open-label, single-arm, phase 2 study. *Lancet Oncol.* (2018) 19:521–36. doi: 10.1016/S1470-2045(18)30144-X
30. Lisberg A, Cummings A, Goldman JW, Bornazyan K, Reese N, Wang T, et al. A phase II study of pembrolizumab in EGFR-mutant, PD-L1+, tyrosine kinase inhibitor naïve patients with advanced NSCLC. *J Thorac Oncol.* (2018) 13:1138–45. doi: 10.1016/j.jtho.2018.03.035
31. Goodman AM, Kato S, Bazhenova L, Patel SP, Frampton GM, Miller V, et al. Tumor mutational burden as an independent predictor of response to immunotherapy in diverse cancers. *Mol Cancer Ther.* (2017) 16:2598–608. doi: 10.1158/1535-7163.MCT-17-0386
32. Le DT, Durham JN, Smith KN, Wang H, Bartlett BR, Aulakh LK, et al. Mismatch repair deficiency predicts response of solid tumors to PD-1 blockade. *Science.* (2017) 357:409–13. doi: 10.1126/science.aan6733
33. Smith KN, Llosa NJ, Cottrell TR, Siegel N, Fan H, Suri P, et al. Persistent mutant oncogene specific T cells in two patients benefitting from anti-PD-1. *J Immunother Cancer.* (2019) 7:40. doi: 10.1186/s40425-018-0492-x
34. Asadi-Ghalehni M, Ghaemmaghami M, Klimka A, Javanmardi M, Navari M, Rasaee MJ. Cancer immunotherapy by a recombinant phage vaccine displaying EGFR mimotope: an *in vivo* study. *Immunopharmacol Immunotoxicol.* (2015) 37:274–9. doi: 10.3109/08923973.2015.1027917
35. Malekzadeh P, Pasetto A, Robbins PF, Parkhurst MR, Paria BC, Jia L, et al. Neoantigen screening identifies broad TP53 mutant immunogenicity in patients with epithelial cancers. *J Clin Invest.* (2019) 129:1109–14. doi: 10.1172/JCI123791
36. Anagnostou V, Smith KN, Forde PM, Niknafs N, Bhattacharya R, White J, et al. Evolution of neoantigen landscape during immune checkpoint blockade in non–small cell lung cancer. *Cancer Discov.* (2017) 7:264–76. doi: 10.1158/1538-7445.AM2017-NG01
37. Consortium APG. AACR Project GENIE: powering precision medicine through an international consortium. *Cancer Discov.* (2017) 7:818–31. doi: 10.1158/2159-8290.CD-17-0151
38. Cafri G, Yossef R, Pasetto A, Deniger DC, Lu YC, Parkhurst M, et al. Memory T cells targeting oncogenic mutations detected in peripheral blood of epithelial cancer patients. *Nat Commun.* (2019) 10:449. doi: 10.1038/s41467-019-08304-z
39. Fehlings M, Jhunjhunwala S, Kowanetz M, O'Gorman WE, Hegde PS, Sumatoh H, et al. Late-differentiated effector neoantigen-specific CD8+ T cells are enriched in peripheral blood of non-small cell lung carcinoma patients responding to atezolizumab treatment. *J Immunother Cancer.* (2019) 7:249. doi: 10.1186/s40425-019-0695-9

40. Gros A, Tran E, Parkhurst MR, Ilyas S, Pasetto A, Groh EM, et al. Recognition of human gastrointestinal cancer neoantigens by circulating PD-1+ lymphocytes. *J Clin Invest.* (2019) 129:4992–5004. doi: 10.1172/JCI127967
41. Liu YY, Yang QF, Yang JS, Cao RB, Liang JY, Liu YT, et al. Characteristics and prognostic significance of profiling the peripheral blood T-cell receptor repertoire in patients with advanced lung cancer. *Int J Cancer.* (2019) 145:1423–31. doi: 10.1002/ijc.32145
42. Yost KE, Satpathy AT, Wells DK, Qi Y, Wang C, Kageyama R, et al. Clonal replacement of tumor-specific T cells following PD-1 blockade. *Nat Med.* (2019) 25:1251–9. doi: 10.1038/s41591-019-0522-3
43. Pan D, Zhou D, Cai W, Wu W, Tan WL, Zhou C, et al. Immunogenicity of Del19 EGFR mutations in Chinese patients affected by lung adenocarcinoma. *BMC Immunol.* (2019) 20:43. doi: 10.1186/s12865-019-0320-1
44. Gonzalez-Galarza FF, Christmas S, Middleton D, Jones AR. Allele frequency net: a database and online repository for immune gene frequencies in worldwide populations. *Nucleic Acids Res.* (2011) 39:D913–9. doi: 10.1093/nar/gkq1128
45. Alspach E, Lussier DM, Miceli AP, Kizhvatov I, DuPage M, Luoma AM, et al. MHC-II neoantigens shape tumour immunity and response to immunotherapy. *Nature.* (2019) 574:696–701. doi: 10.1038/s41586-019-1671-8
46. Koboldt DC, Larson DE, Wilson RK. Using VarScan 2 for germline variant calling and somatic mutation detection. *Curr Protoc Bioinform.* (2013) 44:15–4. doi: 10.1002/0471250953.bi1504s44
47. Raine KM, Van Loo P, Wedge DC, Jones D, Menzies A, Butler AP, et al. ascatNgs: Identifying somatically acquired copy-number alterations from whole-genome sequencing data. *Curr Protoc Bioinform.* (2016) 56:15–9. doi: 10.1002/cpbi.17
48. Shukla SA, Rooney MS, Rajasagi M, Tiao G, Dixon PM, Lawrence MS, et al. Comprehensive analysis of cancer-associated somatic mutations in class I HLA genes. *Nat Biotechnol.* (2015) 33:1152–8. doi: 10.1038/nbt.3344
49. Hoof I, Peters B, Sidney J, Pedersen LE, Sette A, Lund O, et al. NetMHCpan, a method for MHC class I binding prediction beyond humans. *Immunogenetics.* (2009) 61:1–13. doi: 10.1007/s00251-008-0341-z
50. Danilova L, Anagnostou V, Caushi JX, Sidhom JW, Guo H, Chan HY, et al. The mutation-associated neoantigen functional expansion of specific T cells (MANAFEST) assay: a sensitive platform for monitoring antitumor immunity. *Cancer Immunol Res.* (2018) 6:888–99. doi: 10.1158/2326-6066.CIR-18-0129
51. Su S, Hu B, Shao J, Shen B, Du J, Du Y, et al. CRISPR-Cas9 mediated efficient PD-1 disruption on human primary T cells from cancer patients. *Sci Rep.* (2016) 6:20070. doi: 10.1038/srep20070

Conflict of Interest: XL, YiL, ZZ, and YX were employed by the company YuceBio Technology Co.

The remaining authors declare that the research was conducted in the absence of any commercial or financial relationships that could be construed as a potential conflict of interest.

frontiers in Immunology

ORIGINAL RESEARCH
published: 10 August 2020
doi: 10.3389/fimmu.2020.01620

CCND1 Amplification Contributes to Immunosuppression and Is Associated With a Poor Prognosis to Immune Checkpoint Inhibitors in Solid Tumors

Yu Chen[1,2,3†], Yingying Huang[4†], Xuan Gao[5†], Yi Li[4†], Jing Lin[1,2,3], Lizhu Chen[1,2,3], Lianpeng Chang[5], Gang Chen[3,6], Yanfang Guan[5], Leong Kin Pan[7,8], Xuefeng Xia[5], Zengqing Guo[1,2,3], Jianji Pan[2,3,9], Yaping Xu[5], Xin Yi[5] and Chuanben Chen[2,3,9†]*

[1] Department of Medical Oncology, Fujian Medical University Cancer Hospital & Fujian Cancer Hospital, Fuzhou, China, [2] Cancer Bio-immunotherapy Center, Fujian Medical University Cancer Hospital & Fujian Cancer Hospital, Fuzhou, China, [3] Fujian Provincial Key Laboratory of Translational Cancer Medicine, Fuzhou, China, [4] Fujian Medical University Cancer Hospital, Fuzhou, China, [5] Geneplus-Beijing, Beijing, China, [6] Department of Pathology, Fujian Medical University Cancer Hospital & Fujian Cancer Hospital, Fuzhou, China, [7] CCIC Group, Kuok Kim (Macao) Medical Center III, Macao, China, [8] Hui Xian Medical Center, Macao, China, [9] Department of Radiation Oncology, Fujian Medical University Cancer Hospital & Fujian Cancer Hospital, Fuzhou, China

OPEN ACCESS

Edited by:
Said Dermime, National Center for Cancer Care and Research, Qatar

Reviewed by:
Aparna Rao, University of Pittsburgh, United States
Andreas Pircher, Innsbruck Medical University, Austria
Nabil Elhadi Omar, Hamad Medical Corporation, Qatar

***Correspondence:**
Chuanben Chen
ccb@fjmu.edu.cn

[†]These authors have contributed equally to this work

Specialty section:
This article was submitted to Cancer Immunity and Immunotherapy, a section of the journal Frontiers in Immunology

Received: *15 January 2020*
Accepted: *17 June 2020*
Published: *10 August 2020*

Citation:
Chen Y, Huang Y, Gao X, Li Y, Lin J, Chen L, Chang L, Chen G, Guan Y, Pan LK, Xia X, Guo Z, Pan J, Xu Y, Yi X and Chen C (2020) CCND1 Amplification Contributes to Immunosuppression and Is Associated With a Poor Prognosis to Immune Checkpoint Inhibitors in Solid Tumors. Front. Immunol. 11:1620. doi: 10.3389/fimmu.2020.01620

Cyclin D1 (CCND1) amplification relevant to malignant biological behavior exists in solid tumors. The prevalence and utility of *CCND1* amplification as a biomarker for the clinical response to treatment with immune checkpoint inhibitors (ICIs) are unknown. Our study is a preliminary investigation mainly focused on the predictive function of *CCND1* amplification in the tumor microenvironment (TME) in the aspect of genome and transcriptome. We examined the prevalence of *CCND1* amplification and its potential as a biomarker for the efficacy of ICI therapy for solid tumors using a local database ($n = 6{,}536$), The Cancer Genome Atlas (TCGA) database ($n = 10{,}606$), and the Memorial Sloan Kettering Cancer Center (MSKCC) database ($n = 10{,}109$). Comprehensive profiling was performed to determine the prevalence of *CCND1* amplification and the correlation with the prognosis and the response to ICIs. A *CCND1* amplification occurs in many cancer types and correlates with shorter overall survival and inferior outcomes with ICI therapy. Transcriptomic analysis showed various degrees of immune cell exclusion, including cytotoxic cells, T cells, $CD8^+$ T cells, dendritic cells (DCs), and B cells in the TME in a TCGA *CCND1* amplification population. The gene set enrichment analysis suggested that *CCND1* amplification correlates with multiple aggressive, immunosuppressive hallmarks including epithelial–mesenchymal transition, transforming growth factor (TGF)-β signaling, KRAS signaling, phosphoinositide 3-kinase (PI3K)/AKT/mammalian target of rapamycin (mTOR) signaling, p53 pathway, and hypoxia signaling in solid tumors. These findings indicate that *CCND1* amplification may be a key point related to immunosuppression in TME and multiple malignancy hallmarks, and it hinders not only the natural host immune responses but also the efficacy of ICIs.

Keywords: cyclin D1 *(CCND1)*, immune checkpoint inhibitors, prognosis, tumor microenvironment, biomarker

INTRODUCTION

Immunotherapies targeting immune checkpoints have durable antitumor responses in multiple cancer types, which can contribute to a remarkable improvement in treatment outcomes in a subset of patients with advanced cancer (1). This led to the approval of therapeutic inhibitors of programmed cell death 1 (PD-1) pathway, pembrolizumab, nivolumab, and cemiplimab, and of the programmed cell death ligand 1 (PD-L1) pathway, atezolizumab, durvalumab, and avelumab, by the US Food and Drug Administration (FDA) for the treatment of advanced melanoma, non-small-cell lung cancer, renal cell carcinoma, head and neck squamous cell carcinoma (HNSCC), Hodgkin's lymphoma, squamous cell cancer of the skin, and urothelial bladder cancer. Despite this progress, only a minority of patients within each cancer subtype present with a durable response to immune checkpoint inhibitors (ICIs), and the molecular mechanisms of primary resistance remain incompletely understood (2).

The efficiency of PD-1/PD-L1 inhibitors depends on cancer-specific cytotoxic immune cell activation and infiltration into the tumor microenvironment (TME) (2). Cyclin D1 protein encoded by the *CCND1* gene located on human chromosome 11q13.3 is the critical gatekeeping protein in charge of regulating the transition through the restriction point in the G1 phase to S phase of the cell cycle (3). The *CCND1* gene is considered an oncogene, and it reinforces cell proliferation, growth, angiogenesis, and resistance to chemotherapy and radiotherapy (3, 4). Recently, several studies revealed that *CCND1* amplification associates with a negative response to ICIs. In a study by Saada-Bouzid et al. (5), pretreatment tumor tissue samples from patients who present with hyper-progression after treatments of ICIs were retrospectively detected with next-generation sequencing (NGS). Three out of five patients presented with *CCND1* amplification (5). A retrospective study of melanoma also showed that 30 out of 56 patients with innate resistance to anti-PD-1 therapy presented with *CCND1* amplification (6). Although there are currently few reported cases, the clinical phenomena suggest the potential value of *CCND1* amplification as a biomarker for predicting negative therapeutic effects of ICIs.

We hypothesized that *CCND1* amplification may be associated with poor clinical benefits of ICI therapy through suppressing the antitumor immunity in TME. We mainly focused on the predictive function of CCND1 amplification in the TME in the aspect of genome and transcriptome. In this study, we performed an integrative analysis of The Cancer Genome Atlas (TCGA), Geneplus, and Memorial Sloan Kettering Cancer Center (MSKCC) databases to clarify the frequency of amplification of *CCND1*. Importantly, we aimed to explore whether *CCND1* amplification correlates with a poor response to ICIs in solid tumors, for which the potential mechanism may be correlated with events within the TME.

Abbreviations: *CCND1*, cyclin D1; ICIs, immune checkpoint inhibitors; NGS, next-generation sequencing; TCGA, The Cancer Genome Atlas; MSKCC, Memorial Sloan Kettering Cancer Center; OS, overall survival; TMB, tumor mutational burden; TME, tumor microenvironment; PD-1,programmed cell death 1; PD-L1, programmed cell death ligand 1; HNSCC, head and neck squamous cell carcinoma; CNA, copy number alteration; BLCA, bladder urothelial carcinoma; BRCA, breast invasive carcinoma; CHOL, cholangiocarcinoma; ESCA, esophageal carcinoma; LIHC, liver hepatocellular carcinoma; LUSC, lung squamous cell carcinoma; OV, ovarian serous cystadenocarcinoma; SKCM, skin cutaneous melanoma; STAD, stomach adenocarcinoma; MDSCs, myeloid-derived suppressor cells; GSEA, gene set enrichment analysis; CTLA4, cytotoxic T lymphocyte-associated protein 4; DFS, disease-free survival; DCs, dendritic cells.

MATERIALS AND METHODS

Patient Populations

From August 12, 2015, through March 19, 2019, 6,536 tumor tissue samples from 6,536 patients with solid tumors underwent an NGS assay at Geneplus-Beijing (Beijing, China). All procedures were conducted in accordance with the Helsinki Declaration (7) and with approval from the Ethics Committee of Fujian Provincial Cancer Hospital. Written informed consent was obtained from all participants.

Tissue Processing and DNA Extraction

The germline genomic DNA of peripheral blood lymphocytes and frozen tissue samples was extracted using the DNeasy Blood & Tissue Kit (Qiagen, Hilden, Germany). The formalin-fixed, paraffin-embedded (FFPE) tissue samples were isolated using a commercially available kit (Maxwell® 16 FFPE Plus LEV DNA Purification, Qiagen, Hilden, Germany Kit, catalog: AS1135). The DNA concentration was measured using a Qubit fluorometer and the Qubit dsDNA HS (High Sensitivity) Assay Kit (Invitrogen, Carlsbad, CA, USA). The total DNA yield must be $\geq$1 μg, while 260/280 and 260/230 ratios are $\geq$1.8 and 2, respectively.

Library Preparation, Target Capture, and Next-Generation Sequencing

Sequencing was carried out using Illumina 2 × 75-bp paired-end reads on an Illumina HiSeq 3000 instrument according to the manufacturer's recommendations using the KAPA DNA Library Preparation Kit (Kapa Biosystems, Wilmington, MA, USA). Bar-coded libraries were hybridized to a customized panel of 1,021 genes containing whole exons and selected introns of 288 genes and selected regions of 733 genes (**Table S1**). The libraries were sequenced to a uniform median depth (>500×) and assessed for somatic variants including single-nucleotide variants (SNVs), small insertions and deletions (InDels), copy number alterations (CNAs), and gene fusions/rearrangements.

Next-Generation Sequencing Analysis

MuTect2 (version 1.1.4) (8) was employed to identify somatic InDels and SNVs. Contra (v2.0.8) (9) was used to identify CNAs. The CNA was expressed as the ratio of adjusted depth between ctDNA and germline DNA and analyzed using FACETS (10)-with log2ratio thresholds of 0.848 and −0.515 for gain and loss, respectively. Specifically, for the *CCND1* gene, samples with chromosome 11q13.3 alterations were further reviewed for CNAs.

Data Sources

Solid tumors, which had CNAs identified in the data from 10,606 tumor tissue samples from 10,606 patients with solid tumors in the TCGA, were obtained from the Broad Institute Genomic Data Analysis Center (https://gdac.broadinstitute.org/). The TCGA cohort consisted of adrenocortical cancer (ACC, $n = 90$), bladder urothelial carcinoma (BLCA, $n = 408$), breast invasive carcinoma (BRCA, $n = 1{,}080$), cervical and endocervical cancer (CESC, $n = 295$), cholangiocarcinoma (CHOL, $n = 36$), colon and rectum adenocarcinoma (COADREAD, $n = 616$), esophageal carcinoma (ESCA, $n = 184$), glioblastoma multiforme (GBM, $n = 577$), HNSCC ($n = 522$), kidney chromophobe carcinoma (KICH, $n = 66$), kidney clear cell carcinoma (KIRC, $n = 528$), kidney papillary cell carcinoma (KIRP, $n = 288$), lower grade glioma (LGG, $n = 513$), liver hepatocellular carcinoma (LIHC, $n = 370$), lung adenocarcinoma (LUAD, $n = 516$), lung squamous cell carcinoma (LUSC, $n = 501$), mesothelioma (MESO, $n = 87$), ovarian serous cystadenocarcinoma (OV, $n = 579$), pancreatic adenocarcinoma (PAAD, $n = 184$), pheochromocytoma and paraganglioma (PCPG, $n = 162$), prostate adenocarcinoma (PRAD, $n = 492$), sarcoma (SARC, $n = 257$), skin cutaneous melanoma (SKCM, $n = 367$), stomach adenocarcinoma (STAD, $n = 441$), testicular germ cell tumor (TGCT, $n = 150$), thyroid carcinoma (THCA, $n = 499$), thymoma (THYM, $n = 123$), uterine corpus endometrial carcinoma (UCEC, $n = 539$), uterine carcinosarcoma (UCS, $n = 56$), and uveal melanoma (UVM, $n = 80$). Survival information (11) and RSEM-normalized gene-level data from cancers with *CCND1* amplification frequency ranked first to 10th were further downloaded. The data of CHOL were excluded for a limited number of samples ($n = 36$). Patients with *CCND1* amplification or neutral phenotypes were further analyzed. Patients with overall survival (OS) more than 10 days and gene-level data were enrolled as the TCGA pan-cancer cohort ($n = 2{,}633$). The TCGA pan-cancer cohort consisted of BLCA ($n = 247$), BRCA ($n = 714$), ESCA ($n = 122$), HNSCC ($n = 359$), LIHC ($n = 277$), LUSC ($n = 292$), OV ($n = 145$), SKCM ($n = 203$), and STAD ($n = 274$). OS was defined from the date of initial pathologic diagnosis.

We reviewed the CNA data from 10,109 solid tumor tissue samples from 10,109 patients in the MSKCC database who were enrolled as the MSKCC cohort (12). Survival information from cancers with *CCND1* amplification frequency ranked first to 10th was further downloaded. These patients with an OS of more than 10 days were enrolled as the MSKCC pan-cancer cohort ($n = 3{,}629$). Their OS was defined from the date of initial pathologic diagnosis. A total of 1,105 patients treated at MSKCC who had received at least one dose of ICIs had an OS defined from the date of first infusion of any ICI and were enrolled as the MSKCC-IO cohort (13).

To explore the association between *CCND1* amplification and the clinical outcomes of ICIs, we included CNA and clinical data from four clinical cohorts treated with ICIs. The first cohort consisted of 72 patients with melanoma treated with anti-cytotoxic T lymphocyte-associated protein 4 (CTLA-4) therapy (Allen cohort) (14). The second pooled cohort consisted of 464 melanoma patients treated with ICIs (Robert cohort treated with anti-PD-1/L1 or anti-CTLA-4 or combination therapy, Allen and Snyder cohorts treated with anti-CTLA-4 therapy, David cohort treated with anti-PD-1 therapy) (13–16).

Database Analysis for *CCND1* and Tumor Mutational Burden

We analyzed the CNA in the TCGA and MSKCC cohorts. The CN changes, including putative biallelic CNA (+2) or putative biallelic neutral (0), identified using the GISTIC2 (17) algorithm in the TCGA samples and those using the FACETS (10) algorithm in the MSKCC samples, were the focus of our study. For the assessment of tumor mutational burden (TMB), the total number of somatic mutations identified was normalized to the exonic coverage of the respective MSK-IMPACT panel in megabases (13). Mutations in driver oncogenes were not excluded from the analysis (13). For each histology, cases in the top 20th, 40th, 60th, and 80th percentile of TMB were identified (13). Cases in the top 20th percentile of TMB within each histology were enrolled as the TMB-High group ($n = 268$).

Tumor Purity Estimate and Infiltration Levels of Immune Cells

To investigate the immune infiltration status of the tumors, we computed tumor purity using the ESTIMATE (18) (Estimation of STromal and Immune cells in MAlignant Tumor tissues using Expression data) method to analyze immune components and overall stroma in the TCGA pan-cancer cohort. To measure the relative levels of tumor-infiltrating lymphocyte subsets, we then employed gene expression-based computational methods to profile the infiltration levels of 25 immune cell populations in the TCGA pan-cancer cohort. Among the 25 immune cell populations, 24 immune cell populations were calculated using methods named Immune Infiltration Score (IIS) and T cell Infiltration Score (TIS), while infiltration of myeloid-derived suppressor cells (MDSCs) was calculated utilizing an algorithm named Tumor Immune Dysfunction and Exclusion (TIDE) (19, 20).

Gene Set Enrichment Analysis

Based on the hallmark gene sets (21), Gene Set Enrichment Analysis (GSEA) software version 3.0 (Broad Institute) (22) was used to identify the different regulated pathways between the *CCND1* amplification and neutral groups in the TCGA pan-cancer cohort ($|NES| > 1$, NOM P-value < 0.10, FDR q-value < 0.25). For significantly enriched pathways in the amplification group, single-sample gene set enrichment analysis (ssGSEA) was used to calculate the enrichment score in individual samples. The rank-sum test was performed to evaluate the statistical difference.

Statistical Methods

Differences between the two groups were examined by two-tailed, unpaired t-test. Kaplan–Meier survival and multivariate Cox regression analyses were used to analyze associations

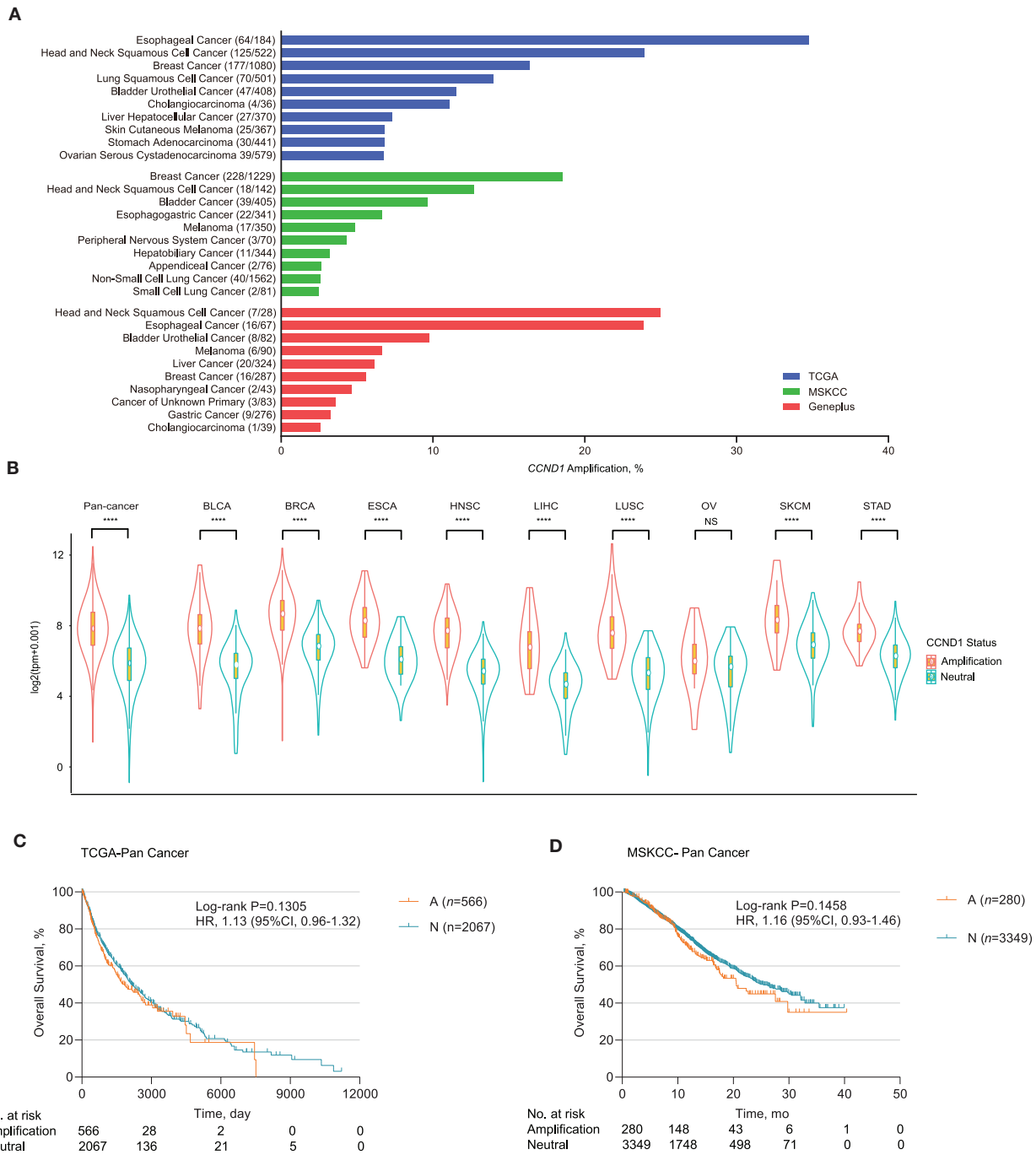

FIGURE 1 | Profile of *cyclin D1 (CCND1)* amplification and association with prognosis. **(A)** Distribution of the top 10 cancer types with the frequency of *CCND1* amplification in The Cancer Genome Atlas (TCGA) (n = 10,606), Memorial Sloan Kettering Cancer Center (MSKCC) (n = 10,109), and Geneplus (n = 6,536) databases. Cancers were sorted according to the frequency of *CCND1* amplification. **(B)** The gene expression profile of *CCND1* between the amplification group and the neutral group in the TCGA pan-cancer cohort (n = 2,633). The white dot represents the median value. The bottom and top of the violins are the 25th and 75th percentiles (interquartile range). Differences between the two groups were evaluated by unpaired t-tests. ns $P \geq 0.05$; $^{*}P < 0.05$; $^{**}P < 1 \times 10^{-2}$; $^{***}P < 1 \times 10^{-3}$; $^{****}P < 1 \times 10^{-4}$. **(C)** Kaplan–Meier survival analysis of overall survival (OS) comparing the *CCND1* amplification and neutral groups in patients in the TCGA pan-cancer cohort (n = 2,633). **(D)** Kaplan–Meier survival analysis of OS comparing the *CCND1* amplification and neutral groups in patients in the MSKCC pan-cancer cohort (n = 3,629).

between *CCND1* status and survival. Log-rank tests were used to determine significant differences of survival curves stratified by TMB. Statistical analyses were performed using SPSS statistical software version 23.0 (SPSS) and Prism analysis and graphic software version 8.0.1 (GraphPad). A two-sided P-value of <0.05 was considered statistically significant.

RESULT

Distribution and Clinical Implication of the *CCND1* Amplification Profile Landscape

We analyzed *CCND1* amplification of 6,536 patients from the Geneplus 1,021 panel in a Chinese population and found that HNSCC had a high *CCND1* amplification in 25.00% of the cases (7/28), followed by ESCA in 23.88% (16/67), BLCA in 9.76% (8/82), and melanoma in 6.67% of cases (6/90) (**Figure 1A** and **Table S2**). Comparison of *CCND1* amplification in 10,606 patients from the TCGA database and 10,109 patients from the MSKCC database revealed that ESCA and breast carcinoma had the highest incidence in the TCGA patients at 34.78% (64/184) and MSKCC patients at 18.55% (228/1,229) databases, respectively (**Figure 1A**). Gene expression analysis from the TCGA database showed that *CCND1* amplification was significantly related to the upregulation of mRNA expression of *CCND1* across the top nine cancer types (TCGA pan-cancer: cancers with *CCND1* amplification frequency ranked first to 10th; CHOL was excluded because of the limited number of samples) (**Figure 1B**).

Next, we examined the association of *CCND1* amplification with clinical outcome for pan-cancer in the TCGA and MSKCC databases. Kaplan–Meier survival analysis showed that *CCND1* amplification was not associated with median OS for pan-cancer in the TCGA database. The median OS for the *CCND1* amplification and *CCND1* neutral groups was 1,838.0 and 2,133.0 days, respectively [$P = 0.1305$, HR 1.13 (95% CI 0.96–1.32); **Figure 1C**]. In the MSKCC database, the median OS for the *CCND1* amplification and *CCND1* neutral groups was 20.6 and 25.4 months, respectively [$P = 0.1458$, HR 1.16 (95% CI 0.93–1.46); **Figure 1D**]. We then further investigated the role of *CCND1* amplification in specific cancer types. We did find a significantly decreased OS for HNSCC in the TCGA database. The median OS for the *CCND1* amplification and *CCND1* neutral groups was 1,079.0 and 2,002.0 days, respectively [$P = 0.0125$, HR 1.51 (95% CI 1.07–2.11); **Figure S1A**]. For melanoma in the MSKCC database, the median OS for the *CCND1* amplification and *CCND1* neutral groups was 13.5 months and not reached [$P = 0.0139$, HR 2.56 (95% CI 0.79–8.29); **Figure S1B**].

CCND1 Amplification Associated With Poor Prognosis in Patients Who Received Immune Checkpoint Inhibitors

We further explored the relationship between *CCND1* amplification and the clinical outcomes of ICIs. Publicly available datasets were utilized for this analysis, including four melanoma clinical cohorts. The Allen cohort (14) included 72 patients with melanoma treated with anti-CTLA-4, among whom six patients were classified as *CCND1* amplification; their disease-free survival (DFS) was inferior to that of 66 patients with the neutral phenotype [2.667 vs. 3.233 months, $P = 0.1196$, HR 2.001 (95% CI 0.5786–6.922); **Figure S1C**]. Then, we performed a pooled analysis on four melanoma cohorts treated with ICIs (the Robert cohort treated with anti-PD-1/L1 or anti-CTLA-4 or combination therapy, the Allen and Snyder cohorts treated with anti-CTLA-4 therapy, and the David cohort treated with anti-PD-1 therapy, $n = 464$) (13–16). A total of 31 patients were classified as having *CCND1* amplification, and their median OS was significantly shorter than 433 patients with a *CCND1* neutral status [18.51 vs. 32.27 months, $P = 0.0426$, HR 1.58 (95% CI 0.9163–2.724); **Figure 2A**].

Based on the impact of *CCND1* amplification as a negative prognostic factor for efficacy of ICIs in melanoma, we further investigated its role in patients with a solid tumor. To validate *CCND1* amplification as a clinical factor associated with poor prognosis in patients with solid tumors treated with ICIs, we performed three analyses. First, a total of 1,105 patients with a variety of cancer types who had received MSKCC-IMPACT testing and at least one dose of ICIs were evaluated and named the MSKCC-IO cohort (13). Fifty-two patients with *CCND1* amplification were identified comprising of 14 melanomas, 11 head and neck carcinomas (HNCs), 11 bladder carcinomas, eight non-small-cell lung carcinomas, five breast carcinomas, three esophagogastric carcinomas, and one glioma (**Table S3**). Across the entire cohort, *CCND1* amplification was associated with a decreased OS. The median OS for the *CCND1* amplification and *CCND1* neutral groups was 11.0 and 18.0 months, respectively [$P = 0.0024$, HR 1.63 (95% CI 1.09–2.43); **Figure 2B**]. We performed a stratified analysis with the melanoma ($n = 231$) and bladder carcinoma patients ($n = 111$) and observed a similar association between *CCND1* amplification with a shorter OS. In melanoma ($n = 231$), the median OS for the *CCND1* amplification and *CCND1* neutral groups was 22.0 and 42.0 months [$P = 0.0029$, HR 2.48 (95% CI 0.99–6.23); **Figure S1D**]. In bladder carcinoma ($n = 111$), the median OS for the *CCND1* amplification and *CCND1* neutral groups was 8.0 and 16.0 months, respectively [$P = 0.0244$, HR 2.17 (95% CI 0.83–5.66); **Figure S1E**].

Recent studies have shown that a high level of TMB associates with improved survival in patients receiving ICIs across a wide variety of cancer types (13, 23). We therefore explored the relationship between *CCND1* amplification and TMB, and their interaction related to ICI efficacy. We compared the TMB between the *CCND1* amplification group and the *CCND1* neutral group in the MSKCC-IO cohort and found no difference between the two groups. The median TMB for the *CCND1* amplification and *CCND1* neutral groups was 6.79 vs. 5.90 ($P = 0.46$; **Figure S2**). We then prepared a stratified analysis of the MSKCC IO-cohort by the percentile of the TMB subgroup. A clear profile demonstrated that the *CCND1* amplification patients did not benefit from ICIs regardless of TMB status (**Figure 2C**). Of note, according to a study by Robert M. Samstein et al. (13), in patients treated with ICIs, there is a significant association between a high level of TMB and a better OS. But in our stratified analysis, in spite of a high level of TMB, patients with *CCND1* amplification have a significantly decreased median OS [10.0 vs. 41.0 months, HR 2.82 (95% CI 1.11–7.20), $P = 0.0003$; **Figure 2D**]. Finally, a multivariable analysis using Cox proportional-hazards regression demonstrated that *CCND1* amplification was significantly associated with a shorter median OS [HR 1.60 (95% CI 1.16–2.21), $P = 0.0040$], with adjustment

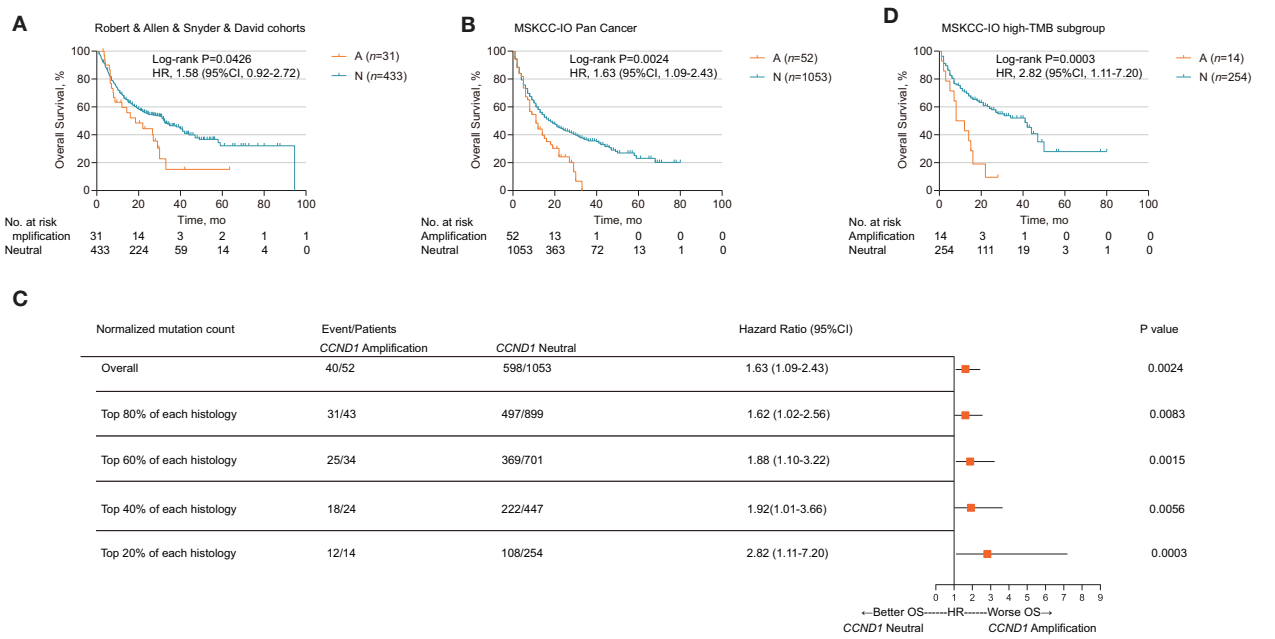

FIGURE 2 | Association of *cyclin D1 (CCND1)* amplification with prognosis in the Memorial Sloan Kettering Cancer Center (MSKCC)-IO cohort. **(A)** Kaplan–Meier survival analysis of overall survival (OS) comparing the *CCND1* amplification and neutral groups in patients with melanoma treated with immune checkpoint inhibitors (ICIs) from the Robert, Allen, Snyder, and David cohorts (n = 464). **(B)** Kaplan–Meier survival analysis of OS comparing the *CCND1* amplification and neutral groups in patients with solid tumors treated with ICIs in the MSKCC-IO pan-cancer cohort (n = 1,105). **(C)** Hazard ratios of *CCND1* status across patients with different levels of tumor mutational burden (TMB) in the MSKCC-IO pan-cancer cohort (n = 1,105). **(D)** Kaplan–Meier survival analysis of OS comparing the *CCND1* amplification and neutral groups in patients with solid tumors treated with ICIs identified with top 20% TMB within each histology in the MSKCC-IO cohort (n = 268).

for TMB, cancer type, age, drug class of ICI, and the year of ICI start (**Table S4**).

Furthermore, we compared the OS in *CCND1* amplification patients who received or did not receive ICIs. In the MSKCC cohort, data from Zehir et al. (12) reported 319 patients with *CCND1* amplification and 46 cases received ICIs. We found that the ICI group has a shorter median OS than the non-ICI group [17.5 vs. 22.6 months, HR 1.258 (95% CI 0.75–2.10), $P = 0.3411$; **Figure S3**]. Taken together, this implies that ICIs would not be useful for treating the *CCND1* amplification population.

CCND1 Amplification Is Significantly Associated With a Signature of Tumor Immunosuppression and Immune Cell Exclusion

Remarkable associations have been observed between the presence of immune cells, especially with tumor-specific T cell infiltration, and/or a T cell-associated inflammatory gene expression signature and the response to ICIs (23, 24). To assess the relationship between *CCND1* amplification and the landscape of immune cell infiltration, we used an algorithm called ESTIMATE (18) to analyze the infiltrating fraction of stromal and immune cells in tumor samples from the TCGA pan-cancer cohort (n = 2,633). We found that the median ESTIMATE score in the *CCND1* amplification group was significantly inferior to that in the neutral group (−849.10 vs. −696.23, $P = 0.0051$; **Figure 3A**). The analysis in nine individual cancer types showed that most cancer types exhibited a similar trend with the exception of melanoma, ESCA, and liver hepatocellular carcinoma. For example, in breast cancer, the *CCND1* amplification group showed a lower median ESTIMATE score (−669.12 vs. −245.99, $P = 0.0130$; **Figure 3A**). In HNSCC, the *CCND1* amplification group also exhibited a lower median ESTIMATE score (−849.10 vs. −716.92, $P = 0.0190$; **Figure 3A**).

To further characterize the levels of distinct immune cell subsets and the signals that are chemotactic for them, we employed a gene expression-based computational method to dissect infiltration of 25 immune cell subsets in the TCGA pan-cancer cohort (19, 20). Strikingly, the analysis of the transcriptomes revealed that, compared with the *CCND1* neutral group, the *CCND1* amplification group had a decrease in the median value of $CD8^+$ T cells (0.0854 vs. 0.0920, $P < 0.001$), cytotoxic cells (−0.1772 vs. −0.1564, $P = 0.0020$), dendritic cells (DCs) (−0.1692 vs. −0.1266, $P < 0.001$), plasmacytoid DC cells (pDCs) (−0.3249 vs. −0.3020, $P < 0.001$), and B cells (−0.1666 vs. −0.1419, $P < 0.001$). There was an increase in T helper cells (0.1677 vs. 0.1603, $P < 0.001$), regulatory T (Treg) cells (0.0240 vs. −0.3954, $P = 0.8890$), activated dendritic cell (−0.0787 vs. 0.0356, $P < 0.001$), and MDSCs (0.0115 vs. −0.0087, $P < 0.001$) (**Figure 3B**).

In the subtype analysis of 25 immune cell components in nine tumor types, we found that various degrees of tumor

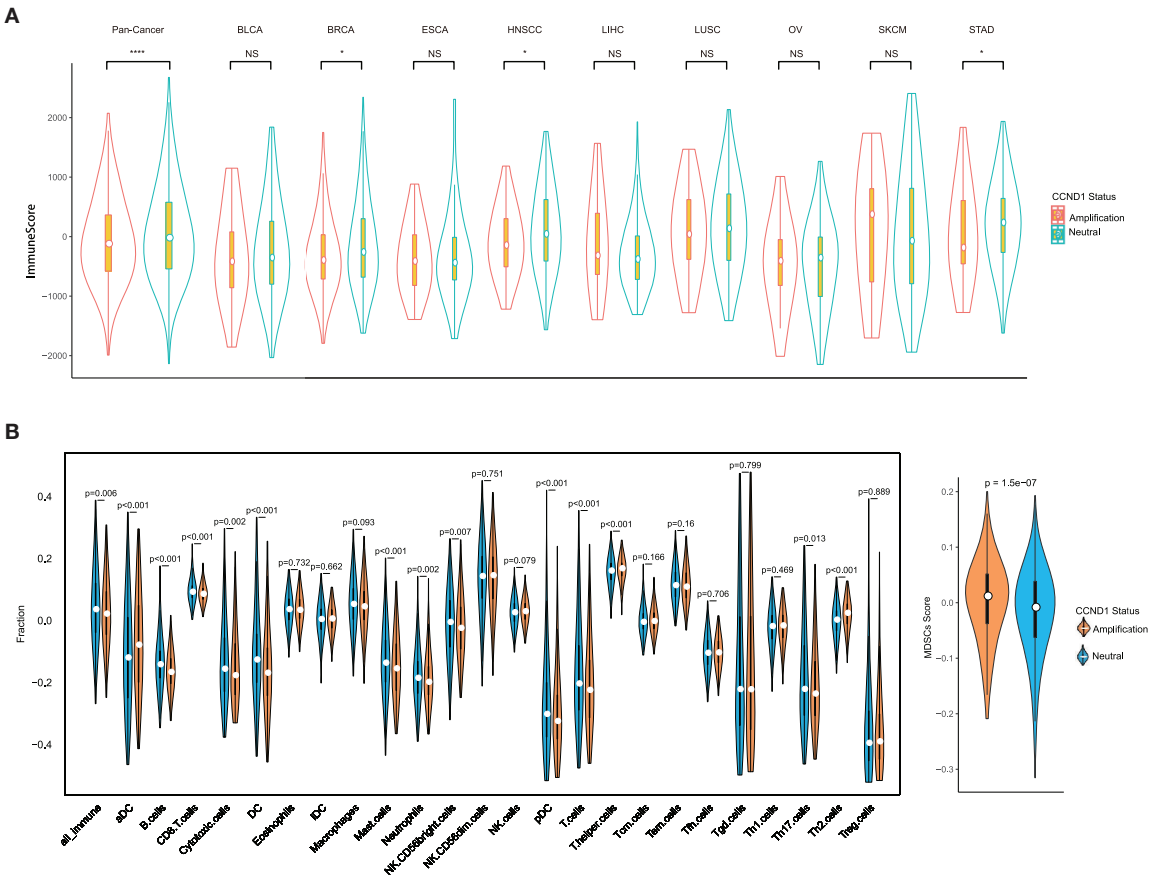

FIGURE 3 | Tumor purity estimate and infiltration levels of immune cells in The Cancer Genome Atlas (TCGA) pan-cancer cohort. **(A)** The ESTIMATE (Estimation of STromal and Immune cells in MAlignant Tumor tissues using Expression data) score of cancers between the *cyclin D1 (CCND1)* amplification group and the neutral group in TCGA pan-cancer cohort (n = 2,633). The white dot represents the median value. The bottom and top of the violins are the 25th and 75th percentiles (interquartile range). Differences between the two groups were evaluated by unpaired t-tests. ns $P \geq 0.05$; *$P < 0.05$; **$P < 1 \times 10^{-2}$; ***$P < 1 \times 10^{-3}$; ****$P < 1 \times 10^{-4}$. **(B)** The measurement of the infiltration levels of 25 immune cell populations between the *CCND1* amplification group and the neutral group in the TCGA pan-cancer cohort (n = 2,633). The median white dot represents the median value, while the upper and lower represent the minimum and maximum values. Differences between the two groups were evaluated by unpaired t-tests.

microenvironmental immunosuppression occurs (**Figure S4**). For example, the median values of B cells (−0.1870 vs. −0.1691, $P < 0.001$), T cells (−0.2160 vs. −0.1935, $P = 0.0090$), $CD8^+$ T cells (0.0914 vs. 0.1009, $P < 0.001$), and DC cells (−0.1810 vs. −0.1465, $P = 0.0170$) were significantly attenuated in the *CCND1* amplification group in breast cancer, while Th2 cells (0.05419 vs. 0.0148, $P < 0.001$) and MDSCs (0.0051 vs. −0.0198, $P = 0.0094$) appear upregulated (**Figure S4**). The signature of immune cell subsets in HNSCC showed a dramatic decrease in median values of cytotoxic cells (−0.1418 vs. −0.0970, $P = 0.0030$), T cells (−0.2357 vs. −0.2056, $P = 0.0010$), $CD8^+$ T cells (0.0730 vs. 0.0761, $P = 0.1310$), DC cells (−0.2267 vs. −0.1796, $P < 0.001$), and B cells (−0.1676 vs. −0.1373, $P < 0.001$), while MDSCs (0.0250 vs. −0.0058, $P < 0.001$) (**Figure S4**).

Multiple Aggressive, Immunosuppressive, and Angiogenic Hallmarks Related With *CCND1* Amplification

To investigate signaling pathways activated for *CCND1* amplification tumors, we performed GSEA comparing the *CCND1* amplification group and the *CCND1* neutral group in the TCGA pan-cancer cohort. GSEA revealed significant differences (false discovery rate-q ≤ 0.25) in the enrichment of the Hallmark database (**Figure 4A**). Notably, gene sets related to epithelial mesenchymal transition, mitotic spindle, myc targets, transforming growth factor (TGF)-β signaling, KRAS signaling, tumor necrosis factor (TNF)-α signaling via nuclear factor (NF)-κB, phosphoinositide 3-kinase (PI3K)/AKT/mammalian target of rapamycin (mTOR) signaling, p53 pathway, mTOR complex 1 (MTORC1) signaling, and the hypoxia signaling pathways

were differentially upregulated in the *CCND1* amplification phenotype (**Figure 4A**). Interestingly, in HNSCC, we also found angiogenesis in the *CCND1* amplification phenotype, while the activities of the interferon-α/β response, interleukin (IL)6-Janus kinase (JAK)-signal transducer and activator of transcription (STAT)3 signaling, and Wnt-β catenin signaling pathways were increased in the neutral phenotype (**Figure S5**).

Since TGF-β (encoded by *TGFB1*), hypoxia-inducible factor (HIF)1A (encoded by *HIF1A*), vascular endothelial growth factors (VEGFs) [encoded by *VEGFA-C*, *placental growth factor (PIGF)*, *VEGF receptor (VEGFR)1-3*], angiopoietin growth factors (encoded by *ANGPT1-2*), MET (encoded by *MET*), hepatocyte growth factor (HGF) (encoded by *HGF*), platelet-derived growth factors (PDGFs) (encoded by *PDGFA-D*, *PDGFRA-B*, *PDGFRL*), fibroblast growth factor (FGF)2 (encoded by *FGF2*), FGFR2 (encoded by *FGFR2*), and adhesion molecules [encoded by *intercellular adhesion molecule* (*ICAM)1*, *vascular cell adhesion molecule (VCAM)1*, *CD34*] might modify the cancer-related immune microenvironment and decrease the efficacy of immunotherapies (25), we analyzed the RNA-Seq data in TCGA focusing on single genes including *TGFB1*, *HIF1A*, *MET*, *HGF*, adhesion molecules, angiopoietin growth factors, PDGF family, and VEGFs family (**Table S5**). In the TME of TCGA pan-cancer cohort, *CCND1* amplification showed a statistically significant correlation with high expression of *TGFB1* (5.293 vs. 5.108, $P < 0.0001$), *VEGFA* (5.992 vs. 5.854, $P = 0.0073$), *VEGFB* (6.458 vs. 6.483, $P = 0.1283$), *ICAM1* (4.721 vs. 4.896, $P = 0.2596$), and *HIF1A* (6.028 vs. 5.761, $P < 0.0001$) in the TME (**Figure 4B** and **Figure S6**). Previous studies had revealed that *VEGFA* has direct or indirect effects on components of the immune system, including suppressing DC maturation and $CD8^+$ T cell proliferation (25) and affecting *ICAM1* to suppress NK cell and T cell trafficking (25), resulting in immunosuppressive outcomes. Another study showed that cyclin D1 (encoded by *CCND1*) may play a key role in the maintenance of VEGFs, and antisense to cyclin D1 could be useful for targeting both cancer cells and blood vessels in tumors (26). Above all, we deduced that anti-VEGFs/VEGFRs may potentially reverse the *CCND1* amplification that is associated with resistance to ICIs.

DISCUSSION

In this study, we comprehensively described the *CCND1* amplification profile in the TCGA and MSKCC databases and in a Chinese population in the Geneplus cohort. We found that *CCND1* amplification can hinder not only the natural host immune response but also the efficacy of ICIs. A *CCND1* amplification may potentially identify a patient population that will not benefit from ICIs irrespective of TMB status.

The *CCND1* located on human chromosome 11q13.3 is considered an oncogene, and it increases cell proliferation, growth, angiogenesis, and resistance to chemotherapy and radiotherapy (3, 4). To our knowledge, our results are the first to reveal that a *CCND1* amplification may significantly correlate with tumorigenesis and attenuation of various types of effector immune cells in the TME, including cytotoxic cells, T cells, $CD8^+$ T cells, DC cells, and B cells, and upregulation of Treg cells and MDSCs. Oncogenes such as *PDGFA-D*, *FGF2*, *HGF*, and *MET* are significantly overexpressed in the *CCND1* amplification group, promoting the development and progression of tumors. Previous studies have shown the role of the cytokine TGF-β, promoting immunosuppression in the TME (2, 20, 27, 28). In our analysis of the TCGA pan-cancer cohort, *CCND1* amplification showed a statistically significant correlation with high mRNA expression of *TGFB1*. More importantly, further study showed significant upregulation of mRNA expression of *VEGFA*, another known factor inducing tumor immune escape and immunotherapy resistance (25), associated with the *CCND1* amplification phenotype.

From the survival analysis in TCGA and MSKCC public databases, we found no significant correlation between *CCND1* amplification with prognosis in the pan-cancer group. There are some reasons to interpret this result. Firstly, the source of samples enrolled in the TCGA and MSKCC databases were diverse, and the clinical pathological characters of patients were complicated. Hence, the differences between cancer types must be taken into account. Secondly, in previous studies, methods such as Fluorescence *in situ* Hybridization (FISH), Chromogenic *in situ* Hybridization (CISH) or Reverse Transcription-Polymerase Chain Reaction (RT-PCR) were used to detect amplification of genes. Some studies used immunohistochemistry to stain cyclin D1. But there was no consistency on the definition of amplification of genes or the high- or low-expression level of cyclin D1 in various cancer types or within the same cancer type. Here, in our study, we used sequencing of genes by a CNV technique to detect amplification of genes. Meanwhile, the analysis of the transcriptome showed that the amplification of *CCND1* was strongly correlated with higher expression level of mRNA. This also increases the credibility of the results and unifies the consistency of the detection. Thirdly, according to our investigation, activations of a variety of oncogenes and deactivations of tumor suppressor genes were observed along with the amplification of CCND1 in different cancer types. Therefore, when the sample is enlarged and after balancing different tumor types, the value of *CCND1*'s impact on prognosis may be weakened.

Nevertheless, the *CCND1* amplification is a potential predictive biomarker for the use of ICIs in patients with solid tumors. In the melanoma pooled cohort, the median OS was shorter in the *CCND1* amplification subgroup. The survival analysis in the MSKCC-IO cohort further verified the negative impact of *CCND1* amplification on the efficacy of ICIs. Strikingly, by comparing *CCND1* amplification with TMB in patients with solid tumors from the MSKCC-IO cohort, we found that the association between *CCND1* amplification and a worse clinical outcome was more distinct in TMB-high patients. This indicates that ICIs may not be useful, and even harmful, to patients with *CCND1* amplification. We propose three hypotheses to explain the impairment for ICI efficacy. First, various types of effector immune cell exclusion and immunosuppression in the TME were found in tumors with *CCND1* amplification. Second, *CCND1* amplification results in high mRNA expression of *TGFB1*, *VEGFA*, and *HIF1A*; these molecules have direct or indirect

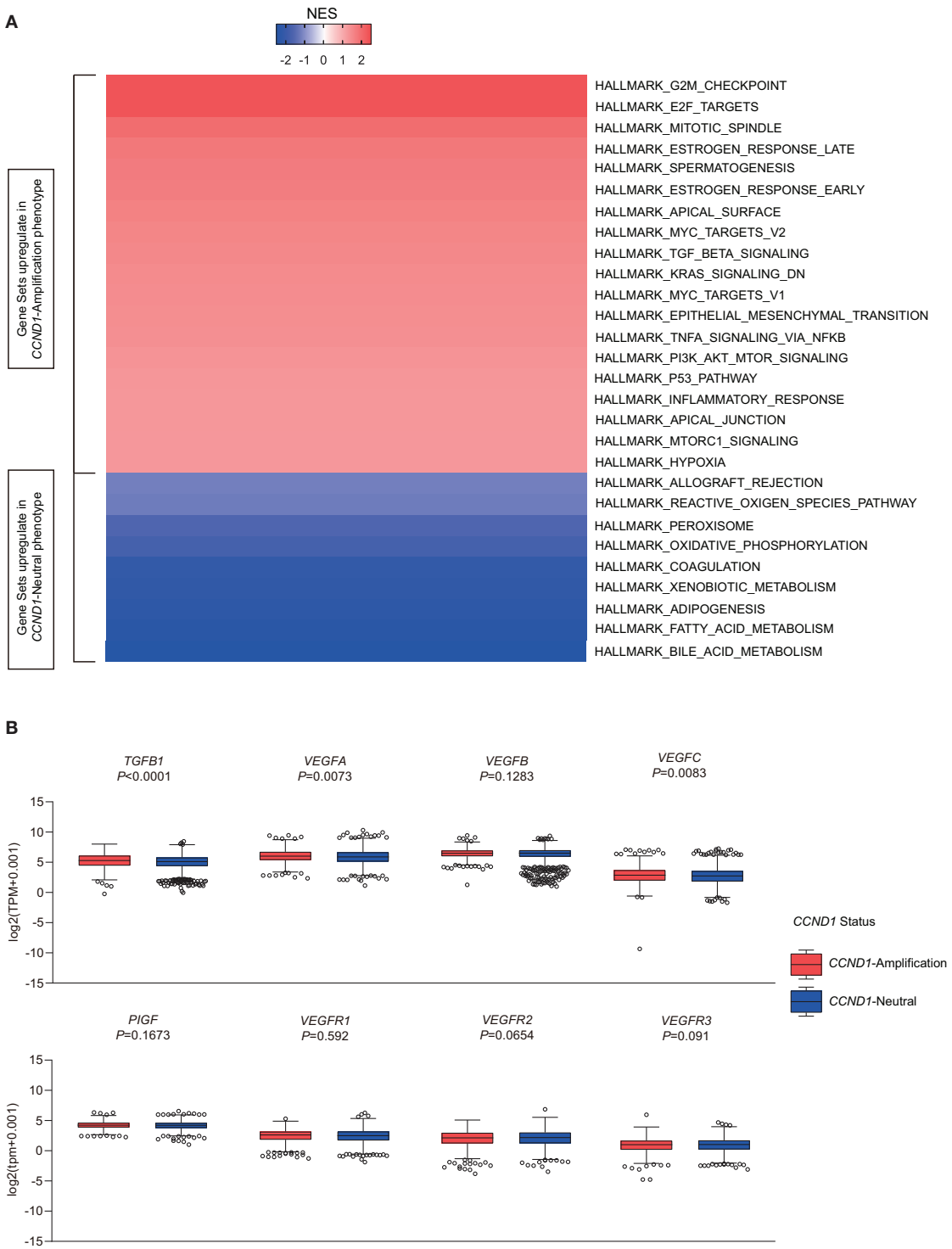

FIGURE 4 | Identification of hallmarks associated with *cyclin D1 (CCND1)* amplification in The Cancer Genome Atlas (TCGA) pan-cancer cohort ($n = 2,633$). **(A)** Different upregulation of inflammatory pathways among the *CCND1* amplification group and the *CCND1* neutral group in the TCGA pan-cancer cohort. The result is expressed according to the normalized enrichment score (NES). **(B)** The box and whiskers plots depict differences in transcript-level changes of *transforming growth factor (TGF)B1*, *vascular endothelial growth factor (VEGF)A–C*, *placental growth factor (PlGF)*, and *VEGF receptor (VEGFR)1–3* between the *CCND1* amplification group and the neutral group in the TCGA pan-cancer cohort. Within each group, the scattered dots represent gene values, and the thick line represents the median value. The bottom and top of the boxes are the 25th and 75th percentiles. Differences between the two groups were determined by unpaired *t*-tests.

negative effects on components of the immune system. Finally, some oncogene pathways are activated in *CCND1* amplification tumor that may lead to acceleration of tumor growth. Recently, a study reported on five patients experiencing hyper-progression who had NGS performed on pretreatment tumor tissue, and it confirmed CNAs in *MDM2*/*MDM4*, *epidermal growth factor receptor (EGFR)*, and several genes located on 11q13 associated with hyper-progression (29). So, these results will establish an important foundation for screening patients who might not benefit from ICI therapy.

Considering the immunosuppression in the TME and overexpression of various oncogenes caused by *CCND1* amplification, patients with such features should avoid ICI monotherapy. Multi-combination strategies including anti-angiogenesis agents or anti-TGF-β agents may eliminate the latent immunosuppressive factors in the TME and reverse the resistance to ICIs.

Our study has some limitations. When *CCND1* amplification is included in the interpretation of cancer prognosis, issues such as tumor type, standardization of detection, and accompanying gene mutation status should be fully considered. The small number of *CCND1* amplification tumors and the rarity of the event suggest that further additional data are warranted. The analysis of additional trials and cohorts will improve the precision of our estimates and the robustness of our findings. Our study is a preliminary investigation mainly focused on the predictive function of *CCND1* amplification in the tumor microenvironment in the aspect of genome and transcriptome. The full implication of *CCND1* amplification remains elusive and requires in-depth studies. Experiments to investigate the direct mechanism of *CCND1* amplification and primary immune resistance should be performed.

These findings indicate that *CCND1* amplification may be a key point related to immunosuppression in the TME and multiple malignancy hallmark; it may be a common mechanism of resistance to ICIs.

DATA AVAILABILITY STATEMENT

The raw data supporting the conclusions of this article will be made available by the authors, without undue reservation, to any qualified researcher.

ETHICS STATEMENT

The studies involving human participants were reviewed and approved by Ethics Committee of Fujian Provincial Cancer Hospital. Written informed consent to participate in this study was provided by the participants' legal guardian/next of kin. Written informed consent was obtained from the individual(s) for the publication of any potentially identifiable images or data included in this article.

AUTHOR CONTRIBUTIONS

YC, YH, XG, and YL were responsible for conducting the study, under the supervision of CC and XY, and contributed to the study design. YC, YH, XG, YL, JL, LChe, YX, GC, YG, LP, XX, ZG, JP, XY, LCha, and CC acquired the data. YC, YH, XG, YL, YX, YG, XX, ZG, JP, XY, and CC performed the data analysis and interpretation. YC, YH, XG, YL, and CC wrote and revised the manuscript. All authors contributed to the article and approved the submitted version.

FUNDING

This work was supported by the Fujian Provincial Health and Family Planning Research Talent Training Program under Grant (numbers 2018-ZQN-13 and 2018-CX-11) and Joint Funds for the Innovation of Science and Technology, Fujian Province under Grant (numbers 2017Y9077 and 2018Y9107).

ACKNOWLEDGMENTS

We appreciate all subjects who participated in this study and wish to thank Dr. Jianping Lu and Dr. Weifeng Zhu (Department of Pathology, Fujian Medical University Cancer Hospital & Fujian Cancer Hospital, Fuzhou, Fujian Province, China) and all colleagues (Cancer Bio-immunotherapy Center, Fujian Medical University Cancer Hospital) for IHC.

SUPPLEMENTARY MATERIAL

The Supplementary Material for this article can be found online at: https://www.frontiersin.org/articles/10.3389/fimmu.2020.01620/full#supplementary-material

REFERENCES

1. Chen DS, Mellman I. Elements of cancer immunity and the cancer-immune set point. *Nature*. (2017) 541:321–30. doi: 10.1038/nature21349
2. Sharma P, Hulieskovan S, Wargo JA, Ribas A. Primary, adaptive, and acquired resistance to cancer immunotherapy. *Cell*. (2017) 168:707–23. doi: 10.1016/j.cell.2017.01.017
3. Malumbres M, Barbacid M. To cycle or not to cycle: a critical decision in cancer. *Nat Rev Cancer*. (2001) 1:222–31. doi: 10.1038/35106065
4. Musgrove EA, Caldon CE, Barraclough J, Stone A, Sutherland RL. Cyclin D as a therapeutic target in cancer. *Nat Rev Cancer*. (2011) 11.8:558–72. doi: 10.1038/nrc3090
5. Saada-Bouzid E, Defaucheux C, Karabajakian A, Coloma VP, Servois V, Paoletti X, et al. Hyperprogression during anti-PD-1/PD-L1 therapy in patients with recurrent and/or metastatic head and neck squamous cell carcinoma. *Ann Oncol*. (2017) 28:1605–11. doi: 10.1093/annonc/mdx178
6. Yu J, Yan J, Guo Q, Chi Z, Tang B, Zheng B, et al. Genetic aberrations in the CDK4 pathway are associated with Innate resistance to PD-1 blockade in Chinese patients with non-cutaneous melanoma. *Clin Cancer Res*. (2019) 25:6511–23. doi: 10.1158/1078-0432.CCR-19-0475
7. Association WM. Declaration of Helsinki. Ethical principles for medical research involving human subjects. *J Indian Med Assoc*. (2009) 14:233–8. doi: 10.1515/9783110208856.233

8. Kristian C, Lawrence MS, Carter SL, Andrey S, David J, Carrie S, et al. Sensitive detection of somatic point mutations in impure and heterogeneous cancer samples. *Nat Biotechnol.* (2013) 31:213–9. doi: 10.1038/nbt.2514
9. Li J, Lupat R, Amarasinghe KC, Thompson ER, Doyle MA, Ryland GL, et al. CONTRA: copy number analysis for targeted resequencing. *Bioinformatics.* (2012) 28:1307–13. doi: 10.1093/bioinformatics/bts146
10. Shen R, Seshan VE. FACETS: allele-specific copy number and clonal heterogeneity analysis tool for high-throughput DNA sequencing. *Nucleic Acids Res.* (2016) 44:e131. doi: 10.1093/nar/gkw520
11. Caesar-Johnson SJ, Demchok JA, Felau I, Kasapi M, Ferguson ML, Hutter CM, et al. An integrated TCGA pan-cancer clinical data resource to drive high-quality survival outcome analytics. *Cell.* (2018) 173:400–16. doi: 10.1016/j.cell.2018.02.052
12. Zehir A, Benayed R, Shah RH, Syed A, Middha S. Mutational landscape of metastatic cancer revealed from prospective clinical sequencing of 10,000 patients. *Nat Med*. (2017) 23:703−13. doi: 10.1038/nm.4333
13. Samstein RM, Lee CH, Shoushtari AN, Hellmann MD, Shen R, Janjigian YY, et al. Tumor mutational load predicts survival after immunotherapy across multiple cancer types. *Nat Genet.* (2019) 51:202–6. doi: 10.1038/s41588-018-0312-8
14. Van Allen EM, Miao D, Schilling B, Shukla SA, Blank C, Zimmer L, et al. Genomic correlates of response to CTLA-4 blockade in metastatic melanoma. *Science.* (2015) 350:207–11. doi: 10.1126/science.aad0095
15. Snyder A, Makarov V, Merghoub T, Yuan J, Zaretsky JM, Desrichard A, et al. Genetic basis for clinical response to CTLA-4 blockade in melanoma. *N Engl J Med.* (2014) 371:2189–99. doi: 10.1056/NEJMoa1406498
16. Liu D, Schilling B. Integrative molecular and clinical modeling of clinical outcomes to PD1 blockade in patients with metastatic melanoma. *Nat Med*. (2019) 25:1916–27. doi: 10.1038/s41591-019-0654-5
17. Mermel CH, Schumacher SE, Hill B, Meyerson ML, Beroukhim R, Getz G. GISTIC2.0 facilitates sensitive and confident localization of the targets of focal somatic copy-number alteration in human cancers. *Genome Biol.* (2011) 12:R41. doi: 10.1186/gb-2011-12-4-r41
18. Yoshihara K, Shahmoradgoli M, Martinez E, Vegesna R, Kim H, Torres-Garcia W, et al. Inferring tumour purity and stromal and immune cell admixture from expression data. *Nat Commun.* (2013) 4:2612. doi: 10.1038/ncomms3612
19. Senbabaoglu Y, Gejman RS, Winer AG, Liu M, Van Allen EM, de Velasco G, et al. Tumor immune microenvironment characterization in clear cell renal cell carcinoma identifies prognostic and immunotherapeutically relevant messenger RNA signatures. *Genome Biol.* (2016) 17:231. doi: 10.1186/s13059-016-1092-z
20. Jiang P, Gu S, Pan D, Fu J, Sahu A, Hu X, et al. Signatures of T cell dysfunction and exclusion predict cancer immunotherapy response. *Nat Med.* (2018) 24:1550–8. doi: 10.1038/s41591-018-0136-1
21. Liberzon A, Birger C, Thorvaldsdã Ttir H, Ghandi M, Mesirov JP, Tamayo P. The Molecular Signatures Database (MSigDB) hallmark gene set collection. *Cell Syst.* (2015) 1:417–25. doi: 10.1016/j.cels.2015.12.004
22. Subramanian A, Tamayo P, Mootha VK, Mukherjee S, Ebert BL, Gillette MA, et al. Gene set enrichment analysis: a knowledge-based approach for interpreting genome-wide expression profiles. *Proc Natl Acad Sci USA.* (2005) 102:15545–50. doi: 10.1073/pnas.0506580102
23. Cristescu R, Mogg R, Ayers M, Albright A, Murphy E, Yearley J, et al. Pan-tumor genomic biomarkers for PD-1 checkpoint blockade-based immunotherapy. *Science.* (2018) 362:eaar3593. doi: 10.1126/science.aar3593
24. Sade-Feldman M, Jiao YJ, Chen JH, Rooney MS, Barzily-Rokni M, Eliane JP, et al. Resistance to checkpoint blockade therapy through inactivation of antigen presentation. *Nat Commun*. (2017) 8:1136. doi: 10.1038/s41467-017-01062-w
25. Khan KA, Kerbel SR. Improving immunotherapy outcomes with anti-angiogenic treatments and vice versa. *Nat Rev Clin Oncol.* (2018) 15:310–24. doi: 10.1038/nrclinonc.2018.9
26. Yasui M, Yamamoto H, Ngan CY, Damdinsuren B, Sugita Y, Fukunaga H, et al. Antisense to cyclin D1 inhibits vascular endothelial growth factor-stimulated growth of vascular endothelial cells: implication of tumor vascularization. *Clin Cancer Res.* (2006) 12:4720–9. doi: 10.1158/1078-0432.CCR-05-1213
27. Mariathasan S, Turley SJ, Nickles D, Castiglioni A, Yuen K, Wang Y, et al. TGFβ attenuates tumour response to PD-L1 blockade by contributing to exclusion of T cells. *Nature.* (2018) 554:544–8. doi: 10.1093/annonc/mdx760.001
28. Tauriello D, Batlle E. TGFβ drives immune evasion in genetically reconstituted colon cancer metastasis. *Nature.* (2018) 554:538. doi: 10.1038/nature25492
29. Singavi AK, Menon S, Kilari D, Alqwasmi A, Ritch PS, Thomas JP. Predictive biomarkers for Hyper-progression (HP) in response to Immune Checkpoint Inhibitors (ICI) – Analysis of Somatic Alterations (SAs). *Ann Oncol*. (2017) 28 (Suppl_5):v403–27. doi: 10.1093/annonc/mdx376

Conflict of Interest: XG, LC, YG, XX, YX, and XY are current employees of Geneplus-Beijing. YG, XX, and XY hold leadership positions and stocks of Geneplus-Beijing.

The remaining authors declare that the research was conducted in the absence of any commercial or financial relationships that could be construed as a potential conflict of interest.

frontiers in Immunology

ORIGINAL RESEARCH
published: 25 August 2020
doi: 10.3389/fimmu.2020.01900

Biomarkers of the Response to Immune Checkpoint Inhibitors in Metastatic Urothelial Carcinoma

Siteng Chen[1†], Ning Zhang[2†], Tao Wang[1], Encheng Zhang[1], Xiang Wang[1] and Junhua Zheng[1*]*

[1] Department of Urology, Shanghai General Hospital, Shanghai Jiao Tong University School of Medicine, Shanghai, China,
[2] Department of Urology, Ruijin Hospital, Shanghai Jiao Tong University School of Medicine, Shanghai, China

The mechanisms underlying the resistance to immune checkpoint inhibitors (ICIs) therapy in metastatic urothelial carcinoma (mUC) patients are not clear. It is of great significance to discern mUC patients who could benefit from ICI therapy in clinical practice. In this study, we performed machine learning method and selected 10 prognostic genes for constructing the immunotherapy response nomogram for mUC patients. The calibration plot suggested that the nomogram had an optimal agreement with actual observations when predicting the 1- and 1.5-year survival probabilities. The prognostic nomogram had a favorable discrimination of overall survival of mUC patients, with area under the curve values of 0.815, 0.752, and 0.805 for ICI response (ICIR) prediction in the training cohort, testing cohort, and combined cohort, respectively. A further decision curve analysis showed that the prognostic nomogram was superior to either mutation burden or neoantigen burden for overall survival prediction when the threshold probability was >0.35. The immune infiltrate analysis indicated that the low ICIR-Score values in mUC patients were significantly related to $CD8^+$ T cell infiltration and immune checkpoint-associated signatures. We also identified differentially mutated genes, which could act as driver genes and regulate the response to ICI therapy. In conclusion, we developed and validated an immunotherapy-responsive nomogram for mUC patients, which could be conveniently used for the estimate of ICI response and the prediction of overall survival probability for mUC patients.

Keywords: metastatic urothelial carcinoma, *PD-L1*, response, machine learning, nomogram

OPEN ACCESS

Edited by:
Maysaloun Merhi, Hamad Medical Corporation, Qatar

Reviewed by:
Bozena Kaminska, Nencki Institute of Experimental Biology (PAS), Poland
Georgi Guruli, Virginia Commonwealth University, United States

***Correspondence:**
Xiang Wang
seanw_hs@163.com
Junhua Zheng
zhengjh0471@sina.com

[†]These authors have contributed equally to this work and share first authorship

Specialty section:
This article was submitted to Cancer Immunity and Immunotherapy, a section of the journal Frontiers in Immunology

Received: *25 March 2020*
Accepted: *15 July 2020*
Published: *25 August 2020*

Citation:
Chen S, Zhang N, Wang T, Zhang E, Wang X and Zheng J (2020) Biomarkers of the Response to Immune Checkpoint Inhibitors in Metastatic Urothelial Carcinoma. Front. Immunol. 11:1900. doi: 10.3389/fimmu.2020.01900

INTRODUCTION

Urothelial carcinoma is one of the most aggressive malignancies, with an estimated 81,400 new cases and 17,980 deaths in the United States in 2020 (1). Up to 10–15% of initially diagnosed patients have metastatic urothelial carcinoma (mUC), with a 5-year survival possibility of 5% worldwide (2, 3). Currently, cisplatin-based combination chemotherapy is identified as the standard first-line therapy for mUC patients (4). However, more than 60% of mUC patients are not suitable for cisplatin treatment (5) due to their poor performance status or other comorbidities, including renal dysfunction, hearing loss, and heart failure (6). Hence, there remain tremendous practical demands for the development of optimal treatments for these patients.

Currently, developments in immune checkpoint inhibitor (ICI) therapy targeting programmed cell death 1 (*PD-1*) and *PD-1* ligand (*PD-L1*) have revolutionized the management of mUC (3, 7).

Compared with traditional chemotherapies, pembrolizumab, a PD-1 blockade drug, demonstrates robust antitumor activity and improves overall survival (OS) by almost 3 months in patients with advanced urothelial carcinoma (7). Unfortunately, only 20–30% of mUC patients achieve response to ICI therapy, and fewer patients could enjoy durable responses for more than 2 years (8). To date, the mechanisms underlying the resistance to ICI therapy in mUC patients are still not clear, suggesting the urgent clinical need for the identification of predictive biomarkers that could discern mUC patients who could benefit from ICI therapy.

Tumor mutational burden (TMB) (3) and DNA mismatch repair (DDR) (9) have been found to be related to the objective response to ICI therapy in mUC patients. However, limitations remain in the clinical application of TMB and DDR mutation status for mUC patients (10). The prognostic model reported by Guru Sonpavde et al. combined genomic and clinical factors to predict the response to anti-*PD-1*/*PD-L1* therapy among 62 patients with advanced urothelial carcinoma (11), and the results also need further validation due to the limited sample size.

In this study, by performing machine learning and nomogram methods, we aimed to create a nomogram model to predict the ICI response and the OS of mUC patients treated with ICI therapy, which could aid in decision-making in clinical practice.

MATERIALS AND METHODS

Patients and RNA Sequencing Data

IMvigor 210 trial was a clinical study (12) exploring the antitumor activity of the PD-L1 inhibitor atezolizumab in patients with mUC. The clinicopathological and the processed gene expression data of 348 mUC patients in IMvigor210 were retrieved from IMvigor210CoreBiologies, a free data resource based on the R environment (13). The baseline characteristics of the mUC patients included sex, race, and tobacco use history; metastatic sites: lymph node (LN) only, visceral, liver, and others; intravesical therapy (BCG) and chemotherapy (platinum); ICI therapy results: complete response (CR), partial response (PR), stable disease (SD), and progressive disease (PD); OS status; and immunotherapy indicators: PD-L1 expression level in immune cells (ICs), tumor cells (TCs), mutation burden per million base pair (Mb), and neoantigen burden per Mb.

The inclusion criteria were as follows: patients with mUC who were platinum refractory or cisplatin-ineligible and treated with atezolizumab, patients with sufficient therapy results (CR, PR, SD, or PD) and follow-up information, and patients with transcriptome RNA sequencing (RNA-seq) data. Patients with missing information on therapy results or survival data were excluded. Finally, 298 patients who met the abovementioned criteria were included and randomly assigned into a training cohort (200 patients) and a testing cohort (98 patients) for the following analyses.

A total of 134 patients with stage IV bladder cancer were also retrieved from The Cancer Genome Atlas (TCGA), as well as their clinical, RNA-seq, and somatic variant data for verification analysis.

Prognostic Nomogram Model Establishment

The RNA-seq data were $\log_2$-transformed before further analysis. Genes with very low expression levels were further filtered out. We used the *limma* package in the R environment to identify differentially expressed genes (DEGs) between ICI response and nonresponse patients with a p value <0.05 and $|\text{fold change}| > 1.5$. The ICI response patients were defined as mUC patients with CR or PR results after receiving the *PD-L1* inhibitor atezolizumab, while the patients with SD or PD results were defined as ICI nonresponse patients. The most useful genes for OS prediction were selected from the top 20 upregulated DEGs and the top 20 downregulated DEGs via the least absolute shrinkage and selection operator (LASSO) method (14) in the training cohort using the *glmnet* package in R. A prognostic nomogram model was then established based on the selected predictive genes via the *rms* and *nomogramEx* packages of R in the training cohort.

Evolution of the Prognostic Nomogram Model

Calibration with bootstrapping was conducted to verify the nomogram-predicted probabilities of 1- and 1.5-year OS by plotting these on the x-axis, with the actual OS plotted on the y-axis. The receiver operating characteristic (ROC) curve was performed to assess the specificity and the sensitivity of the nomogram through the area under the curve (AUC) value. The Kaplan–Meier (KM) curves of OS were compared between the low ICI response score (ICIR-Score) group and the high ICIR-Score group based on the log-rank test. Univariate and multivariate Cox regression analyses were also conducted to determine whether the ICIR-Score was an independent prognostic factor of OS. We also performed decision curve analysis (15) to compare the clinical usefulness of the nomogram, mutation burden (per Mb), and neoantigen burden (per Mb) by quantifying the net benefits at different threshold probabilities though the *rmda* package in R.

Immune Infiltrates and Potential Mechanism Analysis

We estimated the abundances of 22 types of ICs by using CIBERSORT (16). The infiltration scores of the mUC patients were estimated by an immune cell abundance identifier (17). The immunophenoscore based on the expression of major immunocompetence determinants was directly obtained from The Cancer Immunome Atlas for predicting the clinical benefits of tumor immunotherapy (18).

Immune infiltration-related Gene Ontology (GO) biological process and Kyoto Encyclopedia of Genes and Genomes (KEGG) gene sets were enriched via gene set enrichment analysis (GSEA) (19). We also performed somatic variant analysis to detect differentially mutated genes associated with the ICI response via the *maftools* package (20).

Statistical Analysis

Continuous variables were compared by a two-tailed Student's *t*-test or a one-way analysis of variance. Pearson's chi-square test was used to analyze categorical variables. Statistical Package for Social Sciences 24.0 software (SPSS Inc., Chicago, IL, USA) and R were used for statistical analysis. A P-value < 0.05 was regarded as significant.

RESULTS

Clinical Characteristics

The baseline clinical characteristics of the training and the testing cohorts are shown in **Table 1**. Except for the tumor metastasis sites, there was no significant difference in the other medical traits between the two cohorts, which indicated the good performance of the random assignment of mUC patients to the training and the testing cohorts. The baseline clinical characteristics of the TCGA cohort are shown in **Table S1**.

Identification of DEGs and Key Prognostic Genes

Using the *limma* package in the R environment, we identified 457 DEGs between ICI response (CR and PR) and nonresponse (SD and PD) patients, with a cutoff p-value of < 0.05 and |fold change| value over 1.5. Among the 457 DEGs, the top 20 upregulated DEGs and the top 20 downregulated DEGs, which were significantly highly correlated with ICI responsiveness, were further used to identify the most prognostic genes for OS prediction via the LASSO Cox regression method in the training cohort (**Table S2**). As shown in **Figure 1A**, the first vertical line pointed at 10, which equaled the minimum 10-fold cross-validated error. After calculating the active coefficients in **Figure 1B**, 10 key prognostic genes were selected by the LASSO Cox regression model. A further univariate Cox regression analysis was performed and identified that the 10 selected genes were significantly associated with OS in mUC patients receiving ICI therapy (**Table 2**). Finally, 10 prognostic genes, including six OS-favorable genes (*CDH18*, *CXCL10*, *FOXN4*, *SLC6A4*, *CXCL9*, and *PCDH11X*) and four OS-detrimental genes (ITIH2, BNC1, DAPL1, and FGB) from the training cohort, were used for further analysis.

Development and Evaluation of the Prognostic Nomogram

The prognostic nomogram for predicting the OS of mUC patients treated with ICI therapy was constructed based on the 10 selected genes in the training cohort. As shown in **Figure 1C**, each of the 10 selected genes contributed to the total points in the nomogram developed by using the *rms* and the *nomogramEx* packages of R. The total point, which was also called the ICIR-Score, was then acquired by adding the individual points together to predict the 1- and 1.5-year survival probabilities of mUC patients.

The calibration plot revealed that the 1- and 1.5-year survival probabilities predicted by our nomogram model had an excellent agreement with the actual observations (**Figures 2A,D**), indicating that the nomogram had a good ability to accurately predict the survival status of mUC patients treated with ICIs.

TABLE 1 | Baseline characteristics of mUC patients in the training cohort and the testing cohort.

Characteristics	All (%)	Training cohort (%)	Testing cohort (%)	*p* value
Sex				0.852
Male	233 (78.2)	157 (78.5)	76 (77.6)	
Female	65 (21.8)	43 (21.5)	22 (22.4)	
Race				0.529
White	270 (90.6)	182 (91.0)	88 (89.8)	
Asian	7 (2.3)	3 (1.5)	4 (4.1)	
Black	9 (3.0)	6 (3.0)	3 (3.1)	
Other	12 (4.0)	9 (4.5)	3 (3.1)	
ICI response				0.438
CR/PR	68 (22.8)	43 (21.5)	25 (25.5)	
SD/PD	230 (77.2)	157 (78.5)	73 (74.5)	
Intravesical BCG administered				0.370
Yes	67 (22.5)	48 (24.0)	19 (19.4)	
No	231 (77.5)	152 (76.0)	79 (80.6)	
Platinum received				0.852
Yes	233 (78.2)	157 (78.5)	76 (77.6)	
No	65 (21.8)	43 (21.5)	22 (22.4)	
Tobacco use				0.642
Yes	200 (67.1)	136 (68.0)	64 (65.3)	
No	98 (32.9)	64 (32.0)	34 (34.7)	
Metastasis sites				0.018
LN only	51 (17.1)	26 (13.0)	25 (25.5)	
Visceral (include liver)	220 (73.8)	157 (78.5)	63 (64.3)	
Other	27 (9.1)	17 (8.5)	10 (10.2)	
ICs level				0.571
IC0	83 (27.9)	54 (27.0)	29 (29.6)	
IC1	113 (37.9)	80 (40.0)	33 (33.7)	
IC2+	102 (34.2)	66 (33.0)	36 (36.7)	
TCs level				0.804
TC0	239 (80.2)	159 (79.5)	80 (81.6)	
TC1	17 (5.7)	11 (5.5)	6 (6.1)	
TC2+	42 (14.1)	30 (15.0)	12 (12.2)	
Mutation burden (per MB)	10.8 ± 9.4	10.4 ± 8.9	11.4 ± 10.3	0.448
Neoantigen burden (per MB)	1.4 ± 1.6	1.4 ± 1.6	1.3 ± 1.7	0.636

mUC, metastatic urothelial cancer; ICI, immune checkpoint inhibitor; CR, complete response; PR, partial response; SD, stable disease; PD, progressive disease; LN, lymph node; ICs level, PD-L1 expression level on immune cells; TCs level, PD-L1 expression level on tumor cells.

Less accuracy was found in the testing cohort (**Figures 2B,E**), which might be due to the small sample size of the testing cohort. The survival probability predicted by the nomogram had an excellent agreement with the actual observations in the combined cohort (**Figures 2C,F**). A subsequent ROC analysis revealed that our prognostic nomogram had favorable discrimination, with an AUC value of 0.815 (95% confidence interval: 0.754–0.867, $P < 0.0001$) for ICI response prediction in the training cohort (**Figure 2G**). Validation of the prognostic nomogram was

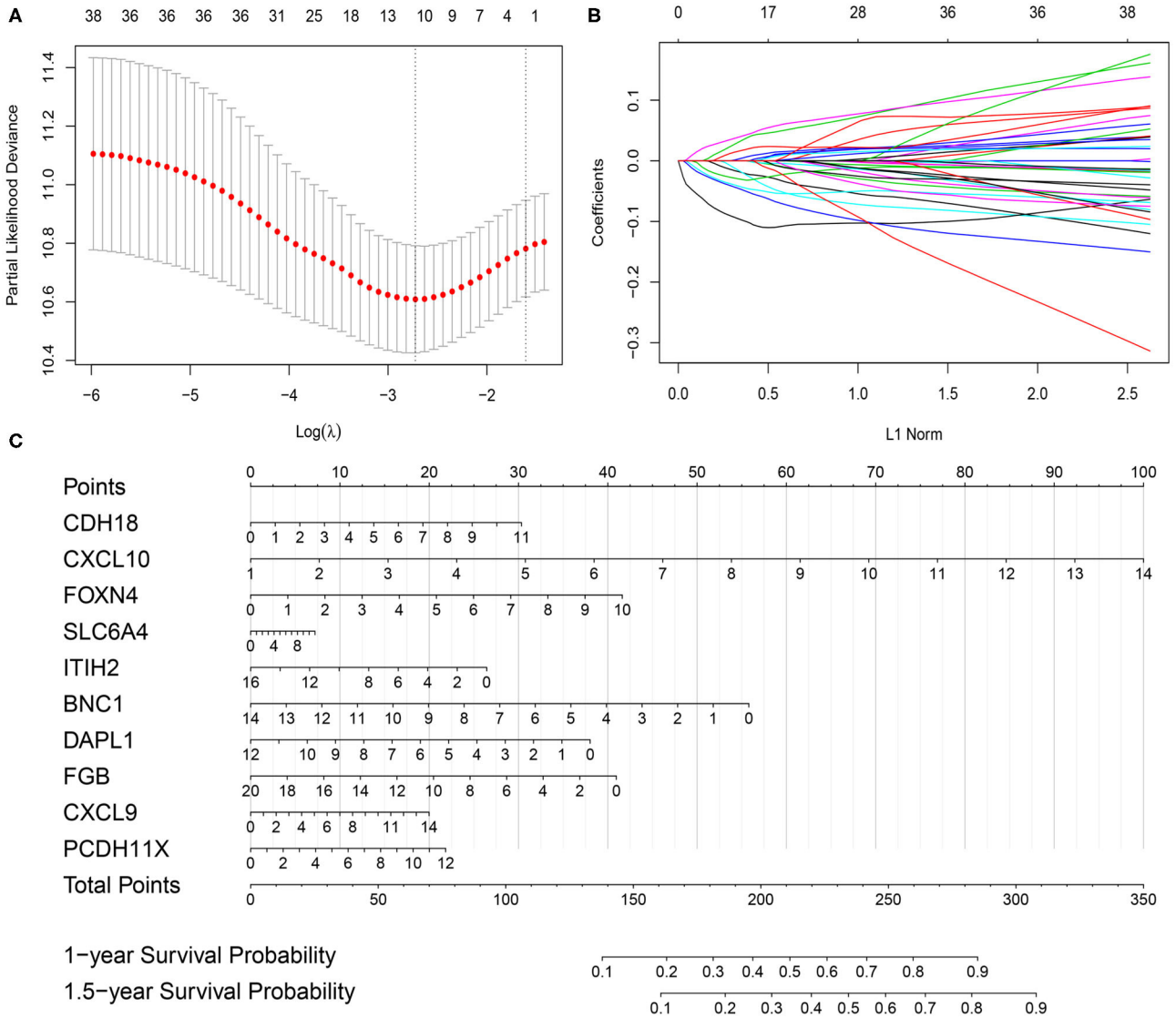

FIGURE 1 | Gene selection via the least absolute shrinkage and selection operator (LASSO) Cox regression model and establishment of the prognostic nomogram model in the training cohort. **(A)** Tenfold cross-validated error. The first vertical line equals the minimum error, whereas the second vertical line shows the cross-validated error within one standard error of the minimum. **(B)** The profile of coefficients in the model at varying levels of penalization plotted against the log (lambda) sequence. **(C)** Nomogram based on selected prognostic genes for the 1- and 1.5-year overall survival predictions in the training cohort. One-year survival probability = 7.9e-08* total points^3 −6.1263e-05 * total points^2 + 0.010410469 * total points + 0.388686628; 1.5-year survival probability = 1.45e-07 * total points^3 −9.7482e-05 * total points^2 + 0.016297495 * total points + 0.019957873.

performed in the testing cohort and the combined cohort, with AUC values of 0.752 (95% confidence interval: 0.654–0.834, $P < 0.0001$) and 0.805 (95% confidence interval: 0.755–0.848, $P < 0.0001$), respectively (**Figures 2H,I**), indicating the good prognostic ability of the nomogram for clinical use.

According to the KM survival analysis, our prognostic nomogram model was able to discriminate patients with poor prognosis from patients with favorable prognosis in both the training and the testing cohorts. The hazard ratios (HRs) of the high- and low-score groups were 3.51 (95% confidence interval: 2.44–5.05, $P < 0.0001$) in the training cohort, 3.11 (95% confidence interval: 1.84–5.26, $P = 0.002$) in the testing cohort, and 3.48 (95% confidence interval: 2.58–4.69, $P < 0.0001$) in the combined cohort (**Figures 2J–L**). Univariate and multivariate Cox regression analyses in the training cohort indicated that our prognostic ICIR-Score could serve as a predictor of OS in mUC patients, independent of other characteristics (**Table 3**).

A further decision curve analysis showed that, when the threshold probability was >0.35, using the prognostic nomogram for OS prediction showed more benefits than either mutation burden or neoantigen burden (**Figure 3**).

TABLE 2 | Univariate Cox regression analyses of 10 genes selected via LASSO analysis based on overall survival in the training cohort.

Characteristics	Cox regression analysis HR (95% CI)	*p* value	LASSO coefficient
Favorable			
CDH18	0.887 (0.809–0.973)	0.011	−0.020244481
CXCL10	0.862 (0.807–0.921)	<0.001	−0.098454694
FOXN4	0.877 (0.805–0.956)	0.003	−0.048390155
SLC6A4	0.896 (0.829–0.968)	0.005	−0.031102883
CXCL9	0.882 (0.831–0.936)	<0.001	−0.019969709
PCDH11X	0.859 (0.788–0.938)	0.001	−0.043952722
Detrimental			
ITIH2	1.075 (1.012–1.141)	0.018	0.004941391
BNC1	1.052 (1.003–1.103)	0.038	0.03469075
DAPL1	1.098 (1.041–1.158)	0.001	0.041243449
FGB	1.046 (1.002–1.091)	0.040	0.017649583

LASSO, least absolute shrinkage and selection operator; HR, hazard ratio; CI, confidence interval.

Low ICIR-Score Values in mUC Patients Were Associated With CD8$^+$ T Cell Infiltration and the Immune-Checkpoint-Associated Signature

As shown in **Figure 4A**, different abundances of ICs were identified between mUC patients with low and high ICIR-Score values. For example, mUC patients with low ICIR-Score values had higher abundances of activated CD8$^+$ T cells, M1 macrophages, and follicular helper T cells. In addition, the low ICIR-Score values in mUC patients were associated with higher expression levels of some chemokines (**Figure 4B**), including *CXCL9* and *CXCL10*, which have been proven to attract dendritic cells and CD8$^+$ T cells (21). In addition, the higher expression levels of MHC molecules and co-inhibitors were also found to be associated with low ICIR-Score values. Correlation analyses indicated that the mRNA expression levels of ICIs, including CD274 (PD-L1), PDCD1 (*PD-1*), *CTLA-4*, *LAG-3*, and *TIM-3* (*HAVCR2*), were inversely correlated with the ICIR-Score (**Figure 4C**).

GSEA revealed that low ICIR-Score values were significantly associated with several immune infiltration-related biological processes, including the T cell receptor signaling pathway, antigen processing and presentation via MHC II, immune response regulating the cell surface receptor signaling pathway, and antigen receptor-mediated signaling pathway (**Figures 4D,E**). A further analysis revealed that, compared with patients in the high ICIR-Score group, the mUC patients in the low-ICIR-Score group were statistically associated with a higher infiltration score (**Figure 4F**), which might account for the probable sensitivity to ICI therapy.

The mutation landscapes of mUC patients with high ICIR-Score values and low ICIR-Score values are shown in **Figure 5A**. Differentially mutated genes, including *EIF4G1*, *CNTNAP2*, *SCAF4*, *MBD6*, *ITGA4*, *AUTS2*, *COL6A6*, *MYCBP2*, *DST*, *NUP107*, and *MYH9* in the low-ICIR-Score group and *RXRA* in the high-ICIR-Score group (**Figure 5B**), might act as driver genes and result in differential responses to ICI therapy in mUC. Higher infiltration scores and immunophenoscores were also identified in mUC patients with low ICIR-Score values in the TCGA cohort (**Figure 5C**).

DISCUSSION

In this study, we designed and validated a gene signature-based nomogram that was associated with ICI response and could predict the OS of mUC patients treated with ICI therapy. Bic-NaSong et al. identified an immunotherapy-responsive molecular subtype of bladder cancer based on a cluster of 1,627 genes, in which a class 3 cluster was reported to be associated with ICI response because of their high rates of alterations in DDR genes and somatic mutations (22). In this study, our prognostic nomogram comprises only 10 prognostic genes, including six OS-favorable genes and four OS-detrimental genes. Among them, *CDH18*, *CXCL10*, *FOXN4*, *SLC6A4*, *CXCL9*, and *PCDH11X* are highly associated with ICI response in patients with mUC.

The mUC patients with clinical benefits from ICI therapy were successfully stratified by the prognostic nomogram in both the training cohort and the testing cohort, with HR values of 3.51 and 3.11, respectively, which facilitated the preoperative individualized prediction of ICI response. Accurate predictions of the 1- and 1.5-year survival probabilities of ICI-treated mUC patients were also observed in this study, indicating the good ability of the prognostic nomogram for OS prediction.

ICI response status is a vital clinical factor for patients receiving anti-*PD-1*/*PD-L1* treatment. In a multicenter clinical trial, the objective response rate of cisplatin-ineligible mUC patients treated with pembrolizumab was 24% (23). The objective response rate to another ICI, atezolizumab, was 23%, and the complete response rate was only 9% (3). Our prognostic nomogram performed well in accurately predicting ICI response in mUC patients, with AUC values up to 0.815 in the training cohort, which indicated a good performance for clinical practice.

A further decision curve analysis showed that, when the threshold probability was >0.35, the prognostic nomogram for OS prediction could add more benefit than either mutation burden or neoantigen burden. TMB has been reported to be a significant predictor for the treatment response to ICIs in urothelial cancer in various studies (3, 13, 22). However, high TMB in mUC patients is not sufficient to predict ICI response (9). In addition, whole-exome sequencing for calculating TMB is expensive, which impedes its widespread use in clinical practice (24). Incorporating only 10 genes, our prognostic nomogram seems to be more cost-effective and time-saving in clinical application.

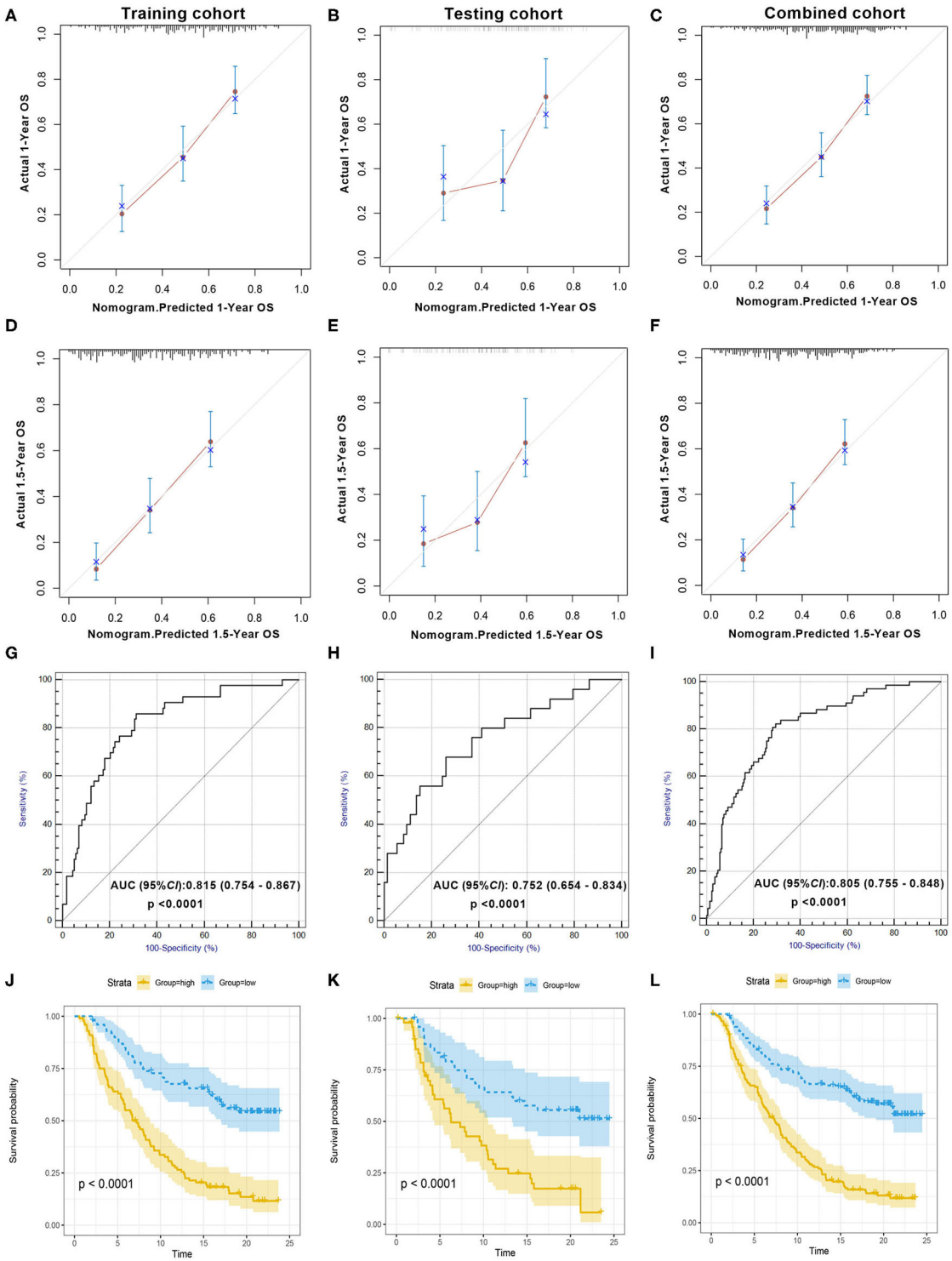

FIGURE 2 | Evaluation of the prognostic nomogram model in the training cohort, testing cohort, and combined cohort. Validity of the predictive performance of the nomogram in the training cohort **(A,D)**, testing cohort **(B,E)**, and combined cohort **(C,F)**. Nomogram-predicted probabilities of 1- and 1.5-year overall survival are plotted on the x-axis; actual overall survival is plotted on the y-axis. ROC curve evaluating the prognostic accuracy of ICI response prediction by nomogram score in the training cohort **(G)**, testing cohort **(H)**, and combined cohort **(I)**. Kaplan–Meier curves of the training cohort **(J)**, testing cohort **(K)**, and combined cohort **(L)**. The median scores of the nomogram in two cohorts were defined as the cutoff value for the high-score and the low-score group, respectively. ROC, receiver operator characteristic; AUC, area under the curve; ICI, immune checkpoint inhibitor.

TABLE 3 | Univariate and multivariate Cox regression analyses of mUC patients based on nomogram score and other characteristics in the training cohort.

Characteristics	Univariate analysis HR (95% CI)	*p* value	Multivariate analysis HR (95% CI)	*p* value
Sex (male vs. female)	1.263 (0.816–1.956)	0.294	/	/
Race (White vs. others)	1.686 (0.824–3.450)	0.153	/	/
Intravesical BCG administered	0.860 (0.565–1.307)	0.480	/	/
Platinum received	0.522 (0.352–0.775)	0.001	0.788 (0.509–1.221)	0.287
Tobacco use history	1.541 (1.041–2.282)	0.031	1.417 (0.935–2.148)	0.100
Metastasis sites				
Visceral vs. LN only	0.585 (0.364–0.940)	0.027	0.597 (0.370–0.963)	0.034
Visceral vs. other	0.796 (0.436–1.453)	0.458	/	/
IC level	1.041 (0.828–1.308)	0.730	/	/
TC level	1.306 (0.818–1.311)	0.772	/	/
Mutation burden (per MB)	1.017 (0.998–1.037)	0.080	/	/
Neoantigen burden (per MB)	1.059 (0.956–1.173)	0.272	/	/
Nomogram score	1.015 (1.011–1.019)	<0.001	1.014 (1.009–1.018)	<0.001

mUC, metastatic urothelial cancer; LN, lymph node; IC Level, PD-L1 expression on immune cells; TC, PD-L1 expression on tumor cells; HR, hazard ratio; CI, confidence interval.

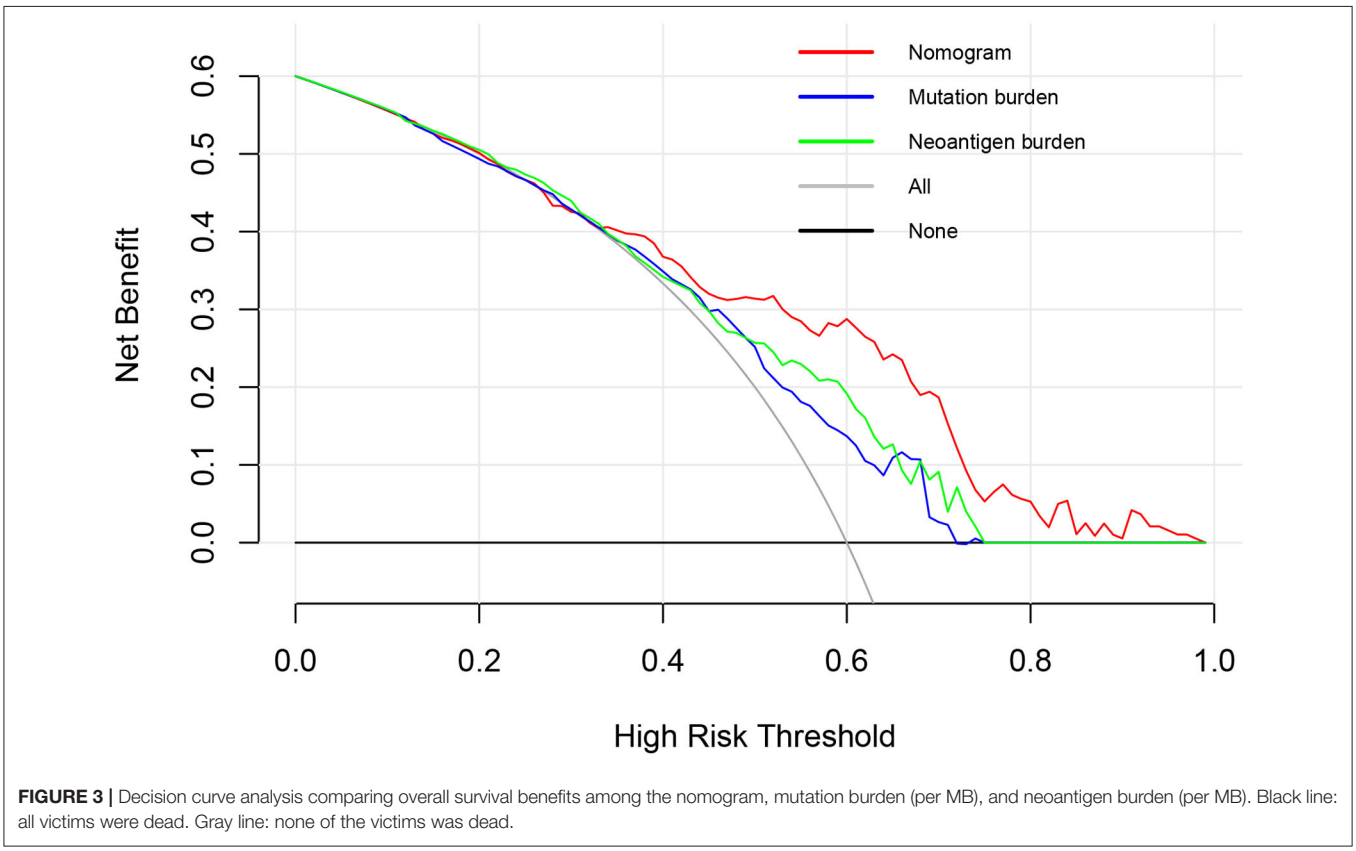

FIGURE 3 | Decision curve analysis comparing overall survival benefits among the nomogram, mutation burden (per MB), and neoantigen burden (per MB). Black line: all victims were dead. Gray line: none of the victims was dead.

The low ICIR-Score values in mUC patients were found to be associated with $CD8^+$ T cell infiltration, conforming to the T cell activation-related biological processes and pathways, which include the T cell receptor signaling pathway and antigen processing and presentation via MHC II.

There are also some notable limitations in our study. First, experimental validation was not performed in this study. The genes used in the nomogram were measured by RNA-seq, which still needs further verification by molecular biology. Second, since this study is a retrospective analysis with data retrieved from IMvigor210CoreBiologies (13), the baseline characteristics of the mUC patients were incomplete. For example, we failed to obtain information about the dose and the schedule of ICIs from IMvigor210CoreBiologies. Third,

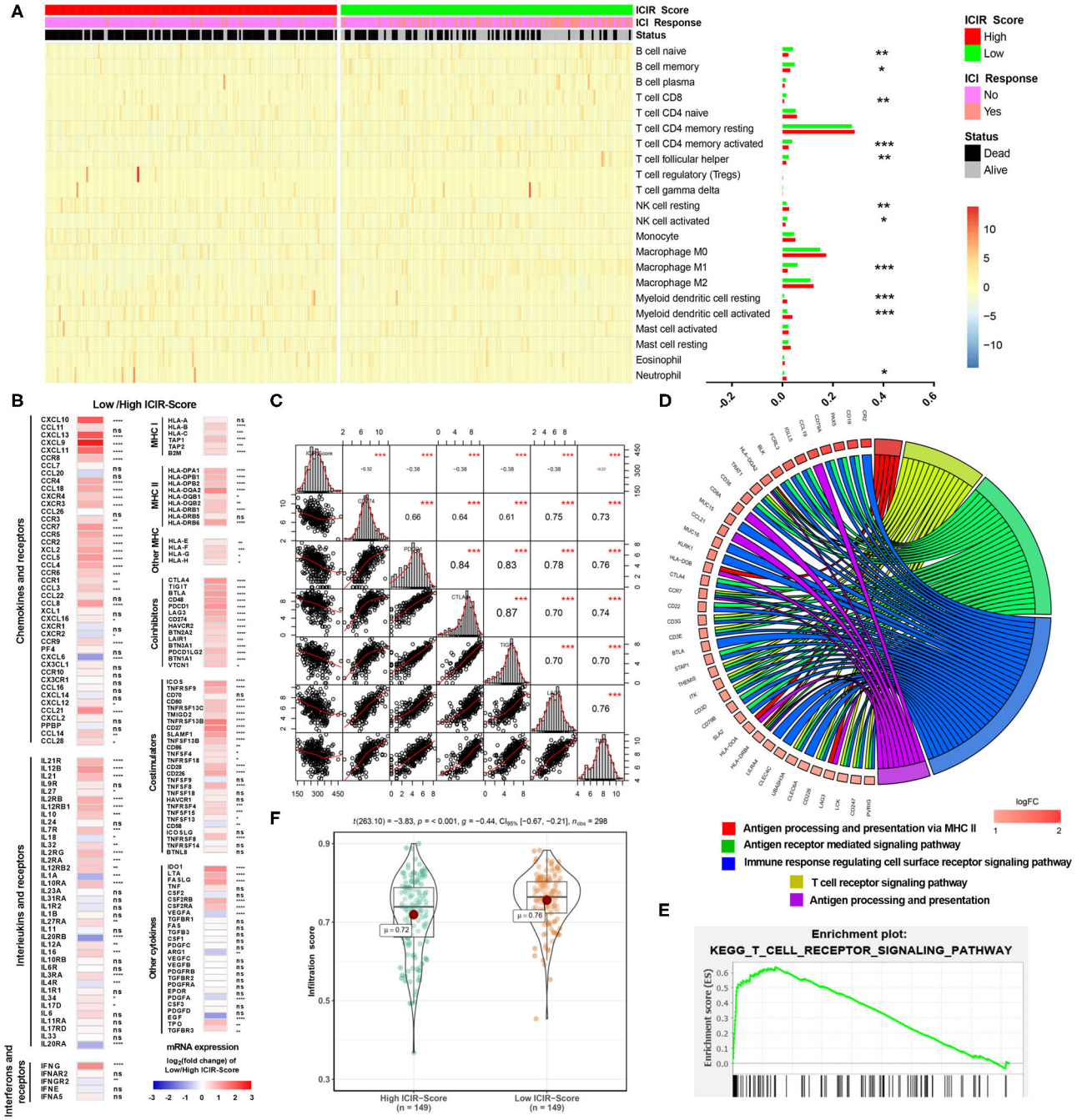

FIGURE 4 | Immune infiltrates and potential mechanism analyses of mUC patients with low ICIR-Score. **(A)** Heatmap and bar graph illustrating the different abundance of 22 immune cell types based on CIBERSORT between mUC patients with high ICIR-Score and low ICIR-Score. **(B)** Expression levels of chemokines, interleukins, interferons, MHC molecules, co-stimulators, co-inhibitors, and other important cytokines and their receptors in mUC patients with low ICIR-Score relative those with high ICIR-Score, shown as $\log_2$(fold change) of expression value of the respective mRNA. **(C)** Correlation analyses of ICIR-Score and expression levels of immune checkpoint inhibitors in mUC patients. **(D,E)** Gene Ontology and Kyoto Encyclopedia of Genes and Genomes analyses of the differentially expressed genes for mUC patients with low ICIR-Score values using gene set enrichment analysis. **(F)** Comparison of infiltration score of mUC patients between high ICIR-Score group and low ICIR-Score group. mUC, metastatic urothelial cancer; ICIR-Score, immune checkpoint inhibitor response score.

some potential medical traits, including physical condition and nutritional status, were neglected. Despite these limitations, this study is the largest cohort study of a prognostic nomogram based on gene signatures for ICI efficacy and OS prediction in patients with mUC. Independent of the pathological stage, our prognostic nomogram could help

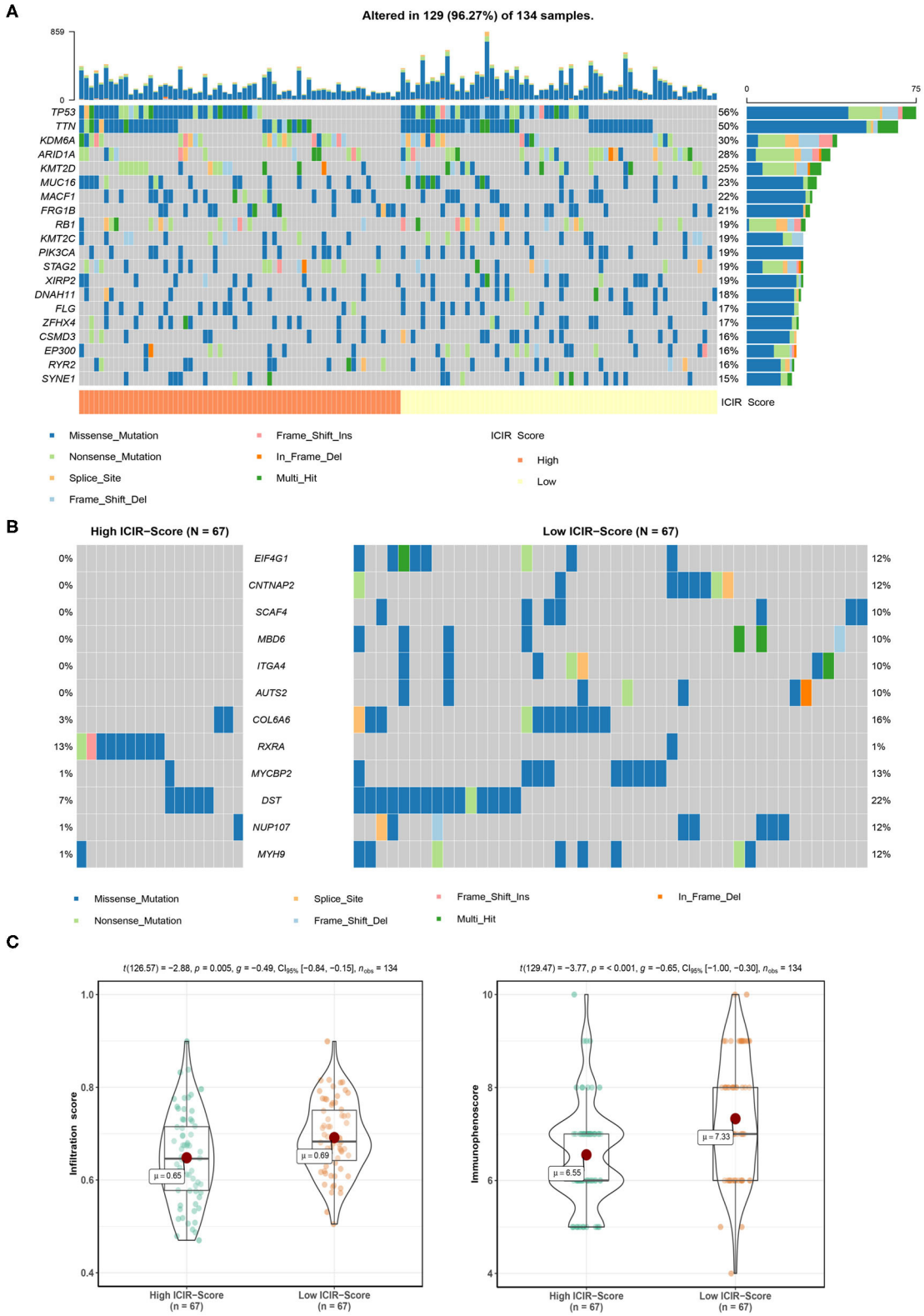

FIGURE 5 | Mutation analysis of mUC patients in The Cancer Genome Atlas cohort. **(A)** Mutation landscape of mUC patients with high ICIR-Score and low ICIR-Score. **(B)** Mutation plot detecting differentially mutated genes between mUC patients in the high ICIR-Score group and the low ICIR-Score group. **(C)** Comparison of infiltration score and immunophenoscore of mUC patients between the high ICIR-Score group and the low ICIR-Score group. mUC, metastatic urothelial cancer; ICIR-Score, immune checkpoint inhibitor response score.

clinicians make more accurate ICI therapy decisions in clinical practice.

In conclusion, based on the 10 prognostic genes associated with ICI therapy, we developed and validated an immunotherapy response nomogram for mUC patients. The prognostic nomogram model has the potential to facilitate the estimation of ICI response and the prediction of OS in patients with mUC, even though experimental validation and prospective validation studies are still needed.

DATA AVAILABILITY STATEMENT

Publicly available datasets were analyzed in this study. This data can be found here: http://research-pub.gene.com/IMvigor210CoreBiologies/.

ETHICS STATEMENT

Ethical review and approval was not required for the study on human participants in accordance with the local legislation and institutional requirements. Written informed consent for participation was not required for this study in accordance with the national legislation and the institutional requirements.

AUTHOR CONTRIBUTIONS

XW, JZ, and SC conceived and designed the study. EZ and TW performed the data collection. SC and NZ analyzed the data and wrote the paper. JZ and SC revised the paper. All the authors read and approved the final manuscript.

FUNDING

This work was supported by the National Natural Science Foundation of China (81972393, 81772705, and 81570607).

SUPPLEMENTARY MATERIAL

The Supplementary Material for this article can be found online at: https://www.frontiersin.org/articles/10.3389/fimmu.2020.01900/full#supplementary-material

REFERENCES

1. Siegel RL, Miller KD, Jemal A. Cancer statistics, (2020). *Cancer J Clin.* (2020) 70:7–30. doi: 10.3322/caac.21590
2. Stein JP, Lieskovsky G, Cote R, Groshen S, Feng AC, Boyd S, et al. Radical cystectomy in the treatment of invasive bladder cancer: long-term results in 1,054 patients. *J Clin Oncol.* (2001) 19:666–75. doi: 10.1200/JCO.2001.19.3.666
3. Balar AV, Galsky MD, Rosenberg JE, Powles T, Petrylak DP, Bellmunt J, et al. Atezolizumab as first-line treatment in cisplatin-ineligible patients with locally advanced and metastatic urothelial carcinoma: a single-arm, multicentre, phase 2 trial. *Lancet.* (2017) 389:67–76. doi: 10.1016/S0140-6736(16)32455-2
4. Alfred Witjes J, Lebret T, Compérat EM, Cowan NC, De Santis M, Bruins HM, et al. Updated 2016 EAU guidelines on muscle-invasive and metastatic bladder cancer. *Eur Urol.* (2017) 71:462–75. doi: 10.1016/j.eururo.2016.06.020
5. Galsky MD, Hahn NM, Rosenberg J, Sonpavde G, Hutson T, Oh WK, et al. Treatment of patients with metastatic urothelial cancer "unfit" for Cisplatin-based chemotherapy. *J Clin Oncol.* (2011) 29:2432–8. doi: 10.1200/JCO.2011.34.8433
6. Bellmunt J, Mottet N, De Santis M. Urothelial carcinoma management in elderly or unfit patients. *EJC Suppl.* (2016) 14:1–20. doi: 10.1016/j.ejcsup.2016.01.001
7. Bellmunt J, de Wit R, Vaughn DJ, Fradet Y, Lee JL, Fong L, et al. Pembrolizumab as second-line therapy for advanced urothelial carcinoma. *N Engl J Med.* (2017) 376:1015–26. doi: 10.1056/NEJMoa1613683
8. Cheng W, Fu D, Xu F, Zhang Z. Unwrapping the genomic characteristics of urothelial bladder cancer and successes with immune checkpoint blockade therapy. *Oncogenesis.* (2018) 7:2. doi: 10.1038/s41389-017-0013-7
9. Teo MY, Seier K, Ostrovnaya I, Regazzi AM, Kania BE, Moran MM, et al. Alterations in DNA damage response and repair genes as potential marker of clinical benefit from PD-1/PD-L1 blockade in advanced urothelial cancers. *J Clin Oncol.* (2018) 36:1685–94. doi: 10.1200/JCO.2017.75.7740
10. Roh W, Chen P-L, Reuben A, Spencer CN, Prieto PA, Miller JP, et al. Integrated molecular analysis of tumor biopsies on sequential CTLA-4 and PD-1 blockade reveals markers of response and resistance. *Sci Transl Med.* (2017) 9:eaah3560. doi: 10.1126/scitranslmed.aah3560
11. Nassar AH, Mouw KW, Jegede O, Shinagare AB, Kim J, Liu C-J, et al. A model combining clinical and genomic factors to predict response to PD-1/PD-L1 blockade in advanced urothelial carcinoma. *Br J Cancer.* (2020) 122:555–63. doi: 10.1038/s41416-019-0686-0
12. Rosenberg JE, Hoffman-Censits J, Powles T, van der Heijden MS, Balar AV, Necchi A, et al. Atezolizumab in patients with locally advanced and metastatic urothelial carcinoma who have progressed following treatment with platinum-based chemotherapy: a single-arm, multicentre, phase 2 trial. *Lancet.* (2016) 387:1909–20. doi: 10.1016/S0140-6736(16)00561-4
13. Mariathasan S, Turley SJ, Nickles D, Castiglioni A, Yuen K, Wang Y, et al. TGFβ attenuates tumour response to PD-L1 blockade by contributing to exclusion of T cells. *Nature.* (2018) 554:544–8. doi: 10.1038/nature25501
14. Tibshirani R. Regression shrinkage and selection via the lasso. *J R Stat Soc.* (1996) 58:267-88. doi: 10.1111/j.2517-6161.1996.tb02080.x
15. Vickers AJ, Cronin AM, Elkin EB, Gonen M. Extensions to decision curve analysis, a novel method for evaluating diagnostic tests, prediction models and molecular markers. *BMC Med Inform Decis Mak.* (2008) 8:53. doi: 10.1186/1472-6947-8-53
16. Newman AM, Steen CB, Liu CL, Gentles AJ, Chaudhuri AA, Scherer F, et al. Determining cell type abundance and expression from bulk tissues with digital cytometry. *Nat Biotechnol.* (2019) 37:773–82. doi: 10.1038/s41587-019-0114-2
17. Miao Y-R, Zhang Q, Lei Q, Luo M, Xie G-Y, Wang H, et al. ImmuCellAI: a unique method for comprehensive T-cell subsets abundance prediction and its application in cancer immunotherapy. *Adv Sci.* (2020) 7:1902880. doi: 10.1002/advs.201902880
18. Charoentong P, Finotello F, Angelova M, Mayer C, Efremova M, Rieder D, et al. Pan-cancer immunogenomic analyses reveal genotype-immunophenotype relationships and predictors of response to checkpoint blockade. *Cell Rep.* (2017) 18:248–62. doi: 10.1016/j.celrep.2016.12.019
19. Subramanian A, Tamayo P, Mootha VK, Mukherjee S, Ebert BL, Gillette MA, et al. Gene set enrichment analysis: a knowledge-based approach for interpreting genome-wide expression profiles. *Proc Natl Acad Sci USA.* (2005) 102:15545–50. doi: 10.1073/pnas.0506580102
20. Mayakonda A, Lin DC, Assenov Y, Plass C, Koeffler HP. Maftools: efficient and comprehensive analysis of somatic variants in cancer. *Genome Res.* (2018) 28:1747–56. doi: 10.1101/gr.239244.118
21. Tekpli X, Lien T, Røssevold AH, Nebdal D, Borgen E, Ohnstad HO, et al. An independent poor-prognosis subtype of breast cancer defined by a distinct tumor immune microenvironment. *Nat Commun.* (2019) 10:5499. doi: 10.1038/s41467-019-13329-5

22. Song B-N, Kim S-K, Mun J-Y, Choi Y-D, Leem S-H, Chu I-S. Identification of an immunotherapy-responsive molecular subtype of bladder cancer. *EBioMedicine*. (2019) 50:238–45. doi: 10.1016/j.ebiom.2019.10.058
23. Balar AV, Castellano D, O'Donnell PH, Grivas P, Vuky J, Powles T, et al. First-line pembrolizumab in cisplatin-ineligible patients with locally advanced and unresectable or metastatic urothelial cancer (KEYNOTE-052): a multicentre, single-arm, phase 2 study. *Lancet Oncol.* (2017) 18:1483–92. doi: 10.1016/S1470-2045(17)30616-2
24. Havel JJ, Chowell D, Chan TA. The evolving landscape of biomarkers for checkpoint inhibitor immunotherapy. *Nat Rev Cancer*. (2019) 19:133–50. doi: 10.1038/s41568-019-0116-x

Conflict of Interest: The authors declare that the research was conducted in the absence of any commercial or financial relationships that could be construed as a potential conflict of interest.

frontiers in Oncology

ORIGINAL RESEARCH
published: 04 September 2020
doi: 10.3389/fonc.2020.01706

ctDNA Concentration, MIKI67 Mutations and Hyper-Progressive Disease Related Gene Mutations Are Prognostic Markers for Camrelizumab and Apatinib Combined Multiline Treatment in Advanced NSCLC

Yao Chen[1†], Xiaobin Li[2†], Guifeng Liu[2], Shifu Chen[2], Mingyan Xu[2], Lele Song[2,3†] and Yina Wang[1*]*

[1] Department of Oncology, First Affiliated Hospital, College of Medicine, Zhejiang University, Hangzhou, China, [2] HaploX Biotechnology, Shenzhen, China, [3] Department of Radiotherapy, The Eighth Medical Center of the Chinese PLA General Hospital, Beijing, China

OPEN ACCESS

Edited by:
Said Dermime, National Center for Cancer Care and Research, Qatar

Reviewed by:
Cristina Maccalli, Sidra Medicine, Qatar
Mona Omar Mohsen, University of Oxford, United Kingdom

***Correspondence:**
Lele Song
songlele@sina.com
Yina Wang
1503099@zju.edu.cn

† These authors have contributed equally to this work

Specialty section:
This article was submitted to Cancer Immunity and Immunotherapy, a section of the journal Frontiers in Oncology

Received: *22 March 2020*
Accepted: *30 July 2020*
Published: *04 September 2020*

Citation:
Chen Y, Li X, Liu G, Chen S, Xu M, Song L and Wang Y (2020) ctDNA Concentration, MIKI67 Mutations and Hyper-Progressive Disease Related Gene Mutations Are Prognostic Markers for Camrelizumab and Apatinib Combined Multiline Treatment in Advanced NSCLC. Front. Oncol. 10:1706. doi: 10.3389/fonc.2020.01706

Immunotherapy by immune checkpoint inhibitors (ICIs) has showed outstanding efficacy in the treatment of advanced non-small cell lung cancer (NSCLC). The combination of immunotherapy with anti-angiogenic therapy exhibited enhanced efficacy in multiline treatment. However, the potential biomarkers for predicting and monitoring the therapeutic response of the combined therapy remain undefined. In this study, we performed a pilot study by prospectively recruiting 22 advanced NSCLC patients who failed to previous lines of chemotherapy, chemoradiotherapy, TKI therapy, surgery, or any combination of the therapies, and investigated the prognostic factors for patients who received anti-PD-1 (Camrelizumab) and anti-angiogenic (Apatinib) combined therapy. The objective response rate (ORR) assessed by an independent radiology review was 22.7%, and the median progression-free survival (PFS) was 5.25 months. We found that high concentration of circulating-free DNA (cfDNA) (HR = 27.75, $P = 0.003$), MIKI67 mutation (HR = 114.11, $P = 0.009$) and gene variations related to hyper-progressive disease (HPD) (HR = 36.85, $P = 0.004$) were independent risk factors and exhibited significant correlation with PFS. Circulating tumor DNA (ctDNA) mutational status was also a predicting indicator for PFS. In contrast, the blood tumor mutational burden (bTMB) could not stratify the clinical benefit in this combined therapy (HR = 0.81, $P = 0.137$). Furthermore, we found that the variant allele fraction (VAF) of mutations in ctDNA was sensitive indicators of therapeutic response and therefore can be used to monitor the tumor relief or progression. In conclusion, cfDNA concentration, MIKI67 mutations and HPD-related mutations were independent risk factors and PFS predictors for multiline combined anti-angiogenic/ICI combined therapy. ctDNA may be a novel monitoring biomarker for therapeutic response and predicting biomarker for prognosis in future combined therapy involving PD-1 blockade.

Keywords: NSCLC, immunotherapy, PD-1, angiogenic, ctDNA, TMB, PFS, Apatinib

INTRODUCTION

Immune checkpoint inhibitors (ICIs), such as programmed death 1 (PD-1)/programmed death ligand 1 (PD-L1) inhibitors have made a significant breakthrough in lung cancer treatment (1–3). Antibody blockade of the PD pathway rectifies immunodeficiency in tumor microenvironment, and empowers CD8+ T cells with the capability to kill tumor cells efficiently (4, 5). Along with success in clinical trials of immunotherapy, many more therapeutic options have appeared for lung cancer patients (6–12).

In patients with previously treated lung cancer, especially patients with wild-type driver genes, ICIs have substantially improved clinical prognosis compared with chemotherapy, as evidenced by an improvement of overall survival (OS) from 9.6 to 13.8 months in OAK cohorts (13). However, the achieved objective response rate (ORR) was less than 20% for anti-PD-1/PD-L1 antibody monotherapy in second-line or higher settings, including Nivolumab, Pembrolizumab, and Atezolizumab (6, 13, 14). Therefore, there is an urgent need to explore appropriate methods for improving the efficacy of immunotherapy and selecting patients potentially benefit from immunotherapy at multiline levels.

Many studies have focused on combination strategies to improve clinical efficacy of ICIs. The combination of Atezolizumab with Bevacizumab, Carboplatin, and Paclitaxel (ABCP) had significantly improved OS (19.2 months vs. 14.7 months) and PFS (8.3 months vs. 6.8 months) for metastatic non-squamous non-small cell lung cancer (NSCLC) in the phase III IMpower150 trial (9). Evidence has also suggested that anti-PD-1 and anti-vascular endothelial growth factor (VEGF) combined therapy may be a more favorable treatment option than any single reagent for NSCLC patients who had failed on the first-line or later treatment, and this therapeutic response was not affected by VEGF mutational status (15–17). CheckMate 227, another phase III trial in advanced NSCLC, suggested that Nivolumab plus Ipilimumab resulted in a longer OS independent of the PD-L1 expression level (18). This could be because the differential immune effects of CTLA-4 vs. PD-1 inhibition recruited effective antitumor immunity from the peripheral compartment, which is increasingly recognized as an important mechanism of response to immunotherapy (19–21). The combination of Pembrolizumab with chemotherapy exhibited superior ORR (57.9% vs. 38.4%), OS (15.9 months vs. 11.3 months) and PFS (6.4 months vs. 4.8 months) compared with placebo group for previously untreated metastatic, squamous NSCLC, demonstrated by the phase III KEYNOTE-407 trial (22). Similarly, in patients with treatment-naïve metastatic non-squamous NSCLC without EGFR or ALK mutations, the combination of standard chemotherapy with Pembrolizumab resulted in significantly longer OS (1-year OS rate: 69.2% vs. 49.4%) and PFS (8.8 months vs. 4.9 months) compared with placebo in KEYNOTE-189 trial (11). Moreover, PEMBRO-RT, a multicenter, randomized phase II study for metastatic NSCLC patients after chemotherapy failure, indicated that the ORR at 12 weeks was improved from 18 to 36% when radiotherapy was combined with Pembrolizumab, although the improvement did not reach statistical significance ($P = 0.07$) (23).

All the above clinical trials suggest that immunotherapy combined with chemotherapy or radiotherapy improved clinical efficacy in NSCLC patients. However, most randomized phase III clinical trials using combined immunotherapy were designed for first-line therapy, and there are few data for NSCLC patients in second-line or higher settings. In this study, we therefore performed a pilot study by recruiting a total of 22 NSCLC patients who failed to previous lines of chemotherapy, chemoradiotherapy, TKI therapy, surgery, or any combination of the therapies, and investigated the clinical efficacy of Camrelizumab, a humanized, high-affinity IgG4-kappa mAb against PD-1, combined with Apatinib, a small molecular drug targeting vascular endothelial growth factor receptor-2 (VEGFR-2). Since the traditional biomarkers for immunotherapy, such as the PD-L1 expression and tumor mutation burden (TMB) appeared to have limited predicting values in several clinical trials using combined immunotherapy (11, 12, 22, 24, 25), we investigated the values of a few new biomarkers in predicting and monitoring the therapeutic response and prognosis in second-line or higher settings when ICI was combined with anti-angiogenic therapy.

MATERIALS AND METHODS

Ethic Approval by Participating Hospitals

All study plans and protocols for the study were submitted to the ethics/licensing committee of the First Affiliated Hospital of Zhejiang University for review and approval before the start of the study, and were approved by the corresponding committee. Confirmation of approval for clinical study was received from the ethics board (approval number: 2018-775-1) before the start of the study. All experiments, methods, procedures and personnel training were carried out in accordance with relevant guidelines and regulations of participating hospitals and laboratories.

Study Design, Patients, and Samples

Patients recruited in this study were advanced NSCLC patients who received at least one line of treatment (chemotherapy or target therapy) and exhibited disease progression, and were recommended for subsequent therapy using Camrelizumab (or SHR-1210, Hengrui Medicine, Jiangsu, China) (200 mg q2w) combined with Apatinib (Hengrui Medicine, Jiangsu, China) (250 mg qd). Blood samples were collected at the First Affiliated Hospital of Zhejiang University. All patients received written informed consent for the use of clinical samples. Patient information was kept anonymous for confidentiality.

A total of 22 advanced lung cancer patients were recruited in this study between July 1, 2018 and October 31, 2019. The baseline characteristics of these patients are described in **Table 1**, and the detailed information has been included in **Table 2**, **Supplementary Tables S2, S3**. The median age of these patients was 61.5 years old (33∼73 years old). Seventeen patients (77.3%) were male and five (22.7%) were female, and all the female patients ($n = 5$) were non-smokers, whereas

TABLE 1 | Patient characteristics grouped by clinicopathological factors.

Clinicopathological factors	Number of patients	Percentage (%)
Total	22	100
Age		
<40	1	4.5
40–49	2	9.1
50–59	3	13.6
60–69	12	54.6
≥70	4	18.2
Gender		
Male	17	77.3
Female	5	22.7
Pathological types		
ADC	10	45.5
SCC	12	54.5
Smoking history		
Yes	15	68.2
No	7	31.8
Stage		
IIIB	5	22.7
IV	17	77.3
Lines of therapy		
2nd	14	63.6
3rd	6	27.3
4th–6th	2	9.1

ADC, adenocarcinoma; SCC, squamous cell carcinoma.

15 (88.2%) male patients had more than 20 pack years of smoking history. The number of lung adenocarcinoma patients (n = 10) was approximately equal to the patients harboring squamous cell carcinoma (n = 12). Seventeen patients (77.3%) were diagnosed with stage IV lung cancer, and five patients were at stage IIIB. Fourteen patients (63.6%) underwent this combined immunotherapy as second-line therapy, and the remaining eight patients (36.4%) received this therapy as third-line or higher treatments. The clinical information of all patients is summarized in **Table 1**. Disease control rate (DCR) and progression free survival (PFS) was used to assess the response of therapy. The expression of PD-L1 was determined before the first-line therapy on primary tumors and not on recurrent or resistant tumors, and immunohistochemistry was performed with Dako PDl-L1 IHC 22C3 pharmDx [Agilent Technology (China) Co., Ltd.] using the 22C3 antibody.

TABLE 2 | The relationship between therapeutic responses and clinicopathological factors.

Clinicopathological factors	DCR	PD	*P*-value
Gender			
Male	11	6	0.61*
Female	2	3	
Histology			
ADC	5	5	0.67*
SCC	8	4	
Smoking history			
Ever	10	5	0.38*
Never	3	4	
Stage			
IIIB	3	2	1*
IV	10	7	
Mutational status in ctDNA			
Negative	7	0	0.017*
Positive	6	9	
bTMB			
High	4	4	0.66*
Low	9	5	
Lines of therapy			
2nd line	9	5	0.66*
3rd–6th line	4	4	
PFS (mean, 95% CI)			
2nd line	9.03 (6.03∼12.02)	3.19 (1.50∼4.88)	0.010#
3rd–6th line	7.83 (0.62∼15.03)	2.10 (0.17∼4.13)	0.088#
TKI-related driver gene status			
With mutations	1	3	0.26*
Without mutations	12	6	

*DCR, disease control rate; PD, progressed disease; ADC, adenocarcinoma; SCC, squamous cell carcinoma; ctDNA, circulating tumor DNA; bTMB, blood tumor mutational burden. *Calibrated Chi-square test or Fisher exact probability test; #unpaired t-test.*

Sample Preparation, Library Construction, Targeted Sequencing, and Data Processing

Blood samples from patients were collected in Ethylene Diamine Tetraacetic Acid (EDTA) tubes and centrifuged at 1600 g for 10 min and at 4°C. The supernatants were further centrifuged at 10,000 × g for 10 min at 4°C, and plasma was harvested and stored at −80°C until further use. Circulating tumor DNA (ctDNA) was extracted from 3 to 3.5 ml plasma using the QIAamp Circulating Nucleic Acid kit (Qiagen, Inc., Valencia, CA, United States) according to the manufacturer's instructions. Blood cell fragments (including peripheral blood lymphocytes and red cells) were preserved at −20°C for further study. We applied the RelaxGene blood DNA system (Tiangen Biotech) to extract genomic DNA from peripheral blood lymphocytes (PBLs) as the normal control for mutation calling from cancer tissues and ctDNA. DNA was quantified with the Qubit 2.0 Fluorometer and the Qubit dsDNA HS assay kit (Thermo Fisher Scientific, Inc., Waltham, MA, United States) according to manufacturer's instructions. Fragmented genomic DNA underwent end-repairing, A-tailing and ligation with indexed adapters sequentially, followed by size selection using Agencourt AMPure XP beads (Beckman Coulter Inc., Brea, CA, United States), and DNA fragments were used for library construction using the KAPA Library Preparation kit (Kapa Biosystems, Inc., Wilmington, MA, United States) according to the manufacturer's protocol. Hybridization-based target enrichment was carried out with HaploX pan-cancer gene

panel (605 cancer-relevant genes, HaploX Biotechnology, gene list is provided in **Supplementary Table S1**) for cancer tissue sequencing. Seven to eight polymerase chain reaction (PCR) cycles, depending on the amount of DNA used, were performed by pre-capture ligation-mediated PCR (Pre-LM-PCR) Oligos (Kapa Biosystems, Inc.) in 50 μl reactions. ctDNA sequencing was then performed on the Illumina Novaseq 6000 system according to the manufacturer's recommendations at an average depth of 20,000×.

Data which meet the following criteria were chosen for subsequent analysis: the ratio of remaining data filtered by fastq in raw data is ≥85%; the proportion of Q30 bases is ≥85%; the ratio of reads on the reference genome is ≥85%; target region coverage ≥98%; average effective sequencing depth in ctDNA is ≥ 3000×. The called somatic variants need to meet the following criteria: the read depth at a position is ≥20×; the variant allele fraction (VAF) is ≥0.5% for ctDNA and ≥2% for PBL genomic DNA; somatic-*P*-value ≤0.01; strand filter ≥1. VAF were calculated for Q30 bases. The copy number variation (CNVs) was detected by CNVkit version 0.9.3[1]. Further analyses of genomic alterations were also performed, including single nucleotide variants (SNVs), CNVs, insertion/deletion (Indels), fusions, and structural variation.

Statistical Analysis

Statistical analysis was performed and figures were plotted with Graphpad Prism 5.0 software (GraphPad Software, Inc., La Jolla, CA, United States). Student *t*-test was performed when two groups were compared, and ANOVA and *post hoc* tests were performed when three or more groups were compared. Chi-square test, calibrated Chi-square test or Fisher exact probability test were performed when rate or percentage was compared for significance. Figures for mutation spectrum were made with the R software[2]. Univariate and multivariate analyses were performed using the SPSS 17.0 software (IBM China Company Limited, Beijing, China). $P < 0.05$ was regarded as statistically significant.

RESULTS

Genetic Alterations Were Capable of Predicting the Therapeutic Response and Prognosis of the Multiline Anti-angiogenic/ICI Combined Therapy

Twenty-two patients involved in this study received Camrelizumab combined with Apatinib therapy (**Table 1**). Fourteen patients received the combined treatment as the second-line therapy, while the rest as the third to sixth line therapy. The ORR and DCR assessed by an independent radiology review were 28.6% (4/14) and 64.3% (9/14), respectively, for the second-line therapy, and were 12.5% (1/8) and 50.0% (4/8), respectively, for the third to sixth line therapy (**Table 2**). All patients were followed up until disease progression (PD) or the end of this study. The progression-free survival (PFS) for all patients ranged from 1.4 to 15.5 months (median at 5.25 months). Data in **Table 2** showed a significantly longer PFS in patients with DCR than those with PD at the second-line therapy ($P = 0.010$, unpaired *t*-test), and similar trend can also be observed with patients at third to sixth line therapy ($P = 0.088$, unpaired *t*-test), while no significant difference was observed in PFS between patients with second-line therapy and patients with third to sixth line therapy (**Table 2**). We stratified all patients into the ADC group and SCC group, and examined the potential correlation between the above factors and patients' response (DCR or PD). It can be observed from **Supplementary Table S2** that the significant difference in PFS between patients with DCR and PD can be observed in SCC patients at second-line level ($P = 0.04$), while a trend of better PFS was also observed with ADC at second-line level ($P = 0.15$).

The mutational spectrum of circulating-free DNA (cfDNA) was established using the pre-therapeutic blood samples (**Figure 1A**). Mutations were detected in cfDNA of 15 patients while not detected in 7 patients. The NGS sequencing yielded a total of 80 somatic SNVs, 19 small insertions/deletions (indels), and 4 CNVs. TP53 (41%), FAT1 (14%), and KMT2D (14%) exhibited the highest mutational frequencies (**Figure 1A**). Few patients carried TKI-related driver gene mutations, including EGFR (one patient), BRAF (one patient), PIK3CA (one patient), and ERBB2 (one patient).

We further explored the potential predicting efficacy of genetic variations on PFS and therapeutic response (**Figures 1B,1C**). Patients with PR and SD were combined into DCR group due to the limited number of patients. It was found that patients with no detectable ctDNA mutations (ctDNA-negative group) showed significantly better PFS than patients with ctDNA mutations (ctDNA-positive group) ($P = 0.017$, Fisher exact probability test), suggesting that the pre-therapeutic ctDNA mutations were predictive for PFS (**Figure 1B** and **Table 2**). Further analysis on ADC and SCC individually revealed that the significant correlation between ctDNA mutational status and response was mainly reflected in ADC ($P = 0.008$, **Supplementary Table S2**). In contrast, the pre-therapeutic blood TMB (bTMB) level was not able to predict the PFS, when the 66.7 percentile bTMB value (6.96 mutations/Mb) was used to discriminate TMB-high (TMB-H) from TMB-low (TMB-L) (**Figure 1B**, **Table 2** and **Supplementary Table S3**). This observation indicates that the predictive capability of bTMB may be compromised in the second-line or multiline combined immunotherapy. Further correlation analysis showed that PFS had significant correlation with the blood cfDNA concentration (Spearman's rho = −0.439, $P = 0.041$), in which patients with better therapeutic response (PR or SD) correlated with longer PFS and lower cfDNA concentration, while no significant correlation can be found between bTMB and blood cfDNA concentration (**Figure 1C** and **Supplementary Table S3**). Furthermore, it appeared that gender, pathological types, smoking history, cancer stage, line of therapy, and the presence of TKI-related driver gene mutations did not affect the therapeutic response (DCR or PD) (**Table 2**). The correlation between

[1]https://github.com/etal/cnvkit

[2]https://www.r-project.org/

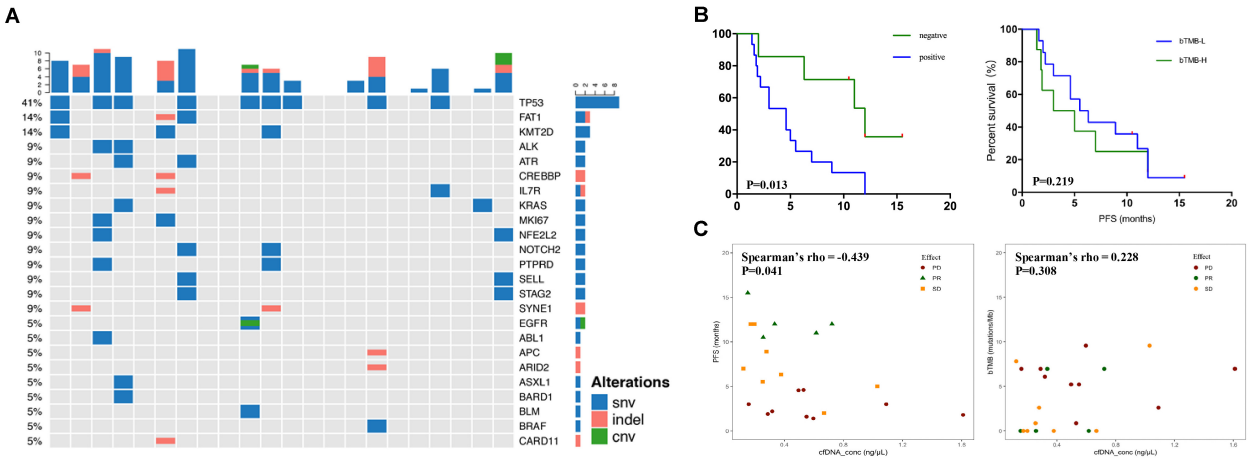

FIGURE 1 | The relationship between blood mutational landscape and therapeutic response. **(A)** The pre-therapeutic blood ctDNA mutational landscape. **(B)** Keplan–Meier survival analysis of patients with negative or positive ctDNA mutation detection (left panel, 7 patients with negative and 15 patients with positive ctDNA mutation detection) or patients with low or high bTMB levels (right panel, 8 patients with high and 14 patients with low bTMB levels). **(C)** Correlation between cfDNA concentration and PFS (left panel) or bTMB (right panel).

PD-L1 expression and PFS (**Supplementary Figure S1A**), bTMB (**Supplementary Figure S1B**), ctDNA concentration (**Supplementary Figure S1C**), and response (**Supplementary Figure S1D**) were investigated, and no clear correlation was identified. In addition, PD-L1 expression levels, whether grouped by positive or negative expression (P = 0.18) or by 50% threshold (P = 0.39), did not show significant stratification on response (**Supplementary Figures S1E,F**).

The relationship between gene variations and PFS was investigated in detail. Kaplan–Meier survival analysis showed that patients with MIKI67 mutations (Log-rank test P = 0.022) or CREBBP mutations (Log-rank test P = 0.049) exhibited significantly worse PFS than those without mutations (**Figures 2A,B**). In contrast, no such difference was observed in patients with or without TP53 mutations (**Figure 2C**). Interestingly, we found that patients who carried mutations in genes related to hyper-progressive diseases (HPDs) (one patient carried EGFR amplification and one patient carried FGF4 amplification) showed significantly worse PFS compared with those without such mutations (Log-rank test P = 0.028) (**Figure 2D**), while no significant difference in PFS was found between patients with or without TKI-related driver gene mutations (**Figure 2E**). Finally, no significant difference was found between patients with second-line therapy and those with third- to sixth-line therapy (**Figure 2F** and **Table 2**).

Multivariate Cox regression analysis (**Figure 3**) was performed using variables with $P \leq 0.3$ as described above (**Figures 1B,C, 2**). The concentration of cfDNA was found to be an independent predictor of PFS (HR = 27.75, P = 0.003), in which higher cfDNA concentration correlated with poorer outcomes (**Figure 3**). Similarly, patients harboring mutations in MIKI67 (HR = 114, P = 0.009) or genes relating to HPDs (HR = 36.85, P = 0.004) were also significantly associated with shorter PFS. Meanwhile, due to the limited number of patients, the ctDNA-negative group did not show more benefit from this combined immunotherapy compared with the ctDNA-positive group, although a trend of difference was observed (HR = 0.19, P = 0.068). As expected, bTMB could not predict the clinical benefits in this combined therapy.

ctDNA Is Capable of Monitoring the Therapeutic Responses of the Multiline Anti-angiogenic/ICI Combined Therapy

We further investigated the potential of blood ctDNA in therapeutic response monitoring. Plasma samples were obtained before and after treatment at key assessment points of therapeutic response in parallel with imaging examination. **Figure 4** shows several examples of patients with distinct therapeutic responses. We found that the changes in variant allelic frequency (VAF) of mutations exhibited identical trend to the changes in target tumor maximal diameter, whether in progressed disease (patient A), partial response (patient B), or in stable disease (patient D). More interestingly, we observed that the VAF of ctDNA decreased significantly in one patients following combined immunotherapy without significant change in tumor size (patient C), but exhibited and a clear cavity inside the tumor. The patient was progression free for 12 months and achieved PR ultimately. These results indicate that dynamics of ctDNA may be more sensitive than imaging examination to monitor the therapeutic response to combined immunotherapy. Furthermore, the regression tree analysis has been performed. PFS, cfDNA concentration, ctDNA detection (negative or positive), bTMB, MIKI67 mutation, CREBBP mutation, TKI-related driver gene mutation, HPDG mutation, TP53 mutation, and lines of therapy were set as the independent variable and the patient risk (determined by the significant factors in **Figure 3**) was set as the dependent variable. Although ctDNA detection appeared to be the only significant factor that may predict the risk of patients, the test was not conclusive as the number of patients involved was limited.

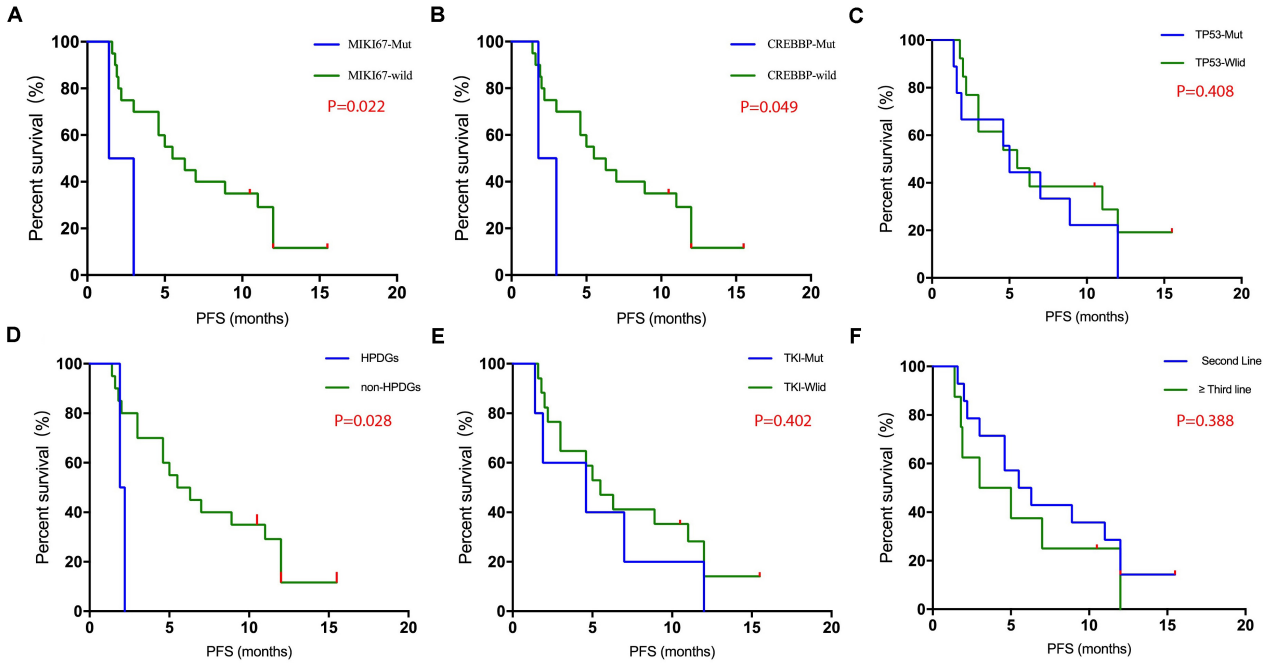

FIGURE 2 | Keplan–Meier survival analysis of various mutational status. The mutational status of MIKI67 (**A**, 2 muts and 20 WTs), CREBBP (**B**, 2 muts and 20 WTs), TP53 (**C**, 12 muts and 10 WTs), HPD genes (**D**, 2 with HPDG alterations and 20 without), TKI-relevant mutations (**E**, 4 with TKI-related mutations and 18 without), and lines of therapy (**F**, 12 at second-line and 10 at higher lines) were compared and shown as indicated.

DISCUSSION

In this study, we prospectively enrolled 22 patients with advanced NSCLC and studied the therapeutic responses and prognostic factors of the combined anti-angiogenic/ICI therapy at second-line and multiline levels. Previous research reported that antiangiogenic drugs can exert immune activation by inhibiting VEGF, promoting dendritic cell maturation, increasing T cell infiltration, and reprogramming the immune microenvironment (26). Therefore, anti-vascular drugs may reverse VEGF-mediated immunosuppression, thereby enhancing the antitumor activity of immunotherapy. Compared with the therapeutic responses of second- or multi-line PD-1 blockade previously reported (13, 14), PD-1 blockade combined with anti-angiogenic drugs had obvious clinical advantages, significantly improving ORR and PFS. This combined therapy could have better ORR, DCR, and PFS in the second-line treatment than the multiline treatment. In this study, we found a trend that the PFS of patients with second-line therapy may be better than that of the 3rd—6th lines of therapy, which supported previous observations. We also found that cfDNA concentration, MIKI67 mutations, and HPD-related gene mutations and potentially ctDNA mutations, were independent risk factors for therapeutic response prediction, while age, gender, lung cancer subtypes, smoking history, and bTMB did not affect the response.

Previous studies have shown that ctDNA was able to predict PFS in the first-line or multi-line immunotherapy of NSCLC (1, 27, 28). Similar capability were confirmed in colorectal cancer (29, 30), breast cancer (31, 32), liver cancer (33), and gastric cancer (34, 35). In this study, we found that ctDNA was also capable of predicting the response of NSCLC to multiline anti-angiogenic/ICI combined therapy. Patients with positive ctDNA exhibited worse prognosis (PFS) than patients with negative ctDNA. This may be due to fact that higher tumor load in ctDNA-positive patients led to poor treatment response and poor tumor remission. It can be concluded from previous and our studies that the survival of ctDNA-positive patients will be worse than ctDNA-negative patients, regardless of single-agent or combined immunotherapy, and regardless of first-line or multi-line therapy. In addition, we also found that the VAF of ctDNA mutations was a good indicator of response of the combined therapy. In this study, prospective collections of blood samples before and after treatment and tests using NGS panel allowed the tracking of multiple genes with fluctuating VAF found in ctDNA. High concordance was found between the change of VAF and the tumor size. Due to the limited number of mutations that can be detected in ctDNA, our observation suggested that targeting a few mutations with high VAF in ctDNA may be sufficient to monitor the therapeutic response. We also found that ctDNA may be more sensitive and have predicting efficacy compared with imaging studies. This is supported by previous reports showing that ctDNA can predict tumor recurrence or remission much earlier than imaging examination (36), which is important for decision-making in therapeutic strategy selection. Therefore, we speculate that if ctDNA is used in combination with imaging, they can better monitor and predict the response and prognosis of patients than using one method alone. In addition, we found that cfDNA

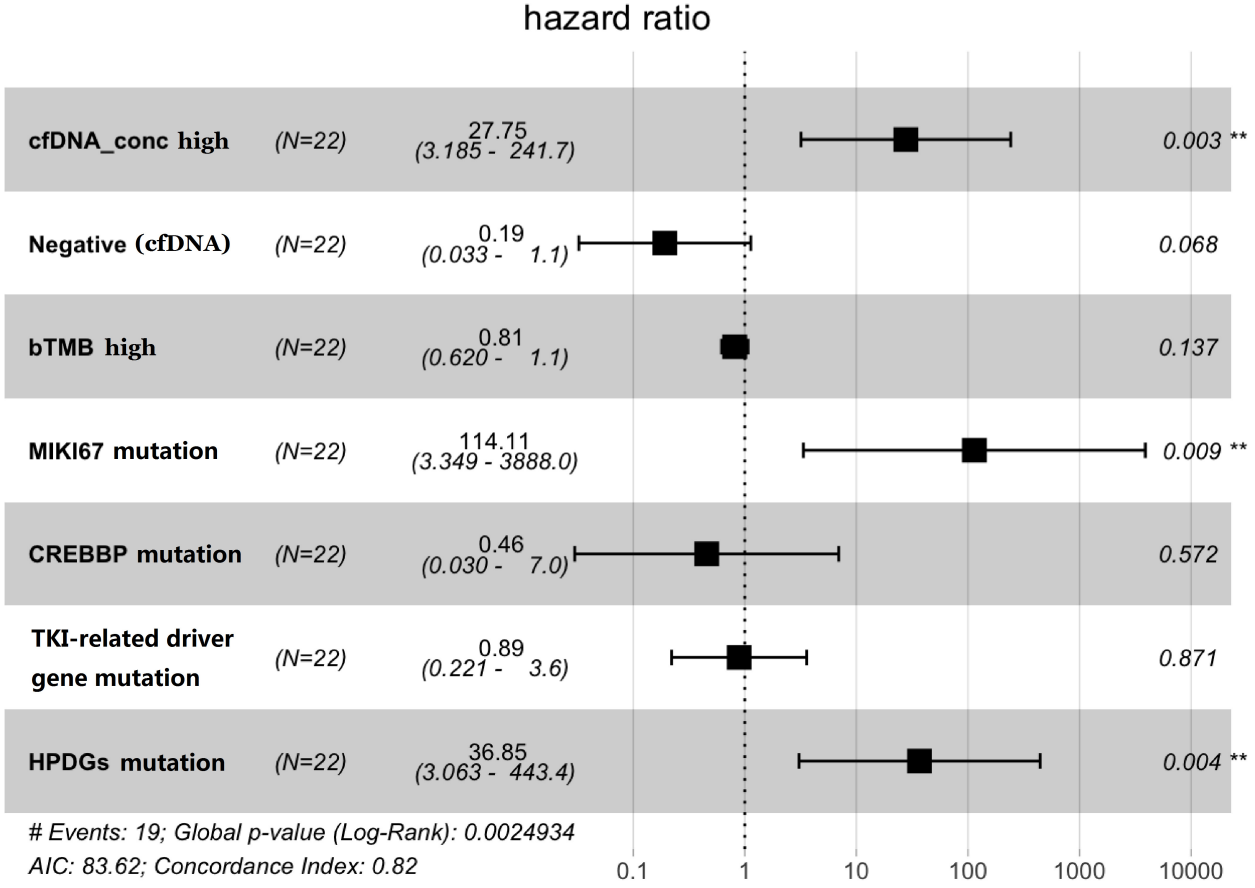

FIGURE 3 | The results of multivariate Cox regression analysis for various potential risk factors. cfDNA concentration (P = 0.003), MIKI67 mutations (P = 0.009), and HPD gene mutations (P = 0.004) were identified as independent risk factors, while a trend of significance can be observed with ctDNA mutations (P = 0.068). Negative (cfDNA) indicates that no mutations in any gene were found in the 605 gene-panel test.

concentration was significantly correlated with PFS and was an independent risk factor for patients, suggesting that the plasma cfDNA level can predict the response and prognosis regardless of the mutational status, which was also supported by previous reports (37–39).

Many studies support the viewpoint that bTMB can be used as a biomarker to predict clinical efficacy in anti-PD-1/PD-L1 immunotherapy. Patients with high bTMB have a better ORR and PFS than patients with low bTMB (1, 40). However, a retrospective analysis of the POPLAR and OAK studies found that bTMB may not effectively distinguish the benefit in OS of patients receiving immunotherapy at second-line or higher (1, 41). Giles et al. (42) recently also found worse PFS and OS in NSCLC patients with higher bTMB in first-line immunotherapy. This suggests us that evidence is still needed to support the effectiveness of bTMB as a biomarker in immunotherapy, especially in multiline combined therapy. We provided such evidence in this article and found that the level of bTMB cannot effectively distinguish the benefit population in second-line and multi-line anti-angiogenic/ICI combined therapy. We speculate that one of the possible reasons is that the combined therapy improved the patients' response, and weakened the stratification of bTMB on the patients' response and prognosis observed in single-agent based immunotherapy.

It has been previously reported that PD-L1 expression can effectively stratify the therapeutic effect of ICIs, and the PD-L1 expression has been approved by the FDA as a companion diagnostic marker for anti-PD-1/PD-L1 treatment. Patients with high PD-L1 expression are more likely to benefit from immunotherapy (43). However, the PEMBRO-RT study found that PFS and OS in patients with PD-L1 high expression were shorter in the second-line immunotherapy combined with radiotherapy for lung cancer (23), also suggesting that the efficacy of biomarkers in multiline combined therapy involving PD1/PD-L1 blockade may be different from previous observations with immunotherapy alone. Ideally, the PD-L1 expression status of all patients with recurrent or resistant tumors should be reexamined, and multiline therapeutic strategies should be established based on the information. However, practically, many patients were reluctant to receive a second biopsy with both PD-L1 test and NGS test, because they believe that immunotherapy combined with other therapies was possibly the only option for them when the disease progressed, and therefore there was no need to repeat the tests anymore. As a

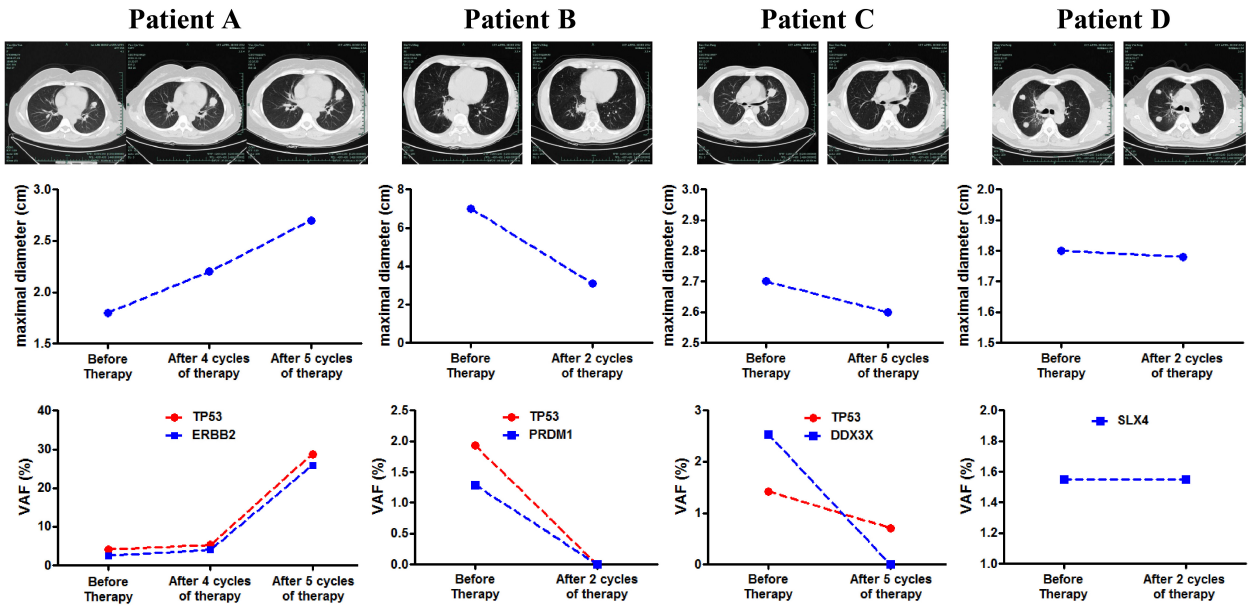

FIGURE 4 | Correlation between tumor diameter change and ctDNA mutational change following the multiline anti-angiogenic/ICI combined therapy. The CT images, tumor diameter changes and VAF changes of blood ctDNA mutations of four patients **(A–D)** were illustrated.

result, the reexamination rate in these patients was very low. We were facing the similar situation in this study. Therefore, we tried to link the PD-L1 expression from primary tumor with the response of 2nd–6th lines therapy to see if we can identify any correlation, while no significant correlation was found, as shown in **supplementary Figure S1**. Another concern is that due to the better response in patients with combined therapy, the effect of stratification by PD-L1 may not be significant anymore, and patients with negative PD-L1 expression may also benefit from the therapy, which was reflected in some recent studies (15–17).

Previous reports have shown that tumors were not effectively controlled and hyperprogression finally developed after immunotherapy in some patients (44). Further clinical studies have shown that these patients may carry genetic alterations, such as EGFR amplification, MDM2/MDM4 amplification, and chromosome 11 band 13-related gene amplification (FGF4, FGF19) (45). In this study, we prospectively enrolled two patients, who carried EGFR amplification and FGF4 amplification, respectively. They quickly developed PD with PFS of 1.9 and 2.2 months, respectively, far lower than those who did not carry hyperprogression-relevant gene mutations. Our observation suggests that the clinical response of patients with hyperprogression-relevant gene mutations was also poor in multiline anti-agiogenic/ICI combined therapy. Similarly, evidence also showed that NSCLC patients with TKI-related driver gene mutations often had poor ORR and PFS in anti-PD-1/PD-L1 treatment, in which the evidence for EGFR mutations and ALK fusions were strong, while other TKI-related driver gene mutations were not confirmed (46, 47). In this study, we compared patients with or without TKI-related driver gene mutations and found no significant differences in PFS between the two groups, suggesting that not all TKI-related driver gene mutations affect anti-angiogenic/ICI combined therapy. Interestingly, we found that two patients with ALK mutations (not fusions) with PFS of 12 and 1.4 months, respectively. The latter had a shorter PFS possibly due to a MIKI67 mutation, since MIKI67 mutations were an independent factor of poor prognosis. Our observation suggests that ALK non-fusion mutations may not affect the response of the combined therapy.

There were some limitations of this study. Firstly, heterogeneity of therapy was a weakness of the study, especially when therapeutic lines from 2nd to 6th were all involved. This is why we stratified the patients into 2nd line and 3rd–6th lines in this study, at least the therapy for 2nd line patients was homogeneous. By comparing these two populations, we found that the PFS of 2nd line treatment might be better than that of 3rd—6th treatment (**Supplementary Table S2**), which was one of main findings in the study. Secondly, two control cohorts, including one Camrelizumab and one Apatinib cohort, should be included to compare with the Camrelizumab and Apatinib combined cohort. However, it is difficult in reality to recruit patients using Camrelizumab or Apatinib alone, since both doctors and patients are aware that patients with combined therapy may potentially respond better than those treated with a single drug, therefore, challenges exist in both practical therapy and ethics if single drug group is recruited in parallel. However, some previous patients using the single drug may be involved as the control cohort. Thirdly, it was unfortunate in this study that we were unable to obtain any tissue samples from patients at advanced therapy stages, and therefore the test for tissue TMB was not possible. This was mainly because patients normally receive the tissue sampling and test when they are first diagnosed (before any therapy), and tissue sampling at later treatment is performed only when specific genetic alterations related to

disease progression are highly suspected. In future study, tissue TMB should be obtained whenever possible, since difference might exist between tissue and blood TMB in therapy guidance. Fourthly, a relatively small cohort was one limitation of the study. For example, **Figure 2** showed all mutations with significant stratification of survival. Due to the limited number of patients with MIKI67 or CREBBP mutants, the conclusion was not solid, although significant stratification was observed. The results need further validation with larger cohort in future.

CONCLUSION

In summary, we found that the combination of anti-angiogenic with PD-1 blockade therapy significantly enhanced the ORR and PFS of NSCLC patients in second-line or multiline treatment. ctDNA concentration, MIKI67 mutation, and HPD-relevant gene mutations were independent risk factors for PFS. The blood ctDNA mutations can potentially identify the benefit population and predict the patients' response and prognosis. In addition, ctDNA detection at series time points can effectively monitor disease relief or progression. Our study provided valuable evidence for treatment strategy selection in the second-line and multiline anti-angiogenic/ICI combined treatment of advanced NSCLC. There were also limitations in this study, mainly due to the limited number of patients included, while more patients should be enrolled in the future to confirm the conclusion of this study.

DATA AVAILABILITY STATEMENT

The datasets presented in this study can be found in online repositories. The names of the repository/repositories and accession number(s) can be found below: Genome Sequence Archive (https://bigd.big.ac.cn/gsa-human/browse/HRA000239).

ETHICS STATEMENT

The studies involving human participants were reviewed and approved by The First Affiliated Hospital of Zhejing University. The patients/participants provided their written informed consent to participate in this study. Written informed consent was obtained from the individual(s) for the publication of any potentially identifiable images or data included in this article.

AUTHOR CONTRIBUTIONS

YW and LS designed the study and proofread the manuscript. YC and XL provided the samples and collected the clinical information and diagnostic information. YC, XL, and LS performed the statistics and wrote the manuscript. GL, SC, and MX performed the sequencing experiments and analyzed the sequencing data. LS submitted the manuscript. All authors contributed to the article and approved the submitted version.

FUNDING

This study was supported by the Special Funds for Strategic Emerging Industry Development of Shenzhen (grant number 20170922151538732) and the Science and Technology Project of Shenzhen (grant number JSGG20180703164202084). This study was also supported by the financial grants from Zhejiang Provincial Natural Science Foundation of China (LY16H160006) and Hangzhou Science and Technology Bureau (20160533 B72). All funders did not participate in the study design, study implementation, data collection, data analysis, data interpretation, and manuscript writing of the study.

SUPPLEMENTARY MATERIAL

The Supplementary Material for this article can be found online at: https://www.frontiersin.org/articles/10.3389/fonc.2020.01706/full#supplementary-material

FIGURE S1 | Correlation of PD-L1 expression level with other markers or patient response or survival. Results of correlation were shown for PD-L1 expression with PFS **(A)**, bTMB **(B)**, ctDNA concentration **(C)**, response **(D)**. The influence of PD-L1 expression (negative or positive) on survival was shown in panel **(E)**, and the influence of PD-L1 expression (<50% or ≥50%)was shown in panel **(F)**. PD-L1 expression level of >1% was considered positive, and PD-L1 expression level of ≥50% was considered high expression. In 15 patients with available PD-L1 expression data, 11 had expression level of >1% and 4 had expression level of ≥50% (**Supplementary Table S3**).

REFERENCES

1. Zhijie W, Jianchun D, Shangli C, Miao H, Hua D, Jun Z, et al. Assessment of blood tumor mutational burden as a potential biomarker for immunotherapy in patients with non-small cell lung cancer with use of a next-generation sequencing cancer gene panel. *JAMA Oncol.* (2019) 5:696–702. doi: 10.1001/jamaoncol.2018.7098
2. Fan Y, Mao W. Immune checkpoint inhibitors in lung cancer: current status and future directions. *Chin Clin Oncol.* (2017) 6:17. doi: 10.21037/cco.2017.02.05
3. Zhang D, Huang J, Zhang C, Guan Y, Guo Q. [Progress on PD-1/PD-L1 checkpoint inhibitors in lung cancer]. *Zhongguo Fei Ai Za Zhi.* (2019) 22:369–79. doi: 10.3779/j.issn.1009-3419.2019.06.07
4. Sanmamed MF, Chen LA. Paradigm shift in cancer immunotherapy: from enhancement to normalization. *Cell.* (2019) 176:677. doi: 10.1016/j.cell.2019.01.008
5. Zhang Y, Chen L. Classification of advanced human cancers based on tumor immunity in the microenvironment (TIME) for cancer immunotherapy. *JAMA Oncol.* (2016) 2:1403–4. doi: 10.1001/jamaoncol.2016.2450
6. Brahmer J, Reckamp KL, Baas P, Crinò L, Eberhardt WE, Poddubskaya E, et al. Nivolumab versus docetaxel in advanced squamous-cell non-small-cell lung cancer. *N Engl J Med.* (2015) 373:123–35. doi: 10.1056/NEJMoa1504627
7. Horn L, Spigel DR, Vokes EE, Holgado E, Ready N, Steins M, et al. Nivolumab versus docetaxel in previously treated patients with advanced non-small-cell lung cancer: two-year outcomes from two randomized, open-label, phase III trials (CheckMate 017 and CheckMate 057). *J Clin Oncol.* (2017) 35:3924–33. doi: 10.1200/JCO.2017.74.3062

8. Dhillon S, Syed YY. Atezolizumab first-line combination therapy: a review in metastatic nonsquamous NSCLC. *Target Oncol.* (2019) 14:759–68. doi: 10.1007/s11523-019-00686-w
9. Socinski MA, Jotte RM, Cappuzzo F, Orlandi F, Stroyakovskiy D, Nogami N, et al. Atezolizumab for first-line treatment of metastatic nonsquamous NSCLC. *N Engl J Med.* (2018) 378:2288–301. doi: 10.1056/NEJMoa1716948
10. Lynch TJ, Bondarenko I, Luft A, Serwatowski P, Barlesi F, Chacko R, et al. Ipilimumab in combination with paclitaxel and carboplatin as first-line treatment in stage IIIB/IV non-small-cell lung cancer: results from a randomized, double-blind, multicenter phase II study. *J Clin Oncol.* (2012) 30:2046–54. doi: 10.1200/JCO.2011.38.4032
11. Gandhi L, Rodríguez-Abreu D, Gadgeel S, Esteban E, Felip E, De Angelis F, et al. Pembrolizumab plus chemotherapy in metastatic non-small-cell lung cancer. *N Engl J Med.* (2018) 378:2078–92. doi: 10.1056/NEJMoa1801005
12. Langer CJ, Gadgeel SM, Borghaei H, Papadimitrakopoulou VA, Patnaik A, Powell SF, et al. Carboplatin and pemetrexed with or without pembrolizumab for advanced, non-squamous non-small-cell lung cancer: a randomised, phase 2 cohort of the open-label KEYNOTE-021 study. *Lancet Oncol.* (2016) 17:1497–508. doi: 10.1016/S1470-2045(16)30498-3
13. Rittmeyer A, Barlesi F, Waterkamp D, Park K, Ciardiello F, von Pawel J, et al. Atezolizumab versus docetaxel in patients with previously treated non-small-cell lung cancer (OAK): a phase 3, open-label, multicentre randomised controlled trial. *Lancet.* (2017) 389:255–65. doi: 10.1016/S0140-6736(16)32517-X
14. Garon EB, Rizvi NA, Hui R, Leighl N, Balmanoukian AS, Eder JP, et al. Pembrolizumab for the treatment of non-small-cell lung cancer. *N Engl J Med.* (2015) 372:2018–28. doi: 10.1056/NEJMoa1501824
15. Zhang F, Huang D, Li T, Zhang S, Wang J, Zhang Y, et al. Anti-PD-1 therapy plus chemotherapy and/or bevacizumab as second line or later treatment for patients with advanced non-small cell lung cancer. *J Cancer.* (2020) 11:741–9. doi: 10.7150/jca.37966
16. Liang H, Wang M. Prospect of immunotherapy combined with anti-angiogenic agents in patients with advanced non-small cell lung cancer. *Cancer Manag Res.* (2019) 11:7707–19. doi: 10.2147/cmar.s212238
17. Rossi A. New options for combination therapy for advanced non-squamous NSCLC. *Expert Rev Respir Med.* (2019) 13:1095–107. doi: 10.1080/17476348.2019.1667233
18. Hellmann MD, Paz-Ares L, Bernabe Caro R, Zurawski B, Kim SW, Carcereny Costa E, et al. Nivolumab plus ipilimumab in advanced non-small-cell lung cancer. *N Engl J Med.* (2019) 381:2020–31. doi: 10.1056/NEJMoa1910231
19. Spitzer MH, Carmi Y, Reticker-Flynn NE, Kwek SS, Madhireddy D, Martins MM, et al. Systemic immunity is required for effective cancer immunotherapy. *Cell.* (2017) 168:487–502.e15.
20. Sade-Feldman M, Yizhak K, Bjorgaard SL, Ray JP, de Boer CG, Jenkins RW, et al. Defining T cell states associated with response to checkpoint immunotherapy in melanoma. *Cell.* (2018) 175:998–1013.e20. doi: 10.1016/j.cell.2018.10.038
21. Yost KE, Satpathy AT, Wells DK, Qi YY, Wang CL, Kageyama R, et al. Clonal replacement of tumor-specific T cells following PD-1 blockade. *Nat Med.* (2019) 25:1251–9. doi: 10.1038/s41591-019-0522-3
22. Paz-Ares L, Luft A, Vicente D, Tafreshi A, Gümüş M, Mazières J, et al. Pembrolizumab plus chemotherapy for squamous non-small-cell lung cancer. *N Engl J Med.* (2018) 379:2040–51. doi: 10.1056/NEJMoa1810865
23. Theelen WSME, Peulen HMU, Lalezari F, van der Noort V, de Vries JF, Aerts JGJV, et al. Effect of pembrolizumab after stereotactic body radiotherapy vs pembrolizumab alone on tumor response in patients with advanced non-small cell lung cancer: results of the PEMBRO-RT Phase 2 randomized clinical trial. *JAMA Oncol.* (2019) 5:1276–82. doi: 10.1001/jamaoncol.2019.1478
24. Gadgeel SM, Stevenson JP, Langer CJ, Gandhi L, Borghaei H, Patnaik A, et al. Pembrolizumab and platinum-based chemotherapy as first-line therapy for advanced non-small-cell lung cancer: phase 1 cohorts from the KEYNOTE-021 study. *Lung Cancer.* (2018) 125:273–81. doi: 10.1016/j.lungcan.2018.08.019
25. Borghaei H, Langer CJ, Gadgeel S, Papadimitrakopoulou VA, Patnaik A, Powell SF, et al. 24-Month overall survival from KEYNOTE-021 Cohort G: pemetrexed and carboplatin with or without pembrolizumab as first-line therapy for advanced nonsquamous non-small cell lung cancer. *J Thorac Oncol.* (2019) 14:124–9. doi: 10.1016/j.jtho.2018.08.004
26. Lacal PM, Graziani G. Therapeutic implication of vascular endothelial growth factor receptor-1 (VEGFR-1) targeting in cancer cells and tumor microenvironment by competitive and non-competitive inhibitors. *Pharmacol Res.* (2018) 136:97–107. doi: 10.1016/j.phrs.2018.08.023
27. Goldberg SB, Narayan A, Kole AJ, Decker RH, Teysir J, Carriero NJ, et al. Early assessment of lung cancer immunotherapy response via circulating tumor DNA. *Clin Cancer Res.* (2018) 24:1872–80. doi: 10.1158/1078-0432.CCR-17-1341
28. Raja R, Kuziora M, Brohawn PZ, Higgs BW, Gupta A, Dennis PA, et al. Early reduction in ctDNA predicts survival in patients with lung and bladder cancer treated with durvalumab. *Clin Cancer Res.* (2018) 24:6212–22. doi: 10.1158/1078-0432.CCR-18-0386
29. Cremolini C, Rossini D, Dell'Aquila E, Lonardi S, Conca E, Del Re M, et al. Rechallenge for patients with RAS and BRAF wild-type metastatic colorectal cancer with acquired resistance to first-line cetuximab and irinotecan: a phase 2 single-arm clinical trial. *JAMA Oncol.* (2019) 5:343–50. doi: 10.1001/jamaoncol.2018.5080
30. Barault L, Amatu A, Siravegna G, Ponzetti A, Moran S, Cassingena A, et al. Discovery of methylated circulating DNA biomarkers for comprehensive non-invasive monitoring of treatment response in metastatic colorectal cancer. *Gut.* (2018) 67:1995–2005. doi: 10.1136/gutjnl-2016-313372
31. Rossi G, Mu Z, Rademaker AW, Austin LK, Strickland KS, Costa RLB, et al. Cell-Free DNA and circulating tumor cells: comprehensive liquid biopsy analysis in advanced breast cancer. *Clin Cancer Res.* (2018) 24:560–8. doi: 10.1158/1078-0432.CCR-17-2092
32. Hrebien S, Citi V, Garcia-Murillas I, Cutts R, Fenwick K, Kozarewa I, et al. Early ctDNA dynamics as a surrogate for progression-free survival in advanced breast cancer in the BEECH trial. *Ann Oncol.* (2019) 30:945–52. doi: 10.1093/annonc/mdz085
33. Lim HY, Merle P, Weiss KH, Yau T, Ross P, Mazzaferro V, et al. Phase II studies with refametinib or refametinib plus sorafenib in patients with RAS-mutated hepatocellular carcinoma. *Clin Cancer Res.* (2018) 24:4650–61. doi: 10.1158/1078-0432.CCR-17-3588
34. Kim ST, Cristescu R, Bass AJ, Kim KM, Odegaard JI, Kim K, et al. Comprehensive molecular characterization of clinical responses to PD-1 inhibition in metastatic gastric cancer. *Nat Med.* (2018) 24:1449–58. doi: 10.1038/s41591-018-0101-z
35. Wang Y, Zhao C, Chang L, Jia R, Liu R, Zhang Y, et al. Circulating tumor DNA analyses predict progressive disease and indicate trastuzumab-resistant mechanism in advanced gastric cancer. *EBioMedicine.* (2019) 43:261–9. doi: 10.1016/j.ebiom.2019.04.003
36. Abbosh C, Birkbak NJ, Wilson GA, Jamal-Hanjani M, Constantin T, Salari R, et al. Phylogenetic ctDNA analysis depicts early-stage lung cancer evolution. *Nature.* (2017) 545:446–51. doi: 10.1038/nature22364
37. Tissot C, Toffart AC, Villar S, Souquet PJ, Merle P, Moro-Sibilot D, et al. Circulating free DNA concentration is an independent prognostic biomarker in lung cancer. *Eur Respir J.* (2015) 46:1773–80. doi: 10.1183/13993003.00676-2015
38. Ai B, Liu H, Huang Y, Peng P. Circulating cell-free DNA as a prognostic and predictive biomarker in non-small cell lung cancer. *Oncotarget.* (2016) 7:44583–95. doi: 10.18632/oncotarget.10069
39. Chen KZ, Lou F, Yang F, Zhang JB, Ye H, Chen W, et al. Circulating Tumor DNA Detection in Early-Stage Non-Small Cell Lung Cancer Patients by Targeted Sequencing. *Sci Rep.* (2016) 6:31985. doi: 10.1038/srep31985
40. Chen YT, Seeruttun SR, Wu XY, Wang ZX. Maximum somatic allele frequency in combination with blood-based tumor mutational burden to predict the efficacy of atezolizumab in advanced non-small cell lung cancer: a pooled analysis of the randomized POPLAR and OAK studies. *Front Oncol.* (2019) 9:1432. doi: 10.3389/fonc.2019.01432
41. Gandara DR, Paul SM, Kowanetz M, Schleifman E, Zou W, Li Y, et al. Blood-based tumor mutational burden as a predictor of clinical benefit in non-small-cell lung cancer patients treated with atezolizumab. *Nat Med.* (2018) 24:1441–8. doi: 10.1038/s41591-018-0134-3
42. Chae YK, Davis AA, Agte S, Pan A, Simon NI, Iams WT, et al. Clinical Implications of circulating tumor DNA tumor mutational burden (ctDNA

TMB) in non-small cell lung cancer. *Oncologist*. (2019) 24:820–8. doi: 10.1634/theoncologist.2018-0433

43. Brahmer JR, Rodríguez-Abreu D, Robinson AG, Hui R, Csõszi T, Fülöp A, et al. Health-related quality-of-life results for pembrolizumab versus chemotherapy in advanced, PD-L1-positive NSCLC (KEYNOTE-024): a multicentre, international, randomised, open-label phase 3 trial. *Lancet Oncol.* (2017) 18:1600–9. doi: 10.1016/S1470-2045(17)30690-3
44. Togasaki K, Sukawa Y, Kanai T, Takaishi H. Clinical efficacy of immune checkpoint inhibitors in the treatment of unresectable advanced or recurrent gastric cancer: an evidence-based review of therapies. *Onco Targets Ther.* (2018) 11:8239–50. doi: 10.2147/OTT.S152514
45. Kim JY, Lee KH, Kang J, Borcoman E, Saada-Bouzid E, Kronbichler A, et al. Hyperprogressive disease during anti-PD-1 (PDCD1) / PD-L1 (CD274) therapy: a systematic review and meta-analysis. *Cancers (Basel).* (2019) 11:699. doi: 10.3390/cancers11111699
46. Mazieres J, Drilon A, Lusque A, Mhanna L, Cortot AB, Mezquita L, et al. Immune checkpoint inhibitors for patients with advanced lung cancer and oncogenic driver alterations: results from the IMMUNOTARGET registry. *Ann Oncol.* (2019) 30:1321–8. doi: 10.1093/annonc/mdz167
47. Santaniello A, Napolitano F, Servetto A, De Placido P, Silvestris N, Bianco C, et al. Tumour microenvironment and immune evasion in EGFR addicted NSCLC: hurdles and possibilities. *Cancers (Basel).* (2019) 11:1419. doi: 10.3390/cancers11101419

Conflict of Interest: XL, GL, SC, MX, and LS are employed by the company HaploX Biotechnology, Co., Ltd.

The remaining authors declare that the research was conducted in the absence of any commercial or financial relationships that could be construed as a potential conflict of interest.

frontiers in Immunology

ORIGINAL RESEARCH
published: 10 September 2020
doi: 10.3389/fimmu.2020.02048

Clinical Implications of Aberrant PD-1 and CTLA4 Expression for Cancer Immunity and Prognosis: A Pan-Cancer Study

Jian-Nan Liu[1†], *Xiang-Shuo Kong*[1†], *Tao Huang*[2,3,4†], *Rui Wang*[5], *Wang Li*[2*] and *Qi-Feng Chen*[2,3,4*]

[1] Department of Oncology, Yantai Yuhuangding Hospital, Yantai, China, [2] Department of Medical Imaging and Interventional Radiology, Sun Yat-sen University Cancer Center, Guangzhou, China, [3] State Key Laboratory of Oncology in South China, Guangzhou, China, [4] Collaborative Innovation Center for Cancer Medicine, Guangzhou, Guangdong, China, [5] Department of Respiratory Oncology, Fushan District People's Hospital, Yantai, China

OPEN ACCESS

Edited by:
Maysaloun Merhi,
Hamad Medical Corporation, Qatar

Reviewed by:
Manel Juan,
Hospital Clínic de Barcelona, Spain
Jan Joseph Melenhorst,
University of Pennsylvania,
United States

***Correspondence:**
Wang Li
liwang@sysucc.org.cn
Qi-Feng Chen
chenqf25@sysucc.org.cn

[†] These authors have contributed equally to this work

Specialty section:
This article was submitted to Cancer Immunity and Immunotherapy, a section of the journal Frontiers in Immunology

Received: 07 May 2020
Accepted: 28 July 2020
Published: 10 September 2020

Citation:
Liu J-N, Kong X-S, Huang T, Wang R, Li W and Chen Q-F (2020) Clinical Implications of Aberrant PD-1 and CTLA4 Expression for Cancer Immunity and Prognosis: A Pan-Cancer Study. Front. Immunol. 11:2048. doi: 10.3389/fimmu.2020.02048

Combination therapy with inhibitors of cytotoxic T lymphocyte-associated protein (CTLA)4 and programmed death (PD)-1 has demonstrated efficacy in cancer patients. However, there is little information on CTLA4 and PD-1 expression levels and their clinical significance across diverse cancers. In this study, we addressed this question by analyzing PD-1 and CTLA4 levels in 33 different types of cancer along with their prognostic significance using The Cancer Genome Atlas (TCGA) and Cancer Cell Line Encyclopedia datasets. Liver hepatocellular carcinoma (LIHC) patients receiving cytokine-induced killer cell (CIK) immunotherapy at Sun Yat-sen University cancer center were enrolled for survival analysis. The correlation between PD-1/CTLA4 expression and cancer immunity was also analyzed. The results showed that PD-1 and CTLA4 transcript levels varied across cancer cell lines, with aberrant expression detected in certain cancer types; Kaplan–Meier analysis with the Cox proportional hazards model showed that this was closely related to overall survival in breast invasive carcinoma, glioblastoma multiforme, head and neck squamous cell carcinoma, acute myeloid leukemialymphoma, uterine corpus endometrial carcinoma, and uveal melanoma in TCGA. High serum PD-1 and CTLA4 levels predicted better survival in LIHC patients receiving CIK therapy. PD-1 and CTLA4 levels were found to be significantly correlated with the degree of tumor cell infiltration using Tumor Immune Estimation Resource, Estimating Relative Subsets of RNA Transcripts, and Estimation of Stromal and immune Cells in Malignant Tumor Tissues Using Expression Data as well as with tumor-infiltrating lymphocyte marker expression; they were also related to tumor mutation burden, microsatellite instability, mismatch repair, and the expression of DNA methyltransferases in some cancer types. Gene set enrichment analysis of 33 cancer types provided further evidence for associations between PD-1/CTLA4 levels and cancer development and immunocyte infiltration. Thus, PD-1 and CTLA4 play important roles in tumorigenesis and tumor immunity and can serve as prognostic biomarkers in different cancer types.

Keywords: pan-cancer, PD-1, CTLA4, prognostic biomarker, cancer immunity

INTRODUCTION

Cancer is a leading cause of death worldwide, and the low efficacy of many existing therapies is a major clinical challenge (1). Molecular-level pan-cancer analyses have provided insights into the common features and heterogeneity of various human malignancies (2). For example, Cancer Cell Line Encyclopedia (CCLE) and The Cancer Genome Atlas (TCGA) were developed based on epigenomic, genomic, proteomic, and transcriptomic data from multiple human cancer cell lines and tissues (3–5). Pan-cancer analyses have also revealed the significance of specific genes and signaling pathways in cancers. For example, tumor hypoxia-associated multi-omic investigations have shown that some molecular variants are correlated with antitumor drug sensitivity or resistance, which has important implications for cancer treatment (6). The expression status of Forkhead box M1 and its relationship to etiology and outcomes of human cancers (7), as well as proteomic and genomic features related to MYC and the proximal MYC network (8) have been reported for 33 cancer types in TCGA. The expression of more than 9,000 genes in TCGA has been characterized in terms of their contribution to the immune phenotype of various cancers (9). Thus, pan-cancer analyses can be useful for the development of new combination treatments and individualized therapies.

The mechanisms of immune evasion by cancer cells are the target of immunotherapies (10). Cytotoxic T lymphocyte-associated protein (CTLA)4 and programmed death (PD)-1 are receptors that attenuate the T cell response (11). Both factors are the immune checkpoint inhibitors with distinct but complementary mechanisms of action. CTLA4 is a target for monoclonal antibody-based drugs that enhance anticancer immunity such as ipilimumab, which was the first CTLA4 inhibitor to be developed and the only one to date that has been approved by the U.S. Food and Drug Administration (FDA) (12). PD-1 is a transmembrane protein that is expressed by immunocytes; blocking PD-1 signaling enhances the anticancer effect of T cells, thereby promoting cancer cell killing. The combination of nivolumab (13)—which targets PD-1—and ipilimumab increased overall survival (OS) in patients with melanoma (14), renal cell carcinoma (15–17), and advanced non-small cell lung cancer (18), and has been approved for the treatment of hepatocellular carcinoma (LIHC) patients previously treated with sorafenib (19).

Although PD-1 and CTLA4 overexpression, mutations, and gene amplification have been reported in certain cancers, the studies had small sample sizes and used different experimental approaches, making it difficult to compare the findings. Additionally, these studies focused on a single or a few

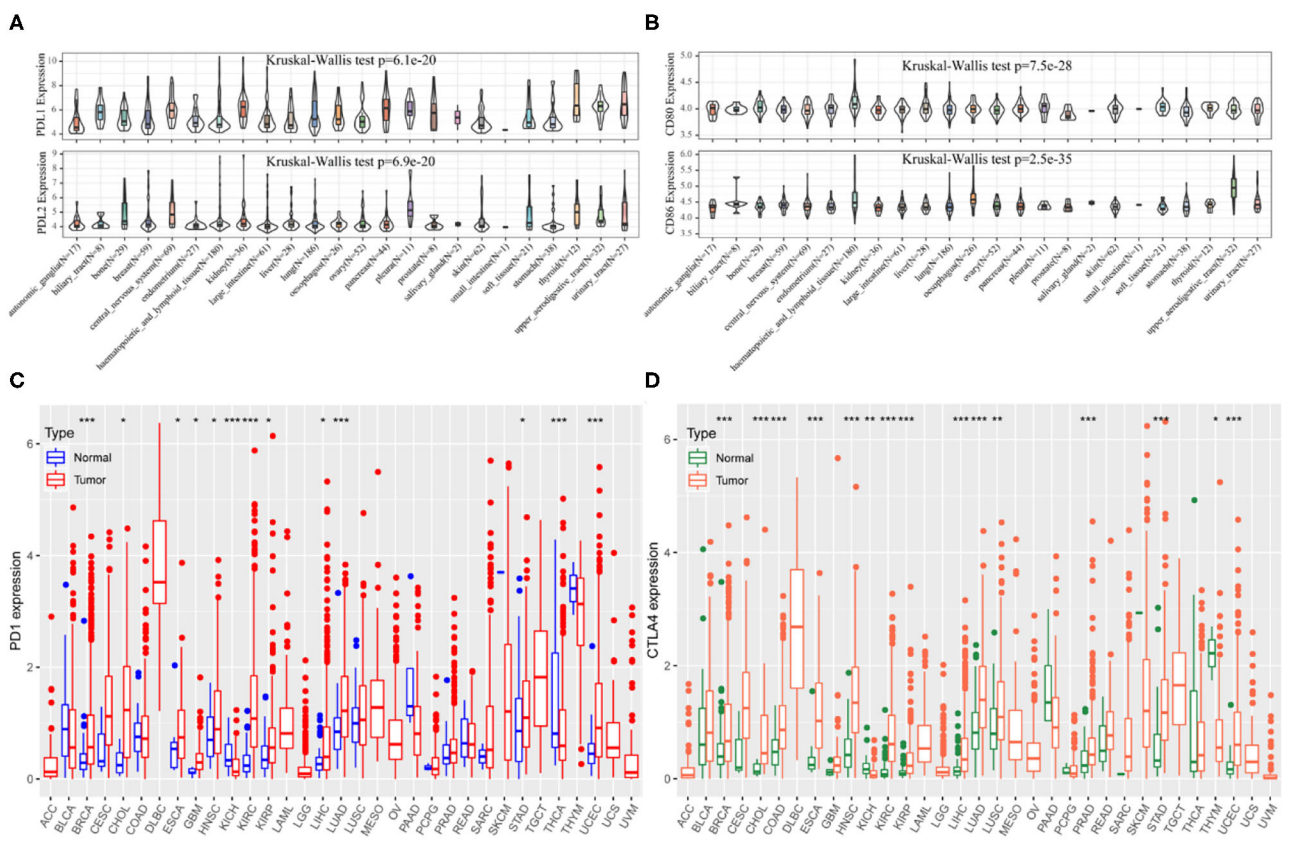

FIGURE 1 | PD-1 and CTLA4 expression in different cancer types. **(A–D)** Expression levels of PD-1 **(A,C)** and CTLA4 **(B,D)** in CCLE **(A,B)** and TCGA **(C,D)** are shown. *$P < 0.05$, **$P < 0.01$, ***$P < 0.001$.

types of cancer; there have been no studies comparing multiple types of cancer. To this end, the present study investigated PD-1 and CTLA4 expression profiles and their prognostic significance in various human malignancies based on large CCLE and TCGA datasets. We also examined the associations between PD-1/CTLA4 expression and the extent of tumor cell infiltration, microsatellite instability (MSI), tumor mutational burden (TMB), DNA methyltransferase (DNMT) levels, and mismatch repair (MMR) in different tumor types by gene set enrichment analysis (GSEA). The results provide important insights into the roles of PD-1 and CTLA4 in anticancer immunity.

MATERIALS AND METHODS

Patient Datasets and Processing

TCGA comprises over 20,000 samples from 33 types of cancer and corresponding non-carcinoma samples. Processed level 3 RNA sequencing data and corresponding clinical annotations were obtained from TCGA using the University of California Santa Cruz cancer genome browser (https://tcga.xenahubs.net; accessed April 2020). CCLE (https://portals.broadinstitute.org/ccle) provides genetic and pharmacologic information from a large number of human tumor models, with RNA sequencing data for over 1,000 cell lines. Ethics approval for use of human data was not required for this part of the study as only open-access datasets were used.

A total of 122 consecutive patients with LIHC (mean age, 46.8 years; range: 22–75 years) who underwent curative resection and received adjuvant cytokine-induced killer (CIK) cell immunotherapy at Sun Yat-sen University Cancer Center between March 2004 and January 2015 were enrolled. Preparation of CIK cells and the treatment schedule are described in our previous study (20). Preoperative patient serum samples were obtained from our hospital's sample bank and analyzed using an anti-PD-1 and -CTLA4 antibody array (RayBiotech, Norcross, GA, USA; product no. QAH-ICM-1-1) according to the manufacturer's instructions. Briefly, the array was incubated with blocking buffer for 1 h before 2-fold–diluted serum samples (60 μl) were added. After overnight incubation at 4°C followed by washes, biotin-conjugated detection antibody was added for 2 h. The array was washed and Alexa Fluor 555-conjugated streptavidin was added for 1 h at room temperature. An InnoScan 300 scanner (Inopsys, Carbonne, France) was used to detect the signals (532 nm excitation); raw data were processed as images and spot intensities using Mapix 7.3.1 software (Innopsys). Serum concentrations of PD-1 and CTLA4 proteins were determined by automatic normalization and calculation. Follow-up was conducted until November 2019, with a median time of 84.3 months (range: 11.6–134.7 months). The primary endpoint was OS. This study was approved by the Ethics Committee of Sun Yat-sen University Cancer Center. All participants provided written, informed consent. The analytical workflow is shown in **Supplementary Figure 1**.

Correlation Between PD-1/CTLA4 Expression and Survival

Data on PD-1 and CTLA4 gene expression for 33 cancer types and adjacent non-carcinoma tissues were extracted from TCGA and used to generate an expression matrix, which was matched

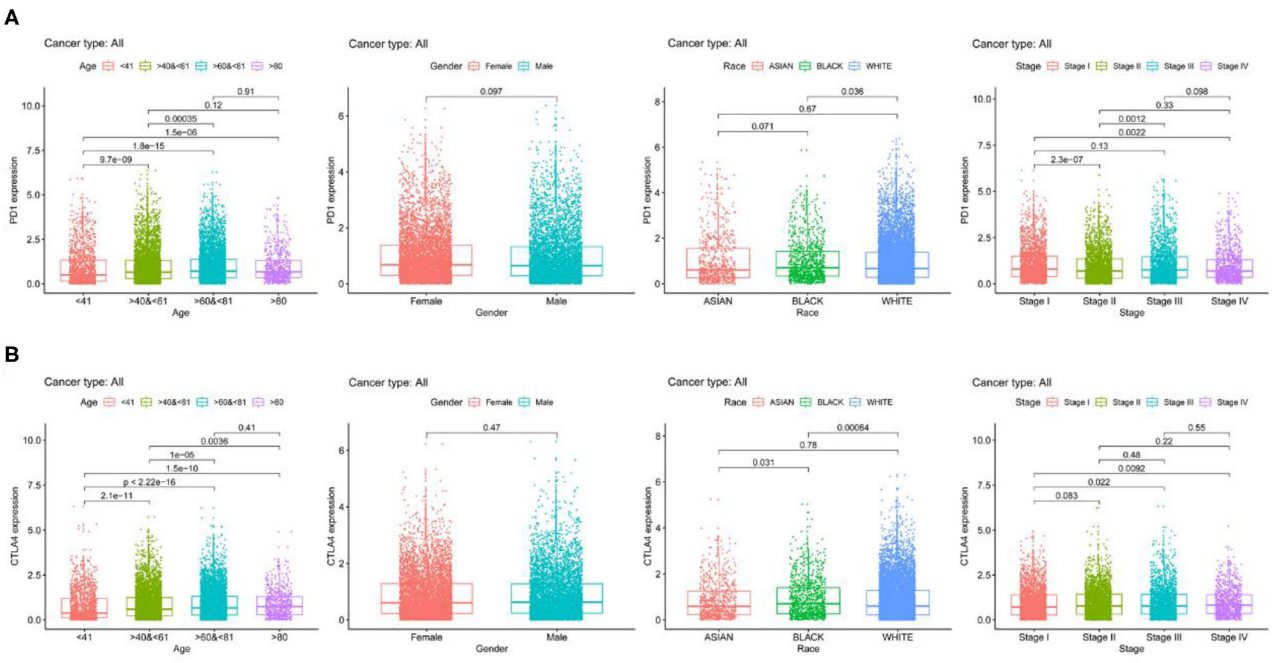

FIGURE 2 | PD-1 and CTLA4 expression across 21 cancer types. **(A,B)** Boxplots of PD-1 **(A)** CTLA4 **(B)** levels.

to clinical information by patient identification number. A univariate Cox proportional hazards model was used to calculate correlations between gene expression and patient survival, where $P < 0.05$ was taken as the threshold for a statistically significant difference for PD-1 and CTLA4 expression in a given cancer relative to normal tissue. A Kaplan–Meier survival analysis was carried out to compare OS of patients in TCGA, which was stratified according to median PD-1 and CTLA4 expression levels with the log-rank test.

Relationship Between PD-1/CTLA4 and Tumor Immunity

Tumor Immune Estimation Resource (TIMER; https://cistrome.shinyapps.io/timer/) allows systemic analysis of immune infiltrates in different cancer types (21) using a deconvolution statistical approach to infer tumor-infiltrating lymphocyte (TIL) counts based on gene expression data (22). Using the TIMER algorithm, we examined the associations between PD-1/CTLA4 levels and the numbers of 6 immune

TABLE 1 | Univariate Cox regression analysis of the associations of PD-1 and CTLA4 expression with patient survival.

Cancer	PD-1-OS			PD-1-PFI			CTLA4-OS			CTLA4-PFI		
	HR	HR (95% CI)	*P*-value	HR	HR (95% CI)	*P*-value	HR	HR (95% CI)	*P*-value	HR	HR (95% CI)	*P*-value
ACC	1.338	0.670–2.675	0.409	0.675	0.281–1.626	0.381	1.305	0.477–3.571	0.605	0.605	0.201–1.825	0.372
BLCA	0.813	0.676–0.977	0.027	0.777	0.645–0.936	0.008	0.826	0.694–0.984	0.032	0.750	0.627–0.896	0.002
BRCA	0.753	0.595–0.953	0.018	0.688	0.538–0.879	0.003	0.845	0.681–1.049	0.127	0.831	0.672–1.028	0.088
CESC	0.683	0.514–0.907	0.008	0.686	0.516–0.912	0.010	0.652	0.482–0.882	0.006	0.581	0.423–0.799	0.001
CHOL	0.979	0.657–1.461	0.919	0.952	0.655–1.383	0.795	0.630	0.286–1.387	0.251	0.388	0.161–0.937	0.035
COAD	1.219	0.872–1.704	0.247	1.130	0.837–1.525	0.424	0.767	0.537–1.095	0.144	0.855	0.631–1.160	0.315
DLBC	0.807	0.461–1.413	0.454	1.203	0.745–1.942	0.451	0.972	0.569–1.660	0.918	1.113	0.701–1.767	0.649
ESCA	1.066	0.745–1.523	0.727	0.909	0.658–1.256	0.564	0.898	0.659–1.225	0.498	0.832	0.628–1.102	0.199
GBM	2.048	1.156–3.628	0.014	1.585	0.894–2.813	0.115	1.307	0.945–1.807	0.106	1.023	0.691–1.515	0.910
HNSC	0.764	0.638–0.914	0.003	0.814	0.679–0.974	0.025	0.725	0.606–0.868	<0.001	0.799	0.671–0.951	0.012
KICH	1.113	0.085–14.499	0.935	1.439	0.280–7.412	0.663	3.155	0.054–185.196	0.580	7.337	0.560–96.103	0.129
KIRC	1.210	1.064–1.375	0.004	1.130	0.995–1.284	0.060	1.619	1.292–2.028	<0.001	1.345	1.080–1.675	0.008
KIRP	1.568	1.241–1.981	<0.001	1.421	1.141–1.769	0.002	1.804	1.054–3.088	0.031	1.651	1.045–2.608	0.032
LAML	1.316	1.021–1.697	0.034	\	\	\	1.452	0.959–2.198	0.078	\	\	\
LGG	3.423	2.153–5.441	<0.001	2.381	1.578–3.594	<0.001	2.671	1.566–4.556	<0.001	3.365	2.057–5.505	<0.001
LIHC	1.009	0.818–1.245	0.935	0.884	0.732–1.069	0.203	1.008	0.740–1.374	0.959	0.918	0.709–1.188	0.516
LUAD	0.978	0.813–1.177	0.814	0.967	0.818–1.143	0.694	0.777	0.638–0.945	0.012	0.884	0.743–1.051	0.161
LUSC	1.007	0.846–1.199	0.934	0.997	0.814–1.220	0.975	1.007	0.837–1.210	0.943	0.947	0.765–1.173	0.617
MESO	1.001	0.781–1.282	0.995	0.983	0.728–1.327	0.912	1.078	0.804–1.446	0.615	0.859	0.572–1.289	0.463
OV	0.885	0.703–1.114	0.297	0.867	0.712–1.055	0.154	0.711	0.508–0.996	0.047	0.739	0.557–0.980	0.035
PAAD	0.952	0.695–1.304	0.759	1.028	0.792–1.334	0.835	0.970	0.715–1.316	0.846	1.034	0.795–1.345	0.803
PCPG	0.770	0.085–6.953	0.816	1.865	0.652–5.333	0.245	0.010	0.000–19.263	0.232	1.411	0.213–9.346	0.721
PRAD	0.728	0.155–3.422	0.687	1.356	0.929–1.980	0.115	0.571	0.109–2.993	0.507	1.358	0.986–1.870	0.061
READ	1.054	0.408–2.718	0.914	0.958	0.441–2.083	0.914	0.974	0.522–1.817	0.934	1.133	0.682–1.882	0.631
SARC	0.853	0.691–1.053	0.139	0.947	0.810–1.108	0.499	0.886	0.663–1.184	0.413	0.965	0.773–1.204	0.751
SKCM	0.764	0.683–0.855	<0.001	0.898	0.823–0.980	0.016	0.783	0.691–0.888	<0.001	0.907	0.823–1.000	0.050
STAD	0.794	0.644–0.978	0.030	0.942	0.768–1.155	0.565	0.775	0.624–0.962	0.021	0.875	0.705–1.085	0.223
TGCT	1.373	0.507–3.717	0.533	0.927	0.686–1.255	0.625	2.026	0.563–7.294	0.280	0.869	0.604–1.250	0.448
THCA	0.706	0.322–1.546	0.384	1.032	0.774–1.375	0.832	0.896	0.384–2.091	0.800	1.207	0.861–1.692	0.276
THYM	0.801	0.423–1.515	0.495	1.108	0.691–1.776	0.669	1.954	1.191–3.203	0.008	1.966	1.343–2.879	0.001
UCEC	0.684	0.530–0.882	0.003	0.709	0.572–0.879	0.002	0.592	0.412–0.852	0.005	0.650	0.483–0.874	0.004
UCS	1.185	0.740–1.899	0.479	0.853	0.524–1.388	0.522	1.073	0.577–1.995	0.824	0.840	0.469–1.503	0.557
UVM	1.905	1.289–2.816	0.001	1.506	1.007–2.253	0.046	3.299	1.299–8.379	0.012	2.088	0.745–5.849	0.161

ACC, adrenocortical carcinoma; BLCA, bladder urothelial carcinoma; BRCA, breast invasive carcinoma; CESC, cervical squamous cell carcinoma and endocervical adenocarcinoma; CHOL, cholangiocarcinoma; COAD, colon adenocarcinoma; DLBC, lymphoid neoplasm diffuse large B-cell lymphoma; ESCA, esophageal carcinoma; GBM, glioblastoma multiforme; HNSC, head and neck squamous cell carcinoma; KICH, kidney chromophobe; KIRC, kidney renal clear cell carcinoma; KIRP, kidney renal papillary cell carcinoma; LAML, acute myeloid Leukemia; LGG, brain lower grade glioma; LIHC, liver hepatocellular carcinoma; LUAD, lung adenocarcinoma; LUSC, lung squamous cell carcinoma; MESO, Mesothelioma; OV, ovarian serous cystadenocarcinoma; PAAD, pancreatic adenocarcinoma; PCPG, pheochromocytoma and paraganglioma; PRAD, prostate adenocarcinoma; READ, Rectum adenocarcinoma; SARC, sarcoma; SKCM, skin cutaneous melanoma; STAD, stomach adenocarcinoma; TGCT, testicular germ cell tumors; THCA, thyroid carcinoma; THYM, thymoma; UCEC, uterine corpus endometrial carcinoma; UCS, uterine carcinosarcoma; UVM, uveal melanoma.

infiltrates—namely, cluster of differentiation [CD]4+ T cells, CD8+ T cells, B cells, neutrophils, dendritic cells, and macrophages.

Estimating Relative Subsets of RNA Transcripts (CIBERSORT) is a metagene tool that can be used to predict the phenotypes of 22 human immunocytes, as previously reported for all TCGA samples (23). In this study, CIBERSORT was used to calculate the relative fractions of the 22 leukocyte types; the correlations between *PD-1/CTLA4 levels and each leukocyte across 33 cancer types was then determined.*

Estimation of Stromal and Immune Cells in Malignant Tumor Tissues Using Expression Data (ESTIMATE) uses gene expression profiles to predict the purity of a tumor based on infiltration of stromal cells/immunocytes (24). The ESTIMATE

FIGURE 3 | Association between PD-1 expression and OS. **(A–I)** Kaplan–Meier analysis of the association between PD-1 expression and OS.

algorithm yields 3 scores based on GSEA of single samples, including (1) stromal score, which reflects the presence of stromal cells in tumor tissue; (2) immune score, which indicates the degree of immunocyte infiltration into tumor tissue; and (3) estimate score, which describes tumor purity. We used the algorithm to estimate both immune and stromal scores for a variety of tumor tissues, and evaluated the associations between the scores and PD-1/CTLA4 levels.

We also examined the associations between PD-1/CTLA4 levels and the expression of TIL markers (25–27). An expression heatmap was generated for gene pairs in specific cancer types and correlations were analyzed with Spearman's rank correlation test.

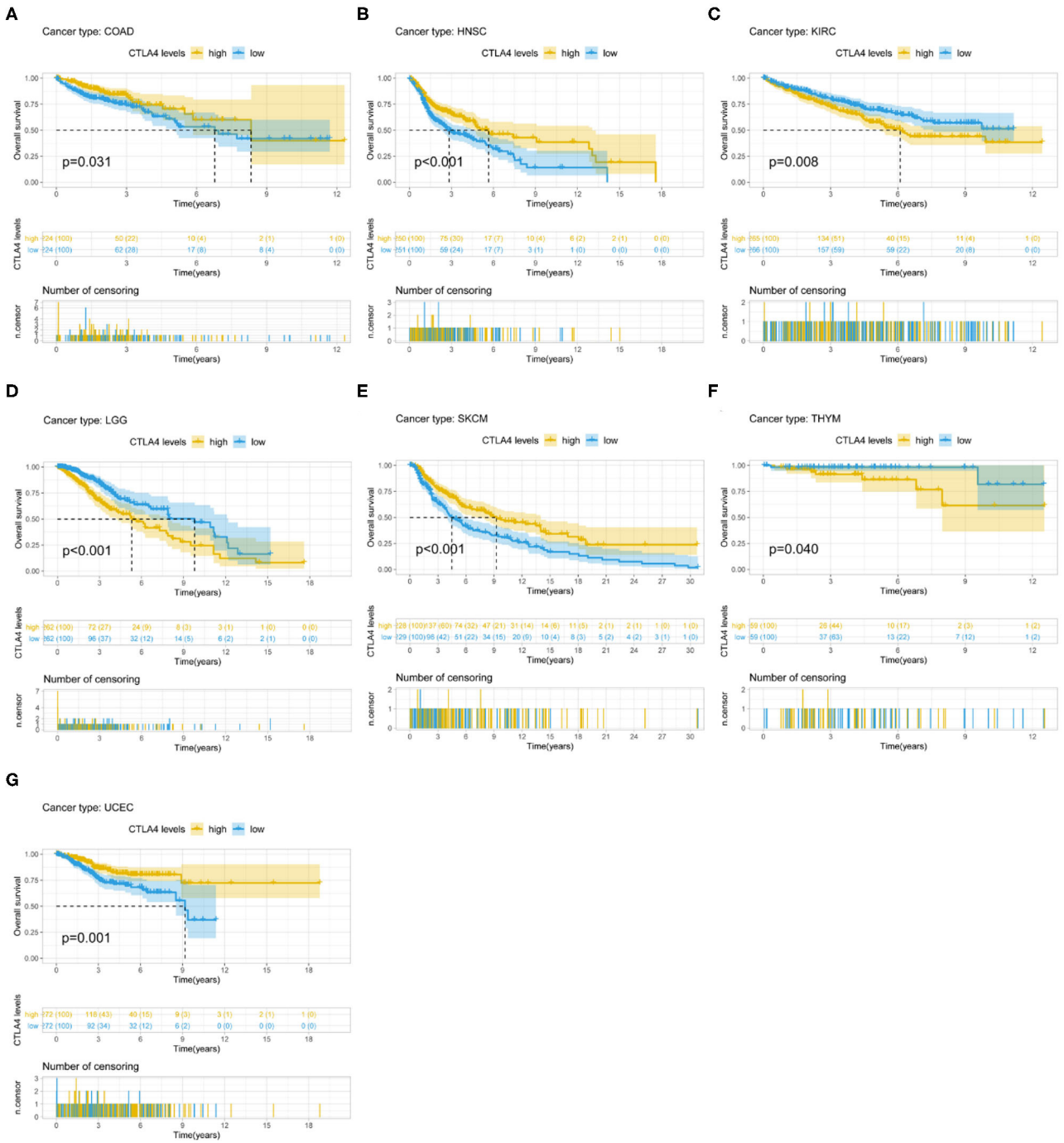

FIGURE 4 | Association between CTLA4 expression and OS. **(A–G)** Kaplan–Meier analysis of the association between CTLA4 expression and OS.

TMB measures the number of mutations in a specific cancer genome and is used as a biomarker to identify patients that are most likely to respond to checkpoint inhibitor therapy (28). We obtained somatic mutation data of all TCGA patients (https://tcga.xenahubs.net), calculated their TMB scores, and then analyzed the correlation between TMB and PD-1/CTLA4 level. MSI is characterized by length polymorphisms of microsatellite sequences resulting from DNA polymerase slippage. Patients with high MSI (MSI-H) cancers benefit from immunotherapy, and MSI is an index used for cancer detection (29). We computed the MSI score of each patient and performed a correlation analysis between MSI and PD-1/CTLA4. MMR, is a DNA repair mechanism in normal cells that corrects DNA replication errors. Gene mutation frequency may be increased in cancer cells as a result of downregulation of MMR genes or defective MMR (29). Here we analyzed the correlation between MMR gene (MutL homolog [MLH]1, MutS homolog [MSH]2, MSH6, postmeiotic segregation increased [PMS]2, and epithelial cell adhesion molecule [EPCAM]) and PD-1/CTLA4 expression levels. DNA methylation has been implicated in tumorigenesis and cancer progression. As DNMT1, DNMT2, DNMT3A, and DNMT3B are the major enzymes involved in DNA methylation (30), we analyzed the correlation between their expression levels and those of PD-1 and CTLA4.

Functional Analysis

We carried out GSEA using the JAVA program (http://software.broadinstitute.org/gsea/index.jsp) to investigate the biological significance of PD-1 and CTLA4 expression levels in tumor tissues. The random sample permutation number was set as 100, and the threshold of significance was $P < 0.05$. The results were visualized with enrichment maps generated using Bioconductor (http://bioconductor.org/) and R v3.6.0 software (R Foundation, Vienna, Austria).

Statistical Analysis

Survival was evaluated as OS (defined as the time from the date of diagnosis to death from any cause) and progression-free survival (PFS; defined as the time until disease progression or death from any cause). The Wilcox log-rank test was used to assess changes in the sum of gene expression z-scores of cancer tissues compared to adjacent normal tissues. Differences in PD-1 and CTLA4 levels between different tumor stages were compared with the Kruskal–Wallis test. Survival was analyzed with Kaplan–Meier curves, the log-rank test, and Cox proportional hazards regression model. Spearman's or Pearson's test was used for correlation analysis. All statistical analyses were performed using R software.

RESULTS

Pan-Cancer Expression Profiles of PD-1 and CTLA4

The CCLE data revealed variable expression of PD-1 and CTLA4 ligands across cancer cell lines (both $P < 0.001$; **Figures 1A,B**). Among the 33 cancer types in TCGA, PD-1 and CTLA4 levels were upregulated in tumor tissues relative to matched non-carcinoma tissues in uterine corpus endometrial carcinoma (UCEC), cholangiocarcinoma (CHOL), breast cancer (BRCA), head-neck squamous cell carcinoma (HNSC), esophageal carcinoma (ESCA), kidney renal papillary

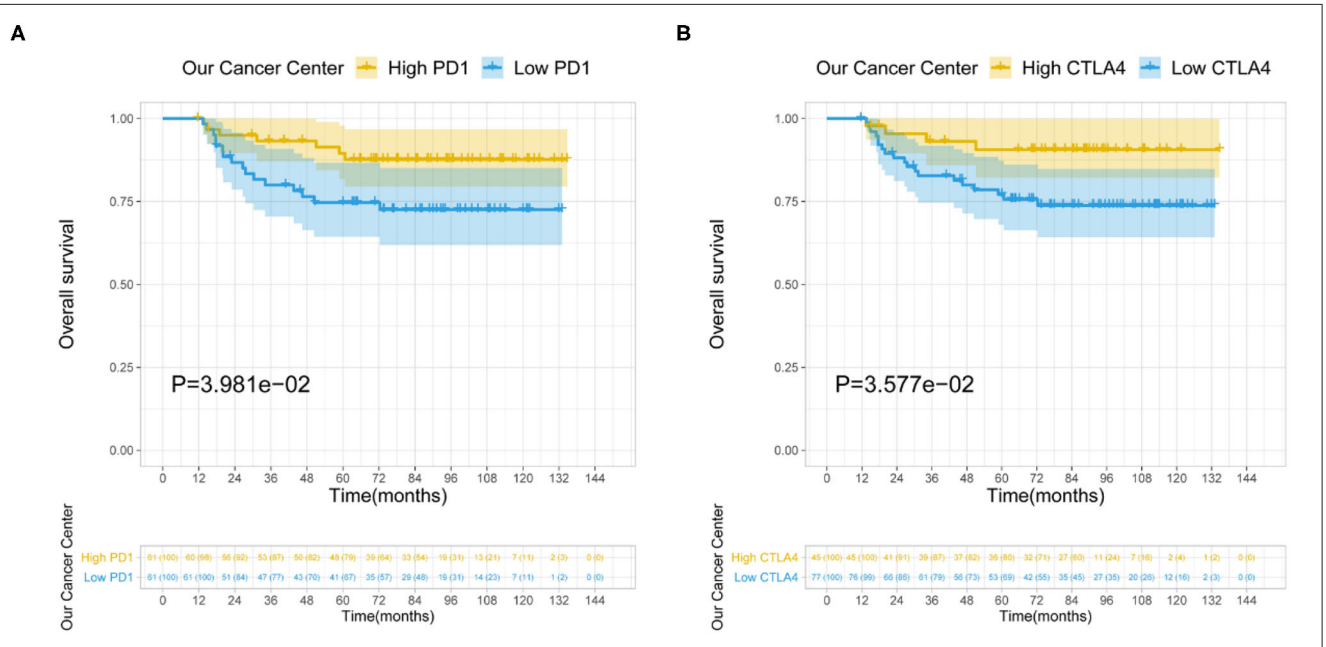

FIGURE 5 | Relationship between serum PD-1/CTLA4 levels and prognosis of LIHC patients receiving CIK therapy. **(A,B)** Serum levels of PD-1 **(A)** and CTLA4 **(B)** are shown.

cell carcinoma (KIRP), kidney renal clear cell carcinoma (KIRC), lung adenocarcinoma (LUAD), LIHC, and stomach adenocarcinoma (STAD); whereas both were downregulated in kidney chromophobe. PD-1 was also upregulated in glioblastoma multiforme (GBM) and downregulated in thyroid cancer (THCA). CTLA4 expression was elevated in colon adenocarcinoma (COAD), lung squamous cell carcinoma (LUSC), and prostate adenocarcinoma (PRAD) and reduced in thymoma (THYM). The expression profiles of PD-1 and CTLA4 in TCGA cohorts are shown in **Figures 1C,D**, respectively, and PD-1 and CTLA4 gene expression matrices for the 33 cancer types in TCGA are shown in **Supplementary Table 1**.

We examined PD-1 and CTLA4 expression according to age, sex, race, and tumor stage and found that older patients had higher expressions of these genes than younger patients, while no differences were observed between sexes (**Figure 2**). Black patients had higher PD-1 and CTLA4 levels than Caucasian patients. PD-1 level was higher whereas CTLA4 level was lower in stage I disease compared to other stages.

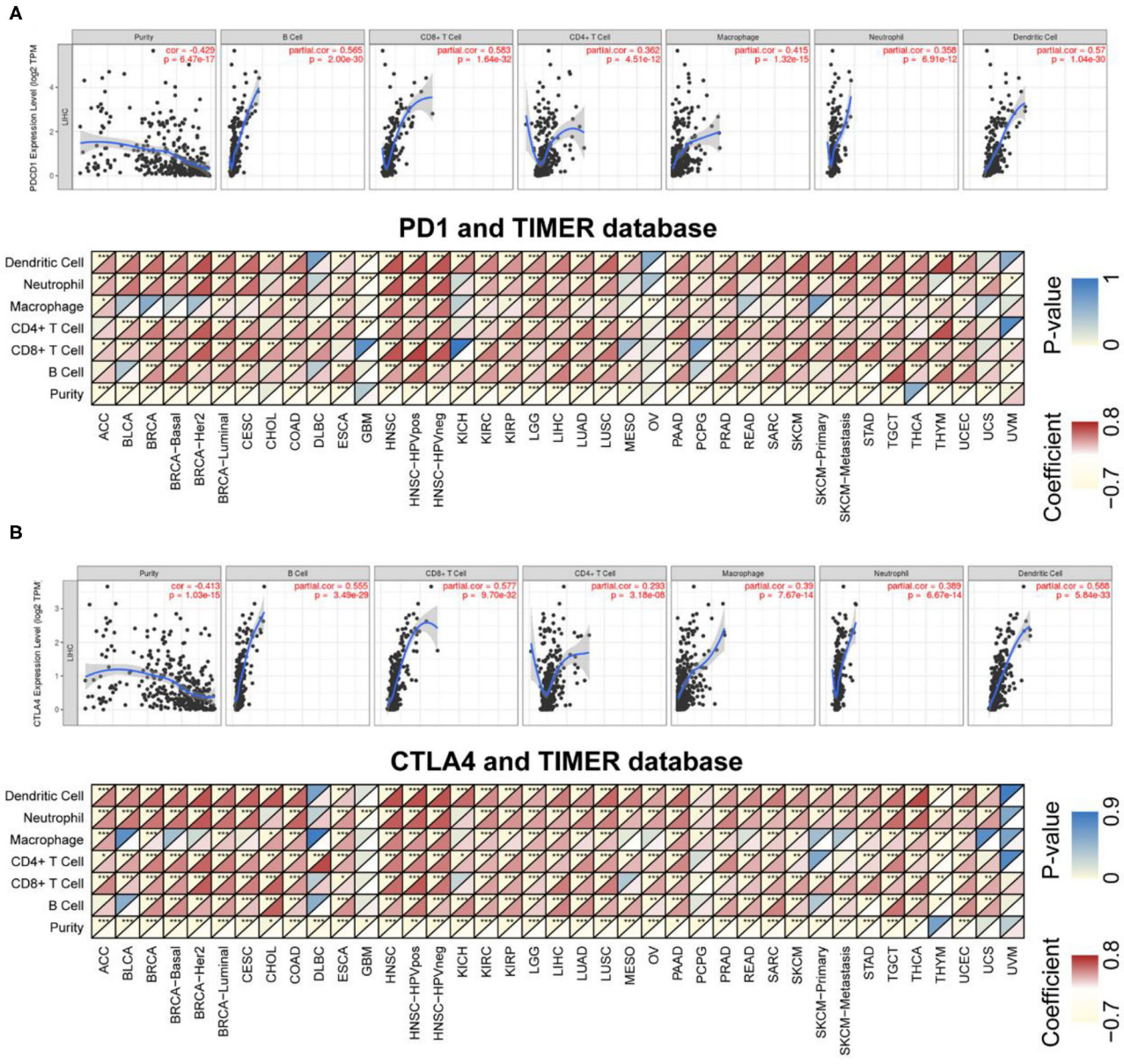

FIGURE 6 | Correlation between PD-1/CTLA4 expression and cancer immunity in TIMER. **(A)**, Top Association between PD-1 level and degree of TIL infiltration in LIHC. (Bottom) TIMER prediction of the association between PD-1 level and degree of TIL infiltration in 33 cancer types. **(B)** TIMER prediction of the relationship between CTLA4 level and degree of TIL infiltration in LIHC and 33 cancer types. For each pair in **(A,B)**, the left top triangle is colored to represent the *P*-value, and the right bottom triangle is colored to represent the Spearman correlation coefficient. $^{*}P < 0.05$, $^{**}P < 0.01$, $^{***}P < 0.001$.

Association Between PD-1/CTLA4 Levels and Survival

PD-1 expression was identified by Cox regression analysis as a prognostic factor for OS in urothelial bladder carcinoma (BLCA), BRCA, cervical squamous cell carcinoma and endocervical adenocarcinoma (CESC), GBM, HNSC, KIRC, acute myeloid leukemia (LAML), STAD, UCEC, and uveal melanoma (UVM) (**Table 1**). The Kaplan–Meier survival analysis showed that subjects with higher PD-1 levels had shorter OS than those with lower levels in GBM ($P = 0.037$), KIRP ($P = 0.040$), LAML ($P = 0.002$), low-grade glioma (LGG) ($P < 0.001$), and UVM ($P < 0.001$). On the other hand, subjects with higher PD-1 levels had longer OS than those with lower levels in BRCA ($P = 0.014$), HNSC ($P = 0.006$), skin cutaneous melanoma (SKCM) ($P < 0.001$), and UCEC ($P < 0.001$) (**Figures 3A–I**).

PD-1 expression was also a prognostic factor for PFS in BLCA, BRCA, CESC, HNSC, KIRP, SKCM, UCEC, and UVM (**Table 1**). The Kaplan–Meier survival analysis showed that patients with higher PD-1 expression had shorter OS than those with lower expression in LGG ($P < 0.001$) and UVM ($P = 0.025$), whereas patients with higher PD-1 levels had longer OS than those with lower PD-1 levels in BRCA ($P = 0.018$), CESC ($P =$

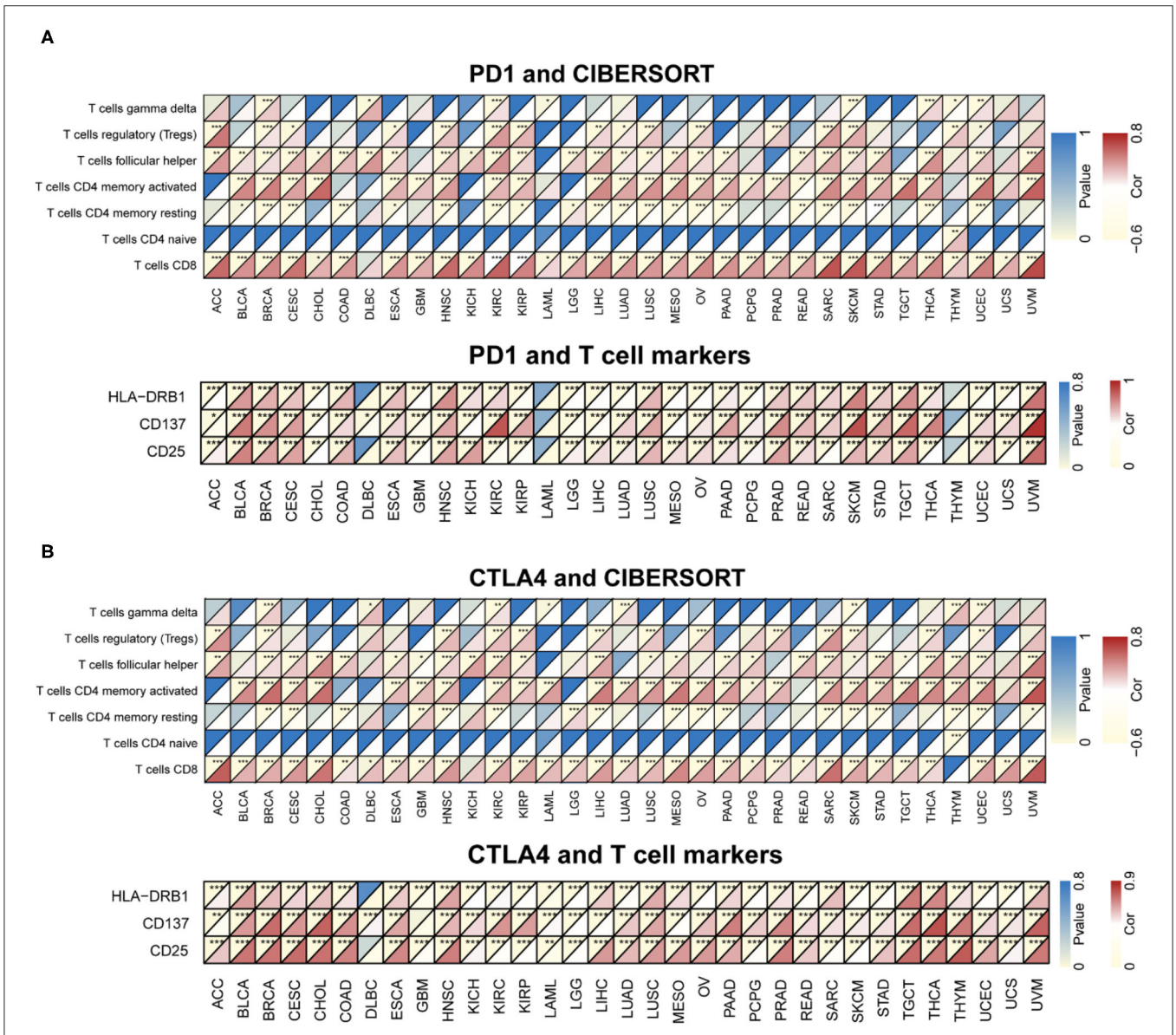

FIGURE 7 | Correlation between PD-1 and CTLA4 expression and cancer immunity in CIBERSORT. **(A,B)** CIBERSORT prediction of the association between PD-1 **(A)** and CTLA4 **(B)** levels and degree of TIL infiltration in 33 cancer types. For each pair, the left top triangle is colored to represent the *P*-value, and the bottom right triangle is colored to represent the Spearman correlation coefficient. $^{*}P < 0.05$, $^{**}P < 0.01$, $^{***}P < 0.001$.

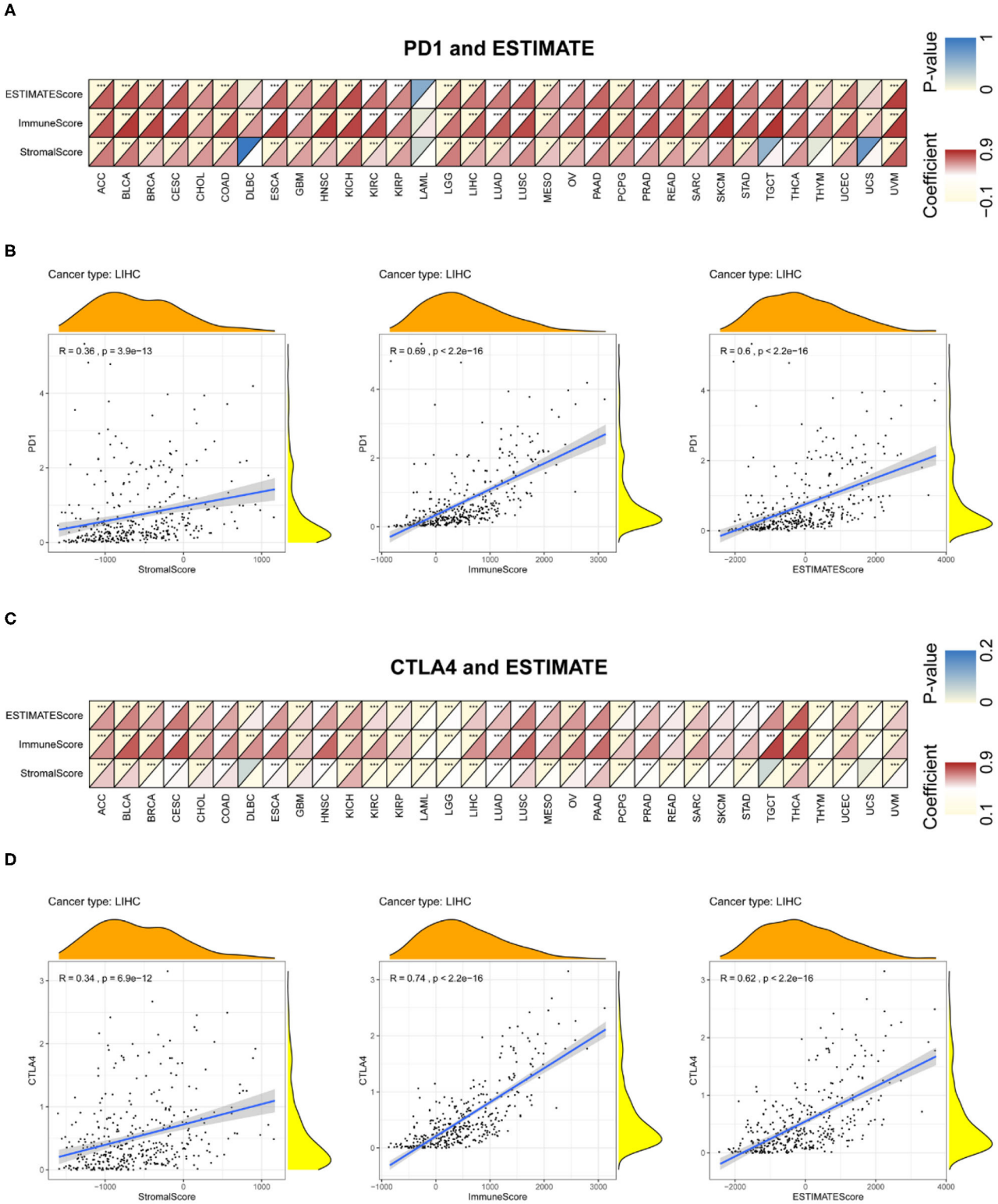

FIGURE 8 | Correlation between PD-1 and CTLA4 expression and cancer immunity in ESTIMATE. ESTIMATE prediction of the relationship between PD-1 **(A,B)** and CTLA4 **(C,D)** levels and the degree of TIL infiltration in 33 cancer types **(A,C)** and LIHC **(B,D)**. For each pair, the top left triangle is colored to represent the *P*-value, and the bottom right triangle is colored to represent the Spearman correlation coefficient. $^{*}P < 0.05$, $^{**}P < 0.01$, $^{***}P < 0.001$.

0.047), SKCM ($P = 0.047$), and UCEC ($P < 0.001$) (**Supplementary Figures 2A–F**).

CTLA4 expression was identified by Cox regression analysis as a prognostic factor for OS in BLCA, BRCA, CESC, GBM, HNSC, KIRC, LAML, STAD, UCEC, and UVM (**Table 1**). The Kaplan–Meier survival analysis showed that patients with higher CTLA4 expression had shorter OS than those with lower CTLA4 expression in KIRC ($P = 0.008$), LGG ($P < 0.001$), and THYM ($P = 0.040$). Meanwhile, patients with higher CTLA4 levels had longer OS than those with lower levels in COAD ($P = 0.031$), HNSC ($P < 0.001$), SKCM ($P < 0.001$), and UCEC ($P = 0.001$) (**Figures 4A–G**).

CTLA4 expression was also a prognostic factor for PFS in BLCA, CESC, CHOL, HNSC, KIRC, KIRP, ovarian serous cystadenocarcinoma (OV), THYM, and UCEC (**Table 1**). The Kaplan–Meier survival analysis showed that patients with higher CTLA4 expression had shorter OS than those with lower expression in KIRC ($P = 0.021$), LGG ($P < 0.001$), and THYM ($P = 0.010$), whereas patients with higher CTLA4 levels had longer OS than those with lower levels in BLCA ($P = 0.011$), HNSC ($P = 0.004$), and UCEC ($P = 0.002$) (**Supplementary Figures 3A–F**).

Among the LIHC patients at our hospital, the median serum PD-1 level was 82.9 μg/μl (range, 7.6–2,886.8); serum CTLA4 was undetectable in 77 patients (63.1%), and the maximum level was 88.6 μg/μl in the others ($n = 45$; 36.9%). The survival analysis showed that among LIHC patients who underwent CIK cell therapy, higher levels of PD-1 ($P = 0.040$) and CTLA4 ($P = 0.036$) were associated with longer OS (**Figure 5**).

Relationship Between PD-1/CTLA4 Levels and Degree of Immune Cell Infiltration

TILs are independent predictors of sentinel lymph node status as well as survival. We examined the correlation between PD-1/CTLA4 levels and the degree of immune cell infiltration in diverse cancer types in TIMER. PD-1 and CTLA4 levels were significantly associated with tumor purity in 35 and 36 cancer types, respectively. Additionally, PD-1 and CTLA4 levels were correlated with the degree of infiltration of CD4+ T cells in 33 and 33 cancer types, respectively; of B cells in 30 and 32 cancer types, respectively; of CD8+ T cells in 32 and 34 cancer types, respectively; of macrophages in 24 and 25 cancer types, respectively; of dendritic cells in 35 and 36 cancer types, respectively; and of neutrophils in 32 and 35 cancer types, respectively. The FDA granted the accelerated approval for the use of PD-1 in combination with CTLA4 for the treatment of LIHC (19). In this study, the association of the degree of immune infiltration with the levels of PD-1 and CTLA4 within LIHC is presented as an example in the top panels of **Figures 6A,B**. While the pan-cancer correlations of immune infiltration level with

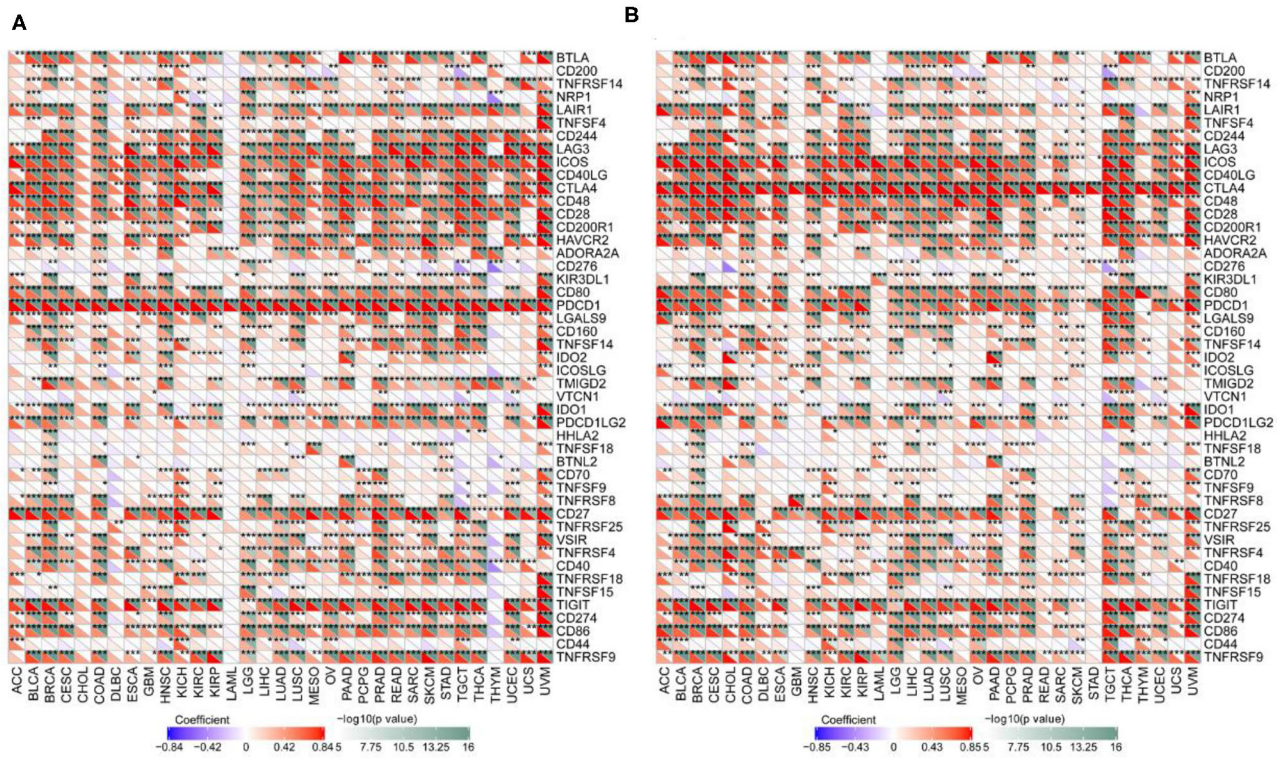

FIGURE 9 | Correlation between PD-1 and CTLA4 levels and expression of immune markers. **(A,B)** Heatmap of the relationship between PD-1 **(A)** and CTLA4 **(B)** levels and expression T cell and other immunocyte markers in 33 cancer types. For each pair, the top right triangle is colored to represent the *P*-value, and the bottom left triangle is colored to represent the correlation coefficient. $^{*}P < 0.05$, $^{**}P < 0.01$, $^{***}P < 0.001$.

PD-1 and CTLA4 expression are present in the bottom panels of **Figures 6A,B** and **Supplementary Table 2**, respectively.

CIBERSORT was used to determine immunocyte profiles in all TCGA patients, and the correlation between 22 immunocytes and PD-1/CTLA4 expression was determined for the 33 cancer types in TCGA (**Supplementary Table 3**). PD-1 and CTLA4 were significantly correlated with CD8+ T cell but not CD4+ naïve T cell counts in most cancers (**Figure 7**). Additionally, the expression of T cell markers (CD25, CD137, and human leukocyte antigen DRB1) was correlated with PD-1 and CTLA4 levels.

Immune and stromal scores for tumor tissues were calculated using ESTIMATE; we then assessed the associations between these scores and PD-1 and CTLA4 expression (**Figure 8** and

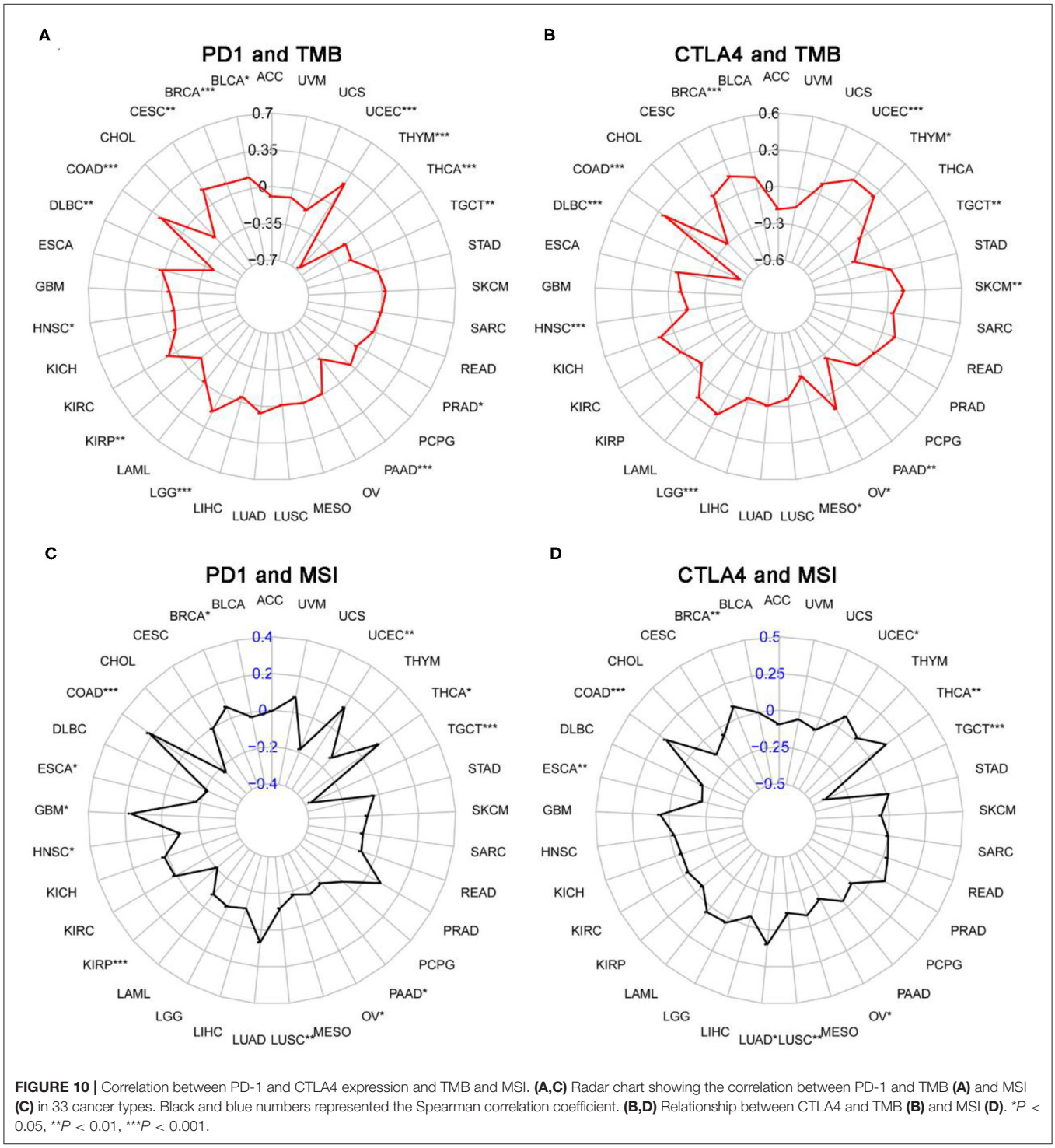

FIGURE 10 | Correlation between PD-1 and CTLA4 expression and TMB and MSI. **(A,C)** Radar chart showing the correlation between PD-1 and TMB **(A)** and MSI **(C)** in 33 cancer types. Black and blue numbers represented the Spearman correlation coefficient. **(B,D)** Relationship between CTLA4 and TMB **(B)** and MSI **(D)**. $^{*}P < 0.05$, $^{**}P < 0.01$, $^{***}P < 0.001$.

Supplementary Table 4). **Figures 8B,D** exhibit the typical results in LIHC. The results showed that PD-1 and CTLA4 levels were significantly correlated with immune and stromal scores as well as estimate scores.

Correlations Between PD-1/CTLA4 and Immune Cell Marker Expression

We examined the associations between TIL markers and PD-1/CTLA4 expression and found that PD-1 and CTLA4 levels were significantly correlated with the expression of T cell and other immunocyte markers (**Figure 9**), suggesting that both factors are involved in the regulation of the immune response to these cancers.

Correlation Analysis of TMB, MSI, MMR, and DNMT Expression

We next examined the associations between PD-1/CTLA4 expression and TMB, MSI, MMR, and DNMT levels (**Supplementary Table 5** and **Figures 10**, **11**). PD-1 expression was correlated with TMB in BRCA, BLCA, COAD, CESC, HNSC, lymphoid neoplasm diffuse large b-cell lymphoma (DLBC), LGG, KIRP, PRAD, pancreatic adenocarcinoma (PAAD), testicular germ cell tumors (TGCT), THCA, THYM, and UCEC (**Figure 10A**); and CTLA4 expression was correlated with TMB in DLBC, BRCA, COAD, OV, HNSC, mesothelioma, LGG, SKCM, UCEC, PAAD, THYM, and TGCT (**Figure 10B**). PD-1 expression was correlated with MSI in COAD, BRCA, GBM, ESCA, OV, KIRP, HNSC, TGCT, LUSC, PAAD, THCA, and UCEC (**Figure 10C**); and CTLA4 expression was correlated with MSI in BRCA, COAD, ESCA, LUAD, LUSC, OV, TGCT, THCA, and UCEC (**Figure 10D**). Correlations between the expression of MMR genes (*MLH1*, *MSH2*, *MSH6*, *PMS2*, and *EPCAM*) and PD-1 and CTLA4 levels are shown in **Figures 11A,B**, respectively; and correlations between the expression of DNA methylation regulatory genes (*DNMT1*, *DNMT2*, *DNMT3A*,

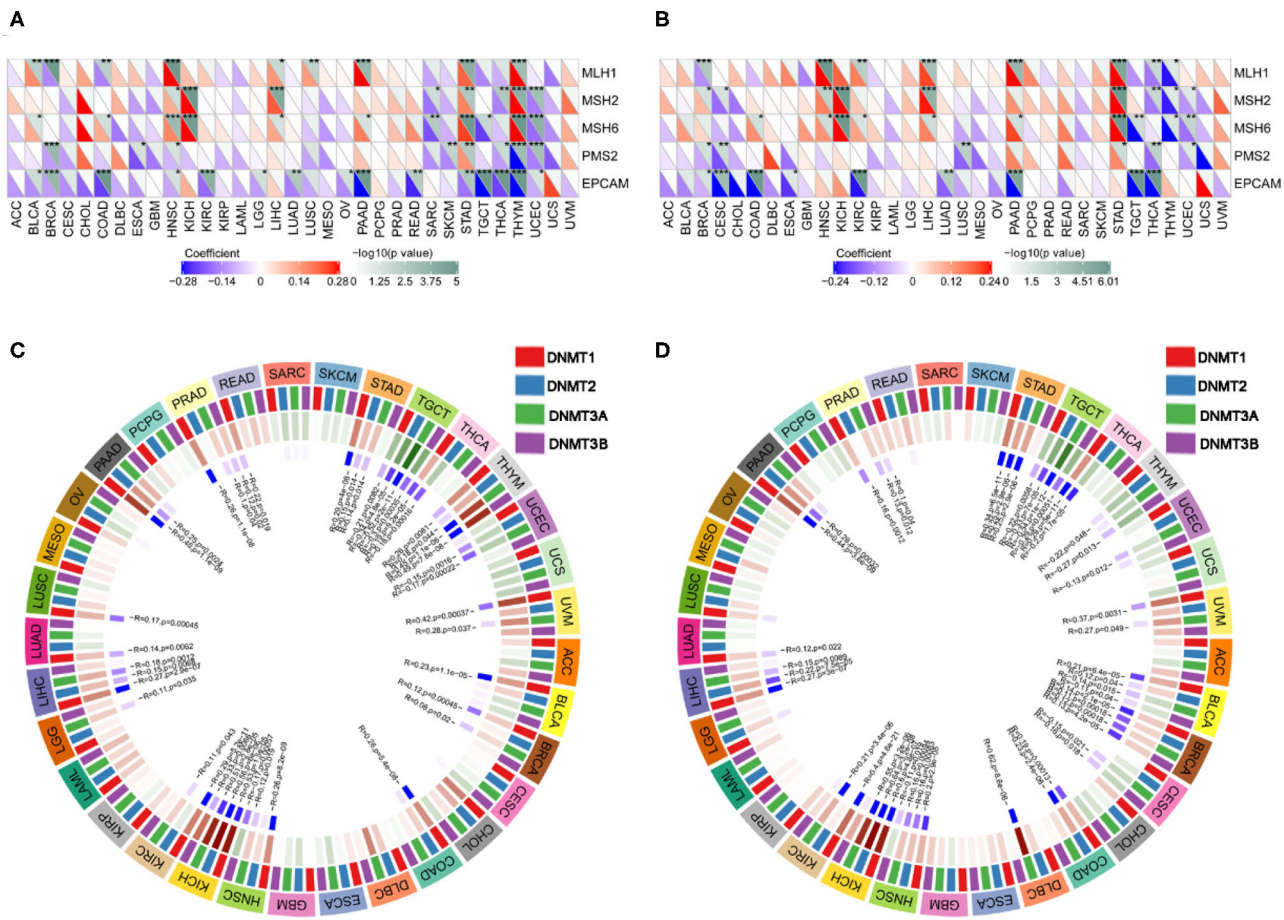

FIGURE 11 | Correlation between PD-1 and CTLA4 expression and MMR and DNMT levels. **(A)** Heatmap of the correlation between PD-1 expression and MMR in 33 cancer types. For each pair, the top right triangle is colored to represent the *P*-value, and the bottom left triangle is colored to represent the Spearman correlation coefficient. **(B,D)** Relationship between CTLA4 level and MMR **(B)** and DNMT levels **(D)**. **(C)** Circle chart of the correlation between PD-1 and DNMT expression in 33 cancer types. The first outer ring represents cancer types; the second ring shows 4 DNMTs; the third ring shows correlation coefficients; the fourth ring is colored to represent *P*-values; and numbers in the inner ring are correlation coefficients and *P*-values.

and *DNMT3B*) and PD-1 and CTLA4 levels are shown in **Figures 11C,D**, respectively.

Functional Analysis

We performed GSEA to assess the biological significance of PD-1 and CTLA4 expression in different cancers. The functional Kyoto Encyclopedia of Genes and Genomes (KEGG) and Hallmark terms for PD-1 and CTLA4 are listed in **Figures 12A,B**, respectively.

DISCUSSION

Combination therapy with immune checkpoint inhibitors including anti–PD-1 and –CTLA4 antibodies shows greater therapeutic efficacy than the monotherapies in several cancers (31–35). In the present study, we used a comprehensive pan-cancer approach to evaluate the clinical significance of PD-1 and CTLA4 expression in a variety of cancers. Our results showed that PD-1 and CTLA4 expression varies across cancer types and that most cancers are characterized by PD-1 and

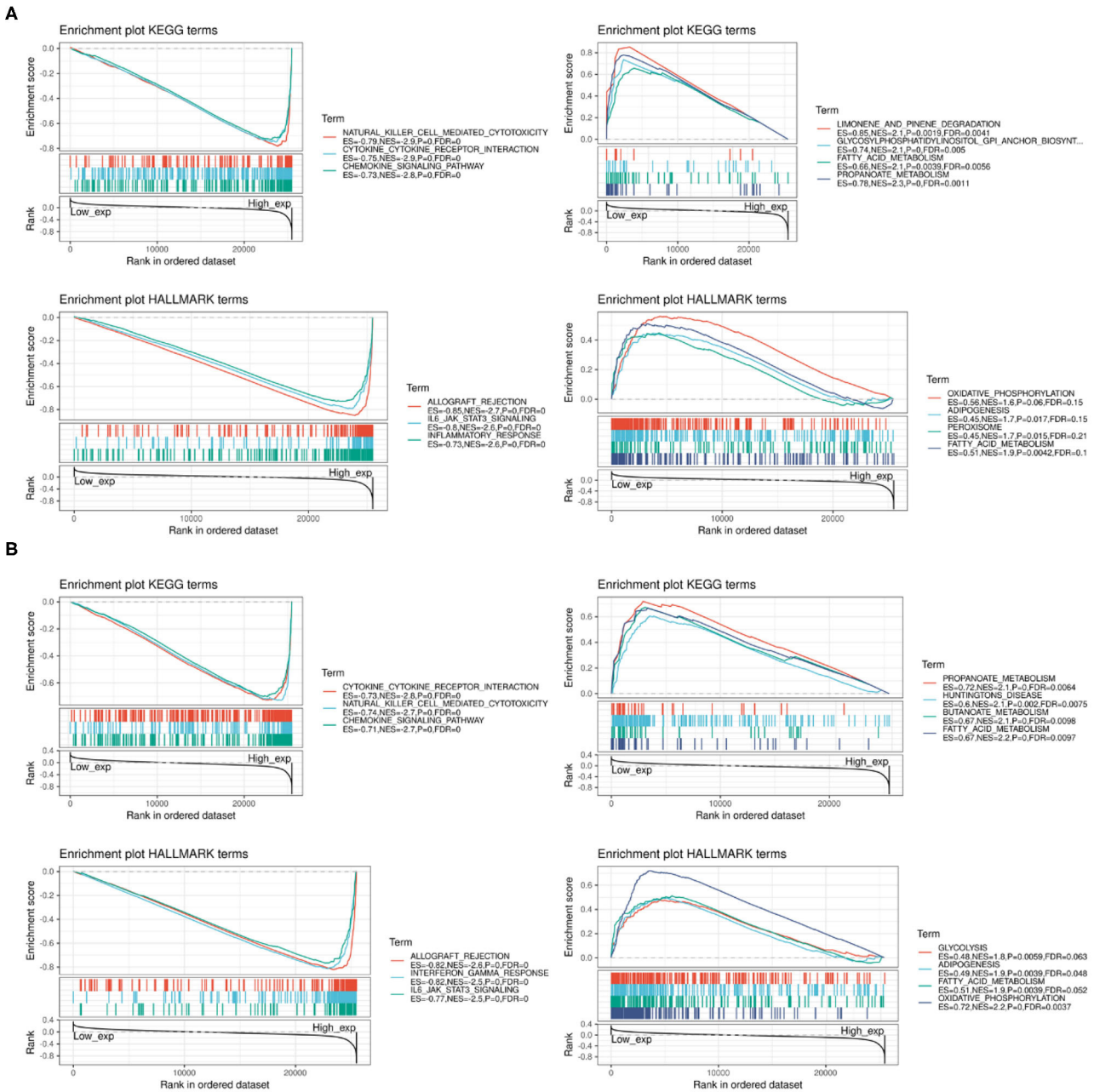

FIGURE 12 | GSEA of top functional terms associated with PD-1 and CTLA4 expression. **(A,B)** Top KEGG and HALLMARK terms related to PD-1 **(A)** and CTLA4 **(B)**.

CTLA4 mutations that lead to their abnormal expression, which can serve as a prognostic biomarker. Serum PD-1 and CTLA4 levels were survival predictor in LIHC patients receiving CIK therapy. Using TIMER, CIBERSORT, and ESTIMATE, we found that PD-1 and CTLA4 overexpression was associated with TIL infiltration, immune scores, and immune marker expression. Furthermore, PD-1 and CTLA4 levels were correlated with TMB, MSI, MMR, and the expression of DNMTs. We also identified KEGG and Hallmark terms that are associated with PD-1 and CTLA4 expression.

Identifying aberrantly expressed genes in tumors is important for the development of individualized treatments, which can improve therapeutic outcomes (36). Pan-cancer analyses can reveal the functional significance of PD-1 and CTLA4 in cancers (37, 38). Here we examined PD-1 and CTLA4 expression in a large and diverse set of samples from CCLE, which provides gene expression data for future experiments, and from TCGA, which provides genomic and survival data that may be useful for clinical investigations. Consistent with previous reports (39, 40), we found that PD-1 was more highly expressed in older cancer patients, indicating that checkpoint inhibitor treatment may more effective in this group. Additionally, Black patients had higher PD-1 and CTLA4 levels than Caucasian or Asian patients, suggesting better outcomes following immunotherapy.

Our results showed that PD-1 and CTLA4 are implicated in cancer immunity, as evidenced by the association between PD-1 and CTLA4 levels and the degree of infiltration of immunocytes in the TIMER and CIBERSORT analyses. The ESTIMATE method has been used to assess genomic data in various cancers, including the prediction of clinical outcomes in GBM and SKCM (41, 42). We determined immune and stromal scores based on TCGA data and found that PD-1 and CTLA4 levels were correlated with ESTIMATE scores as well as the expression of TIL markers.

Gene mutations are the major cause of cancer development (43), and specific mutations predict treatment response and prognosis (44, 45). TMB affects the generation of immunogenic peptides, thereby affecting patients' response to immune checkpoint inhibitor treatment (46, 47). Additionally, TMB and MSI reflect the production of new antibodies, with the latter being linked to increased TMB (48). In cervical squamous cell carcinoma and adrenocortical carcinoma, MSI-H was associated with an abnormally high mutation frequency (49). Thus, MSI is an important predictor of tumor development (29). MSI testing is recommended in the National Comprehensive Cancer Network guidelines for all colorectal cancer subtypes, as early detection of MSI-H can reduce mortality (50). Cancer cells with MMR deficiency (dMMR) can generate heterologous antigens that are recognized by T cells. PD-1 inhibitors are highly effective against MSI-H solid tumors (51); accordingly, the FDA has approved the use of the anti–PD-1 immunotherapy pembrolizumab for the treatment of MSI-H/dMMR solid tumors (51). Thus, TMB, MSI, and MMR can be used to predict therapeutic responses. In this study, we showed that PD-1 and CTLA4 levels were correlated with TMB and MSI in BRCA, COAD, TGCT, and UCEC. However, it remains to be determined whether the combination of PD-1 and CTLA4 inhibitors has greater efficacy than monotherapy in these cancers. Epigenetic modifications modulate gene expression and can be exploited by tumor cells to evade immune surveillance. A potential therapeutic strategy to circumvent this problem is to combine immune checkpoint and methylase inhibitors (30). PD-1 and CTLA4 have been implicated in various pathways related to immune function (52, 53). We carried out GSEA to identify clinically relevant pathways that may provide clues for future research. Taken together, our findings provided clues for the roles of PD-1 and CTLA4 in cancer immunity. However, these results should be interpreted with caution since checkpoint inhibitor treatment not analyzed in our work. And more experiments are needed to demonstrate our results, such as immunohistochemistry.

In conclusion, the results of our pan-cancer analysis indicate that PD-1 and CTLA4 are useful prognostic biomarkers in some cancer types. Importantly, we found that PD-1/CTLA4 expression is associated with cancer immunity. The integrative omics-based workflow in this study can serve as a basis for developing and testing hypotheses regarding novel targets in cancer treatment.

DATA AVAILABILITY STATEMENT

All datasets presented in this study are included in the article/**Supplementary Material**.

AUTHOR CONTRIBUTIONS

J-NL, WL, and Q-FC conceived of and designed the study. J-NL, X-SK, TH, WL, and Q-FC performed the literature search, generated the figures and tables, and wrote the manuscript. J-NL, TH, X-SK, and RW collected, analyzed the data, and critically reviewed the manuscript. WL and Q-FC supervised the study and reviewed the manuscript. All authors contributed to the article and approved the submitted version.

ACKNOWLEDGMENTS

We thank Ms. Yue-Ming Du for encouraging Q-FC to pursue his career in medicine.

SUPPLEMENTARY MATERIAL

The Supplementary Material for this article can be found online at: https://www.frontiersin.org/articles/10.3389/fimmu.2020.02048/full#supplementary-material

Supplementary Figure 1 | Overall study design.

Supplementary Figure 2 | Association between PD-1 level and PFS. **(A–I)** Kaplan–Meier analysis of the association between PD-1 expression and PFS.

Supplementary Figure 3 | Association between CTLA4 level and PFS. **(A–F)** Kaplan–Meier analysis of the association between CTLA4 expression and PFS.

Supplementary Table 1 | PD-1 and CTLA4 expression across 33 cancers.

Supplementary Table 2 | Associations between PD-1/CTLA4 expression levels and CD4+ and CD8+ T cell, B cell, dendritic cell, neutrophil, and macrophage counts based on TIMER.

Supplementary Table 3 | Association between PD-1/CTLA4 expression levels and immunocyte marker expression as determined using CIBERSORT.

Supplementary Table 4 | Associations between PD-1/CTLA4 expression levels and ESTIMATE scores.

Supplementary Table 5 | Associations between PD-1/CTLA4 expression levels and TMB and MSI.

REFERENCES

1. Bray F, Ferlay J, Soerjomataram I, Siegel RL, Torre LA, Jemal A. Global cancer statistics 2018: GLOBOCAN estimates of incidence and mortality worldwide for 36 cancers in 185 countries. *CA: Cancer J Clin.* (2018) 68:394–424. doi: 10.3322/caac.21492
2. Cancer Genome Atlas Research N, Weinstein JN, Collisson EA, Mills GB, Shaw KR, Ozenberger BA, et al. The cancer genome atlas pan-Cancer analysis project. *Nat Genet.* (2013) 45:1113–20. doi: 10.1038/ng.2764
3. Li W, Chen QF, Huang T, Shen L, Huang ZL, Wu P. Profiles of m(6)A RNA methylation regulators for the prognosis of hepatocellular carcinoma. *Oncol Lett.* (2020) 19:3296–306. doi: 10.3892/ol.2020.11435
4. Huang ZL, Li W, Chen QF, Wu PH, Shen LJ. Eight key long non-coding RNAs predict hepatitis virus positive hepatocellular carcinoma as prognostic targets. *World J Gastroint Oncol.* (2019) 11:983–97. doi: 10.4251/wjgo.v11.i11.983
5. Cancer Cell Line Encyclopedia C, Genomics of Drug Sensitivity in Cancer C. Pharmacogenomic agreement between two cancer cell line data sets. *Nature.* (2015) 528:84–7. doi: 10.1038/nature15736
6. Ye Y, Hu Q, Chen H, Liang K, Yuan Y, Xiang Y, et al. Characterization of hypoxia-associated molecular features to aid hypoxia-targeted therapy. *Nat Metabo.* (2019) 1:431–44. doi: 10.1038/s42255-019-0045-8
7. Barger CJ, Branick C, Chee L, Karpf AR. Pan-cancer analyses reveal genomic features of FOXM1 overexpression in cancer. *Cancers.* (2019) 11:251. doi: 10.3390/cancers11020251
8. Schaub FX, Dhankani V, Berger AC, Trivedi M, Richardson AB, Shaw R, et al. Pan-cancer alterations of the MYC oncogene and its proximal network across the cancer genome atlas. *Cell Syst.* (2018) 6:282–300 e2.
9. Danaher P, Warren S, Lu R, Samayoa J, Sullivan A, Pekker I, et al. Pan-cancer adaptive immune resistance as defined by the tumor inflammation signature (TIS): results from The cancer genome atlas (TCGA). *J Immunother Cancer.* (2018) 6:63. doi: 10.1186/s40425-018-0367-1
10. Vaddepally RK, Kharel P, Pandey R, Garje R, Chandra AB. Review of indications of FDA-approved immune checkpoint inhibitors per NCCN guidelines with the level of evidence. *Cancers.* (2020) 12:738. doi: 10.3390/cancers12030738
11. Chen L, Flies DB. Molecular mechanisms of T cell co-stimulation and co-inhibition. *Nat Rev Immunol.* (2013) 13:227–42. doi: 10.1038/nri3405
12. Schadendorf D, Hodi FS, Robert C, Weber JS, Margolin K, Hamid O, et al. Pooled Analysis of long-term survival data from phase II and phase III trials of ipilimumab in unresectable or metastatic melanoma. *J Clin Oncol.* (2015) 33:1889–94. doi: 10.1200/JCO.2014.56.2736
13. Larkin J, Minor D, D'Angelo S, Neyns B, Smylie M, Miller WH, et al., et al. Overall survival in patients with advanced melanoma who received nivolumab versus investigator's choice chemotherapy in checkmate 037: a randomized, controlled, open-label phase III trial. *J Clin Oncol.* (2018) 36:383–90. doi: 10.1200/JCO.2016.71.8023
14. Larkin J, Chiarion-Sileni V, Gonzalez R, Grob JJ, Rutkowski P, Lao CD, et al. Five-year survival with combined nivolumab and ipilimumab in advanced melanoma. *N Engl J Med.* (2019) 381:1535–46. doi: 10.1056/NEJMoa1910836
15. Motzer RJ, Tannir NM, McDermott DF, Aren Frontera O, Melichar B, Choueiri TK, et al. Nivolumab plus Ipilimumab versus sunitinib in advanced renal-cell carcinoma. *N Engl J Med.* (2018) 378:1277–90. doi: 10.1056/NEJMoa1712126
16. Cella D, Grunwald V, Escudier B, Hammers HJ, George S, Nathan P, et al. Patient-reported outcomes of patients with advanced renal cell carcinoma treated with nivolumab plus ipilimumab versus sunitinib (CheckMate 214): a randomised, phase 3 trial. *Lancet Oncol.* (2019) 20:297–310. doi: 10.1016/S1470-2045(18)30778-2
17. Motzer RJ, Rini BI, McDermott DF, Aren Frontera O, Hammers HJ, Carducci MA, et al. Nivolumab plus ipilimumab versus sunitinib in first-line treatment for advanced renal cell carcinoma: extended follow-up of efficacy and safety results from a randomised, controlled, phase 3 trial. *Lancet Oncol.* (2019) 20:1370–85. doi: 10.1016/S1470-2045(19)30413-9
18. Hellmann MD, Paz-Ares L, Bernabe Caro R, Zurawski B, Kim SW, Carcereny Costa E, et al. Nivolumab plus Ipilimumab in advanced non-small-cell lung cancer. *N Engl J Med.* (2019) 381:2020–31. doi: 10.1056/NEJMoa1910231
19. Wright K. FDA approves nivolumab plus ipilimumab for the treatment of advanced HCC. *Oncology.* (2020) 34:693606.
20. Li T, Fan J, Wang B, Traugh N, Chen Q, Liu JS, et al. TIMER: A web server for comprehensive analysis of tumor-infiltrating immune cells. *Cancer Res.* (2017) 77:e108–10. doi: 10.1158/0008-5472.CAN-17-0307
21. Li B, Severson E, Pignon JC, Zhao H, Li T, Novak J, et al. Comprehensive analyses of tumor immunity: implications for cancer immunotherapy. *Genome Biol.* (2016) 17:174. doi: 10.1186/s13059-016-1028-7
22. Chen QF, Li W, Wu PH, Shen LJ, Huang ZL. Significance of tumor-infiltrating immunocytes for predicting prognosis of hepatitis B virus-related hepatocellular carcinoma. *World J Gastroenterol.* (2019) 25:5266–82. doi: 10.3748/wjg.v25.i35.5266
23. Yoshihara K, Shahmoradgoli M, Martinez E, Vegesna R, Kim H, Torres-Garcia W, et al. Inferring tumour purity and stromal and immune cell admixture from expression data. *Nat Commun.* (2013) 4:2612. doi: 10.1038/ncomms3612
24. Siemers NO, Holloway JL, Chang H, Chasalow SD, Ross-MacDonald PB, Voliva CF, et al. Genome-wide association analysis identifies genetic correlates of immune infiltrates in solid tumors. *PLoS ONE.* (2017) 12:e0179726. doi: 10.1371/journal.pone.0179726
25. Danaher P, Warren S, Dennis L, D'Amico L, White A, Disis ML, et al. Gene expression markers of tumor infiltrating leukocytes. *J Immunother Cancer.* (2017) 5:18. doi: 10.1186/s40425-017-0215-8
26. Pan JH, Zhou H, Cooper L, Huang JL, Zhu SB, Zhao XX, et al. LAYN is a prognostic biomarker and correlated with immune infiltrates in gastric and colon cancers. *Front Immunol.* (2019) 10:6. doi: 10.3389/fimmu.2019.00006
27. Krieger T, Pearson I, Bell J, Doherty J, Robbins P. Targeted literature review on use of tumor mutational burden status and programmed cell death ligand 1 expression to predict outcomes of checkpoint inhibitor treatment. *Diagnos Pathol.* (2020) 15:6. doi: 10.1186/s13000-020-0927-9
28. Li K, Luo H, Huang L, Luo H, Zhu X. Microsatellite instability: a review of what the oncologist should know. *Cancer Cell Int.* (2020) 20:16. doi: 10.1186/s12935-019-1091-8
29. Dan H, Zhang S, Zhou Y, Guan Q. DNA methyltransferase inhibitors: catalysts for antitumour immune responses. *OncoTargets Ther.* (2019) 12:10903–16. doi: 10.2147/OTT.S217767
30. Antonia SJ, Lopez-Martin JA, Bendell J, Ott PA, Taylor M, Eder JP, et al. Nivolumab alone and nivolumab plus ipilimumab in recurrent small-cell lung cancer (CheckMate 032): a multicentre, open-label, phase 1/2 trial. *Lancet Oncol.* (2016) 17:883–95. doi: 10.1016/S1470-2045(16)30098-5
31. Hammers HJ, Plimack ER, Infante JR, Rini BI, McDermott DF, Lewis LD, et al. Safety and efficacy of nivolumab in combination with ipilimumab in metastatic renal cell carcinoma: the checkmate 016 study. *J Clini Oncol.* (2017) 35:3851–8. doi: 10.1200/JCO.2016.72.1985
32. Hellmann MD, Rizvi NA, Goldman JW, Gettinger SN, Borghaei H, Brahmer JR, et al. Nivolumab plus ipilimumab as first-line treatment for advanced non-small-cell lung cancer (CheckMate 012): results of an open-label, phase 1, multicohort study. *Lancet Oncol.* (2017) 18:31–41. doi: 10.1016/S1470-2045(16)30624-6
33. Larkin J, Chiarion-Sileni V, Gonzalez R, Grob JJ, Cowey CL, Lao CD, et al. Combined nivolumab and ipilimumab or monotherapy in untreated melanoma. *N Engl J Med.* (2015) 373:23–34. doi: 10.1056/NEJMc1509660
34. Wolchok JD, Kluger H, Callahan MK, Postow MA, Rizvi NA, Lesokhin AM, et al. Nivolumab plus ipilimumab in advanced melanoma. *N Engl J Med.* (2013) 369:122–33. doi: 10.1056/NEJMoa1302369
35. Andre F, Mardis E, Salm M, Soria JC, Siu LL, Swanton C. Prioritizing targets for precision cancer medicine. *Ann Oncol.* (2014) 25:2295–303. doi: 10.1093/annonc/mdu478

36. Cao Z, Zhang S. An integrative and comparative study of pan-cancer transcriptomes reveals distinct cancer common and specific signatures. *Sci Rep.* (2016) 6:33398. doi: 10.1038/srep33398
37. Cava C, Bertoli G, Colaprico A, Olsen C, Bontempi G, Castiglioni I. Integration of multiple networks and pathways identifies cancer driver genes in pan-cancer analysis. *BMC Genom.* (2018) 19:25. doi: 10.1186/s12864-017-4423-x
38. Jeske SS, Schuler PJ, Doescher J, Theodoraki MN, Laban S, Brunner C, et al. Age-related changes in T lymphocytes of patients with head and neck squamous cell carcinoma. *Immun Ageing.* (2020) 17:3. doi: 10.1186/s12979-020-0174-7
39. Kasanen H, Hernberg M, Makela S, Bruck O, Juteau S, Kohtamaki L, et al. Age-associated changes in the immune system may influence the response to anti-PD1 therapy in metastatic melanoma patients. *Cancer Immunol Immunother.* (2020) 69:717–30. doi: 10.1007/s00262-020-02497-9
40. Jia D, Li S, Li D, Xue H, Yang D, Liu Y. Mining TCGA database for genes of prognostic value in glioblastoma microenvironment. *Aging.* (2018) 10:592–605. doi: 10.18632/aging.101415
41. Yang S, Liu T, Nan H, Wang Y, Chen H, Zhang X, et al. Comprehensive analysis of prognostic immune-related genes in the tumor microenvironment of cutaneous melanoma. *J Cell Physiol.* (2020) 235:1025–35. doi: 10.1002/jcp.29018
42. Martincorena I, Campbell PJ. Somatic mutation in cancer and normal cells. *Science.* (2015) 349:1483–9. doi: 10.1126/science.aab4082
43. Sanz-Garcia E, Argiles G, Elez E, Tabernero J. BRAF mutant colorectal cancer: prognosis, treatment, and new perspectives. *Ann Oncol.* (2017) 28:2648–57. doi: 10.1093/annonc/mdx401
44. Allegra CJ, Rumble RB, Hamilton SR, Mangu PB, Roach N, Hantel A, et al. Extended RAS gene mutation testing in metastatic colorectal carcinoma to predict response to anti-epidermal growth factor receptor monoclonal antibody therapy: American society of clinical oncology provisional clinical opinion update 2015. *J Clin Oncol.* (2016) 34:179–85. doi: 10.1200/JCO.2015.63.9674
45. Wu HX, Wang ZX, Zhao Q, Chen DL, He MM, Yang LP, et al. Tumor mutational and indel burden: a systematic pan-cancer evaluation as prognostic biomarkers. *Ann Translat Med.* (2019) 7:640. doi: 10.21037/atm.2019.10.116
46. Havel JJ, Chowell D, Chan TA. The evolving landscape of biomarkers for checkpoint inhibitor immunotherapy. *Nat Rev Cancer.* (2019) 19:133–50. doi: 10.1038/s41568-019-0116-x
47. Chalmers ZR, Connelly CF, Fabrizio D, Gay L, Ali SM, Ennis R, et al. Analysis of 100,000 human cancer genomes reveals the landscape of tumor mutational burden. *Genome Med.* (2017) 9:34. doi: 10.1186/s13073-017-0424-2
48. Bonneville R, Krook MA, Kautto EA, Miya J, Wing MR, Chen HZ, et al. Landscape of microsatellite instability across 39 cancer types. *JCO Preci Oncol.* (2017) 2017. doi: 10.1200/PO.17.00073
49. Benson AB, 3rd, Venook AP, Cederquist L, Chan E, Chen YJ, Cooper HS, et al. Colon cancer, version 1.2017, NCCN clinical practice guidelines in oncology. *J Natl Comprehen Cancer Netw.* (2017) 15:370–98. doi: 10.6004/jnccn.2017.0036
50. Diaz LA Jr, Le DT. PD-1 blockade in tumors with mismatch-repair deficiency. *N Engl J Med.* (2015) 373:1979. doi: 10.1056/NEJMc1510353
51. Yu Y. Molecular classification and precision therapy of cancer: immune checkpoint inhibitors. *Front Med.* (2018) 12:229–35. doi: 10.1007/s11684-017-0581-0
52. Mannick JB, Del Giudice G, Lattanzi M, Valiante NM, Praestgaard J, Huang B, et al. mTOR inhibition improves immune function in the elderly. *Sci Trans Med.* (2014) 6:268ra179. doi: 10.1126/scitranslmed.3009892
53. Bagherzadeh Yazdchi S, Witalis M, Meli AP, Leung J, Li X, Panneton V, et al. Hippo pathway kinase Mst1 is required for long-lived humoral immunity. *J Immunol.* (2019) 202:69–78. doi: 10.4049/jimmunol.1701407

Conflict of Interest: The authors declare that the research was conducted in the absence of any commercial or financial relationships that could be construed as a potential conflict of interest.

frontiers in Immunology

ORIGINAL RESEARCH
published: 15 September 2020
doi: 10.3389/fimmu.2020.01933

Construction of a Prognostic Immune Signature for Squamous-Cell Lung Cancer to Predict Survival

*Rui-Lian Chen[1], Jing-Xu Zhou[1], Yang Cao[1], Ling-Ling Sun[1], Shan Su[2], Xiao-Jie Deng[3], Jie-Tao Lin[1], Zhi-Wei Xiao[1], Zhuang-Zhong Chen[1], Si-Yu Wang[4] and Li-Zhu Lin[1]**

[1] Integrative Cancer Centre, The First Affiliated Hospital of Guangzhou University of Chinese Medicine, Guangzhou, China, [2] Department of Oncology, Guangzhou Chest Hospital, Guangzhou, China, [3] Department of Oncology, Shenzhen People's Hospital, The Second Clinical Medical College of Jinan University, Shenzhen, China, [4] Department of Thoracic Surgery, Sun Yat-sen University Cancer Center, Guangzhou, China

OPEN ACCESS

Edited by:
Maysaloun Merhi,
Hamad Medical Corporation, Qatar

Reviewed by:
Aparna Rao,
University of Pittsburgh, United States
Jinquan Cai,
Harbin Medical University, China

***Correspondence:**
Li-Zhu Lin
lizhulin26@yahoo.com

Specialty section:
This article was submitted to Cancer Immunity and Immunotherapy, a section of the journal Frontiers in Immunology

Received: 13 April 2020
Accepted: 17 July 2020
Published: 15 September 2020

Citation:
Chen R-L, Zhou J-X, Cao Y, Sun L-L, Su S, Deng X-J, Lin J-T, Xiao Z-W, Chen Z-Z, Wang S-Y and Lin L-Z (2020) Construction of a Prognostic Immune Signature for Squamous-Cell Lung Cancer to Predict Survival. Front. Immunol. 11:1933. doi: 10.3389/fimmu.2020.01933

Background: Limited treatment strategies are available for squamous-cell lung cancer (SQLC) patients. Few studies have addressed whether immune-related genes (IRGs) or the tumor immune microenvironment can predict the prognosis for SQLC patients. Our study aimed to construct a signature predict prognosis for SQLC patients based on IRGs.

Methods: We constructed and validated a signature from SQLC patients in The Cancer Genome Atlas (TCGA) using bioinformatics analysis. The underlying mechanisms of the signature were also explored with immune cells and mutation profiles.

Results: A total of 464 eligible SQLC patients from TCGA dataset were enrolled and were randomly divided into the training cohort (n = 232) and the testing cohort (n = 232). Eight differentially expressed IRGs were identified and applied to construct the immune signature in the training cohort. The signature showed a significant difference in overall survival (OS) between low-risk and high-risk cohorts ($P < 0.001$), with an area under the curve of 0.76. The predictive capability was verified with the testing and total cohorts. Multivariate analysis revealed that the 8-IRG signature served as an independent prognostic factor for OS in SQLC patients. Naive B cells, resting memory CD4 T cells, follicular helper T cells, and M2 macrophages were found to significantly associate with OS. There was no statistical difference in terms of tumor mutational burden between the high-risk and low-risk cohorts.

Conclusion: Our study constructed and validated an 8-IRG signature prognostic model that predicts clinical outcomes for SQLC patients. However, this signature model needs further validation with a larger number of patients.

Keywords: squamous-cell lung cancer, prognostic, immune-related genes, signature, immune cells, mutation profiles

INTRODUCTION

Lung cancer is the most commonly diagnosed cancer and the first leading cause of cancer-related mortality worldwide, making it a major public health concern (1). In 2018, there were an estimated 2,093,876 new cases, and 1,761,007 deaths from lung cancer worldwide (1). There are two common histological types of non-small cell lung cancer (NSCLC): adenocarcinoma carcinoma, which accounts for 70% of NSCLC cases, and squamous carcinoma, which accounts for 30% of cases. Standard treatments, including chemotherapy, radiotherapy, and surgical resection, have improved the prognosis of early stage squamous-cell lung cancer (SQLC) (2). However, it is difficult to prevent metastasis and recurrence of SQLC, which is considered responsible for most SQLC deaths (3). Platinum-based doublet chemotherapy, the standard therapy for advanced SQLC, only obtained poor efficacy, with a median overall survival (OS) of 12.1 months (4). The utility of targeted drugs had brought significant improvements on OS and the quality of life for advanced NSCLC patients (5, 6). However, driver gene alterations are rarely found in SQLC patients, so the benefit from targeted agents is limited (7). Furthermore, most novel drugs, including pemetrexed and bevacizumab, have been approved in the treatment for lung cancer but not for squamous-cell subtype because of the adverse events (8, 9). Thus, there are limited treatment strategies available for SQLC patients. Checkpoint inhibitors, including anti-cytotoxic T lymphocyte antigen 4 (CTLA4), anti-programmed cell death (PD-1), or anti-programmed cell death-ligand 1 (PD-L1), have brought impressive clinical benefit for various cancer types (10, 11). Due to the remarkable response, pembrolizumab was approved as the first-line treatment for recurrent or metastatic SQLC by the United States Food and Drug Administration and National Medical Products Administration of China (12).

Recent studies have shown that several promising biomarkers might help to select patients who were appropriate candidates for immunotherapy (13, 14). PD-L1 protein expression has been reported to predict the response of checkpoint inhibitors (15, 16). Previous studies have indicated that the tumor mutation burden (TMB) and T-cell infiltration levels were related to the efficacy of immunotherapy (13, 17). However, there is no consensus on the biomarkers that can predict prognosis for SQLC patients. The tumor biology and immune microenvironment were so complicated that a single biomarker may be unable to sufficiently predict the clinical outcomes of immunotherapy.

Several studies have demonstrated that immune signatures played an important role in predicting the prognosis of patients with cancers, such as ovarian cancer, colorectal cancer, and cervical cancer. However, few studies have explored whether immune-related genes (IRGs) could be biomarkers for predicting the prognosis of SQLC. Furthermore, diverse treatment outcomes of PD-1 or PD-L1 inhibitors were observed in SQLC patients (12, 18). Therefore, an immune signature of SQLC based on IRGs is urgently needed to predict clinical outcomes. The aim of the current study was to establish an immune signature that predicts the prognosis of SQLC patients based on IRGs or tumor immune microenvironment (TIME). Furthermore, we explored the relationships of the immune signature and the clinical characteristics, immune cell infiltration, and mutation data. This immune signature may help clinicians to provide more precise immunotherapy for SQLC patients.

MATERIALS AND METHODS

Clinical Samples and Data Acquisition

Transcriptome mRNA-sequencing data and clinical information of SQLC patients were downloaded from The Cancer Genome Atlas (TCGA) data portal[1]. These data contained 49 normal and 502 primary SQLC tissues. The raw count data were downloaded for further analyses. Clinical information was also downloaded and extracted from the Immunology Database and Analysis Portal (ImmPort) database[2]. ImmPort is an important foundation of immunology research, which updates immunology data accurately and timely. This database provides a list of IRGs that are involved in the process of immune activity for cancer researchers (19).

Differentially Expressed Gene Analysis

To select the IRGs involved in the development of SQLC, differentially expressed genes (DEGs) between tumor and normal samples were identified with the limma package[3]. A differential gene expression analysis was performed with a false discovery rate (FDR) < 0.05 and a log2 fold change > 1 as the cutoff values. A list of IRGs was derived from Immport. We identified differently expressed immune-related genes (DE IRGs) at point intersection between the IRGs list and all DEGs. Functional enrichment analyses were performed to investigate the potential molecular mechanisms of the DE IRGs with gene ontology (GO) and Kyoto Encyclopedia of Genes and Genomes (KEGG) enrichment using DAVID. Terms in GO and KEGG with an FDR < 0.05 were considered significantly enriched.

Development and Validation of the Immune-Related Signature for SQLC

Squamous-cell lung cancer patients from TCGA data were randomly divided into two cohorts, including the training cohort and the testing cohort. The training cohort was used to identify the prognostic immune-related signature and to develop a prognostic immune-related risk model. The testing cohort was used to validate its prognostic capability. We performed a univariate Cox proportional hazard regression analysis to identify the correlation between DE IRGs and OS in the training cohort. To minimize overfitting and to identify the best gene model, survival-related DE IRGs ($P < 0.05$) were evaluated with a least absolute shrinkage and selection operator (LASSO) (20). The risk score was established with the following formula: risk score = expression gene 1 *coefficient + expression gene 2 *coefficient + . . . + expression gene n *coefficient (21). The risk score was calculated for each patient in the training and testing

[1]https://cancergenome.nih.gov

[2]https://immport.niaid.nih.gov

[3]https://Bioconductor.org/packages/limma

cohorts based on this model. SQLC patients were divided into the high- and low-risk groups based on the median cutoff of the risk score. We validated the prognostic ability of the immune-related signature by calculating the area under the curve (AUC) and evaluating the survival difference between the high- and low-risk groups (22).

TMB Analysis

The mutation data for SQLC patients were obtained from the TCGA data portal, and analyzed with maftools (23). For each patient, the TMB score was calculated as follows: (total mutations/total covered bases) $\times 10^6$ (24).

Tumor-Infiltrating Immune Cells

We used gene expression RNA-sequencing data from TCGA to estimate the proportions of 22 types of infiltrating immune cells with the CIBERSORT algorithm following the procedure as previously reported (25).

Statistical Analysis

Differences among variables were analyzed with independent *t* tests, chi-square tests, non-parametric tests, or ANOVA tests. Univariate cox regression analysis and multivariate cox regression were conducted to assess the prognostic effect of the immune signature and clinical characteristics including gender, age, clinical stage, and TNM stage. Statistical analyses were conducted with SPSS 22.0 and R software, version 3.6.1. The heatmap was generated with R package "pheatmap" and the volcano plot was generated with R package "ggplot2". A two-sided $P < 0.05$ was considered statistically significant.

RESULTS

Clinical Characteristics

A total of 502 SQLC patients were identified in the TCGA cohort. In order to reduce the effect of follow-up time on short term, patients with follow-up time less than 30 days were not included in our study. Thus, a total of 464 patients were enrolled, including 344 (74.1%) male and 120 (25.9%) female patients. These SQLC patients were randomly divided into the training cohort ($n = 232$) and the testing cohort ($n = 232$). No significant difference was observed in terms of the clinical characteristics between these two cohorts. The clinical characteristics of the patients are listed in **Supplementary Table S1**.

Identification of DE IRGs

We identified 8527 DEGs for SQLC, including 5803 up-regulated and 2724 down-regulated genes (**Supplementary Figure S1**). We extracted 587 DE IRGs from the set of DEGs, comprising 287 up-regulated and 300 down-regulated genes (**Figures 1A,B**). Gene functional enrichment analysis indicated that these genes were significantly enriched in important inflammatory pathways, including leukocyte migration, regulation of inflammatory response, regulation of immune effector process, and lymphocyte-mediated immunity (**Figure 1C**). KEGG pathway analysis highlighted the six ranked pathways that were enriched among the DE IRGs: "cytokine–cytokine receptor interaction", "neuroactive ligand–receptor interaction", "viral protein interaction with cytokine and cytokine receptor", "chemokine signaling pathway", "rheumatoid arthritis", and "JAK-STAT signaling pathway" (**Figure 1D**).

Construction of Immune-Related Risk Signatures in SQLC

We performed a univariate Cox regression analysis to explore the association between OS and these 587 DE IRGs identified above. A total of 32 DE IRGs were significantly associated with the OS of SQLC patients in the training cohort ($P < 0.05$). LASSO analysis was performed with these 32 survival-associated IRGs in order to minimize overfitting. Eight DE IRGs were utilized to construct the immune signature (**Figure 2**). The prognostic model was established with the linear combination of the expression levels of the 8-IRGs weighted by their relative coefficient in multivariate Cox regression analysis as follows: risk score = (*MMP12* $\times$ 0.00332) + (*PLAU* $\times$ 0.00434) + (*IGHD3-22* $\times$ 0.00460) + (*IGKV1D-17* $\times$ 0.03535) + (*CGA* $\times$ 0.66283) + (*SPP1* $\times$ 0.00072) + (*AGTR2*$\times$ 0.10901) + (*NR4A1* $\times$ 0.02224) (**Supplementary Table S2**). We calculated risk scores for each patient in the training cohort based on the expression of the eight IRGs and their relative coefficient. A total of 232 patients in the training group were divided into a high-risk cohort ($n = 166$) and a low-risk cohort ($n = 166$) based on their median risk score. A significant difference in OS was observed between the high-risk and low-risk cohorts [median OS, 4.56 vs 7.40 years; hazard ratio (HR), 2.21; 95% CI, 1.44–3.41, $P < 0.001$] (**Figure 3A**). The AUC for the 8-IRG signature was 0.76 at 1 year for OS (**Figure 3B**). The distribution of the risk score and survival status and the expression of 8-IRGs in the training cohort were presented in **Figures 3C–E**.

Evaluating the Predictive Value of the 8-IRG Signature

The predictive capability of the 8-IRG signature was verified with the testing cohort and the total cohort. As previously described, there were 125 high-risk and 107 low-risk patients in the testing cohort. The patients in the high-risk cohort had a significant shorter median OS than those in the low-risk cohort (median OS, 3.93 vs 6.47 years; HR, 1.84; 95% CI, 1.20–2.84; $P = 0.005$; **Figure 4A**). The AUC of 1 year was 0.63 (**Figure 4B**). The distribution of the risk score, survival status, and the expression of 8-IRGs in the testing cohort are shown in **Figures 4C–E**. Similarly, SQLC patients in the total cohort were divided into low-risk ($n = 223$) and high-risk ($n = 241$) groups. The median OS in the high-risk cohort was inferior than that of the low-risk cohort (median OS, 4.34 vs 7.00 years; HR, 2.04; 95% CI, 1.50 to 2.76, $P < 0.001$; **Supplementary Figure S2a**). The AUC of 1 year in the total cohort was 0.69 (**Supplementary Figure S2b**). The distribution of the risk score, survival

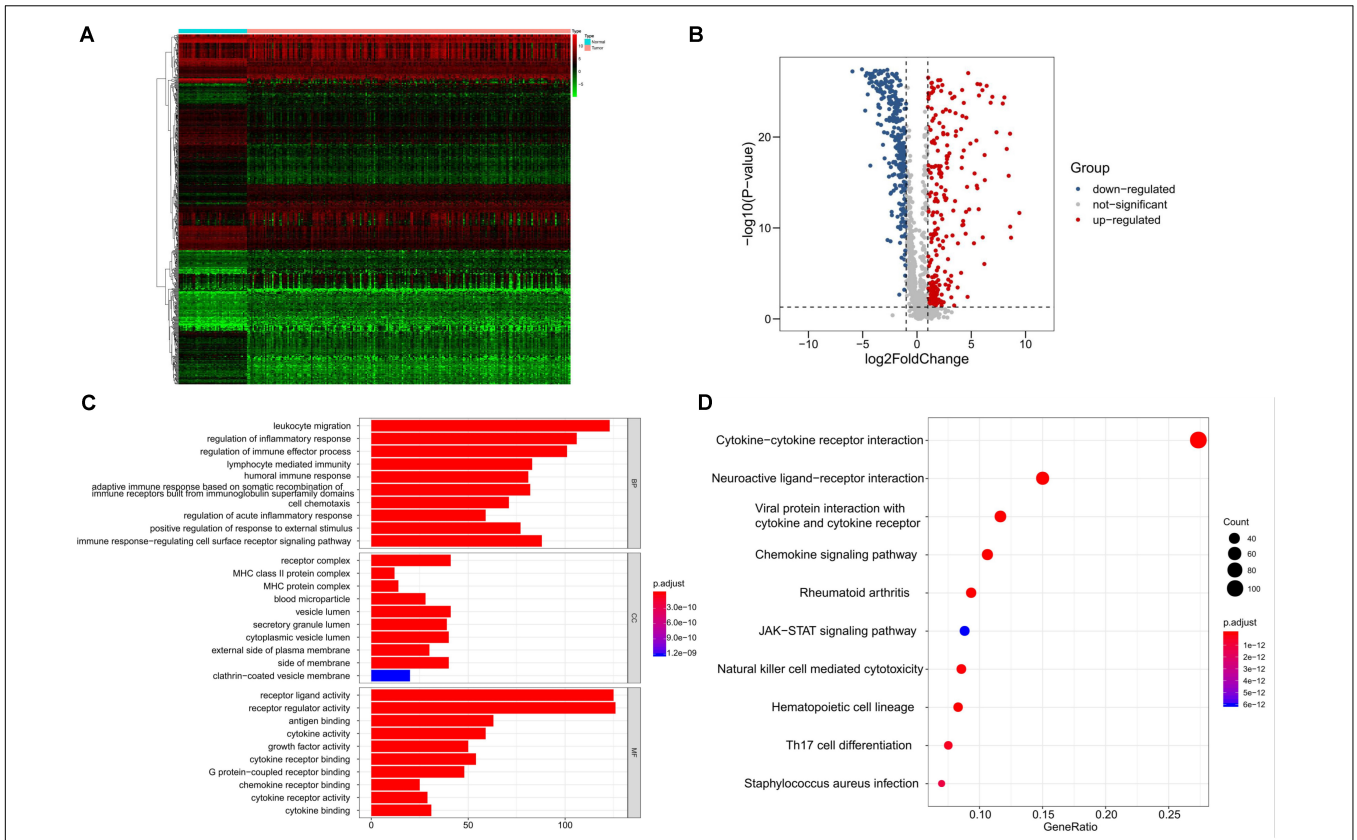

FIGURE 1 | Identification and functional enrichment analyses of differentially expressed immune-related genes in SQLC from training cohort. **(A)** Heatmap of differentially expressed immune-related genes. **(B)** Volcano plot of differentially expressed immune-related genes. **(C)** Gene ontology analysis. **(D)** The top 10 most significant Kyoto Encyclopedia of Genes and Genomes pathways.

status, and the expression of 8-IRGs in the total cohort are presented in **Supplementary Figures S2c–e**.

Association Between the Immune-Related Risk Signature and the Clinical Outcome

A univariate Cox regression model was conducted to explore the association between clinical characteristics, OS, and the 8-IRG risk signature in the total SQLC cohort (**Table 1**). The immune-related risk signature could independently predict OS in the total cohort (HR, 1.60; 95% CI, 1.17–2.19, $P = 0.003$). Multivariate Cox regression analysis suggested that the immune-related risk signature could act as an independent prognosis predictor for OS (HR, 1.94; 95% CI, 1.38–2.72, $P < 0.001$). The relationships between the immune signature and clinical characteristics were also explored. No significant difference of risk scores was found in terms of age, gender, clinical stage, T stage, and N stage (**Supplementary Figure S3**).

TIME Changing and the Immune-Related Risk Signature

We applied RNA-sequencing data to assess the relative proportion of the 22 immune cells in each SQLC sample with CIBERSORT (**Figure 5A**). The abundances of the immune cell types in the 8-IRG signature low- and high-risk cohorts are presented in **Supplementary Table S4**. Among the 22 immune cell types, the proportions of follicular helper T cells, naïve B cells, and activated NK cells were low in the 8-IRG signature high-risk group. The abundances of resting memory CD4 T cells, M2 macrophages, and neutrophils were high in the 8-IRG signature high-risk group (**Figure 5B**). The proportions of naïve B cells, resting memory CD4 T cells, follicular helper T cells, and M2 macrophages were significantly associated with OS. For the 8-IRG signature in the low-risk cohort, the abundance level of resting memory CD4 T cells and M2 macrophages was low and showed a significant association with superior OS, whereas the abundance levels of naïve B cells and follicular helper T cells were high and were associated with inferior OS (**Figures 5C–F**).

Tumor Mutation Profile and the Immune-Related Risk Signature

We explored the relationship between the mutation profile and the immune-related risk signature in TCGA SQLC patients with available somatic mutation data. The 30 ranked, mutated genes in the low-risk and high-risk cohorts are illustrated in **Figures 6A,B**. The top 10 mutated genes in SQLC patients

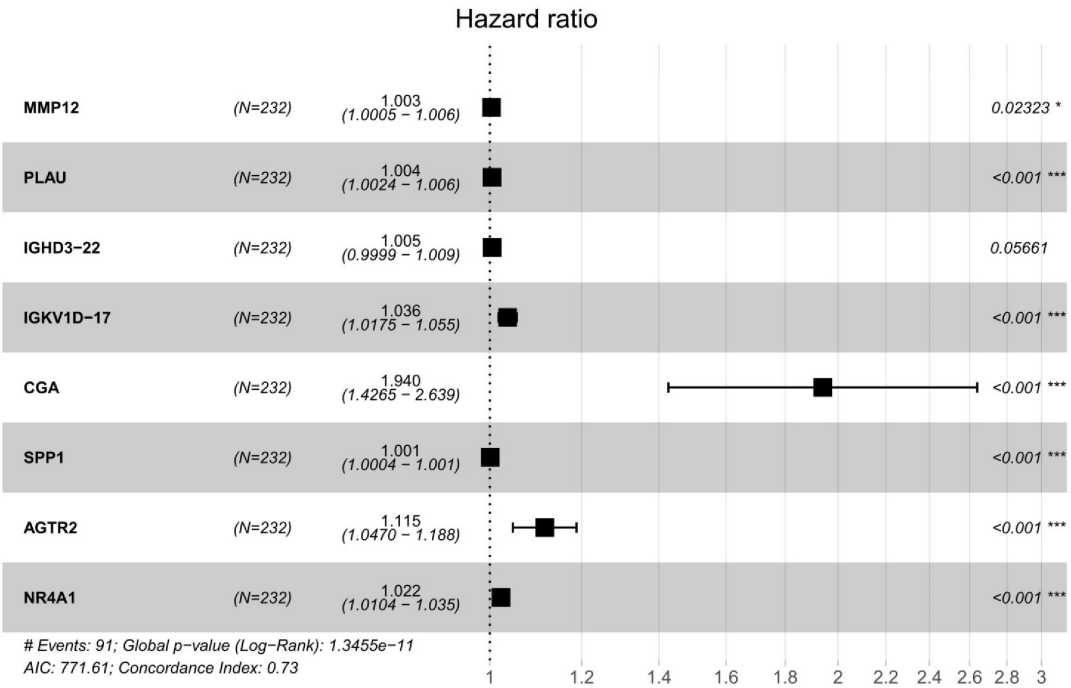

FIGURE 2 | Forest plot of the multivariable Cox model of each gene in 8-IRG risk signature.

were *TP53*, *TIN*, *CSMD3*, *MUC16*, *RYR2*, *SYNE1*, *USH2A*, *LRP1B*, *ZFHX4*, and *FAM135B*. There were no statistical differences in terms of TMB between the high-risk and low-risk cohorts (P = 0.121; **Figure 6C**). No significant difference in OS was found in the high- or low-TMB cohorts (P = 0.657; **Figure 6D**).

DISCUSSION

Several clinical trials have shown that checkpoint inhibitors were superior to chemotherapy for SQLC patients (12, 18). However, SQLC patients have shown limited improved clinical outcomes from immunotherapy. Thus, it is important to identify and develop potential biomarkers for predicting prognosis in SQLC patients treated with immunotherapy.

Early studies have demonstrated that PD-L1 expression, T-cell receptor clonality, TMB, and T-cell infiltration levels may be associated with the clinical response to immunotherapy (13, 17). However, due to the complexity of tumor biology and the immune microenvironment, a single biomarker could not be sufficiently predictive of clinical outcomes to immunotherapy (26). It may be necessary to apply the integration genomics and transcriptomic to improve the accuracy of predictions. Furthermore, as the TIME served as a critical role in tumor progression, it is important to explore an immune-related model to predict the prognosis of SQLC patients and identify patients who would obtain clinical benefit from immunotherapy.

To the best of our knowledge, it was the first immune-related signature prognostic model for SQLC patients based on RNA-sequencing data. In our study, we firstly presented the gene mutation profiles and the relative proportion of 22 immune cells of SQLC from TCGA dataset. Besides, the relationships between TMB, proportion of immune cells, and SQLC prognosis were firstly systematic exploration in our article.

Our study established and validated an immune-related risk signature model for SQLC from TCGA dataset. A total of eight DE IRGs with prognostic value were included in the signature. Among these genes, six (*MMP12*, *PLAU*, *IGHD3-22*, *IGKV1D-17*, *CGA*, and *SPP1*) were up-regulated in SQLC tissues compared with normal samples, while two (*AGTR2* and *NR4A1*) were down-regulated. *PLAU* and *MMP12* have been reported to be associated with aberrant regulation of gene function and poor prognosis for lung carcinoma (27–30). *SPP1* has been reported as an independent risk biomarker prognostic evaluation of patients with lung adenocarcinoma (31). *NR4A1* has been considered as a member of the orphan nuclear receptor superfamily of transcription factors (32). In our study, *NR4A1* was down-regulated in the SQLC tissues compared with the normal tissues. However, *NR4A1* has been reported to be overexpressed in multiple types of carcinomas in previous reports, and play a critical role in survival or cell proliferation in cervical, lymphoma, pancreatic, lung, and colon cancer cells. *NR4A1* has been found to be involved in promoting cancer invasion and metastasis (33–35). A previous research showed that *AGTR2* was under-expressed in lung adenocarcinoma and played a role in the pathology of adenocarcinoma (36). *CGA* gene was identified as a new estrogen receptor a (ERa) responsive gene in human breast cancer cells and a member of a novel dysregulated pathway in prostate cancer (37–39). *IGKV1-17* gene was reported to be rarely expressed by normal cells and play a critical role

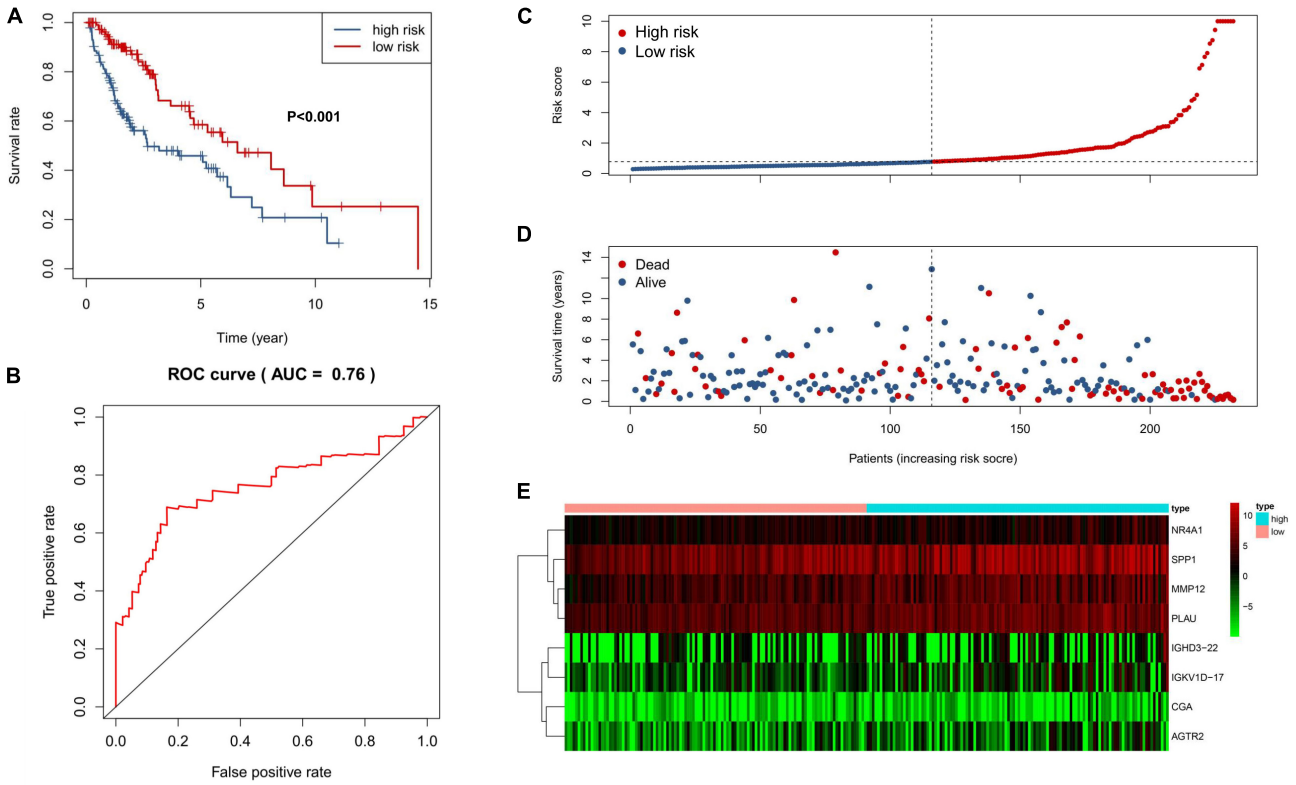

FIGURE 3 | Construction of an 8-IRG signature in the training cohort. **(A)** Kaplan-Meier curve analysis of overall survival of SQLC patients in high- and low-risk groups. **(B)** ROC curves analysis of 1 year. Risk score distribution **(C)**, survival status **(D)**, and heatmap of expression profiles **(E)** for patients in high- and low-risk groups by the 8-IRG signature.

in the development of SLE-nephritis (40). *IGHD* gene served as suppressor genes in the recurrence of triple-negative breast cancer (41). Although the role of the remaining *CGA*, *IGHD3-22*, and *IGKV1D-17* genes in lung cancer patients has not been previously reported, they might play an important role as potential biomarkers.

We found that four IRGs encoded cytokines or cytokine receptors, including *CGA*, *SPP1*, *AGTR2*, and *NR4A1* genes. Cytokines and cytokine receptors have been reported to modulate the tumor microenvironment and promote the development of cancer, which may contribute to disease progression and a worse prognosis for SQLC patients in the high-risk group (42–44). Significant differences in OS were found between patients with high-risk and low-risk scores. Furthermore, our signature was significantly associated with the prognosis of SQLC patients in the training, testing, and total cohorts. Our 8-IRG signature has acted as an independent prognostic factor in OS for SQLC patients in both the univariate and the multivariate Cox regression analyses. These results demonstrated that the signature might be a useful tool for predicting prognosis.

Our signature had also shown relationships with immune cells. CIBERSORT was applied to assess the relative abundances of 22 immune cells types in each SQLC sample. Our study showed that the proportion of resting memory CD4 T cells, M2 macrophages, and neutrophils were positively correlated with 8-IRG risk score, and the proportion of follicular helper T cells, naïve B cells, and activated NK cells were negatively associated with the 8-IRG risk score. Furthermore, high abundance levels of resting memory CD4 T cells and M2 macrophages were found in the high-risk cohort, which was associated with poorer OS. Low abundance levels of naïve B cells and follicular helper T cells were found in the high-risk cohort, which was associated with better OS. High proportion of M2 macrophage was reported to be correlated with a poor response to immunotherapy (45). These results may contribute to the poor prognosis in the high-risk cohort.

We also performed gene mutation analysis to explore the possible mechanisms of the 8-IRG signature in the high- and low-risk groups. However, there was no significant difference in TMB between the 8-IRG signature high-risk group and low-risk group. Furthermore, our study showed that TMB was not associated with OS, which was not consistent with the results of previously reported studies (17, 46). However, a recent study showed that there was no significant correlation between TMB and the prognosis of lung cancer patients treated with pembrolizumab (26). According to the NCCN guideline for NSCLC patients, TMB is an evolving biomarker that may be helpful to select patients for immunotherapy, but there is no consensus on how to measure TMB in clinical practices (14).

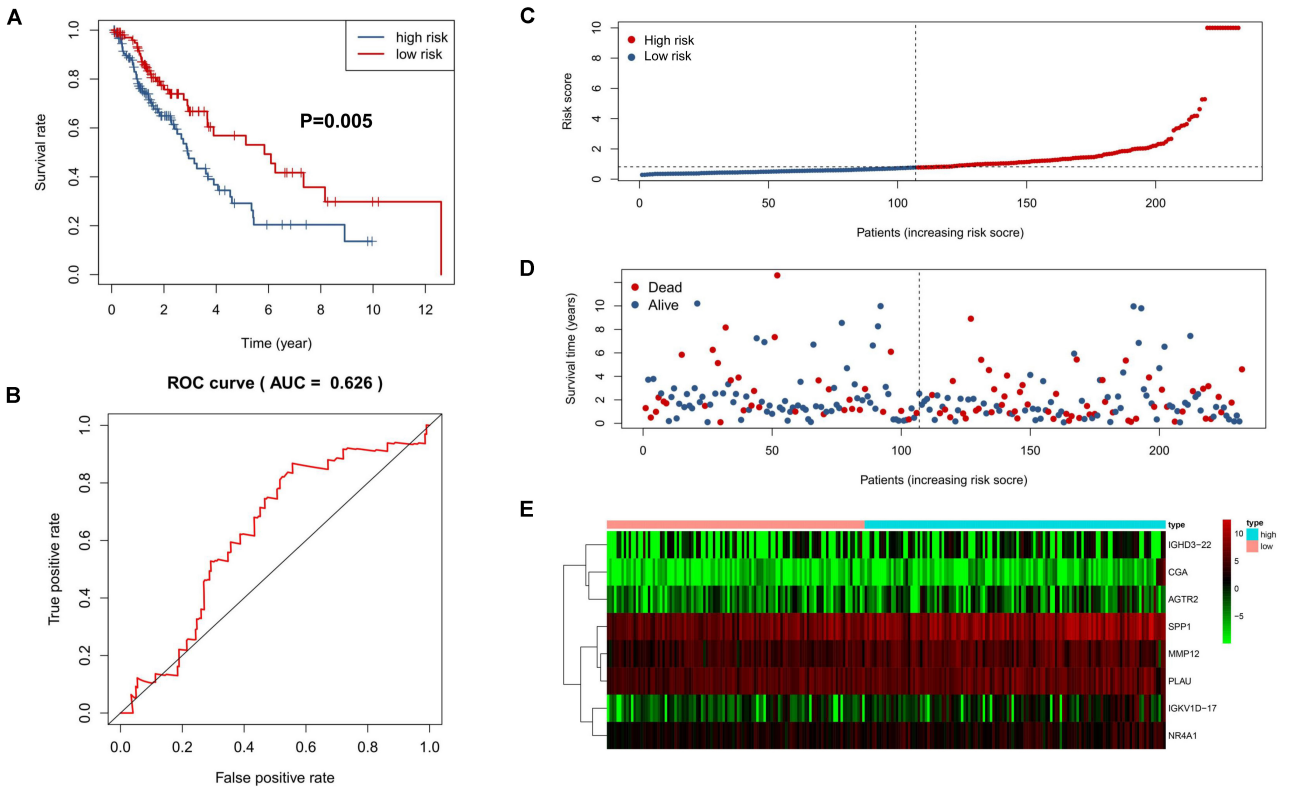

FIGURE 4 | Validation of an 8-IRG signature in the validating cohort. **(A)** Kaplan-Meier curve analysis of overall survival of SQLC patients in high- and low-risk groups. **(B)** ROC curves analysis of 1 year. Risk score distribution **(C)**, survival status **(D)**, and heatmap of expression profiles **(E)** for patients in high- and low-risk groups by the 8-IRG signature.

TABLE 1 | Univariate and multivariate Cox regression analysis of SQLC.

Variables	Univariate analysis		Multivariate analysis	
	Hazard ratio (95% CI)	*P* value	Hazard ratio (95% CI)	*P* value
Age (≤65 vs. >65)	1.237 (0.908–1.686)	0.178	1.285 (0.932–1.771)	0.126
Gender (male vs. female)	0.899 (0.637–1.268)	0.544	0.800(0.562–1.138)	0.215
Tumor stage				
T1	1		1	
T2	1.274 (0.859–1.890)	0.229	1.302(0.862–1.969)	0.210
T3	1.972 (1.204–3.231)	0.007	2.245 (1.093–4.612)	0.028
T4	2.491 (1.308–4.744)	0.005	3.250 (1.288–8.196)	0.013
N stage				
N0	1		1	
N1	1.205 (0.862–1.684)	0.275	1.361 (0.780–2.374)	0.278
N2	1.405 (0.862–2.292)	0.173	1.521 (0.622–3.722)	0.358
N3	2.987 (0.733–12.174)	0.127	5.574 (1.005–30.929)	0.049
Clinical stage				
I	1		1	
II	1.235 (0.871–1.750)	0.236	0.918 (0.507–1.661)	0.777
III	1.784 (1.229–2.591)	0.002	0.874 (0.330–2.315)	0.787
IV	2.251 (0.707–7.166)	0.170	1.579 (0.419–5.959)	0.500
8-IRG risk score (low vs high)	1.600 (1.168–2.193)	0.003	1.937 (1.382–2.715)	<0.001

HR, hazard ratio; CI, confidence interval; IRG, immune-related genes.

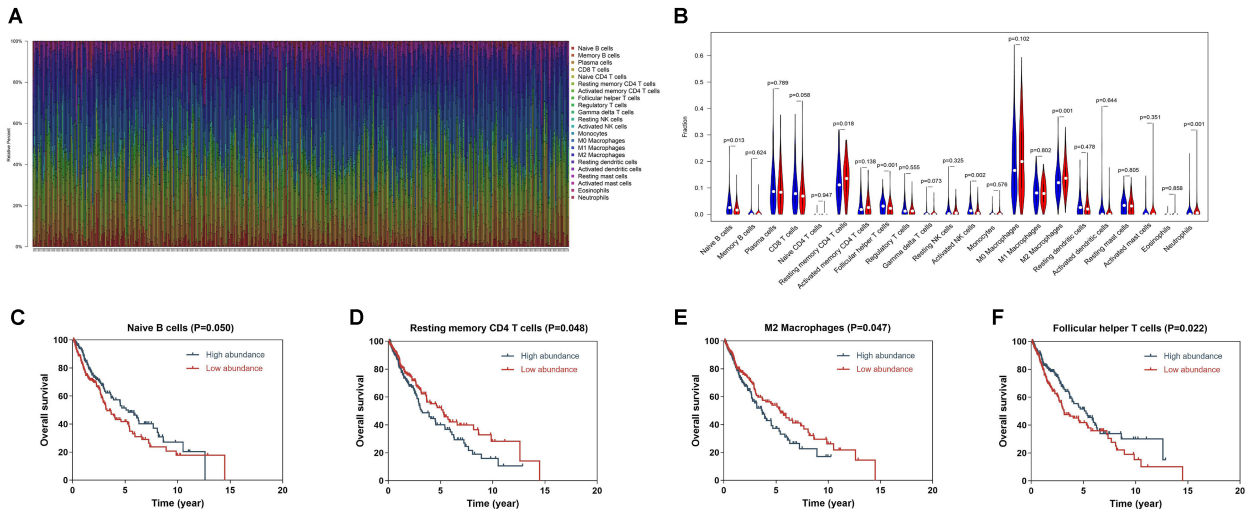

FIGURE 5 | (A) Bar chart of the relative proportion of the 22 immune cells in each SQLC sample. **(B)** The association of immune cells infiltration and the immune-related risk signature in SQLC. A red violin and a blue violin represent the 8-IRG signature high-risk and low-risk groups. The white points inside the violin represent median values. **(C–F)** The association of immune cells infiltration and OS in TCGA SQLC dataset. **(C)** Naïve B cells; **(D)** Resting memory CD4 T cells; **(E)** M2 macrophages; **(F)** Follicular helper T cells.

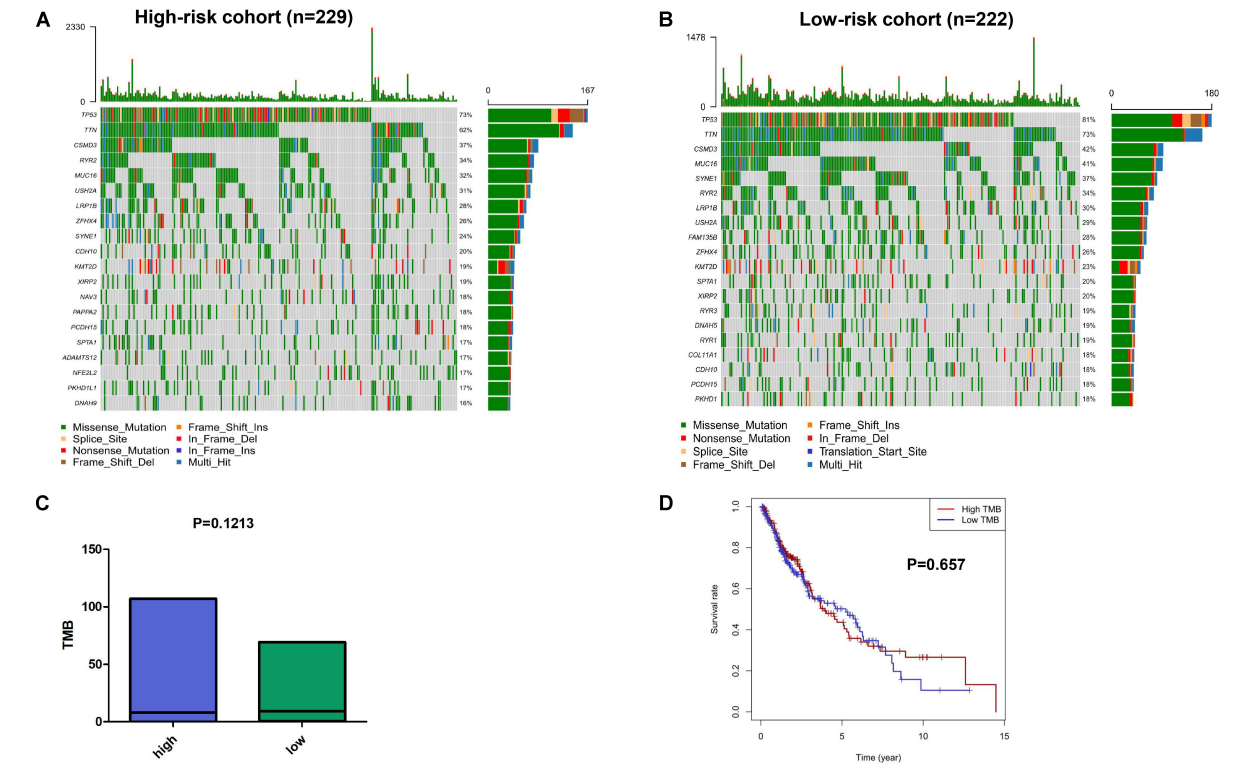

FIGURE 6 | The mutation profiles and TMB among low-risk and high-risk groups. Mutation profile of low-risk **(A)** and high-risk **(B)** groups. **(C)** The relationship between the immune-related risk signature and TMB. **(D)** The association of TMB and OS in TCGA SQLC dataset.

Despite these promising results, there were several limitations in our study. First, the immune-related signature model was established and validated with gene profiles from the public dataset. Second, the proportion of Asian SQLC patients was small in the TCGA cohort. Thus, it is still unclear whether this signature model will be effective for Asian SQLC patients. Further studies should incorporate with a larger number of SQLC patients from Asia and the clinical practice.

CONCLUSION

Our study constructed and validated an 8-IRG signature prognostic model to predict clinical outcomes for SQLC patients, which may provide a deeper understanding of immunotherapy. However, this signature model for SQLC needs further validation with a larger number of patients.

DATA AVAILABILITY STATEMENT

The gene expression RNA-sequencing data, mutation data, and clinical information of SQLC patients in our study were downloaded from the TCGA data portal (https://portal.gdc.cancer.gov). The comprehensive list of IRGs was obtained from the ImmPort database (https://immport.niaid.nih.gov).

AUTHOR CONTRIBUTIONS

R-LC made contributions to conception, design, and data analysis and wrote the manuscript. SS, X-JD, and L-LS analyzed the data. J-TL, Z-WX, Z-ZC, and S-YW gave suggestions on study design, discussed, and interpreted the data. J-XZ, YC, and L-ZL designed and supervised the study. All authors read and approved the final version of the manuscript.

FUNDING

This study was supported by a grant from the National Administration of Traditional Chinese Medicine: 2019 Project of building evidence-based practice capacity for TCM (No. 2019xzzx—zl001), the Pilot project of Integrated traditional Chinese and Western medicine clinical collaboration for major and difficult diseases (lung cancer), and the National Natural Science Foundation of China (Grant Numbers 81973775 and 81973815).

SUPPLEMENTARY MATERIAL

The Supplementary Material for this article can be found online at: https://www.frontiersin.org/articles/10.3389/fimmu.2020.01933/full#supplementary-material

REFERENCES

1. Bray F, Ferlay J, Soerjomataram I, Siegel RL, Torre LA, Jemal A. Global cancer statistics 2018: GLOBOCAN estimates of incidence and mortality worldwide for 36 cancers in 185 countries. *CA Cancer J Clin*. (2018) 68:394–424. doi: 10.3322/caac.21492
2. Gridelli C, Rossi A, Carbone DP, Guarize J, Karachaliou N, Mok T, et al. Non-small-cell lung cancer. *Nat Rev Dis Primers*. (2015) 1:15009. doi: 10.1038/nrdp.2015.9
3. Socinski MA, Obasaju C, Gandara D, Hirsch FR, Bonomi P, Bunn PA Jr., et al. Current and emergent therapy options for advanced squamous cell lung cancer. *J Thorac Oncol*. (2018) 13:165–83. doi: 10.1016/j.jtho.2017.11.111
4. Socinski MA, Bondarenko I, Karaseva NA, Makhson AM, Vynnychenko I, Okamoto I, et al. Weekly nab-paclitaxel in combination with carboplatin versus solvent-based paclitaxel plus carboplatin as first-line therapy in patients with advanced non-small-cell lung cancer: final results of a phase III trial. *J Clin Oncol*. (2012) 30:2055–62. doi: 10.1200/JCO.2011.39.5848
5. Maemondo M, Inoue A, Kobayashi K, Sugawara S, Oizumi S, Isobe H, et al. Gefitinib or chemotherapy for non-small-cell lung cancer with mutated EGFR. *N Engl J Med*. (2010) 362:2380–8. doi: 10.1056/NEJMoa0909530
6. Solomon BJ, Mok T, Kim DW, Wu YL, Nakagawa K, Mekhail T, et al. First-line crizotinib versus chemotherapy in ALK-positive lung cancer. *N Engl J Med*. (2014) 371:2167–77. doi: 10.1056/NEJMoa1408440
7. An SJ, Chen ZH, Su J, Zhang XC, Zhong WZ, Yang JJ, et al. Identification of enriched driver gene alterations in subgroups of non-small cell lung cancer patients based on histology and smoking status. *PLoS One*. (2012) 7:e40109. doi: 10.1371/journal.pone.0040109
8. Sandler A, Gray R, Perry MC, Brahmer J, Schiller JH, Dowlati A, et al. Paclitaxel-carboplatin alone or with bevacizumab for non-small-cell lung cancer. *N Engl J Med*. (2006) 355:2542–50. doi: 10.1056/NEJMoa061884
9. Scagliotti G, Hanna N, Fossella F, Sugarman K, Blatter J, Peterson P, et al. The differential efficacy of pemetrexed according to NSCLC histology: a review of two Phase III studies. *Oncologist*. (2009) 14:253–63. doi: 10.1634/theoncologist.2008-0232
10. Xu C, Chen YP, Du XJ, Liu JQ, Huang CL, Chen L, et al. Comparative safety of immune checkpoint inhibitors in cancer: systematic review and network meta-analysis. *BMJ*. (2018) 363:k4226. doi: 10.1136/bmj.k4226
11. Schachter J, Ribas A, Long GV, Arance A, Grob JJ, Mortier L, et al. Pembrolizumab versus ipilimumab for advanced melanoma: final overall survival results of a multicentre, randomised, open-label phase 3 study (KEYNOTE-006). *Lancet*. (2017) 390:1853–62. doi: 10.1016/S0140-6736(17)31601-X
12. Paz-Ares L, Luft A, Vicente D, Tafreshi A, Gumus M, Mazieres J, et al. Pembrolizumab plus chemotherapy for squamous non-small-cell lung cancer. *N Engl J Med*. (2018) 379:2040–51. doi: 10.1056/NEJMoa1810865
13. Gibney GT, Weiner LM, Atkins MB. Predictive biomarkers for checkpoint inhibitor-based immunotherapy. *Lancet Oncol*. (2016) 17:e542–51. doi: 10.1016/S1470-2045(16)30406-5
14. National Comprehensive Cancer Network (NCCN) *Clinical Practice Guidelines in Oncology. Non-Small Cell Lung Cancer, Version 2,2020*. (2020). Available online at: https://www.nccn.org/professionals/physician_gls/pdf/nscl.pdf (accessed January 26, 2020).
15. Reck M, Rodriguez-Abreu D, Robinson AG, Hui R, Csoszi T, Fulop A, et al. Updated analysis of KEYNOTE-024: pembrolizumab versus platinum-based chemotherapy for advanced non-small-cell lung cancer with PD-L1 tumor proportion score of 50% or greater. *J Clin Oncol*. (2019) 37:537–46. doi: 10.1200/JCO.18.00149
16. Goodman AM, Piccioni D, Kato S, Boichard A, Wang HY, Frampton G, et al. Prevalence of PDL1 amplification and preliminary response to immune checkpoint blockade in solid tumors. *JAMA Oncol*. (2018) 4:1237–44. doi: 10.1001/jamaoncol.2018.1701
17. Samstein RM, Lee CH, Shoushtari AN, Hellmann MD, Shen R, Janjigian YY, et al. Tumor mutational load predicts survival after immunotherapy across multiple cancer types. *Nat Genet*. (2019) 51:202–6. doi: 10.1038/s41588-018-0312-8
18. Brahmer J, Reckamp KL, Baas P, Crino L, Eberhardt WE, Poddubskaya E, et al. Nivolumab versus docetaxel in advanced squamous-cell non-small-cell lung cancer. *N Engl J Med*. (2015) 373:123–35. doi: 10.1056/NEJMoa1504627
19. Bhattacharya S, Andorf S, Gomes L, Dunn P, Schaefer H, Pontius J, et al. ImmPort: disseminating data to the public for the future of immunology. *Immunol Res*. (2014) 58:234–9. doi: 10.1007/s12026-014-8516-1
20. Sauerbrei W, Royston P, Binder H. Selection of important variables and determination of functional form for continuous predictors in multivariable model building. *Stat Med*. (2007) 26:5512–28. doi: 10.1002/sim.3148
21. Chen HY, Yu SL, Chen CH, Chang GC, Chen CY, Yuan A, et al. A five-gene signature and clinical outcome in non-small-cell lung cancer. *N Engl J Med*. (2007) 356:11–20. doi: 10.1056/NEJMoa060096

22. Lorent M, Giral M, Foucher Y. Net time-dependent ROC curves: a solution for evaluating the accuracy of a marker to predict disease-related mortality. *Stat Med*. (2014) 33:2379–89. doi: 10.1002/sim.6079
23. Mayakonda A, Lin DC, Assenov Y, Plass C, Koeffler HP. Maftools: efficient and comprehensive analysis of somatic variants in cancer. *Genome Res*. (2018) 28:1747–56. doi: 10.1101/gr.239244.118
24. Robinson DR, Wu YM, Lonigro RJ, Vats P, Cobain E, Everett J, et al. Integrative clinical genomics of metastatic cancer. *Nature*. (2017) 548:297–303. doi: 10.1038/nature23306
25. Newman AM, Liu CL, Green MR, Gentles AJ, Feng W, Xu Y, et al. Robust enumeration of cell subsets from tissue expression profiles. *Nat Methods*. (2015) 12:453–7. doi: 10.1038/nmeth.3337
26. Langer C, Gadgeel S, Borghaei S, Patnaik A, Powell S, Gentzler R, et al. KEYNOTE-021: TMB and outcomes for carboplatin and pemetrexed with or without pembrolizumab for nonsquamous NSCLC.OA04.05. *J Thorac Oncol*. (2019) 14:S216. doi: 10.1016/j.jtho.2019.08.426
27. Watanabe T, Miura T, Degawa Y, Fujita Y, Inoue M, Kawaguchi M, et al. Comparison of lung cancer cell lines representing four histopathological subtypes with gene expression profiling using quantitative real-time PCR. *Cancer Cell Int*. (2010) 10:2. doi: 10.1186/1475-2867-10-2
28. Ning P, Wu Z, Hu A, Li X, He J, Gong X, et al. Integrated genomic analyses of lung squamous cell carcinoma for identification of a possible competitive endogenous RNA network by means of TCGA datasets. *PeerJ*. (2018) 6:e4254. doi: 10.7717/peerj.4254
29. Gao C, Zhuang J, Li H, Liu C, Zhou C, Liu L, et al. Exploration of methylation-driven genes for monitoring and prognosis of patients with lung adenocarcinoma. *Cancer Cell Int*. (2018) 18:194. doi: 10.1186/s12935-018-0691-z
30. Liu L, Shi M, Wang Z, Lu H, Li C, Tao Y, et al. A molecular and staging model predicts survival in patients with resected non-small cell lung cancer. *BMC Cancer*. (2018) 18:966. doi: 10.1186/s12885-018-4881-9
31. Li S, Yang R, Sun X, Miao S, Lu T, Wang Y, et al. Identification of SPP1 as a promising biomarker to predict clinical outcome of lung adenocarcinoma individuals. *Gene*. (2018) 679:398–404. doi: 10.1016/j.gene.2018.09.030
32. Lee SO, Li X, Khan S, Safe S. Targeting NR4A1 (TR3) in cancer cells and tumors. *Expert Opin Ther Targets*. (2011) 15:195–206. doi: 10.1517/14728222.2011.547481
33. Zhou F, Drabsch Y, Dekker TJ, De Vinuesa AG, Li Y, Hawinkels LJ, et al. Nuclear receptor NR4A1 promotes breast cancer invasion and metastasis by activating TGF-beta signalling. *Nat Commun*. (2014) 5:3388. doi: 10.1038/ncomms4388
34. Lacey A, Rodrigues-Hoffman A, Safe S. PAX3-FOXO1A expression in rhabdomyosarcoma is driven by the targetable nuclear receptor NR4A1. *Cancer Res*. (2017) 77:732–41. doi: 10.1158/0008-5472.CAN-16-1546
35. Delgado E, Boisen MM, Laskey R, Chen R, Song C, Sallit J, et al. High expression of orphan nuclear receptor NR4A1 in a subset of ovarian tumors with worse outcome. *Gynecol Oncol*. (2016) 141:348–56. doi: 10.1016/j.ygyno.2016.02.030
36. Goldstein B, Trivedi M, Speth RC. Alterations in gene expression of components of the renin-angiotensin system and its related enzymes in lung cancer. *Lung Cancer Int*. (2017) 2017:6914976. doi: 10.1155/2017/6914976
37. Bieche I, Parfait B, Le Doussal V, Olivi M, Rio MC, Lidereau R, et al. Identification of CGA as a novel estrogen receptor-responsive gene in breast cancer: an outstanding candidate marker to predict the response to endocrine therapy. *Cancer Res*. (2001) 61:1652–8.
38. Bièche I, Parfait B, Noguès C, Andrieu C, Vidaud D, Spyratos F, et al. The CGA gene as new predictor of the response to endocrine therapy in ER alpha-positive postmenopausal breast cancer patients. *Oncogene*. (2001) 20:6955–9. doi: 10.1038/sj.onc.1204739
39. Bièche I, Latil A, Parfait B, Vidaud D, Laurendeau I, Lidereau R, et al. CGA gene (coding for the alpha subunit of glycoprotein hormones) overexpression in ER alpha-positive prostate tumors. *Eur Urol*. (2002) 41:335–41. doi: 10.1016/s0302-2838(02)00020-9
40. Suzuki N, Harada T, Mihara S, Sakane T. Characterization of a germline Vk gene encoding cationic anti-DNA antibody and role of receptor editing for development of the autoantibody in patients with systemic lupus erythematosus. *J Clin Invest*. (1996) 98:1843–50. doi: 10.1172/jci118985
41. Hsu H-M, Chu C-M, Chang Y-J, Yu J-C, Chen C-T, Jian C-E, et al. Six novel immunoglobulin genes as biomarkers for better prognosis in triple-negative breast cancer by gene co-expression network analysis. *Sci Rep*. (2019) 9:4484. doi: 10.1038/s41598-019-40826-w
42. Zhu J, Petit PF, Van Den Eynde BJ. Apoptosis of tumor-infiltrating T lymphocytes: a new immune checkpoint mechanism. *Cancer Immunol Immunother*. (2019) 68:835–47. doi: 10.1007/s00262-018-2269-y
43. Hansen W. Neuropilin 1 guides regulatory T cells into VEGF-producing melanoma. *Oncoimmunology*. (2013) 2:e23039. doi: 10.4161/onci.23039
44. Abolhassani M, Aloulou N, Chaumette MT, Aparicio T, Martin-Garcia N, Mansour H, et al. Leptin receptor-related immune response in colorectal tumors: the role of colonocytes and interleukin-8. *Cancer Res*. (2008) 68:9423–32. doi: 10.1158/0008-5472.CAN-08-1017
45. Sharma P, Hu-Lieskovan S, Wargo JA, Ribas A. Primary, adaptive, and acquired resistance to cancer immunotherapy. *Cell*. (2017) 168:707–23. doi: 10.1016/j.cell.2017.01.017
46. Fang W, Ma Y, Yin JC, Hong S, Zhou H, Wang A, et al. Comprehensive genomic profiling identifies novel genetic predictors of response to anti-PD-(L)1 therapies in non-small cell lung cancer. *Clin Cancer Res*. (2019) 25:5015–26. doi: 10.1158/1078-0432.CCR-19-0585

Conflict of Interest: The authors declare that the research was conducted in the absence of any commercial or financial relationships that could be construed as a potential conflict of interest.

frontiers in Immunology

REVIEW
published: 25 September 2020
doi: 10.3389/fimmu.2020.578349

Leveraging Endogenous Dendritic Cells to Enhance the Therapeutic Efficacy of Adoptive T-Cell Therapy and Checkpoint Blockade

Mie Linder Hübbe[1], *Ditte Elisabeth Jæhger*[2], *Thomas Lars Andresen*[2] *and Mads Hald Andersen*[1]*

[1] National Center for Cancer Immune Therapy (CCIT-DK), Department of Oncology, Copenhagen University Hospital Herlev, Copenhagen, Denmark, [2] Department of Health Technology, Technical University of Denmark, Kongens Lyngby, Denmark

OPEN ACCESS

Edited by:
Maysaloun Merhi, Hamad Medical Corporation, Qatar

Reviewed by:
Amer Najjar, University of Texas MD Anderson Cancer Center, United States
Fabian Benencia, Ohio University, United States

***Correspondence:**
Mads Hald Andersen
mads.hald.andersen@regionh.dk

Specialty section:
This article was submitted to Cancer Immunity and Immunotherapy, a section of the journal Frontiers in Immunology

Received: *30 June 2020*
Accepted: *26 August 2020*
Published: *25 September 2020*

Citation:
Hübbe ML, Jæhger DE, Andresen TL and Andersen MH (2020) Leveraging Endogenous Dendritic Cells to Enhance the Therapeutic Efficacy of Adoptive T-Cell Therapy and Checkpoint Blockade. Front. Immunol. 11:578349. doi: 10.3389/fimmu.2020.578349

Adoptive cell therapy (ACT), based on treatment with autologous tumor infiltrating lymphocyte (TIL)-derived or genetically modified chimeric antigen receptor (CAR) T cells, has become a potentially curative therapy for subgroups of patients with melanoma and hematological malignancies. To further improve response rates, and to broaden the applicability of ACT to more types of solid malignancies, it is necessary to explore and define strategies that can be used as adjuvant treatments to ACT. Stimulation of endogenous dendritic cells (DCs) alongside ACT can be used to promote epitope spreading and thereby decrease the risk of tumor escape due to target antigen downregulation, which is a common cause of disease relapse in initially responsive ACT treated patients. Addition of checkpoint blockade to ACT and DC stimulation might further enhance response rates by counteracting an eventual inactivation of infused and endogenously primed tumor-reactive T cells. This review will outline and discuss therapeutic strategies that can be utilized to engage endogenous DCs alongside ACT and checkpoint blockade, to strengthen the anti-tumor immune response.

Keywords: cancer immunotherapy, immune checkpoint blockade, combination therapies, T-cell therapy, dendritic cells

INTRODUCTION

The ability of the immune system to recognize and eliminate cancer cells has paved the way for the development of cancer immunotherapies that target components of the immune system to mobilize a tumor-reactive immune response (1). Adoptive cell therapy (ACT) using T cells is an example of a cancer immunotherapy that has become a potentially curative option for subgroups of patients with melanoma and hematological malignancies (2). ACT is based on a systemic treatment with tumor-reactive autologous T cells that are obtained from tumor biopsies or blood samples,

expanded *in vitro* and infused back to the patient (3, 4). This process can involve selection of tumor-reactive clones or genetic modification to generate chimeric antigen receptor (CAR) T cells or T cell receptor (TCR) modified T cells that recognize cancer-specific antigens (5). ACT using tumor infiltrating lymphocytes (TILs) is being used to treat patients with advanced stage melanoma and have mounted durable complete responses in up to 20% of treated patients (6, 7). CAR-T cells targeting the shared tumor antigen CD19 have been used to treat adult and pediatric patients suffering from B-cell acute lymphocytic leukemia (8), reaching up to 90% response rate in some clinical trials (9).

Clinical success of ACT has been correlated with the ability of the transferred T cells to undergo post-infusion priming and expansion, which is dependent on the phenotype of infused T cells (10–12) as well as antigen presentation and activation of dendritic cells (DCs) in the tumor-draining lymph node (tdLN) (13–15). Following priming and expansion, the therapeutic efficacy of the transferred T cells is dependent on their ability to engraft the tumor and maintain their effector functions. Thus, even sufficiently primed T cells can lose their tumor-reactivity due to escape mechanisms adapted by the tumor (16, 17), such as downregulation of the cognate antigen (18). Accordingly, it has been found that many patients treated with CAR-T cells targeting CD19 eventually suffer from relapse with CD19-negative leukemias (19, 20). Tumor escape has also been described in melanoma patients treated with TILs, where ACT was found to alter the antigenic landscape by causing target antigen downregulation (21). Relapse caused by loss of antigen can be ameliorated by the engagement of endogenous T cells to facilitate recognition of a broader tumor antigen repertoire (22–24). This phenomenon, denoted epitope spreading, is facilitated by peripheral, migratory DCs that transport antigen from the tumor to the tdLN, where naïve, endogenous tumor-reactive T cells can be primed (25) (**Figure 1**). Thereby the engagement of DCs alongside ACT can help to facilitate a broader and durable therapeutic response.

Another major obstacle to clinically efficient ACT is an eventual inactivation of infused and endogenously primed T cells via engagement of immune checkpoints, such as programmed cell death protein 1 (PD-1) and cytotoxic T-lymphocyte-associated protein 4 (CTLA-4), expressed by activated T cells (26). Checkpoint blockade has been a major milestone in the field of cancer immunotherapy and has shown remarkable clinical success (27). Accordingly, in 2018, the discovery that inhibition of negative immune regulation through checkpoint inhibition could be utilized for cancer therapy was awarded with the Nobel Prize jointly to James P. Allison and Tasuku Honjo (28). Immune checkpoint engagement results in an inactivation of T cells through binding of PD-1, expressed by activated T cells, to programmed death-ligand 1 (PD-L1), expressed by cells of the tumor stroma, e.g., cancer cells and other immune cells. Priming and activation of T cells can also be inhibited by interaction between CD28 on T cells and CTLA-4 expressed by regulatory T cells (Tregs) (26). In order to become activated, T cells must receive co-stimulatory signals from antigen presenting cells, such as DCs, through interaction between CD28 and B7 (CD80 or CD86) and Tregs can prevent this interaction by hijacking B7 through binding to CTLA-4, thereby blocking the binding between CD28 and B7. Antibody-based blocking of PD-1 or PD-L1 can therefore prevent inhibition of activated T cells whereas CTLA-4 blockade can enhance the priming of T cells.

Besides PD-1 and CTLA-4, other co-inhibitory receptors that influence anti-tumor immune responses have been discovered. In particular Lag-3 and T cell immunoreceptor with Ig and ITIM domains (TIGIT) are of interest in this respect and blockade of these receptors are being explored in clinical trials.

Lag-3 is upregulated by activated CD4+ and CD8+ T cells, it structurally resembles the CD4 co-receptor and binds MHC class II molecules with high affinity (29). Lag-3 is also expressed by Tregs and Lag-3 blockade has been shown to abrogate the suppressive functions of Tregs. Lag-3+ Tregs produces high amounts of IL-10 and transforming growth factor beta (TGF-β) and expand in tumor tissue of patients with melanoma and colorectal cancer (30). In pre-clinical cancer models, Lag-3 expression has been found to be co-expressed with PD-1 on tumor-infiltrating CD4+ and CD8+ T cells and co-blockade of Lag-3 and PD-1 can improve the proliferation and cytokine production of tumor-antigen specific CD8+ T cells (31). Also, Lag-3 blockade has been shown to have a synergistic therapeutic effect in combination with tumor antigen vaccination (32).

TIGIT is expressed by activated T cells, NK cells memory T cells and a subset of Tregs. TIGIT binds to CD155 and CD112 that are expressed by antigen-presenting cells (APCs), T cells and other non-hematopoietic cells, including tumor cells. Engagement of TIGIT to CD155 on DCs has been shown to inhibit IL-12p40 production and instead induce IL-10 production, thereby rendering DCs tolerogenic rather than inflammatory (33). In this way, TIGIT can indirectly inhibit the priming of tumor-reactive T cells but TIGIT engagement can also directly induce T cell inhibition by blocking T cell activation, proliferation, and acquisition of effector functions (34). In Tregs, TIGIT expression marks a phenotype that suppresses pro-inflammatory type I and type 17 responses and TIGIT engagement on Tregs has been shown to induce IL-10 secretion (35). TIGIT has been shown to be highly expressed by TILs in melanoma patients (36) and in murine tumors, the most dysfunctional TIL phenotype is CD8+ T cells that co-express TIGIT, PD-1, Tim-3, and Lag-3 (37). Consequently, in melanoma patients, co-blockade of PD-1 and TIGIT has been shown to improve proliferation, cytokine production and degranulation of CD8+ TILs (36).

The use of PD-1 and CTLA-4 blockers has been shown to increase the durable response rates and overall survival of responding patients when administered as monotherapies. However, the clinical benefits of the checkpoint blockers as monotherapies are limited by relatively low objective response rates, e.g., 10–16% for ipilimimab and 30–40% for nivolumab and pembrolizumab in metastatic melanoma patients (38–40). The combined treatment of ACT and checkpoint blockade has however been explored with encouraging results. ACT in combination with blockade of both PD-1 and CTLA-4 has shown particularly good effects (41), most likely because the anti-PD-1 treatment counteracts PD-L1-mediated inactivation of T cells

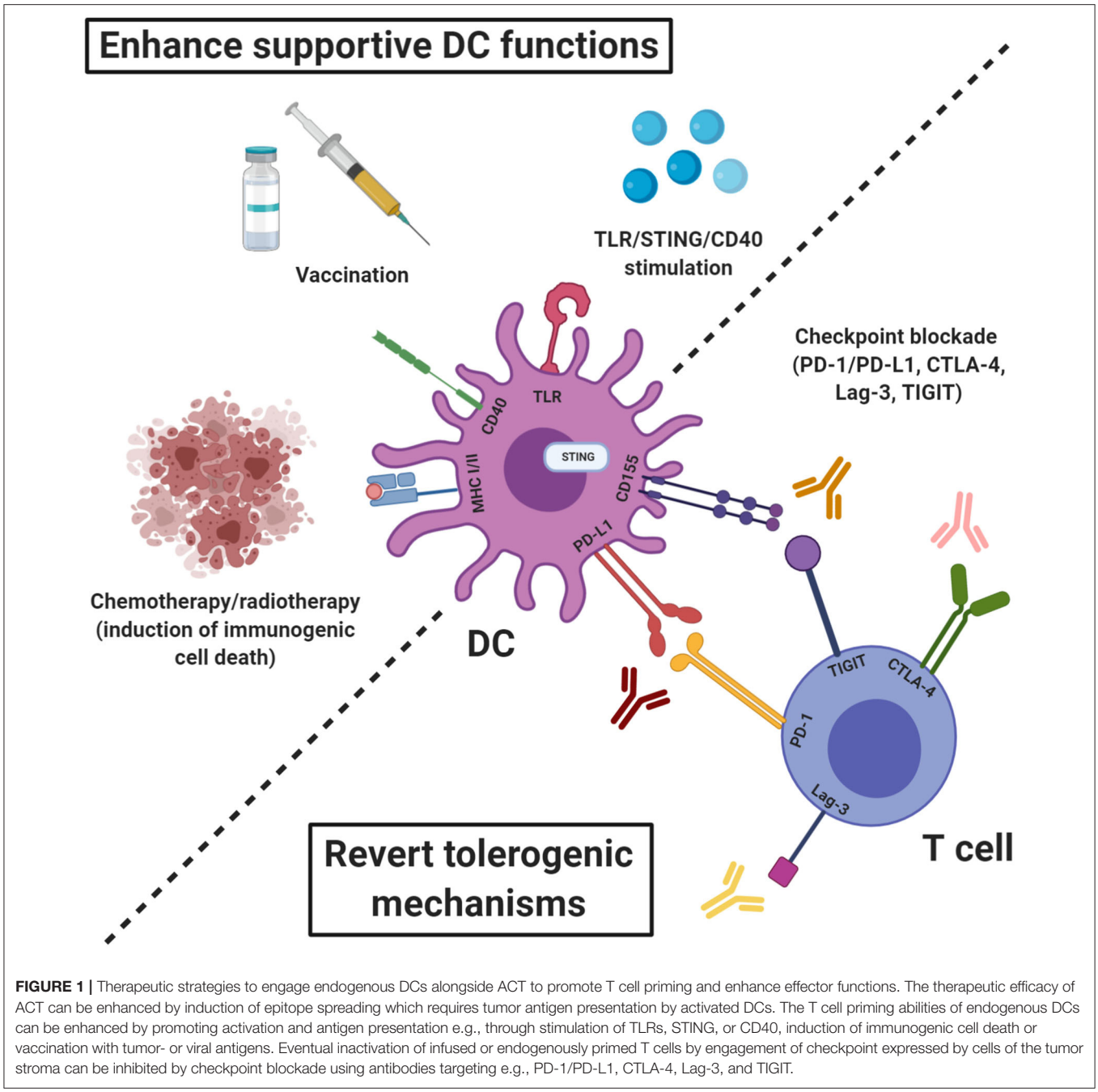

FIGURE 1 | Therapeutic strategies to engage endogenous DCs alongside ACT to promote T cell priming and enhance effector functions. The therapeutic efficacy of ACT can be enhanced by induction of epitope spreading which requires tumor antigen presentation by activated DCs. The T cell priming abilities of endogenous DCs can be enhanced by promoting activation and antigen presentation e.g., through stimulation of TLRs, STING, or CD40, induction of immunogenic cell death or vaccination with tumor- or viral antigens. Eventual inactivation of infused or endogenously primed T cells by engagement of checkpoint expressed by cells of the tumor stroma can be inhibited by checkpoint blockade using antibodies targeting e.g., PD-1/PD-L1, CTLA-4, Lag-3, and TIGIT.

whereas anti-CTLA-4 enhances priming of endogenous tumor-reactive T cells (42, 43). The combination of ACT and anti-PDL1/PD-1 or CTLA-4 might be of particular relevance as release of IFN-γ by T cells in the TME has been shown to induce checkpoint expression in both stromal cells and myeloid cell subsets, thereby constituting a negative feedback loop which hinders the continuous function of infused T cells (44, 45).

Clinical studies evaluating the efficacy of Lag-3 and TIGIT inhibition are still in early phases and despite encouraging results, the majority of patients still fail to respond to PD-1 or CTLA-4 blockade as mono- or combination therapy. This lack of sustained therapeutic responses can partly be attributed to the actions of other immune suppressive mechanisms in the tumor, e.g., secretion of amino acid depleting enzymes [such as Arginase-1 and Indolamin-2,3-dioxygenase (IDO)], TGF-β or IL-10 (46). For this reason, it can be necessary to include additional treatments that counteract these immunosuppressive mechanisms. There are several therapeutic strategies that can be utilized for this purpose, but particularly stimulation of endogenous DCs represents an interesting approach.

In this review, we will discuss strategies, that have been described pre-clinically and clinically, to improve the efficacy of

ACT and immune checkpoint blockade by engaging endogenous DCs to support the effector functions of infused and endogenous tumor-reactive T cells. Our primary focus will be on CD8+ T cells and the subsets of DCs that that are essential for stimulating a tumor-reactive T cell response, i.e. cross-presenting conventional type 1 dendritic cells (cDC1s) and type I interferon (IFN) producing plasmacytoid DCs (pDCs).

DENDRITIC CELL SUBTYPES AND THEIR ROLE IN T CELL PRIMING

In order to become activated and gain an effector phenotype, naïve T cells must to be introduced to their cognate antigen presented by activated APCs in the context of MHC molecules. DCs are the most effective type of APCs and they are indispensable for initiating an anti-tumor response (47). The outcome of an interaction between a DC and a T cell is however critically dependent on the activation status of the DC. Consequently, antigen presentation by DCs in the absence of co-stimulatory molecules or in the presence of co-inhibitory signals can result in induction of antigen-specific CD8+ T cell tolerance (48) or expansion of antigen-specific regulatory T cells (Tregs) (49, 50). The tolerogenic DCs can be induced by IL-10 that causes downregulation of co-stimulatory molecules and decreases the secretion of inflammatory chemokines (51). Priming of tumor-reactive T cells can therefore only be achieved if there is availability of tumor antigens in an inflammatory environment that also facilitates DC activation. DCs can become activated by pathogen-associated molecular patterns (PAMPs), inflammatory cytokines, and damage-associated molecular patterns (DAMPs) (52). Activation of DCs stimulates intrinsic processes necessary for T cell priming, including accumulation of MHC class I molecules in MHC loading intracellular compartments for enhanced cross-presentation (53), upregulation of co-stimulatory molecules (54) and secretion of T cell promoting cytokines (55).

Due to the pivotal role of the DC activation status on T cell priming, tumor infiltration of immature or otherwise functionally deficient DCs presents an obstacle for efficient ACT. Non-activated tumor-associated DCs can contribute to the induction of a tolerable environment that both limits the effector functions of infused T cells and affects priming of endogenous T cells (56). It is therefore relevant to discuss therapeutic strategies that can increase the availability of tumor antigens and enhance DC activation as adjuvant therapies to ACT. Enhancing the tumor antigen presentation and DC activation will not only remove a potential barrier to T cell functions, but also enhance post-infusion priming of T cells and support the mobilization of an endogenous T cell response.

Conventional Dendritic Cells

cDCs are the most effective types of APCs and they are dedicated to the continuous sampling of antigen. Precursors to cDCs are released from the bone marrow where after they enter lymphoid organs or other peripheral sites and develop into migratory or resident DC subsets (57). The migratory DCs travel to the local lymph nodes (LNs) via the afferent lymph, where they are able to mature and function (58, 59). Both human and murine cDCs can be divided into cDC1s and cDC2s and these subtypes can be further discriminated on the basis of surface marker and transcription factor expression (**Table 1**). An important difference between cDC1s and cDC2s is their ability to perform cross-presentation (60), which is a process where exogenous derived antigens are internalized, processed and presented on MHC I molecules. Cross-presentation is a pre-requisite for induction of a tumor reactive cytotoxic T cell response because it enables the presentation of exogenous tumor antigens on MHC class I molecules, which are normally presented on MHC class II molecules. cDC1s are known to excel at cross-presentation of antigen to CD8+ T cells and they are the main producers of IL-12 (61, 62). In contrast, cDC2s orchestrate CD4+ T helper responses (60).

TABLE 1 | Main markers of dendritic cell subtypes.

	Human	Murine
cDC1	**Surface markers** MHC II, CD11c, XCR1, CD141, CLEC9A **Transcription factors** BATF3, IRF8	**Surface markers** MHC II, CD11c, XCR1, CD8a/CD103 **Transcription factors** BATF3, IRF8
cDC2	**Surface markers** MHC II, CD11c, CD1c, CD172a **Transcription factors** IRF4	**Surface markers** MHC II, CD11c, CD11b, CD172a **Transcription factors** IRF4
pDC	**Surface markers** MHC II, CD11c, CD123, CD303, CD304 **Transcription factors** TCF4 (E2-2), BCL11A	**Surface markers** MHC II, CD11c, Siglec-H, Ly-6C **Transcription factors** TCF4 (E2-2)

In a cancer immunotherapy context, the important function of intra-tumoural CD103+ cDC1s has been well-described pre-clinically and via their function as the primary producers of the T cell recruiting chemokine CXCL10, they are known to be essential for tumor-homing of effector T cells (63). Furthermore, migratory cDC1s are critical for the continuous trafficking of tumor antigens to the draining LN in a CCR7-dependent process (64, 65).

Plasmacytoid Dendritic Cells

pDCs are unique in their ability to rapidly produce vast amounts of type I IFNs (IFN-α/β) in response to TLR stimulation (66). In contrast to cDCs, pDCs develop fully in the bone marrow where after they traffic to secondary lymphoid organs (67). Activated pDCs are known to augment CD8+ T cell responses, even in the absence of specific antigen stimulation (68). In addition, studies indicate that TLR-activated pDCs can function as cross-presenting cells (69–71) and even have direct cytotoxic effects (72, 73).

The ability of pDCs to produce vast amounts of type I IFNs upon activation is important for induction of cancer immunity (74, 75). A pre-clinical study reported that tumor rejection was dependent on secretion of type I IFNs (76) and

this observation has later been seconded by a study reporting that production of type I IFNs by DCs were required for priming of tumor-reactive T cells and tumor elimination (77). Type I IFNs have been found to promote cross-priming of CD8+ T cells (78), enhance the division of activated CD8+ T cells (79) and stimulate intratumoural accumulation of cross-presenting DCs (80). Stimulating production of type I IFNs by pDCs therefore a feasible strategy to augment tumor-reactivity.

STRATEGIES TO ENGAGE ENDOGENOUS DCS FOR IMPROVED ACT EFFICACY

Because engagement of DCs alongside ACT is pivotal for broadening the tumor-reactive response, it is relevant to explore treatment strategies that can be used to stimulate DC activation and/or antigen presentation. In this review, the focus will be on pre-conditioning with chemotherapeutics or radiotherapy, peptide or DC-based vaccination, stimulation with toll-like receptor (TLR) agonists or stimulator of interferon genes (STING) agonists, and CD40 ligation as adjuvant treatments to ACT and checkpoint inhibition.

Pre-conditioning With Chemotherapeutics or Radiotherapy

It is well-established that ACT following lymphodepletion can enhance anti-tumor reactivity in murine and human hosts (81–83), and lymphodepleting pre-conditioning is a standard treatment before T cell infusion in human patients (84). Lymphodepletion refers to an elimination of endogenous lymphocytes, which can be achieved by treatment with a low dose of radiotherapy (RT) or a chemotherapeutic agent, typically cyclophosphamide (CPX) and Fludarabine. Lymphodepletion results in a more pronounced tumor regression than observed with ACT alone and there are several proposed mechanisms behind the improved immunity. Depletion of immune cell subsets that can suppress tumor-reactive T cells, in particular Tregs, has been suggested as an important feature of pre-conditioning before ACT. Pre-clinically, a single treatment with a low dose of doxorubicin or paclitaxel was found to reduce the amount of Tregs and increase the amount of adoptively transferred CD8+ T cells in EG.7-OVA tumors, compared to tumors of mice treated only with chemotherapy or ACT. In this study, it was also found that the frequency of myeloid derived suppressor cells (MDSCs), that can inhibit tumor-reactive T cells through secretion of anti-inflammatory cytokines and amino acid depletion, decreased in the combination treatment groups (85). In a clinical study with metastatic melanoma patients, pre-conditioning with non-myeloablative chemotherapy before adoptive transfer of TILs was likewise shown to decrease the frequency of peripheral CD4+ FoxP3+ Tregs, which in turn correlated with an improved response to the ACT (86). Another proposed mechanism for enhanced ACT efficacy after pre-conditioning is an increased availability of homeostatic cytokines for the infused T cells (87). Under normal physiological circumstances, IL-7, IL-15, and IL-21 exert a supportive role for endogenous T cells because they stimulate homeostatic proliferation. Lymphodepletion, as a result of pre-conditioning, results in a decrease in the endogenous T cell population, which in turn increases the availability of IL-7, IL-15, and IL-21 to support proliferation of adoptively transferred T cells (81).

Enhanced functionality of APCs, in particular DCs, is also believed to play an important role in mediating the enhanced anti-tumor reactivity of adoptively transferred T cells following pre-conditioning (88–90). A pre-clinical study demonstrated that pre-conditioning with CPX enhanced the proliferative capacity of bone marrow-derived DC precursors (91). Compared to untreated control mice, bone marrow harvested from CPX-treated mice generated higher numbers of DCs with the ability to become activated in response to TLR stimulation and prime T cells *in vitro*. These results were in line with previous findings demonstrating that lymphodepletion with a single dose of CPX induced expansion of immature DCs that could be detected in the peripheral blood 8–16 days post treatment (92). Pre-conditioning with CPX followed by a DC based vaccine has also been found to enhance the anti-tumor response in murine hosts, even in the absence of ACT (93), suggesting that CPX stimulates priming of endogenous T cells. Another proposed mechanism, behind the enhanced DC function following pre-conditioning, is induction of immunogenic cancer cell death, which is a result of the anti-proliferative and cytotoxic effects of chemotherapy or ionizing radiation (94–96). Immunogenic cell death involves exposure of several plasma membrane markers that enhances DC functions, e.g., HSP70 and calreticulin that stimulates cross-presentation of tumor derived antigens and phagocytosis, repectively (97). In response to plasma membrane markers associated with immunogenic cell death, DCs become activated and release cytokines, which supports the process of creating a pro-inflammatory environment for T cell priming and activation (98). Immunogenic cell death is also a determining factor for antigen trafficking and presentation by DCs in the tdLN (99). In particular RT is known to induce immunogenic cell death and is therefore a potent DC stimulator. RT also influences APCs directly by inducing cell-intrinsic changes that affect the activation status. This was demonstrated in a study where a single high dose of local RT promoted the activation and functional maturation of a human antigen-presenting cell line through intrinsic DNA damage and p53 activation (100). Also a RT-dependent release of Type I IFNs has been found to be an important contributor to activation of tumor infiltrating innate immune cells, including DCs (101). On the contrary, RT might increase the secretion of TGF-β, which in turn can inhibit the activation and maturation of DCs, and pre-clinical studies have shown that TGF-β blockade enhances the efficacy of RT (102, 103). Negative effects on APCs and consequently the anti-tumor immunity have however also been reported as an effect of RT. In a pre-clinical study, a single dose of RT was found to cause a significant decrease in the amount of CD8+ DCs in murine spleens, which correlated with a switch from a Th1 to a Th2 T cell response (104). In the same study, an analysis of blood samples from RT-treated patients revealed a significant decrease in the frequency of circulating BDCA3+ DCs. Evidently, RT can affect APC function and consequently the anti-tumor immunity in different ways. The main outcome does however seem to be

mostly favorable for supporting anti-tumor T cell priming and pre-conditioning using RT or chemotherapy remains to be a well-established therapeutic strategy that enhances the efficacy of ACT.

Vaccination

Pre-clinical and clinical studies have demonstrated that the *in vivo* expansion, persistence and poly-functionality of infused T cells can be enhanced by providing post-transfer vaccination. Vaccination can facilitate post-infusion priming of adoptively transferred T cells, which stimulates the expansion and functionality and enhances the tumor-reactivity. Clinical trials combining ACT and post-infusion vaccination with viral or tumor antigens are in early stages and with a primary focus on evaluating safety and applicability but encouraging findings have been reported.

Several strategies for enhancing the post-infusion effect of adoptively transferred T cells by vaccination have been explored. One of these is to exploit the ability of viral antigens to stimulate potent T cell activation and expansion, as well as promoting central memory formation. A recent study demonstrated that vaccination with Epstein Barr Virus (EBV) antigen improved the persistence of CD19 CAR T cells modified to recognize EBV in relapsed pediatric acute lymphoblastic leukemia patients (105). In this study, donor Epstein–Barr virus (EBV)-specific cytotoxic T-cells were genetically modified to express a CD19CAR to enhance the long-term persistence of the transferred T cells but also to facilitate a more physiologically relevant expansion of the CARs and avoid cytokine mediated toxicities. An initial patient cohort treated only with the EBV CD19CARs showed poor post-infusion persistence and expansion, but EVB CD19CARs combined with post-infusion EBV vaccination showed enhanced persistence without induction of cytokine release syndrome, neurotoxicity or graft vs. host disease. Another study evaluated the effects of combining a DC-based vaccine with cytomegalovirus (CMV) antigens and CMV-specific T cell transfer in glioblastoma patients (106). CMV-antigens have previously been found to be expressed by GBM which in this study was leveraged to enhance the expansion and persistence of adoptively transferred CMV pp65-specific T cells. For this study, autologous DCs were transfected with CMV pp65 mRNA and infused following adoptive T cell transfer. The results showed that DC vaccination with the CMV pp65 mRNA gave an increase in the frequency of polyfunctional CMV pp65-specific CD8+ T cells with simultaneous expression of IFN-γ and TNF-α. This increase in polyfunctional antigen-specific T cells correlated with an improved overall survival.

Stimulating TAA-specific adoptively transferred T cells with post-infusion TAA vaccination has also shown promising results in pre-clinical and clinical trials. Recently, a pre-clinical study found that the persistence and activity of infused CAR-T cells could be enhanced by a tumor antigen vaccination (107). Results from this study showed that the CAR-T cells could undergo post-infusion priming in lymphoid organs which triggered extensive expansion and enhanced anti-tumor efficacy. These results were in line with findings from a previous study demonstrating that a DC-based tumor antigen vaccination significantly enhanced the proliferation, cytokine production and tumor infiltration of infused T cells (108).

Other clinical trials have reported encouraging results related to the objective clinical response of cancer patients treated with the ACT and post-infusion TAA vaccination. In line with these findings, a clinical phase II trial reported an improved 5 year recurrence-free and prolonged overall survival of patients with invasive hepatocellular carcinoma who received a post-operative DC based vaccine combined with ACT (109). This treatment was based on autologous tumor lysate pulsed DCs and transfer of activated T cells.

Recent research has provided evidence of the existence of so-called "anti-regulatory T cells" that recognize immunosuppressive molecules (110, 111). Studies have shown that both human cancer patients and healthy individuals have CD8+ and CD4+ T cells that can respond to factors associated with immune suppression, such as PD-L1 (112), arginase-1 (113), arginase-2 (114), and IDO (115, 116). The existence of anti-regulatory T cells represents an interesting potential of vaccinating against immune suppressive subsets that express these immunomodulatory molecules, e.g., M2 macrophages, MDSCs, and Tregs. Accordingly, an interesting study showed that the immunogenicity of a DC-based vaccine against p53 could be enhanced by co-stimulation with a PD-L1 derived epitope (117). This could potentially be one mechanism to counter-act the inflammation-induced suppressive mechanisms that can counter-act the anti-tumor effects of T cells.

The ability to combine ACT with vaccination, either with viral antigens or TAAs, represents an interesting approach to enhance the efficacy of ACT. The persistence of infused T cells have been linked to therapeutic efficacy (118, 119) and because post-transfer vaccination has been shown to enhance the persistence of infused T cells, future studies should further explore the concept of enhancing ACT with post-infusion vaccination.

TLR Stimulation

A well-established way to activate DCs is by stimulation with TLR agonists. TLRs are a type of pattern recognition receptors (PRRs) that comprise a group of endosomal and plasma-membrane associated proteins expressed on DCs and other innate immune cells, such as macrophages (120). TLRs are conventionally used as vaccine adjuvants (121) and when DCs or macrophages are stimulated through TLRs, a process of activation and maturation is initiated which results in secretion of T cell activating cytokines such as TNF-α, IL-6, IL-12, and type I IFNs (122). To this date, three TLR agonists have been approved by US regulatory agencies to treat cancer patients; (1) Imiquimod, a TLR7 agonist used to treat superficial basal cell carcinoma, (2) Bacillus Calmette-Guérin (BCG), supposedly stimulating TL2, TLR3, and TLR9, used to treat non-invasive transitional cell carcinoma of the bladder, and (3) monophosphoryl lipid A (MPL) stimulating TLR4 and used in a prophylactic vaccine against HPV-virus (123).

TLR stimulation can be used in combination with tumor antigen delivery to ensure activation of antigen presenting DCs. TLR stimulation can however also be used as an adjuvant

treatment to other cancer therapies that induce tumor antigen release, such as RT. The combination of TLR stimulation and RT has been explored in pre-clinical studies with encouraging results. A study reported that intravenous administration of the TLR7 agonist resiquimod (R848) in combination with RT lead to clearance of established tumors in murine lymphoma models (124). The treatment effect was associated with expansion of tumor-antigen specific CD8+ cells and improved survival of the treated mice. These results were in line with findings from other pre-clinical studies demonstrating that TLR7/8 agonists can be potent adjuvants to RT by boosting antigen-presentation by DCs in subcutaneous and orthotopic mouse models of colorectal and pancreatic cancer (125). Similarly, systemic administration of a TLR7 agonist in combination with RT has been shown to prime a tumor-reactive CD8+ T cell response and result in improved survival in syngeneic models of colorectal carcinoma and fibrosarcoma (126). The combination of RT and TLR stimulation is interesting because the RT-induced availability of tumor antigens at the tumor site can be exploited to stimulate an endogenous tumor response. RT acts directly on cancer cells and introduce DNA damage that, if left unrepaired, results in cell death (95, 96). This can stimulate an anti-tumor T cell response, when APCs engulf (parts of) dying cancer cells for subsequent T cell priming. In this setting, TLR stimulation can feed into the circle of events and boost activation and antigen-presentation of DCs that enhances the T cell priming.

To the best of our knowledge, no clinical trials evaluating the effect of enhancing ACT efficacy by TLR stimulation have so far been completed. Pre-clinical studies have however described the use of TLR stimulation to augment ACT with encouraging results. A recent study reported that the administration of the TLR4 agonist Lipopolysaccharid (LPS) could augment the tumor-reactivity of adoptively transferred pmel-1 CD8+ T cells in mice with established B16.F10 tumors (127). Administration of MPL and the TLR9 agonist CpG ODN likewise potentiated the anti-tumor activity of infused CD8+ T cells. These results were in line with findings from a previous study demonstrating that TLR3 stimulation and a tumor antigen vaccination increased the expansion and anti-tumor efficacy of adoptively transferred antigen-specific pmel-1 CD8+ T cells in pre-conditioned B16.F10 tumor-bearing mice (92).

Although TLR agonists are effective vaccine adjuvants, the overall beneficial effect of TLR stimulation as cancer immunotherapy is debated. The concept is complicated by the fact that TLRs are not only expressed by immune cells but also by cancer cells (128) and TLR expression by cancer cells has been linked to metastasis in breast cancer (129) and esophageal squamous cell carcinoma (130). Accordingly, the reported effects of TLR treatment as a cancer immunotherapy have been mixed (123, 131), reflecting issues with toxicity and supposedly the complexity of TLR expression in the tumor microenvironment. Therefore, additional research is needed to further elucidate the effect of TLR stimulation as a cancer immunotherapy and current issues related to safety and administration of TLR agonists have to be resolved.

STING Agonists

Given the importance of type I IFNs in cancer immunity, efforts have been put into identifying pathways that are responsible for or linked to secretion of type I IFNs. Recent findings have pointed toward a crucial role for the STING pathway in this process (132). STING is an adapter molecule that becomes activated by cyclic dinucleotides generated by cyclic GMP-AMP synthase, which in turn is activated by cytosolic DNA. Activated STING phosphorylates interferon regulatory factor 3 (IRF3) that directly contributes to type I IFN gene transcription (133). One study found that spontaneous tumor-reactive CD8+ T cell priming was defective in STING$^{-/-}$ mice and that STING pathway activation and IFN-β production correlated with DNA detection in tumor infiltrating DCs (134). The STING pathway therefore appears to be involved in detecting the presence of a tumor to drive DC activation and subsequent T cell priming against tumor associated antigens.

STING agonists have been shown to have therapeutic implications for stimulating anti-tumor T cell reactivity. Pre-clinical studies have described that treatment with STING agonists can induce an increase in the abundance and functionality of tumor-infiltrating cytotoxic T cells associated with tumor regression (135–137) and STING stimulation has also been shown to antagonize expansion of immune suppressive myeloid derived suppressor cells (138). Interestingly, a pre-clinical study recently demonstrated that co-delivery of a STING agonist and CAR-T cells resulted in elimination of tumor cells that were not recognized by adoptively transferred CAR-T cells as monotherapy (139). The combined delivery of a STING agonist and CAR-T cells resulted in a synergistic activation of APCs and was associated with prolonged survival and protection against tumor escape. These results indicate that STING activation might enhance the effect of CAR-T cell therapy by broadening the tumor-reactive T cell response.

Given the ability of STING to stimulate priming of tumor-reactive T cells through DC activation, it is likely that STING activation can enhance epitope spreading when combined with ACT. The combination of STING and checkpoint inhibitors is being tested in clinical settings and has been shown to enhance the therapeutic response to chemotherapy in patients with ovarian cancer (140). A study done in a pre-clinical model of head and neck cancer also demonstrated that the combined treatment of STING and PD-1 blockade could enhance local and systemic immunity and reverse adaptive resistance to chemotherapy (141). The ability to (re)establish tumor immunity using STING and checkpoint inhibition indicates that STING activation can expand pre-existing tumor reactivity, perhaps by broadening the tumor response. STING activation could thereby support the therapeutic efficacy of adoptively transferred T cells by activating APCs that in turn can cross-prime endogenous tumor-reactive T cells.

CD40 Stimulation

Another well-established mechanism, which is implicated in priming of tumor-reactive T cells, is engagement of the CD40/CD40L axis. CD40 is a member of the Tumor necrosis factor (TNF) receptor family and is expressed by a range of

different cell types including DCs, B cells, platelets and non-hematopoietic cells such as endothelial cells, fibroblasts and some types of cancer cells (142). Ligation of CD40 on DCs has been found to upregulate the expression of co-stimulatory molecules (e.g., CD80 and CD86) and MHC molecules, induce secretion of pro-inflammatory cytokines and enhancing the antigen processing machinery (143). Stimulation with CD40 agonists has been shown to stimulate the T cell priming abilities of DCs and lead to potent anti-tumor T cell immunity in pre-clinical models. Early mechanistic studies also demonstrated that CD40 stimulation can enhance the efficacy of tumor antigen vaccination (144, 145), induce activation of endogenous CD4+ T cells (144) and reverse cytotoxic T cell tolerance (145). Interestingly, pre-clinical studies indicate that activated CD8+ T cells are able to boost IL-12 production by DCs through expression of CD40L. Consequently, this could provide a positive feedback loop for adoptively transferred T cells through the engagement of DCs (146).

The ability of CD40 stimulation to enhance the efficacy of ACT has been evaluated in different pre-clinical models. Recently, a study showed that lymphodepleting WBI in combination with CD40 stimulation enhanced the accumulation of infused T cells in a murine pancreatic tumor model (147). Here it was demonstrated that the combination of CD40 stimulation, WBI and ACT enhanced the proliferation of infused T cells, promoted high levels of tumor inflammation and was associated with tumor regression and prolonged survival of treated mice. These findings were in line with observations from a previous study, where CD40 stimulation was shown to boost the anti-tumor activity of ACT in murine B16.F10 tumors (148). Here, a monoclonal antibody targeting CD40 was combined with ACT and administration of IL-2. This combination improved the expansion of the infused T cells and was associated with tumor regression. The results also showed that the T cell expansion was dependent on IL-12 and expression of CD80 and CD86 by endogenous DCs.

The use of CD40 agonists has also been tested as cancer immunotherapy in clinical settings. A paper recently summarized the long-term outcomes of a phase I study of agonistic CD40 antibody and CTLA-4 treatment of metastatic melanoma patients (149). Here it was found that the therapy was associated with increased tumor T cell infiltration, T cell reinvigoration and T cell clonal expansion. The positive effects of CD40 stimulation on T cell priming can however not necessarily be attributed to DC stimulation alone. Co-stimulatory signaling through CD40/CD40L interaction influences not only DCs but also macrophages and in particular B cells. CD40 stimulation promotes the survival and expansion of B cells and supports their development into antibody-secreting plasma cells and memory B cells. CD40 stimulated B cells also undergo somatic hyper-mutation of the Ig, which gives and enhanced antigen-affinity (150). Importantly, since B cells can also function as APCs, it is possible that the enhanced T cell functions as a result of CD40 stimulation can be attributed to the effects of both activated B cells and DCs. Collectively, findings from pre-clinical and clinical studies indicate that CD40 agonists, via the ability of CD40 stimulation to enhance APC functions and T cell priming, could be a feasible adjuvant therapy to ACT.

DISCUSSION

The post-infusion performance of adoptively transferred T cells is critically dependent on several factors, in particular the composition of the TME that can favor or suppress the tumor-reactivity of the T cells. Studies have also linked the post-infusion performance to the differentiation status of the adoptively transferred T cells, with less differentiated T cells, such as naïve or stem cell memory T cells, having greater capacity for expansion and persistence after transfer. The T cells used for ACT typically have a more differentiated effector T cell phenotype at the time of infusion, because the *in vitro* expansion step of the process involves activating and stimulating T cell proliferation to reach a large number of cells. This activation and stimulation of T cells induce a stepwise differentiation process, which ultimately leads to generation of T cells with a terminally differentiated and short-lived effector phenotype that is suboptimal for ACT (151). Because T cells with a less differentiated phenotype have greater post-infusion expansion and persistence potential (10, 12), efforts are being put into designing strategies to maintain the less differentiated phenotype of T cells used for ACT. These strategies include optimizing the T cell culture conditions to preserve a less differentiated phenotype during expansion. This can be done e.g., by adding specific (combinations of) cytokines (152, 153), small molecule inhibitors (154, 155) or co-stimulatory molecules (156, 157) to the culture medium. Another strategy is to generate antigen-specific T cells that are induced from pluripotent stem cells (158, 159). The less differentiated T cells are however critically dependent on post-infusion priming with their cognate antigen to have any tumor-reactivity, which can be provided through endogenous DC stimulation. Therefore, if T cells with e.g., a stem cell memory phenotype are being used for ACT, it could be favorable to combine the T cell infusion with post-infusion vaccination with the cognate antigen of the T cells. If T cells with a more differentiated phenotype, such as effector memory, are being infused, the secretion of pro-inflammatory cytokines might be sufficient for enhancing the post-infusion expansion and persistence. When choosing the optimal add-on therapy to ACT, it is therefore important to take into consideration the differentiation status of the infused T cells.

In addition to the examples given above, another emerging strategy is to modify the T cell product prior to infusion, thereby "arming" the T cells with the ability to engage endogenous DCs. Recent pre-clinical studies have investigated ACT with genetically modified T cells expressing membrane-anchored IL-12 (160), which is known to increase co-stimulation by dendritic cells. In addition, T cells engineered to express the DC-recruiting cytokine FLT3L, was recently shown to enhance efficacy and support epitope spreading after ACT therapy (161). With the advancements made within engineering of T cells for ACT, it is feasible to include the DC-priming strategy—not only as an add-on treatment, but also as an intrinsic property of the transferred T cells.

CONCLUDING REMARKS

The concept of ACT has been manifested as a promising therapeutic option for a subgroup of patients with melanoma and hematological malignancies. To further improve the therapeutic efficacy of ACT, and to broaden the application to other types of solid cancers, it is necessary to expand our knowledge on factors that can enhance the post-infusion persistence and functionality of transferred T cells. Engagement of DCs, as an adjuvant therapy to ACT, can stimulate a broader tumor-reactive response by priming endogenous T cells and facilitate post-infusion priming of adoptively transferred T cells. Accordingly, the combination of ACT and DC-activating treatments such as TLR or STING agonists, as well as CD40 stimulation and vaccination with viral or tumor antigens, has been found to have implications for the *in vivo* expansion, persistence and polyfunctionality of infused T cells. Engagement of activated DCs alongside ACT has also been associated with improved tumor control and prolonged survival in pre-clinical models. The addition of checkpoint blockade alongside ACT and DC stimulation can be utilized to counteract an eventual inactivation of tumor-reactive T cells and might provide an additional synergistic effect. The combination of ACT, treatments that activates and/or induces antigen presentation of DCs and checkpoint blockade therefore represents an interesting therapeutic strategy that potentially can enhance the efficacy and broaden the applicability of ACT in the future.

AUTHOR CONTRIBUTIONS

MH and DJ did the literature search and wrote the review. TA and MA revised and approved the final version of the review. All authors contributed to the article and approved the submitted version.

FUNDING

During the writing of this review, DJ and MH have been employed with funding received from the Independent Research Fund Denmark and Herlev Hospital. The funders were not involved in the compilation of the review.

REFERENCES

1. Chen DS, Mellman I. Oncology meets immunology: the cancer-immunity cycle. *Immunity*. (2013) 39:1–10. doi: 10.1016/j.immuni.2013.07.012
2. Met Ö, Jensen KM, Chamberlain CA, Donia M, Svane IM. Principles of adoptive T cell therapy in cancer. *Semin Immunopathol.* (2019) 41:49–58. doi: 10.1007/s00281-018-0703-z
3. Rosenberg SA, Spiess P, Lafreniere R. A new approach to the adoptive immunotherapy of cancer with tumor-infiltrating lymphocytes. *Science.* (1986) 233:1318–21. doi: 10.1126/science.3489291
4. Boon T, van der Bruggen P. Human tumor antigens recognized by T lymphocytes. *J Exp Med.* (1996) 183:725–9. doi: 10.1084/jem.183.3.725
5. Kershaw MH, Westwood JA, Darcy PK. Gene-engineered T cells for cancer therapy. *Nat Rev Cancer*. (2013) 13:525–41. doi: 10.1038/nrc3565
6. Rosenberg SA, Yang JC, Sherry RM, Kammula US, Hughes MS, Phan GQ, et al. Durable complete responses in heavily pretreated patients with metastatic melanoma using T-cell transfer immunotherapy. *Clin Cancer Res.* (2011) 17:4550–7. doi: 10.1158/1078-0432.CCR-11-0116
7. Besser MJ, Shapira-Frommer R, Treves AJ, Zippel D, Itzhaki O, Hershkovitz L, et al. Clinical responses in a phase II study using adoptive transfer of short-term cultured tumor infiltration lymphocytes in metastatic melanoma patients. *Clin Cancer Res.* (2010) 16:2646–55. doi: 10.1158/1078-0432.CCR-10-0041
8. Park JH, Geyer MB, Brentjens RJ. CD19-targeted CAR T-cell therapeutics for hematologic malignancies: interpreting clinical outcomes to date. *Blood.* (2016) 127:3312–20. doi: 10.1182/blood-2016-02-629063
9. Maude SL, Laetsch TW, Buechner J, Rives S, Boyer M, Bittencourt H, et al. Tisagenlecleucel in children and young adults with B-Cell lymphoblastic leukemia. *N Engl J Med.* (2018) 378:439–48. doi: 10.1056/NEJMoa1709866
10. Zhou J, Shen X, Huang J, Hodes RJ, Rosenberg SA, Robbins PF. Telomere length of transferred lymphocytes correlates with *in vivo* persistence and tumor regression in melanoma patients receiving cell transfer therapy. *J Immunol.* (2005) 175:7046–52. doi: 10.4049/jimmunol.175.10.7046
11. Hinrichs CS, Borman ZA, Cassard L, Gattinoni L, Spolski R, Yu Z, et al. Adoptively transferred effector cells derived from naive rather than central memory CD8+ T cells mediate superior antitumor immunity. *Proc Natl Acad Sci USA.* (2009) 106:17469–74. doi: 10.1073/pnas.0907448106
12. Klebanoff CA, Gattinoni L, Torabi-Parizi P, Kerstann K, Cardones AR, Finkelstein SE, et al. Central memory self/tumor-reactive CD8+ T cells confer superior antitumor immunity compared with effector memory T cells. *Proc Natl Acad Sci USA.* (2005) 102:9571–6. doi: 10.1073/pnas.0503726102
13. McDonnell AM, Currie AJ, Brown M, Kania K, Wylie B, Cleaver A, et al. Tumor cells, rather than dendritic cells, deliver antigen to the lymph node for cross-presentation. *Oncoimmunology.* (2012) 1:840–6. doi: 10.4161/onci.20493
14. Marzo AL, Lake RA, Lo D, Sherman L, McWilliam A, Nelson D, et al. Tumor antigens are constitutively presented in the draining lymph nodes. *J Immunol.* (1999) 162:5838–45.
15. Munn DH, Mellor AL. The tumor-draining lymph node as an immune-privileged site. *Immunol Rev.* (2006) 213:146–58. doi: 10.1111/j.1600-065X.2006.00444.x
16. Khong HT, Nicholas Restifo P. Natural selection of tumor variants in the generation of "tumor escape" phenotypes. *Nat Immunol.* (2006) 3:999–1005. doi: 10.1038/ni1102-999
17. Sharma P, Hu-Lieskovan S, Wargo JA, Ribas A. Primary, adaptive, and acquired resistance to cancer immunotherapy. *Cell.* (2017) 168:707–23. doi: 10.1016/j.cell.2017.01.017
18. Olson BM, McNeel DG. Antigen loss and tumor-mediated immunosuppression facilitate tumor recurrence. *Expert Rev Vaccines.* (2012) 11:1315–7. doi: 10.1586/erv.12.107
19. Brown CE, Mackall CL. CAR T cell therapy: inroads to response and resistance. *Nat Rev Immunol.* (2019) 19:73–4. doi: 10.1038/s41577-018-0119-y
20. Gardner R, Wu D, Cherian S, Fang M, Hanafi LA, Finney O, et al. Acquisition of a CD19-negative myeloid phenotype allows immune escape of MLL-rearranged B-ALL from CD19 CAR-T-cell therapy. *Blood.* (2016) 127:2406–10. doi: 10.1182/blood-2015-08-665547
21. Verdegaal EME, de Miranda NFCC, Visser M, Harryvan T, van Buuren MM, Andersen RS, et al. Neoantigen landscape dynamics during human melanoma–T cell interactions. *Nature.* (2016) 536:91–5. doi: 10.1038/nature18945
22. Pilon SA, Kelly C, Wei W-Z. Broadening of epitope recognition during immune rejection of ErbB-2-positive tumor prevents growth of ErbB-2-negative tumor. *J Immunol.* (2003) 170:1202–8. doi: 10.4049/jimmunol.170.3.1202
23. Heckler M, Dougan SK. Unmasking pancreatic cancer: epitope spreading after single antigen chimeric antigen receptor T-cell therapy in a human phase I trial. *Gastroenterology.* (2018) 155:11–4. doi: 10.1053/j.gastro.2018.06.023
24. Walsh SR, Lichty BD, Wan Y. Endogenous T cells prevent tumor immune escape following adoptive T cell therapy. *J Clin Invest.* (2019) 129:5400–10. doi: 10.1172/JCI126199

25. Johnson LA, Sanchez-Perez L, Suryadevara CM, Sampson JH. Chimeric antigen receptor engineered T cells can eliminate brain tumors and initiate long-term protection against recurrence. *Oncoimmunology*. (2014) 3:e944059. doi: 10.4161/21624011.2014.944059
26. Pardoll DM. The blockade of immune checkpoints in cancer immunotherapy. *Nat Rev Cancer*. (2012) 12:252–64. doi: 10.1038/nrc3239
27. Costa R, Carneiro BA, Agulnik M, Rademaker AW, Pai SG, Villaflor VM, et al. Toxicity profile of approved anti-PD-1 monoclonal antibodies in solid tumors: a systematic review and meta-analysis of randomized clinical trials. *Oncotarget*. (2017) 8:8910–20. doi: 10.18632/oncotarget.13315
28. Guo ZS. The 2018 Nobel Prize in medicine goes to cancer immunotherapy (editorial for BMC cancer). *BMC Cancer*. (2018) 18:1086. doi: 10.1186/s12885-018-5020-3
29. Huard B, Prigent P, Tournier M, Bruniquel D, Triebel F. CD4/major histocompatibility complex class II interaction analyzed with CD4- and lymphocyte activation gene-3 (LAG-3)-Ig fusion proteins. *Eur J Immunol.* (1995) 25:2718–21. doi: 10.1002/eji.1830250949
30. Camisaschi C, Casati C, Rini F, Perego M, De Filippo A, Triebel F, et al. LAG-3 expression defines a subset of CD4 + CD25 high Foxp3 + regulatory T cells that are expanded at tumor sites. *J Immunol.* (2010) 184:6545–51. doi: 10.4049/jimmunol.0903879
31. Matsuzaki J, Gnjatic S, Mhawech-Fauceglia P, Beck A, Miller A, Tsuji T, et al. Tumor-infiltrating NY-ESO-1-specific CD8+ T cells are negatively regulated by LAG-3 and PD-1 in human ovarian cancer. *Proc Natl Acad Sci USA*. (2010) 107:7875–80. doi: 10.1073/pnas.1003345107
32. Grosso JF, Kelleher CC, Harris TJ, Maris CH, Hipkiss EL, De Marzo A, et al. LAG-3 regulates CD8+ T cell accumulation and effector function in murine self- and tumor-tolerance systems. *J Clin Invest*. (2007) 117:3383–92. doi: 10.1172/JCI31184
33. Yu X, Harden K, Gonzalez LC, Francesco M, Chiang E, Irving B, et al. The surface protein TIGIT suppresses T cell activation by promoting the generation of mature immunoregulatory dendritic cells. *Nat Immunol.* (2009) 10:48–57. doi: 10.1038/ni.1674
34. Joller N, Hafler JP, Brynedal B, Kassam N, Spoerl S, Levin SD, et al. Cutting edge: TIGIT has T cell-intrinsic inhibitory functions. *J Immunol.* (2011) 186:1338–42. doi: 10.4049/jimmunol.1003081
35. Joller N, Lozano E, Burkett PR, Patel B, Xiao S, Zhu C, et al. Treg cells expressing the coinhibitory molecule TIGIT selectively inhibit proinflammatory Th1 and Th17 cell responses. *Immunity*. (2014) 40:569–81. doi: 10.1016/j.immuni.2014.02.012
36. Chauvin JM, Pagliano O, Fourcade J, Sun Z, Wang H, Sander C, et al. TIGIT and PD-1 impair tumor antigen-specific CD8+ T cells in melanoma patients. *J Clin Invest.* (2015) 125:2046–58. doi: 10.1172/JCI80445
37. Kurtulus S, Sakuishi K, Ngiow SF, Joller N, Tan DJ, Teng MWL, et al. TIGIT predominantly regulates the immune response via regulatory T cells. *J Clin Invest.* (2015) 125:4053–62. doi: 10.1172/JCI81187
38. Stephen Hodi F, O'Day SJ, McDermott DF, Weber RW, Sosman JA, Haanen JB, et al. Improved survival with ipilimumab in patients with metastatic melanoma. *N Engl J Med.* (2010) 8:711–34. doi: 10.1056/NEJMoa1003466
39. Robert C, Thomas L, Bondarenko I, O'Day S, Weber J, Garbe C, et al. Ipilimumab plus dacarbazine for previously untreated metastatic melanoma. *N Engl J Med.* (2011) 364:2517–26. doi: 10.1056/NEJMoa1104621
40. Robert C, Long GV, Brady B, Dutriaux C, Maio M, Mortier L, et al. Nivolumab in previously untreated melanoma without BRAF mutation. *N Engl J Med.* (2015) 372:320–30. doi: 10.1056/NEJMoa1412082
41. Shi LZ, Goswami S, Fu T, Guan B, Chen J, Xiong L, et al. Blockade of CTLA-4 and PD-1 enhances adoptive t-cell therapy efficacy in an ICOS-mediated manner. *Cancer Immunol Res.* (2019) 7:1803–12. doi: 10.1158/2326-6066.CIR-18-0873
42. Fiegle E, Doleschel D, Koletnik S, Rix A, Weiskirchen R, Borkham-Kamphorst E, et al. Dual CTLA-4 and PD-L1 blockade inhibits tumor growth and liver metastasis in a highly aggressive orthotopic mouse model of colon cancer. *Neoplasia*. (2019) 21:932–44. doi: 10.1016/j.neo.2019.07.006
43. Seidel JA, Otsuka A, Kabashima K. Anti-PD-1 and anti-CTLA-4 therapies in cancer: mechanisms of action, efficacy, and limitations. *Front Oncol.* (2018) 8:86. doi: 10.3389/fonc.2018.00086
44. Thibaut R, Bost P, Milo I, Cazaux M, Lemaître F, Garcia Z, et al. Bystander IFN-γ activity promotes widespread and sustained cytokine signaling altering the tumor microenvironment. *Nat Cancer*. (2020) 1:302–14. doi: 10.1038/s43018-020-0038-2
45. Benci JL, Xu B, Qiu Y, Wu TJ, Dada H, Twyman-Saint Victor C, et al. Tumor interferon signaling regulates a multigenic resistance program to immune checkpoint blockade. *Cell*. (2016) 167:1540–54. doi: 10.1016/j.cell.2016.11.022
46. Shimizu K, Iyoda T, Okada M, Yamasaki S, Fujii SI. Immune suppression and reversal of the suppressive tumor microenvironment. *Int Immunol.* (2018) 30:445–55. doi: 10.1093/intimm/dxy042
47. Pfirschke C, Siwicki M, Liao HW, Pittet MJ. Tumor microenvironment: no effector t cells without dendritic cells. *Cancer Cell*. (2017) 31:614–5. doi: 10.1016/j.ccell.2017.04.007
48. Probst HC, McCoy K, Okazaki T, Honjo T, Van Den Broek M. Resting dendritic cells induce peripheral CD8+ T cell tolerance through PD-1 and CTLA-4. *Nat Immunol.* (2005) 6:280–6. doi: 10.1038/ni1165
49. Darrasse-Jèze G, Deroubaix S, Mouquet H, Victora GD, Eisenreich T, Yao K, et al. Feedback control of regulatory T cell homeostasis by dendritic cells *in vivo*. *J Exp Med*. (2009) 206:1853–62. doi: 10.1084/jem.20090746
50. Jonuleit H, Schmitt E, Schuler G, Knop J, Enk AH. Induction of interleukin 10–producing, nonproliferating CD4 + T cells with regulatory properties by repetitive stimulation with allogeneic immature human dendritic cells. *J Exp Med.* (2000) 192:1213–22. doi: 10.1084/jem.192.9.1213
51. Clausen BE, Girard-Madoux MJH. IL-10 control of dendritic cells in the skin. *Oncoimmunology*. (2013) 2:8–10. doi: 10.4161/onci.23186
52. Reis E Sousa C. Activation of dendritic cells: translating innate into adaptive immunity. *Curr Opin Immunol.* (2004) 16:21–5. doi: 10.1016/j.coi.2003.11.007
53. Nair-Gupta P, Baccarini A, Tung N, Seyffer F, Florey O, Huang Y, et al. TLR signals induce phagosomal MHC-I delivery from the endosomal recycling compartment to allow cross-presentation. *Cell*. (2014) 158:506–21. doi: 10.1016/j.cell.2014.04.054
54. McLellan AD, Starling GC, Williams LA, Hock BD, Hart DNJ. Activation of human peripheral blood dendritic cells induces the CD86 co-stimulatory molecule. *Eur J Immunol.* (1995) 25:2064–8. doi: 10.1002/eji.1830250739
55. Wenzel J, Uerlich M, Haller O, Bieber T, Tueting T. Enhanced type I interferon signaling and recruitment of chemokine receptor CXCR3-expressing lymphocytes into the skin following treatment with the TLR7-agonist imiquimod. *J Cutan Pathol.* (2005) 32:257–62. doi: 10.1111/j.0303-6987.2005.00297.x
56. Waisman A, Lukas D, Clausen BE, Yogev N. Dendritic cells as gatekeepers of tolerance. *Semin Immunopathol.* (2017) 39:153–63. doi: 10.1007/s00281-016-0583-z
57. Shortman K, Naik SH. Steady-state and inflammatory dendritic-cell development. *Nat Rev Immunol.* (2007) 7:19–30. doi: 10.1038/nri1996
58. Villadangos JA, Schnorrer P. Intrinsic and cooperative antigen-presenting functions of dendritic-cell subsets *in vivo*. *Nat Rev Immunol.* (2007) 7:543–55. doi: 10.1038/nri2103
59. Huang SW, Chang SH, Mu SW, Jiang HY, Wang ST, Kao JK, et al. Imiquimod activates p53-dependent apoptosis in a human basal cell carcinoma cell line. *J Dermatol Sci.* (2016) 81:182–91. doi: 10.1016/j.jdermsci.2015.12.011
60. Eisenbarth SC. Dendritic cell subsets in T cell programming: location dictates function. *Nat Rev Immunol.* (2019) 19:89–103. doi: 10.1038/s41577-018-0088-1
61. Böttcher JP, Reis e Sousa C. The role of type 1 conventional dendritic cells in cancer immunity. *Trends Cancer*. (2018) 4:784–92. doi: 10.1016/j.trecan.2018.09.001
62. Cance JC, Crozat K, Dalod M, Mattiuz R. Are conventional type 1 dendritic cells critical for protective antitomor immunity and how? *Front Immunol.* (2019) 10:9. doi: 10.3389/fimmu.2019.00009
63. Spranger S, Dai D, Horton B, Gajewski TF. Tumor-residing Batf3 dendritic cells are required for effector T cell trafficking and adoptive T cell therapy. *Cancer Cell*. (2017) 31:711–23. doi: 10.1016/j.ccell.2017.04.003
64. Roberts EW, Broz ML, Binnewies M, Headley MB, Nelson AE, Wolf DM, et al. Critical role for CD103+/CD141+ dendritic cells bearing CCR7 for tumor antigen trafficking and priming of T cell immunity in melanoma. *Cancer Cell*. (2016) 30:324–36. doi: 10.1016/j.ccell.2016.06.003
65. Clatworthy MR, Aronin CEP, Mathews RJ, Morgan NY, Smith KGC, Germain RN. Immune complexes stimulate CCR7-dependent

dendritic cell migration to lymph nodes. *Nat Med.* (2014) 20:1458–63. doi: 10.1038/nm.3709
66. Fitzgerald-Bocarsly P, Dai J, Singh S. Plasmacytoid dendritic cells and type I IFN: 50 years of convergent history. *Cytokine Growth Factor Rev.* (2008) 19:3–19. doi: 10.1016/j.cytogfr.2007.10.006
67. Villadangos JA, Young L. Antigen-presentation properties of plasmacytoid dendritic cells. *Immunity*. (2008) 29:352–61. doi: 10.1016/j.immuni.2008.09.002
68. Masuta Y, Yamamoto T, Natsume-Kitatani Y, Kanuma T, Moriishi E, Kobiyama K, et al. An antigen-free, plasmacytoid dendritic cell–targeting immunotherapy to bolster memory CD8 + T cells in nonhuman primates. *J Immunol.* (2018) 200:2067–75. doi: 10.4049/jimmunol.1701183
69. Mouriès J, Moron G, Schlecht G, Escriou N, Dadaglio G, Lederc C. Plasmacytoid dendritic cells efficiently cross-prime naive T cells *in vivo* after TLR activation. *Blood*. (2008) 112:3713–22. doi: 10.1182/blood-2008-03-146290
70. Tel J, Schreibelt G, Sittig SP, Mathan TSM, Buschow SI, Cruz LJ, et al. Human plasmacytoid dendritic cells efficiently cross-present exogenous Ags to CD8+ T cells despite lowerAg uptake than myeloid dendritic cell subsets. *Blood*. (2013) 121:459–67. doi: 10.1182/blood-2012-06-435644
71. Tel J, Sittig SP, Blom RAM, Cruz LJ, Schreibelt G, Figdor CG, et al. Targeting uptake receptors on human plasmacytoid dendritic cells triggers antigen cross-presentation and robust type I IFN secretion. *J Immunol.* (2013) 191:5005–12. doi: 10.4049/jimmunol.1300787
72. Stary G, Bangert C, Tauber M, Strohal R, Kopp T, Stingl G. Tumoricidal activity of TLR7/8-activated inflammatory dendritic cells. *J Exp Med.* (2007) 204:1441–51. doi: 10.1084/jem.20070021
73. Drobits B, Holcmann M, Amberg N, Swiecki M, Grundtner R, Hammer M, et al. Imiquimod clears tumors in mice independent of adaptive immunity by converting pDCs into tumor-killing effector cells. *J Clin Invest.* (2012) 122:575–85. doi: 10.1172/JCI61034
74. Cella M, Jarrossay D, Facchetha F, Alebardi O, Nakajima H, Lanzavecchia A, et al. Plasmacytoid monocytes migrate to inflamed lymph nodes and produce large amounts of type I interferon. *Nat Med.* (1999) 5:919–23. doi: 10.1038/11360
75. Swiecki M, Colonna M. The multifaceted biology of plasmacytoid dendritic cells. *Nat Rev Immunol.* (2015) 15:471–85. doi: 10.1038/nri3865
76. Dunn GP, Bruce AT, Sheehan KCF, Shankaran V, Uppaluri R, Bui JD, et al. A critical function for type I interferons in cancer immunoediting. *Nat Immunol.* (2005) 6:722–29. doi: 10.1038/ni1213
77. Diamond MS, Kinder M, Matsushita H, Mashayekhi M, Dunn GP, Archambault JM, et al. Type I interferon is selectively required by dendritic cells for immune rejection of tumors. *J Exp Med.* (2011) 208:1989–2003. doi: 10.1084/jem.20101158
78. Lorenzi S, Mattei F, Sistigu A, Bracci L, Spadaro F, Sanchez M, et al. Type I IFNs control antigen retention and survival of CD8 + dendritic cells after uptake of tumor apoptotic cells leading to cross-priming. *J Immunol.* (2011) 186:5142–50. doi: 10.4049/jimmunol.1004163
79. Starbeck-Miller GR, Xue H-H, Harty JT. IL-12 and type I interferon prolong the division of activated CD8 T cells by maintaining high-affinity IL-2 signaling *in vivo*. *J Exp Med.* (2013) 211:105–20. doi: 10.1084/jem.20130901
80. Fuertes MB, Kacha AK, Kline J, Woo SR, Kranz DM, Murphy KM, et al. Host type I IFN signals are required for antitumor CD8+ T cell responses through CD8α+ dendritic cells. *J Exp Med.* (2011) 208:2005–16. doi: 10.1084/jem.20101159
81. Klebanoff CA, Khong HT, Antony PA, Palmer DC, Restifo NP. Sinks, suppressors and antigen presenters: how lymphodepletion enhances T cell-mediated tumor immunotherapy. *Trends Immunol.* (2005) 26:111–7. doi: 10.1016/j.it.2004.12.003
82. Dudley ME, Yang JC, Sherry R, Hughes MS, Royal R, Kammula U, et al. Adoptive cell therapy for patients with metastatic melanoma: evaluation of intensive myeloablative chemoradiation preparative regimens. *J Clin Oncol.* (2008) 26:5233–9. doi: 10.1200/JCO.2008.16.5449
83. Dudley ME, Wunderlich JR, Yang JC, Sherry RM, Topalian SL, Restifo NP, et al. Adoptive cell transfer therapy following non-myeloablative but lymphodepleting chemotherapy for the treatment of patients with refractory metastatic melanoma. *J Clin Oncol.* (2005) 23:2346–57. doi: 10.1200/JCO.2005.00.240
84. Gattinoni L, Powell DJ, Rosenberg SA, Restifo NP. Adoptive immunotherapy for cancer: building on success. *Nat Rev Immunol.* (2006) 6:383–93. doi: 10.1038/nri1842
85. Hsu FT, Chen TC, Chuang HY, Chang YF, Hwang JJ. Enhancement of adoptive T cell transfer with single low dose pretreatment of doxorubicin or paclitaxel in mice. *Oncotarget*. (2015) 6:44134–50. doi: 10.18632/oncotarget.6628
86. Yao X, Ahmadzadeh M, Lu YC, Liewehr DJ, Dudley ME, Liu F, et al. Levels of peripheral CD4 +FoxP3 + regulatory T cells are negatively associated with clinical response to adoptive immunotherapy of human cancer. *Blood*. (2012) 119:5688–96. doi: 10.1182/blood-2011-10-386482
87. Gattinoni L, Finkelstein SE, Klebanoff CA, Antony PA, Palmer DC, Spiess PJ, et al. Removal of homeostatic cytokine sinks by lymphodepletion enhances the efficacy of adoptively transferred tumor-specific CD8 $^{+}$ T cells. *J Exp Med.* (2005) 202:907–12. doi: 10.1084/jem.20050732
88. Salem ML, Cole DJ. Dendritic cell recovery post-lymphodepletion: a potential mechanism for anti-cancer adoptive T cell therapy and vaccination. *Cancer Immunol Immunother.* (2010) 59:341–53. doi: 10.1007/s00262-009-0792-6
89. Schiavoni G, Sistigu A, Valentini M, Mattei F, Sestili P, Spadaro F, et al. Cyclophosphamide synergizes with type I interferons through systemic dendritic cell reactivation and induction of immunogenic tumor apoptosis. *Cancer Res.* (2011) 71:768–78. doi: 10.1158/0008-5472.CAN-10-2788
90. Torihata H, Ishikawa F, Okada Y, Tanaka Y, Uchida T, Suguro T, et al. Irradiation up-regulates CD80 expression through two different mechanisms in spleen B cells, B lymphoma cells, and dendritic cells. *Immunology*. (2004) 112:219–27. doi: 10.1111/j.1365-2567.2004.01872.x
91. Salem ML, El-Naggar SA, Cole DJ. Cyclophosphamide induces bone marrow to yield higher numbers of precursor dendritic cells *in vitro* capable of functional antigen presentation to T cells *in vivo*. *Cell Immunol.* (2010) 261:134–43. doi: 10.1016/j.cellimm.2009.11.011
92. Salem ML, Diaz-Montero CM, Al-Khami AA, El-Naggar SA, Naga O, Montero AJ, et al. Recovery from cyclophosphamide-induced lymphopenia results in expansion of immature dendritic cells which can mediate enhanced prime-boost vaccination antitumor responses in vivo when stimulated with the TLR3 agonist Poly(I:C). *J Immunol.* (2009) 182:2030–40. doi: 10.4049/jimmunol.0801829
93. Liu JY, Wu Y, Zhang XS, Yang JL, Li HL, Mao YQ, et al. Single administration of low dose cyclophosphamide augments the antitumor effect of dendritic cell vaccine. *Cancer Immunol. Immunother.* (2007) 56:1597–604. doi: 10.1007/s00262-007-0305-4
94. Bloy N, Pol J, Manic G, Vitale I, Eggermont A, Galon J, et al. Trial watch: radioimmunotherapy for oncological indications. *Oncoimmunology*. (2014) 3:e1214790. doi: 10.4161/21624011.2014.954929
95. Casares N, Pequignot MO, Tesniere A, Ghiringhelli F, Roux S, Chaput N, et al. Caspase-dependent immunogenicity of doxorubicin-induced tumor cell death. *J Exp Med.* (2005) 202:1691–701. doi: 10.1084/jem.20050915
96. Prise KM, O'Sullivan JM. Radiation-induced bystander signalling in cancer therapy. *Nat Rev Cancer*. (2009) 9:351–60. doi: 10.1038/nrc2603
97. Tesniere A, Panaretakis T, Kepp O, Apetoh L, Ghiringhelli F, Zitvogel L, et al. Molecular characteristics of immunogenic cancer cell death. *Cell Death Differ.* (2008) 15:3–12. doi: 10.1038/sj.cdd.4402269
98. Galluzzi L, Buqué A, Kepp O, Zitvogel L, Kroemer G. Immunogenic cell death in cancer and infectious disease. *Nature*. (2016) 17:97–111. doi: 10.1038/nri.2016.107
99. Bonnotte B, Favre N, Moutet M, Fromentin A, Solary E, Martin M, et al. Role of tumor cell apoptosis in tumor antigen migration to the draining lymph nodes. *J Immunol.* (2000) 164:1995–2000. doi: 10.4049/jimmunol.164.4.1995
100. Parker JJ, Jones JC, Strober S, Knox SJ. Characterization of direct radiation-induced immune function and molecular signaling changes in an antigen presenting cell line. *Clin Immunol.* (2013) 148:44–55. doi: 10.1016/j.clim.2013.03.008
101. Burnette BC, Liang H, Lee Y, Chlewicki L, Khodarev NN, Weichselbaum RR, et al. The efficacy of radiotherapy relies upon induction of type I interferon-dependent innate and adaptive immunity. *Cancer Res.* (2011) 71:2488–96. doi: 10.1158/0008-5472.CAN-10-2820
102. Bouquet F, Pal A, Pilones KA, Demaria S, Hann B, Akhurst RJ, et al. TGFβ1 inhibition increases the radiosensitivity of breast cancer cells *in vitro*

and promotes tumor control by radiation *in vivo*. *Clin Cancer Res.* (2011) 17:6754–65. doi: 10.1158/1078-0432.CCR-11-0544
103. Young KH, Newell P, Cottam B, Friedman D, Savage T, Baird JR, et al. TGFβ inhibition prior to hypofractionated radiation enhances efficacy in preclinical models. *Cancer Immunol Res.* (2014) 2:1011–22. doi: 10.1158/2326-6066.CIR-13-0207
104. Liu H, Li B, Jia X, Ma Y, Gu Y, Zhang P, et al. Radiation-induced decrease of CD8 + dendritic cells contributes to Th1/Th2 shift. *Int Immunopharmacol.* (2017) 46:178–85. doi: 10.1016/j.intimp.2017.03.013
105. Rossig C, Pule M, Altvater B, Saiagh S, Wright G, Ghorashian S, et al. Vaccination to improve the persistence of CD19CAR gene-modified T cells in relapsed pediatric acute lymphoblastic leukemia. *Leukemia*. (2017) 31:1087–95. doi: 10.1038/leu.2017.39
106. Reap EA, Suryadevara CM, Batich KA, Sanchez-Perez L, Archer GE, Schmittling RJ, et al. Dendritic cells enhance polyfunctionality of adoptively transferred T cells that target cytomegalovirus in glioblastoma. *Cancer Res.* (2018) 78:256–64. doi: 10.1158/0008-5472.CAN-17-0469
107. Ma L, Dichwalkar T, Chang JYH, Cossette B, Garafola D, Zhang AQ, et al. Enhanced CAR-T cell activity against solid tumors by vaccine boosting through the chimeric receptor. *Science.* (2019) 365:162–8. doi: 10.1126/science.aav8692
108. Lou Y, Wang G, Lizée G, Kim GJ, Finkelstein SE, Feng C, et al. Dendritic cells strongly boost the antitumor activity of adoptively transferred T cells *in vivo*. *Cancer Res.* (2004) 64:6783–90. doi: 10.1158/0008-5472.CAN-04-1621
109. Shimizu K, Kotera Y, Aruga A, Takeshita N, Katagiri S, Ariizumi SI, et al. Postoperative dendritic cell vaccine plus activated T-cell transfer improves the survival of patients with invasive hepatocellular carcinoma. *Hum Vaccines Immunother.* (2014) 10:970–6. doi: 10.4161/hv.27678
110. Andersen MH. The T-win® technology: immune-modulating vaccines. *Semin Immunopathol.* (2019) 41:87–95. doi: 10.1007/s00281-018-0695-8
111. Klausen U, Holmberg S, Holmström MO, Jørgensen NGD, Grauslund JH, Svane IM, et al. Novel strategies for peptide-based vaccines in hematological malignancies. *Front Immunol.* (2018) 9:2264. doi: 10.3389/fimmu.2018.02264
112. Munir S, Lundsager MT, Jørgensen MA, Hansen M, Petersen TH, Bonefeld CM, et al. Inflammation induced PD-L1-specific T cells. *Cell Stress*. (2019) 3:319–27. doi: 10.15698/cst2019.10.201
113. Jørgensen MA, Holmström MO, Martinenaite E, Riley CH, Hasselbalch HC, Andersen MH. Spontaneous T-cell responses against Arginase-1 in the chronic myeloproliferative neoplasms relative to disease stage and type of driver mutation. *Oncoimmunology*. (2018) 7:1–8. doi: 10.1080/2162402X.2018.1468957
114. Emilie Weis-Banke S, Linder Hübbe M, Orebo Holmström M, Aaboe Jørgensen M, Kloch Bendtsen S, Martinenaite E, et al. The metabolic enzyme arginase-2 is a potential target for novel immune modulatory vaccines. *Oncoimmunology*. (2020) 9:1–16. doi: 10.1080/2162402X.2020.1771142
115. Sørensen RB, Hadrup SR, Svane IM, Hjortsø MC, Straten PT, Andersen MH. Indoleamine 2,3-dioxygenase specific, cytotoxic T cells as immune regulators. *Blood*. (2011) 117:2200–10. doi: 10.1182/blood-2010-06-288498
116. Bjoern J, Iversen TZ, Nitschke NJ, Andersen MH, Svane IM. Safety, immune and clinical responses in metastatic melanoma patients vaccinated with a long peptide derived from indoleamine 2,3-dioxygenase in combination with ipilimumab. *Cytotherapy*. (2016) 18:1043–55. doi: 10.1016/j.jcyt.2016.05.010
117. Munir Ahmad S, Martinenaite E, Hansen M, Junker N, Borch TH, Met Ö, et al. PD-L1 peptide co-stimulation increases immunogenicity of a dendritic cell-based cancer vaccine. *Oncoimmunology*. (2016) 5:e1202391. doi: 10.1080/2162402X.2016.1202391
118. Powell J, Rosenberg El-Gamil SA, Li YF, Zhou J, Huang J, Paul Robbins DF, et al. Cutting edge: persistence of transferred lymphocyte clonotypes correlates with cancer regression in patients receiving cell transfer therapy. *J Immunol.* (2004) 173:7125–30. doi: 10.4049/jimmunol.173.12.7125
119. Zhou J, Dudley ME, Rosenberg SA, Robbins PF. Persistence of multiple tumor-specific T-cell clones is associated with complete tumor regression in a melanoma patient receiving adoptive cell transfer therapy. *J Immunother.* (2005) 28:53–62. doi: 10.1097/00002371-200501000-00007
120. Schreibelt G, Tel J, Sliepen KHEWJ, Benitez-Ribas D, Figdor CG, Adema GJ, et al. Toll-like receptor expression and function in human dendritic cell subsets: implications for dendritic cell-based anti-cancer immunotherapy. *Cancer Immunol Immunother.* (2010) 59:1573–82. doi: 10.1007/s00262-010-0833-1
121. Duthie MS, Windish HP, Fox CB, Reed SG. Use of defined TLR ligands as adjuvants within human vaccines. *Immunol Rev.* (2011) 239:178–96. doi: 10.1111/j.1600-065X.2010.00978.x
122. Cen X, Liu S, Cheng K. The role of toll-like receptor in inflammation and tumor immunity. *Front Pharmacol.* (2018) 9:878. doi: 10.3389/fphar.2018.00878
123. Smith M, García-Martínez E, Pitter MR, Fucikova J, Spisek R, Zitvogel L, et al. Trial watch: toll-like receptor agonists in cancer immunotherapy. *Oncoimmunology*. (2018) 7:e1526250. doi: 10.1080/2162402X.2018.1526250
124. Dovedi SJ, Melis MHM, Wilkinson RW, Adlard AL, Stratford IJ, Honeychurch J, et al. Plenary paper systemic delivery of a TLR7 agonist in combination with radiation primes durable antitumor immune responses in mouse models of lymphoma. *Blood*. (2013) 121:251–9. doi: 10.1182/blood-2012-05-432393
125. Schölch S, Rauber C, Tietz A, Rahbari NN, Bork U, Schmidt T, et al. Radiotherapy combined with TLR7/8 activation induces strong immune responses against gastrointestinal tumors. *Oncotarget*. (2015) 6:4663-76. doi: 10.18632/oncotarget.3081
126. Adlard AL, Dovedi SJ, Telfer BA, Koga-Yamakawa E, Pollard C, Honeychurch J, et al. A novel systemically administered toll-like receptor 7 agonist potentiates the effect of ionizing radiation in murine solid tumor models. *Int J Cancer*. (2014) 135:820–9. doi: 10.1002/ijc.28711
127. Nelson MH, Bowers JS, Bailey SR, Diven MA, Fugle CW, Kaiser ADM, et al. Toll-like receptor agonist therapy can profoundly augment the antitumor activity of adoptively transferred CD8+ T cells without host preconditioning. *J Immunother Cancer*. (2016) 4:6. doi: 10.1186/s40425-016-0110-8
128. Sato Y, Goto Y, Narita N, Hoon DSB. Cancer cells expressing toll-like receptors and the tumor microenvironment. *Cancer Microenviron.* (2009) 2:205–14. doi: 10.1007/s12307-009-0022-y
129. González-Reyes S, Marín L, González L, González LO, Del Casar JM, Lamelas ML, et al. Study of TLR3, TLR4 and TLR9 in breast carcinomas and their association with metastasis. *BMC Cancer*. (2010) 10:665. doi: 10.1186/1471-2407-10-665
130. Sheyhidin I, Nabi G, Hasim A, Zhang RP, Ainiwaer J, Ma H, et al. Overexpression of TLR3, TLR4, TLR7 and TLR9 in esophageal squamous cell carcinoma. *World J Gastroenterol.* (2011) 17:3745. doi: 10.3748/wjg.v17.i32.3745
131. Griffiths EA, Srivastava P, Matsuzaki J, Brumberger Z, Wang ES, Kocent J, et al. NY-ESO-1 vaccination in combination with decitabine induces antigen-specific T-lymphocyte responses in patients with myelodysplastic syndrome. *Clin Cancer Res.* (2018) 24:1019–29. doi: 10.1158/1078-0432.CCR-17-1792
132. Ishikawa H, Barber GN. STING is an endoplasmic reticulum adaptor that facilitates innate immune signalling. *Nature*. (2008) 455:674–8. doi: 10.1038/nature07317
133. Sun L, Wu J, Du F, Chen X, Chen ZJ. Cyclic GMP-AMP synthase is a cytosolic DNA sensor that activates the type I interferon pathway. *Science.* (2013) 339:786–91. doi: 10.1126/science.1232458
134. Woo SR, Fuertes MB, Corrales L, Spranger S, Furdyna MJ, Leung MYK, et al. STING-dependent cytosolic DNA sensing mediates innate immune recognition of immunogenic tumors. *Immunity*. (2014) 41:830–42. doi: 10.1016/j.immuni.2014.10.017
135. Jing W, McAllister D, Vonderhaar EP, Palen K, Riese MJ, Gershan J, et al. STING agonist inflames the pancreatic cancer immune microenvironment and reduces tumor burden in mouse models. *J Immunother Cancer*. (2019) 7:115. doi: 10.1186/s40425-019-0573-5
136. Corrales L, Glickman LH, McWhirter SM, Kanne DB, Sivick KE, Katibah GE, et al. Direct activation of STING in the tumor microenvironment leads to potent and systemic tumor regression and immunity. *Cell Rep.* (2015) 11:1018–30. doi: 10.1016/j.celrep.2015.04.031
137. Demaria O, De Gassart A, Coso S, Gestermann N, Di Domizio J, Flatz L, et al. STING activation of tumor endothelial cells initiates spontaneous and therapeutic antitumor immunity. *Proc Natl Acad Sci USA*. (2015) 112:15408–13. doi: 10.1073/pnas.1512832112

138. Zhang C-X, Ye S-B, Ni J-J, Cai T-T, Liu Y-N, Huang D-J, et al. STING signaling remodels the tumor microenvironment by antagonizing myeloid-derived suppressor cell expansion. *Cell Death Differ.* (2019) 26:2314–28. doi: 10.1038/s41418-019-0302-0
139. Smith TT, Moffett HF, Stephan SB, Opel CF, Dumigan AG, Jiang X, et al. Biopolymers codelivering engineered T cells and STING agonists can eliminate heterogeneous tumors. *J Clin Invest.* (2017) 127:2176–91. doi: 10.1172/JCI87624
140. Ghaffari A, Peterson N, Khalaj K, Vitkin N, Robinson A, Francis JA, et al. Sting agonist therapy in combination with pd-1 immune checkpoint blockade enhances response to carboplatin chemotherapy in high-grade serous ovarian cancer. *Br J Cancer.* (2018) 119:440–9. doi: 10.1038/s41416-018-0188-5
141. Moore E, Clavijo PE, Davis R, Cash H, Van Waes C, Kim Y, et al. Established T cell-inflamed tumors rejected after adaptive resistance was reversed by combination STING activation and PD-1 pathway blockade. *Cancer Immunol Res.* (2016) 4:1061–71. doi: 10.1158/2326-6066.CIR-16-0104
142. Richards DM, Sefrin JP, Gieffers C, Hill O, Merz C. Concepts for agonistic targeting of CD40 in immuno-oncology. *Hum Vaccin Immunother.* (2020) 16:377–87. doi: 10.1080/21645515.2019.1653744
143. O'Sullivan BJ, Thomas R. CD40 ligation conditions dendritic cell antigen-presenting function through sustained activation of NF-κB. *J Immunol.* (2002) 168:5491–8. doi: 10.4049/jimmunol.168.11.5491
144. Sotomayor EM, Borrello I, Tubb E, Rattis FM, Bien H, Lu Z, et al. Conversion of tumor-specific CD4+ T-cell tolerance to T-cell priming through *in vivo* ligation of cd40. *Nat Med.* (1999) 5:780–7. doi: 10.1038/10503
145. Diehl L, Den Boer AT, Schoenberger SP, Van Der Voort EIH, Schumacher TNM, Melief CJM, et al. CD40 activation *in vivo* overcomes peptide-induced peripheral cytotoxic T-lymphocyte tolerance and augments anti-tumor vaccine efficacy. *Nat Med.* (1999) 5:774–9. doi: 10.1038/10495
146. Tay NQ, Lee CPD, Chua YL, Prabhu N, Gascoigne NRJ, Kemeny DM. CD40L expression allows CD8+ T cells to promote their own expansion and differentiation through dendritic cells. *Front Immunol.* (2017) 8:1484. doi: 10.3389/fimmu.2017.01484
147. Ward-Kavanagh LK, Kokolus KM, Cooper TK, Lukacher AE, Schell TD. Combined sublethal irradiation and agonist anti-CD40 enhance donor T cell accumulation and control of autochthonous murine pancreatic tumors. *Cancer Immunol Immunother.* (2018) 67:639–52. doi: 10.1007/s00262-018-2115-2
148. Liu C, Lewis CM, Lou Y, Xu C, Peng W, Yang Y, et al. Agonistic antibody to CD40 boosts the antitumor activity of adoptively transferred T cells *in vivo*. *J Immunother.* (2012) 35:276–82. doi: 10.1097/CJI.0b013e31824e7f43
149. Bajor DL, Mick R, Riese MJ, Huang AC, Sullivan B, Richman LP, et al. Long-term outcomes of a phase I study of agonist CD40 antibody and CTLA-4 blockade in patients with metastatic melanoma. *Oncoimmunology.* (2018) 7:e1468956. doi: 10.1080/2162402X.2018.1468956
150. Chand Dakal T, Dhabhai B, Agarwal D, Gupta R, Nagda G, Meena AR, et al. Mechanistic basis of co-stimulatory CD40-CD40L ligation mediated regulation of immune responses in cancer and autoimmune disorders. *Immunobiology.* (2020) 225:151899. doi: 10.1016/j.imbio.2019.151899
151. Gattinoni L, Klebanoff CA, Palmer DC, Wrzesinski C, Kerstann K, Yu Z, et al. Acquisition of full effector function *in vitro* paradoxically impairs the *in vivo* antitumor efficacy of adoptively transferred CD8+ T cells. *J Clin Invest.* (2005) 115:1616–26. doi: 10.1172/JCI24480
152. Li Y, Bleakley M, Yee C. IL-21 influences the frequency, phenotype, and affinity of the antigen-specific CD8 T cell response. *J Immunol.* (2005) 175:2261–9. doi: 10.4049/jimmunol.175.4.2261
153. Zeng R, Spolski R, Finkelstein SE, Oh SK, Kovanen PE, Hinrichs CS, et al. Synergy of IL-21 and IL-15 in regulating CD8+ T cell expansion and function. *J Exp Med.* (2005) 201:139–48. doi: 10.1084/jem.20041057
154. Mousset CM, Hobo W, Ji Y, Fredrix H, De Giorgi V, Allison RD, et al. *Ex vivo* AKT-inhibition facilitates generation of polyfunctional stem cell memory-like CD8+ T cells for adoptive immunotherapy. *Oncoimmunology.* (2018) 7:e1488565. doi: 10.1080/2162402X.2018.1488565
155. Sabatino M, Hu J, Sommariva M, Gautam S, Fellowes V, Hocker JD, et al. Generation of clinical-grade CD19-specific CAR-modified CD81 memory stem cells for the treatment of human B-cell malignancies Marianna. *Blood.* (2016) 127:1117–27. doi: 10.1182/blood-2015-11-683847
156. Kondo T, Morita R, Okuzono Y, Nakatsukasa H, Sekiya T, Chikuma S, et al. Notch-mediated conversion of activated T cells into stem cell memory-like T cells for adoptive immunotherapy. *Nat Commun.* (2017) 8:1–14. doi: 10.1038/ncomms15338
157. Chacon JA, Wu RC, Sukhumalchandra P, Molldrem JJ, Sarnaik A, Pilon-Thomas S, et al. Co-stimulation through 4-1BB/CD137 improves the expansion and function of CD8+ melanoma tumor-infiltrating lymphocytes for adoptive T-cell therapy. *PLoS ONE.* (2013) 8:e0060031. doi: 10.1371/journal.pone.0060031
158. Minagawa A, Yoshikawa T, Yasukawa M, Hotta A, Kunitomo M, Iriguchi S, et al. Enhancing T cell receptor stability in rejuvenated iPSC-derived T cells improves their use in cancer immunotherapy. *Cell Stem Cell.* (2018) 23:850–8. doi: 10.1016/j.stem.2018.10.005
159. Vizcardo R, Masuda K, Yamada D, Ikawa T, Shimizu K, Fujii SI, et al. Regeneration of human tumor antigen-specific T cells from iPSCs derived from mature CD8+ T cells. *Cell Stem Cell.* (2013) 12:31–6. doi: 10.1016/j.stem.2012.12.006
160. Zhang L, Davies JS, Serna C, Yu Z, Restifo NP, Rosenberg SA, et al. Enhanced efficacy and limited systemic cytokine exposure with membrane-anchored interleukin-12 T-cell therapy in murine tumor models. *J Immunother Cancer.* (2020) 8:210. doi: 10.1136/jitc-2019-000210
161. Lai J, Mardiana S, House IG, Sek K, Henderson MA, Giuffrida L, et al. Adoptive cellular therapy with T cells expressing the dendritic cell growth factor Flt3L drives epitope spreading and antitumor immunity. *Nat Immunol.* (2020) 21:914–26. doi: 10.1038/s41590-020-0676-7

Conflict of Interest: The authors declare that the research was conducted in the absence of any commercial or financial relationships that could be construed as a potential conflict of interest.

frontiers in Immunology

REVIEW
published: 06 October 2020
doi: 10.3389/fimmu.2020.02023

Predictive Biomarkers of Immune Checkpoint Inhibitors-Related Toxicities

Ya Xu[1†], *Yang Fu*[2†], *Bo Zhu*[3], *Jun Wang*[4*] *and Bicheng Zhang*[1*]

[1] Cancer Center, Renmin Hospital of Wuhan University, Wuhan, China, [2] Department of Oncology, Xiangyang Hospital, Hubei University of Chinese Medicine, Xiangyang, China, [3] Institute of Cancer, Xinqiao Hospital, Army Medical University, Chongqing, China, [4] Department of Oncology, The First Affiliated Hospital of Shandong First Medical University, Jinan, China

The emergence and continuous development of immune checkpoint inhibitors (ICIs) therapy brings a revolution in cancer therapy history, but the major hurdle associated with their usage is the concomitant ICIs-related toxicities that present a challenge for oncologists. The toxicities may involve non-specific symptoms of multiple systems as for the unique mechanism of formation, which are not easily distinguishable from traditional toxicities. A few of these adverse events are self-limiting and readily manageable, but others may limit treatment, cause interruption and need to be treated with methylprednisolone or tumor necrosis factor-α (TNF-α) antibody infliximab, and even directly threaten life. Early accurate recognition and adequate management are critical to the patient's prognosis and overall survival (OS). Several biomarkers such as the expression of programmed cell death ligand 1 (PD-L1), tumor mutation burden (TMB), and microsatellite instability-high (MSI-H)/mismatch repair-deficient (dMMR) have been proved to be the predictors for anti-tumor efficacy of ICIs, but there is a gap in clinical needs for effective biomarkers that predict toxicities and help filter out the patients who may benefit most from these costly therapies while avoiding major risks of toxicities. Here, we summarize several types of risk factors correlated with ICIs-related toxicities to provide a reference for oncologists to predict the occurrence of ICIs-related toxicities resulting in a timely process in clinical practice.

Keywords: immune checkpoint inhibitor, toxicity, predictive biomarker, PD-1, PD-L1

OPEN ACCESS

Edited by:
Maysaloun Merhi,
Hamad Medical Corporation, Qatar

Reviewed by:
Loredana Ruggeri,
University of Perugia, Italy
Jeff K. Davies,
Queen Mary University of London, United Kingdom

***Correspondence:**
Bicheng Zhang
bichengzhang@hotmail.com
Jun Wang
ggjun2005@126.com

[†]These authors have contributed equally to this work

Specialty section:
This article was submitted to Cancer Immunity and Immunotherapy, a section of the journal Frontiers in Immunology

Received: *11 May 2020*
Accepted: *27 July 2020*
Published: *06 October 2020*

Citation:
Xu Y, Fu Y, Zhu B, Wang J and Zhang B (2020) Predictive Biomarkers of Immune Checkpoint Inhibitors-Related Toxicities. Front. Immunol. 11:2023. doi: 10.3389/fimmu.2020.02023

INTRODUCTION

The development of ICIs has changed the systemic treatments of tumors and rewritten history. Even as advanced stage therapy, ICIs have enjoyed unprecedented success in many types of cancers including malignant melanoma (1), non-small cell lung cancer (NSCLC) (2), small cell lung cancer (3), metastatic bladder cancer (4), and urothelial carcinoma (5), etc. Because of such an effective anti-tumor immune response, the Food and Drug Administration (FDA) has approved ICIs for more than thirty indications. With the unprecedented objective response rates (ORR) as well as durable responses across many tumor types, the clinical application of ICIs continues to expand in various combinations including ICIs monotherapy or combination with chemotherapy, radiotherapy, anti-angiogenic agents, or other ICIs.

ICIs are a novel category of drugs that are essentially humanized monoclonal antibodies, which activate T cells and relieve the immune system to recognize and assault cancer cells by targeting

cytotoxic T lymphocyte-associated antigen-4 (CTLA-4) (CD152), programmed cell death protein 1 (PD-1), or programmed cell death ligand 1 (PD-L1). However, the unleashing immune response could increase autoimmunity and cause a plethora of immune-related toxicities, termed ICIs-related toxicities, which can potentially affect any tissue and organs of patients (mainly including gut, skin, endocrine glands, liver, and lung) (**Figure 1**).

With unclear mechanisms, ICIs-related toxicities may require discontinuation of immunotherapy. Furthermore, because of the early onset and fulminant progression, some severe toxicities are even life-threatening (such as myocarditis, serious colitis, and pneumonia). Oncologists are facing huge challenges in optimizing outcomes during the use of ICIs, which is expected to increase significantly in the years to come. Assuming most toxicities are mild and reversible when detected early and properly managed, searching for predictive biomarkers for the ICIs-related toxicities remain essential for early recognition and appropriate clinical management. Identifying predictive biomarkers to distinguish patients most likely to suffer immune-related adverse events (irAEs) from overall individuals will avoid severe toxicity risk and decrease treatment costs.

This review focuses on summarizing a variety of potential biomarkers from different sources for ICIs-related toxicities and discussing the unique considerations relevant to patients' treating (**Figure 2**).

PREDICTIVE BIOMARKERS FOR CTLA-4 INHIBITORS-RELATED TOXICITIES

CTLA-4 plays a pivotal role in inducing peripheral tolerance and maintaining immunologic homeostasis but it is believed to be a negative regulator within the anti-tumor immunity. Specifically, CTLA-4 and CD28 are homologous receptors of T cells, which share a pair of ligands, B7 molecules (CD80 and CD86) expressed on the surface of antigen-presenting cells (APCs) (6). CTLA-4 binds with B7 molecules or detaches them away on APCs in the lymph nodes, causing T cell activation to be inhibited during the primary phase (7). The recombinant fully human immunoglobulin (Ig) monoclonal antibodies, such as ipilimumab and tremelimumab, activate T cells by forming a CTLA-4 pathway blockade at an early stage, of which the former was the first FDA approved inhibitor for unrespectable or metastatic melanoma based on significantly improved survival data in March 2011 (8). However, ICIs-related toxicities were accompanied with the enhanced anti-tumor responses following the CTLA-4 blockade. Ipilimumab-related all grade and 3–4 grade toxicities rates were 86.8 and 28.6%, respectively, which mainly affected gastrointestinal, skin, and renal system (9), while tremelimumab commonly led to gastrointestinal events, dermatologic events, and fatigue (10). Recently, several studies have looked for predictive biomarkers of CTLA-4 inhibitors-related toxicities. Key results are summarized in **Table 1**.

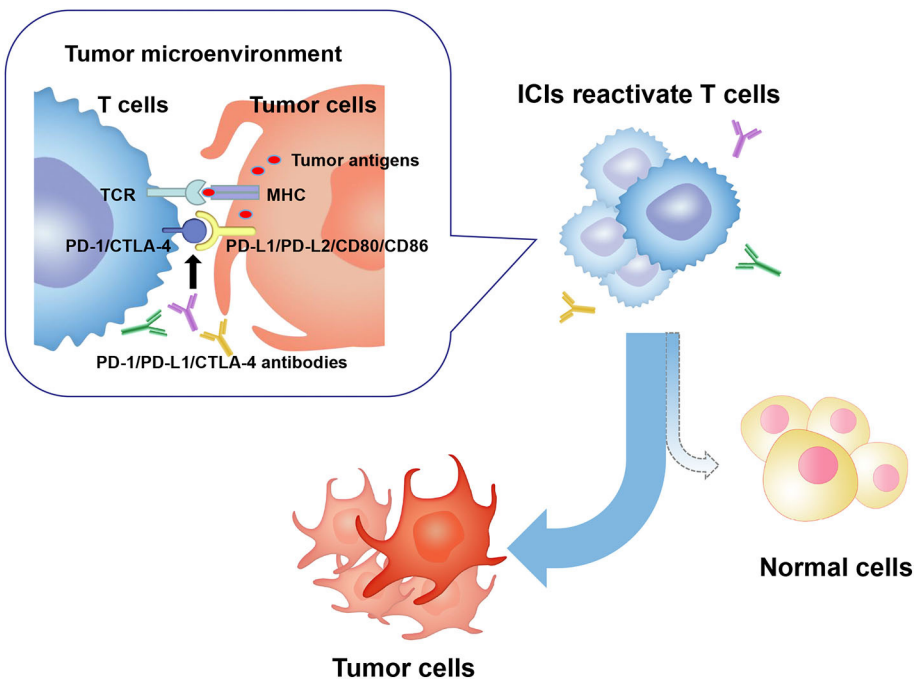

FIGURE 1 | In the tumor microenvironment, PD-1/CTLA-4 molecules on activated T cells are up-regulated and combined to PD-L1/PD-L2 or CD80/CD86 molecules on tumor cells. Consequently, T cell activity is inhibited, and an immunosuppressive microenvironment is formed, which leads to tumor cells escaping the immune surveillance and growing wildly. ICIs restore anti-tumor activity of T cells by targeting and blocking PD-1 or CTLA-4 signaling pathway. Activated T cells kill tumor cells and may attack normal human tissue cells, forming ICIs-related toxicities. PD-1, programmed cell death protein 1; PD-L1/2, programmed cell death ligand 1/2; CTLA-4, cytotoxic T lymphocyte-associated antigen-4; ICIs, immune checkpoint inhibitors; MHC, major histocompatibility complex; TCR, T cell receptor.

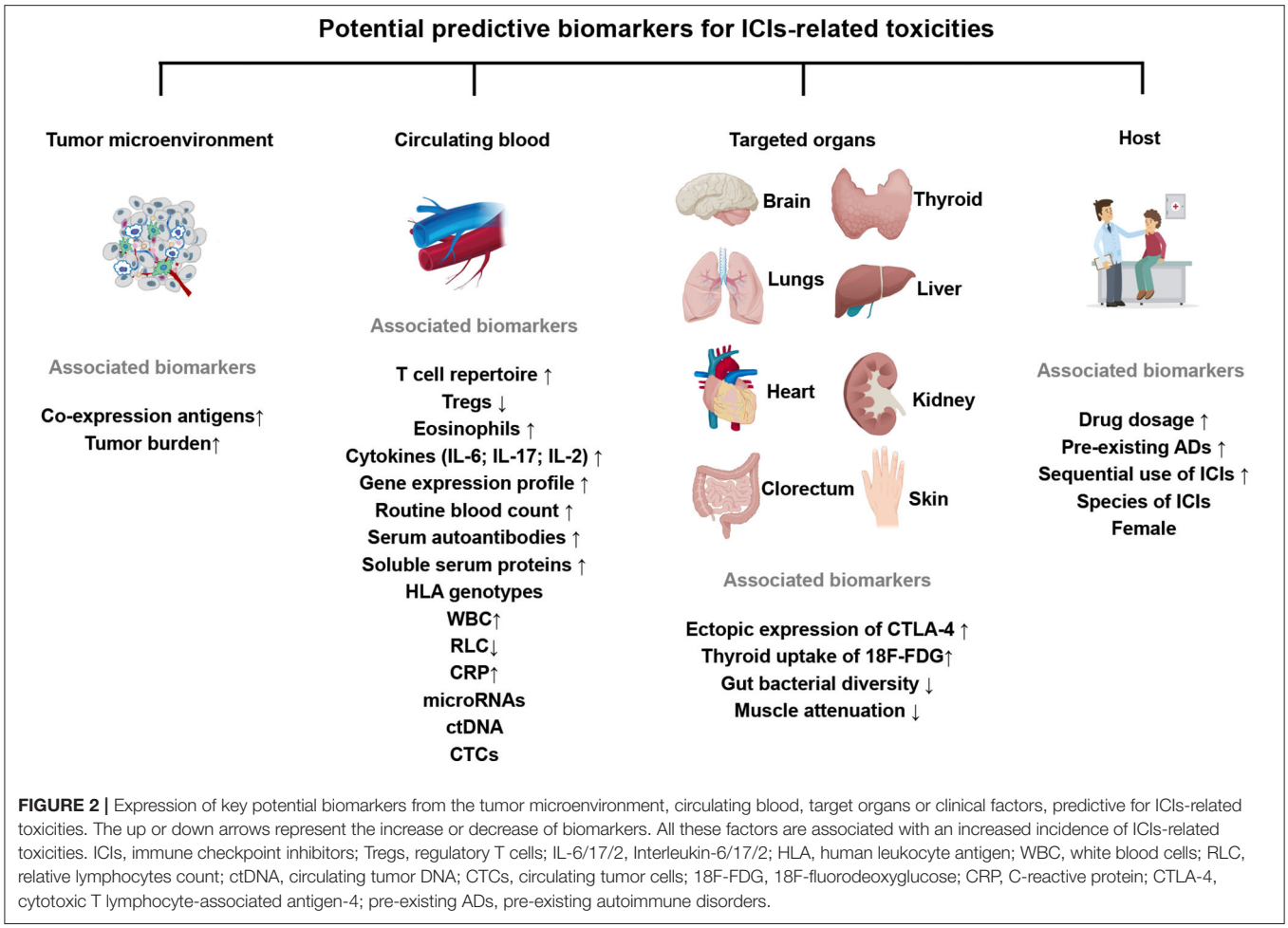

FIGURE 2 | Expression of key potential biomarkers from the tumor microenvironment, circulating blood, target organs or clinical factors, predictive for ICIs-related toxicities. The up or down arrows represent the increase or decrease of biomarkers. All these factors are associated with an increased incidence of ICIs-related toxicities. ICIs, immune checkpoint inhibitors; Tregs, regulatory T cells; IL-6/17/2, Interleukin-6/17/2; HLA, human leukocyte antigen; WBC, white blood cells; RLC, relative lymphocytes count; ctDNA, circulating tumor DNA; CTCs, circulating tumor cells; 18F-FDG, 18F-fluorodeoxyglucose; CRP, C-reactive protein; CTLA-4, cytotoxic T lymphocyte-associated antigen-4; pre-existing ADs, pre-existing autoimmune disorders.

Biomarkers From Circulating Blood

T Cell Repertoire

Since CTLA-4 blockade leads to the proliferation of circulating T cells, the diversity of the T cell receptor (TCR) repertoire as well as the expanse of the T cell repertoire are increased simultaneously (25). The clonal expansion of CD8+ T cells occurred predating the onset of grade 2–3 ipilimumab-related toxicities (11), patients with ipilimumab-related toxicities exhibited greater diversity of CD4+ and CD8+ T cells (12), indicating that the early diversification of the T cell repertoire appeared to present with the development of ipilimumab-related toxicities as well as an efficacious prostate-specific antigen responses (12). In total, the checkpoint blockade therapy with subsequent T cell repertoire diversification immediately can be both detrimental and beneficial for patients with cancer, suggesting that oncologists should be more cautious about this indicator.

Tregs

Regulatory T cells (Tregs) are a kind of CD4+ T cells that inhibit immunopathology or autoimmune disease *in vivo* by influencing the activity of other cell types. The expression of CTLA-4 on Tregs directly influenced its homeostasis and the function of preventing autoimmunity, the loss of CTLA-4 promoted the expansion of Tregs (6). Zhang's group reported that ipilimumab could prevent CTLA-4 recycling by lysosomal degradation and be less effective in intratumor Tregs depletion and rejection of large established tumors. Notably, the CTLA-4 inactivation led to irAEs (26). The selective depletion of tumor-infiltrating Tregs enhanced by preserving CTLA-4 recycling led to the cancer therapeutic effect of anti-CTLA-4 antibodies (27). That is to say, the depletion of tumor-infiltrating Tregs was closely related to CTLA-4-related toxicities and CTLA-4 molecule inactivation. It was reported that a low baseline proportion of peripheral blood $CD4^+$ Tregs was associated with subsequent colitis caused by ipilimumab (13), consistent with previous views that Tregs were capable of suppressing autoimmune diseases (ADs).

Eosinophils

A retrospective analysis informed that the growth count of circulating eosinophils during treatment with ipilimumab was associated with ICIs-related toxicity occurrence (14, 15). Furthermore, biopsies of diseased tissue about ipilimumab-associated hepatitis (28), rash (29), and colitis (16) showed the inflammatory infiltrate was similar, and all contained with eosinophils. Similarly, immunohistochemistry revealed the

TABLE 1 | Predictive biomarkers for CTLA-4 inhibitor-related toxicities.

Marker	Cancer type (sample size)	Source	Measurement methods	Drugs	Correlation
T cell repertoire (11)	Metastatic prostate cancer (*N* = 27)	Blood	TCR β-chains sequencing	Ipilimumab	Early clonal expansion of CD8 T-cell clones preceded the development of 2-3 CTLA-4-related toxicities
T cell repertoire (12)	Prostate cancer (*N* = 42)	Blood	TCR β-chains sequencing	Ipilimumab	Patients with CTLA-4-related toxicities exhibited greater diversity of $CD4^+$ and $CD8^+$ T cells
Tregs (13)	Metastatic melanoma (*N* = 26)	Blood	Absolute cell counts	Ipilimumab	A low baseline proportion of peripheral blood CD4+ Tregs was associated with subsequent colitis caused by ipilimumab
Eosinophils (14, 15)	Melanoma (*N* = 156) /(*N* = 43)	Blood	Absolute cell counts	Ipilimumab	The growth count of circulating eosinophils during treatment with ipilimumab was associated with CTLA-4-related toxicities occurrence
Neutrophils (16)	Melanoma (*N* = 115)	Tissue	Biopsy	Ipilimumab	The inflammation of neutrophils was associated with the occurrence of dysregulation of gastrointestinal immunity
IL-6 (17)	Metastatic melanoma (*N* = 140)	Blood	Chemoluminescent immunoenzymatic method	Ipilimumab	Baseline IL-6 serum levels was significantly and independently associated with higher risk of severe toxicity
IL-17 (18)	Metastatic melanoma (*N* = 52)	Blood	Chemoluminescent immunoenzymatic method	Ipilimumab	The fluctuations in blood IL-17 levels was associated with the development and the resolution of colitis symptoms in individually
IL-17 (19)	Metastatic melanoma (*N* = 35)	Blood	Chemoluminescent immunoenzymatic method	Ipilimumab	The baseline serum IL-17 levels were significantly higher in patients with grade 3 diarrhea/colitis
sMICA (20)	Advanced melanoma (*N* = 77)	Serum	ELISA	Ipilimumab	The increased of baseline sMICA related to a lower frequency of ipilimumab-related toxicities
Ectopic expression of CTLA-4 (21)	Advanced melanoma/ prostate cancer (*N* = 20)	Tissue	RT-PCR and Western blotting	Ipilimumab	Ectopic expression of CTLA-4 was associated with the onset of hypophysitis
Sex (17)	Metastatic melanoma (*N* = 140)	Clinical characteristics	Logistic regression	Ipilimumab	Female faced higher risk of irAEs
Baseline gut microbiota (13)	Metastatic melanoma (*N* = 26)	Fecal	Next generation metagenomic sequencing	Ipilimumab	Ipilimumab-related colitis was associated with decreased bacterial diversity
Baseline gut microbiota (22)	Metastatic melanoma (*N* = 115)	Fecal	Next generation metagenomic sequencing	Ipilimumab	The bacteroidetes phylum bacteria were more abundant in the faces of the patients who were resistant to ipilimumab-induced colitis
MA (23)	Metastatic melanoma (*N* = 84)	Body composition	CT	Ipilimumab	The decrease of MA significantly associated with high-grade ipilimumab-related toxicities
Pre-existing ADs (24)	Advanced melanoma (*N* = 30)	Clinicopathologic characteristic	Data collection	Ipilimumab	50% of patients with pre-existing ADs experienced exacerbations of their autoimmune or grade 3–5 -CTLA-4-related toxicities

CTLA-4, cytotoxic T lymphocyte-associated antigen-4; TCR, T cell receptor; Tregs, regulatory T cells; sMICA, soluble major histocompability complex class I chain-related protein A; ELISA, enzyme-linked immunoassay; IL-6/17, interleukin-6/17; MA, muscle attenuation; CT, computed tomography; Pre-existing ADs, pre-existing and early changes in autoimmune disorders.

infiltration of CD4+ and CD8+ T cells and highly activated effector cells of affected skin and gut correlated with ipilimumab-related toxicities intensity (30).

IL-6

Interleukin (IL)-6 is a pleiotropic inflammatory cytokine acting as a keystone factor in infection, cancer and inflammation. The blocking of immune checkpoints increases cytokine release including IL-6. Notably, low baseline IL-6 serum level was an independent risk factor for ICIs-related toxicities (17). Lower baseline levels of IL-6, IL-8, and sCD25 were associated with subsequent colitis in metastatic melanoma patients treated with ipilimumab (13).

IL-17

Compared with no colitis patients, serum IL-17 levels were significantly higher in patients with CTLA-4-related colitis; furthermore, the growth and fall in blood IL-17 levels were, respectively, associated with the development and the resolution of colitis symptoms individually (18). A significant association was demonstrated between baseline circulating IL-17 levels and the later progress of grade 3 diarrhea/colitis after the neoadjuvant treatment of ipilimumab (19). All these studies consistently

showed a positive correlation between IL-17 levels and CTLA-4-related toxicities.

Other Serum Protein

The release of soluble major histocompability complex class I chain-related protein A (sMICA) compromised natural killer (NK)- cell cytotoxicity, resulting in the tumor's escape from immunosurveillance (31, 32). A visible association was found between a higher baseline serum level of sMICA and lower frequency of ipilimumab-related toxicities (20).

Gene Expression Profile

The increased expression of CD177 and CEACAM1 genes, markers of neutrophils activation, were found associated with gastrointestinal toxicity occurrence (33). Similarly, using whole-blood RNA transcript-based models from a169-gene panel, a 16-gene signature (including CARD12, CCL3, CCR3, CXCL1, F5, FAM210B, GADD45A, IL18bp, IL2RA, IL5, IL8, MMP9, PTGS2, SOCS3, TLR9, and UBE2C) was identified to be predictive of tremelimumab-related gastrointestinal toxicities as well as to discriminate patients developing grade 0–1 from grade 2–4 diarrhea/colitis (34).

Biomarkers From Target Organs

Ectopic Expression of CTLA-4

Hypophysitis induced by ipilimumab in about 4% of patients may be attributed to the ectopic expression of CTLA-4 in the pituitary glands, which has been proved at both RNA and protein levels. Furthermore, pituitary antibodies were negative at baseline, increased in the 7 patients with hypophysitis but remained negative in the 13 patients without it (21). In other words, the CTLA-4 molecular expressed ectopically in the pituitary glands or the development of pituitary antibodies may be predictors for the appearance of ipilimumab-related pituitary toxicities.

Baseline Gut Microbiota

In recent years, intestinal commensal bacteria has gradually become a popular research direction. Commensal bacteria in the colonic microbiota showed an immunomodulatory effect. For example, the members of Bacteroidetes phylum can limit inflammation by stimulating Tregs differentiation (35). More specifically, colitis was associated with decreased bacterial diversity, the microbiota of patients prone to develop ipilimumab-induced colitis was enriched in Firmicutes at baseline, but others abundant with high proportions of Bacteroidetes phylum in the feces seemed resistant to ipilimumab-induced colitis (13). Besides, a lack of genetic pathways involved in polyamine transport and B vitamin biosynthesis was associated with an increased risk of colitis (22). These affirm the accurately predicted value of the intestinal bacterial spectrum and genome as potential biomarkers for identifying patients who are at risk of developing CTLA-4-related colitis.

Muscle Attenuation

With computed tomography (CT), low muscle attenuation (MA) were independent factors significantly associated with high-grade ipilimumab-related toxicities in metastatic melanoma (23).

Biomarkers From the Host

Valpione et al. (17) found female sex was significantly associated with a higher risk of several ipilimumab-related toxicities, Specifically, abnormal thyroid function happened more frequently in female patients (36).

Compared with 3 and 10 mg/kg dosage of ipilimumab, it showed an ∼50% rate of increase of grade 3–5 toxicities and an increased count of toxicities-related death with the higher dosage group (37). Similarly, the incidence level of all grade adverse events with anti-CTLA-4 treatment was 61% for 3 mg/kg dosage and 79% for 10 mg/kg (38). These dose effects corroborated that the dosage decided the risk of developing ipilimumab-related adverse events.

PREDICTIVE BIOMARKERS FOR PD-1/PD-L1 INHIBITORS-RELATED TOXICITIES

PD-1 molecule is an inhibitory receptor that was expressed on activated T cells and avoids unwanted inflammation and tissue damage caused by the excessive activation of T cells. But tumor cells take advantage of immune-tolerance mechanisms by up-regulating the expression of PD-1 ligands, PD-L1 (B7-H1), and PD-L2 (B7-DC). Subsequently, the binding of PD-1 and its ligands in the peripheral tissues inhibits those already activated T cells in the immune response. The production of monoclonal antibodies target the PD-1/PD-L1 signaling pathway to mobilize the host autoimmune system's anti-tumor potential. PD-1/PD-L1 monoclonal antibodies significantly improve the survival of patients with advanced malignancies compared to chemotherapy, and they are now being used as the second-line, or even first-line treatment in many types of cancers. However, it can also provoke powerful autoimmune reactions in other organ systems, classified as PD-1/PD-L1 inhibitors-related toxicities. PD-1-related serious adverse events were reported to occur at a percentage of 11% with a 1% rate of PD-1-related deaths (39). Key results about predictive markers for PD-1/PD-L1 inhibitors-related toxicities are summarized in **Table 2**.

Biomarkers From Circulating Blood

Routine Blood Count

The routine blood count is a basic and routine examination for clinical tumor inpatients. After univariate analysis and multivariate analysis in routine blood count data, an increased white blood cells (WBC) count and decreased relative lymphocytes count (RLC) were independent factors associated with lung/gastrointestinal toxicities (40). The baseline Absolute eosinophils count $>240/\mu L$ or relative eosinophils count could be useful biomarkers to predict PD-1-related endocrine toxicities (48). Besides, numerous neutrophils infiltrated into the skin of one of the nivolumab-associated psoriasiform dermatitis

TABLE 2 | Predictive biomarkers for PD-1/PD-L1 inhibitors-related toxicities.

Marker	Cancer type (smple size)	Source	Measurement methods	Drugs	Correlation
Routine blood count (40)	Melanoma ($N = 101$)	Blood	The count of blood cells	Nivolumab	An increased WBC count and decreased RLC were independently associated with lung/gastrointestinal toxicities
TgAbs and TPOAbs (41)	cancer ($N = 66$)	Blood	TOSOH	Nivolumab	The baseline TgAbs and TPOAbs levels were associated with the development of thyroiditis
TgAbs and TPOAbs (42)	Advanced NSCLC ($N = 137$)	Blood	TOSOH	PD-1 inhibitors	Thyroid dysfunction was more frequent among patients with pre-existing antithyroid antibodies
Rheumatoid factor (42)	Advanced NSCLC ($N = 137$)	Blood	TOSOH	PD-1 inhibitors	Skin reactions were more frequent among patients with pre-existing rheumatoid factor
TgAbs and TPOAbs (43)	Advanced malignant diseases ($N = 26$)	Blood	TOSOH	PD-1 inhibitors	The pre-existing and early increase ($\leq$4 weeks) in TgAbs and TPOAbs levels were found to be associated with PD-1-related thyroid toxicities
Tg (43)	Advanced malignant diseases ($N = 26$)	Blood	Chemiluminescence immunoassay	PD-1 inhibitors	The early increase in Tg levels were strongly associated with development of thyroid irAEs
sCD163 and CXCL5 (44)	Advanced melanoma ($N = 46$)	Blood	ELISA	Nivolumab	The serum absolute level of serum sCD163 was significantly increased in patients with nivolumab-related toxicities, accompaning by an increasing trend of CXCL5
Pre-existing ADs (45)	Advanced melanoma ($N = 119$)	Clinicopathologic characteristic	Data collection	PD-1 inhibitors	20 (38%) patients had a flare of ADs requiring immunosuppression, 2 (3%) patients experienced a recurrence toxicities the same with ipilimumab while 23 (34%) developed new toxicities
Pre-existing ADs (46)	NSCLC($N = 56$)	Clinicopathologic characteristic	Data collection	PD-(L)1 inhibitors	55% patients developed an ADs flare and/or ICIs-related toxicities
Pre-existing ICIs-related toxicities (47)	Metastatic melanoma ($N = 80$)	Clinical characteristic	Data collection	PD-1inhibitors	31 patients experienced clinically significant recurrent or distinct toxicities

WBC, white blood cells; RLC, relative lymphocytes count; TgAbs, anti-thyroglobulin antibodies; TPOAbs, anti-thyroid peroxidase antibodies; sCD163, soluble CD163; PD-1, programmed cell death protein 1; PD-L1, programmed cell death-ligand 1; NSCLC, non-small-cell lung cancer; ICIs, immune checkpoint inhibitors; Tg, thyroglobulin; ADs, autoimmune diseases; TOSOH, electrochemiluminescent immunoassay; ELISA, enzyme-linked immunosorbent assay; irAEs, immune related adverse events.

patients (49). It is manifested that these factors could be a prompting signal of PD-1-related toxicity occurrence.

Th1

CD4+ helper T cells (Th) 1 are key regulators in the tumor immune microenvironment and have a crucial role in activating cytotoxic T lymphocytes, participating in the pathological response process of inflammatory bowel disease (IBD) and rheumatoid arthritis (RA). Previous study showed that the subepithelial layer was enriched with CD4+ T cells in colitis induced by CTLA-4 inhibitors (50). The increased numbers of Th1 in tumors was reported to be associated with an improved response to immune therapies (51). By contrast, the presence of high CD4+ and low CD8+ tumor-infiltrating lymphocyte levels were independent predictors of poor progression-free survival (PFS), while the former was positively correlated with late tumor stage (52). Infiltration of Th1 in the colon suggested that the development of nivolumab-related colitis is associated with Th1 dominant response (53).

Serum Autoantibodies

Hypothyroidism was observed in 8.6% of metastatic melanoma patients treated with nivolumab (54), thyroid dysfunction has been reported to be one of the most frequent nivolumab-related adverse events. Compared with those patients free of thyroiditis, the baseline anti-thyroglobulin antibodies (TgAbs) and anti-thyroid peroxidase antibodies (TPOAbs) levels were significantly higher in destructive thyroiditis patients (41), the appearance of thyroid dysfunction during PD-1 treatment closely associated with anti-thyroid antibodies (55). Toi et al. (42) assessed the relationship between the safety and efficacy of anti-PD-1 treatment and preexisting autoimmune markers, found that the clinical outcomes, including PFS, ORR, and disease control rate, were significantly better among patients with any of the preexisting antibodies positive. Moreover, thyroid dysfunction was more frequent among patients with preexisting thyroid autoantibodies (TgAbs and TPOAbs) (20 vs. 1%, $P < 0.001$) while skin toxicities were more frequent among patients with preexisting rheumatoid factors (47 vs. 24%, $P = 0.02$). In addition, the pre-existing and early increasing ($\leq$4 weeks) serum thyroid autoantibodies levels were found to be associated with ICIs-related thyroid toxicities (43). The homology of tumor-associated antigen NY-ESO-1 with thyroid autoantigens leads to the cross presentation, which might partly explain the mechanisms of PD-1/PD-L1 related thyroid toxicities (56).

PD-1/PD-L1 related autoimmune diabetes (type 1 diabetes mellitus, T1DM) were rare with an incidence of 1% ∼53% of which had at least one positive islet autoantibody (57) and 21% had two or more (58). A Hispanic boy with insulin autoantibody and islet antigen 2 antibody-positive, was reported to suffer from T1DM which presented with acute progression to hyperglycemia and diabetic ketoacidosis after treated with pembrolizumab because of the progression of classical Hodgkin lymphoma (59). Briefly, the autoantibodies would be great potential predicting indicators for these endocrine toxicities with genetic disposition, which need to be detected before ICIs to assess risk.

Soluble Serum Proteins

Immune-mediated myocarditis was rare but presented unique clinical challenges due to non-specific presentation, exclusive diagnosis, and potentially life-threatening consequences, and the time-critical need to differentiate it from other causes of cardiac dysfunction. In some cases, the common cardiotoxicity markers, troponins, and BNP were found to be raised (60, 61), circulating anti-conductive tissue autoantibodies (ACTA) was suggested as a possible biomarker (62). The true incidence of ICIs-included cardiotoxicity is presently unknown, the biomarkers are needed for early identification and diagnosis of myocarditis because of the fatal consequences. Since the serum absolute levels of serum soluble CD163 (sCD163) and CXCL5 were significantly increased in patients who developed nivolumab-related toxicities, the absolute level of sCD163 and CXCL5 may serve as possible prognostic biomarkers (44). Besides, low serum albumin was reported as an independent risk factor for PD-1-related pneumonitis (63). The baseline and early increase (before 4 weeks) in serum thyroglobulin (Tg) levels were strongly associated with the development of thyroid irAEs (43). C-reactive protein (CRP) level and IL-6 were observed to reflect the clinical course of colitis clearly, which exposed the potentiality nivolumab-related toxicities predictive value (53).

HLA Genotypes

As we know, the human leukocyte antigen (HLA) genotypes are strongly associated with many kinds of autoimmune diseases. For example, the HLA B27 was identified as the susceptibility gene of ankylosing spondylitis (AS); HLA-DR3 was reported as the main predisposing allele for autoimmune thyroid diseases (64). Susceptible HLA genotypes dominated by DR4 were present in 76% patients with PD-1/PD-L1 related T1DM (58). The dominance of susceptible HLA genotypes indicates the potentiality in identifying patients who are at the highest risk of suffering from T1DM during ICIs treatment.

Biomarkers From the Host

Similarly to CTLA-4, compared with men, women were more likely to develop all grades of PD-1-related toxicities (mainly including pneumonitis and endocrinopathies). Interestingly, endocrinopathies were more common in premenopausal women than postmenopausal women or men (67 vs. 60 vs. 46%) (65). The female sex is known as one of the risk factors for autoimmune diseases, which provides us with an idea that differences in sex hormone levels in patients may affect the incidence of toxicity. It reminds us that in the era of precision treatment, we need to record the clinical characteristics and baseline hormone level status of patients before treatment in more detail.

Other Biomarkers

Because of the non-invasive, intuitive, and fast advantages, imaging examination plays an irreplaceable role for cancer patients in diagnosing, staging, curative effect evaluation, and adverse events detection in clinical practice. With the 18F-fluorodeoxyglucose (18F-FDG) positron emission tomography-computed tomography (PET/CT), thyroid gland diffuse increased 18F-FDG uptake was observed in majority of patients at the period of PD-1-related thyroid toxicities suffering (45, 46). the baseline thyroid uptake of 18F-FDG increased the risk of nivolumab induced thyroid toxicity development (47). Therefore, with dynamic imaging monitoring, the dynamic changes of thyroid 18F-FDG uptake may predict PD-1 related markers of thyroid toxicity. Additionally, with chest CT, the baseline fibrosis score $\geq$1 (0–5) was the only risk factor for PD-1-related pneumonitis (66).

COMBINED PREDICTIVE BIOMARKERS

Because of the similar onset mechanism, there were some overlaps between PD-1, PD-L1, and CTLA-4 blockades related toxicity spectra, indicating the presence of common predictors.

Biomarkers From Circulating Blood

Circulating Blood Cells

Since the elevated baseline neutrophil-to-lymphocyte ratio (NLR) and absolute neutrophil counts were significantly correlated with poor outcome data of immunotherapies, a neutrophil-based index was suggested as biomarkers for risk-group stratification (67). Neutrophils are the main components of inflammatory infiltration; higher-grade colitis was associated with endoscopic inflammation (68). Lamina propria infiltration by neutrophils was associated with the occurrence of dysregulation of gastrointestinal immunity after the CTLA-4 was blocked (16). Low NLR and low platelet-to-lymphocyte ratio at baseline were confirmed as independent predictive markers of the development of ICIs-related toxicities (69). Besides, early changes in B cells induced by inhibitors combined-treatment predicted higher rates of higher-grade ICIs-related-toxicities after therapy (70). Taken together these findings suggest a potential predictive role of circulating blood cells as markers for ICIs-related-toxicities development in a category of patients, which is easy to measure in daily practice.

Serum Pro-inflammatory Cytokines

Blood markers, such as the raised serum levels of lactate dehydrogenase and CRP were identified as risk factors for poor survival in patients treated with ICIs (71). In view of the finding of 11 significantly upregulated cytokines (including proinflammatory cytokines such as IL-1α, IL-2, and IFN-α2) in patients with severe toxicities at baseline and early during

ICIs treatment, these were integrated into a single toxicity score and validated to predict for high grade ICIs-related toxicities in patients treated with combination immunotherapy (72). In addition, a significant serum IL-6 levels increase in patients with psoriasis-afflicted or other ICIs-related toxicities after nivolumab treatment while decreases were observed in non-afflicted metastatic melanoma patients (49).

Anti-CTLA-4 antibodies could regulate the unfolding of autoimmune diabetes (73). PD-1/PD-L1 binding played an important role in preventing the onset of diabetes in mouse models (74). The existence of PD-1 or CTLA-4 genetic polymorphisms in humans was linked to series of autoimmune diseases (ADs) susceptibility, which mainly included RA, AS, T1DM, and graves' disease. For different genotypes, the correlation with ADs was inconsistent (75–77). Indeed, ICIs treatment can cause or exacerbate ADs including T1DM (78), Immune checkpoint-associated gene polymorphisms may be potential predictors of ICIs-related autoimmune toxicity, but still need to be validated in clinical practice.

Biomarkers From Tumor Microenvironment

Co-expression Antigens

A case report which made the post-mortem evaluation and analyzed the immune infiltrated tissues (including skeletal muscle and myocardium) and tumor in two melanoma patients suffered from fulminant myocarditis after the combination treatment with ipilimumab and nivolumab, presented the most abundant TCR type increases in one of the patients. Additionally, tumors in the two patients expressed abundant desmin and troponin which belonged to the muscle-specific antigen (61). These may be interpreted that the presence of common antigens between tumor and healthy tissue caused the myocarditis, supporting with recent views that the cross-presentation of shared antigens might lead to autoimmunity in patients treated with ICIs.

Tumor Burden

According to the Response Evaluation Criteria in Solid Tumors version 1.1 (RECST 1.1), tumor burden was defined as the sum of the longest diameters for a maximum of five target lesions and up to two lesions per organ and accessed by CT (79). A higher tumor burden was a significant independent predictor of severe irAEs ($P = 0.03$) (80) and poorer survival ($P < 0.01$) (79).

Biomarkers From the Host

ICIs may trigger a higher risk of toxicity among patients with pre-existing autoimmune disorders (ADs) or inflammatory diseases, which excluded such patients from most clinical trials involving ICIs therapy and the relevant data were limited (24). These situations led to a gap in clinical needs for those patients. Patients with pre-existing ADs (including RA, psoriasis, IBD, systemic lupus erythematosus, multiple sclerosis, and autoimmune thyroiditis) treated with ipilimumab, 50% of those experienced exacerbations of their autoimmune or grade 3–5 ICIs-related toxicities (24). Then, after identifying another 119 melanoma patients with pre-existing ADs and/or ipilimumab-related adverse events treated with PD-1 blockades, 38% patients experienced a flare of ADs requiring immunosuppression, 3% suffered a recurrence toxicity while 34% developed new toxicities (81). A 55% rate of patients developed an ADs flare and/or an ICIs-related toxicity in PD-1/PD-L1 antibodies treated NSCLC patients with ADs (82). A serious case of metastatic melanoma patients resumed PD-1 therapy after suffering from combination ICIs treated-related toxicities, ultimately, 39% of patients experienced clinically significant recurrent or distinct toxicities (83). Recently, multivariable analyses showed whether the pre-existing ADs identified by strict criteria or relaxed criteria were both associated with the ICIs-related toxicities diagnosis during hospitalization therapy resumption (84). These results consistently indicated that pre-existing ADs may be a predictor of toxicity. Notably, ICIs could be considered in this setting with vigilant clinical monitoring after a detailed and comprehensive assessment on the risk vs. benefit for each case.

As a matter of fact, ICIs-related toxicities in different tumor types showed a regular pattern. For instance, gastrointestinal and skin toxicities were more common in melanoma patients. Compared with melanoma, NSCLC had a higher rate of pneumonitis. Arthritis and myalgia happened more frequently in melanoma patients compared to renal cell carcinoma where pneumonitis and dyspnoea were more endemic (85).

Generally, PD-1-related toxicities were different from CTLA-4. Compared with PD-1 inhibitors, more high-grade toxicities occurred in patients treated with CTLA-4 inhibitors (86). Specifically, all grades colitis, hypophysis, and rash were more common with CTLA-4 inhibitors, whereas PD-1 inhibitors had increased risk for development of pneumonitis, hypothyroidism, arthralgia, and vitiligo (85). There was a greater risk of hyperthyroidism in patients with PD-1 inhibitors than PD-L1 inhibitors. Even as for PD-1 inhibitors, the rates of hyperthyroidism were significantly different between nivolumab and pembrolizumab (87). That is to say, the species of ICIs are closely related to the occurrence of different toxicities. For patients with different basic conditions, the choice of ICIs is important to the overall efficacy and safety of the patient.

Combination strategies of ICIs have been suggested to expose synergistic effects on the activation of anti-tumor immune response and increase the response rates in patients, which may offer promising future cancer treatments (88–90). Because of immunotherapy resistance or toxicity, sequential therapy with two or more ICIs to prolong survival in cancer patients is becoming more common in clinical practice (91). However, ICIs-based combination therapy leads to a relatively high incidence of ICIs-related toxicities coexisting with improved efficacy (92, 93). Severe ICIs-related pneumonitis (94), fulminant cardiotoxicities (95) or other severe toxicities (91) were observed in lung cancer patients re-treated with PD-(L)1 inhibitors after having experienced previous ICIs treatment, indicating that the sequential and combined use of ICIs treatment for patients may predict higher frequency of toxicity. Likewise, the incidence of ICIs-related pneumonitis was marginally higher in those lung cancer patients who received prior chest radiotherapy than patients who did not (96); Curative-intent chest radiotherapy

may increase the risk of any grade ICIs-related pneumonitis (97). Therefore, great caution is needed in patients receiving ICIs in combination or sequel.

DISCUSSIONS

Immunotherapy represents a major breakthrough for several cancers, but only 20–30% of patients with malignancies respond to ICIs. Unfortunately, the incidence of any-grade irAEs is more than 50%, including a significant proportion of serious and occasionally life-threatening irAEs, and treatment-related deaths occur in up to 2% of patients (98). Based on this, tumor immunotherapy requires the selection of the most beneficial population based on minimizing the risk of irAEs. Looking for highly efficient and specific predictive biomarkers is an urgent problem during the current stage of the explosive application of immunotherapy. Identification and investigation of potential biomarkers that may predict the development of ICIs-related toxicities are areas of active research. Several potential biomarkers have been reported to show the early predicative value of ICIs-related toxicities, which mainly taken from circulating blood, affected organs, tumor microenvironment, and clinical parameters.

Generally, biomarkers from affected organs or tumor microenvironments requires tissue biopsy, which is useful for predicting the biological behavior, especially for high heterogeneous tumor tissue (99). Besides, histopathological and immunohistochemical are mature clinical routine examination methods. However, tumor and immune microenvironments may change dynamically during tumor development and treatment. It is necessary to dynamically observe biomarkers to accurately reflect the actual state at different time points which requires repeated biopsy, but the invasive procedures are inevitable steps which are not allowed to be used often and may cause additional side effects such as infection. In these subtypes, the gut microbiota is an exceptional biomarker, as it can be collected from the patient's feces without intrusive steps. Therefore, it has unique clinical application value in this view and needs further verification in prospective studies. Compared with biopsy samples from tumor tissue, circulating blood sample is more available because of negligible invasion, it is an ideal access to monitor the shift of biomarkers in peripheral blood for predicting the development of ICIs-related toxicities. Circulating blood-based liquid biopsy holds a high position in oncology because of the unique advantages and wide clinical applications, such as estimating overall tumor heterogeneity, dynamic tracking temporal-based tumor heterogeneity, and assessing response to therapy early in real time (100). In the age of precision medicine, with the development of cutting-edge molecular diagnostics, soluble immune checkpoint molecule, exosomal protein, exosomal microRNA, circulating tumor cells (CTCs), and circulating tumor DNA (ctDNA) were established to be closely correlated with tumor diagnosis, staging, monitoring, and prognosis (100–105). These molecules played critical roles in tumorigenesis and tumor progression; therefore, they demonstrated a promising predictive value at the clinical treatment efficacy and ICIs-related adverse events. Advances in technologies such as sequencing will bring more translational research and clear mechanisms of action, making the treatment of cancer patients more personalized and efficient. For example, the pre-exciting thyroid autoantibodies were significantly associated with subsequent PD-1 related toxicities and with the clinical benefits (42). Some other potential clinical factors predictive for severe ICIs-related toxicities have also been proposed, including family history of ADs, tumors infiltration and location, previous viral infections (HIV or hepatitis B virus) and the concomitant use of medicines with known autoimmune toxicities (106, 107). Additionally, monitoring muscle attenuation, tumor burden and thyroid 18F-FDG uptake through imaging examinations is also the preferred solution, because it is relatively convenient, quick and non-invasive. From a practical clinical perspective, these data are relatively simple to collect and do not require additional financial burden on patients, most biomarkers are practical.

The oncologists should be familiar with every patient in detailed medical history and basic conditions (included but not limited to routine blood counts, lymphocyte typing, cytokine and autoantibody detection, and gender, age, basic immune status, and other general situation) before immunotherapy, watch out for any new or worsening symptoms as well as detailed and dynamic but comprehensive auxiliary inspection during the treatment, evaluate it in time and treat these toxicities. For example, tocilizumab can target inhibit IL-6 in order to prevent the increased of IL-6 and stop related toxicities (108); patients with high titer of TgAbs and TPOAbs who developed to grade 2 hypothyroidisms early take a moderate dosage of L-T4 therapy throughout (43). Then, a close follow up is also necessary after treatment.

Identification of biomarkers that predict the onset of ICIs-related toxicities has great relevance in clinical practice, as it could help identify patients earlier that are particularly susceptible to distinct forms of immunotherapy-induced adverse events, and consequently facilitate proper preemptive management and not only reduce the risk of severe toxicities, discontinuation of medication or obstruction of efficacy but also the costs of treatment. Since a single biomarker change is often related to a certain type of toxicity, it is necessary to increase the types of biomarker and combine them, with dynamic and continuous monitoring, in order to comprehensively analyze the risk of toxicity in patients and perform treatment, benefit in survival but also improve the quality of life on the premise of maximization.

In conclusion, we summarized multiple kinds of potential biomarkers and discussed their respective advantages and disadvantages. Firstly, additional studies are still needed to confirm the predictive value of potential biomarkers and identify other risk factors for irAEs to ICIs helping to determine the patients who are able to maximize the therapeutic benefits while minimizing irAEs. Secondly, with the changes of the immune microenvironment and tumor status in tumor patients at different stages, most biomarkers require dynamic monitoring and combined analyzing so as to predict the possible risks and development direction more comprehensively and accurately and deal with them in time. Thirdly, irAEs

predictive biomarkers are still in the exploratory stage recently. We insist that oncologists should examine different kinds of potential biomarkers as comprehensively as possible in clinical practice, to comprehensively assess the risk-benefit ratio for individual patients and maximize therapeutic benefits while minimizing irAEs. In the future, the focus should perhaps be on effective screening of the benefit-seeking population through the diversified detection based on liquid biopsy and the combination of new immune toxicities related biomarkers. Furthermore, precision strategy should be applied in irAE management according to patient's toxicity features associated with cellular and molecular mechanisms including T cell activation, and inflammatory responses.

AUTHOR CONTRIBUTIONS

YX, YF, BZ, JW, and BZ analyzed the literatures and studies and wrote the manuscript. YX and YF contributed equally to this work. All authors contributed to the article and approved the submitted version.

REFERENCES

1. Maio M, Grob JJ, Aamdal S, Bondarenko I, Robert C, Thomas L, et al. Five-year survival rates for treatment-naive patients with advanced melanoma who received ipilimumab plus dacarbazine in a phase III trial. *J Clin Oncol*. (2015) 33:1191–6. doi: 10.1200/JCO.2014.56.6018
2. Horn L, Spigel DR, Vokes EE, Holgado E, Ready N, Steins M, et al. Nivolumab versus docetaxel in previously treated patients with advanced non-small-cell lung cancer: two-year outcomes from two randomized, open-label, phase III trials (CheckMate 017 and CheckMate 057). *J Clin Oncol*. (2017) 35:3924–33. doi: 10.1200/JCO.2017.74.3062
3. Horn L, Mansfield AS, Szczesna A, Havel L, Krzakowski M, Hochmair MJ, et al. First-line atezolizumab plus chemotherapy in extensive-stage small-cell lung cancer. *N Engl J Med*. (2018) 379:2220–9. doi: 10.1056/NEJMoa1809064
4. Powles T, Eder JP, Fine GD, Braiteh FS, Loriot Y, Cruz C, et al. MPDL3280A (anti-PD-L1) treatment leads to clinical activity in metastatic bladder cancer. *Nature*. (2014) 515:558–62. doi: 10.1038/nature13904
5. Bellmunt J, de Wit R, Vaughn DJ, Fradet Y, Lee JL, Fong L, et al. Pembrolizumab as second-line therapy for advanced urothelial carcinoma. *N Engl J Med*. (2017) 376:1015–26. doi: 10.1056/NEJMoa1613683
6. Rowshanravan B, Halliday N, Sansom DM. CTLA-4: a moving target in immunotherapy. *Blood*. (2018) 131:58–67. doi: 10.1182/blood-2017-06-741033
7. Qureshi OS, Zheng Y, Nakamura K, Attridge K, Manzotti C, Schmidt EM, et al. Trans-endocytosis of CD80 and CD86: a molecular basis for the cell-extrinsic function of CTLA-4. *Science*. (2011) 332:600–3. doi: 10.1126/science.1202947
8. Hodi FS, O'Day SJ, McDermott DF, Weber RW, Sosman JA, Haanen JB, et al. Improved survival with ipilimumab in patients with metastatic melanoma. *N Engl J Med*. (2010) 363:711–23. doi: 10.1056/NEJMoa1003466
9. Xu C, Chen YP, Du XJ, Liu JQ, Huang CL, Chen L, et al. Comparative safety of immune checkpoint inhibitors in cancer: systematic review and network meta-analysis. *BMJ*. (2018) 363:k4226. doi: 10.1136/bmj.k4226
10. Ribas A, Kefford R, Marshall MA, Punt CJ, Haanen JB, Marmol M, et al. Phase III randomized clinical trial comparing tremelimumab with standard-of-care chemotherapy in patients with advanced melanoma. *J Clin Oncol*. (2013) 31:616–22. doi: 10.1200/JCO.2012.44.6112
11. Subudhi SK, Aparicio A, Gao J, Zurita AJ, Araujo JC, Logothetis CJ, et al. Clonal expansion of CD8 T cells in the systemic circulation precedes development of ipilimumab-induced toxicities. *Proc Natl Acad Sci U.S.A*. (2016) 113:11919–24. doi: 10.1073/pnas.1611421113
12. Oh DY, Cham J, Zhang L, Fong G, Kwek SS, Klinger M, et al. Immune toxicities elicted by CTLA-4 blockade in cancer patients are associated with early diversification of the T-cell repertoire. *Cancer Res*. (2017) 77:1322–30. doi: 10.1158/0008-5472.CAN-16-2324
13. Chaput N, Lepage P, Coutzac C, Soularue E, Le Roux K, Monot C, et al. Baseline gut microbiota predicts clinical response and colitis in metastatic melanoma patients treated with ipilimumab. *Ann Oncol*. (2017) 28:1368–79. doi: 10.1093/annonc/mdx108
14. Schindler K, Harmankaya K, Kuk D, Mangana J, Michielin O, Hoeller C, et al. Correlation of absolute and relative eosinophil counts with immune-related adverse events in melanoma patients treated with ipilimumab. *J Clin Oncol*. (2014) 32(Suppl. 15):9096. doi: 10.1200/jco.2014.32.15_suppl.9096
15. Coana YP, Wolodarski M, Poschke I, Yoshimoto Y, Yang Y, Nystrom M, et al. Ipilimumab treatment decreases monocytic MDSCs and increases CD8 effector memory T cells in long-term survivors with advanced melanoma. *Oncotarget*. (2017) 8:21539–53. doi: 10.18632/oncotarget.15368
16. Berman D, Parker SM, Siegel J, Chasalow SD, Weber J, Galbraith S, et al. Blockade of cytotoxic T-lymphocyte antigen-4 by ipilimumab results in dysregulation of gastrointestinal immunity in patients with advanced melanoma. *Cancer Immun*. (2010) 10:11.
17. Valpione S, Pasquali S, Campana LG, Piccin L, Mocellin S, Pigozzo J, et al. Sex and interleukin-6 are prognostic factors for autoimmune toxicity following treatment with anti-CTLA4 blockade. *J Transl Med*. (2018) 16:94. doi: 10.1186/s12967-018-1467-x
18. Callahan MK, Yang A, Tandon S, Xu Y, Subudhi SK, Roman RA, et al. Evaluation of serum IL-17 levels during ipilimumab therapy: correlation with colitis. *J Clin Oncol*. (2011) 29(Suppl. 15):2505. doi: 10.1200/jco.2011.29.15_suppl.2505
19. Tarhini AA, Zahoor H, Lin Y, Malhotra U, Sander C, Butterfield LH, et al. Baseline circulating IL-17 predicts toxicity while TGF-beta1 and IL-10 are prognostic of relapse in ipilimumab neoadjuvant therapy of melanoma. *J Immunother Cancer*. (2015) 3:39. doi: 10.1186/s40425-015-0081-1
20. Felix J, Cassinat B, Porcher R, Schlageter MH, Maubec E, Pages C, et al. Relevance of serum biomarkers associated with melanoma during follow-up of anti-CTLA-4 immunotherapy. *Int Immunopharmacol*. (2016) 40:466–73. doi: 10.1016/j.intimp.2016.09.030
21. Iwama S, De Remigis A, Callahan MK, Slovin SF, Wolchok JD, Caturegli P. Pituitary expression of CTLA-4 mediates hypophysitis secondary to administration of CTLA-4 blocking antibody. *Sci Transl Med*. (2014) 6:230ra45. doi: 10.1126/scitranslmed.3008002
22. Dubin K, Callahan MK, Ren B, Khanin R, Viale A, Ling L, et al. Intestinal microbiome analyses identify melanoma patients at risk for checkpoint-blockade-induced colitis. *Nat Commun*. (2016) 7:10391. doi: 10.1038/ncomms10391
23. Daly LE, Power DG, O'Reilly A, Donnellan P, Cushen SJ, O'Sullivan K, et al. The impact of body composition parameters on ipilimumab toxicity and survival in patients with metastatic melanoma. *Br J Cancer*. (2017) 116:310–7. doi: 10.1038/bjc.2016.431
24. Johnson DB, Sullivan RJ, Ott PA, Carlino MS, Khushalani NI, Ye F, et al. Ipilimumab therapy in patients with advanced melanoma and preexisting autoimmune disorders. *JAMA Oncol*. (2016) 2:234–40. doi: 10.1001/jamaoncol.2015.4368
25. Cha E, Klinger M, Hou Y, Cummings C, Ribas A, Faham M, et al. Improved survival with T cell clonotype stability after anti-CTLA-4 treatment in cancer patients. *Sci Transl Med*. (2014) 6:238ra70. doi: 10.1126/scitranslmed.3008211
26. Zhang Y, Du X, Liu M, Tang F, Zhang P, Ai C, et al. Hijacking antibody-induced CTLA-4 lysosomal degradation for safer and more effective cancer immunotherapy. *Cell Res*. (2019) 29:609–27. doi: 10.1038/s41422-019-0184-1
27. Liu Y, Zheng P. Preserving the CTLA-4 checkpoint for safer and more effective cancer immunotherapy. *Trends Pharmacol Sci*. (2020) 41:4–12. doi: 10.1016/j.tips.2019.11.003
28. Johncilla M, Misdraji J, Pratt DS, Agoston AT, Lauwers GY, Srivastava A, et al. Ipilimumab-associated hepatitis: clinicopathologic

characterization in a series of 11 cases. *Am J Surg Pathol*. (2015) 39:1075–84. doi: 10.1097/PAS.0000000000000453
29. Lacouture ME, Wolchok JD, Yosipovitch G, Kahler KC, Busam KJ, Hauschild A. Ipilimumab in patients with cancer and the management of dermatologic adverse events. *J Am Acad Dermatol*. (2014) 71:161–9. doi: 10.1016/j.jaad.2014.02.035
30. Hodi FS, Mihm MC, Soiffer RJ, Haluska FG, Butler M, Seiden MV, et al. Biologic activity of cytotoxic T lymphocyte-associated antigen 4 antibody blockade in previously vaccinated metastatic melanoma and ovarian carcinoma patients. *Proc Natl Acad Sci U.S.A*. (2003) 100:4712–7. doi: 10.1073/pnas.0830997100
31. Kloess S, Huenecke S, Piechulek D, Esser R, Koch J, Brehm C, et al. IL-2-activated haploidentical NK cells restore NKG2D-mediated NK-cell cytotoxicity in neuroblastoma patients by scavenging of plasma MICA. *Eur J Immunol*. (2010) 40:3255–67. doi: 10.1002/eji.201040568
32. Huang B, Sikorski R, Sampath P, Thorne SH. Modulation of NKG2D-ligand cell surface expression enhances immune cell therapy of cancer. *J Immunother*. (2011) 34:289–96. doi: 10.1097/CJI.0b013e31820e1b0d
33. Shahabi V, Berman D, Chasalow SD, Wang L, Tsuchihashi Z, Hu B, et al. Gene expression profiling of whole blood in ipilimumab-treated patients for identification of potential biomarkers of immune-related gastrointestinal adverse events. *J Transl Med*. (2013) 11:75. doi: 10.1186/1479-5876-11-75
34. Friedlander P, Wood K, Wassmann K, Christenfeld AM, Bhardwaj N, Oh WK. A whole-blood RNA transcript-based gene signature is associated with the development of CTLA-4 blockade-related diarrhea in patients with advanced melanoma treated with the checkpoint inhibitor tremelimumab. *J Immunother Cancer*. (2018) 6:90. doi: 10.1186/s40425-018-0408-9
35. Faith JJ, Ahern PP, Ridaura VK, Cheng J, Gordon JI. Identifying gut microbe-host phenotype relationships using combinatorial communities in gnotobiotic mice. *Sci Transl Med*. (2014) 6:220ra11. doi: 10.1126/scitranslmed.3008051
36. Morganstein DL, Lai Z, Spain L, Diem S, Levine D, Mace C, et al. Thyroid abnormalities following the use of cytotoxic T-lymphocyte antigen-4 and programmed death receptor protein-1 inhibitors in the treatment of melanoma. *Clin Endocrinol*. (2017) 86:614–20. doi: 10.1111/cen.13297
37. Ascierto PA, Del Vecchio M, Robert C, Mackiewicz A, Chiarion-Sileni V, Fernandez AMA, et al. Overall survival (OS) and safety results from a phase 3 trial of ipilimumab (IPI) at 3 mg/kg vs 10 mg/kg in patients with metastatic melanoma (MEL). *Ann Oncol*. (2016) 27(Suppl. 6):vi379. doi: 10.1093/annonc/mdw379.01
38. Bertrand A, Kostine M, Barnetche T, Truchetet ME, Schaeverbeke T. Immune related adverse events associated with anti-CTLA-4 antibodies: systematic review and meta-analysis. *BMC Med*. (2015) 13:211. doi: 10.1186/s12916-015-0455-8
39. Topalian SL, Hodi FS, Brahmer JR, Gettinger SN, Smith DC, McDermott DF, et al. Safety, activity, and immune correlates of anti-PD-1 antibody in cancer. *N Engl J Med*. (2012) 366:2443–54. doi: 10.1056/NEJMoa1200690
40. Fujisawa Y, Yoshino K, Otsuka A, Funakoshi T, Fujimura T, Yamamoto Y, et al. Fluctuations in routine blood count might signal severe immune-related adverse events in melanoma patients treated with nivolumab. *J Dermatol Sci*. (2017) 88:225–31. doi: 10.1016/j.jdermsci.2017.07.007
41. Kobayashi T, Iwama S, Yasuda Y, Okada N, Tsunekawa T, Onoue T, et al. Patients with antithyroid antibodies are prone to develop destructive thyroiditis by nivolumab: a prospective study. *J Endocr Soc*. (2018) 2:241–51. doi: 10.1210/js.2017-00432
42. Toi Y, Sugawara S, Sugisaka J, Ono H, Kawashima Y, Aiba T, et al. Profiling preexisting antibodies in patients treated with anti-PD-1 therapy for advanced non-small cell lung cancer. *JAMA Oncol*. (2019) 5:376–83. doi: 10.1001/jamaoncol.2018.5860
43. Kurimoto C, Inaba H, Ariyasu H, Iwakura H, Ueda Y, Uraki S, et al. Predictive and sensitive biomarkers for thyroid dysfunctions during treatment with immune-checkpoint inhibitors. *Cancer Sci*. (2020) 111:1468–77. doi: 10.1111/cas.14363
44. Fujimura T, Sato Y, Tanita K, Kambayashi Y, Otsuka A, Fujisawa Y, et al. Serum levels of soluble CD163 and CXCL5 may be predictive markers for immune-related adverse events in patients with advanced melanoma treated with nivolumab: a pilot study. *Oncotarget*. (2018) 9:15542–51. doi: 10.18632/oncotarget.24509
45. De Filette J, Jansen Y, Schreuer M, Everaert H, Velkeniers B, Neyns B, et al. Incidence of thyroid-related adverse events in melanoma patients treated with pembrolizumab. *J Clin Endocrinol Metab*. (2016) 101:4431–39. doi: 10.1210/jc.2016-2300
46. Delivanis DA, Gustafson MP, Bornschlegl S, Merten MM, Kottschade L, Withers S, et al. Pembrolizumab-induced thyroiditis: comprehensive clinical review and insights into underlying involved mechanisms. *J Clin Endocrinol Metab*. (2017) 102:2770–80. doi: 10.1210/jc.2017-00448
47. Yamauchi I, Yasoda A, Matsumoto S, Sakamori Y, Kim YH, Nomura M, et al. Incidence, features, and prognosis of immune-related adverse events involving the thyroid gland induced by nivolumab. *PLoS ONE*. (2019) 14:e0216954. doi: 10.1371/journal.pone.0216954
48. Nakamura Y, Tanaka R, Maruyama H, Ishitsuka Y, Okiyama N, Watanabe R, et al. Correlation between blood cell count and outcome of melanoma patients treated with anti-PD-1 antibodies. *Jpn J Clin Oncol*. (2019) 49:431–7. doi: 10.1093/jjco/hyy201
49. Tanaka R, Okiyama N, Okune M, Ishitsuka Y, Watanabe R, Furuta J, et al. Serum level of interleukin-6 is increased in nivolumab-associated psoriasiform dermatitis and tumor necrosis factor-alpha is a biomarker of nivolumab recativity. *J Dermatol Sci*. (2017) 86:71–3. doi: 10.1016/j.jdermsci.2016.12.019
50. Coutzac C, Adam J, Soularue E, Collins M, Racine A, Mussini C, et al. Colon immune-related adverse events: anti-CTLA-4 and anti-PD-1 blockade induce distinct immunopathological entities. *J Crohns Colitis*. (2017) 11:1238–46. doi: 10.1093/ecco-jcc/jjx081
51. Gooden MJ, de Bock GH, Leffers N, Daemen T, Nijman HW. The prognostic influence of tumour-infiltrating lymphocytes in cancer: a systematic review with meta-analysis. *Br J Cancer*. (2011) 105:93–103. doi: 10.1038/bjc.2011.189
52. Han S, Zhang C, Li Q, Dong J, Liu Y, Huang Y, et al. Tumour-infiltrating CD4(+) and CD8(+) lymphocytes as predictors of clinical outcome in glioma. *Br J Cancer*. (2014) 110:2560–68. doi: 10.1038/bjc.2014.162
53. Yoshino K, Nakayama T, Ito A, Sato E, Kitano S. Severe colitis after PD-1 blockade with nivolumab in advanced melanoma patients: potential role of Th1-dominant immune response in immune-related adverse events: two case reports. *BMC Cancer*. (2019) 19:1019. doi: 10.1186/s12885-019-6138-7
54. Larkin J, Chiarion-Sileni V, Gonzalez R, Grob JJ, Cowey CL, Lao CD, et al. Combined nivolumab and ipilimumab or monotherapy in untreated melanoma. *N Engl J Med*. (2015) 373:23–34. doi: 10.1056/NEJMoa1504030
55. Osorio JC, Ni A, Chaft JE, Pollina R, Kasler MK, Stephens D, et al. Antibody-mediated thyroid dysfunction during T-cell checkpoint blockade in patients with non-small-cell lung cancer. *Ann Oncol*. (2017) 28:583–9. doi: 10.1093/annonc/mdw640
56. Vita R, Guarneri F, Agah R, Benvenga S. Autoimmune thyroid disease elicited by NY-ESO-1 vaccination. *Thyroid*. (2014) 24:390–4. doi: 10.1089/thy.2013.0170
57. De Filette JMK, Pen JJ, Decoster L, Vissers T, Bravenboer B, Van der Auwera BJ, et al. Immune checkpoint inhibitors and type 1 diabetes mellitus: a case report and systematic review. *Eur J Endocrinol*. (2019) 181:363–74. doi: 10.1530/EJE-19-0291
58. Stamatouli AM, Quandt Z, Perdigoto AL, Clark PL, Kluger H, Weiss SA, et al. Collateral damage: insulin-dependent diabetes induced with checkpoint inhibitors. *Diabetes*. (2018) 67:1471–80. doi: 10.2337/dbi18-0002
59. Samoa RA, Lee HS, Kil SH, Roep BO. Anti-PD-1 therapy associated type 1 diabetes in a pediatric patient with relapsed classical Hodgkin lymphoma. *Diabetes Care*. (2020) 43:2293–95. doi: 10.2337/dc20-0740
60. Laubli H, Balmelli C, Bossard M, Pfister O, Glatz K, Zippelius A. Acute heart failure due to autoimmune myocarditis under pembrolizumab treatment for metastatic melanoma. *J Immunother Cancer*. (2015) 3:11. doi: 10.1186/s40425-015-0057-1
61. Johnson DB, Balko JM, Compton ML, Chalkias S, Gorham J, Xu Y, et al. Fulminant myocarditis with combination immune checkpoint blockade. *N Engl J Med*. (2016) 375:1749–55. doi: 10.1056/NEJMoa1609214
62. Caio G. Myocarditis with immune checkpoint blockade. *N Engl J Med*. (2017) 376:291–2. doi: 10.1056/NEJMc1615251
63. Fukihara J, Sakamoto K, Koyama J, Ito T, Iwano S, Morise M, et al. Prognostic impact and risk factors of immune-related pneumonitis in patients with

non-small-cell lung cancer who received programmed death 1 inhibitors. *Clin Lung Cancer*. (2019) 20:442–50.e444. doi: 10.1016/j.cllc.2019.07.006
64. Inaba H, De Groot LJ, Akamizu T. Thyrotropin receptor epitope and human leukocyte antigen in graves' disease. *Front Endocrinol*. (2016) 7:120. doi: 10.3389/fendo.2016.00120
65. Duma N, Abdel-Ghani A, Yadav S, Hoversten KP, Reed CT, Sitek AN, et al. Sex differences in tolerability to anti-programmed cell death protein 1 therapy in patients with metastatic melanoma and non-small cell lung cancer: are we all equal? *Oncologist*. (2019) 24:e1148–55. doi: 10.1634/theoncologist.2019-0094
66. Yamaguchi T, Shimizu J, Hasegawa T, Horio Y, Inaba Y, Yatabe Y, et al. Pre-existing pulmonary fibrosis is a risk factor for anti-PD-1-related pneumonitis in patients with non-small cell lung cancer: a retrospective analysis. *Lung Cancer*. (2018) 125:212–17. doi: 10.1016/j.lungcan.2018.10.001
67. Ferrucci PF, Ascierto PA, Pigozzo J, Del Vecchio M, Maio M, Antonini Cappellini GC, et al. Baseline neutrophils and derived neutrophil-to-lymphocyte ratio: prognostic relevance in metastatic melanoma patients receiving ipilimumab. *Ann Oncol*. (2016) 27:732–8. doi: 10.1093/annonc/mdw016
68. Wang Y, Abu-Sbeih H, Mao E, Ali N, Qiao W, Trinh VA, et al. Endoscopic and histologic features of immune checkpoint inhibitor-related colitis. *Inflamm Bowel Dis*. (2018) 24:1695–705. doi: 10.1093/ibd/izy104
69. Pavan A, Calvetti L, Dal Maso A, Attili I, Del Bianco P, Pasello G, et al. Peripheral blood markers identify risk of immune-related toxicity in advanced non-small cell lung cancer treated with immune-checkpoint inhibitors. *Oncologist*. 24:1128–36. doi: 10.1634/theoncologist.2018-0563
70. Das R, Bar N, Ferreira M, Newman AM, Zhang L, Bailur JK, et al. Early B cell changes predict autoimmunity following combination immune checkpoint blockade. *J Clin Invest*. (2018) 128:715–20. doi: 10.1172/JCI 96798
71. Heppt MV, Heinzerling L, Kahler KC, Forschner A, Kirchberger MC, Loquai C, et al. Prognostic factors and outcomes in metastatic uveal melanoma treated with programmed cell death-1 or combined PD-1/cytotoxic T-lymphocyte antigen-4 inhibition. *Eur J Cancer*. (2017) 82:56–65. doi: 10.1016/j.ejca.2017.05.038
72. Lim SY, Lee JH, Gide TN, Menzies AM, Guminski A, Carlino MS, et al. Circulating cytokines predict immune-related toxicity in melanoma patients receiving anti-PD-1-based immunotherapy. *Clin Cancer Res*. (2019) 25:1557–63. doi: 10.1158/1078-0432.CCR-18-2795
73. Luhder F, Hoglund P, Allison JP, Benoist C, Mathis D. Cytotoxic T lymphocyte-associated antigen 4 (CTLA-4) regulates the unfolding of autoimmune diabetes. *J Exp Med*. (1998) 187:427–32. doi: 10.1084/jem.187.3.427
74. Rajasalu T, Brosi H, Schuster C, Spyrantis A, Boehm BO, Chen L, et al. Deficiency in B7-H1 (PD-L1)/PD-1 coinhibition triggers pancreatic beta-cell destruction by insulin-specific, murine CD8 T-cells. *Diabetes*. (2010) 59:1966–73. doi: 10.2337/db09-1135
75. Lee YH, Bae SC, Kim JH, Song GG. Meta-analysis of genetic polymorphisms in programmed cell death 1. Associations with rheumatoid arthritis, ankylosing spondylitis, and type 1 diabetes susceptibility. *Z Rheumatol*. (2015) 74:230–9. doi: 10.1007/s00393-014-1415-y
76. Gunavathy N, Asirvatham A, Chitra A, Jayalakshmi M. Association of CTLA-4 and CD28 gene polymorphisms with type 1 diabetes in South Indian population. *Immunol Invest*. (2019) 48:659–71. doi: 10.1080/08820139.2019.1590395
77. Chen X, Hu Z, Liu M, Li H, Liang C, Li W, et al. Correlation between CTLA-4 and CD40 gene polymorphisms and their interaction in graves' disease in a Chinese Han population. *BMC Med Genet*. (2018) 19:171. doi: 10.1186/s12881-018-0665-y
78. Gauci ML, Boudou P, Baroudjian B, Vidal-Trecan T, Da Meda L, Madelaine-Chambrin I, et al. Occurrence of type 1 and type 2 diabetes in patients treated with immunotherapy (anti-PD-1 and/or anti-CTLA-4) for metastatic melanoma: a retrospective study. *Cancer Immunol Immunother*. (2018) 67:1197–208. doi: 10.1007/s00262-018-2178-0
79. Dercle L, Ammari S, Champiat S, Massard C, Ferte C, Taihi L, et al. Rapid and objective CT scan prognostic scoring identifies metastatic patients with long-term clinical benefit on anti-PD-1/-L1 therapy. *Eur J Cancer*. (2016) 65:33–42. doi: 10.1016/j.ejca.2016.05.031
80. Sakata Y, Kawamura K, Ichikado K, Shingu N, Yasuda Y, Eguchi Y, et al. The association between tumor burden and severe immune-related adverse events in non-small cell lung cancer patients responding to immune-checkpoint inhibitor treatment. *Lung Cancer*. (2019) 130:159–61. doi: 10.1016/j.lungcan.2019.02.011
81. Menzies AM, Johnson DB, Ramanujam S, Atkinson VG, Wong ANM, Park JJ, et al. Anti-PD-1 therapy in patients with advanced melanoma and preexisting autoimmune disorders or major toxicity with ipilimumab. *Ann Oncol*. (2017) 28:368–76. doi: 10.1093/annonc/mdw443
82. Leonardi GC, Gainor JF, Altan M, Kravets S, Dahlberg SE, Gedmintas L, et al. Safety of programmed death-1 pathway inhibitors among patients with non-small-cell lung cancer and preexisting autoimmune disorders. *J Clin Oncol*. (2018) 36:1905–12. doi: 10.1200/JCO.2017.77.0305
83. Pollack MH, Betof A, Dearden H, Rapazzo K, Valentine I, Brohl AS, et al. Safety of resuming anti-PD-1 in patients with immune-related adverse events (irAEs) during combined anti-CTLA-4 and anti-PD1 in metastatic melanoma. *Ann Oncol*. (2018) 29:250–5. doi: 10.1093/annonc/mdx642
84. Kehl KL, Yang S, Awad MM, Palmer N, Kohane IS, Schrag D. Pre-existing autoimmune disease and the risk of immune-related adverse events among patients receiving checkpoint inhibitors for cancer. *Cancer Immunol Immunother*. (2019) 68:917–26. doi: 10.1007/s00262-019-02321-z
85. Khoja L, Day D, Wei-Wu Chen T, Siu LL, Hansen AR. Tumour- and class-specific patterns of immune-related adverse events of immune checkpoint inhibitors: a systematic review. *Ann Oncol*. (2017) 28:2377–85. doi: 10.1093/annonc/mdx286
86. Robert C, Schachter J, Long GV, Arance A, Grob JJ, Mortier L, et al. Pembrolizumab versus ipilimumab in advanced melanoma. *N Engl J Med*. (2015) 372:2521–32. doi: 10.1056/NEJMoa1503093
87. Barroso-Sousa R, Barry WT, Garrido-Castro AC, Hodi FS, Min L, Krop IE, et al. Incidence of endocrine dysfunction following the use of different immune checkpoint inhibitor regimens: a systematic review and meta-analysis. *JAMA Oncol*. (2018) 4:173–82. doi: 10.1001/jamaoncol.2017.3064
88. Boutros C, Tarhini A, Routier E, Lambotte O, Ladurie FL, Carbonnel F, et al. Safety profiles of anti-CTLA-4 and anti-PD-1 antibodies alone and in combination. *Nat Rev Clin Oncol*. (2016) 13:473–86. doi: 10.1038/nrclinonc.2016.58
89. Rotte A. Combination of CTLA-4 and PD-1 blockers for treatment of cancer. *J Exp Clin Cancer Res*. (2019) 38:255. doi: 10.1186/s13046-019-1259-z
90. Rotte A, Jin JY, Lemaire V. Mechanistic overview of immune checkpoints to support the rational design of their combinations in cancer immunotherapy. *Ann Oncol*. (2018) 29:71–83. doi: 10.1093/annonc/mdx686
91. Santini FC, Rizvi H, Plodkowski AJ, Ni A, Lacouture ME, Gambarin-Gelwan M, et al. Safety and efficacy of re-treating with immunotherapy after immune-related adverse events in patients with NSCLC. *Cancer Immunol Res*. (2018) 6:1093–9. doi: 10.1158/2326-6066.CIR-17-0755
92. Wolchok JD, Chiarion-Sileni V, Gonzalez R, Rutkowski P, Grob JJ, Cowey CL, et al. Overall survival with combined nivolumab and ipilimumab in advanced melanoma. *N Engl J Med*. (2017) 377:1345–56. doi: 10.1056/NEJMoa1910836
93. Hellmann MD, Callahan MK, Awad MM, Calvo E, Ascierto PA, Atmaca A, et al. Tumor mutational burden and efficacy of nivolumab monotherapy and in combination with ipilimumab in small-cell lung cancer. *Cancer Cell*. (2018) 33:853–61.e4. doi: 10.1016/j.ccell.2018.04.001
94. Liang X, Guan Y, Zhang B, Liang J, Wang B, Li Y, et al. Severe immune-related pneumonitis with PD-1 inhibitor after progression on previous PD-L1 inhibitor in small cell lung cancer: a case report and review of the literature. *Front Oncol*. (2019) 9:1437. doi: 10.3389/fonc.2019.01437
95. Liu SY, Huang WC, Yeh HI, Ko CC, Shieh HR, Hung CL, et al. Sequential blockade of PD-1 and PD-L1 causes fulminant cardiotoxicity-from case report to mouse model validation. *Cancers*. (2019) 11:580. doi: 10.3390/cancers11040580
96. Hwang WL, Niemierko A, Hwang KL, Hubbeling H, Schapira E, Gainor JF, et al. Clinical outcomes in patients with metastatic lung cancer treated with PD-1/PD-L1 inhibitors and thoracic radiotherapy. *JAMA Oncol*. (2018) 4:253–5. doi: 10.1001/jamaoncol.2017.3808
97. Voong KR, Hazell SZ, Fu W, Hu C, Lin CT, Ding K, et al. (2019). Relationship between prior radiotherapy and checkpoint-inhibitor pneumonitis in patients with advanced non-small-cell lung cancer. *Clin Lung Cancer*. 20:e470–9. doi: 10.1016/j.cllc.2019.02.018

98. Puzanov I, Diab A, Abdallah K, Bingham CO, Brogdon C, Dadu R, et al. Managing toxicities associated with immune checkpoint inhibitors: consensus recommendations from the Society for Immunotherapy of Cancer (SITC) Toxicity Management Working Group. *J Immunother Cancer*. (2017) 5:95. doi: 10.1186/s40425-017-0300-z
99. Shioga T, Kondo R, Ogasawara S, Akiba J, Mizuochi S, Kusano H, et al. Usefulness of tumor tissue biopsy for predicting the biological behavior of hepatocellular carcinoma. *Anticancer* Res. (2020) 40:4105–13. doi: 10.21873/anticanres.14409
100. Diaz LA, JR, Bardelli A. Liquid biopsies: genotyping circulating tumor DNA. *J Clin Oncol*. (2014) 32:579–86. doi: 10.1200/JCO.2012.45.2011
101. Gu D, Ao X, Yang Y, Chen Z, Xu X. Soluble immune checkpoints in cancer: production, function and biological significance. *J Immunother Cancer*. (2018) 6:132. doi: 10.1186/s40425-018-0449-0
102. Li W, Li C, Zhou T, Liu X, Liu X, Li X, et al. Role of exosomal proteins in cancer diagnosis. *Mol Cancer*. (2017) 16:145. doi: 10.1186/s12943-017-0706-8
103. Bidard FC, Peeters DJ, Fehm T, Nole F, Gisbert-Criado R, Mavroudis D, et al. Clinical validity of circulating tumour cells in patients with metastatic breast cancer: a pooled analysis of individual patient data. *Lancet Oncol*. (2014) 15:406–14. doi: 10.1016/S1470-2045(14)70069-5
104. De Rubis G, Rajeev Krishnan S, Bebawy M. Liquid biopsies in cancer diagnosis, monitoring, and prognosis. *Trends Pharmacol Sci*. (2019) 40:172–86. doi: 10.1016/j.tips.2019.01.006
105. He Y, Deng F, Yang S, Wang D, Chen X, Zhong S, et al. Exosomal microRNA: a novel biomarker for breast cancer. *Biomark Med*. (2018) 12:177–88. doi: 10.2217/bmm-2017-0305
106. Champiat S, Lambotte O, Barreau E, Belkhir R, Berdelou A, Carbonnel F, et al. Management of immune checkpoint blockade dysimmune toxicities: a collaborative position paper. *Ann Oncol*. (2016) 27:559–74. doi: 10.1093/annonc/mdv623
107. Manson G, Norwood J, Marabelle A, Kohrt H, Houot R. Biomarkers associated with checkpoint inhibitors. *Ann Oncol*. (2016) 27:1199–206. doi: 10.1093/annonc/mdw181
108. Amlani A, Barber C, Fifi-Mah A, Monzon J. Successful treatment of cytokine release syndrome with IL-6 blockade in a patient transitioning from immune-checkpoint to MEK/BRAF inhibition: a case report and review of literature. *Oncologist*. (2020) 25:e1120–23. doi: 10.1634/theoncologist.2020-0194

Conflict of Interest: The authors declare that the research was conducted in the absence of any commercial or financial relationships that could be construed as a potential conflict of interest.

frontiers in Immunology

ORIGINAL RESEARCH
published: 09 October 2020
doi: 10.3389/fimmu.2020.563653

Pretreatment Peripheral B Cells Are Associated With Tumor Response to Anti-PD-1-Based Immunotherapy

*Shumin Yuan[1], Yuqing Liu[2], Brian Till[3], Yongping Song[4] and Zibing Wang[1]**

[1] Department of Immunotherapy, Affiliated Cancer Hospital of Zhengzhou University & Henan Cancer Hospital, Zhengzhou, China, [2] Third Affiliated Hospital of Xinxiang Medical College, Xinxiang, China, [3] Clinical Research Division, Fred Hutchinson Cancer Research Center, Seattle, WA, United States, [4] Department of Hematology, Affiliated Cancer Hospital of Zhengzhou University & Henan Cancer Hospital, Zhengzhou, China

Identification of reliable biomarkers to predict efficacy of immune checkpoint inhibitors and to monitor relapse in cancer patients receiving this therapy remains one of the main objectives of cancer immunotherapy research. We found that the pretreatment B cell number in the peripheral blood differed significantly between responders and non-responders to anti-PD-1-based immunotherapy. Patients with various cancer types achieving a clinical response had a significantly lower number of B cells compared with those with progressive disease. Patients who progressed from partial response to progressive disease exhibited a gradually increased number of circulating B cells. Our findings suggest that B cells represent a promising biomarker for anti-PD-1-based immunotherapy responses and inhibit the effect of PD-1 blockade immunotherapy. Thus, preemptive strategies targeting B cells may increase the efficacy of PD-1 blockade immunotherapy in patients with solid tumors.

Keywords: immunotherapy, immune checkpoint inhibitor, PD-1, biomarker, B cells

OPEN ACCESS

Edited by:
Said Dermime, National Center for Cancer Care and Research, Qatar

Reviewed by:
Zong Sheng Guo, University of Pittsburgh, United States
Ala-Eddin Al Moustafa, Qatar University, Qatar
Monther Al-alwan, King Faisal Specialist Hospital & Research Centre, Saudi Arabia

***Correspondence:**
Zibing Wang
zlyywzb2118@zzu.edu.cn

Specialty section:
This article was submitted to Cancer Immunity and Immunotherapy, a section of the journal Frontiers in Immunology

Received: *19 May 2020*
Accepted: *13 August 2020*
Published: *09 October 2020*

Citation:
Yuan S, Liu Y, Till B, Song Y and Wang Z (2020) Pretreatment Peripheral B Cells Are Associated With Tumor Response to Anti-PD-1-Based Immunotherapy. Front. Immunol. 11:563653. doi: 10.3389/fimmu.2020.563653

INTRODUCTION

Therapeutic blocking of the programmed death-1 (PD-1) pathway has recently been shown to be a promising strategy for treating solid tumors, rendering long-term survival possible (1). However, only a minority of patients benefit from this treatment. Identification of reliable predictors of response to PD-1 blockade is therefore of utmost importance for determining the most appropriate therapy candidates. PD-L1 overexpression is the most logical biomarker to predict patient response to anti-PD-1 therapy; however, various shortcomings limit its clinical utility, including variability in detection antibodies and differing immunohistochemistry cutoffs (2). Other reports suggest that potential biomarkers could include tumor-infiltrating lymphocytes, mutational burden, and immune gene signatures (3). However, the main obstacle for these biomarkers is the need to obtain tumor biopsies, which is often not feasible, especially for patients with poor performance status or who need to begin therapy urgently. More importantly, even the use of these tumor-based factors fails to reliably identify potentially responsive patients.

Blood is the ideal biological specimen for identifying biomarkers, due to its availability. Hence, analysis of circulating biomarkers as an alternative method is much more convenient for clinical application. Recently, several studies have reported that the proportion of circulating myeloid-derived suppressor cells (MDSCs) differed significantly between responders and non-responders following immunotherapy; patients with a lower frequency of MDSCs had enhanced immune responses when compared with patients who had high MDSC levels (4–8). Furthermore, a recent

TABLE 1 | Characteristics of patients enrolled in this study.

	Number (*n*, %)	BCELL (%)	TCELL (%)	NKCELL (%)
Tumor type	Malignant melanoma (*n* = 11, 13.92%)	10.05 ± 1.83	68.30 ± 3.04	15.66 ± 2.10
	Lung cancer (*n* = 16, 20.25%)	8.36 ± 0.5	65.79 ± 2.15	21.30 ± 2.44
	Sarcoma (*n* = 8, 10.13%)	7.45 ± 2.36	70.85 ± 2.40	17.1 ± 2.65
	Renal carcinoma (*n* = 12, 15.19%)	7.08 ± 1.78	72.14 ± 2.68	16.72 ± 3.07
	Mammary cancer (*n* = 3, 3.80%)	12.77 ± 1.98	61.63 ± 4.64	19.97 ± 4.04
	Cervical carcinoma (*n* = 5, 6.33%)	21.22 ± 7.49	58.78 ± 10.24	20.78 ± 9.50
	Liver cancer (*n* = 7, 8.86%)	8.81 ± 2.11	66.24 ± 4.07	22.71 ± 4.59
	Lymphoma (*n* = 3, 3.80%)	7.87 ± 5.59	72.17 ± 3.07	17.05 ± 2.38
	Pancreatic cancer (*n* = 2, 2.53%)	4.59 ± 0.35	66.60 ± 8.50	21.05 ± 0.25
	Thymic carcinoma (*n* = 2, 2.53%)	29 ± 26.5	52.40 ± 28.60	12.85 ± 9.15
	Esophageal cancer (*n* = 22.53%)	7.65 ± 1.25	57.20 ± 4.50	26.55 ± 1.65
	Oophoroma (*n* = 1, 1.27%)			
	Oropharynx malignant tumor (*n* = 1, 1.27%)			
	Ulreter carcinoma (*n* = 1, 1.27%)			
	Orchioncus (*n* = 1, 1.27%)			
	Carcinoma tubae (*n* = 1, 1.27%)			
	Gallbladder carcinoma (*n* = 1, 1.27%)			
	Intramedullary glioma (*n* = 1, 1.27%)			
	Vular cystadenocarcinoma (*n* = 1, 1.27%)			
Gender	Male (*n* = 42, 53.16%)	7.14 ± 0.87	67.73 ± 1.53	19.20 ± 1.51
	Female (*n* = 37, 46.84%)	13.32 ± 1.83	65.73 ± 2.2	17.52 ± 1.56
Age (years)	≤65 (*n* = 66, 83.54%)	11.05 ± 1.18	66.68 ± 1.43	18.94 ± 1.49
	>65 (*n* = 13, 16.46%)	5.65 ± 1.01	67.37 ± 3.32	22.66 ± 2.68
Clinical response	PD (*n* = 36, 45.57%)	13.24 ± 1.39	65.09 ± 1.66	17.58 ± 1.67
	SD (*n* = 18, 22.78%)	7.21 ± 1.31	70.05 ± 2.26	18.16 ± 1.92
	PR (*n* = 25, 31.65%)	7.47 ± 2.18	66.92 ± 2.95	21.92 ± 2.36

study found that a set of MDSC-related microRNAs are associated with resistance to treatment with immune checkpoint inhibitors (9). These studies suggest that circulating MDSCs are a potential biomarker for predicting the response to immunotherapy. A recent study investigated the correlation between circulating B cells and clinical response as well as adverse effects in 39 patients with advanced melanoma receiving anti-PD-1 or anti-cytotoxic T lymphocyte-associated protein 4 (CTLA-4) therapy alone, or in combination (10). Although this study did not find a correlation between B cells and clinical response to immunotherapy, it demonstrated that checkpoint blockade immunotherapy led to changes in circulating B cells (10).

In the present study, we set out to identify a reliable biomarker that can be used to predict the response to anti-PD-1-based immunotherapy, and our results strongly suggest that pretreatment levels of B cells are highly predictive of immunotherapy response.

MATERIALS AND METHODS

Study Subjects and Samples

Whole peripheral blood samples from cancer patients were aseptically collected by venipuncture before or after anti-PD-1-based immunotherapy and prepared using a stain-lyse-no-wash procedure to provide white blood cells labeled with fluorescence-linked CD3, CD4, CD8, CD19, CD45, CD16, and CD56 antibodies (BD Multitest 6-color TBNK reagent). Lymphocyte absolute counts and subset percentages are automatically calculated using BD FACSCanto clinical software. The absolute numbers (cells/μL) of positive cells in the sample are determined by comparing cellular events to bead events. The percentages of subsets are obtained by gating the lymphocyte population.

Statistical Analysis

Data were analyzed using GraphPad Prism Software (GraphPad Software Inc.). Unless otherwise indicated, the results are presented as mean ± standard deviation. The results were analyzed using 2-tailed unpaired or paired Student's *t*-tests. A *p*-value <0.05 was considered significant.

RESULTS

Patients and Treatments

A total of 79 patients treated with anti-PD-1-based therapy were included in the study. A detailed listing of patients and treatment characteristics is presented in **Table 1**. All patients received at least one prior systemic

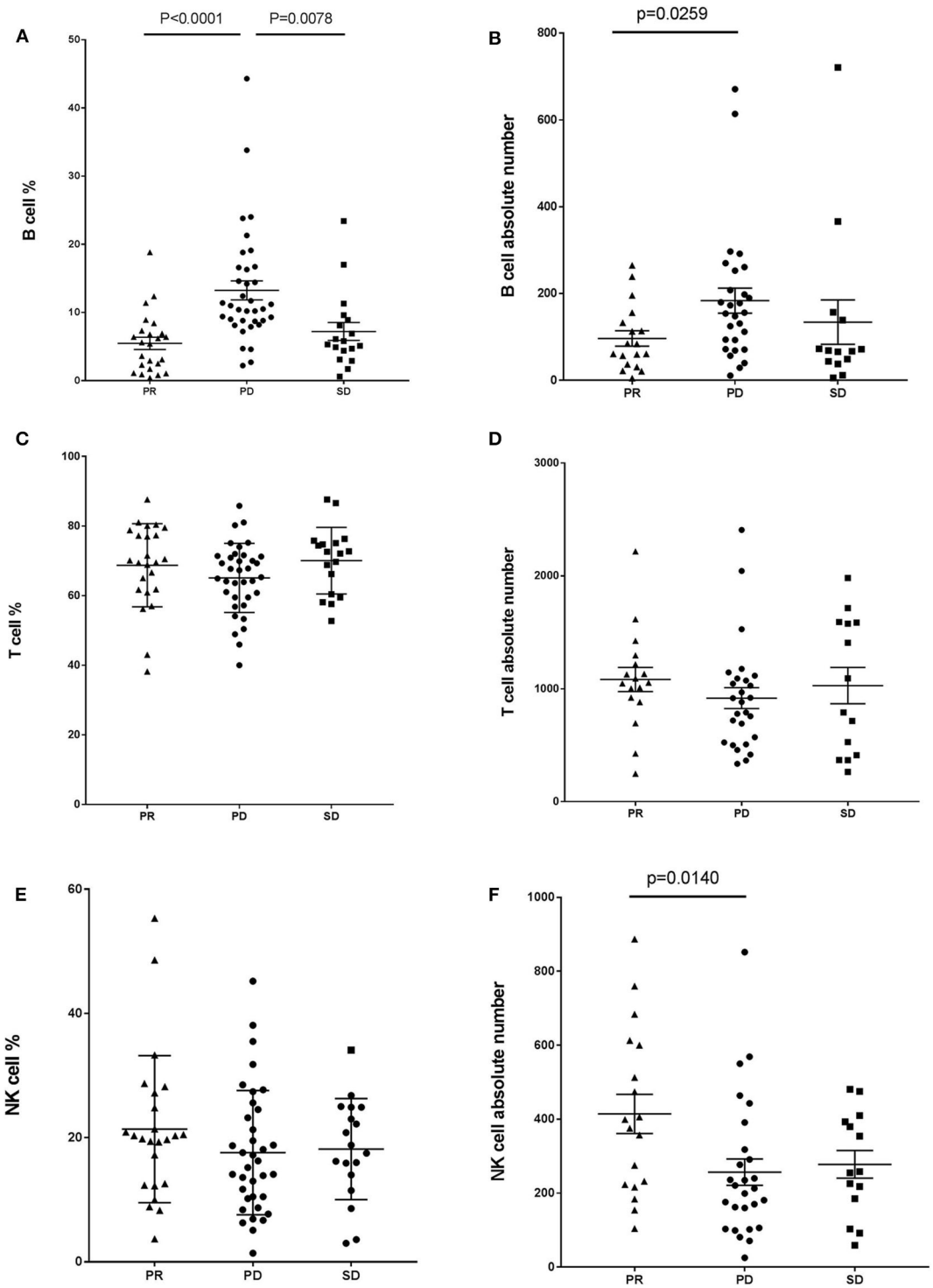

FIGURE 1 | Baseline B cell number correlates with response in cancer patients with anti-PD-1-based immunotherapy. Whole blood cells, obtained from patients before treatment with anti-PD-1-based therapy, were stained and analyzed using flow cytometry. Shown are baseline frequencies, which were expressed as a percentage of total lymphocytes (gated from an CD45 PerCP vs. SSC dot plot) according to clinical response, and absolute number, which were expressed as cells/μL of B cells **(A,B)**, T cells **(C,D)**, and NK cells **(E,F)**. A *t*-test was conducted to test for differences between groups.

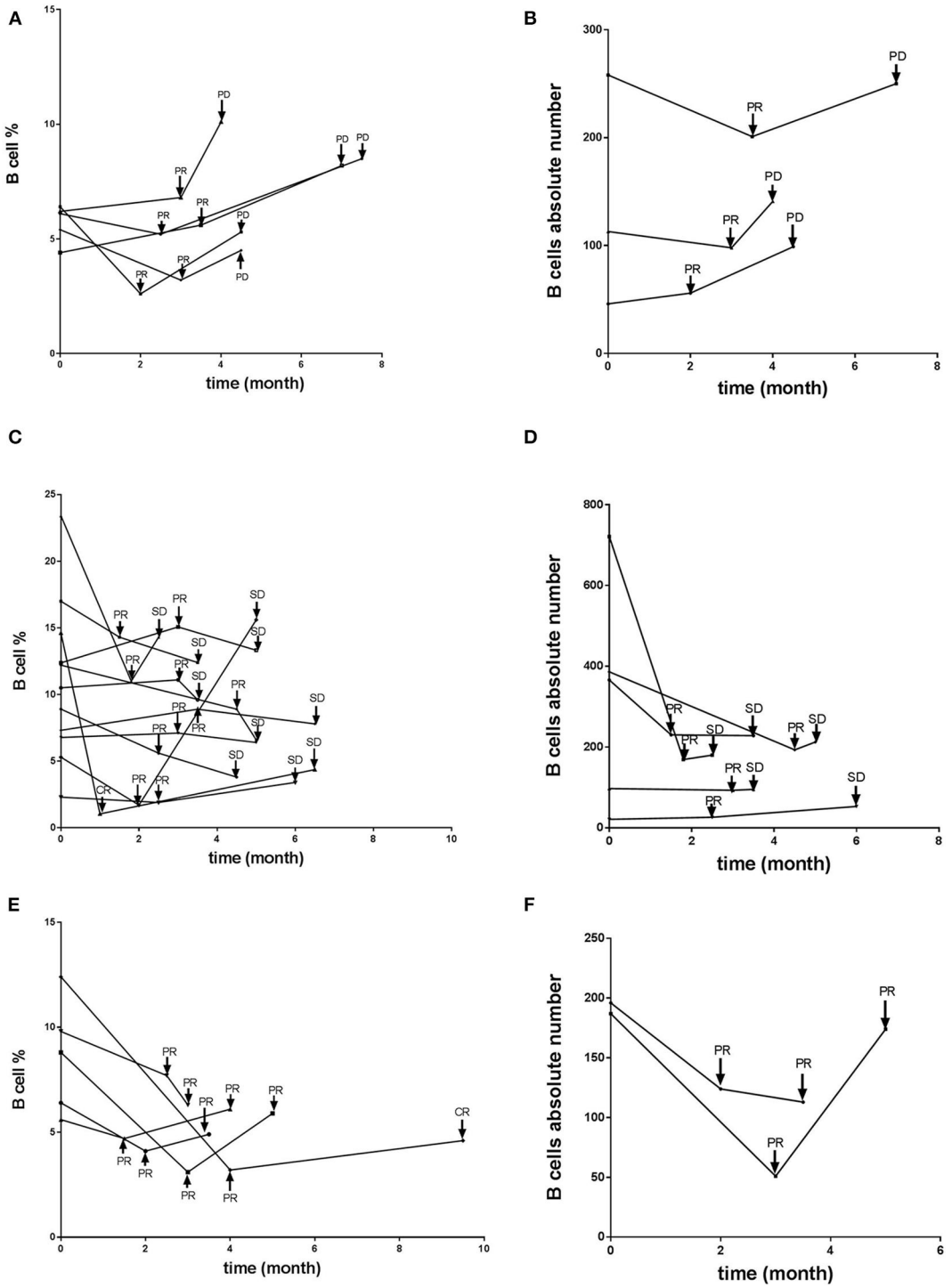

FIGURE 2 | B cell number correlates with progression in patients with PR receiving anti-PD-1-based immunotherapy. Whole blood cells, obtained from patients with PR before and at various timepoints after treatment receiving anti-PD-1-based therapy, were stained and analyzed using flow cytometry. Shown are changes of B cell percentages and absolute numbers in patients with PR who **(A,B)** later developed PD over time, with time of relapse shown with arrows, **(C,D)** maintained stable disease, or **(E,F)** further improved the PR over time.

treatment before anti-PD-1-based therapy. Combination immunotherapy approaches involved chemotherapy, radiotherapy, antiangiogenic therapy, and adoptive T-cell therapy. The tumor response was assessed in accordance with the Response Evaluation Criteria In Solid Tumors (RECIST) 1.1. This approach has four response categories:

complete response (CR), partial response (PR), stable disease (SD) and progressive disease (PD). Of response-evaluable patients, 31.7% achieved a PR, 22.8% had SD, and 45.6% developed PD, which resulted in a disease control rate of 54.4% (**Table 1**).

Baseline B Cell Number Correlates With Efficacy in Cancer Patients With Anti-PD-1-Based Immunotherapy

We analyzed the absolute lymphocyte counts and lymphocyte subset percentages in the peripheral blood of 78 cancer patients prior to treatment with anti-PD-1-based therapy and evaluated the association with clinical efficacy. A significant difference in the proportion of B cells between responders and non-responders to combination immunotherapy was observed. Patients achieving a PR had a significantly lower frequency of CD19+ B cells compared with that in the patients with PD (**Figure 1A**). We also found this difference in patients with SD when comparing with patients with PD (**Figure 1A**). In contrast, no difference was observed in the frequency of CD3+ T cells or CD16+CD56+ natural killer (NK) cells between patients with PD and PR (**Figures 1C,E**). In addition, no difference was observed in the proportion of T cells or NK cells between patients with PD and SD (**Figures 1C,E**). Similar results were observed when absolute numbers of lymphocyte subsets were analyzed (**Figures 1B,D**), except that the value of NK cells was higher in PR patients (**Figure 1F**). Together, these results indicated that the frequency of B cells in the peripheral blood is associated with efficacy of immunotherapy and might be a potential biomarker for predicting response in patients who receive anti-PD-1-based therapy.

B Cell Frequency Correlates With Progression in Patients With PR Receiving Anti-PD-1-Based Immunotherapy

We next explored whether B cell frequency is able to predict tumor relapse in patients who achieve a PR. Among the 21 patients who achieved a PR, five progressed to PD (PR-PD), 11 exhibited no change (PR-SD), and five had further improvement in their PR over time (PR-PR). B cell counts and imaging studies were performed after every 2–4 cycles of PD-1-based anti-tumor therapy. Most of the patients who progressed from PR to PD exhibited a gradually increased number of circulating B cells (**Figures 2A,B**), which was not observed in patients who maintained SD or had an improved PR (**Figures 2C–F**). We also evaluated the association between T cells as well as NK cells and tumor development. No changes were observed whether these patients with PR further improved the PR, maintained SD, or developed PD (data not shown). As of the most recent follow-up, none of the patients in PR-PR or PR-SD groups have relapsed. Together, these data indicate that B cell number might represent a reliable biomarker for monitoring tumor relapse in patients with PR.

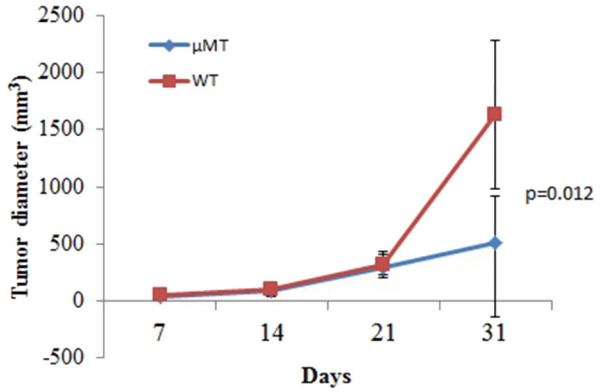

FIGURE 3 | B cell absence leads to delay of tumor growth. WT or μMT mice were injected s.c. with 1 × 105 TSA tumor cells and observed for 31 days ($n = 5$ in each group). Three-dimensional tumor growth was serially measured using calipers and tumor volumes calculated. The average tumor volume (± SD) among all the mice in each group over time is shown.

B Cell Absence Leads to Delay of Tumor Growth

The aforementioned clinical observation that B cell number is associated with tumor growth suggested that B cell presence might be detrimental to anti-tumor immunity of the host. We tested this hypothesis using a murine model of mammary carcinoma. TSA cells were injected s.c. at day 0 into both syngeneic immunocompetent BALB/c mice as well as μMT mice, which lack B cells but produce normal levels of granulocytes and CD4+ and CD8+ T cells (11). As shown in **Figure 3**, tumors in the wild-type mice proliferated rapidly. In contrast, the rate of proliferation was significantly reduced in μMT mice. Together, these data suggest that absence of B cells enhances anti-tumor responses.

DISCUSSION

In the present study, we retrospectively reviewed patients treated with anti-PD-1-based therapy at our center in recent years. We found that patients who developed PD following therapy had a higher number of B cells than those achieving SD and PR, suggesting that B cells in the peripheral blood may impact the efficacy of PD-1-based immunotherapy and might be a potential biomarker for patients who receive this treatment. In addition, an increase in B cell frequency may also be a biomarker identifying patients at high risk for imminent cancer progression after an initial response. These findings need to be confirmed in larger prospective studies enrolling patients with specific cancer types, since this study included a wide variety of cancers.

This study is consistent with our previously published finding that the presence of B cells inhibits induction of T cell-dependent anti-tumor immunity (11). In that study, μMT mice immunized with irradiated TSA cells and challenged 2 weeks later with a lethal dose of the same tumor typically rejected the tumor, whereas nearly all wild-type mice developed a tumor (11). These

data suggested, consistent with the present results, that B cells are possibly another negative regulatory factor, in addition to PD-1/PD-L1 co-inhibitory signals, in inducing immune tolerance. PD-1 blockade in combination with B cell inactivation or depletion might be a promising way to achieve more potent responses in tumor immunotherapy.

In conclusion, the data reported herein show that B cells represent a potential predictive biomarker for anti-PD-1-based immunotherapy responses. Preemptive strategies targeting B cells and/or MDSCs may increase the efficacy of PD-1 blockade immunotherapy in patients with solid tumors.

DATA AVAILABILITY STATEMENT

The raw data supporting the conclusions of this article will be made available by the authors, without undue reservation.

ETHICS STATEMENT

The study protocol was approved by the IRB of Affiliated Cancer Hospital of Zhengzhou University. All participants gave their informed written consent.

AUTHOR CONTRIBUTIONS

SY and YL performed experiments, analyzed data, and wrote the manuscript. BT, YS, and ZW analyzed data and edited the manuscript. ZW designed and supervised the study.

FUNDING

This work was supported by National Natural Science Foundation of China (Grant Nos. 81972690, 81000914, and 81272526).

ACKNOWLEDGMENTS

The authors thank Dr. Torsten Juelich for linguistic assistance during the preparation of this manuscript.

SUPPLEMENTARY MATERIAL

The Supplementary Material for this article can be found online at: https://www.frontiersin.org/articles/10.3389/fimmu.2020.563653/full#supplementary-material

REFERENCES

1. Ribas A, Wolchok JD. Cancer immunotherapy using checkpoint blockade. *Science.* (2018) 359:1350–5. doi: 10.1126/science.aar4060
2. Patel SP, Kurzrock R. PD-L1 expression as a predictive biomarker in cancer immunotherapy. *Mol Cancer Ther.* (2015) 14:847–56. doi: 10.1158/1535-7163.MCT-14-0983
3. Gibney GT, Weiner LM, Atkins MB. Predictive biomarkers for checkpoint inhibitor-based immunotherapy. *Lancet Oncol.* (2016) 17:e542–51. doi: 10.1016/S1470-2045(16)30406-5
4. Finkelstein SE, Iclozan C, Bui MM, Cotter MJ, Ramakrishnan R, Ahmed J, et al. Combination of external beam radiotherapy (EBRT) with intratumoral injection of dendritic cells as neo-adjuvant treatment of high-risk soft tissue sarcoma patients. *Int J Radiat Oncol Biol Phys.* (2012) 82:924–32. doi: 10.1016/j.ijrobp.2010.12.068
5. Kitano S, Postow MA, Ziegler CG, Kuk D, Panageas KS, Cortez C, et al. Computational algorithm-driven evaluation of monocytic myeloid-derived suppressor cell frequency for prediction of clinical outcomes. *Cancer Immunol Res.* (2014) 2:812–21. doi: 10.1158/2326-6066.CIR-14-0013
6. Meyer C, Cagnon L, Costa-Nunes CM, Baumgaertner P, Montandon N, Leyvraz L, et al. Frequencies of circulating MDSC correlate with clinical outcome of melanoma patients treated with ipilimumab. *Cancer Immunol Immunother.* (2014) 63:247–57. doi: 10.1007/s00262-013-1508-5
7. Martens A, Wistuba-Hamprecht K, Foppen MG, Yuan J, Postow MA, Wong P, et al. Baseline peripheral blood biomarkers associated with clinical outcome of advanced melanoma patients treated with ipilimumab. *Clin Cancer Res.* (2016) 22:2908–18. doi: 10.1158/1078-0432.CCR-15-2412
8. Gebhardt C, Sevko A, Jiang H, Lichtenberger R, Reith M, Tarnanidis K, et al. Myeloid cells and related chronic inflammatory factors as novel predictive markers in melanoma treatment with ipilimumab. *Clin Cancer Res.* (2015) 21:5453–9. doi: 10.1158/1078-0432.CCR-15-0676
9. Huber V, Vallacchi V, Fleming V, Hu X, Cova A, Dugo M, et al. Tumor-derived microRNAs induce myeloid suppressor cells and predict immunotherapy resistance in melanoma. *J Clin Invest.* (2018) 128:5505–16. doi: 10.1172/JCI98060
10. Das R, Bar N, Ferreira M, Newman AM, Zhang L, Bailur JK, et al. Early B cell changes predict autoimmunity following combination immune checkpoint blockade. *J Clin Invest.* (2018) 128:715–20. doi: 10.1172/JCI96798
11. Qin Z, Richter G, Schuler T, Ibe S, Cao X, Blankenstein T. B cells inhibit induction of T cell-dependent tumor immunity. *Nat Med.* (1998) 4:627–30. doi: 10.1038/nm0598-627

Conflict of Interest: The authors declare that the research was conducted in the absence of any commercial or financial relationships that could be construed as a potential conflict of interest.

frontiers in Immunology

REVIEW
published: 14 October 2020
doi: 10.3389/fimmu.2020.587014

Characteristics of TCR Repertoire Associated With Successful Immune Checkpoint Therapy Responses

*Joel Kidman[1,2], Nicola Principe[1,2], Mark Watson[3], Timo Lassmann[4], Robert A. Holt[5], Anna K. Nowak[1,6], Willem Joost Lesterhuis[1,2,4], Richard A. Lake[1,2] and Jonathan Chee[1,2]**

[1] National Centre for Asbestos Related Diseases, Institute of Respiratory Health, University of Western Australia, Perth, WA, Australia, [2] School of Biomedical Sciences, University of Western Australia, Perth, WA, Australia, [3] Institute for Immunology and Infectious Diseases, Murdoch University, Perth, WA, Australia, [4] Telethon Kids Institute, Perth, WA, Australia, [5] Canada's Michael Smith Genome Sciences Centre, Vancouver, BC, Canada, [6] School of Medicine, University of Western Australia, Perth, WA, Australia

OPEN ACCESS

Edited by:
Said Dermime,
National Center for Cancer Care and Research, Qatar

Reviewed by:
Anastasia Minervina,
Institute of Bioorganic Chemistry (RAS), Russia
Benny Chain,
University College London, United Kingdom

***Correspondence:**
Jonathan Chee
jonathan.chee@uwa.edu.au

Specialty section:
This article was submitted to Cancer Immunity and Immunotherapy, a section of the journal Frontiers in Immunology

Received: 24 July 2020
Accepted: 23 September 2020
Published: 14 October 2020

Citation:
Kidman J, Principe N, Watson M, Lassmann T, Holt RA, Nowak AK, Lesterhuis WJ, Lake RA and Chee J (2020) Characteristics of TCR Repertoire Associated With Successful Immune Checkpoint Therapy Responses. Front. Immunol. 11:587014. doi: 10.3389/fimmu.2020.587014

Immunotherapies have revolutionized cancer treatment. In particular, immune checkpoint therapy (ICT) leads to durable responses in some patients with some cancers. However, the majority of treated patients do not respond. Understanding immune mechanisms that underlie responsiveness to ICT will help identify predictive biomarkers of response and develop treatments to convert non-responding patients to responding ones. ICT primarily acts at the level of adaptive immunity. The specificity of adaptive immune cells, such as T and B cells, is determined by antigen-specific receptors. T cell repertoires can be comprehensively profiled by high-throughput sequencing at the bulk and single-cell level. T cell receptor (TCR) sequencing allows for sensitive tracking of dynamic changes in antigen-specific T cells at the clonal level, giving unprecedented insight into the mechanisms by which ICT alters T cell responses. Here, we review how the repertoire influences response to ICT and conversely how ICT affects repertoire diversity. We will also explore how changes to the repertoire in different anatomical locations can better correlate and perhaps predict treatment outcome. We discuss the advantages and limitations of current metrics used to characterize and represent TCR repertoire diversity. Discovery of predictive biomarkers could lie in novel analysis approaches, such as network analysis of amino acids similarities between TCR sequences. Single-cell sequencing is a breakthrough technology that can link phenotype with specificity, identifying T cell clones that are crucial for successful ICT. The field of immuno-sequencing is rapidly developing and cross-disciplinary efforts are required to maximize the analysis, application, and validation of sequencing data. Unravelling the dynamic behavior of the TCR repertoire during ICT will be highly valuable for tracking and understanding anti-tumor

immunity, biomarker discovery, and ultimately for the development of novel strategies to improve patient outcomes.

Keywords: checkpoint immunotherapy, tumor immunology, T cell receptor, immunogenomics, dynamic analysis

INTRODUCTION

Immunotherapies that harness T cell responses against cancer have changed cancer treatment. Therapies such as immune checkpoint therapy (ICT) and adoptive T cell transfer now play a critical role in the treatment of solid and blood malignancies. In-depth understanding of the biology that underlies immunotherapy success or failure is crucial for treatment monitoring and improving current therapies. Cutting edge high-throughput sequencing and flow cytometry have enabled multi-faceted profiling of T cells, evaluating immune receptor composition, antigen specificity, epigenetic and functional status of T cells, greatly contributing to our understanding of how the anti-tumor T cell responds especially in the context of ICT.

ICT IS A REVOLUTIONARY CANCER THERAPY, BUT NOT ALL PATIENTS RESPOND

Treatment with antibodies that block inhibitory receptors, such as cytotoxic T lymphocyte associated protein 4 (CTLA-4), programmed death receptor 1 (PD-1), or its ligand PD-L1, can lead to durable complete responses in some patients depending on the cancer type (1). CTLA-4 blockade has been the most successful in metastatic melanoma, while responses in other cancers such as non-small cell lung (NSCLC) (2, 3), Hodgkin's lymphoma (4), Merkel-cell carcinoma (5), triple-negative breast cancer (6), renal cell carcinoma (7), urothelial bladder (8, 9) and squamous cell carcinoma of the head and neck (10) are common with anti-PD-1/PD-L1 therapy.

Despite these promising results, it is difficult to predict whether an individual will benefit from ICT or not. ICT removes T cell suppression indiscriminately, causing immune related adverse events in up to 90% of treated patients, with serious autoimmune-like toxicity observed in approximately 2–5% of treated patients (11). Immune related adverse events are observed with either anti-CTLA-4 or anti-PD1/L1 therapy and increase in incidence with combination therapy. ICT is also expensive, costing approximately USD6,000 to 20,000 per patient each month, depending on the cancer type and treatment schedule (12). Importantly, only a minority of patients respond to ICT, highlighting a need to develop accurate biomarkers of response. The most clinically advanced, pre-treatment biomarkers of ICT responses include $CD8^+$ T cell tumor infiltration (13, 14), intra-tumoral PD-L1 expression (13, 15), tumor mutation burden and neo-antigen burden (16, 17). However, these have poor positive and negative predictive value as pre-treatment biomarkers of ICT response and are not reproducible across all cancers.

MEASUREMENTS OF DYNAMIC CHANGE IN THE IMMUNE SYSTEM COULD OFFER A BIOMARKER OF ICT RESPONSE

Although a pre-treatment predictor of ICT response would be ideal, an early on-treatment biomarker could also have value. We previously argued the therapeutic response to ICT can be visualized as a critical state transition of a complex system because of its dichotomous nature; some patients experience rapid tumor regression, but other patients do not benefit from ICT at all (18). In such complex, highly connected systems, not all determinants of response can be found in pre-treatment. Small differences in the initial state (*e.g.* minor differences in T cell repertoire) can be easily amplified in cascading events, resulting in a dramatic shift in the system state. Biomarkers could be identified between the start of treatment and when the critical state transition occurs. In the context of ICT, dynamic changes in features of the immune system, such as the T cell repertoire shortly after initiation of treatment, could inform ICT responses and biomarker development. We envisage that a dynamic biomarker will complement existing ones and facilitate clinical decisions once treatment has started. For example, dynamic biomarkers would allow the identification of patients with 'pseudoprogression' (an initial increase in tumor diameter due to immune cell infiltration and edema, followed by regression) who would benefit from continuing therapy, and it would identify early-on patients who will not benefit, thus limiting side effects and reducing the substantial costs associated with continued treatment. Characterizing the T cell repertoire is useful for developing potential dynamic biomarkers of ICT response, and there are different technologies used to approach this.

SEQUENCING TECHNOLOGY IS IMPORTANT FOR THE CHARACTERIZATION OF TCR REPERTOIRES

Fine characterization of T cell repertoires is made possible by the application of high-throughput sequencing. Immune specificity is derived from T cell receptors (TCRs) expressed on the surface of all T cells that bind to peptides in the context of major histocompatibility complex (MHC) proteins. Conventional T cells express a vast range of TCRs, and each TCR is typically composed of a heterodimer of α and β chains. This diversity is generated during random, somatic rearrangement of variable (V), joining (J), and diversity (D) gene segments in TCR chains (19). Most TCR diversity arises from the β chain because it

utilizes an additional D segment (**Figure 1**). Furthermore, the process of gene rearrangement adds and removes random nucleotides between segments (20), forming a hyper-variable third complementarity-determining region (CDR3) that is a key component of specificity. Although an upper bound of 10^{16} possible unique TCR$\alpha\beta$ pairs can occur, 10^4 unique TCRβs can be typically routinely sampled in human peripheral blood samples (21, 22). In this review, we refer to TCR repertoire as the collection of TCRs within a given T cell population.

Sequencing across the CDR3 region of TRBV gene in either bulk populations of cells or at the single-cell level can be used to fingerprint a repertoire (21, 23, 24). There are several well-established TCR sequencing protocols, which involve targeted PCRs to generate amplicons across the CDR3 region. We briefly review commonly used protocols, as in-depth assessment and head-to-head comparisons of different techniques have been reviewed elsewhere (25–27).

TCR sequencing libraries can be prepared from genomic DNA (gDNA) or messenger RNA (mRNA) starting material, both with pros and cons (28). Essentially, DNA is more stable and can be isolated from frozen or FFPE samples, whereas there are more TCR RNA transcripts compared to the single copy of rearranged DNA. Multiple fixed forward and reverse primers specific to TCR Vβ, and TCR Jβ gene segments respectively are used in multiplex PCRs to generate TCR libraries (24). Because there are multiple TCR Vβ and TCR Jβ gene combinations, multiplex PCR is required to cover most variations (24). The benefit of the DNA approach is the direct quantification of single TCR clones as each T cell contains one TCRβ gene rearrangement. However, transcriptional information is only contained in RNA. Both RNA and gDNA based TCRseq have well documented methods and choosing one is dependent on individual use cases.

5′ rapid amplification of cDNA ends (5′RACE) with template switching oligonucleotides is the most widely used RNA based approach to generate TCR sequencing libraries (29). This approach incorporates an adaptor site at the 5′ end of a TCR template during first strand synthesis, paired with a 3′ primer specific for the TCR constant region. Subsequent PCR amplification is performed with primers specific for 3′ end and the 5′ adaptor sequence. 5′RACE is widely used because it circumvents the need for multiple fixed primers. RNA approaches measure expressed TCRβs, but quantification of clonal expansion is challenging when sequencing bulk populations of T cells, because multiple copies of the same TCR could be expressed within a single cell (30). In a recent study, matched samples underwent single-cell and bulk TCR sequencing, and the proportion of each unique TCRβ sequence highly correlated between the two approaches (31). This suggests that TCR transcript counts detected by bulk TCRseq can be representative of T cell clonal expansion, rather than increased expression of TCRs in a limited number of cells.

Regardless of starting material, PCR-based approaches are often susceptible to amplification bias, which distort the relative abundances of the sequenced products. A challenge lies in distinguishing genuine rare clones from sequencing errors, especially if sequences differ by a few nucleotides. Errors can be corrected during analysis. For example, low frequency TCR clones are often clustered with highly similar clones with significantly greater frequencies because it is more likely the sequence differences arising from these clones are due to error. We also highlight the utility of unique molecular identifiers

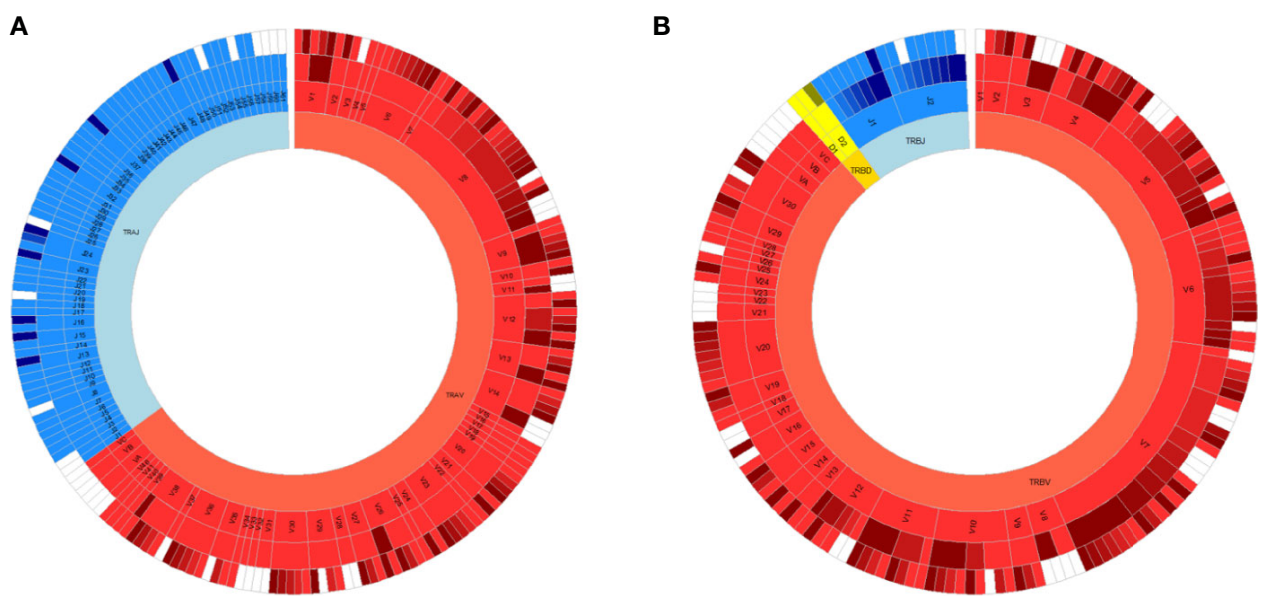

FIGURE 1 | All germline VDJ gene segments of the human T cell receptor. Variable (V) genes in red, diversity (D) genes in yellow and joining (J) genes in blue. From outmost ring to innermost ring are the V (D)J sub-group, V (D)J group, and alpha **(A)**/beta **(B)** chains. Non-functional alleles are in white.

(UMIs) or adjusting primer concentrations to correct this error (32–34). UMIs are strings of random nucleotides added between the adaptor sequence and oligonucleotides of the template switching primer. During first-strand synthesis, each cDNA template is tagged with a UMI which is carried through the entire PCR and sequencing process. Post sequencing analysis identifies sequences that originate from the same starting priming molecule based on UMI sequence, allowing for correction of any PCR bias and sequencing errors. Longer UMI sequences lower the chance of identical but distinct RNA molecules binding the same UMI (35). UMIs of 9 to 12 nucleotides are used in most RNA based TCR sequencing protocols because it provides coverage for a typical range of 10^5 to 10^8 distinct TCR transcripts. Repeated deep sequencing of human peripheral blood T cells identified a lower bound of 10^6 unique TCRβ chains in a repertoire (36). With 12 nucleotide UMIs there is sufficient coverage to sequence each unique human peripheral blood TCRβ at most 100 times. Both DNA and RNA based bulk TCRseq approaches are now available through commercial services or kits. While it is generally accepted that current TCR sequencing methods will not capture the entirety of repertoire diversity in an individual (36), there is significant overlap between different bulk TCR sequencing approaches in capturing the most abundant and frequent TCRs.

Single-cell analysis is at the forefront of TCR sequencing technology. In addition to sequencing TCRs, single-cell sequencing interrogates transcriptional activity of individual cells, linking T cell phenotype and specificity (37). With single-cell technology, each cDNA molecule is barcoded to a unique cell in a microfluidic droplet. UMIs are added and amplicon libraries are similarly generated for sequencing. Sequencing reads from individual cells are identified through their unique barcodes. Single-cell fluidic platforms such as 10× Chromium capture transcript and TCR information from up to 10,000 of individual cells in parallel. Bulk TCRseq captures 10^5 transcripts that provides more opportunity to sample low expanded T cell clones. Although bulk TCRseq does not provide transcriptomic information, it gives a more accurate estimation of diversity than single-cell sequencing, and is considerably cheaper. Both single-cell and bulk TCR sequencing approaches have been used in combination because they offer complementary information (reviewed in later sections). The accessibility of the assays has led to an increase in its use in immuno-oncology studies to characterize T cell repertoires, especially in the context of response/non-response to ICT.

TCR REPERTOIRES CAN BE CHARACTERIZED BY DIFFERENT METRICS

It is important to understand how multiple TCR clones are distributed in T cell repertoires of patients that respond to ICT. As TCRseq data sets typically contain millions of TCR sequences, with unique TCR clonotypes expressed at variable frequencies, diversity metrics adapted from ecological studies are used to characterize the relative distributions of multiple TCR clones. These metrics are one-dimensional scores that estimate the distribution of species in any given system. In the case of TCR repertoires, each unique TCR clone represents a unique species, and the abundance of each clone represents the number of members of that species. The fraction of every unique species (unique TCR clone) over the total number of T cells (total TCRs) in the repertoire is calculated, weighted, summed and normalized to produce a summary statistic. The most commonly used metrics to characterize repertoire diversity in published studies are based on Shannon's and Simpson's diversity indices (38, 39). These scores range between maximum clonality (with one clone occupying the whole repertoire) and maximum evenness (with all clones occurring equally). The degree of T cell clonal expansion is estimated with these values. Importantly, diversity scores allow for statistical comparisons between different TCR repertoires within (for example before and after treatment) and between patients. Perturbations in TCR repertoire, such as changes in TCR diversity reflect immunological processes that can be analyzed to understand antigen-specific T cell responses. ICT-induced clonal expansion of antigen-specific T cells results in a reduction of TCR diversity. Conversely, increased migration of T cells into the tumor due to ICT could be reflected in an increase of TCR diversity. The diversity index also offers a possible stratification score for developing a biomarker of responsiveness to therapy, but this requires further validation. Diversity indices are one of few widely used metrics to characterize TCR repertoires in ICT (40).

Another common metric used to characterize similarities or differences in TCR repertoires is the Morisita–Horn index (41). It accounts for both the number and abundance of shared TCRs between two repertoires, and its score ranges between zero (no overlap) and one (all clones overlapping at similar frequencies). An advantage of performing TCR sequencing on serial samples is the ability to track dynamic changes in TCR clonotypes over time. For time course data, not only frequencies of individual TCR clonotypes are measured, but overlap metrics have been used as well (42). For example, an increased Morisita–Horn Index between two sequential samples could reflect the persistence and expansion of TCR clonotypes over time (43). Changes in TCR overlap and diversity over time are important dynamic measurements that could be informative of ICT outcomes, and have been assessed in different studies (44–47).

ANTI-CTLA-4 MONOTHERAPY REMODELS THE BLOOD TCR REPERTOIRE

Studies investigating TCR repertoire and ICT are difficult to compare because they differ in the type of cancer, type of sample (blood or tumor biopsy), and timing (pre-treatment or post-treatment) of sample collected, genetic material used for

sequencing (gDNA or RNA), and different diversity metrics used for analysis. Our next section will focus on anti-CTLA-4 and anti-PD-1/PD-L1 separately, as they are the most commonly used antibodies in the clinic and have different mechanisms of action (48, 49).

CTLA-4 blockade appears to broaden blood $CD8^+$ T cell responses against tumor associated antigens, increasing the number of tumor-specificities measured by peptide-MHC multimer staining when pre- and post-blood samples were compared (50). TCRβ sequencing performed in separate studies support this, as anti-CTLA-4 increases the total number of unique TCR clones and increases TCR diversity in the blood (51). Although significant changes in TCR diversity were not observed in all studies (43, 52), an important observation with anti-CTLA-4 monotherapy is that highly different repertoires were observed pre- and post-treatment, as measured by low overlap indices (43, 48). This suggests that anti-CTLA-4 treatment drives a rapid influx of new T cell clones and broadens the circulating TCR repertoire, with minimal clonal expansion of T cells within the blood (51). The broadening of the T cell repertoire is indiscriminate in its specificity, as increased blood TCR diversity has been linked to immune-related side effects (48, 53).

Patients with a high pre-treatment blood TCR diversity score experienced more clinical benefit and increased survival with anti-CTLA-4 monotherapy in some studies (43, 54), but not others (48, 55, 56). TCR diversity scores from pre-treatment blood samples are highly variable because the peripheral blood contains the most heterogeneous populations of T cells. Although anti-CTLA-4 reshapes the blood TCR repertoire, some TCR clonotypes are still found before and after treatment. The persistence and expansion of high-frequency TCR clonotypes post-treatment correlate with survival in some studies (43, 51). There is no clear consensus on how TCR diversity in whole blood samples correlates with anti-CTLA-4 response.

ANTI-CTLA-4 DRIVES CLONAL EXPANSION OF TUMOR INFILTRATING LYMPHOCYTES

There is limited clinical data about dynamic changes in tumor TCR repertoire diversity upon anti-CTLA-4 monotherapy. A reduction in overall TCR diversity (measured by Shannon's Diversity) post-treatment compared to pre-treatment was reported in a melanoma study (57) but not in a breast cancer study (52). When TCR clones were tracked, anti-CTLA-4 drove polyclonal, rather than oligoclonal expansion of TCR clones within the tumor (52). Recent studies highlight that bystander T cells specific for non-tumor antigens can infiltrate tumors, obscuring the ability to analyze the anti-tumor T cell response (58). A significant challenge lies in distinguishing tumor-specific TCRs from the bystanders. Furthermore, most early clinical studies were performed with limited samples, and the effects of anti-CTLA-4 monotherapy are not clear because anti-CTLA-4 is mostly administered in combination with anti-PD-1/L1 or other adjuvant therapies in clinical studies. Furthermore, serial tumor biopsies are limited for most cancers. Hence preclinical models have been widely used to study the effects of anti-CTLA-4 on tumor TCR repertoires.

In murine studies, the effects of anti-CTLA-4 monotherapy on tumor TCR diversity are model-dependent. Treatment of breast tumors (4T1, E0771) results in reduced tumor TCR diversity compared to untreated tumors, and this reduction in diversity is accompanied by expansion of dominant TIL clones (59, 60). However, similar changes are not observed in murine melanoma (61, 62). B16 tumors did not respond to anti-CTLA-4 monotherapy in these studies, likely contributing to the discrepancy. *In vivo* anti-CTLA-4 treatment increases the frequency of neo-antigen specific tumor-infiltrating T cells in other responsive murine cancer lines, suggesting that clonal expansion of T cells, and reduction in tumor TCR diversity is a feature that accompanies anti-CTLA-4 treatment (63, 64). In most preclinical studies, tumors from treated vs untreated animals are compared, unlike clinical studies where serial samples from the same individual can be studied. This has to be taken into consideration when studying dynamic changes in murine models, as individual mice have highly private tumor TCR repertoires even though they are genetically identical, and were inoculated with ostensibly similar cancer cell lines (60, Nicola Principe et al., 2020) (manuscript under review). This highlights the challenge of developing a TCR based dynamic biomarker of response from tumor samples.

NUANCED ANALYSIS OF PD-1^+ BLOOD T CELLS MIGHT OFFER A BIOMARKER TO RESPONSE TO PD-1/L1 BLOCKADE

Peripheral blood T cells are heterogeneous and include naïve, effector and memory T cells. Bulk TCR sequencing is often performed on all PBMCs, and TCR distributions within these different T cell subsets are lost. This could explain why some studies show an association between TCR diversity and response to ICT, but not others. Focusing TCR diversity analysis on a phenotypically distinct subset of blood T cells could provide a more accurate biomarker of response, compared to analysis of whole blood samples. Peripheral PD-1^+ T cells represents one such population, as $CD8^+$PD-1^+ are the primary T cells which PD-1 blockade acts, are clonally expanded, and are enriched for tumor-specific T cells (65–67). TCR diversity of select populations of T cells can be derived from sequencing flow cytometry sorted populations. Patients with high pre-treatment TCR diversity, and reduced diversity post anti-PD-1 treatment in their $CD8^+$PD-1^+ T cell population had longer progression-free survival. Importantly, these associations with treatment outcomes were not observed when TCR sequencing was performed on blood $CD8^+$ T cells (66, 68).

EXPANSION OF INTRA-TUMORAL TCR CLONOTYPES IS A FEATURE OF RESPONSE TO ANTI-PD-1 THERAPY

A pre-treatment tumor TCRβ repertoire with reduced diversity correlates with clinical response to anti-PD-1 therapy in some melanoma, and lung cancer patient cohorts (13, 17, 40), but not others (69, 70). In pancreatic ductal carcinomas, post-treatment but not pre-treatment TCRβ clonality was associated with response to anti-PD-1 (43). Patients who were refractory to anti-CTLA-4 therapy, but who responded to subsequent anti-PD-1 therapy had a more clonal TCRβ repertoire before and after PD-1 blockade (57). In studies where subsequent biopsies could be profiled, expansion of a greater number of TCRβ clonotypes between pre- and on-treatment samples was observed in responders compared to a smaller number of expanded clonotypes in non-responders (13, 40, 57, 70). Even though the timing of biopsies varied between studies, expansion in tumor TCRβ clonotypes suggests antigen-specific T cell proliferation and is likely to be a key feature of successful responses to anti-PD-1 therapy.

Some studies have described dynamic changes in tumor and blood TCR repertoire, providing insight into how the T cell response changes when ICT treatment is administered. However, the utility of the TCR repertoire as a dynamic biomarker of ICT response is still limited, and we discuss some of the current limitations in the next section.

IMPROVING HOW TCR REPERTOIRE DATA IS REPRESENTED

The most frequently used diversity metrics, including Shannon's and Simpson's indices are useful to generate a single numerical score to estimate repertoire diversity of millions of TCR sequences (71). However descriptive information, such as oligo- or monoclonality is lost when data is compressed like this. For example, two repertoires with the same numerical Shannon's or Simpson's diversity values can have vastly different repertoires, especially in how the most abundant clones are distributed (**Figures 2A, B**). Renyi entropy can be used to graphically represent how abundant clones are distributed in relation to the rare clones within a given repertoire, in addition to assigning a numerical value to repertoire diversity (**Figure 2C**) (72). For example, the gradient of the slope increases as the distribution of the repertoire becomes more monoclonal.

Another common feature of bulk TCR sequencing data is the large number of unique TCR clones that occur once only. These low-frequency TCRs can skew Shannon's and Simpson's indices, increasing the diversity score in the presence of a few dominant clones. Ecological diversity metrics were designed to account for rare species, but it is unclear if a rare, unique TCRβ sequence belongs to a rare T cell clone, or a sequencing artefact. Even if it was the former, it is likely that only the most abundant clonotypes are of biological relevance. Hence, modified diversity metrics that only account for the more abundant TCR clonotypes have been used to characterize repertoires, and stratify patients. Top 10 clones or the top 50% of the most abundant clones have been used to represent TCR repertoire diversity (62). A recent melanoma study highlighted ICT response correlated with a higher number of large clones (clones occupying greater than 0.5% of the total repertoire) in the blood (31).

Diversity indices are highly sensitive to the sequencing depth and absolute number of TCRs sampled in each repertoire. Comparisons of diversity measurements are only meaningful if repertoires have sufficient sampling and similar repertoire sizes. The absolute number of TCRs and unique TCRs from individual samples are important data that should be presented for understanding and comparing TCR repertoire diversity. A challenge with developing a predictive biomarker based on

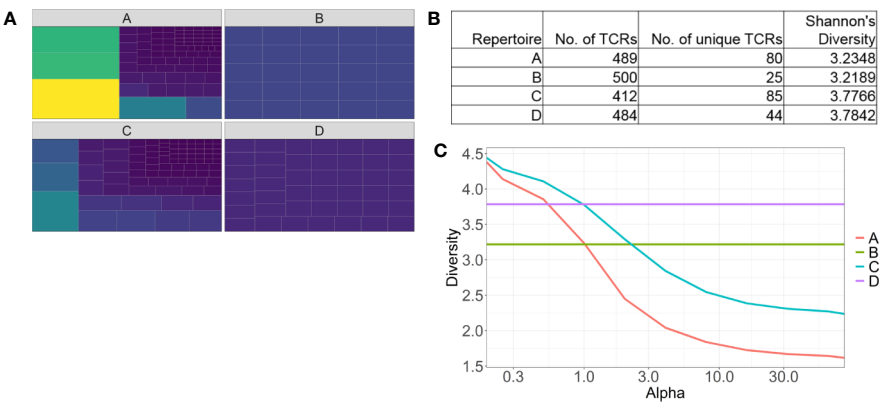

FIGURE 2 | Identifying pitfalls in one-dimensional T cell receptor diversity metrics. **(A)** Tree maps of four examples of TCR repertoires. Each tile is a unique clone, and the size of each tile represents the abundance of each clone. **(B)** Table of summary statistics of the four repertoires, highlighting different distributions of TCRs can have similar diversity scores. **(C)** Representative Renyi diversity plots of the four repertoire examples. Features of each line/curve on the plot, such as the gradient and where the curve intersects the y-axis, correspond to different repertoire features.

TCR diversity is the variation in how repertoire diversity is measured between different studies and the lack of validation of these metrics used to stratify ICT responders and non-responders.

MOVING BEYOND DIVERSITY: NOVEL APPROACHES TO STUDY TCR REPERTOIRES

Recent studies have approached TCR repertoire analysis utilizing novel computational approaches. Some unique TCRβ CDR3 sequences only differ from others by a single or few amino acids. A novel approach to studying TCR repertoires is to account for sequence similarity, with the underlying assumption that TCRs specific for the same antigen will have similar CDR3 amino acid sequences. Clustering highly similar sequences, and mapping them as networks can reveal interesting properties about TCR repertoire structure. The most abundant, public TCRβ CDR3 sequences are highly conserved between healthy individuals, more so than previously expected (73). When clustering approaches are applied to longitudinal blood samples, changes in the connectivity of TCR clusters over time distinguished healthy and tumor bearing mice (74). ICT possibly alters TCR networks in patients over time (73). Mapping TCR networks based on amino acid motifs within the CDR3 region potentially offers a more robust biomarker of response to therapy than TCR diversity measurement by Shannon's alone (75).

Some key papers describe how a clustering approach identified shared amino acid motifs within CDR3 regions of common virus (influenza, CMV) epitope specific TCR repertoires (76, 77). If tumor-epitope associated TCR clusters can be identified, the expansion and contraction of these clusters can be tracked over time and might be expected to correlate better with response. Heterogeneity in tumor antigens between patients and the lack of TCR sequencing data of tumor-specific T cells are significant hurdles to this. It is also likely that such an approach would be suited to shared tumor antigens, such as tumor differentiation or viral associated tumor antigens.

As a further consideration, it is important to recognize that the nucleotide sequence within TCRβ CDR3 regions can be redundant, with receptors having identical amino acid sequences but different nucleotide sequences. TCR convergence in peripheral blood, defined as the frequency of unique TCRβ nucleotide sequences that share a CDR3 amino acid sequence with at least one other clone, correlated with response to anti-CTLA-4 in a small cohort of patients (42).

High dimensional analysis comparing amino acid residues or nucleotide bases between millions of TCR sequences is now possible, giving us unprecedented information about TCR repertoires and how they relate to anti-tumor immunity. Although these approaches are at an early stage, the use of novel analytic approaches could inform our understanding of the TCR repertoire structure in the context of tumor immunology and assist development of a TCR based dynamic biomarker of response.

CLONAL DIVERSITY OF MEMORY CD8$^+$ T CELL SUBSETS MIGHT OFFER A DYNAMIC BIOMARKER OF ICT RESPONSE

Another approach to develop a novel biomarker of response is to focus on the clonal diversity within a population of relevant T cells. Most existing studies perform bulk TCR sequencing on whole blood and tumor samples, without the capacity to differentiate heterogeneous T cell populations that differ in phenotype and function. We would anticipate that changes in TCR diversity, such as clonal expansion within a population of T cells would be more robust biomarkers of response to ICT, compared to TCR diversity derived from unsorted T cells.

The advent of single-cell technology that incorporates transcriptome and TCR profiling now permits the assignment of T cell clones to a phenotype or phenotype cluster. This has the potential to provide unprecedented insight into the dynamics of phenotype change within T cell clones and how those changes relate to ICT treatment response. Recent papers highlight the role of memory CD8$^+$ T cells in ICT therapy, identifying tissue resident memory (TRM) and effector memory-like CD8$^+$ T cell subsets as potential predictors of positive outcomes to ICT therapy.

A specialized subset of resident memory T cells reside in tissues to mount an effective, rapid local immune response. TRM cells are canonically identified by surface expression of CD69 and CD103 and reside in organs such as the skin and lung and within solid tumors. CD8$^+$CD103$^+$ tumor infiltrating T cells often correlate with better prognosis and outcomes in multiple cancers (68, 78–87). Clonally expanded TRM expressed PD-1 and correlated with effective anti-PD-1 therapy in lung cancer patients. Single-cell analysis of TRM from these responding patients demonstrated increased expression of cytotoxicity genes in these populations (88).

Single-cell analysis of CD8$^+$ T cells from melanoma biopsies revealed that ICT responders are enriched with effector memory like T cells that express genes associated with memory, activation and cell survival (IL-7R, TCF7), but not residency (89). The transcription factor TCF7 is critical for CD8$^+$ T cell proliferation, differentiation (90), especially in the context of anti-PD-1 therapy (91, 92). Importantly, TCF7 expression was validated in a different patient cohort and found to associate with responses to ICT (89). A limitation to acquiring dynamic data of TRM or TIL subsets is the difficulty in obtaining serial on-treatment tumor biopsies for study.

When serial peripheral blood T cells were analyzed using single-cell phenotyping, responders to both anti-PD-1 and anti-PD-1/anti-CTLA-4 exhibited more expanded T cell clones than non-responders in PBMCs post-treatment (31). Some highly expanded clones appeared to differentially express genes associated with cytotoxicity (such as granzyme B, perforin, ITGB1, and CCL4), compared to the non-expanded clones (31). In another study, a subset of clonally expanded memory T cells characterized by CD27$^-$CCR7$^-$ were found in the

peripheral blood of patients responding to ICT (93). In these patients, response to immunotherapy correlated with a subset of clonally expanded T cells identified by single-cell RNAseq, representing a potential biomarker of response.

Although single-cell sequencing is a powerful tool, the costs are very high. It does, however, provide novel insights that can be tested with bulk TCRseq and flow cytometry analysis. A more cost effective T cell based biomarker might lie in TCR analysis of a subset of effector T cells. Further work is required to identify surface markers that define memory T cell subsets of interest across multiple studies. Lastly, the approach of combining TCR sequencing and flow cytometry analysis to develop a biomarker of response is agnostic to antigens and would be useful when tumor antigens are not well defined.

CONCLUSION

Immune checkpoint therapy has changed the therapeutic landscape allowing the word "cure" to enter the oncologist's lexicon at least for a subset of hitherto incurable cancer patients. Methods to stratify cancer patients who will benefit most from therapy are desperately needed because of the high cost of treatment and the potential for adverse reaction without clinical benefit. The specificity of the immune system allows us to leverage T cell receptor sequencing as a potential biomarker of patient outcomes. T cell proliferation and differentiation is a dynamic process so serial samples are likely to boost the predictive potential of TCRseq on ICT outcomes. Sequencing of specific subsets of T cells will also improve predictive power as the downstream effectors and additional targets of ICT are identified. Immune cell phenotyping and receptor sequencing combined in single-cell RNAseq is beginning to provide the greatest depth of analysis and is likely to better stratify patients by predicted outcomes. The current challenge is to make single-cell RNAseq more accessible by overcoming technical barriers and developing robust mathematical and statistical models to accurately interpret the wealth of information. The last 10 years of cancer immunology research have demonstrated an acceleration in treatment, diagnostic and predictive capacity that ensure the future contains better outcomes for all cancer patients.

AUTHOR CONTRIBUTIONS

JK wrote the article. JC edited and conceived the article. NP, TL, AN, MW, RH, WL, and RL provided critical review and edited the article. All authors contributed to the article and approved the submitted version.

FUNDING

JK receives a stipend from the iCare Dust Diseases Board. JC receives funding from the iCare Dust Diseases Board, Cancer Council Western Australia and the University of Western Australia Raine Foundation. WL is supported by a Simon Lee Fellowship, an NHMRC Fellowship and a Cancer Council WA fellowship. The National Centre for Asbestos Related Diseases receives funding as an NHMRC Centre of Research Excellence.

REFERENCES

1. Hodi FS, O'Day SJ, McDermott DF, Weber RW, Sosman JA, Haanen JB, et al. Improved Survival with Ipilimumab in Patients with Metastatic Melanoma. *New Engl J Med* (2010) 363(8):711–23. doi: 10.1056/nejmoa1003466
2. Brahmer J, Reckamp KL, Baas P, Crinò L, Eberhardt WEE, Poddubskaya E, et al. Nivolumab versus Docetaxel in Advanced Squamous-Cell Non–Small-Cell Lung Cancer. *New Engl J Med* (2015) 373(2):123–35. doi: 10.1056/NEJMoa1504627
3. Reck M, Rodríguez-Abreu D, Robinson AG, Hui R, Csőszi T, Fülöp A, et al. Pembrolizumab versus Chemotherapy for PD-L1–Positive Non–Small-Cell Lung Cancer. *New Engl J Med* (2016) 375(19):1823–33. doi: 10.1056/NEJMoa1606774
4. Ansell SM, Lesokhin AM, Borrello I, Halwani A, Scott EC, Gutierrez M, et al. PD-1 Blockade with Nivolumab in Relapsed or Refractory Hodgkin's Lymphoma. *New Engl J Med* (2015) 372(4):311–9. doi: 10.1056/NEJMoa1411087
5. Nghiem PT, Bhatia S, Lipson EJ, Kudchadkar RR, Miller NJ, Annamalai L, et al. PD-1 Blockade with Pembrolizumab in Advanced Merkel-Cell Carcinoma. *New Engl J Med* (2016) 374(26):2542–52. doi: 10.1056/NEJMoa1603702
6. Schmid P, Adams S, Rugo HS, Schneeweiss A, Barrios CH, Iwata H, et al. Atezolizumab and Nab-Paclitaxel in Advanced Triple-Negative Breast Cancer. *New Engl J Med* (2018) 379(22):2108–21. doi: 10.1056/NEJMoa1809615
7. Motzer RJ, Escudier B, McDermott DF, George S, Hammers HJ, Srinivas S, et al. Nivolumab versus Everolimus in Advanced Renal-Cell Carcinoma. *New Engl J Med* (2015) 373(19):1803–13. doi: 10.1056/NEJMoa1510665
8. Bellmunt J, De Wit R, Vaughn DJ, Fradet Y, Lee J-L, Fong L, et al. Pembrolizumab as Second-Line Therapy for Advanced Urothelial Carcinoma. *New Engl J Med* (2017) 376(11):1015–26. doi: 10.1056/NEJMoa1613683
9. Massard C, Gordon MS, Sharma S, Rafii S, Wainberg ZA, Luke J, et al. Safety and Efficacy of Durvalumab (MEDI4736), an Anti–Programmed Cell Death Ligand-1 Immune Checkpoint Inhibitor, in Patients With Advanced Urothelial Bladder Cancer. *J Clin Oncol* (2016) 34(26):3119–25. doi: 10.1200/JCO.2016.67.9761
10. Ferris RL, Blumenschein G, Fayette J, Guigay J, Colevas AD, Licitra L, et al. Nivolumab for Recurrent Squamous-Cell Carcinoma of the Head and Neck. *New Engl J Med* (2016) 375(19):1856–67. doi: 10.1056/NEJMoa1602252
11. Michot JM, Bigenwald C, Champiat S, Collins M, Carbonnel F, Postel-Vinay S, et al. Immune-related adverse events with immune checkpoint blockade: a comprehensive review. *Eur J Cancer* (2016) 54:139–48. doi: 10.1016/j.ejca.2015.11.016
12. Tartari F, Santoni M, Burattini L, Mazzanti P, Onofri A, Berardi R. Economic sustainability of anti-PD-1 agents nivolumab and pembrolizumab in cancer patients: Recent insights and future challenges. *Cancer Treat Rev* (2016) 48:20–4. doi: 10.1016/j.ctrv.2016.06.002
13. Tumeh PC, Harview CL, Yearley JH, Shintaku IP, Taylor EJM, Robert L, et al. PD-1 blockade induces responses by inhibiting adaptive immune resistance. *Nature* (2014) 515(7528):568–71. doi: 10.1038/nature13954
14. Wei SC, Levine JH, Cogdill AP, Zhao Y, Anang N-AAS, Andrews MC, et al. Distinct Cellular Mechanisms Underlie Anti-CTLA-4 and Anti-PD-1 Checkpoint Blockade. *Cell* (2017) 170(6):1120–33.e17. doi: 10.1016/j.cell.2017.07.024
15. Borghaei H, Paz-Ares L, Horn L, Spigel DR, Steins M, Ready NE, et al. Nivolumab versus Docetaxel in Advanced Nonsquamous Non–Small-Cell

Lung Cancer. *New Engl J Med* (2015) 373(17):1627–39. doi: 10.1056/NEJMoa1507643
16. Samstein RM, Lee C-H, Shoushtari AN, Hellmann MD, Shen R, Janjigian YY, et al. Tumor mutational load predicts survival after immunotherapy across multiple cancer types. *Nat Genet* (2019) 51(2):202–6. doi: 10.1038/s41588-018-0312-8
17. Forde PM, Chaft JE, Smith KN, Anagnostou V, Cottrell TR, Hellmann MD, et al. Neoadjuvant PD-1 Blockade in Resectable Lung Cancer. *New Engl J Med* (2018) 378(21):1976–86. doi: 10.1056/nejmoa1716078
18. Lesterhuis WJ, Bosco A, Millward MJ, Small M, Nowak AK, Lake RA. Dynamic versus static biomarkers in cancer immune checkpoint blockade: unravelling complexity. *Nat Rev Drug Discovery* (2017) 16(4):264–72. doi: 10.1038/nrd.2016.233
19. Chien Y-H, Gascoigne NRJ, Kavaler J, Lee NE, Davis MM. Somatic recombination in a murine T-cell receptor gene. *Nature* (1984) 309 (5966):322–6. doi: 10.1038/309322a0
20. Okazaki K, Davis DD, Sakano H. T cell receptor β gene sequences in the circular DNA of thymocyte nuclei: Direct evidence for intramolecular DNA deletion in V-D-J joining. *Cell* (1987) 49: (4):477–85. doi: 10.1016/0092-8674(87)90450-8
21. Freeman JD, Warren RL, Webb JR, Nelson BH, Holt RA. Profiling the T-cell receptor beta-chain repertoire by massively parallel sequencing. *Genome Res* (2009) 19(10):1817–24. doi: 10.1101/gr.092924.109
22. Mora T, Walczak AM. How many different clonotypes do immune repertoires contain? *Curr Opin Syst Biol* (2019) 18(December 2019):104–10. doi: 10.1016/j.coisb.2019.10.001
23. Redmond D, Poran A, Elemento O. Single-cell TCRseq: paired recovery of entire T-cell alpha and beta chain transcripts in T-cell receptors from single-cell RNAseq. *Genome Med* (2016) 8(1). doi: 10.1186/s13073-016-0335-7
24. Robins HS, Campregher PV, Srivastava SK, Wacher A, Turtle CJ, Kahsai O, et al. Comprehensive assessment of T-cell receptor β-chain diversity in αβ T cells. *Blood* (2009) 114(19):4099–107. doi: 10.1182/blood-2009-04-217604
25. Rosati E, Dowds CM, Liaskou E, Henriksen EKK, Karlsen TH, Franke A. Overview of methodologies for T-cell receptor repertoire analysis. *BMC Biotechnol* (2017) 17(1):61–77. doi: 10.1186/s12896-017-0379-9
26. Friedensohn S, Khan TA, Reddy ST. Advanced Methodologies in High-Throughput Sequencing of Immune Repertoires. *Trends Biotechnol* (2017) 35(3):203–14. doi: 10.1016/j.tibtech.2016.09.010
27. Woodsworth DJ, Castellarin M, Holt RA. Sequence analysis of T-cell repertoires in health and disease. *Genome Med* (2013) 5(10):98. doi: 10.1186/gm502
28. Heather JM, Ismail M, Oakes T, Chain B. High-throughput sequencing of the T-cell receptor repertoire: pitfalls and opportunities. *Briefings Bioinf* (2018) 19 (4):554–65. doi: 10.1093/bib/bbw138
29. Zhu YY, Machleder EM, Chenchik A, Li R, Siebert PD. Reverse Transcriptase Template Switching: A SMART™ Approach for Full-Length cDNA Library Construction. *BioTechniques* (2001) 30(4):892–7. doi: 10.2144/01304pf02
30. Paillard F, Sterkers G, Vaquero C. Transcriptional and post-transcriptional regulation of TcR, CD4 and CD8 gene expression during activation of normal human T lymphocytes. *EMBO J* (1990) 9(6):1867–72. doi: 10.1002/j.1460-2075.1990.tb08312.x
31. Fairfax BP, Taylor CA, Watson RA, Nassiri I, Danielli S, Fang H, et al. Peripheral CD8+ T cell characteristics associated with durable responses to immune checkpoint blockade in patients with metastatic melanoma. *Nat Med* (2020) 26(2):193–9. doi: 10.1038/s41591-019-0734-6
32. Turchaninova MA, Davydov A, Britanova OV, Shugay M, Bikos V, Egorov ES, et al. High-quality full-length immunoglobulin profiling with unique molecular barcoding. *Nat Protoc* (2016) 11(9):1599–616. doi: 10.1038/nprot.2016.093
33. Ma K-Y, He C, Wendel BS, Williams CM, Xiao J, Yang H, et al. Immune Repertoire Sequencing Using Molecular Identifiers Enables Accurate Clonality Discovery and Clone Size Quantification. *Front Immunol* (2018) 9:33. doi: 10.3389/fimmu.2018.00033
34. Shugay M, Britanova OV, Merzlyak EM, Turchaninova MA, Mamedov IZ, Tuganbaev TR, et al. Towards error-free profiling of immune repertoires. *Nat Methods* (2014) 11(6):653–5. doi: 10.1038/nmeth.2960
35. Sheward DJ, Murrell B, Williamson C. Degenerate Primer IDs and the Birthday Problem. *Proc Natl Acad Sci* (2012) 109(21):E1330–E. doi: 10.1073/pnas.1203613109
36. Warren RL, Freeman JD, Zeng T, Choe G, Munro S, Moore R, et al. Exhaustive T-cell repertoire sequencing of human peripheral blood samples reveals signatures of antigen selection and a directly measured repertoire size of at least 1 million clonotypes. *Genome Res* (2011) 21(5):790–7. doi: 10.1101/gr.115428.110
37. De Simone M, Rossetti G, Pagani M. Single Cell T Cell Receptor Sequencing: Techniques and Future Challenges. *Front Immunol* (2018) 9:1638. doi: 10.3389/fimmu.2018.01638
38. Shannon CE. A Mathematical Theory of Communication. *Bell System Tech J* (1948) 27(3):379–423. doi: 10.1002/j.1538-7305.1948.tb01338.x
39. Simpson EH. Measurement of Diversity. *Nature* (1949) 163(4148):688–. doi: 10.1038/163688a0
40. Riaz N, Havel JJ, Makarov V, Desrichard A, Urba WJ, Sims JS, et al. Tumor and Microenvironment Evolution during Immunotherapy with Nivolumab. *Cell* (2017) 171(4):934–49.e16. doi: 10.1016/j.cell.2017.09.028
41. Rempala GA, Seweryn M. Methods for diversity and overlap analysis in T-cell receptor populations. *J Math Biol* (2013) 67(6-7):1339–68. doi: 10.1007/s00285-012-0589-7
42. Looney TJ, Topacio-Hall D, Lowman G, Conroy J, Morrison C, Oh D, et al. TCR Convergence in Individuals Treated With Immune Checkpoint Inhibition for Cancer. *Front Immunol* (2020) 10:2985. doi: 10.3389/fimmu.2019.02985
43. Hopkins AC, Yarchoan M, Durham JN, Yusko EC, Rytlewski JA, Robins HS, et al. T cell receptor repertoire features associated with survival in immunotherapy-treated pancreatic ductal adenocarcinoma. *JCI Insight* (2018) 3(13):e122092. doi: 10.1172/jci.insight.122092
44. Carreno BM, Magrini V, Becker-Hapak M, Kaabinejadian S, Hundal J, Petti AA, et al. A dendritic cell vaccine increases the breadth and diversity of melanoma neoantigen-specific T cells. *Science* (2015) 348(6236):803–8. doi: 10.1126/science.aaa3828
45. Lu Y-C, Zheng Z, Robbins PF, Tran E, Prickett TD, Gartner JJ, et al. An Efficient Single-Cell RNA-Seq Approach to Identify Neoantigen-Specific T Cell Receptors. *Mol Ther* (2018) 26(2):379–89. doi: 10.1016/j.ymthe.2017.10.018
46. Miller BC, Sen DR, Al Abosy R, Bi K, Virkud YV, Lafleur MW, et al. Subsets of exhausted CD8+ T cells differentially mediate tumor control and respond to checkpoint blockade. *Nat Immunol* (2019) 20(3):326–36. doi: 10.1038/s41590-019-0312-6
47. Chapuis AG, Desmarais C, Emerson R, Schmitt TM, Shibuya KC, Lai IP, et al. Tracking the fate and origin of clinically relevant adoptively transferred CD8+T cells in vivo. *Sci Immunol* (2017) 2(8):eaal2568. doi: 10.1126/sciimmunol.aal2568
48. Robert L, Tsoi J, Wang X, Emerson R, Homet B, Chodon T, et al. CTLA4 Blockade Broadens the Peripheral T-Cell Receptor Repertoire. *Clin Cancer Res* (2014) 20(9):2424–32. doi: 10.1158/1078-0432.CCR-13-2648
49. Wei SC, Anang N-AAS, Sharma R, Andrews MC, Reuben A, Levine JH, et al. Combination anti–CTLA-4 plus anti–PD-1 checkpoint blockade utilizes cellular mechanisms partially distinct from monotherapies. *Proc Natl Acad Sci* (2019) 116(45):22699–709. doi: 10.1073/pnas.1821218116
50. Kvistborg P, Philips D, Kelderman S, Hageman L, Ottensmeier C, Joseph-Pietras D, et al. Anti-CTLA-4 therapy broadens the melanoma-reactive CD8+ T cell response. *Science Transl Med* (2014) 6: (254):254ra128–254ra12. doi: 10.1126/scitranslmed.3008918
51. Cha E, Klinger M, Hou Y, Cummings C, Ribas A, Faham M, et al. Improved Survival with T Cell Clonotype Stability After Anti-CTLA-4 Treatment in Cancer Patients. (2014) 6: (238):238ra70–ra70. doi: 10.1126/scitranslmed.3008211
52. Page DB, Yuan J, Redmond D, Wen YH, Durack JC, Emerson R, et al. Deep Sequencing of T-cell Receptor DNA as a Biomarker of Clonally Expanded TILs in Breast Cancer after Immunotherapy. *Cancer Immunol Res* (2016) 4 (10):835–44. doi: 10.1158/2326-6066.cir-16-0013
53. Oh DY, Cham J, Zhang L, Fong G, Kwek SS, Klinger M, et al. Immune Toxicities Elicted by CTLA-4 Blockade in Cancer Patients Are Associated with Early Diversification of the T-cell Repertoire. *Cancer Res* (2017) 77(6):1322–30. doi: 10.1158/0008-5472.CAN-16-2324

54. Postow MA, Manuel M, Wong P, Yuan J, Dong Z, Liu C, et al. Peripheral T cell receptor diversity is associated with clinical outcomes following ipilimumab treatment in metastatic melanoma. *J ImmunoTher Cancer* (2015) 3:23. doi: 10.1186/s40425-015-0070-4
55. Hogan SA, Courtier A, Cheng PF, Jaberg-Bentele NF, Goldinger SM, Manuel M, et al. Peripheral Blood TCR Repertoire Profiling May Facilitate Patient Stratification for Immunotherapy against Melanoma. *Cancer Immunol Res* (2019) 7(1):77–85. doi: 10.1158/2326-6066.CIR-18-0136
56. Subudhi SK, Aparicio A, Gao J, Zurita AJ, Araujo JC, Logothetis CJ, et al. Clonal expansion of CD8 T cells in the systemic circulation precedes development of ipilimumab-induced toxicities. *Proc Natl Acad Sci USA* (2016) 113(42):11919–24. doi: 10.1073/pnas.1611421113
57. Roh W, Chen P-L, Reuben A, Spencer CN, Prieto PA, Miller JP, et al. Integrated molecular analysis of tumor biopsies on sequential CTLA-4 and PD-1 blockade reveals markers of response and resistance. *Sci Trans Med* (2017) 9(379):eaah3560. doi: 10.1126/scitranslmed.aah3560
58. Simoni Y, Becht E, Fehlings M, Loh CY, Koo SL, Teng KWW, et al. Bystander CD8(+) T cells are abundant and phenotypically distinct in human tumour infiltrates. *Nature* (2018) 557(7706):575–9. doi: 10.1038/s41586-018-0130-2
59. Rudqvist N-P, Pilones KA, Lhuillier C, Wennerberg E, Sidhom J-W, Emerson RO, et al. Radiotherapy and CTLA-4 Blockade Shape the TCR Repertoire of Tumor-Infiltrating T Cells. *Cancer Immunol Res* (2018) 6(2):139–50. doi: 10.1158/2326-6066.CIR-17-0134
60. Crosby EJ, Wei J, Yang XY, Lei G, Wang T, Liu C-X, et al. Complimentary mechanisms of dual checkpoint blockade expand unique T-cell repertoires and activate adaptive anti-tumor immunity in triple-negative breast tumors. *OncoImmunology* (2018) 7(5):e1421891. doi: 10.1080/2162402X.2017.1421891
61. Twyman-Saint Victor C, Rech AJ, Maity A, Rengan R, Pauken KE, Stelekati E, et al. Radiation and dual checkpoint blockade activate non-redundant immune mechanisms in cancer. *Nature* (2015) 520(7547):373–7. doi: 10.1038/nature14292
62. Hosoi A, Takeda K, Nagaoka K, Iino T, Matsushita H, Ueha S, et al. Increased diversity with reduced "diversity evenness" of tumor infiltrating T-cells for the successful cancer immunotherapy. *Sci Rep* (2018) 8(1):1058. doi: 10.1038/s41598-018-19548-y
63. Ma S, Chee J, Fear VS, Forbes CA, Boon L, Dick IM, et al. Pre-treatment tumor neo-antigen responses in draining lymph nodes are infrequent but predict checkpoint blockade therapy outcome. *OncoImmunology* (2019) 9 (1):1684714. doi: 10.1080/2162402X.2019.1684714
64. Fehlings M, Simoni Y, Penny HL, Becht E, Loh CY, Gubin MM, et al. Checkpoint blockade immunotherapy reshapes the high-dimensional phenotypic heterogeneity of murine intratumoural neoantigen-specific CD8+ T cells. *Nat Commun* (2017) 8(1):562. doi: 10.1038/s41467-017-00627-z
65. Pasetto A, Gros A, Robbins PF, Deniger DC, Prickett TD, Matus-Nicodemos R, et al. Tumor- and Neoantigen-Reactive T-cell Receptors Can Be Identified Based on Their Frequency in Fresh Tumor. *Cancer Immunol Res* (2016) 4(9):734–43. doi: 10.1158/2326-6066.CIR-16-0001
66. Gros A, Parkhurst MR, Tran E, Pasetto A, Robbins PF, Ilyas S, et al. Prospective identification of neoantigen-specific lymphocytes in the peripheral blood of melanoma patients. *Nat Med* (2016) 22(4):433–8. doi: 10.1038/nm.4051
67. Huang AC, Postow MA, Orlowski RJ, Mick R, Bengsch B, Manne S, et al. T-cell invigoration to tumour burden ratio associated with anti-PD-1 response. *Nature* (2017) 545(7652):60–5. doi: 10.1038/nature22079
68. Han J, Duan J, Bai H, Wang Y, Wan R, Wang X, et al. TCR Repertoire Diversity of Peripheral PD-1+CD8+ T Cells Predicts Clinical Outcomes after Immunotherapy in Patients with Non–Small Cell Lung Cancer. *Cancer Immunol Res* (2020) 8(1):146–54. doi: 10.1158/2326-6066.CIR-19-0398
69. Johnson DB, Frampton GM, Rioth MJ, Yusko E, Xu Y, Guo X, et al. Targeted Next Generation Sequencing Identifies Markers of Response to PD-1 Blockade. *Cancer Immunol Res* (2016) 4(11):959–67. doi: 10.1158/2326-6066.CIR-16-0143
70. Amaria RN, Reddy SM, Tawbi HA, Davies MA, Ross MI, Glitza IC, et al. Neoadjuvant immune checkpoint blockade in high-risk resectable melanoma. *Nat Med* (2018) 24(11):1649–54. doi: 10.1038/s41591-018-0197-1
71. Laydon DJ, Bangham CRM, Asquith B. Estimating T-cell repertoire diversity: limitations of classical estimators and a new approach. *Philos Trans R Soc B: Biol Sci* (2015) 370(1675):20140291. doi: 10.1098/rstb.2014.0291
72. Joshi K, Robert de Massy M, Ismail M, Reading JL, Uddin I, Woolston A, et al. Spatial heterogeneity of the T cell receptor repertoire reflects the mutational landscape in lung cancer. *Nat Med* (2019) 25(10):1549–59. doi: 10.1038/s41591-019-0592-2
73. Madi A, Poran A, Shifrut E, Reich-Zeliger S, Greenstein E, Zaretsky I, et al. T cell receptor repertoires of mice and humans are clustered in similarity networks around conserved public CDR3 sequences. *eLife* (2017) 6:e22057. doi: 10.7554/eLife.22057
74. Priel A, Gordin M, Philip H, Zilberberg A, Efroni S. Network Representation of T-Cell Repertoire— A Novel Tool to Analyze Immune Response to Cancer Formation. *Front Immunol* (2018) 9:2913. doi: 10.3389/fimmu.2018.02913
75. Sidhom JW, Bessell CA, Havel JJ, Kosmides A, Chan TA, Schneck JP. ImmunoMap: A Bioinformatics Tool for T-cell Repertoire Analysis. *Cancer Immunol Res* (2018) 6(2):151–62. doi: 10.1158/2326-6066.CIR-17-0114
76. Dash P, Fiore-Gartland AJ, Hertz T, Wang GC, Sharma S, Souquette A, et al. Quantifiable predictive features define epitope-specific T cell receptor repertoires. *Nature* (2017) 547(7661):89–93. doi: 10.1038/nature22383
77. Glanville J, Huang H, Nau A, Hatton O, Wagar LE, Rubelt F, et al. Identifying specificity groups in the T cell receptor repertoire. *Nature* (2017) 547 (7661):94–8. doi: 10.1038/nature22976
78. Savas P, Virassamy B, Ye C, Salim A, Mintoff CP, Caramia F, et al. Single-cell profiling of breast cancer T cells reveals a tissue-resident memory subset associated with improved prognosis. *Nat Med* (2018) 24(7):986–93. doi: 10.1038/s41591-018-0078-7
79. Mami-Chouaib F, Blanc C, Corgnac S, Hans S, Malenica I, Granier C, et al. Resident memory T cells, critical components in tumor immunology. *J Immunother Cancer* (2018) 6(1):87. doi: 10.1186/s40425-018-0399-6
80. Wang ZQ, Milne K, Derocher H, Webb JR, Nelson BH, Watson PH. CD103 and Intratumoral Immune Response in Breast Cancer. *Clin Cancer Res* (2016) 22(24):6290–7. doi: 10.1158/1078-0432.CCR-16-0732
81. Duhen T, Duhen R, Montler R, Moses J, Moudgil T, De Miranda NF, et al. Co-expression of CD39 and CD103 identifies tumor-reactive CD8 T cells in human solid tumors. *Nat Commun* (2018) 9(1):2724. doi: 10.1038/s41467-018-05072-0
82. Workel HH, Komdeur FL, Wouters MCA, Plat A, Klip HG, Eggink FA, et al. CD103 defines intraepithelial CD8+ PD1+ tumour-infiltrating lymphocytes of prognostic significance in endometrial adenocarcinoma. *Eur J Cancer* (2016) 60:1–11. doi: 10.1016/j.ejca.2016.02.026
83. Webb JR, Milne K, Watson P, Deleeuw RJ, Nelson BH. Tumor-Infiltrating Lymphocytes Expressing the Tissue Resident Memory Marker CD103 Are Associated with Increased Survival in High-Grade Serous Ovarian Cancer. *Clin Cancer Res* (2014) 20(2):434–44. doi: 10.1158/1078-0432.CCR-13-1877
84. Webb JR, Wick DA, Nielsen JS, Tran E, Milne K, McMurtrie E, et al. Profound elevation of CD8+ T cells expressing the intraepithelial lymphocyte marker CD103 (αE/β7 Integrin) in high-grade serous ovarian cancer. *Gynecol Oncol* (2010) 118:(3):228–36. doi: 10.1016/j.ygyno.2010.05.016
85. Komdeur FL, Prins TM, Van De Wall S, Plat A, Wisman GBA, Hollema H, et al. CD103+ tumor-infiltrating lymphocytes are tumor-reactive intraepithelial CD8+ T cells associated with prognostic benefit and therapy response in cervical cancer. *OncoImmunology* (2017) 6(9):e1338230. doi: 10.1080/2162402X.2017.1338230
86. Ganesan A-P, Clarke J, Wood O, Garrido-Martin EM, Chee SJ, Mellows T, et al. Tissue-resident memory features are linked to the magnitude of cytotoxic T cell responses in human lung cancer. *Nat Immunol* (2017) 18(8):940–50. doi: 10.1038/ni.3775
87. Li R, Liu H, Cao Y, Wang J, Chen Y, Qi Y, et al. Identification and validation of an immunogenic subtype of gastric cancer with abundant intratumoural CD103+CD8+ T cells conferring favourable prognosis. *Br J Cancer* (2020) 122(10):1525–34. doi: 10.1038/s41416-020-0813-y
88. Clarke J, Panwar B, Madrigal A, Singh D, Gujar R, Wood O, et al. Single-cell transcriptomic analysis of tissue-resident memory T cells in human lung cancer. *J Exp Med* (2019) 216(9):2128–49. doi: 10.1084/jem.20190249
89. Sade-Feldman M, Yizhak K, Bjorgaard SL, Ray JP, De Boer CG, Jenkins RW, et al. Defining T Cell States Associated with Response to Checkpoint Immunotherapy in Melanoma. *Cell* (2018) 175(4):998–1013.e20. doi: 10.1016/j.cell.2018.10.038
90. Zhou X, Yu S, Zhao D-M, Harty JT, Badovinac VP, Xue H-H. Differentiation and Persistence of Memory CD8+ T Cells Depend on T Cell Factor 1. *Immunity* (2010) 33(2):229–40. doi: 10.1016/j.immuni.2010.08.002

91. Siddiqui I, Schaeuble K, Chennupati V, Fuertes Marraco SA, Calderon-Copete S, Pais Ferreira D, et al. Intratumoral Tcf1+PD-1+CD8+ T Cells with Stem-like Properties Promote Tumor Control in Response to Vaccination and Checkpoint Blockade Immunotherapy. *Immunity* (2019) 50(1):195–211.e10. doi: 10.1016/j.immuni.2018.12.021
92. Kurtulus S, Madi A, Escobar G, Klapholz M, Nyman J, Christian E, et al. Checkpoint Blockade Immunotherapy Induces Dynamic Changes in PD-1–CD8+ Tumor-Infiltrating T Cells. *Immunity* (2019) 50(1):181–94.e6. doi: 10.1016/j.immuni.2018.11.014
93. Valpione S, Galvani E, Tweedy J, Mundra PA, Banyard A, Middlehurst P, et al. Immune awakening revealed by peripheral T cell dynamics after one cycle of immunotherapy. *Nat Cancer* (2020) 1(2):210–21. doi: 10.1038/s43018-019-0022-x

Conflict of Interest: The authors declare that the research was conducted in the absence of any commercial or financial relationships that could be construed as a potential conflict of interest.

frontiers in Immunology

ORIGINAL RESEARCH
published: 19 October 2020
doi: 10.3389/fimmu.2020.576914

A Novel Signature of 23 Immunity-Related Gene Pairs Is Prognostic of Cutaneous Melanoma

*Ya-Nan Xue[1], Yi-Nan Xue[2], Zheng-Cai Wang[1], Yong-Zhen Mo[3], Pin-Yan Wang[4] and Wei-Qiang Tan[1]**

[1] Department of Plastic Surgery, Sir Run Run Shaw Hospital, Zhejiang University School of Medicine, Hangzhou, China, [2] Department of Biological Science, College of Chemistry and Life Sciences, Zhejiang Normal University, Jinhua, China, [3] Key Laboratory of Carcinogenesis and Cancer Invasion of the Chinese Ministry of Education, Cancer Research Institute, Central South University, Changsha, China, [4] Department of Neurosurgery, The Third Xiangya Hospital, Central South University, Changsha, China

In this study, we aimed to identify an immune-related signature for predicting prognosis in cutaneous melanoma (CM). Sample data from The Cancer Genome Atlas (TCGA; n = 460) were used to develop a prognostic signature with 23 immune-related gene pairs (23 IRGPs) for CM. Patients were divided into high- and low-risk groups using the TCGA and validation datasets GSE65904 (n = 214), GSE59455 (n = 141), and GSE22153 (n = 79). The ability of the 23-IRGP signature to predict CM was precise, with the stratified high-risk groups showing a poor prognosis, and it had a significant predictive power when used for immune microenvironment and biological analyses. We subsequently established a novel promising prognostic model in CM to determine the association between the immune microenvironment and CM patient results. This approach may be used to discover signatures in other diseases while avoiding the technical biases associated with other platforms.

Keywords: immune related gene pairs (IRGPs), cutaneous melanoma (CM), immune micro-environment, prognosis, immune check point

OPEN ACCESS

Edited by:
Maysaloun Merhi,
Hamad Medical Corporation, Qatar

Reviewed by:
Zoltan Vereb,
University of Szeged, Hungary
Sheng Yang,
Southeast University, China

***Correspondence:**
Wei-Qiang Tan
tanweixxxx@zju.edu.cn

Specialty section:
This article was submitted to Cancer Immunity and Immunotherapy, a section of the journal Frontiers in Immunology

Received: *27 June 2020*
Accepted: *29 September 2020*
Published: *19 October 2020*

Citation:
Xue Y-N, Xue Y-N, Wang Z-C, Mo Y-Z, Wang P-Y and Tan W-Q (2020) A Novel Signature of 23 Immunity-Related Gene Pairs Is Prognostic of Cutaneous Melanoma. Front. Immunol. 11:576914. doi: 10.3389/fimmu.2020.576914

INTRODUCTION

The incidence of cutaneous melanoma (CM) is increasing more rapidly than any other cancer, and accounts for about 132,000 new cases and 65,000 deaths worldwide annually (1). CM is the most lethal form of skin cancer and is a serious public health concern. The primary clinical feature of CM is early stage metastasis, which is one of the most significantly increasing cancers in the United States (2). Siegel et al. reported that in 2018, it had been 91,270 new cases and 9,320 deaths in the United States, owing to this disease (3).

As most diagnoses are made in the terminal stage, surgical results are often poor. At present, chemotherapy is the first line of treatment for CM (4), although many cases respond poorly to such regimens due to a high prevalence of adverse drug reactions and resistance to chemotherapeutic agents.

CM is associated with strong immunogenicity; thus, immunotherapy is a promising treatment alternative (5). Initial clinical trials using interferon-α (6) and high-dose interleukin-2 for advanced cases of CM (7) reported successful results. In addition, immune checkpoint inhibitors (ICIs), such

monoclonal antibodies against cytotoxic T-lymphocyte-associated protein (CTLA-4) (8) and programmed cell death protein 1 (PD-1) (9), have provided meaningful results in the clinical outcomes against advanced melanoma, as demonstrated by improved survival and a greater curative effect for an increasing proportion of patients with CM.

However, despite broad efforts to identify novel prognostic biomarkers, the clinical behavior of CM remains unpredictable, rendering the prediction of survival time and tumor stage particularly difficult (10). Therefore, novel biomarkers and patient-tailored treatments are greatly needed, especially for patients at higher risk of recurrence. Although the immune system plays an essential role in the development and progression of CM (11), few immunity-related genes (IRGs) have been identified for use as tumor markers for prognosis. Nowadays, many recent CM investigations have several limitations such as studies only one or a few immunity-related biomarkers, small sample datasets, lack of follow-up validations or lack of detailed and comprehensive immunity-related studies. Moreover, many studies have reported that genetic mutations and the interactions between the tumor and its microenvironment can impact the biological features and malignant potential of CM. Considering that many immunity-related treatments have shown significant therapeutic effects, identification of the interactions between cancer cells and the host immune response is especially important (12, 13).

In this study, 23 IRGs associated with CM were identified from the whole transcriptome sequencing (RNA-seq) data retrieved from The Cancer Genome Atlas (TCGA) (14) and the ImmPort dataset (15). Then, three microarray datasets (GSE65904, GSE59455, and GSE22153) were selected from the Gene Expression Omnibus (GEO) database (16) to verify the usefulness of this 23 IRG pair (IRGP) signature for the prognosis of CM. Moreover, the possible relationships between clinical pathological factors and the prognostic signature were explored to validate the predictive efficacy and accuracy of the IRGP. Finally, analyses of immune cell infiltration, the tumor microenvironment, and biological functions of different risk groups based on the 23 IRGPs were performed.

MATERIALS AND METHODS

CM Patient Data

In this retrospective study, four independent RNA-seq datasets and clinical data from diverse, high-throughput sequencing platforms were comprehensively analyzed. A CM dataset (n = 460) was downloaded from the TCGA data portal (https://portal.gdc.cancer.gov) and randomly assigned to a training dataset (n = 230) or a testing dataset (n = 230). In addition, the GSE65904 (n = 214), GSE59455 (n = 141), and GSE22153 (n = 79) datasets were downloaded from the GEO database (http://www.ncbi.nlm.nih.gov/geo/) for validation of the IRGP signature. In total, 905 samples were available for analysis. A file containing 1534 IRGs that was downloaded from the ImmPort database (https://immport.niaid.nih.gov) and the CIBERSORT analytical tool (https://cibersort.stanford.edu/) were used to determine an estimation of the abundances of 22 distinct cell types in a mixed cell population based on gene expression data. Immunohistochemical images of CM patients were downloaded from The Human Protein Atlas dataset (http://www.proteinatlas.org/). All data was available for free from website.

Data Preprocessing

All data were preprocessed using R software (version 3.6.2). If more than one probe was matched to the same target gene, the average value of the probe was calculated to replace the expression level of the single gene. If there were multiple samples from the same patient, the average value of each gene was used as the expression level of that gene.

Establishment of Prognostic IRGPs Based on the TCGA Dataset

The TCGA CM dataset was randomly divided into a training group and a testing group by R package "caret" with the ratio of training group samples to test group samples is 0.5. The distribution of CM patients gender ($p = 0.068$), age ($p = 0.047$), clinical stage ($p = 0.036$), follow-up time ($p < 0.0001$), death rate ($p < 0.0001$) and the number of CM samples in the dichotomies was similar between the two groups (17, 18). The GSE65904, GSE59455, and GSE2215 datasets were employed as the validation group. IRGs with relatively high variation (median absolute deviation >0.5) were extracted from the platforms, as described previously. For the pairwise comparison of a specific sample, two IRGs were paired off, and if the expression of the first IRG was higher than that of the second, the two IRGs were merged as an IRGP and assigned a score of 1; otherwise, a score of 0 was assigned. Then, IRGPs with score of 1 or 0 in over 80% of the specimens both in the training and testing groups were selected as potential prognostic IRGPs. Based on the results of a log-rank test, IRGPs with a false discovery rate (FDR) <0.001 (n = 23) were retained and entered into a least absolute shrinkage and selection operator (LASSO) penalized Cox regression model (iterations = 1000). The median value of the risk score was used as a cut-off to divide the patients into high- and low-risk groups. Next, a heat map, risk score map, state map of overall survival (OS), and 1-, 3-, and 5-year receiver operating characteristic (ROC) curves were created, and the concordance (C)-index was calculated. Then, the IRGPs were integrated with other clinical factors to construct a nomogram and a calibration curve. Finally, univariate and multivariate Cox regression analyses were performed to determine whether the 23 IRGPs were independent from other clinical parameters.

Verification and Assessment of the IRGP Signature for the Prediction of OS

The TCGA testing dataset and three microarray data files were selected to validate the signature comprised of 23 IRGPs. Every dataset was stratified into high- and low-risk groups based on the cut-off value of the prognostic signature. Next, the log-rank test and Cox analysis were performed, and a graph of OS was created

to calculate the C-index between the high- and low-risk groups in each dataset. Finally, the signature of the 23 IRGPs was compared to the 1-, 3-, and 5-year area under the ROC curves (AUCs) and the C-indices.

Immune Cell Infiltration in CM

The CIBERSORT analytical tool (19) was used to explore the enrichment of immune cells in the two CM risk groups. CIBERSORT is a tool used for deconvolution of the expression matrix of immune cell subtypes based on the principle of linear support vector regression, which can estimate the enrichment of various immune cell types in CM. Based on the CIBERSORT results, a radar chart of significantly differentially expressed IRGs between the two risk groups was constructed. All procedures were performed using R software (version 3.6.2).

Biological Function Analysis of the 23 IRGPs

Gene ontology (GO) and Kyoto Encyclopedia of Genes and Genomes (KEGG) pathways analyses of the two risk groups were performed using the R bioconductor package "fgsea." GO analysis and KEGG pathways files (c5.all.v7.0.symbols.gmt and c2.cp.kegg.v7.1.symbols.gmt, respectively) were downloaded from the Gene Set Enrichment Analysis (GSEA) website (https://www.gsea-msigdb.org/gsea/datasets.jsp) (20). Gene sets with an FDR-adjusted probability (p) value <0.05 were considered statistically significant.

Statistical Analysis

All statistical analyses were performed using the software packages R (version 3.6.2; www.r-project.org) and Prism 8 (GraphPad Software Inc., San Diego, CA, USA). Training group and testing group were randomly divided by R package "caret". OS curves were plotted using the R packages "survival" and "survminer." A heat map of the IRGPs, risk score map, and OS status graph were created using the R package "pheatmap." A model of prognostic IRGPs was established using the R package "glmnet" (21). Univariate and multivariate Cox regression analyses were performed using the R package "survival." ROC curves were constructed using the R package "survivalROC." A nomogram and calibration curves were plotted using the R packages "rms," "foreign," and "survival." The C-index was computed using the R package "Hmsic." Immune cell infiltration was processed with the R packages "e701," "limma," and "fmsb" (22). The tumor environment plot, based on the R package "estimate" (23), and the expression levels of six single key genes were determine using the R package "ggpubr." GO and KEGG analyses were conducted using the R package "fgsea."

RESULTS

Establishment, Definition, and Genetic Variation of the IRGP Signature

A flowchart of the establishment and validation of the 23 IRGPs is presented in **Figure 1**. The TCGA dataset was divided into a training dataset (n = 230) and a testing dataset (n = 230) (**Table S2**). Filter analysis was applied to establish a prognostic model of 1,811 unique IRGs that were obtained from the ImmPort database (accessed on January 4, 2020). In total, 620 IRGs with a median absolute deviation >0.5 were common among the datasets. After removing any IRGPs with a score of 0 or 1 in <20% or >80% of the samples in the TCGA training and testing datasets, a total of 74,750 IRGPs remained. Of these, 6,800 prognostic IRGPs were significantly associated with OS (FDR <

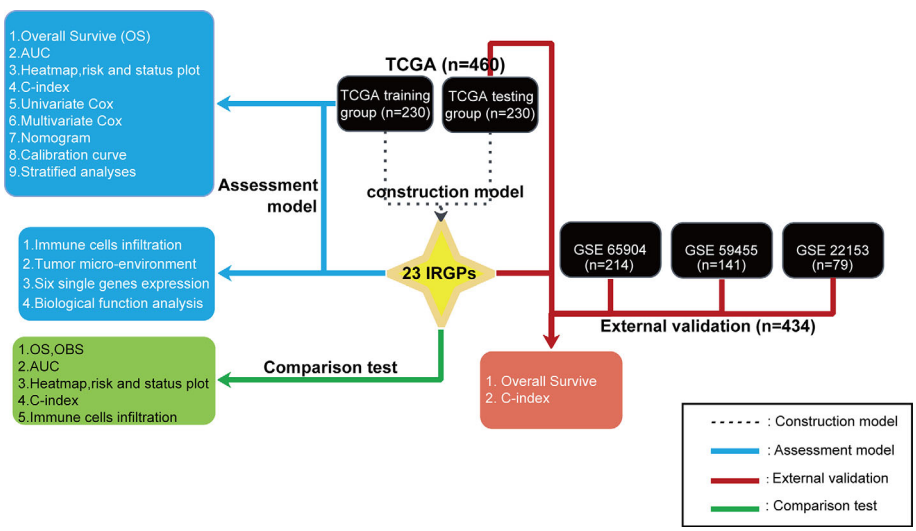

FIGURE 1 | A flowchart of the establishment and validation of 23 IRGPs. The TCGA data were divided into a training cohort (230), which was applied to identify potential IRGPs, and a testing cohort (230). A validate cohort of the datasets GSE65904, GSE59455, and GSE22153 was used to verify the 23 IRGPs, which were also compared to the IRGP-OBS and IRGs.

0.001), as determined by log-rank testing. Finally, 23 IRGPs consisted of 39 IRGs were selected for the LASSO penalized Cox regression model (**Figure 3A**), including 39 unique IRGs, most of which encoded molecules related to antimicrobials and cytokines (**Table 1**). Furthermore, we conducted Principal Component Analysis (PCA), bioligical function analysis and genetic and expression variation of the 39 unique IRGs using GEPIA web (gepia.cancer-pku.cn/), Metascape (https://metascape.org/gp/index.html) and R package "RCircos" and "GenVisR". We found that the genes expressed in TCGA tumor samples were independent parts, compared to TCGA normal sample (only one sample), GTEx normal skin exposed samples or not to the sun (**Figure 2A**). What's more, **Figure 2D** showed 39 IRGs were positively correlated with cancer immune-related biological functions, including cytokine-mediated signaling pathway, defense response to other organism, Influenza A, response to interferon-gamma, and type I interferon signaling pathway. We first summarized the incidence of copy number variations and somatic mutations of 39 IRGs in CM. The investigation of CNV alteration frequency showed that only 12 IRGs had alteration, and most were focused on the deletion in copy number, while CYBB, NGFR and BIRC5 had a widespread frequency of CNV amplification (**Figure 2B**). The location of CNV alteration of 12 IRGs on chromosomes was shown in **Figure 2C**. Among 460 samples downloaded from TCGA-CM mutation dataset, 253 experienced mutations of 39 IRGs, with frequency 53.94%. We found that the LTBP2 exhibited the highest mutation frequency followed by PLXNB2, while almost antigen processing and presentation molecules (HSPA1A, ICAM1, and PSME1) as well as cytokines (CCL17 and LHB) did not show any mutations in CM samples (**Figure 2E**). Further analyses revealed a significant mutation co-occurrence relationship between IKBKE and CYBB, IKBKE and CD8A, GPB2 and CD8A, GNLY and CD40, LYZ and TNFSF10, along with GPB2 and PSME1 (**Figure S1**). To explore whether the above genetic variations influenced the expression of 39 IRGs in CM patients, we investigated the mRNA expression levels of genes between skin normal samples (GTEx skin normal sample and TCGA skin normal sample) and tumor samples, and found that the alterations of mutation could be the prominent impact factors resulting in perturbations on the 39 IRGs expression. Compared to normal skin tissues, 39 IRGs with high mutation obviously lower expression in CM samples (e.g., LTBP2, CD86, EDNRA, TRIM22, CYBB, STC1, GBP2, and RNASEL), and vice versa (e.g., LHB, PSME1, CCL17, ICAM1, ISG15, and BIRC5) (**Figure 2E** and **Figure S2**). The above analyses presented the highly heterogeneity of genetic and expressional alteration landscape in 39 IRGs between normal and CM tissues, indicating that the expression imbalance of 39 IRGs played a important role in the CM occurrence and progression.

Twenty-three IRGPs were used to calculate a risk score to predict the 5-year OS rate of each patient in the training cohort. The analysis of the 5-year dependent ROC curve revealed that the best cut-off value of the 23 IRGPs to stratify patients in the training cohort and testing cohort into the high- or low-risk group was −0.674 (**Figure 4A**). These data suggested that the high-risk group had a higher risk index than the low-risk group. A higher risk score means a higher number of deaths (**Figures 3B, C**), indicating that OS was significantly poorer for the high-risk group than for the low-risk group ($p < 0.001$; **Figure 3E**). As shown in **Figure 3D**, the AUC values (24) for the 1-, 3-, and 5-year OS rates of the training cohort were 0.909, 0.901, and 0.912 (**Table S3**), respectively, and the C-index was 0.775 [95% confidence interval (CI) = 0.748–0.802] (**Figure 6E**). Moreover, the AUC values for the 1-, 3-, 5-year OS rates of the testing cohort and TCGA dataset was also shown in **Table S3**. A nomogram of OS was created by combining all of the clinicopathological factors, including age, sex, tumor stage, and the IRGP risk score, to predict the prognosis of CM (**Figure 4C**). The IRGP risk score made a major contribution to the nomogram, and the 1-, 3-, and 5-year calibration curves (**Figure 4B**) demonstrated the promising predictive ability of the nomogram, moreover, the nomograms of TCGA-test dataset and TCGA dataset were shown in **Figure S7**. The 1-, 3-, and 5-year calibration curves of TCGA-test dataset and TCGA dataset were shown in **Figures S9** and **S10**.

Univariate and multivariate Cox proportional hazards regression analyses of the TCGA dataset were performed to further assess the prognostic accuracy of the IRGPs for other clinical elements. The results of the univariate and multivariate Cox analyses showed that the signature of the 23 IRGPs and clinical factors, such as tumor stage, were indeed predictive of prognosis. However, although the IRGP signature was highly predictive of prognosis, the p-value was notably low (**Figures 5A, B** and **Table 2**).

Stratified analyses of patient age, tumor stage, and sex were also conducted. First, all patients in the TCGA training dataset were stratified by age into a young dataset (age ≤ 65 years) or an old dataset (age > 65 years), where OS was expected to be better for the younger patients ($p = 0.029$, **Figure 5C**). Then, all patients from the TCGA training dataset were further divided into an early onset dataset (stages I and II) or a later onset dataset (stages III and IV). Similar results were observed for the late dataset ($p = 0.002$, **Figure 5D**). Finally, all patients were stratified by sex into a male dataset or a female dataset. As shown in **Figure 5E**, there was little difference in the OS rate between males and females ($p = 0.543$), possibly due to the small number of samples.

Collectively, the results indicate that the predictive ability of the 23-IRGP signature was independent of other clinical parameters and was predictive of OS of CM patients.

Verification of Ability of the 23-IRGP Signature to Predict OS

To determine whether the 23-IRGP signature had consistent prognostic value in different risk groups, the validation datasets GES65904 (n = 214), GSE59455 (n = 141), and GSE54467 (n = 79) were applied for external validation. The risk score of each patient was calculated using the same 23-IRGP prognostic signature. Then, based on the median risk score, the patients were assigned to the low- or high-risk group. Interestingly, OS was poorer in the high-risk group (**Figures 6A–D**). The results of multivariate Cox regression analysis (**Table 2**) showed that, after

TABLE 1 | Information on the 23-IRGP.

Gene Pair1	Full Name	Immune Processes	Gene Pair2	Full Name	Immune Processes	Coefficient
CD8A	CD8a molecule	Antigen_Processing_and_Presentation, Antimicrobials, TCRsignalingPathway	LTBP2	latent transforming growth factor beta binding protein 2	Cytokines	–0.009639653
HSPA1A	heat shock 70kDa protein 1A	Antigen_Processing_and_Presentation	LYZ	lysozyme (renal amyloidosis)	Antimicrobials	0.098898359
HSPA1A	heat shock 70kDa protein 1A	Antigen_Processing_and_Presentation	GBP2	guanylate binding protein 2, interferon-inducible	Antimicrobials	0.06573857
HSPA1A	heat shock 70kDa protein 1A	Antigen_Processing_and_Presentation	LTBP3	latent transforming growth factor beta binding protein 3	Cytokines	0.00106882
ICAM1	intercellular adhesion molecule 1	Antigen_Processing_and_Presentation, NaturalKiller_Cell_Cytotoxicity	PLXNB2	plexin B2	Chemokine_Receptors, Cytokine_Receptors	-0.039340917
PSME1	proteasome (prosome, macropain) activator subunit 1 (PA28 alpha)	Antigen_Processing_and_Presentation	NENF	neuron derived neurotrophic factor	Cytokines	–0.008677831
ZC3HAV1L	zinc finger CCCH-type, antiviral 1-like	Antimicrobials	CMTM8	CKLF-like MARVEL transmembrane domain containing 8	Cytokines	0.037052249
APOBEC3G	apolipoprotein B mRNA editing enzyme, catalytic polypeptide-like 3G	Antimicrobials	IKBKE	inhibitor of kappa light polypeptide gene enhancer in B-cells, kinase epsilon	Antimicrobials	-0.511310011
CYBB	cytochrome b-245, beta polypeptide	Antimicrobials	SEMA7A	semaphorin 7A, GPI membrane anchor (John Milton Hagen blood group)	Chemokines, Cytokines	–0.0389128
TRIM5	tripartite motif-containing 5	Antimicrobials	SOS1	son of sevenless homolog 1 (Drosophila)	NaturalKiller_Cell_Cytotoxicity, TCRsignalingPathway	–0.064111635
TNFSF10	tumor necrosis factor (ligand) superfamily, member 10	Antimicrobials, Cytokines, NaturalKiller_Cell_Cytotoxicity, TNF_Family_Members	STC1	stanniocalcin 1	Cytokines	–0.089600117
RNASEL	ribonuclease L (2',5'-oligoisoadenylate synthetase-dependent)	Antimicrobials	TRIM22	tripartite motif-containing 22	Antimicrobials	0.019575179
RARRES3	retinoic acid receptor responder (tazarotene induced) 3	Antimicrobials	DDX17	DEAD (Asp-Glu-Ala-Asp) box polypeptide 17	Antimicrobials	–0.036983795
CD40	CD40 molecule, TNF receptor superfamily member 5	Antimicrobials, Cytokine_Receptors	BIRC5	baculoviral IAP repeat-containing 5	Antimicrobials	–0.008823763
ISG15	ISG15 ubiquitin-like modifier	Antimicrobials	NENF	neuron derived neurotrophic factor	Cytokines	–0.225283963
GNLY	granulysin	Antimicrobials	EDNRA	endothelin receptor type A	Chemokine_Receptors, Cytokine_Receptors	–0.027334821
IRF7	interferon regulatory factor 7	Antimicrobials	AKT1	v-akt murine thymoma viral oncogene homolog 1	BCRSignalingPathway, TCRsignalingPathway	–0.035142572
TRIM22	tripartite motif-containing 22	Antimicrobials	CCL17	chemokine (C-C motif) ligand 17	Antimicrobials, Chemokines, Cytokines	–0.270054236
BIRC5	baculoviral IAP repeat-containing 5	Antimicrobials	NGFR	nerve growth factor receptor (TNFR superfamily, member 16)	Cytokine_Receptors	0.211653036
GBP2	guanylate binding protein 2, interferon-inducible	Antimicrobials	PLXNA1	plexin A1	Chemokine_Receptors, Cytokine_Receptors	–0.031264198
GBP2	guanylate binding protein 2, interferon-inducible	Antimicrobials	SHC4	SHC (Src homology 2 domain containing) family, member 4	NaturalKiller_Cell_Cytotoxicity	–0.09011139
PTK2B	PTK2B protein tyrosine kinase 2 beta	Antimicrobials, NaturalKiller_Cell_Cytotoxicity	LHB	luteinizing hormone beta polypeptide	Cytokines	–0.397220258
CD86	CD86 molecule	Antimicrobials	IL1RN	interleukin 1 receptor antagonist	Cytokines, Interleukins	–0.018374851

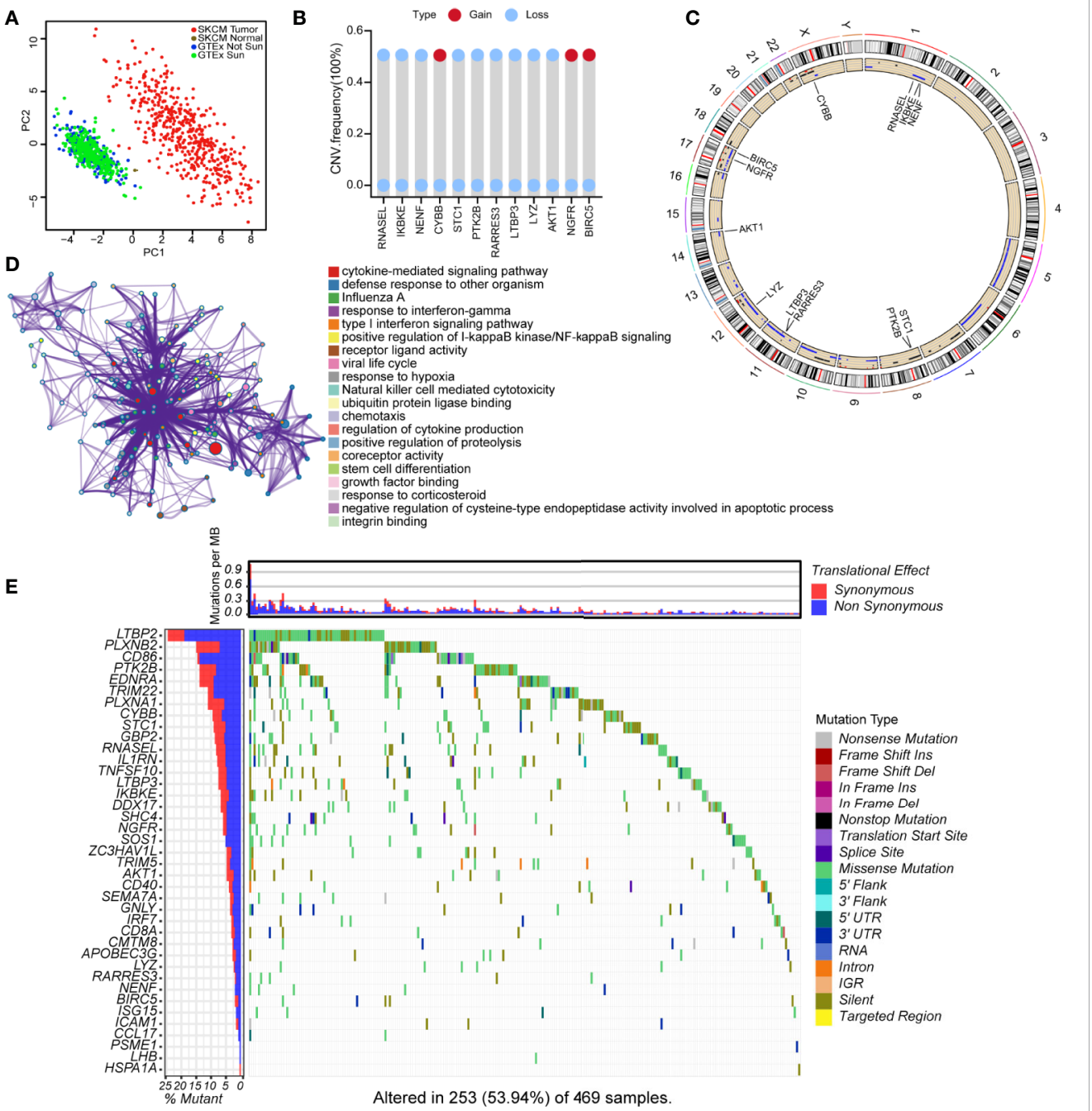

FIGURE 2 | Landscape of genetic and expression variation of 39 IRGs in CM. **(A)** the Principal Component Analysis (PCA) of 39 unique IRGs to distinguish tumors and normal samples in TCGA cohort and GTEx normal skin cohort. Normal samples and tumor samples were identified without intersection, indicating the two subgroups were well distinguished based on the expression profiles of 39 IRGs. GTEx normal skin exposed sun were marked green, GTEx normal skin not exposed sun were marked blue, TCGA normal sample were marked gray and TCGA tumor samples were marked with red. **(B)** The CNV variation frequency of 12 IRGs in TCGA cohort. The blue dot meaning deletion frequency and the red dot meaning amplification frequency. The height of the column represented the alteration frequency. **(C)** The location of CNV alteration of 12 IRGs on 23 chromosomes using TCGA cohort. **(D)** The biological functional enrichment analysis and interaction network of enriched terms for 39 IRGs. **(E)** The mutation frequency of 39 IRGs in 460 patients with CM from TCGA mutation dataset. Each column represented individual patients. The number on the left showed the mutation frequency in each gene. The upper barplot showed the mutations per MB, Synonymous, red; Non Synonymous, blue. The right annotation list showed the different variant type.

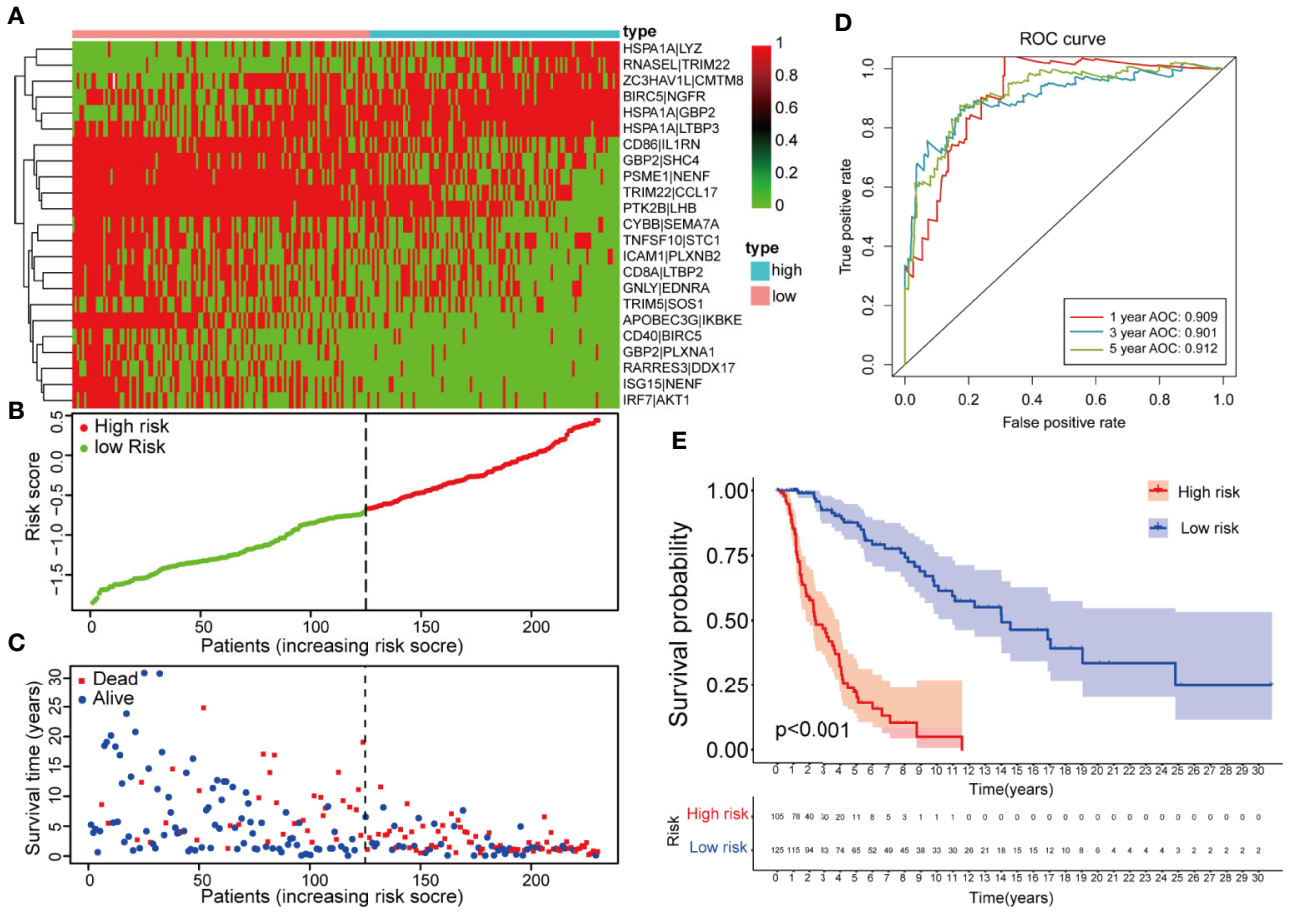

FIGURE 3 | Establishment and assessment of a 23-IRGP signature. **(A)** A heat map of the risk scores of the 23 IRGPs. **(B)** According to the 23 IRGPs, the training cohort was divided into high and low immune risk groups. The red and green points represent the risk scores of the high and low risk groups, respectively. **(C)** A plot of OS based on the 23 IRGPs. The red points represent deaths, while the blue points represent survivors. **(D)** The AUCs for 1-, 3-, and 5-year OS in the training cohort were 0.909, 0.901, and 0.912, respectively. **(E)** According to the OS curve, OS was poorer for the high risk group as compared to the low risk group in the training cohort ($p < 0.001$).

adjustment for age, sex, and tumor stage (age is a continuous variable), the risk score from the 23-IRGP signature was an independent prognostic factor in the testing dataset [hazard ratio (HR) = 2.08, 95% CI = 1.41–2.75, p = 0.0002] and TCGA dataset (HR = 2.08, 95% CI = 1.41–2.75, p = 0.0002), as well as the GSE datasets [GSE65904 (HR = 5.11, 95% CI = 3.12–7.10, p = 0.009), GSE59455 (HR = 1.64, 95% CI = 0.94–2.34, p = 0.042), and GSE22153 (HR = 2.07, 95% CI = 1.16–2.98, p = 0.014)]. Finally, the C-index values for the TCGA training dataset, TCGA test dataset, TCGA dataset, GSE65904, GSE59455, and GSE22153 datasets were 0.775 (95% CI = 0.748–0.802), 0.636 (95% CI = 0.585–0.687), 0.650 (95% CI = 0.609–0.691), 0.691 (95% CI = 0.653–0.729), 0.557 (95% CI = 0.508–0.606), and 0.610 (95% CI = 0.537–0.683), respectively (**Figure 6E**), the AUC values for the 1-, 3-, 5-year OS rates of the these datasets were also shown in **Table S3**. Moreover, the nomograms and the 1-, 3-, and 5-year calibration curves of three GSE validation datasets were shown in **Figures S8**, and **S11–S13**.

Immune Cell Infiltration, the Tumor Microenvironment, Potential of 23-IRGP as an Indicator of Response to Immunotherapy, and Analysis of Six Key Genes

Reportedly, the infiltration of immune cells is associated with the prognosis of CM patients. The CIBERSORT analytical tool can be used to estimate the abundances of immune cell subsets and has been used in many previous studies of the cancer microenvironment. Therefore, the CIBERSORT analytical tool was applied to estimate the relative abundances of 22 different immune cells for each patient. A comparative summary of the CIBERSORT output resulting from the two risk groups is shown in **Figure 7A**. Immune cells, such as M0, M1, and M2 macrophages; plasma cells; activated CD4+ memory T cells; monocytes; CD8+ T cells; follicular helper T cells; and gamma delta T cells, were enriched in the risk groups. As shown in **Figures 7B, D**, M0 macrophages (p = 0.004) and M2 macrophages

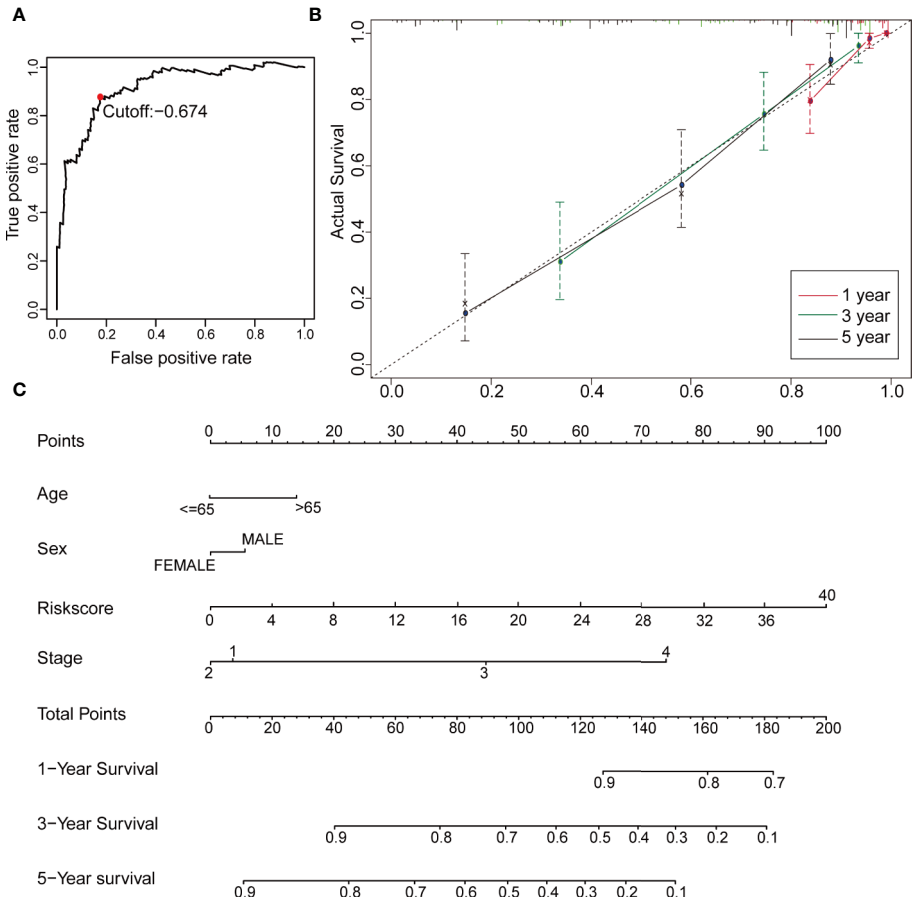

FIGURE 4 | Construction of a Robust nomogram in TCGA training dataset. **(A)** A time-dependent ROC curve for IRGPs in the training and testing dataset. An IRGP score of –0.674 was used as a cut-off to assign patients to the high- or low-risk group. **(B)** The 1-, 3-, and 5-year calibration curves of the nomogram. **(C)** A nomogram of OS was established by 23-IRGP risk score and other clinicopathological parameters.

($p = 0.003$) were significantly high in the high-risk group, while the abundances of M1 macrophages ($p = 0.001$), activated CD4+ memory T cells ($p = 0.005$), monocytes ($p = 0.047$), plasma cells ($p = 0.011$), CD8+ T cells ($p = 0.028$), follicular helper T cells ($p = 0.017$), and gamma delta T cells ($p = 0.014$) were significantly enriched in the low-risk group (**Figures 7C, E–J**). Then, we estimated the tumor microenvironment (TME) in the two groups and found that the high-risk group had a higher tumor purity with lower immune cells and stromal cell infiltration (**Figure 8A**). Furthermore, as 23-IRGP had a potential of indicator of response to CM immunotherapy, the relationship between the 23-IRGP and ICIs, namely PD-1, PD-L1, and CTLA-4, were investigated. As shown in the **Figure S14**, the 23-IRGP was markedly negatively related with PD-1 and PD-L1 (rho = 0.321 and $p < 0.001$ for PD-1, and rho = 0.203 and $p < 0.001$ for PD-L1) (**Figures S14A, B**), and positively correlated with CTLA-4 (rho = 0.085 and $p = 0.145$, without statistical significance). Moreover, three ICIs were found to be highly expressed in the low-risk group of 23-IRGP prognosis signature (**Figures 8B–D**), and this result indicated that patients with low risk presented obviously higher expression levels of immune checkpoint genes (PD-1, PD-L1) compared with those in the high risk group ($p < 0.001$ for PD-1, and $p < 0.001$ for PD-L1) (**Figures 8B, C**), which demonstrated that the PD-1 and PD-L1 are involved in better immunotherapy efficacy, and their high expression is associated with better prognosis. The effect of cross-talk between 23-IRGP and ICIs on CM patients' survival was shown in **Figures S14D–F**. According to the Meng Zhou et al. (25), we divided TCGA-CM patients into four clusters according to the connection of 23-IRGP and ICIs, and survival comparisons of three ICIs were presented among the four clusters. In PD-1 and PD-L1, Survival rate results showed that the 23-IRGP could significantly differentiate the result of patients with the same or similar levels of PD-1 and PD-L1 ($P < 0.001$, log-rank test) (**Figures S14D, E**). Relative to other three clusters, patients who had low 23-IRGP value with high level of PD-1 or PD-L1 were likely to have best survival results. However, patients who had high 23-IRGP value with low level of PD-1 or PD-L1 expression tended to the poorest consequence compared with the other three clusters (**Figures S14D, E**). Meanwhile, patients who had low level PD-1 or PD-L1 with low 23-IRGP value had better survival outcomes than the patients that had low PD-1 or PD-L1 with high 23-IRGP value. Furthermore, no obvious statistical

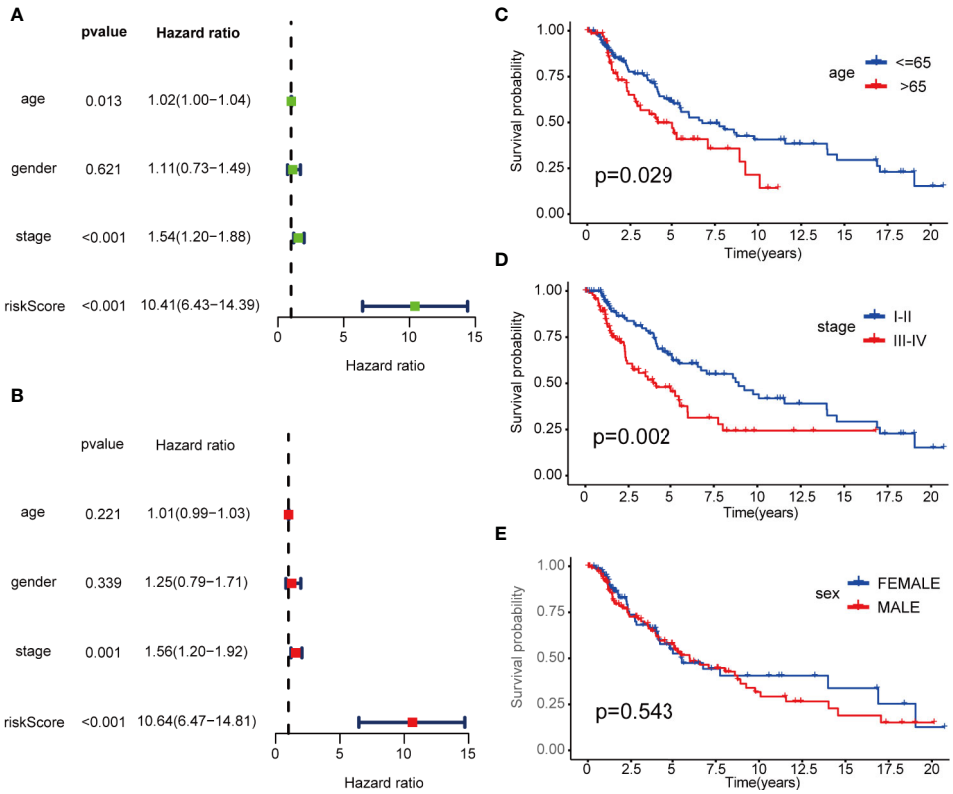

FIGURE 5 | Cox proportional hazards model and stratified analysis of the training cohort revealed 23-IRGP was a independent prognostic factors. **(A)** Age, stage and risk score were the independent prognostic factors in Univariate Cox analysis. **(B)** Stage and risk score were the independent prognostic factors in Multivariate Cox analysis. Stratified analyses applied by age (p = 0.029) **(C)**, tumor stage (p = 0.002) **(D)** and sex (p = 0.543) **(E)** demonstrated the predictive of 23-IRGP in OS of CM patients.

significance was identified between the expression level of CTLA-4 and survival results for patients with 23-IRGP (P = 0.063, log- rank test) (**Figure S14F**). Collectively, these investigations between the 23-IRGP and ICIs made us to speculate that the 23-IRGP may have a predictive ability of the response to CM immunotherapy. Kalaora et al. reported that that the among melanoma patients, overexpression of PSMB8 and PSMB9 was predictive for better survival and improved response to immune-checkpoint inhibitors (26), and these genes were highly expressed in the low-risk group (**Figures 8E, F**). Interestingly, the PRAME gene, which is an independent biomarker of uveal melanoma metastasis (27), was also significant expressed in the high-risk group (**Figure 8G**). These results correlated with the immunohistochemical results downloaded from The Human Protein Atlas dataset (THPA) (**Figures 8H–Q**), which showed no results for CTLA-4, while the other five genes were expressed in melanoma tissue. Furthermore, in GEPIA, patients with high PD-1, PD-L1, CTLA-4, PSMB8, and PSMB9 expression showed better OS (**Figures S3A–E**). cBioPortal (https://www.cbioportal.org/) was used to determine the mutation rates of the different genes. According to the results, the probability of mutation for PD-1, PD-L1, CTLA-4, PSMB8, and PSMB9 were 5%, 1.9%, 1.6%, 5%, and 4% (**Figure S4A**), respectively. Poor OS was observed in cases where these genes were mutated (**Figure S4B**). In addition, in the GEPIA analysis, PRAME had no significant effect on OS (**Figure S3F**). However, further study will be needed to verify this result.

Biological Function Analysis in the High-Risk Group Stratified by the 23-IRGP Signature

First, GSEA was used to investigate the results of the GO and KEGG pathway analyses between the high- and low-risk groups using genes that were more highly expressed in the high-risk group than the low-risk group. According to the GO analysis results, these genes were positively correlated with skin-related biological functions, including keratinization, epidermal cell differentiation, keratin filament, intermediate filament cytoskeleton, and skin development (padj < 0.05). A bubble graph of the 16 GO terms enriched in the high-risk group with a padj value < 0.05 is presented in **Figure S5**. Information on every GO term is provided in **Table S1**. As shown in **Figure S6**, several melanoma progression-related pathways, including oxidative phosphorylation (28, 29), retinol metabolism (30–32), and ribosome (33, 34), were significantly upregulated in the high-risk group (padj < 0.05). Collectively, the results obtained using the IRGP signature provide evidence of the molecular mechanisms affected by CM and, thus, the predictive power of this signature for the prognosis of CM patients.

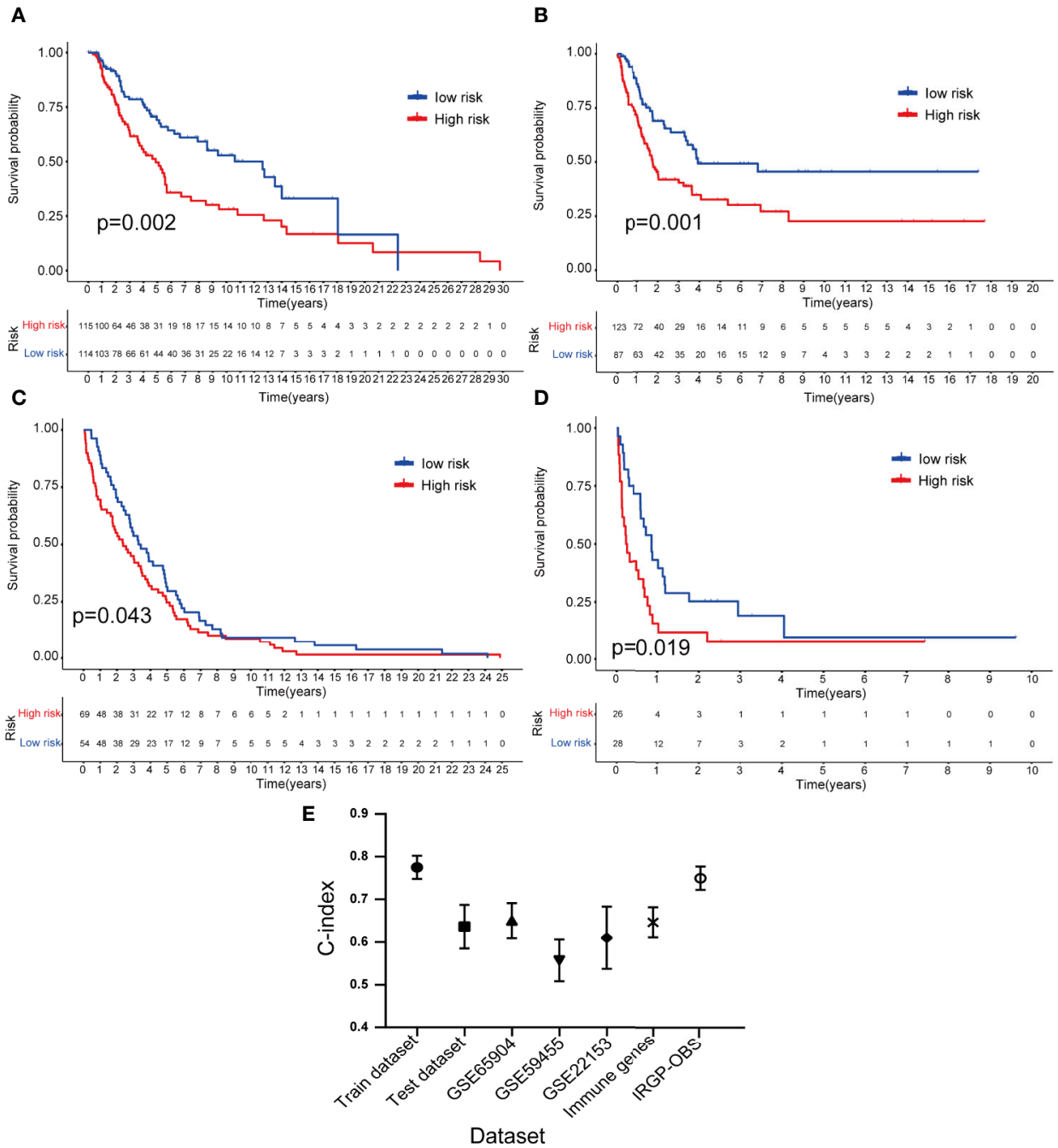

FIGURE 6 | Validation of the 23-IRGP signature. As indicated, OS was poorer for the high-risk group than the low-risk group of the testing cohort **(A)**. Datasets GES65904 **(B)**, GSE59455 **(C)**, and GSE54467 **(D)**. These results showed that the 23-IRGP signature had good predictive ability ($p < 0.05$) **(E)**. The C-index values for the TCGA training, testing cohorts and TCGA dataset, as well as the datasets GES65904, GSE59455, GSE54467, IRGs and IRGP-OBS were 0.775 (95% CI = 0.748–0.802), 0.636 (95% CI = 0.585–0.687), 0.691 (95% CI = 0.653–0.729), 0.650 (95% CI = 0.609–0.691), 0.557 (95% CI = 0.508–0.606), 0.610 (95% CI = 0.537–0.683), 0.647 (95% CI = 0.612–0.682), 0.751 (95% CI = 0.716–0.786), respectively.

Comparison of IRGP Signature Model and Others in CM

TCGA-CM dataset includes primary and metastatic samples, the primary samples submitted to sequence were initially diagnosed melanoma samples; however, the metastatic samples for sequencing were always from follow-up patients instead of initially diagnosed samples. So the TCGA-CM dataset did not always adopt the initially diagnosed melanoma samples for sequencing. So we established another prognostic model in CM determine the effectiveness of this approach according to the observed survival interval (OBS), which

TABLE 2 | Univariate Cox and Multivariate Cox analysis of clinicopathological factors and risk signatures.

Variable	Univariate Cox analysis of clinicopathologicalfactors and risk signatures			Multivariate Cox analysis of clinicopathologicalfactors and risk signatures		
TCGA-train dataset						
id	HR	95% CI	p-value	HR	95% CI	p-value
age	1.02	1.00–1.04	0.013	1.01	0.99–1.03	0.221
gender	1.11	0.73–1.49	0.621	1.25	0.79–1.71	0.339
stage	1.54	1.20–1.88	0.001	1.56	1.20–1.92	0.001
riskScore	10.41	6.43–14.39	1.49E-21	10.64	6.47–14.81	1.15E-20
TCGA-test dataset						
id	HR	95% CI	p-value	HR	95% CI	p-value
age	1.02	1.01–1.03	0.002	1.02	1.01–1.03	0.002
gender	0.94	0.60–1.28	0.805	0.84	0.53–1.15	0.469
stage	1.27	1.02–1.52	0.036	1.3	1.03–1.57	0.029
riskScore	2.12	1.44–2.80	0	2.08	1.41–2.75	0.0002
TCGA dataset						
id	HR	95% CI	p-value	HR	95% CI	p-value
age	1.02	1.01–1.03	0.011	1.01	0.98–1.04	0.010
gender	1.04	0.60–1.48	0.701	1.02	0.61–1.43	0.412
stage	1.42	1.31–1.63	0.006	1.13	0.83–1.43	0.008
riskScore	6.32	2.14–10.50	0.002	5.11	3.12–7.10	0.009
GSE65904 validation dataset						
id	HR	95% CI	p-value	HR	95% CI	p-value
age	0.99	0.98–1.01	0.567	1	0.99–1.02	0.592
gender	1.37	0.90–1.84	0.143	1.31	0.86–1.76	0.205
stage	2.35	1.53–3.17	8.55E-05	2.77	1.78–3.76	5.53E-06
riskScore	1.76	1.34–2.18	4.48E-05	1.98	1.49–2.47	1.87E-06
GSE59455 validation dataset						
id	HR	95% CI	p-value	HR	95% CI	p-value
age	0.99	0.98–1.00	0.177	0.99	0.98–1.00	0.112
gender	1.24	0.84–1.64	0.283	1.17	0.80–1.54	0.421
stage	0.77	0.67–0.87	0	0.76	0.66–0.86	8.68E-05
riskScore	1.35	0.78–1.92	0.141	1.64	0.94–2.34	0.042
GSE22153 validation dataset						
id	HR	95% CI	p-value	HR	95% CI	p-value
age	1.01	0.99–1.03	0.372	1.01	0.99–1.03	0.547
gender	0.99	0.55–1.43	0.967	1.32	0.71–1.93	0.378
stage	1.69	0.66–2.72	0.27	1.05	0.33–1.77	0.938
riskScore	1.95	1.15–2.75	0.013	2.07	1.16–2.98	0.014

could be defined as the time interval from TCGA sampling to patient death or last follow-up (35). As is shown in **Figures 9A, B**, IRGP-OBS prognostic signature divided the TCGA training dataset and testing dataset into a low- or high-risk OBS group, respectively, with cut off value −1.433 (**Figure 9D**). Both in training and testing groups, high-risk group had a poor OBS than low-risk group. As shown in **Figure 9C**, the AUC values for the 1-, 3-, and 5-year OS rates of the training cohort were 0.946, 0.928, and 0.957, respectively, and the C-index was 0.751 (95% CI = 0.716–0.786) (**Figure 6E**). It is worth noting that, group's immune cells infiltration of IRGP-OBS had a similar trend with 23-IRPG's (**Figure 9E**). In this study, both IRGP prognostic and 23-IRGP prognostic models had predictive power of immune cells infiltration, with high AUC value and C-index value.

The 23-IRGP prognostic signature was also compared with the prognostic signatures of individual IRGs. First, as the TCGA CM data had only one normal sample, the samples from the Genotype-Tissue Expression dataset (36) and TCGA CM dataset were merged. Then, significant differentially expressed IRGs were selected. Next, the LASSO penalized Cox regression model was applied to the TCGA clinical dataset, and 24 prognostic IRGs were selected for the final risk scoring model (**Figure 10A**). Most of the 24 prognostic IRGs coded for molecules related to antimicrobials and cytokines. The IRGs significantly stratified the TCGA dataset patients into a low- or high-risk OS group. These data suggested that the high-risk group had a higher risk index than the low-risk group, as a higher risk score was associated with a higher risk of death (**Figures 10B, C**). Moreover, the high-risk group had a significantly poorer OS than the low-risk group ($p < 0.001$) (**Figure 10E**). As shown in **Figure 10D**, the AUC values of the 1-, 3-, and 5-year OS rates were 0.731, 0.760, and 0.749, respectively, and the C-index was 0.647 (95% CI = 0.612–0.682) (**Figure 6E**). Collectively, these results demonstrate that the prognostic signatures of these IRGs had predictive ability but with a smaller AUC and lower C-index than the 23-IRGP signature, demonstrating that the 23-IRGP signature was the more precise predictive model in CM.

DISCUSSION

CM is a solid malignant tumor with strong immunogenicity with a rapidly increasing incidence rate worldwide. Since the approval of

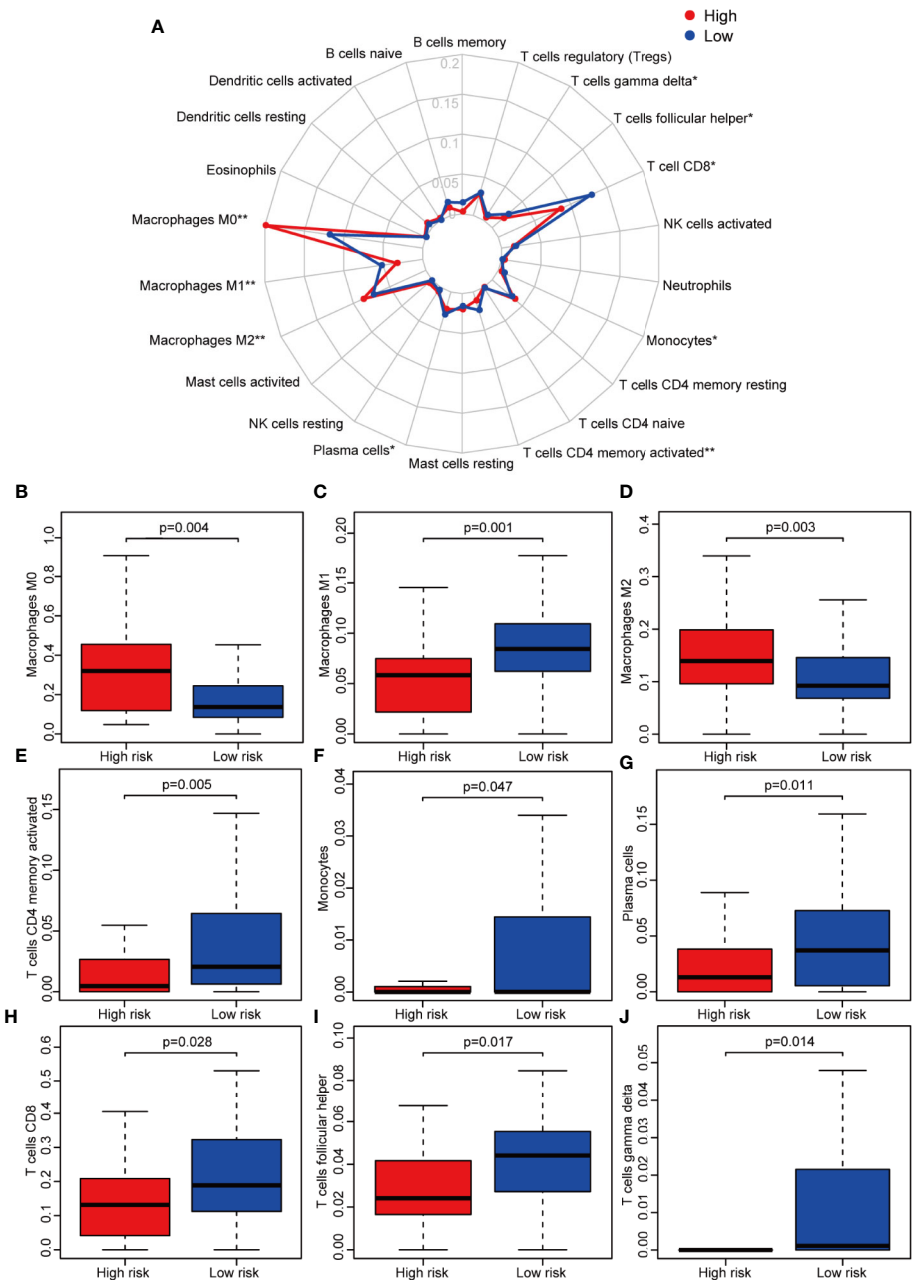

FIGURE 7 | Immune infiltration status of the 23 IRGPs. **(A)** Summary of the abundances of 22 types of immune cells, as estimated with the use of the CIBERSORT analytical tool for different risk groups. **(B–J)** The abundance distribution of specific immune cells within different risk groups. The abundances of M0 macrophages ($p = 0.004$) and M2 macrophages ($p = 0.003$) were significantly greater in the high risk group, while the abundances of M1 macrophages ($p = 0.001$), activated CD4+ memory T cells ($p = 0.005$), monocytes ($p = 0.047$), plasma cells ($p = 0.011$), CD8+ T cells ($p = 0.028$), follicular helper T cells ($p = 0.017$), and gamma delta T cells ($p = 0.014$) were significantly enriched in the low risk group. *$p < 0.05$, **$p < 0.01$ (t-test).

interferon-α for the treatment of CM in 1995, the potential of other immunotherapies have received much attention from researchers (37). Like with many other tumors, immune checkpoint (PD-1/PD-L1 and CTLA-4) blockade therapy has also become a target clinical. In 2011, ipilimumab, which targets CTLA-4, provided a major breakthrough in the clinical treatment of CM and was subsequently approved for marketing by the Food and Drug Administration (FDA). Ipilimumab is the first antibody drug to prolong the OS of patients with metastatic cancer (38). However, ipilimumab has been associated with some toxicity; thus, other immune surveillance sites have since been investigated, which has led to phase III clinical studies of the anti-PD-1

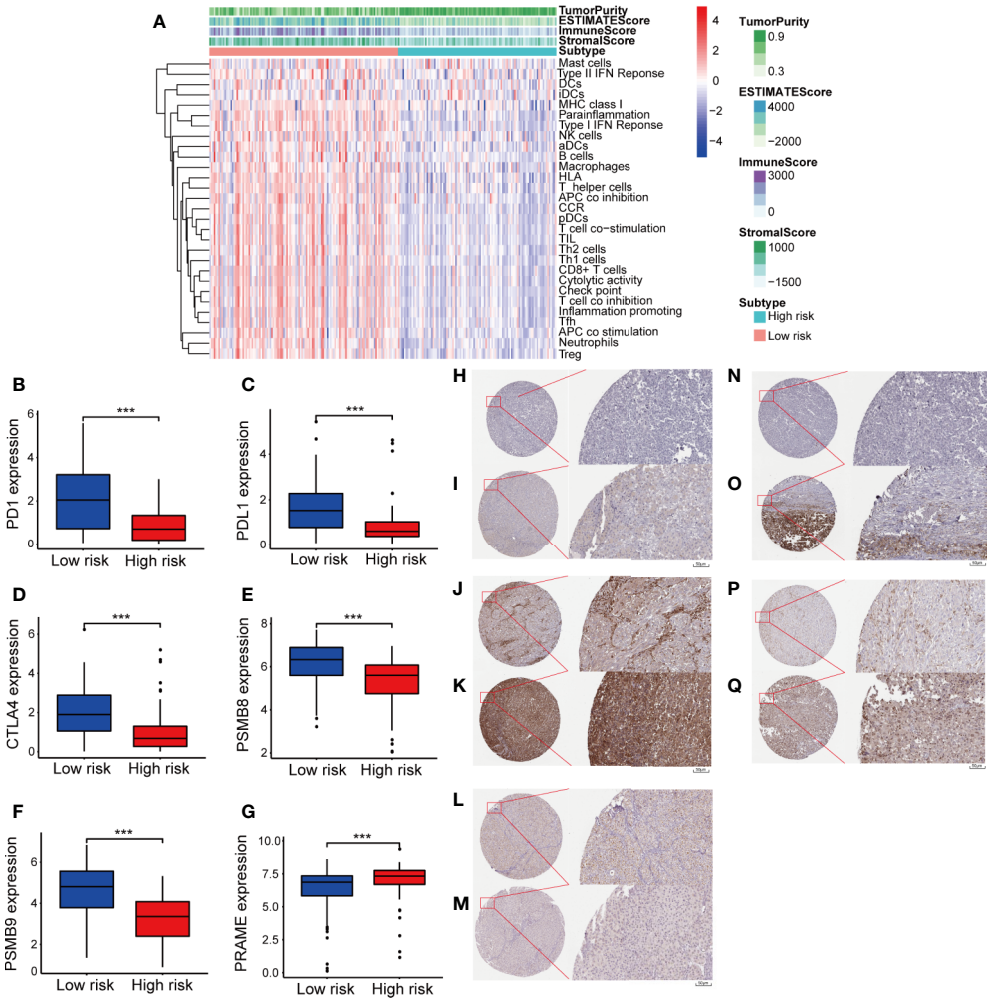

FIGURE 8 | Tumor micro-environment (TME) and key genes expression in two different groups. In TME, "TumorPurity" is the percentage of tumor cells, "ImmuneScore" is the percentage of Immune cells, "StromalScore" is the percentage of stromal cells, "EstimateScore" is the percentage that merge the "ImmuneScore" and "StromalScore". as we can see, high risk group had higher tumor purity with lower immune cells and stromal cells infiltration **(A)**. In low immune risk group, PD-1, PD-L1, CTLA-4, PSMB8, and PSMB9 were highly expressed **(B–F)**. PRAME were significant expressed in high risk group **(G)**. **(H)** IHC result of PD-1 protein in high risk group. Staining, not detected; intensity, negative; quantity, none; location, none. **(I)** IHC result of PD-1 protein in low risk group. Staining, low; intensity, weak; quantity, 75%–25%; location, cytoplasmic/membranous. **(J)** IHC result of PD-L1 protein in high risk group. Staining, not detected; intensity, negative; quantity, none; location, none. **(K)** IHC result of PD-L1 protein in low risk group. Staining, high; intensity, Strong; quantity, >75%; location, cytoplasmic/membranous. **(L)** IHC result of PSMB8 protein in high risk group. Staining, low; intensity, moderate; quantity, <25%; location, cytoplasmic/membranous nuclear. **(M)** IHC result of PSMB8 protein in low risk group. Staining, high; intensity, Strong; quantity, >75%; location, cytoplasmic/membranous nuclear. **(N)** IHC result of PSMB9 protein in high risk group. Staining, not detected; intensity, negative; quantity, none; location, none. **(O)** IHC result of PSMB9 protein in low risk group. Staining, medium; intensity, moderate; quantity, >75%; location, cytoplasmic/membranous nuclear. **(P)** IHC result of PRAME protein in high risk group. Staining, medium; intensity, moderate; quantity, 75%–25%; location, cytoplasmic/membranous. **(Q)** IHC result of PRAME protein in low risk group. Staining, not detected; intensity, weak; quantity, <25%; location, cytoplasmic/membranous. ***$p < 0.01$ (t-test).

antibody drugs pembrolizumab and nivolumab. These drugs were approved for use by the FDA in September and December 2014, respectively. With lower anti-drug resistance and higher clinical safety, these anti-PD-1 antibody drugs offer hope to patients with advanced unresectable or metastatic CM (39, 40). Given that the results of single antibody drugs are limited and the many links between the occurrence and development of CM, a multiple-immune therapy strategy may have more prospects (41). It is, therefore, necessary to develop a prognostic signature using IRGs.

Due to the technical bias of sequencing platforms, gene expression data must be preprocessed for standardization, which is particularly significant when establishing prognostic signatures. To achieve robust prognosis prediction without the technical bias associated with different platforms, prognostic signatures of IRGPs can be established by pairwise comparison, which does not require preprocessing for data standardization. IRGP scores are calculated based on the expression levels of IRGs in the same sample. As such, the

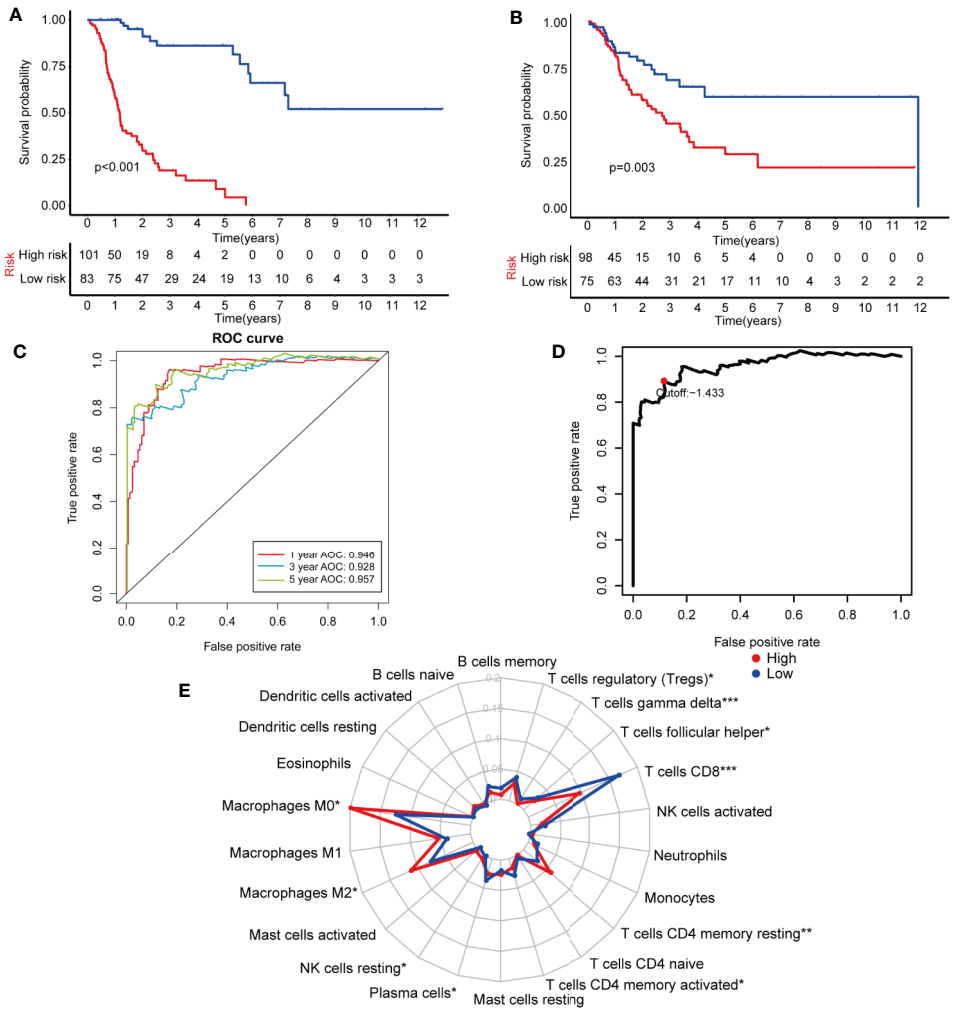

FIGURE 9 | Establishment and assessment of the IRGP-OBS. **(A)** According to the OBS curve, OBS was poorer for the high risk group as compared to the low risk group in the training cohort ($p < 0.001$). **(B)** According to the OBS curve, OBS was poorer for the high risk group as compared to the low risk group in the training cohort ($p = 0.003$). **(C)** The AUCs for 1-, 3-, and 5-year OS in the training cohort were 0.946, 0.928, and 0.957, respectively. **(D)** A time-dependent ROC curve for IRGP-OBS in the training and testing dataset. An IRGP score of −1.433 was used as a cut-off to assign patients to the high- or low-risk group. **(E)** The abundances of M0 macrophages ($p = 0.013$), M2 macrophages ($p = 0.049$), T cells CD4 memory resting ($p = 0.001$) and NK cells resting ($p = 0.035$) were significantly greater in the high risk group, while the abundances of CD8+ T cells ($p < 0.001$), plasma cells ($p = 0.043$), follicular helper T cells ($p = 0.025$), gamma delta T cells ($p < 0.001$), T cells regulatory ($p = 0.019$), T cells CD4 memory activated ($p = 0.011$) were significantly enriched in the low risk group. *$p < 0.05$, **$p < 0.01$, ***$p < 0.001$ (t-test).

prognostic signature is not only able to overcome the batch effects of different platforms, but also does not require the scaling and normalization of data. In CM prognostic model, based on the AUC and C-index values, the prediction capability of IRGPs is more promising when compared with prognostic checkpoint (AUC = 0.729) (42), prognostic DNA methylation (AUC = 0.822) (43), prognostic IRGs that require preprocessing for data standardization. Moreover, this approach has been reported to be robust in other cancer-related studies (44, 45).

Given that the results of TCGA-CM dataset is made up of primary and metastatic samples, and the metastatic samples for sequencing were always from follow-up patients instead of initially diagnosed samples, IRGP-OBS prognostic model were established to make a predict comparison with 23-IRGP. As we expected, both IRGP-OBS model and 23-IRGP model had precious prediction capability with high AUC and C-index values. In addition, many researchers of CM also regarded OS as golden standard to evaluate the model predict power (43, 46), and there is no significantly different trend in immune cell infiltration in our study. Collectively, IRGP model could be well applied to survival probability and immune cell infiltration of CM patients, providing reference for immunotherapy.

In the present study, an IRGP signature was established using a LASSO penalized Cox regression model to predict OS in CM patients. The prognostic signature of the 23 IRGPs consisted of 46 unique IRGs. Most of the genes in the immune signature encoded molecules related to antimicrobials and cytokines, which play important roles in the response to stimuli and the immune

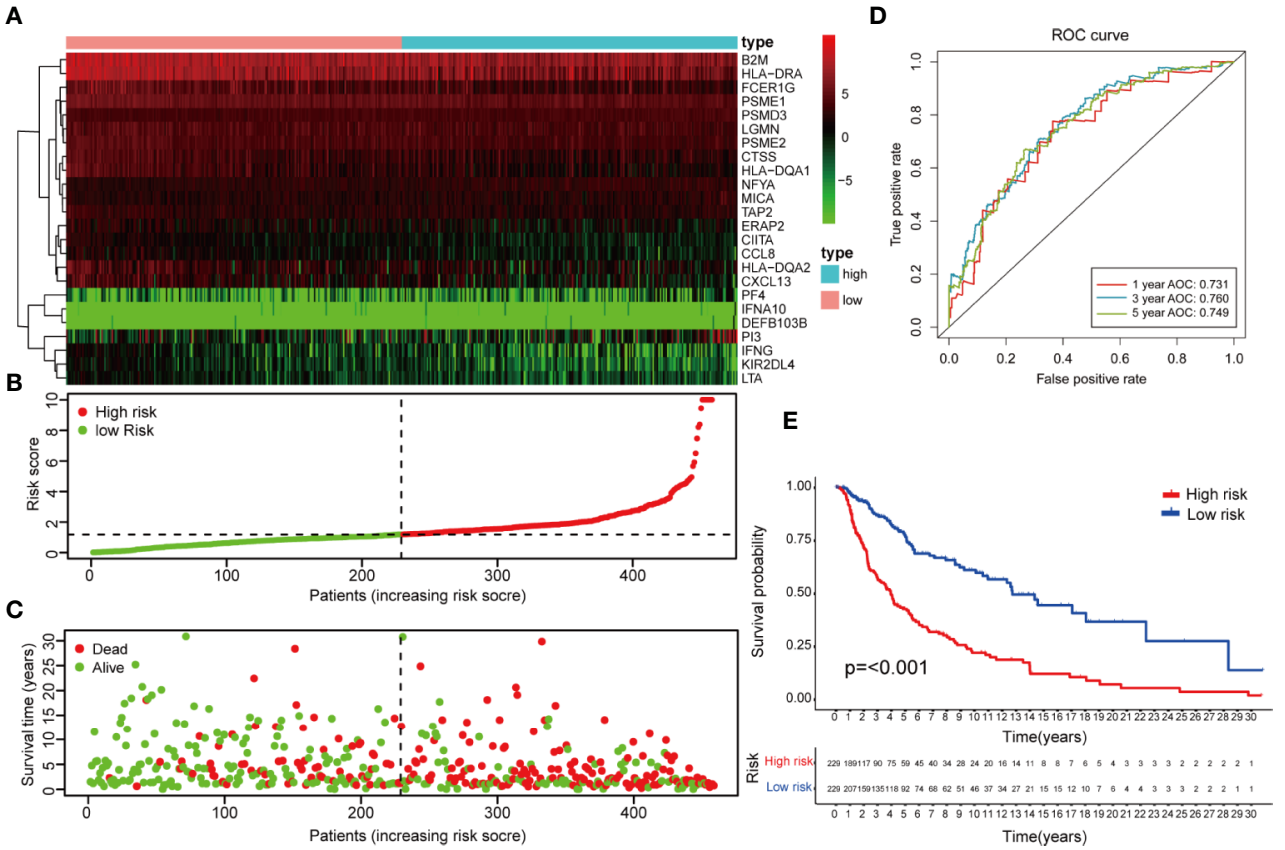

FIGURE 10 | Identification of IRGs and comparison with IRGPs. **(A)** A heat map of the patient risk scores of the 24 IRGs. **(B)** Based on the 24 IRGs, patients in the TCGA dataset were assigned to the high- or low-immune risk groups. The red and green points represent the risk scores of the high and low risk groups, respectively. **(C)** A plot of OS based on the 24 IRGs. The red points represent deaths and blue points represent survivors. **(D)** The AUCs for 1-, 3-, and 5-year OS in the training cohort were 0.731, 0.760, and 0.749, respectively. **(E)** According to the OS curve, OS was poorer for the high risk group as compared to the low risk group in the training cohort ($p < 0.001$). These results showed that the prognostic signature of the IRGs had good predictive power, but with a smaller AUC and lower C-index (0.610 in **Figure 5E**) than the 23 IRGPs signature. Therefore, the 23-IRGP was more precisely predictive for CM.

microenvironment. Many of these IRGs have be shown to be related to cancer development and prognosis, expression of serine/threonine kinase 1 promotes melanoma metastasis (47), serum levels of C-C motif chemokine ligand 17 (CCL17) are an independent prognostic marker of distant metastasis of melanoma, and patients with 43% of patients with high CCL17 levels survived to 3 years (48). Singh et al. found that activation of intratumoral cluster of differentiation 40 induced T cell-mediated eradication of melanoma in the brain (49). Smith et al. discovered that endothelin 1 was enhanced in treated melanomas and conferred drug resistance *via* endothelin receptor type A (50). Ribonuclease L has been reported to interact with microRNA-146a as a sex-specific factor in melanoma (51), and semaphorin 7A has been found to reduce the pulmonary metastasis of melanoma (52).

In this study, according to 23-IRGP signature, ICIs, including PD-1, PD-L1, and CTLA-4, were highly expressed in the low-risk group which had better survival. When exploring the relationship between PD-1/PD-L1 and the 23-IRGP value, the 23-IRGP signature presented significant relationship with PD-1/PD-L1 expression. Moreover, the interaction between ICIs and the 23-IRGP indicated a combined prognostic effect on patient survival. M2 macrophages have been shown to promote growth and are related to poorer OS in melanoma patients, while M1 macrophages support tumor destruction and antigen presentation (53). Yamaguchi et al. found that anti-PD-1 antibody (nivolumab) therapy increased the activated effector memory phenotypes of central memory T cells and subsets of CD4+ and CD8+ central memory T cells, as well as Th1 plus T-helper follicular 1 cells (54), indicating that these immune cells can prolong patient survival when they are activated. The results of the present study revealed a significant increase in the abundance of infiltrating M0 and M2 macrophages in the high-risk immune group, while the abundances of infiltrating M1 macrophages, activated memory CD4+ T cells, CD8+ T cells, follicular helper T cells, monocytes, plasma cells, and gamma delta T cells were greater in the low-risk immune group, which was found to have a better survival rate. In addition, both the mRNA analysis and immunohistochemistry results showed that the high-risk group had higher tumor purity and lower infiltration of immune cells and stromal cells. Meanwhile, low-risk group had higher immune

checkpoint inhibitors indicating that patients in the low-risk group may have better outcomes with immunotherapy. Nowadays, ICIs provide a new way to cacer immunotherapy, when exploring the relationship 23-IRGP signature and ICIs, 23-IRGP signature showed closely connections with ICIs expression. Moreover, the relationship between 23-IRGP and ICIs indicated an integrated prognostic power on patient OS, which is associated with previous result that M1 macrophages, activated CD4+ memory T cells, monocytes, plasma cells, CD8+ T cells, follicular helper T cells, and gamma delta T cells infiltration and ICIs expression may make a difference on patients' OS and patients' immunotherapy effect. Collectively, it may suggested that the 23-IRGP may have a predictive ability of the response to CM immunotherapy (25).

In our previous study, overexpression of PSMB8 and PSMB9 was found to be predictive of better survival and improved response to immune-checkpoint inhibitors. This was reflected in the low-risk group in the present study, in which PSMB8 and PSMB9 were highly expressed, indicating that the low-risk group had better survival rate and immunotherapy effect. Moreover, this indicates that a mutation in these genes will result in poor OS. Unexpectedly, PRAME, which acts as an independent biomarker in uveal melanoma metastasis, was also significantly expressed in the high-risk group, indicating that PRAME may also be a biomarker in CM. However, further study will be needed to verify these results. Thus, our research outcomes were closely in line with those of previous studies, demonstrating the precise predictive power of our platform (55).

The 23-IRGP signature identified three pathways (i.e., oxidative phosphorylation, retinol metabolism, and ribosome) that were highly related to the invasiveness of melanoma, suggesting that a high-risk score was correlated with increased melanoma metastasis and poorer survival. These results indicated the capability of the IRGP signature for predicting tumor invasion in CM patients.

Nevertheless, there were some limitations to this study that should be addressed. First, the 23-IRGP prognostic signature was based on a retrospective study using the TCGA CM dataset and validated using three microarray datasets from the GEO dataset. Thus, these results should be validated against other datasets with different sample attributes in a prospective cohort. Second, as the 23 IRGPs were used to construct a prognostic signature model, different prognostic signature models are needed for comparison. Third, further validation of the 23 IRGPs by quantitative real-time polymerase chain reaction, western blotting, and immunohistochemical analyses will be needed before this approach can be applied clinically. Fourth, due to the fact that the relevant CM data (such as patients that received PD-1, PD-L1, and CTLA-4 treatment) cannot be obtained, the analysis of cross-talk between the signature and ICIs cannot be compensated systematically at present.

CONCLUSIONS

In conclusion, our findings indicate that our prognostic signature established using 23 IRGPs is a novel, promising model for predicting the prognosis of CM, indicating an association between the immune microenvironment and CM. This approach can be used to discover signatures in other diseases without the technical bias associated with different platforms.

DATA AVAILABILITY STATEMENT

Publicly available datasets were analyzed in this study. This data can be found here: TCGA dataset (https://www.cancer.gov/about-nci/organization/ccg/research/structural-genomics/tcga); GEO dataset (https://www.ncbi.nlm.nih.gov/gds/): GSE65904, GSE59455, and GSE22153.

AUTHOR CONTRIBUTIONS

Ya-NX conceptualized the project, all data analysis and wrote the first draft of the manuscript. Yi-NX, Z-CW, Y-ZM, and P-YW contributed to processing, analysis, and interpretation of the data. W-QT contributed to guide the data analysis, and manuscript writing. All authors contributed to the article and approved the submitted version.

FUNDING

This study was supported by the National Natural Science Foundation of China (No. 81671918), the National Key Research Program of China (No. 2016YFC1101004), and Zhejiang Provincial Medical and Healthy Science Foundation of China (No. 2019ZD028 and 2018KY874).

ACKNOWLEDGMENTS

This article has been released as a pre-print at Research Square, DOI:10.21203/rs.3.rs-38060/v1.

SUPPLEMENTARY MATERIAL

The Supplementary Material for this article can be found online at: https://www.frontiersin.org/articles/10.3389/fimmu.2020.576914/full#supplementary-material

REFERENCES

1. W. H. Organization. *Skin cancers*. (2020). Retrieved from https://www.who.int/uv/faq/skincancer/en/index1.html
2. Miller AJ, Mihm MC Jr. Melanoma. *N Engl J Med* (2006) 355(1):51–65. doi: 10.1056/NEJMra052166
3. Siegel RL, Miller KD, Jemal A. Cancer statistics, 2018. *CA Cancer J Clin* (2018) 68(1):7–30. doi: 10.3322/caac.21442
4. Furue M, Kadono T. Melanoma therapy: Check the checkpoints. *J Dermatol* (2016) 43(2):121–4. doi: 10.1111/1346-8138.13257
5. Sullivan RJ, Atkins MB, Kirkwood JM, Agarwala SS, Clark JII, Ernstoff MS, et al. An update on the Society for Immunotherapy of Cancer consensus

statement on tumor immunotherapy for the treatment of cutaneous melanoma: version 2.0. *J Immunother Cancer* (2018) 6(1):44. doi: 10.1186/s40425-018-0362-6
6. Yamazaki N, Uhara H, Wada H, Matsuda K, Yamamoto K, Shimamoto T, et al. Phase I study of pegylated interferon-alpha-2b as an adjuvant therapy in Japanese patients with malignant melanoma. *J Dermatol* (2016) 43(10):1146–53. doi: 10.1111/1346-8138.13338
7. Kirkwood JM, Ibrahim JG, Sondak VK, Richards J, Flaherty LE, Ernstoff MS, et al. High- and low-dose interferon alfa-2b in high-risk melanoma: first analysis of intergroup trial E1690/S9111/C9190. *J Clin Oncol* (2000) 18 (12):2444–58. doi: 10.1200/jco.2000.18.12.2444
8. Peggs KS, Quezada SA, Korman AJ, Allison JP. Principles and use of anti-CTLA-4 antibody in human cancer immunotherapy. *Curr Opin Immunol* (2006) 18(2):206–13. doi: 10.1016/j.coi.2006.01.011
9. Sharpe AH, Wherry EJ, Ahmed R, Freeman GJ. The function of programmed cell death 1 and its ligands in regulating autoimmunity and infection. *Nat Immunol* (2007) 8(3):239–45. doi: 10.1038/ni1443
10. Cirenajwis H, Ekedahl H, Lauss M, Harbst K, Carneiro A, Enoksson J, et al. Molecular stratification of metastatic melanoma using gene expression profiling: Prediction of survival outcome and benefit from molecular targeted therapy. *Oncotarget* (2015) 6(14):12297–309. doi: 10.18632/oncotarget.3655
11. Perez-Guijarro E, Yang HH, Araya RE, El Meskini R, Michael HT, Vodnala SK, et al. Multimodel preclinical platform predicts clinical response of melanoma to immunotherapy. *Nat Med* (2020) 26(5):781–91. doi: 10.1038/s41591-020-0818-3
12. Osella-Abate S, Ribero S, Sanlorenzo M, Maule MM, Richiardi L, Merletti F, et al. Risk factors related to late metastases in 1,372 melanoma patients disease free more than 10 years. *Int J Cancer* (2015) 136(10):2453–7. doi: 10.1002/ijc.29281
13. Ribero S, Moscarella E, Ferrara G, Piana S, Argenziano G, Longo C. Regression in cutaneous melanoma: a comprehensive review from diagnosis to prognosis. *J Eur Acad Dermatol Venereol* (2016) 30(12):2030–7. doi: 10.1111/jdv.13815
14. Tomczak K, Czerwinska P, Wiznerowicz M. The Cancer Genome Atlas (TCGA): an immeasurable source of knowledge. *Contemp Oncol (Pozn)* (2015) 19(1a):A68–77. doi: 10.5114/wo.2014.47136
15. Bhattacharya S, Andorf S, Gomes L, Dunn P, Schaefer H, Pontius J, et al. ImmPort: disseminating data to the public for the future of immunology. *Immunol Res* (2014) 58(2-3):234–9. doi: 10.1007/s12026-014-8516-1
16. Edgar R, Domrachev M, Lash AE. Gene Expression Omnibus: NCBI gene expression and hybridization array data repository. *Nucleic Acids Res* (2002) 30(1):207–10. doi: 10.1093/nar/30.1.207
17. Zhao K, Xu L, Li F, Ao J, Jiang G, Shi R, et al. Identification of hepatocellular carcinoma prognostic markers based on 10-immune gene signature. *Biosci Rep* (2020) 40(8):BSR20200894. doi: 10.1042/bsr20200894
18. Liu J, Mei J, Li S, Wu Z, Zhang Y. Establishment of a novel cell cycle-related prognostic signature predicting prognosis in patients with endometrial cancer. *Cancer Cell Int* (2020) 20:329. doi: 10.1186/s12935-020-01428-z
19. Newman AM, Liu CL, Green MR, Gentles AJ, Feng W, Xu Y, et al. Robust enumeration of cell subsets from tissue expression profiles. *Nat Methods* (2015) 12(5):453–7. doi: 10.1038/nmeth.3337
20. Subramanian A, Tamayo P, Mootha VK, Mukherjee S, Ebert BL, Gillette MA, et al. Gene set enrichment analysis: a knowledge-based approach for interpreting genome-wide expression profiles. *Proc Natl Acad Sci U.S.A.* (2005) 102(43):15545–50. doi: 10.1073/pnas.0506580102
21. Engebretsen S, Bohlin J. Statistical predictions with glmnet. *Clin Epigenet* (2019) 11(1):123. doi: 10.1186/s13148-019-0730-1
22. Ritchie ME, Phipson B, Wu D, Hu Y, Law CW, Shi W, et al. limma powers differential expression analyses for RNA-sequencing and microarray studies. *Nucleic Acids Res* (2015) 43(7):e47. doi: 10.1093/nar/gkv007
23. Yoshihara K, Shahmoradgoli M, Martinez E, Vegesna R, Kim H, Torres-Garcia W, et al. Inferring tumour purity and stromal and immune cell admixture from expression data. *Nat Commun* (2013) 4:2612. doi: 10.1038/ncomms3612
24. Pencina MJ, D'Agostino RB, D'Agostino RB Jr., Vasan RS. Evaluating the added predictive ability of a new marker: from area under the ROC curve to reclassification and beyond. *Stat Med* (2008) 27(2):157–72; discussion 207-12. doi: 10.1002/sim.2929
25. Zhou M, Zhang Z, Bao S, Hou P, Yan C, Su J, et al. Computational recognition of lncRNA signature of tumor-infiltrating B lymphocytes with potential implications in prognosis and immunotherapy of bladder cancer. *Brief Bioinform* (2020) 00(00):1–13. doi: 10.1093/bib/bbaa047
26. Kalaora S, Lee JS, Barnea E, Levy R, Greenberg P, Alon M, et al. Immunoproteasome expression is associated with better prognosis and response to checkpoint therapies in melanoma. *Nat Commun* (2020) 11 (1):896. doi: 10.1038/s41467-020-14639-9
27. Field MG, Decatur CL, Kurtenbach S, Gezgin G, van der Velden PA, Jager MJ, et al. PRAME as an Independent Biomarker for Metastasis in Uveal Melanoma. *Clin Cancer Res* (2016) 22(5):1234–42. doi: 10.1158/1078-0432.Ccr-15-2071
28. Ho J, de Moura MB, Lin Y, Vincent G, Thorne S, Duncan LM, et al. Importance of glycolysis and oxidative phosphorylation in advanced melanoma. *Mol Cancer* (2012) 11:76. doi: 10.1186/1476-4598-11-76
29. Salhi A, Jordan AC, Bochaca II, Izsak A, Darvishian F, Houvras Y, et al. Oxidative Phosphorylation Promotes Primary Melanoma Invasion. *Am J Pathol* (2020) 190(5):1108–17. doi: 10.1016/j.ajpath.2020.01.012
30. Amann PM, Luo C, Owen RW, Hofmann C, Freudenberger M, Schadendorf D, et al. Vitamin A metabolism in benign and malignant melanocytic skin cells: importance of lecithin/retinol acyltransferase and RPE65. *J Cell Physiol* (2012) 227(2):718–28. doi: 10.1002/jcp.22779
31. Hassel JC, Amann PM, Schadendorf D, Eichmuller SB, Nagler M, Bazhin AV. Lecithin retinol acyltransferase as a potential prognostic marker for malignant melanoma. *Exp Dermatol* (2013) 22(11):757–9. doi: 10.1111/exd.12236
32. Amann PM, Czaja K, Bazhin AV, Ruhl R, Skazik C, Heise R, et al. Knockdown of lecithin retinol acyltransferase increases all-trans retinoic acid levels and restores retinoid sensitivity in malignant melanoma cells. *Exp Dermatol* (2014) 23(11):832–7. doi: 10.1111/exd.12548
33. El Hassouni B, Sarkisjan D, Vos JC, Giovannetti E, Peters GJ. Targeting the Ribosome Biogenesis Key Molecule Fibrillarin to Avoid Chemoresistance. *Curr Med Chem* (2019) 26(33):6020–32. doi: 10.2174/0929867326666181203133332
34. Scull CE, Zhang Y, Tower N, Rasmussen L, Padmalayam I, Hunter R, et al. Discovery of novel inhibitors of ribosome biogenesis by innovative high throughput screening strategies. *Biochem J* (2019) 476(15):2209–19. doi: 10.1042/bcj20190207
35. Xiong J, Bing Z, Guo S. Observed Survival Interval: A Supplement to TCGA Pan-Cancer Clinical Data Resource. *Cancers (Basel)* (2019) 11(3):280. doi: 10.3390/cancers11030280
36. Human genomics. The Genotype-Tissue Expression (GTEx) pilot analysis: multitissue gene regulation in humans. *Science* (2015) 348(6235):648–60. doi: 10.1126/science.1262110
37. Girotti MR, Saturno G, Lorigan P, Marais R. No longer an untreatable disease: how targeted and immunotherapies have changed the management of melanoma patients. *Mol Oncol* (2014) 8(6):1140–58. doi: 10.1016/j.molonc.2014.07.027
38. Hoag H. Drug development: a chance of survival. *Nature* (2014) 515(7527): S118–20. doi: 10.1038/515S118a
39. Hodi FS, Chiarion-Sileni V, Gonzalez R, Grob JJ, Rutkowski P, Cowey CL, et al. Nivolumab plus ipilimumab or nivolumab alone versus ipilimumab alone in advanced melanoma (CheckMate 067): 4-year outcomes of a multicentre, randomised, phase 3 trial. *Lancet Oncol* (2018) 19(11):1480–92. doi: 10.1016/s1470-2045(18)30700-9
40. Schadendorf D, Hodi FS, Robert C, Weber JS, Margolin K, Hamid O, et al. Pooled Analysis of Long-Term Survival Data From Phase II and Phase III Trials of Ipilimumab in Unresectable or Metastatic Melanoma. *J Clin Oncol* (2015) 33(17):1889–94. doi: 10.1200/jco.2014.56.2736
41. Kaufman HL, Kirkwood JM, Hodi FS, Agarwala S, Amatruda T, Bines SD, et al. The Society for Immunotherapy of Cancer consensus statement on tumour immunotherapy for the treatment of cutaneous melanoma. *Nat Rev Clin Oncol* (2013) 10(10):588–98. doi: 10.1038/nrclinonc.2013.153
42. Subrahmanyam PB, Dong Z, Gusenleitner D, Giobbie-Hurder A, Severgnini M, Zhou J, et al. Distinct predictive biomarker candidates for response to anti-CTLA-4 and anti-PD-1 immunotherapy in melanoma patients. *J Immunother Cancer* (2018) 6(1):18. doi: 10.1186/s40425-018-0328-8

43. Guo W, Zhu L, Zhu R, Chen Q, Wang Q, Chen JQ. A four-DNA methylation biomarker is a superior predictor of survival of patients with cutaneous melanoma. *Elife* (2019) 8:e44310. doi: 10.7554/eLife.44310
44. Li B, Cui Y, Diehn M, Li R. Development and Validation of an Individualized Immune Prognostic Signature in Early-Stage Nonsquamous Non-Small Cell Lung Cancer. *JAMA Oncol* (2017) 3(11):1529–37. doi: 10.1001/jamaoncol.2017.1609
45. Zhang L, Zhu P, Tong Y, Wang Y, Ma H, Xia X, et al. An immune-related gene pairs signature predicts overall survival in serous ovarian carcinoma. *Onco Targets Ther* (2019) 12:7005–14. doi: 10.2147/ott.S200191
46. Emran AA, Nsengimana J, Punnia-Moorthy G, Schmitz U, Gallagher SJ, Newton-Bishop J, et al. Study of the Female Sex Survival Advantage in Melanoma-A Focus on X-Linked Epigenetic Regulators and Immune Responses in Two Cohorts. *Cancers (Basel)* (2020) 12(8):2082. doi: 10.3390/cancers12082082
47. Cho JH, Robinson JP, Arave RA, Burnett WJ, Kircher DA, Chen G, et al. AKT1 Activation Promotes Development of Melanoma Metastases. *Cell Rep* (2015) 13(5):898–905. doi: 10.1016/j.celrep.2015.09.057
48. Weide B, Allgaier N, Hector A, Forschner A, Leiter U, Eigentler TK, et al. Increased CCL17 serum levels are associated with improved survival in advanced melanoma. *Cancer Immunol Immunother* (2015) 64(9):1075–82. doi: 10.1007/s00262-015-1714-4
49. Singh M, Vianden C, Cantwell MJ, Dai Z, Xiao Z, Sharma M, et al. Intratumoral CD40 activation and checkpoint blockade induces T cell-mediated eradication of melanoma in the brain. *Nat Commun* (2017) 8 (1):1447. doi: 10.1038/s41467-017-01572-7
50. Smith MP, Rowling EJ, Miskolczi Z, Ferguson J, Spoerri L, Haass NK, et al. Targeting endothelin receptor signalling overcomes heterogeneity driven therapy failure. *EMBO Mol Med* (2017) 9(8):1011–29. doi: 10.15252/emmm.201607156
51. Sangalli A, Orlandi E, Poli A, Maurichi A, Santinami M, Nicolis M, et al. Sex-specific effect of RNASEL rs486907 and miR-146a rs2910164 polymorphisms' interaction as a susceptibility factor for melanoma skin cancer. *Melanoma Res* (2017) 27(4):309–14. doi: 10.1097/cmr.0000000000000360
52. Ma B, Herzog EL, Lee CG, Peng X, Lee CM, Chen X, et al. Role of chitinase 3-like-1 and semaphorin 7a in pulmonary melanoma metastasis. *Cancer Res* (2015) 75(3):487–96. doi: 10.1158/0008-5472.Can-13-3339
53. Lopez-Janeiro A, Padilla-Ansala C, de Andrea CE, Hardisson D, Melero I. Prognostic value of macrophage polarization markers in epithelial neoplasms and melanoma. A systematic review and meta-analysis. *Mod Pathol* (2020) 33 (8):1458–65. doi: 10.1038/s41379-020-0534-z
54. Yamaguchi K, Mishima K, Ohmura H, Hanamura F, Ito M, Nakano M, et al. Activation of central/effector memory T cells and T-helper 1 polarization in malignant melanoma patients treated with anti-programmed death-1 antibody. *Cancer Sci* (2018) 109(10):3032–42. doi: 10.1111/cas.13758
55. Xue Y, Xue Y, Wang Z, Mo Y, Wang P, Tan W. A Novel Signature of 23 Immunity-related Gene Pairs is Prognostic of Cutaneous Melanoma. *PREPRINT*. doi: 10.21203/rs.3.rs-38060/v1. (Posted 29 Jun, 2020) available at Rsearch Square.

Conflict of Interest: The authors declare that the research was conducted in the absence of any commercial or financial relationships that could be construed as a potential conflict of interest.

frontiers in Immunology

SYSTEMATIC REVIEW
published: 21 October 2020
doi: 10.3389/fimmu.2020.01354

Diagnosis and Management of Hematological Adverse Events Induced by Immune Checkpoint Inhibitors: A Systematic Review

Nabil E. Omar[1†], Kareem A. El-Fass[2†], Abdelrahman I. Abushouk[3], Noha Elbaghdady[4], Abd Elmonem M. Barakat[5], Ahmed E. Noreldin[6], Dina Johar[7], Mohamed Yassin[8], Anas Hamad[1], Shereen Elazzazy[1] and Said Dermime[9]*

[1] Pharmacy Department, National Center for Cancer Care and Research, Hamad Medical Corporation, Doha, Qatar, [2] Department of Pharmacy Practice, College of Clinical Pharmacy, King Faisal University, Hofuf, Saudi Arabia, [3] Division of Cardiology, Department of Medicine, Harvard Medical School, Boston, MA, United States, [4] Clinical Pharmacy Department, School of Pharmacy, New Giza University, Giza, Egypt, [5] Faculty of Veterinary Medicine, Damanhour University, Damanhour, Egypt, [6] Department of Histology and Cytology, Faculty of Veterinary Medicine, Damanhour University, Damanhour, Egypt, [7] Basic Sciences Department, Faculty of Medicine, Algalala University, Suez, Egypt, [8] Medical Oncology-Hematology Section, National Center for Cancer Care and Research, Hamad Medical Corporation, Doha, Qatar, [9] National Centre for Cancer Care and Research, Hamad Medical Corporation, Doha, Qatar

OPEN ACCESS

Edited by:
Zhihai Qin,
Institute of Biophysics (CAS), China

Reviewed by:
Ryota Tanaka,
University of Tsukuba, Japan
Wei Chen,
Stanford University, United States

***Correspondence:**
Dina Johar
umjohar@myumanitoba.ca;
dinajohar@gmail.com

[†]These authors have contributed equally to this work

Specialty section:
This article was submitted to Cancer Immunity and Immunotherapy, a section of the journal Frontiers in Immunology

Received: *01 February 2020*
Accepted: *27 May 2020*
Published: *21 October 2020*

Citation:
Omar NE, El-Fass KA, Abushouk AI, Elbaghdady N, Barakat AEM, Noreldin AE, Johar D, Yassin M, Hamad A, Elazzazy S and Dermime S (2020) Diagnosis and Management of Hematological Adverse Events Induced by Immune Checkpoint Inhibitors: A Systematic Review. Front. Immunol. 11:1354. doi: 10.3389/fimmu.2020.01354

There has been less volume of literature focusing on the Immune-related Hematological Adverse Drug Events (Hem-irAEs) of Immune Checkpoint Inhibitors (ICPis) in cancer patients. Furthermore, there has been no consensus about the management of hematological toxicity from immunotherapy in the recently published practice guidelines by the European Society for Medical Oncology (ESMO). We conducted a systematic review of case reports/series to describe the diagnosis and management of potentially rare and unrecognized Hem-irAEs. We searched Medline, OVID, Web of Science for eligible articles. Data were extracted on patient characteristics, Hem-irAEs, and management strategies. We performed quality assessment using the Pierson-5 evaluation scheme and causality assessment using the Naranjo scale. Our search retrieved 49 articles that described 118 cases. The majority of patients had melanoma (57.6%) and lung cancer (26.3%). The most common Hem-irAEs reported with ICPis (such as nivolumab, ipilimumab, and pembrolizumab) were thrombocytopenia, hemolytic and aplastic anemias. Less reported adverse events included agranulocytosis and neutropenia. Steroids were commonly used to treat these adverse events with frequent success. Other used strategies included intravenous immunoglobulins (IVIG), rituximab, and transfusion of blood components. The findings of this review provide more insights into the diagnosis and management of the rarely reported Hem-irAEs of ICPis.

Keywords: immune checkpoint inhibitors, immune-related adverse events, ipilimumab, pembrolizumab, nivolumab, atezolizumab, durvalumab, avelumab

INTRODUCTION

In the past decade, the enthusiasm for connecting the immune system and malignancy has expanded. Exploiting the host's immune system to treat cancers depends on immune surveillance: the ability of the immune system to identify foreign neo-antigens and target them for elimination (1). Immune checkpoint receptors, i.e., cytotoxic T-lymphocyte-associated protein 4 CTLA4 antibody ipilimumab, and programmed cell death protein-1 (PD-1) are critical for the physiological responses of the immune system. Checkpoint signaling triggers immune tolerance of T-cell activation to avoid autoimmunity and the adverse effects of excessive inflammatory responses. Tumor cells utilize these mechanisms to avoid destruction by the immune system (2).

In August, 18, 2010, the FDA approved the CTLA-4 ipilimumab antibody as the first ICPi for the treatment of metastatic melanoma (3). The filing was based on results from the primary analysis of the pivotal MDX010-020 trial, which were published online in the New England Journal of Medicine and presented in June 2010 during a plenary session at the 46th Annual Meeting of the American Society of Clinical Oncology (3). Despite its approval, ICPis have not been widely used except in the last 2 years. Recently, PD-1 inhibitors were approved for the treatment of non-small cell lung cancer (NSCLC) (4). Following their approval, these immunotherapeutics became integral parts of the treatment protocols against melanoma and NSCLC. Furthermore, they have shown promising responses [objective response rates (ORRs)] against different cancers, including mismatch repair deficient colorectal cancer (60%) and Hodgkin's disease (65–85%) (5).

Although the side effects of immunotherapy are less than chemotherapeutic agents (4), immunotherapy still may cause dermatological (reticular, maculopapular erythematous rash, and mucositis), gastrointestinal (diarrhea and colitis), hepatic (elevation of liver enzymes in serum), and endocrine adverse effects (involving pituitary, adrenal, or thyroid glands). This is because the immune response triggered by these drugs is not completely tumor-specific (6). The management of their adverse events usually includes various forms and regimens of corticosteroids (7).

With the expanding use of ICPis in clinical practice, more rare side effects are being discovered. Some Hem-irAEs were described, including immune thrombocytopenia, autoimmune hemolytic anemia, agranulocytosis, or pure red cell aplasia (8). The evidence focusing on the Hem-irAEs of ICPis is scarce. Moreover, there is no consensus on the management of hematologic toxicity from immunotherapy in the recently published practice guideline by ESMO (9). We aimed to evaluate the published literature on this topic and summarize the successful management approaches of the rare side effects.

Abbreviations: Hem-irAEs, Hematological Immune-Related Adverse Events; ICPis, Immune Checkpoint Inhibitors; ITP, Immune Thrombocytopenia; IVIG, Intravenous Immunoglobulins; ESMO, The European Society for Medical Oncology; CTLA4, Cytotoxic T-Lymphocyte-Associated Protein 4; PD-1, Programmed Cell Death Protein-1; SCLC, Small Cell Lung Carcinoma; NSCLC, Non-Small Cell Lung Cancer; ORRs, Objective Response Rates; PRISMA, Preferred Reporting Items for Systematic Reviews and Meta-Analyses; CD8, Cluster of Differentiation 8; IVATG, Intravenous Anti-thymocyte Globulin; CSF, Colony Stimulating Factor; G-CSF, Granulocyte Colony Stimulating Factor; GM-CSF, Granulocyte-Macrophage Colony Stimulating Factor; RBC, Red Blood Cells; AEC, Absolute Eosinophil Count; AHA, Autoimmune Hemolytic Anemia; IFN-α, Interferon alpha; CTCAE, Common Terminology Criteria of Adverse Events.

METHODS

Data Sources and Searches

We commenced this study in May 2018 and included all available updates published since 2008 till the present time.

We conducted literature search using different databases: Medline, OVID, and Web of Science. Furthermore, we searched the gray literature; conference proceedings; using Web of Conferences, Open Grey up to January 2019. We searched the bibliographies of relevant studies for any eligible case reports/series up to January 2019. The flow of the article selection process is presented in the graphical abstract as Preferred Reporting Items for Systematic Reviews and Meta-Analyses (PRISMA) figure. We used no time limit to date.

We used well-defined keywords. The search terms are listed in Appendix 1. The following keywords: (immune checkpoint inhibitors), (ICPis), (immunotherapy) (ipilimumab), (programmed cell death), (Programmed Cell Death 1 Receptor), (Programmed death ligand), (pembrolizumab), (nivolumab), (atezolizumab), (durvalumab), (avelumab) (adverse drug reaction), (adverse effects) (hematological adverse effect), Immune related adverse event (pancytopenia), (immune thrombocytopenic purpura), (thrombocytopenia), (leucopenia), (anemia) and (neutropenia) were entered, and the search was limited to articles in English. A summary of the 49 enrolled studies, clustered based on the medication used and Hem-irAEs experienced is shown in **Table 1**.

Initial screening of the eligible articles was done independently by two authors NO and NE. The articles were screened first based on their titles and abstracts, and then the full text was reviewed to decide the eligibility. Any conflict was solved by a third author KE. Only full-text articles published in peer-reviewed journals were retrieved for review according to the following criteria. AA, MY, AH, SE contributed to data analysis.

Inclusion Criteria

1. Case reports/series of solid tumors;
2. Reporting Hem-irAEs;
3. Using ICPis, monotherapy or combinations either as part of a clinical trial or during clinical practice;
4. English language;
5. Adults or pediatrics.

Exclusion Criteria

6. Other irAEs than Hem-irAEs;
7. Non-solid tumors;
8. Article reporting side effects which are not immune related;
9. Use other medications than ICPis causing Hem-irAEs;

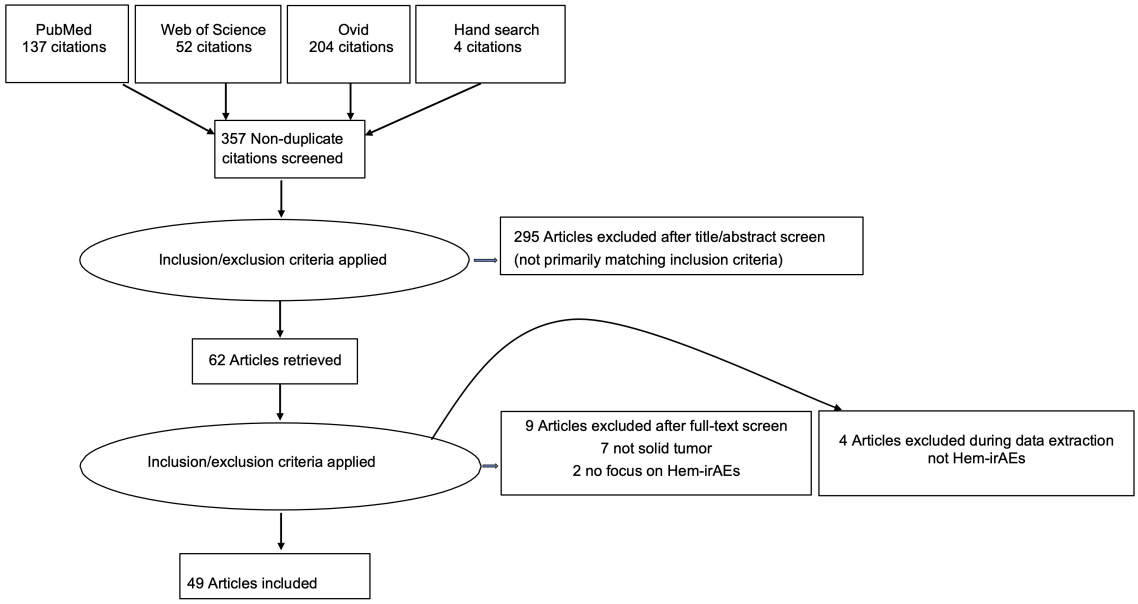

GRAPHICAL ABSTRACT 1 | The flow of the article selection process is presented as PRISMA.

10. Use of non-FDA approved ICPis up to the date of data extraction.

Data Extraction and Quality Assessment

Data was extracted by NO and NE, then was revised by KE. The extracted data included type of cancer, ICPis, number of cases, Hem-irAEs, onset of the adverse events, management of Hem-irAEs, and management outcomes. We used the Pierson-5 evaluation scheme (57) to assess quality of case reports based on 5 domains: documentation, uniqueness, educational value, objectivity, and interpretation as shown in **Table 2**. Each domain is scored, for example (0, 1, or 2 points, the upper score is 10 points). When a case report scores 9–10 points, the report contributes to the literature; a 6–8 points indicates validity and clinical value of the report are doubtful; a 5 points or less indicates insufficient quality. The assessment was carried out by KE and a random sample was crosschecked by NO and NE.

Causality Assessment

Each case report was assessed according to Naranjo scale (58) for causality as shown in **Supplementary Table 1**. Naranjo scale was used for causality assessment of the case reports, that allows categorical classification of adverse events as "definite," "probable," "possible," or "doubtful" based on the answers to 10 questions. One investigator KE carried out the assessment and NO and NE randomly re-checked it.

RESULTS

Patient Characteristics

Patient characteristics are described in **Table 3**. One hundred and eighteen cases were identified in 49 articles. The median age of cases was 54 years (range 32–85 years). The majority of cases were males ($n = 73$, 61.8%). Most patients had melanoma (57.6%) and lung cancer (26.3%). Other cancer sites included prostate ($n = 1$), bladder ($n = 1$), glioblastoma multiforme ($n = 1$), renal cell carcinoma ($n = 4$), and others ($n = 10$). Fifty three (44.9%) cases were labeled as stage 4, two cases as stage 3, one case as locally advanced disease, while in 61 (51.7%) cases, the stage of cancer was not mentioned. Twenty one (17.8%) cases were confirmed to have bone metastasis, while 55 (46.6%) cases did not have bone metastasis and no data were mentioned for the remaining 42 (35.5%) cases.

Thirty seven (31.3%) cases were treated with radiotherapy, while 38 (32.2%) cases did not receive radiotherapy and no history of exposure to radiotherapy in 43 (36.5%) cases.

Heavily pretreated patients were defined as patients who previously received two or more lines of treatment; 56 (47.5%) cases were heavily pretreated; 50 (42.4) cases received only one previous line of treatment; 5 cases were treatment naïve. With respect to history of autoimmune or hematological disorders before the use of ICPis; no data was provided in 73 (61.8%) cases, while 18 (15.3%) cases had history of either autoimmune or hematological disorder before ICPis usage, while 27 (22.9%) cases did not have history. A bone marrow biopsy was done to confirm the Hem-irAEs in 71 (61.2%) cases, but it was not done in 19 (16.1%) cases. The grade of Hem-irAEs was labeled as grade 2 in 3 cases, grade 3 in 5 cases, grade 4 in 50 (42.3%) case, and grade 5 in 2 cases.

Nivolumab

Seventeen case studies (out of 49) reported Hem-irAEs with nivolumab in 20 cases (13 lung cancer, 5 melanoma, 1 cutaneous squamous cell carcinoma, and 1 glioblastoma). Anemia was reported in 7 cases; two had aplastic anemia and five had

TABLE 1 | Summary of available literature about immune check point inhibitors-associated hematological adverse effects.

References	Therapeutic agent	Diagnosis	Number of cases	Hematological adverse effect/s	Occurred after how many cycles/days post ICPis	Intervention or management of hematological adverse effect/s	Outcome of hematological adverse effect/s management
(10)	Pembrolizumab	Metastatic melanoma	Case A	Immune thrombocytopenia	A: 1st cycle	A: three boluses of methylprednisolone and two infusions of immunoglobulins (2 g/kg). Followed by oral corticosteroid therapy then tapered down B: a course of corticosteroid was initiated (1 mg/kg/d)	Resolved Resolved
			Case B		B: NA		
(11)	Pembrolizumab	Metastatic melanoma	1	Immune thrombocytopenia	After the 2nd dose of pembrolizumab	Steroids	Ineffective
(12)	Pembrolizumab	Metastatic melanoma	1	Pancytopenia	The 18th cycle	High dose prednisolone and a 5 day course of IVIG therapy	Resolved after IVIG course
(13)	Pembrolizumab	Metastatic melanoma	1	Warm antibody autoimmune hemolytic anemia and pure red cell aplasia	The 3rd cycle	High dose glucocorticoids	Pure red cell aplasia flared when prednisone tapered to 20 mg Subsequent treatment with one dose of IVIG enabled tapering of the glucocorticoids
(14)	Pembrolizumab	Stage 4 lung adenocarcinoma	1	Sever neutropenia	The 2nd cycle	G-CSF, IV solumedrol, IVIG, cyclosporine A	Recovered
(15)	Pembrolizumab	Metastatic bladder cancer	1	Hemophagocytic lymphohistiocytosis	NA	Etoposide and dexamethasone	NA
(16)	Pembrolizumab	Metastatic NSCLC	1	Evan's syndrome	After the 18th cycle	Pembrolizumab discontinuation and prednisone, azathioprine, cyclophosphamide, and IVIG therapy combined with erythropoietin injections and transfusion, then weekly rituximab and re-initiation of high dose prednisone	Resolved
(17)	Pembrolizumab	Stage 3a lung adenocarcinoma	1	Exacerbation of autoimmune hemolytic anemia	17 days after the 1st cycle	IV steroids and blood transfusion	Recovered but patient died 33 days later
(18)	Pembrolizumab	Metastatic melanoma	1	Autoimmune hemolytic anemia	The 4th cycle	IV steroids	Recovered
(19)	Pembrolizumab	Metastatic melanoma	1	Autoimmune hemolytic anemia	The 3rd cycle	Steroids, rituximab and pembrolizumab discontinuation	Resolved
(20)	Nivolumab	Metastatic melanoma	1	Severe anemia and thrombocytopenia (Bicytopenia)	The 6th cycle	RBCs, platelet transfusion and high dose IV methylprednisolone	Ineffective
(21)	Nivolumab	Metastatic NSCLC	1	Severe pancytopenia	After the 3rd cycle	IV steroids, G-CSF and IVIG	Ineffective

(Continued)

TABLE 1 | Continued

References	Therapeutic agent	Diagnosis	Number of cases	Hematological adverse effect/s	Occurred after how many cycles/days post ICPis	Intervention or management of hematological adverse effect/s	Outcome of hematological adverse effect/s management
(22)	Nivolumab	Metastatic NSCLC	1	Exacerbation of underlying immune thrombocytopenia	After the 9th cycle	IV romiplostim, withholding of nivolumab	Recovered and nivolumab resumed
(23)	Nivolumab	Metastatic NSCLC	1	Immune Thrombocytopenia	After the 6th cycle	Discontinuation of nivolumab, platelet transfusions were given for 4 weeks then IV steroids	Resolved
(24)	Nivolumab	Metastatic NSCLC	1	Immune-mediated thrombocytopenia and hypothyroidism	After the 2nd cycle	IV steroids, levothyroxine and discontinuation of nivolumab	Recovered
(25)	Nivolumab	Metastatic melanoma	1	Severe thrombocytopenia, ITP	Before the 3rd dose	Prednisolone, IVIG, romiplostim and platelet transfusion	Resolved
(4)	Nivolumab	Metastatic NSCLC	1	Severe agranulocytosis	The 2nd cycle	3 doses of IVIG without improvement, then oral 1.5 mg/kg/day prednisone for 3 days without improvement, count improved after high dose IV methylprednisolone	Resolved only after high dose methylprednisolone (3 mg/kg IV)
(26)	Nivolumab	Metastatic NSCLC	Case A Case B	Severe complicated neutropenia	Case A: the 5th cycle Case B: after the 9th cycle	Case A: G-CSF, IV steroids Case B: G-CSF, IV steroids	Case A: ineffective and patient passed away 13 days later Case B: ineffective
(8)	Nivolumab	Stage IV adenocarcinoma of the lung	Case A Case B Case C	Bone marrow failure as an immune-related aplastic anemia	NA	A: IVIG, antibiotics 4 RBCs units, and 3 platelets units B: prednisone 1 mg/kg, norethandrolone, G-CSF, 4 RBCs and 9 platelets units C: prednisolone 1 mg/kg IVIG, G-CSF, antibiotics, 20 RBCs and 15 platelets units	A: no response to IVIG, death at 1 month of febrile neutropenia B: partial and transient response to steroids, persistent pancytopenia ongoing at 4 months C: no response to steroids and IVIG, death at 3 months from acute coronary syndrome
(27)	Nivolumab	Metastatic melanoma	1	Symptomatic warm autoimmune hemolytic anemia	The 4th cycle	Discontinuation of nivolumab and prednisone	Resolved
(28)	Nivolumab	Metastatic cutaneous squamous cell carcinoma and CLL	1	Hemolytic anemia	The 8th cycle	Discontinuation of nivolumab and prednisone	Anemia recovered after 2 weeks
(29)	Nivolumab	Stage 4 lung adenocarcinoma	1	Autoimmune hemolytic anemia	The 2nd cycle	Prednisolone	Ineffective
(30)	Nivolumab	Glioblastoma multiforme	1	Aplastic anemia	After the 2nd cycle	G-CSF, eltrombopag and blood transfusion	Ineffective, death 73 days after the 2nd dose of nivolumab

(Continued)

TABLE 1 | Continued

References	Therapeutic agent	Diagnosis	Number of cases	Hematological adverse effect/s	Occurred after how many cycles/days post ICPis	Intervention or management of hematological adverse effect/s	Outcome of hematological adverse effect/s management
(31)	Nivolumab	Metastatic melanoma	1	Pure red cell aplasia	The 31st cycles	IV steroids and blood transfusion, nivolumab was discontinued	Recovered
(32)	Nivolumab	Metastatic melanoma	1	Severe allograft rejection and autoimmune hemolytic anemia	NA	IV steroids	Recovered
(33)	Nivolumab	Stage 4 NSCLC	1	Immunotherapy-associated hemophagocytic syndrome	After the 2nd dose	IV steroids	Resolved with tumor regression
(34)	Nivolumab	Metastatic lung squamous cell carcinoma	1	Acquired hemophilia A	After 17 months from the 1st cycle	Oral steroids then IV cyclophosphamide and factor VII	Resolved
(35)	Ipilimumab	Metastatic melanoma	1	Autoimmune pancytopenia	8 days after the 4th cycle	High dose corticosteroids Erythropoietin 30,000 IU/wk, N-plate 1 mg/kg/wk, filgrastim 10 mg/kg/d and IVIG	Pancytopenia was resistant to high dose oral corticosteroids and to hematopoietic growth factors, but resolved after IVIG injection
(36)	Ipilimumab	Metastatic melanoma	1	Pancytopenia	After 36 weeks	Growth factors, transfusions, antibiotics, immunoglobulins, and immunosuppressive therapy (cyclosporine)	Ineffective
(37)	Ipilimumab	Metastatic melanoma	1	Pancytopenia with cerebral hemorrhage and respiratory insufficiency	Unknown	Steroids	Ineffective
(38)	Ipilimumab	Metastatic melanoma	1	thrombocytopenia	Day 12 after the 2nd cycle	1 mg/kg prednisolone and 1 g/kg IVIG	Resolved
(39)	Ipilimumab	Metastatic melanoma	1	Immune-mediated thrombocytopenia.	After the 1st cycle	IV steroids, platelet transfusion, oral steroids and ipilimumab discontinuation	Effective
(40)	Ipilimumab	Metastatic melanoma	1	Acute grade 4 neutropenia	14 days after the 4th cycle	CSF, steroids and IVIG	Neutropenia did not respond to CSF and steroids, it rapidly improved after administration of IVIG
(41)	Ipilimumab	Metastatic melanoma	1	Febrile neutropenia with agranulocytosis	14 days after administration of the 3rd cycle	Filgrastim, meropenem, fluconazole IV, and 2 mg/kg of methylprednisolone (120 mg) IV daily, and was discharged on 128 mg oral methylprednisolone daily	Ineffective

(Continued)

TABLE 1 | Continued

References	Therapeutic agent	Diagnosis	Number of cases	Hematological adverse effect/s	Occurred after how many cycles/days post ICPis	Intervention or management of hematological adverse effect/s	Outcome of hematological adverse effect/s management
(42)	Ipilimumab	Metastatic melanoma	Case A Case B Case C	A: hemolytic autoimmune anemia B: severe leukopenia and febrile neutropenia C: severe anemia and leukopenia	A: after the 3rd cycle B: after the 3rd cycle C: after treatment discharge (48 weeks from initial dose), during follow up	A: high dose methylprednisolone and blood transfusion B: antibiotics, GM-CSF and high doses of IV Methylprednisolone followed by tapering C: oral corticosteroids prednisone 1 mg/kg/day and GM-CSF for 1 week	A: resolved B: resolved C: resolved
(43)	Ipilimumab	Stage IIIB melanoma	1	Neutropenia	After the 4th cycle	- Oral steroids, - IV cyclosporine, - IVIG, - G-CSF, - IVATG	Resolved after 7.5 weeks from the 4th dose
(44)	Ipilimumab	Metastatic melanoma	1	Large granular lymphocytosis with severe neutropenia	After the 3rd cycle	Discontinuation of ipilimumab, IV antibiotics, G-CSF, IVIG, IV steroids, IVATG, IV cyclosporine	Resolved after IVATG plus cyclosporine and steroids
(45)	Ipilimumab	Metastatic melanoma	1	Acquired hemophilia A	After the 3rd cycle	IV steroid, factor VII and tranexamic acid	Effective, bleeding stopped
(46)	Ipilimumab	Metastatic melanoma	1	Immune-mediated red cell aplasia	After the 9th cycle	Oral prednisone at 1 mg/kg /day with little change in his transfusion requirement after 4 weeks, he received IVIG	Poor response to corticosteroids and rapid clinical benefit from IVIG
(47)	Ipilimumab	Metastatic melanoma	1	Hemophagocytic syndrome	After the 2nd cycle	IV steroids and IV etoposide	Ineffective
(48)	Durvalumab	NSCLC	1	A fatal allo- and immune-mediated thrombocytopenia	Two months after cessation of treatment with the PD-L1 inhibitor	Platelet transfusion daily for 12 days and polyvalent immunoglobulins (25 g/day for 4 days) and steroid treatment (1 mg/kg)	No improvement and death occurred 36 days after the 1st transfusion due to intra-alveolar hemorrhage
(49)	Avelumab	Metastatic Merkel cell carcinoma	1	Lethal thrombocytopenia	After the 4th cycle	IV steroids, IVIG	Ineffective, patient died 1 month of ITP
(50)	Ipilimumab and nivolumab	Case A: melanoma stage IIb Case B: metastatic melanoma	Case A Case B	Severe thrombocytopenia	A: The 1st cycle B: 43 days after nivolumab monotherapy and 8 days after ipilimumab monotherapy	A: 1st dose of steroids and IVIG, then rituximab B: prednisone, IVIG, and rituximab, cessation of ipilimumab	A: no response to steroids or IVIG, recovered after 4 doses of rituximab B: Resolved
(51)	Ipilimumab plus nivolumab	Metastatic melanoma	1	Aplastic anemia	After four courses of the combined treatment, followed by five courses of nivolumab in 3 days	Daily treatment with prednisone (1 mg/kg), and G-CSF	At the 11th day of hospitalization patient suffered brain hemorrhage with rapid fatal outcome

(Continued)

TABLE 1 | Continued

References	Therapeutic agent	Diagnosis	Number of cases	Hematological adverse effect/s	Occurred after how many cycles/days post ICPis	Intervention or management of hematological adverse effect/s	Outcome of hematological adverse effect/s management
(52)	Ipilimumab and nivolumab	Metastatic melanoma	1	Autoimmune hemolytic anemia	The 2nd cycle	Multiple blood transfusions and started on pulse dose steroids using 1,000 mg of IV methylprednisolone daily for 3 days then course of oral prednisone, had AHA after re-challenging with immunotherapy which responded faster to rituximab	First occurrence responded gradually to corticosteroid Due to slow response to steroids after the 2nd occurrence of AHA; rituximab added, and the patient responded well to it
(53)	Case A: ipilimumab Case B: pembrolizumab Case C: pembrolizumab Case D: ipilimumab and nivolumab	A: prostate cancer B: metastatic melanoma C: SCLC D: metastatic melanoma	A B C D	A: neutropenia B: hemolytic anemia C: hemolytic anemia D: hemolytic anemia	A: after the 2nd cycle of ipilimumab B: After 3 weeks of immunotherapy C: After 2 weeks of pembrolizumab D: on day 33	A: Methylprednisolone at 1 mg/kg every 12 h IV for 3 consecutive days and subsequent oral prednisone at 1 mg/kg daily B: IV methylprednisolone 1 mg/kg once daily for 3 days and then transitioned to oral prednisone 1 mg/kg daily for 2 additional weeks C: prednisone at 1 mg/kg/d D: prednisone 1 mg/kg/d initially which was increased to 2 mg/kg/d after day 38 when platelet count dropped to 5,000/μL IVIG 1 g/kg/d for 2 days for presumed immune thrombocytopenia	A: Resolved B: Resolved C: Resolved D: Resolved
(54)	Pembrolizumab ($n = 17$), nivolumab ($n = 7$), and durvalumab ($n = 2$)	Melanoma ($n = 20$), renal cell carcinoma ($n = 3$), other tumor types ($n = 3$)	26	Increase in AEC	After a median of 3.0 months after the 1st cycle	NA	NA
(55)	Ipilimumab and nivolumab	Metastatic melanoma	1	Aplastic anemia	Two weeks following the 2nd cycle	IV methylprednisone 70 mg/ day for 8 days, followed by a prednisone taper.	Recovery
(56)	Nivolumab ($n = 20$), pembrolizumab ($n = 14$), and atezolizumab ($n = 1$)	Melanoma ($n = 15$), NSCLC ($n = 12$), and other types of cancers ($n = 8$)	35	Neutropenia 9 (26%), anemia 9 (26%), thrombocytopenia 9 (26%), pancytopenia or aplastic anemia 5 (14%), bicytopenia 2 (6%), and pure red cell aplasia 1(3%)	Median time to onset was 10.1 weeks	22 (63%) of 35 patients were given steroids orally, 5 (14%) were given steroids IV and orally, 11 (31%) had IVIG, and 7 (20%) had rituximab	21 (60%) of patients recovered

ICPi, Immune Check Point inhibitors; IVIG, Intravenous Immunoglobulin; IVATG, Intravenous Anti-thymocyte Globulin; CSF, Colony Stimulating Factor; G-CSF, Granulocyte Colony Stimulating Factor; GM-CSF, Granulocyte-Macrophage Colony Stimulating Factor; RBC, Red Blood Cells; NA, Not Available; ITP, Idiopathic Thrombocytopenic Purpura; SCLC, Small Cell Lung Carcinoma; AEC, Absolute Eosinophil Count; NSCLC, Non-Small Cell Lung Carcinoma; AHA, Autoimmune Hemolytic Anemia.

TABLE 2 | Number of case reports with different scores for the five domains of Pierson-5 scale.

Domain/score	0	1	2
Documentation	3	9	42
Uniqueness	12	23	19
Educational value	3	29	22
Objectivity	1	19	34
Interpretation	1	8	45

hemolytic anemia. Thrombocytopenia was reported in five cases. Bone marrow failure was reported in three cases, pancytopenia in one case, neutropenia in one case, red cell aplasia in one case, hemophagocytic syndrome in one case, agranulocytosis in one case and acquired hemophilia A in one case.

Treatment was reported for all patients. Resolution of the adverse events was reported in 11 cases (55%) and treatment was ineffective in 8 cases (40%). One case showed partial and transient response to treatment. In the 11 cases that showed response, the most common treatment for Hem-irAEs was IV corticosteroids, however, IV romiplostim, platelets transfusion, IVIG, and oral steroids were used. Many patients had to discontinue nivolumab with the treatment used.

Another two-case series reported Hem-irAEs with nivolumab in 27 cases. An increase in the absolute eosinophil count was reported by Bernard-Tessier et al. (54). No treatment was mentioned in this report. Delanoy et al. (56) reported neutropenia, anemia, thrombocytopenia, pancytopenia, bicytopenia, pure red cell aplasia with nivolumab, pembrolizumab, and atezolizumab. Twenty one patients had resolved symptoms with oral steroids, IV steroids, IVIG, and rituximab.

Ipilimumab

Fourteen articles reported Hem-irAEs with ipilimumab in 16 cases (15 melanomas and one with prostate cancer). The adverse events reported were neutropenia (5 cases), pancytopenia (3 cases), leukopenia (3 cases), thrombocytopenia (2 cases), anemia (2 cases), and 5 cases showed one of the following adverse events: agranulocytosis, lymphocytosis, hemophagocytic syndrome, acquired hemophilia A, and red cell aplasia. Eleven cases (68.75%) recovered after treatment. Steroids (8 cases) and IVIG (7 cases) were the most commonly used treatments.

Pembrolizumab

Twelve reports described Hem-irAEs with pembrolizumab in 13 cases (7 melanomas, 4 lung cancer, and 1 bladder cancer). In these cases, hemolytic anemia was reported in five cases and thrombocytopenia in two cases. Neutropenia, pancytopenia, red cell aplasia, hemophagocytic lymphohistiocytosis, and Evan's syndrome were reported in one case each. Adverse events were resolved in 11 cases. Steroids (whether IV or oral) were used in all the managed cases, and IVIG was used in five cases.

Combination of Ipilimumab—Nivolumab

This combination of ipilimumab and nivolumab, used to treat metastatic melanoma, was associated with Hem-irAEs in 6 cases (5 reports). Thrombocytopenia, aplastic anemia, and hemolytic anemia were reported in two cases each. The adverse events were resolved in 5 cases. One case died with refractory aplastic anemia. Rituximab was a commonly used treatment; one patient with thrombocytopenia recovered after 4 doses of rituximab following IVIG failure. The second occurrence of hemolytic anemia in one of the cases resolved with rituximab use.

Durvalumab

A fatal allo- and immune-mediated thrombocytopenia was reported with durvalumab use in one NSCLC case. Platelet transfusion, polyvalent immunoglobulins and steroid treatments were used to treat the patient without improvement.

Avelumab

One patient with metastatic Merkel cell carcinoma developed lethal immune thrombocytopenia (ITP) after avelumab administration. Treatments with steroids and IVIG were ineffective and the patient died after 1 month from initial diagnosis.

Concerning the treatment of Hem-irAEs reported, steroids were the most commonly used (80/118, 67.7%), with a failure rate of (16/80 = 20%) out of 118 cases. Other treatment options included IVIG, rituximab, and combination of the three options at varying doses.

Quality Assessment

Table 2 shows quality assessment of the extracted citations using Pierson-5. The number of case reports is based on five domains: uniqueness, documentation, objectivity, interpretation, and educational value. Every domain is scored with 2 points, the upper score is 10 points. Naranjo scale was used for causality assessment of the case reports, that allows categorical classification of adverse events as "definite," "probable," "possible," or "doubtful" based on the answers to 10 questions.

Fifty-four case reports were retrieved from the literature and assessed. Out of the 54 reports, 5 (9.2%) could not be assessed, since the data presented were insufficient for assessment for 4 of them, while 1 study was an observational study. Seven cases (12.9%) were rated as "of insufficient quality for publication" because they scored 5 or less. The second case reported in Shiuan et al. (50) got zero score in the five domains. Twenty-six studies (48.1%) were assessed as "reader should be cautious about validity and clinical value of the report" because they scored 7–8. Twenty-one cases (38.8%) were rated as "likely to be a worthwhile contribution to the literature" as they scored 9–10.

Causality Assessment

Eight studies were ranked as "possible" adverse drug reaction, scoring 3 (one study) and 4 (7 studies). Two studies were not assessed because their data were insufficient. Sixteen studies were ranked as "probable" adverse drug reaction as they scored between 5 and 8. No cases were ranked as "definite" or "doubtful" adverse drug reaction.

TABLE 3 | Characteristics of the described patients in the eligible case reports.

References	Therapeutic agent	Age	Gender	Stage of the disease	Bone metastasis Y, N, or NA	How many line/s of therapy before ICPi	History of radiotherapy Y or N	History of autoimmune or hematological disorder/s before ICPi	Bone marrow Biopsy done Y or N	Grade of Hem-IRAEs according to the (CTCAE)
(10)	Pembrolizumab	34	M	4 locally advanced	NA	4 lines	Y	NA	Y	NA
Case a		51	F		N	None	N	None	Y	NA
Case b										
(11)	Pembrolizumab	73	M	4	Y	3 lines	Y	IFN-α Hashimoto thyroiditis mild thrombocytopenia	N	NA
(12)	Pembrolizumab	52	F	4	N	1 line	N	None	Y	4
(13)	Pembrolizumab	52	F	4	N	2 lines	Y	Autoimmune hepatitis	Y	NA
(14)	Pembrolizumab	73	F	4	NA	1 line	NA	Autoimmune myositis (in remission)	N	4
(15)	Pembrolizumab	76	M	4	NA	NA	NA	NA	Y	NA
(16)	Pembrolizumab	67	M	4	N	2 lines	Y	NA	N	NA
(17)	Pembrolizumab	82	M	3a	N	1 line	N	Chronic anemia	Y	NA
(18)	Pembrolizumab	79	F	4	Y	1 line	Y	None	N	NA
(19)	Pembrolizumab	78	M	4	NA	1 line	NA	NA	N	NA
(20)	Nivolumab	73	M	4	N	2 lines	Y	Moderate macrocytic anemia and mild thrombocytopenia	Y	4
(21)	Nivolumab	56	M	4	N	1 line	NA	None	Y	NA
(22)	Nivolumab	32	M	4	Y	3 lines	Y	Mild ITP	N	NA
(23)	Nivolumab	78	M	4	Y	1 line	N	Early stage lymphoma (in remission)	Y	4
(24)	Nivolumab	62	M	4	NA	2 lines	NA	Asymptomatic Hashimoto's thyroiditis	Y	NA
(25)	Nivolumab	79	F	4	N	1 line	N	NA	N	4
(4)	Nivolumab	74	F	4	Y	1 line	Y	Ulcerative colitis (in remission)	Y	NA
(26)	Nivolumab	73	M	Both cases were stage	N	4 lines	N	None	N	4
Case a		74	M	4	N	3 lines	N	Treated intermediate grade follicular lymphoma	Y	4
Case b										
(8)	Nivolumab	73	F	All 3 cases were stage	N	2 lines	Y	None	Y	Sever cytopenias, grade
Case a		70	M	4	N	3 lines	N	None	Y	3 or higher
Case b		78	M		Y	1 line	Y	None	Y	
Case c										
(27)	Nivolumab	85	M	4	N	2 lines	N	None	N	NA
(28)	Nivolumab	82	M	4	Y	2 lines	Y	CLL	N	NA
(29)	Nivolumab	70	M	4	NA	1 line	N	NA	N	NA
(30)	Nivolumab	57	F	4	N	2 lines	Y	None	Y	4
(31)	Nivolumab	70	F	4	N	1 line	Y	None	Y	NA
(32)	Nivolumab	73	M	4	NA	NA	NA	None	Y	NA

(Continued)

TABLE 3 | Continued

References	Therapeutic agent	Age	Gender	Stage of the disease	Bone metastasis Y, N, or NA	How many line/s of therapy before ICPi	History of radiotherapy Y or N	History of autoimmune or hematological disorder/s before ICPi	Bone marrow Biopsy done Y or N	Grade of Hem-IRAEs according to the (CTCAE)
(33)	Nivolumab	63	F	4	NA	3 lines	NA	None	Y	NA
(34)	Nivolumab	68	M	4	NA	1 line	NA	None	N	NA
(35)	Ipilimumab	77	F	4	N	2 lines	N	History of regressive thyroiditis	Y	4
(36)	Ipilimumab	NA	NA	4	NA	Heavily pretreated	NA	NA	NA	4
(37)	Ipilimumab	NA	NA	4	NA	NA	NA	NA	NA	4
(38)	Ipilimumab	57	M	4	Y	1 line	Y	None	Y	4
(39)	Ipilimumab	54	M	4	N	1 line	N	None	Y	4
(40)	Ipilimumab	42	F	4	N	5 lines	Y	None	Y	4
(41)	Ipilimumab	35	M	4	Y	1 line	Y	None	Y	4
(42)	Ipilimumab	68	F	All 3 cases were stage	N	1 line	NA	NA	N	NA
Case a		49	F	4	Y	1 line	Y	NA	Y	
Case b		70	M		N	1 line	N	NA	Y	
Case c										
(43)	Ipilimumab	54	M	3b	N	None	N	None	Y	NA
(44)	Ipilimumab	74	F	4	NA	1 line	NA	NA	Y	4
(45)	Ipilimumab	42	M	4	Y	3 lines	N	None	N	NA
(46)	Ipilimumab	55	M	4	N	3 lines	N	None	Y	NA
(47)	Ipilimumab	52	F	4	N	1 line	Y	Indolent lymphoplasmocytic lymphoma	Y	NA
(48)	Durvalumab	39	M	4	NA	None	NA	None	Y	4
(49)	Avelumab	77	M	4	N	None	N	B12 and folic acid deficiency	Y	4
(50)	Ipilimumab and	47	F	2b		1 line	N	NA	Y	4
Case a	nivolumab	45	F	4		None	N	Thrombocytopenia	N	
Case b										
(51)	Ipilimumab plus nivolumab	48	F	4	NA	NA	NA	NA	Y	NA
(52)	Ipilimumab and nivolumab	43	F	4	N	NA	Y	None	N	NA
(53)	Case a:	64	M	4	N	3 lines	NA	None	N	NA
Case a	Ipilimumab	58	F	4	N	NA	NA	None	Y	
Case b	Case b:	62	M	4	NA	1 line	Y	NA	N	
Case c	Pembrolizumab	64	M	4	NA	NA	NA	None	N	
Case d	Case c: Pembrolizumab Case d: Ipilimumab and nivolumab									

(Continued)

TABLE 3 | Continued

References	Therapeutic agent	Age	Gender	Stage of the disease	Bone metastasis Y, N, or NA	How many line/s of therapy before ICPi	History of radiotherapy Y or N	History of autoimmune or hematological disorder/s before ICPi	Bone marrow Biopsy done Y or N	Grade of Hem-IRAEs according to the (CTCAE)
(54) (26 cases)	Pembrolizumab ($n = 17$) Nivolumab ($n = 7$) Durvalumab ($n = 2$)	58#	19 M 7 F	Miscellaneous	NA	Median: 1 [Range 0–7]	NA	NA	NA	NA
(55)	Ipilimumab and nivolumab	51	M	4	N	1 line	Y	None	Y	4
(56) (35 cases)	Nivolumab ($n = 20$) Pembrolizumab ($n = 14$) atezolizumab ($n = 1$)	65**	21 M 14 F	Miscellaneous	10 Y 25 N	Median: 2 [Range 1–3]	16 Y 19 N	The 3 cases had a history of b-c 2	Y	Grade 2 $n = 3$ Grade 3 $n = 5$ Grade 4 $n = 25$ Grade 5 $n = 2$

*#age range (3–87), **age range (51–75). Y, yes; N, no; NA, not available; ITP, immune thrombocytopenia; IFN-α, Interferon alpha; CTCAE, Common Terminology Criteria of Adverse Events.*

For pembrolizumb case reports (13 reports), 8 of them (61.5%) were assessed as probable Hem-irAEs. Next to pembrolizumab, nivolumab (20 reports), 12 of which (60%) were assessed as probable, then comes ipilimumab (14 reports), 8 of which (57%) were assessed as probable. For the combination of ipilimumab and nivolumab (6 reports), 3 of them (50%) were assessed as probable. Finally, only one case report was assessed for durvalamab where the causality assessment yielded as a possible Hem-irAEs.

DISCUSSION

Immunotherapeutics are increasingly used in cancer patients. However, adverse events can limit their use and may result in serious adverse outcomes, including death. While some adverse events have been well-described in clinical trials (e.g., dermatitis and colitis), other inflammatory and autoimmune manifestations are reported. Case reports can provide vital clues and signals to identify rare but serious events and can generate hypotheses that can direct ongoing scientific research. We conducted a systematic review of case reports/series of patients treated with checkpoint blockade to identify the scope of rare Hem-irAEs that may occur with these therapies. We included publications that had adequate description of the clinical manifestations of the patients reported.

This systematic review showed thrombocytopenia, hemolytic and aplastic anemias as the most commonly associated with ICPis use, i.e., nivolumab, ipilimumab, and pembrolizumab. Less reported adverse events included agranulocytosis and neutropenia. Steroids (either intravenous or oral) were commonly used to treat these adverse events with frequent success. Other strategies used IVIG, rituximab and transfusion of blood components.

The mechanisms of the recorded adverse events in the included articles remain elusive. The most plausible theory is activation of T-cells, leading to the secretion of different cytokines from T-helper cells and consequent tissue infiltration with cluster of differentiation 8 (CD8) T-cytotoxic cells (59). Another suggested mechanism was immune-mediated dysfunction in hematopoietic cell maturation and proliferation, yet, the exact intermediate mechanism is unknown (20). The response to steroids in the majority of these cases potentiates the theory of immune-mediated mechanisms that occur centrally (in the bone marrow) or peripherally (in the circulation).

We used the Naranjo scale to infer causality of the reported adverse event to the used ICPi drug. Although data were not available for some reports, we showed possible or probable causality in several included reports. In some of these reports, the ICPi was the only new treatment introduced and the events diminished after the drug withdrawal. Further, the temporal relationship between ICPis administration and the occurrence of the adverse effect implicates these drugs. Hem-irAEs are known to occur within 12 to 16 weeks of treatment initiation (60).

As reflected from the causality assessment results, the majority of cases reported were "probable"; being at the near top of the

causality continuum of the Naranjo scale (just before definite). Consequently, the association between ICPis and Hem-irAEs cannot be ignored.

This review provides insights into the proper management strategies for Hem-irAEs. Previously, it was thought that cancer patients receiving immunotherapy should not receive immunosuppressive drugs. This view has significantly changed over the past few years and the use of immunosuppressive agents has been proven not to impair the efficacy of ICPis (61). Corticosteroids should be the first resource and some reports highlighted the benefit of high dose steroids therapy. In grade 3/4 adverse events, the ICPis should be discontinued and steroids can later be tapered off in 4 to 6 weeks with close monitoring of blood counts (7). Other immunosuppressive drugs as IVIG, rituximab or tumor necrosis factor antagonists may also be effective. In case the immunosuppressive therapy is prolonged, immunization against pneumocystis is recommended (4).

Definitions of the side effects in the registries of rare events are poor. Therefore, we focused on the qualitative features such as demographic characteristics of patients, diagnosis and management. We did not perform quantitative analysis of these case reports because risk analysis was not possible. Randomized clinical trials were not related to our objective and were excluded in this systematic review. Limiting the inclusion criteria to studies published in English was challenging. However, a former analysis showed that this language limitation does not usually alter the study results (62).

Future case reports/series should follow a standardized approach in reporting their patients characteristics and findings. Further attention should be given to Hem-irAEs in ICPis randomized controlled trials to provide higher quality data in this regard. Moreover, the mechanisms of these adverse events should be investigated on the molecular and cellular levels to specify more effective pharmacological interventions. The management of Hem-irAEs in patients receiving ICPis needs evidence-based guidelines to inform future practice and research in this area.

Concerning the factors that may have predisposed patients to the adverse effects, there was no clear pattern for age. Patients characteristics were heterogenous for age with high interpatient variability with median age of 54 years and wide range 32–85 years. For gender, most patients were males ($n = 73$, 61.8%); although the percentage is not conclusive, it warrants further investigations and more research.

There was no predictor for the response to treatment. However, steroids were the most commonly used option. This can be explained secondary to its relative availability, low cost, and physicians' experience compared to other options. Furthermore, steroid was not always successful (20% failure rate) which implies seeking other treatment options and keeping patients on steroids for Hem-irAEs closely monitored.

CONCLUSION

Although rare, Hem-irAEs are serious adverse events that may be associated with checkpoint blockade therapy. Depending on the grade of the adverse event, the ICPi therapy may be discontinued and steroid therapy should be initiated. Steroids were the most commonly management strategy with considerable failure rate. There were no detected underlying factors predicting the outcome to steroid therapy. Other promising management strategies for some events include IVIG, rituximab, and transfusion of blood components.

FUTURE RESEARCH RECOMMENDATION

Further research should focus on the plausible mechanisms contributing to these adverse events, to develop more specific management strategies.

DATA AVAILABILITY STATEMENT

Datasets are available on request from the authors.

AUTHOR CONTRIBUTIONS

NO and NE extracted eligible articles. KE-F conducted initial screening of the eligible articles. Any conflict was solved by KE-F. The assessment was carried out by KE-F. A random sample was cross checked by NO and NE. AA, MY, AH, and SE contributed to the analysis. DJ, AA, AB, and AN contributed to writing of the manuscript and discussion. SD contributed to the discussion and reviewing the scientific background. All authors approved the article for submission.

FUNDING

This work was funded by the Medical Research Center, Hamad Medical Corporation, Qatar, as part of MRC-01-20-376 grant.

SUPPLEMENTARY MATERIAL

The Supplementary Material for this article can be found online at: https://www.frontiersin.org/articles/10.3389/fimmu.2020.01354/full#supplementary-material

REFERENCES

1. Mellman I, Coukos G, Dranoff G. Cancer immunotherapy comes of age. *Nature.* (2011) 480:480–9. doi: 10.1038/nature10673
2. Pico de Coaña Y, Choudhury A, Kiessling R. Checkpoint blockade for cancer therapy : revitalizing a suppressed immune system. *Trends Mol Med.* (2015) 21:482–91. doi: 10.1016/j.molmed.2015.05.005
3. Hodi FS, O'Day SJ, McDermott DF, Weber RW, Sosman JA, Haanen JB, et al. Improved survival with ipilimumab in patients with metastatic melanoma. *N Engl J Med.* (2010) 363:711–23. doi: 10.1056/NEJMx100063
4. Tabchi S, Weng X, Blais N. Severe agranulocytosis in a patient with metastatic non-small-cell lung cancer treated with nivolumab. *Lung Cancer.* (2016) 99:123–6. doi: 10.1016/j.lungcan.2016.06.026

5. Champiat S, Lambotte O, Barreau E, Belkhir R, Berdelou A, Carbonnel F, et al. Management of immune checkpoint blockade dysimmune toxicities: a collaborative position paper. *Ann Oncol.* (2016) 27:559–74. doi: 10.1093/annonc/mdv623
6. Spallarossa P, Meliota G, Brunelli C, Arboscello E, Ameri P, Dessalvi CC, et al. Potential cardiac risk of immune-checkpoint blockade as anticancer treatment: what we know, what we do not know, and what we can do to prevent adverse effects. *Med Res Rev.* (2018) 38:1447–68. doi: 10.1002/med.21478
7. Fay AP, Moreira RB, Nunes Filho PRS, Albuquerque C, Barrios CH. The management of immune-related adverse events associated with immune checkpoint blockade. *Expert Rev Qual Life Cancer Care.* (2016) 1:89–97. doi: 10.1080/23809000.2016.1142827
8. Michot JM, Vargaftig J, Leduc C, Quere G, Burroni B, Lazarovici J, et al. Immune-related bone marrow failure following anti-PD1 therapy. *Eur J Cancer.* (2017) 80:1–4. doi: 10.1016/j.ejca.2017.04.004
9. Haanen JBAG, Carbonnel F, Robert C, Kerr KM, Peters S, Larkin J, et al. Management of toxicities from immunotherapy: ESMO Clinical Practice Guidelines for diagnosis, treatment and follow-up. *Ann Oncol.* (2017) 28:iv119–42. doi: 10.1093/annonc/mdx225
10. Le Roy A, Kempf E, Ackermann F, Routier E, Robert C, Turpin A, et al. Two cases of immune thrombocytopenia associated with pembrolizumab. *Eur J Cancer.* (2016) 54:172–4. doi: 10.1016/j.ejca.2015.10.073
11. Pföhler C, Eichler H, Burgard B, Krecké N, Müller CSL, Vogt T. A case of immune thrombocytopenia as a rare side effect of an immunotherapy with PD1-blocking agents for metastatic melanoma. *Transfus Med Hemother.* (2017) 44:426–8. doi: 10.1159/000479237
12. Atwal D, Joshi KP, Ravilla R, Mahmoud F. Pembrolizumab-Induced pancytopenia: a case report. *Perm J.* (2017) 21:17–004. doi: 10.7812/TPP/17-004
13. Nair R, Gheith S, Nair SG. Immunotherapy-associated hemolytic anemia with pure red-cell aplasia. *N Engl J Med.* (2016) 374:1096–7. doi: 10.1056/NEJMc1509362
14. Barbacki A, Maliha PG, Hudson M, Small D. A case of severe pembrolizumab-induced neutropenia. *Anticancer Drugs.* (2018) 29:817–9. doi: 10.1097/CAD.0000000000000661
15. Shah D, Shrestha R, Ramlal R, Hatton J, Saeed H. Pembrolizumab associated hemophagocytic lymphohistiocytosis. *Ann Oncol.* (2017) 28:1403. doi: 10.1093/annonc/mdx113
16. Lott A, Butler M, Leighl N, Cserti-Gazdewich CM. Evan's syndrome associated with pembrolizumab therapy in metastatic non-small cell lung cancer. *Blood.* (2015) 126:4543. doi: 10.1182/blood.V126.23.4543.4543
17. Ogawa K, Ito J, Fujimoto D, Morita M, Yoshizumi Y, Ariyoshi K, et al. Exacerbation of autoimmune hemolytic anemia induced by the first dose of programmed death-1 inhibitor pembrolizumab: a case report. *Invest New Drugs.* (2018) 36:509–12. doi: 10.1007/s10637-018-0561-5
18. Robilliard B, Arnaud E, Gastaud L, Broner J. A case of pembrolizumab-induced autoimmune haemolytic anaemia with polymyalgia rheumatica. *Eur J Cancer.* (2018) 103:281–3. doi: 10.1016/j.ejca.2018.07.318
19. Sherbeck JP, Hugan S, Novak B, Ahmed A, Cooling L. IGT84: pembrolizumab induced autoimmune hemolytic anemia with possible. In: *American Association of Blood Banks (AABB) Annual Meeting.* (2018) 1–2.
20. Inadomi K, Kumagai H, Arita S, Tsuruta N, Takayoshi K, Mishima K, et al. Bi-cytopenia possibly induced by anti-PD-1 antibody for primary malignant melanoma of the esophagus: a case report. *Medicine.* (2016) 95:e4283. doi: 10.1097/MD.0000000000004283
21. Tokumo K, Masuda T, Miyama T, Miura S, Yamaguchi K, Sakamoto S, et al. Nivolumab-induced severe pancytopenia in a patient with lung adenocarcinoma. *Lung Cancer.* (2018) 119:21–4. doi: 10.1016/j.lungcan.2018.02.018
22. Bagley SJ, Kosteva JA, Evans TL, Langer CJ. Immune thrombocytopenia exacerbated by nivolumab in a patient with non-small-cell lung cancer. *Cancer Treat Commun.* (2016) 6:20–3. doi: 10.1016/j.ctrc.2016.02.009
23. Karakas Y, Yuce D, Kilickap S. Immune thrombocytopenia induced by nivolumab in a metastatic non-small cell lung cancer patient. *Oncol Res Treat.* (2017) 40:621–2. doi: 10.1159/000477968
24. Jotatsu T, Oda K, Yamaguchi Y, Noguchi S, Kawanami T, Kido T, et al. Immune-mediated thrombocytopenia and hypothyroidism in a lung cancer patient treated with nivolumab. *Immunotherapy.* (2018) 10:85–91. doi: 10.2217/imt-2017-0100
25. Kanameishi S, Otsuka A, Nonomura Y, Fujisawa A, Endo Y, Kabashima K. Idiopathic thrombocytopenic purpura induced by nivolumab in a metastatic melanoma patient with elevated PD-1 expression on B cells. *Ann Oncol.* (2016) 27:546–47. doi: 10.1093/annonc/mdv580
26. Turgeman I, Wollner M, Hassoun G, Bonstein L, Bar-Sela G. Severe complicated neutropenia in two patients with metastatic non-small-cell lung cancer treated with nivolumab. *Anticancer Drugs.* (2017) 28:811–4. doi: 10.1097/CAD.0000000000000520
27. Kong BY, Micklethwaite KP, Swaminathan S, Kefford RF, Carlino MS. Autoimmune hemolytic anemia induced by anti-PD-1 therapy in metastatic melanoma. *Melanoma Res.* (2016) 26:202–4. doi: 10.1097/CMR.0000000000000232
28. Schwab KS, Heine A, Weimann T, Kristiansen G, Brossart P. Development of hemolytic anemia in a nivolumab-treated patient with refractory metastatic squamous cell skin cancer and chronic lymphatic leukemia. *Case Rep Oncol.* (2016) 9:373–8. doi: 10.1159/000447508
29. Palla AR, Kennedy D, Mosharraf H, Doll D. Autoimmune hemolytic anemia as a complication of nivolumab therapy. *Case Rep Oncol.* (2016) 9:691–7. doi: 10.1159/000452296
30. Comito RR, Badu LA, Forcello N. Nivolumab-induced aplastic anemia: a case report and literature review. *J Oncol Pharm Pract.* (2019) 25:221–5. doi: 10.1177/1078155217726159
31. Yuki A, Takenouchi T, Takatsuka S, Ishiguro T. A case of pure red cell aplasia during nivolumab therapy for cardiac metastatic melanoma. *Melanoma Res.* (2017) 27:635–7. doi: 10.1097/CMR.0000000000000392
32. Deltombe C, Garandeau C, Renaudin K, Hourmant M. Severe allograft rejection and autoimmune hemolytic anemia after anti-PD1 therapy in a kidney transplanted patient. *Transplantation.* (2017) 101:e291. doi: 10.1097/TP.0000000000001861
33. Takeshita M, Anai S, Mishima S, Inoue K. Coincidence of immunotherapy-associated hemophagocytic syndrome and rapid tumor regression. *Ann Oncol.* (2016) 28:mdw537. doi: 10.1093/annonc/mdw537
34. Kato R, Hayashi H, Sano K, Handa K, Kumode T, Ueda H, et al. Nivolumab-induced hemophilia a presenting as gastric ulcer bleeding in a patient with NSCLC. *J Thorac Oncol.* (2018) 13:e239–41. doi: 10.1016/j.jtho.2018.06.024
35. du Rusquec P, Saint-Jean M, Brocard A, Peuvrel L, Khammari A, Quéreux G, et al. Ipilimumab-induced autoimmune pancytopenia in a case of metastatic melanoma. *J Immunother.* (2014) 37:348–50. doi: 10.1097/CJI.0000000000000041
36. Di Giacomo AM, Danielli R, Calabrò L, Bertocci E, Nannicini C, Giannarelli D, et al. Ipilimumab experience in heavily pretreated patients with melanoma in an expanded access program at the University Hospital of Siena (Italy). *Cancer Immunol Immunother.* (2011) 60:467–77. doi: 10.1007/s00262-010-0958-2
37. Zimmer L, Vaubel J, Mohr P, Hauschild A, Utikal J, Simon J, et al. Phase II DeCOG-study of ipilimumab in pretreated and treatment-naïve patients with metastatic uveal melanoma. *PLoS ONE.* (2015) 10:e0118564. doi: 10.1371/journal.pone.0118564
38. Ahmad S, Lewis M, Corrie P, Iddawela M. Ipilimumab-induced thrombocytopenia in a patient with metastatic melanoma. *J Oncol Pharm Pract.* (2012) 18:287–92. doi: 10.1177/1078155211411001
39. Kopecký J, Trojanová P, Kubeček O, Kopecký O. Treatment possibilities of ipilimumab-induced thrombocytopenia–case study and literature review. *Jpn J Clin Oncol.* (2015) 45:381–4. doi: 10.1093/jjco/hyu222
40. Akhtari M, Waller EK, Jaye DL, Lawson DH, Ibrahim R, Papadopoulos NE, et al. Neutropenia in a patient treated with ipilimumab (anti–CTLA-4 Antibody). *J Immunother.* (2009) 32:322–4. doi: 10.1097/CJI.0b013e31819aa40b
41. Wozniak S, Mackiewicz-Wysocka M, Krokowicz Ł, Kwinta Ł, Mackiewicz J. Febrile neutropenia in a metastatic melanoma patient treated with ipilimumab - case report. *Oncol Res Treat.* (2015) 38:105–8. doi: 10.1159/000377650
42. Simeone E, Grimaldi AM, Esposito A, Curvietto M, Palla M, Paone M, et al. Serious haematological toxicity during and after ipilimumab treatment: a case series. *J Med Case Rep.* (2014) 8:240. doi: 10.1186/1752-1947-8-240

43. Ban-Hoefen M, Burack R, Sievert L, Sahasrabudhe D. Ipilimumab-induced neutropenia in melanoma. *J Investig Med High Impact Case Rep.* (2016) 4:232470961666183. doi: 10.1177/2324709616661835
44. Wei G, Nwakuche U, Cadavid G, Ajaz A, Seiter K, Liu D. Large granular lymphocytosis with severe neutropenia following ipilimumab therapy for metastatic melanoma. *Exp Hematol Oncol.* (2012) 1:3. doi: 10.1186/2162-3619-1-3
45. Delyon J, Mateus C, Lambert T. Hemophilia A induced by ipilimumab. *N Engl J Med.* (2012) 366:280–1. doi: 10.1056/NEJMc1113863
46. Gordon IO, Wade T, Chin K, Dickstein J, Gajewski TF. Immune-mediated red cell aplasia after anti-CTLA-4 immunotherapy for metastatic melanoma. *Cancer Immunol Immunother.* (2009) 58:1351–3. doi: 10.1007/s00262-008-0627-x
47. Michot JM, Pruvost R, Mateus C, Champiat S, Voisin AL, Marabelle A, et al. Fever reaction and haemophagocytic syndrome induced by immune checkpoint inhibitors. *Ann Oncol.* (2018) 29:518–20. doi: 10.1093/annonc/mdx701
48. Leroy L, Lafarge X, Blouin L, Bijou F, Durrieu F, Olivier E, et al. A fatal allo- and immune-mediated thrombocytopenia with a PD-L1 inhibitor. *Ann Oncol.* (2018) 29:514–5. doi: 10.1093/annonc/mdx693
49. Kratzsch D, Simon JC, Pönitzsch I, Ziemer M. Lethal thrombocytopenia in a patient treated with avelumab for metastatic Merkel cell carcinoma. *J Dtsch Dermatol Ges.* (2018) 17:73–5. doi: 10.1111/ddg.13722
50. Shiuan E, Beckermann KE, Ozgun A, Kelly C, McKean M, McQuade J, et al. Thrombocytopenia in patients with melanoma receiving immune checkpoint inhibitor therapy. *J Immunother Cancer.* (2017) 5:8. doi: 10.1186/s40425-017-0210-0
51. Helgadottir H, Kis L, Ljungman P, Larkin J, Kefford R, Ascierto PA, et al. Lethal aplastic anemia caused by dual immune checkpoint blockade in metastatic melanoma. *Ann Oncol.* (2017) 28:1672–3. doi: 10.1093/annonc/mdx177
52. Khan U, Ali F, Khurram MS, Zaka A, Hadid T. Immunotherapy-associated autoimmune hemolytic anemia. *J Immunother Cancer.* (2017) 5:15. doi: 10.1186/s40425-017-0214-9
53. Sun Y, Lee SK, Oo TH, Rojas-Hernandez CM. Management of immune-mediated cytopenias in the era of cancer immunotherapy. *J Immunother.* (2018) 41:32–4. doi: 10.1097/CJI.0000000000000194
54. Bernard-Tessier A, Jeanville P, Champiat S, Lazarovici J, Voisin AL, Mateus C, et al. Immune-related eosinophilia induced by anti-programmed death 1 or death-ligand 1 antibodies. *Eur J Cancer.* (2017) 81:135–7. doi: 10.1016/j.ejca.2017.05.017
55. Meyers DE, Hill WF, Suo A, Jimenez-Zepeda V, Cheng T, Nixon NA. Aplastic anemia secondary to nivolumab and ipilimumab in a patient with metastatic melanoma: a case report. *Exp Hematol Oncol.* (2018) 7:4–9. doi: 10.1186/s40164-018-0098-5
56. Delanoy N, Michot JM, Comont T, Kramkimel N, Lazarovici J, Dupont R, et al. Haematological immune-related adverse events induced by anti-PD-1 or anti-PD-L1 immunotherapy: a descriptive observational study. *Lancet Haematol.* (2019) 6:e48–57. doi: 10.1016/S2352-3026(18)30175-3
57. Pierson DJ. How to read a case report (or teaching case of the month). *Respir Care.* (2009) 54:1372–8.
58. Naranjo CA, Busto U, Sellers EM, Sandor P, Ruiz I, Roberts EA, et al. A method for estimating the probability of adverse drug reactions. *Clin Pharmacol Ther.* (1981) 30:239–45. doi: 10.1038/clpt.1981.154
59. Quirk SK, Shure AK, Agrawal DK. Immune-mediated adverse events of anticytotoxic T lymphocyte-associated antigen 4 antibody therapy in metastatic melanoma. *Transl Res.* (2015) 166:412–24. doi: 10.1016/j.trsl.2015.06.005
60. Weber JS, Dummer R, de Pril V, Lebb? C, Hodi FS. Patterns of onset and resolution of immune-related adverse events of special interest with ipilimumab: detailed safety analysis from a phase 3 trial in patients with advanced melanoma. *Cancer.* (2013) 119:1675–82. doi: 10.1002/cncr.27969
61. Horvat TZ, Adel NG, Dang TO, Momtaz P, Postow MA, Callahan MK, et al. Immune-related adverse events, need for systemic immunosuppression, and effects on survival and time to treatment failure in patients with melanoma treated with ipilimumab at memorial sloan kettering cancer center. *J Clin Oncol.* (2015) 33:3193–8. doi: 10.1200/JCO.2015.60.8448
62. Moher D, Pham B, Klassen TP, Schulz KF, Berlin JA, Jadad AR, et al. What contributions do languages other than English make on the results of meta-analyses?. *J Clin Epidemiol.* (2000) 53:964–72. doi: 10.1016/S0895-4356(00)00188-8

Conflict of Interest: The authors declare that the research was conducted in the absence of any commercial or financial relationships that could be construed as a potential conflict of interest.

frontiers in Immunology

CLINICAL TRIAL
published: 09 November 2020
doi: 10.3389/fimmu.2020.595035

Peptide Vaccination Against PD-L1 With IO103 a Novel Immune Modulatory Vaccine in Multiple Myeloma: A Phase I First-in-Human Trial

Nicolai Grønne Jørgensen[1,2], Uffe Klausen[1,2], Jacob Handlos Grauslund[1], Carsten Helleberg[2], Thomas Granum Aagaard[2], Trung Hieu Do[2], Shamaila Munir Ahmad[1], Lars Rønn Olsen[3], Tobias Wirenfeldt Klausen[2], Marie Fredslund Breinholt[4], Morten Hansen[1], Evelina Martinenaite[1], Özcan Met[1,5], Inge Marie Svane[1], Lene Meldgaard Knudsen[2†] and Mads Hald Andersen[1,5*†]*

[1] National Center for Cancer Immune Therapy (CCIT-DK), Department of Oncology, Copenhagen University Hospital, Herlev, Denmark, [2] Department of Hematology, Copenhagen University Hospital, Herlev, Denmark, [3] Department of Health Technology, Technical University of Denmark, Kgs. Lyngby, Denmark, [4] Department of Pathology, Copenhagen University Hospital, Herlev, Denmark, [5] Department of Immunology and Microbiology, University of Copenhagen, Copenhagen, Denmark

Background: Immune checkpoint blockade with monoclonal antibodies targeting programmed death 1 (PD-1) and its ligand PD-L1 has played a major role in the rise of cancer immune therapy. We have identified naturally occurring self-reactive T cells specific to PD-L1 in both healthy donors and cancer patients. Stimulation with a PD-L1 peptide (IO103), activates these cells to exhibit inflammatory and anti-regulatory functions that include cytotoxicity against PD-L1–expressing target cells. This prompted the initiation of the present first-in-human study of vaccination with IO103, registered at clinicaltrials.org (NCT03042793).

Methods: Ten patients with multiple myeloma who were up to 6 months after high dose chemotherapy with autologous stem cell support, were enrolled. Subcutaneous vaccinations with IO103 with the adjuvant Montanide ISA 51 was given up to fifteen times during 1 year. Safety was assessed by the common toxicity criteria for adverse events (CTCAE). Immunogenicity of the vaccine was evaluated using IFNγ enzyme linked immunospot and intracellular cytokine staining on blood and skin infiltrating lymphocytes from sites of delayed-type hypersensitivity. The clinical course was described.

Results: All adverse reactions to the PD-L1 vaccine were below CTCAE grade 3, and most were grade 1–2 injection site reactions. The total rate of adverse events was as expected for the population. All patients exhibited peptide specific immune responses in peripheral blood mononuclear cells and in skin-infiltrating lymphocytes after a delayed-type hypersensitivity test. The clinical course was as expected for the population. Three of 10 patients had improvements of responses which coincided with the vaccinations.

OPEN ACCESS

Edited by:
Said Dermime, National Center for Cancer Care and Research, Qatar

Reviewed by:
Antonio Curti, University of Bologna, Italy
Viktor Umansky, German Cancer Research Center (DKFZ), Germany

***Correspondence:**
Mads Hald Andersen
mads.hald.andersen@regionh.dk
Nicolai Grønne Jørgensen
nicolai.groenne.dahlager.joergensen.01@regionh.dk

[†]These authors have contributed equally to this work

Specialty section:
This article was submitted to Cancer Immunity and Immunotherapy, a section of the journal Frontiers in Immunology

Received: *14 August 2020*
Accepted: *14 October 2020*
Published: *09 November 2020*

Citation:
Jørgensen NG, Klausen U, Grauslund JH, Helleberg C, Aagaard TG, Do TH, Ahmad SM, Olsen LR, Klausen TW, Breinholt MF, Hansen M, Martinenaite E, Met Ö, Svane IM, Knudsen LM and Andersen MH (2020) Peptide Vaccination Against PD-L1 With IO103 a Novel Immune Modulatory Vaccine in Multiple Myeloma: A Phase I First-in-Human Trial. Front. Immunol. 11:595035. doi: 10.3389/fimmu.2020.595035

Conclusion: Vaccination against PD-L1 was associated with low toxicity and high immunogenicity. This study has prompted the initiation of later phase trials to assess the vaccines efficacy.

Clinical Trial Registration: clinicaltrials.org, identifier NCT03042793.

Keywords: peptide, vaccination, PD-L1, first-in-human, myeloma

INTRODUCTION

The development of monoclonal antibodies that block immune checkpoint molecules (ICB) has launched a new era in the treatment of malignancies. However, ICB treatment benefits a minority of patients with cancer and is associated with side effects (1, 2). We have recently explored whether ICBs can also be targeted by peptide vaccination. Such a vaccine could potentially combine the low toxicity of vaccination with a therapy that mitigates cancer-imposed immune inhibition.

In preclinical studies, we have demonstrated that the ICB programmed death ligand 1 (PD-L1) is recognized by T cells in both healthy donors and cancer patients (3). These PD-L1–reactive T cells can be activated by peptide stimulation. From the signal peptide of PD-L1, we developed a highly immunogenic 19-amino-acid peptide, designated IO103. IO103-stimulated PD-L1–specific T cells are cytotoxic to cancer cell lines, including melanoma, renal cell carcinoma, breast cancer, leukemia, and chronic myeloproliferative neoplasms (4–7). *In vitro* stimulation with PD-L1 peptide boosted immune responses to a dendritic cell (DC) vaccine (8). Similarly, immune responses to PD-L1 have been observed in multiple myeloma (MM) (Jørgensen et al., in preparation).

In MM, T cells and natural killer (NK) cells in the tumor microenvironment exhibit upregulated PD-1, and MM cells, osteoclasts, and DCs are often PD-L1$^+$ (9–16). The PD-1/PD-L1 pathway indirectly promotes myeloma progression by causing failure of immune control. Moreover, bone marrow (BM) stromal cells induce myeloma cells to express PD-L1, inducing increased tumor cell proliferation and reduced susceptibility to chemotherapy (17). PD-L1 expression is often detected on plasma cells in extramedullary plasmacytomas of late-stage disease (18). Furthermore, PD-1 levels on T cells in myeloma patients are negatively correlated with survival (19), and PD-L1 upregulation on MM cells is common among patients with relapsed or refractory MM and associated with an aggressive phenotype (20). However, PD-1 blockade does not exhibit single-agent activity in MM (21), and initial promising data regarding combination therapy with PD-1 ICB and immunomodulatory drugs with dexamethasone was not confirmed in randomized trials (22, 23). The present study was initiated before these randomized trials were halted by the FDA in 2017.

Peptide vaccination has shown promising results in early-stage neoplasia, and combined with chemotherapy (24). High-dose chemotherapy with autologous stem cell support (HDT)-mediated lymphodepletion yields a decreased Treg/CD8$^+$ ratio, which theoretically should favor immunotherapy post-HDT (25, 26). Furthermore, in preclinical studies, homeostatic cytokine-driven peripheral T-cell expansion after lymphodepletion reportedly aids the establishment of antitumor responses to vaccines, prompting several studies of post-HDT immune therapy (27, 28). Hence, we chose to vaccinate patients as they were in post-HDT remission.

Based on previous studies of therapeutic cancer vaccines, we expected a low level of adverse reactions. The impressive preclinical immunogenicity of the peptide led us to expect the induction of strong immune responses to IO103. Here, we present the results from a phase I first-in-human study of subcutaneous vaccination with IO103 emulsified with the adjuvant Montanide.

SUBJECTS AND METHODS

Study Design

In this first-in-human open-label single-armed study, the safety and immunogenicity of vaccinations using the PD-L1 peptide IO103 with the adjuvant Montanide was evaluated. Patients were enrolled at Herlev and Gentofte University Hospital, Copenhagen, Denmark, between February and November of 2017. The study was conducted in accordance with the Helsinki Declaration, and Good Clinical Practice (GCP) recommendations. All participants gave written informed consent before enrollment. The protocol was approved by the Ethics Committee of the Capital Region of Denmark, the National Board of Health, and the Danish Data Protection Agency, and registered at www.clinicaltrials.gov (NCT03042793; date of registration: February 2, 2017). Blood samples were obtained from a reference cohort of unvaccinated patients (n = 6) with MM and who concurrently received the same standard-of-care treatment as the vaccinated patients, after they gave written informed consent in an observational study approved by the Ethics Committee of the Capital Region of Denmark (Approval no. H-17010084). In the same study, serum was sampled from patients with smoldering multiple myeloma (n = 10).

With no previous human exposure to this vaccine to perform statistical power calculations, a sample size of 10 individuals was chosen based on experience from similar studies. Eligibility criteria included Eastern Cooperative Oncology Group performance status of ≤2, no severe comorbidities or autoimmune diseases, and no signs of myeloma relapse. Cytogenetic analyses were not required. **Supplementary Table 1** presents full inclusion and exclusion criteria. Patients with MM were enrolled to receive vaccination once they were in remission, between 4 weeks to 6 months post-HDT. No additional maintenance treatment was given. All patients received zoledronic acid to minimize the rate of skeletal osteolytic lesions.

Treatment

Vaccination with a long peptide forces uptake and presentation by antigen presenting cells, whereas vaccination with short peptides (9–10 amino acids) could lead to merely coating HLA molecules. Thus, vaccination with long peptides permits inclusion of patients without HLA-type restriction, and is associated with stimulation of both $CD4^+$ and $CD8^+$ T cells (29). In this study, patients were administered subcutaneous vaccinations containing 100 µg IO103, a 19-amino-acid peptide (FMTYWHLLNAFTVTVPKDL) from the signal peptide of PD-L1 (PolyPeptide Laboratories, France). The peptide was dissolved in dimethylsulfoxide (DMSO), sterile filtered, and frozen at –20° Celsius (NUNC™ CryoTubes™ CryoLine System™ Internal Thread, Sigma-Aldrich). At ≤2 h before administration, the peptide was thawed and dissolved in sterile water for injection. Immediately before injection, the dissolved peptide was emulsified 1:1 with the adjuvant Montanide ISA-51 (Seppic Inc. Paris, France) to a total volume of 1 ml (30). Vaccinations were administered by subcutaneous injection every two weeks, repeated six times, and then once every 4 weeks until reaching a total of 15 vaccines.

Clinical Evaluation

Adverse events were assessed according to CTCAE v.4.03. Patients were followed with frequent blood samples including a full myeloma panel and electrocardiograms. Clinical response was evaluated following International Myeloma Working Group (IMWG) response criteria (31). Time to next treatment was calculated from autologous stem cell transplant (ASCT) until initiation of next treatment.

Blood and Bone Marrow Samples

Blood samples for isolation of serum and peripheral blood mononuclear cells (PBMCs) were obtained at baseline, after three vaccinations, after six vaccinations, and after 15 vaccinations or at relapse. Samples were kept at room temperature (RT) for ≤5 h until handling. PBMCs were isolated by gradient centrifugation of heparinized blood on Lymphoprep (STEMCELL Technologies) in LeucoSep tubes (Greiner Bio-One). Isolated PBMCs were cryopreserved in 90% human serum (Sigma-Aldrich) with 10% DMSO (Sigma-Aldrich) using controlled-rate freezing (Cool-Cell, Biocision) in a –80°C freezer. The next day, the ampules were transferred to –140°C. To obtain serum samples, blood was collected in 8-ml Vacuette gel tubes containing clot activator (Greiner Bio-One). The tubes were centrifuged, and serum was stored at –140°C. Serum and PBMCs were stored in 1.8-ml NUNC™ CryoTubes™ CryoLine System™ Internal Thread (Sigma-Aldrich).

Heparinized bone marrow samples (10 ml in a heparinized tube) were obtained at baseline, after six vaccines, and after 15 vaccines or at relapse. The samples were subjected to red blood cell lysis by adding Ortho-Lysing Buffer diluted 10× in H_20, followed by centrifugation and incubation for 15 min in the dark. The remaining cells were cryopreserved following the same procedure as for PBMCs.

Delayed-Type Hypersensitivity and Skin-Infiltrating Lymphocytes

Presence of tumor-specific T cells in biopsies from delayed-type hypersensitivity (DTH) testing post-vaccination is correlated with clinical outcome (32). We assessed the presence of vaccine-reactive cells at DTH sites after six vaccinations. On the lower back, we performed three intradermal injections of IO103 without adjuvant and one control injection of aqueous solvent containing DMSO without peptide. At 48 h post-DTH injection, skin reaction was measured, and punch biopsies were taken from the sites of IO103-containing injections and cut into fragments. Fragments were cultured in 24-well plates for 3–5 weeks in RPMI-1640 with 10% human serum and 100 U/ml interleukin-2 (IL-2) with penicillin, streptomycin, and fungizone. Three times weekly, half the medium was replaced with fresh medium containing IL-2. Skin-infiltrating lymphocytes (SKILs) emigrated from the biopsies. After 3–5 weeks, SKILs were harvested and tested in ELISPOT assays (see below). The remaining SKILs were cryopreserved, as described for PBMCs.

IFNγ ELISpot Assay

To assess T-cell responses against IO103, indirect interferon gamma Enzyme-Linked ImmunoSPOT (IFNγ-ELISpot) assays were performed as previously described (3). PBMCs were stimulated once *in vitro* to increase assay sensitivity (33). Briefly, cryopreserved PBMCs were thawed and stimulated once with IO103 at RT in 24-well plates with 0.5 ml X-VIVO medium. After 2 h, 1.5 ml X-VIVO medium with 5% human serum was added, and the plate was incubated at 37°C under 5% CO_2. The next day, IL-2 was added, yielding a concentration of 120 U/ml. After 5–10 days, stimulated PBMCs were added to a 96-well nitrocellulose plate (MultiScreen, MAIP N45; Millipore) precoated with anti-IFNγ-mAb (mAb 1-DIK, Mabtech, Sweden). IO103 was added, and the cells were incubated overnight. Next day, the plates were washed, biotinylated secondary anti-INFγ mAb (Mabtech) was added, and the plates were incubated for 2 h at RT. Then, the plates were washed, Streptavidin-enzyme conjugate (AP-Avidin; Calbiochem/Invitrogen Life Technologies) was added, and the plates were incubated for 1 h at RT, and then washed again. Finally, the enzyme substrate NBT/BCIP (Invitrogen Life Technologies) was added, and the resulting spots were counted using the ImmunoSpot Series 2.0 Analyser (CTL Analyser). Maximum count was set to 500 spots/well. Raw data are available upon request.

IFNγ-ELISPOT assays on PBMCs were run in triplicate with 2.2–3.0 × 10^5 cells/well. For graphic representation, numbers were normalized to 2.2 × 10^5 cells/well. IFNγ-ELISPOT assays on SKILs were run in triplicate or quadruplicate with 3 × 10^5 cells/well, using a reversed sequence of the IO103 peptide as a control. IFNγ-ELISPOT assays on BM samples were hampered by low viability and high background, but singlets were run from all time points from one patient.

Flow Cytometry on PBMCs

Cryopreserved PBMCs were thawed in wash buffer (0.5% BSA, 2 mM EDTA in PBS) at 37°C, and Fc-receptors blocked by incubation with human IgG (20 mcg/ml). PBMCs were

stained in three panels using the following antibodies: CD3-FITC, CD56-PE, CD11c-PE, CD8-PerCP, HLA-DR-PerCP, CD27-BV421, CD25-BV421, CD4-BV510, CD28-PE-Cy7, CD3-PE-Cy7, CD19-PE-Cy7, CD127-PE-Cy7, CD45RA-APC, CD56-BV510 (all from BD Bioscience, NJ, United States), CCR7-PE, PD-1-APC, CD14-BV421 (all from Biolegend, California, United States), CD16-FITC (Dako, Glostrup, Denmark), and NiR live-dead reagent for APC-Cy7 channel (Invitrogen-Thermo Fischer, United States). Two panels for analyzing regulatory T cells (Tregs) were run: one with intracellular FoxP3-PE and one with only surface markers, including CCR7-PE. Both Treg panels included CD45RA-FITC, CD4-PerCP, CD127-PE-Cy7, CCR4-APC, CD25-BV421, and CD15s-BV510. Samples were incubated with relevant antibodies for 20 min in the dark at 4°C, washed, and then analyzed on a FACS Canto II flow cytometer (BD) and analyzed using FACSDiva Software version 8.0.1 (BD). T cells in the CD4 and CD8 compartments were characterized by examining live singlet events in the PBMC (lymphocyte and monocyte) gate in the forward and side scatter plot. Naïve T cells were characterized as $CCR7^{+}CD45RA^{+}$, central memory (CM) as $CCR7^{+}CD45RA^{-}$, effector memory as $CCR7^{-}CD45RA^{-}$, and effector memory RA^{+} (EMRA) as $CCR7^{-}CD45RA^{+}$. Tregs were gated on PBMCs, singlets, live cells, and subsequently on $CD4^{+}$ cells. **Supplementary Figure 10** presents the gating strategy for Tregs. Myeloid DCs ($LIN^{-}CD11c^{+}HLA\text{-}DR^{+}CD14^{-}CD16^{-}$) and non-classical monocytes ($LIN^{-}CD11c^{+}HLA\text{-}DR^{+}CD14^{-}CD16^{+}$) were gated from the Lineage (CD3/CD19/CD56) and CD14 negative and CD11c, HLA-DR positive fraction of PBMCs. To analyze SKILs' cytokine secretion capability, intracellular cytokine staining was performed on SKILs incubated 5 h with or without 5 μg/ml IO103 (37°C, 5% CO_2). GolgiPlug (BD) was applied before staining with CD3-APC-H7, CD4-PerCP/FITC, CD8-Pacific Blue/PerCP, and Horizon Fixable Viability Stain 510 (BD). The cells were fixed and permeabilized with Fixation/Permeabilization Buffer (eBioscience), following the manufacturer's instructions, and then intracellularly stained using IFNγ-PE-Cy7/APC (eBioscience) and TNF-APC/BV421 (eBioscience). Relevant isotype controls were used to support correct compensation and confirm antibody specificity.

Cytokines in Serum

Cytokines in serum samples were measured using the MSD Mesoscale V-Plex Human Cytokine 30-plex Kit (Catalog No. K15054D-1), following the manufacturer's instructions, except that the samples were diluted four-fold instead of two-fold.

Statistical Analysis

Responses in ELISpot assays were determined using the previously described distribution-free resampling (DFR) method as described by Moodie et al. (34). The Wilcoxon matched-pairs signed-rank test was used to compare responses to IO103 between baseline and later time points. For flow cytometry samples, the unpaired Mann-Whitney was used to compare lymphocyte subsets in vaccinated patients versus the reference cohort at an individual time point. As this exploratory analysis was descriptive and done *post hoc*, no formal multiple testing corrections were performed. p values ≤ 0.05 were considered significant. All analyses were performed in Graphpad Prism v 8.0 (GraphPad Software. Inc.).

For cytokine heatmaps each protein/cytokine was normalized by subtracting the mean value and dividing by standard deviation of the logarithmic transformed values. The normalized values for the cytokines for each subject were

TABLE 1 | Patient characteristics.

	Age	Sex	ECOG PS	Comorbidity	Type of paraprotein	LDH at diagnosis	Cytogenetics at diagnosis	ISS/R-ISS at diagnosis	Time from HDT to start of vaccination (days)
Patient 1	70	F	0	Hypertension, Cholecystectomy	Lambda	262	Not enough material	2/2	188
Patient 2	69	M	0	Hypertension, Hypercholesterolemia, CABG, BCC	Kappa	188	amp1q(80%), t(11:14) (100%) = High risk	1/1	70
Patient 3	58	F	1	Hypertension, multinodular goiter	Lambda	246	Normal FISH = Standard risk	3/3	131
Patient 4	58	M	1	None	IgG kappa	172	t(11:14)(91%) = Standard risk	3/2	43
Patient 5	60	F	1	Inguinal hernea	Lambda	141	t(11:14)(96%) = Standard risk	3/3	61
Patient 6	59	M	1	None	IgG kappa	220	del(13q14.3)(96%) del1p (97%) = High risk	1/2	82
Patient 7	60	F	1	Hypertension, Spinal stenosis operata	IgG kappa	260	Not enough material	3/2	41
Patient 8	61	M	1	None	Biclonal IgG kappa IgA kappa	142	Not enough material	2/2	50
Patient 9	69	M	1	None	IgG kappa	175	Not done	Missing	28
Patient 10	39	M	1	None	IgG kappa	148	Not possible	2/2	83

Patient 9 had previously been transplanted, and was enrolled after a HDT treating first relapse.
HDT, high dose chemotherapy with autologous stem cell transplant; ISS, International Staging System; LDH, lactate dehydrogenase.

shown in the heatmap. The dendrograms and ordering of subjects and cytokines were performed by hierarchical clustering using Ward's method. Distances between cytokines were calculated by 1 – r, where r is the Pearson correlation coefficient and distances between subjects by Euclidian distance. The R function "agnes" in the "cluster" package was used for clustering.

RESULTS

Patient Characteristics

Our study population included 10 patients with MM (4 female and 6 male; mean age, 60.3 years; age range: 39–70), who had undergone HDT treatment within 1–6 months. **Table 1** shows patient characteristics. Nine patients were included after first-line induction therapy with HDT. Induction therapy comprised standard of care therapy of cyclophosphamide, bortezomib, and dexamethasone (Cy-Vel-Dex) for all but one patient who instead received bortezomib, thalidomide, and dexamethasone (VTD, patient 4) due to renal insufficiency at diagnosis. Patient 9 was included after Cy-Vel-Dex and HDT, following relapse occurring 18 years after primary double transplantation. Five patients lacked cytogenetic data from diagnosis. FISH was performed on BM samples at inclusion, but the low tumor burden post-HDT prohibited cytogenetic analysis. All included patients received at least 6 vaccines and are included in the data set.

Adverse Events

Infections are common in patients with MM, and the infection rate is further increased for at least one1 year post-HDT. The rate of infections and other adverse events was as expected for the population (**Table 2**). Adverse events considered potentially related to vaccination were most commonly injection site reactions and were all transient of nature (**Table 2**). No adverse events above grade 2 were deemed related to the vaccine. No autoimmune adverse events were observed.

Immune Responses in Blood

PBMCs from blood samples were assessed using indirect ELISPOT assays against IO103. No or little response to the vaccine occurred at baseline, while all patients exhibited a response to IO103 during the vaccination course (**Figures 1A–D**). To assess whether immune responses to IO103 would normally occur post-HDT, we ran IO103 ELISPOT on our reference cohort at similar time points as in the vaccinated patients. Consistent with our previous data, we observed spontaneous immune responses to IO103 before HDT. These responses were not observed post-HDT in the unvaccinated reference cohort (**Figure 1E**), likely due to the strong lympho-depleting chemotherapy.

Immune Responses in the Skin

Nine patients consented to DTH testing before the seventh vaccine. The cells from one patient (patient 3) were accidentally infected in culture. All eight evaluable patients had a positive skin induration of more than double the diameter of the control injection. SKILs could be grown from skin biopsies of all patients, and all were strongly reactive to the vaccine as evaluated by IFNγ-ELISPOT (**Figure 2A**). IL2-expanded SKILs were mainly $CD4^+$ T cells (data not shown). Intracellular cytokine staining after stimulation with IO103 revealed that these $CD4^+$ SKILs secreted tumor necrosis factor alfa (TNF-α) and a minor fraction also secreted IFN-γ (**Figures 2B, C**).

TABLE 2 | AEs total adverse events during vaccinations.

Relation to therapy*	Adverse event	No. of patients	Grade 1	Grade 2	Grade 3
Cy-Vel-Dex induction, HDT, myeloma or unrelated	Cold	6	6		
	Respiratory tract infection	3	1		2
	Influenza	2		1	1
	Urinary tract infection	2		2	
	Abscessus	1		1	
	Conjunctivitis	1		1	
	Fungal skin infection	1		1	
	Flu-like viral infection	1		1	
	Gastroenteritis	1		1	
	Herpes reactivation	1		1	
	Sinusitis	1		1	
	Tonsillitis	1			3
	Cough	2	2		
	Diarrhoea	2	2		
	Basal cell carcinoma	1			1
	Constipation	1	1		
	Creatinin increase	1	1		
	Hernia, inguinal	1			1
	Nausea	1		1	
	Palpitations	1		1	
	Sore throat	1	1		
	Tendernes of jaw	1	1		
	Artroscopic miniscus manipulation	1			1
PD-L1 vaccine (IO103)	Injection site reaction	9	6	3	
	Pruritus	3	2	1	
	Myalgia	3	1	2	
	Artralgia	2		2	
	Sore nipple	2	2		
	Dry skin	1	1		
	Lymphopenia	1	1		
	Cough	1	1		
	Dermatitis	1		1	
	Rash	2	1	1	
	Swelling of bursa olecrani	1	1		

**Investigator deemed whether adverse events were related or possibly related to the experimental treatment or to other causes. Injection site reactions included local erythema, oedema, and pruritus. Non-tender subcutaneous lumps up to 1 cm in diameter could linger up to months, as is seen commonly with the deposition of the adjuvant Montanide. Cy-Vel-Dex, cyclophosphamide-bortezomib-dexamethazone; HDT, high-dose chemotherapy with autologous stem cell transplantation.*

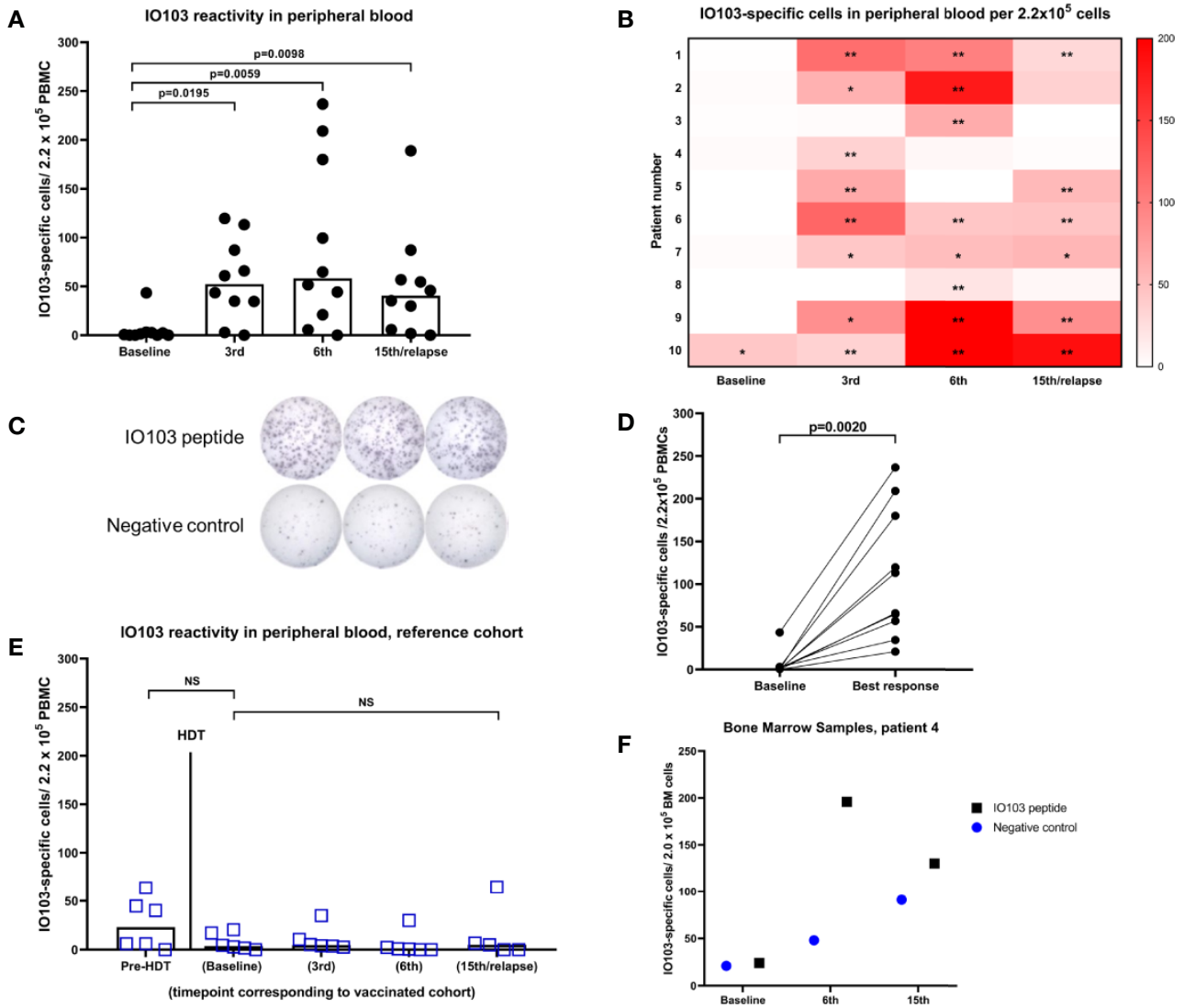

FIGURE 1 | IFNγ-ELISPOT immune responses against IO103. **(A)** responses in PBMCs in vaccinated patients (bars represent median); **(B)** Heatmap of responses in PBMCs per vaccinated per time point. (*DFRx1; **DFRx2); **(C)** representative example of ELISPOT-wells with response; **(D)** best response in PBMCs in vaccinated patients; **(E)** responses in unvaccinated reference cohort including time point before HDT (All p-values: Wilcoxon matched-pairs signed rank test); **(F)** IFNγ-ELISPOT responses against IO103 in bone marrow samples from patient 4.

Immune Responses in the Bone Marrow

ELISPOT assays on cryopreserved BM samples had a very high background signal due to ex vivo cell death. Reduced viability of BM mononuclear cells is well known (35). The fact that these BM samples were taken in the recovery from HDT, may have decreased the viability further. The low viability of the immune cells in the BM samples did not permit in depth immune monitoring with functional living cells. Nonetheless, singlet samples were run with only modest background in one of three tested patients, and in samples from this patient, a strong immune response to IO103 was seen in the BM (**Figure 1F**).

Lymphocytes

An exploratory analysis of lymphocyte phenotypes was performed comparing samples from the vaccinated patients to samples from the unvaccinated reference cohort. Vaccinated patients 1, 3, 6, and 10 were not included in these comparisons, since these patients did not have synchronous reference cohort samples for comparison. An inversion of the CD4/CD8 ratio following HDT was seen in the unvaccinated cohort, and the vaccinated patients had a similar ratio at baseline (**Supplementary Figures 1A, B**). A significantly lower level of CD4 cells in vaccinated patients after 15th vaccination or relapse

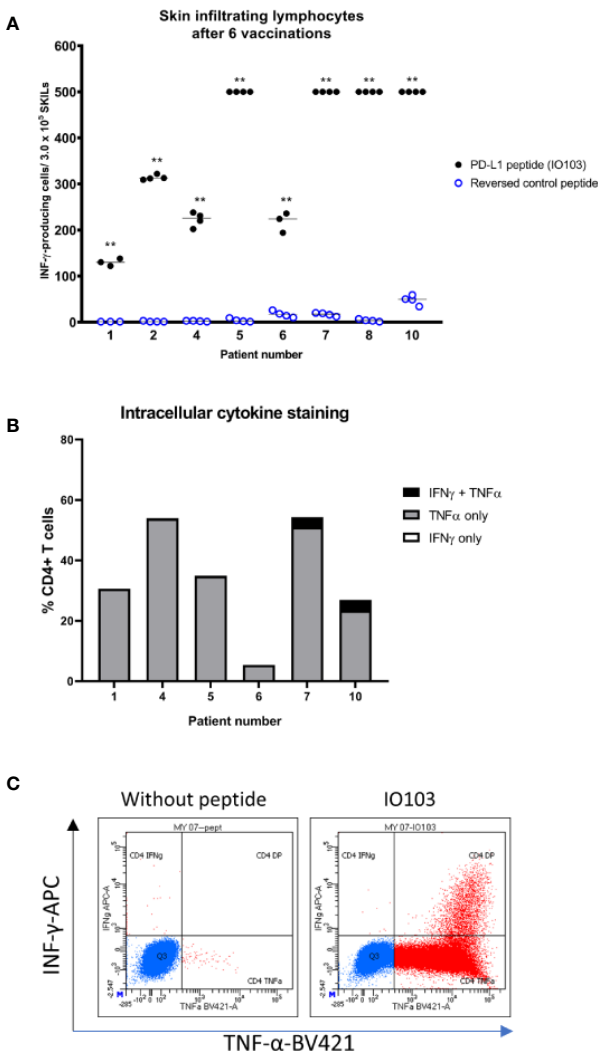

FIGURE 2 | Immune responses to the vaccine in the skin. **(A)** IFNγ-ELISPOT responses against the PD-L1 peptide IO103 of skin infiltrating lymphocytes after delayed type hypersensitivity reaction performed after 6 vaccines. 300,000 cells per well. Samples were run in triplicate or quadruplicate. **DFRx2; **(B)** intracellular cytokine staining (ICS) of SKILs. Almost all cells were CD4+ (not shown). Two out of six evaluable patients had TNFα- and INFγ-double positive SKILs; **(C)** example of a double positive ICS (patient 7).

was seen. Gating of differentiation stages did not reveal significant differences and exhibited substantial interindividual variance. Naïve cell repopulation post-HDT did not significantly differ in samples from vaccinated patients compared to the reference population (**Supplementary Figures 2** and **3**). The level of Tregs was not found to be significantly different compared to the reference population (**Figures 3A–D**). The FoxP3$^+$ Treg levels of all vaccinated patients are shown in **Supplementary Figure 12**. Levels of DCs in peripheral blood samples did not show significant differences compared to the reference population (**Supplementary Figure 13**).

Clinical Course

Before vaccinations, four patients were in complete response (CR) or better, and five had very good partial response (VGPR). At the data cut-off (May 14, 2020; mean follow-up, 36.5 months), 2/10 patients had not started their next treatment, and 8/10 were still alive (**Supplementary Figure 4**). The relapse rate was as expected for the population.

Three patients exhibited improved depth of response during vaccination therapy: patient 2 at day 145 post-ASCT (after 5 vaccines), patient 5 at day 161 (6 vaccines), and patient 7 at day 168 (7 vaccines) (**Figure 4**).

Patients 3 and 7 showed declining levels of M component/ involved light chain during vaccinations; however, both exhibited slow biochemical relapse after completing vaccinations. As a study amendment, these two patients were revaccinated to test if a stabilization or decline could be induced. In patient 3, revaccination did not decrease the tumor marker slope (**Supplementary Figure 7**). In patient 7, the M-component slope decreased briefly along with revaccinations (**Supplementary Figure 8**).

Patient 8 exhibited an early rapid clinical relapse, which was fatal despite initiation of therapy with daratumumab, lenalidomide, and dexamethasone. At this time, the patient had received 11 vaccines. We explored possible correlations between immune data and clinical course. Patients who did and did not relapse during the vaccination course did not differ in ELISPOT responses to IO103 in blood samples (**Supplementary Figure 5**). However, the two earliest relapsing patients (patients 8 and 9) showed baseline cytokine profiles that grouped apart from the remaining vaccinated patients in unsupervised analysis (**Supplementary Figures 6A, B**). Furthermore, two patients (patients 8 and 4) with early relapses had the lowest ELISPOT responses to IO103 in PBMCs (**Figure 1C**), and the highest Treg levels in PBMCs even at baseline (**Supplementary Figure 11**).

During the vaccination course, patient 2 exhibited significant regression of concurrent basal cell carcinoma (BCC), and patient 6 exhibited spontaneous BCC clearance that was macroscopically complete, such that planned surgery was cancelled. In patient 6, BCC recurred, coinciding with biochemical relapse of MM.

DISCUSSION

The vaccine was generally well tolerated, and the frequency of adverse events was as expected in the patient population. Adverse events that were related or possibly related to vaccination with IO103 were mild (CTCAE grade 1–2) and reversible, and most frequently injection site reactions.

PD-L1 is expressed on cancer cells and non-cancerous cells in the tumor microenvironment, on normal antigen-presenting cells and placental cells, and frequently on cells in an inflammatory microenvironment, since its expression is primarily regulated by interferons (36). We recently demonstrated that inflammation alone induces PD-L1–specific T cells (37). The fact that PD-L1–specific T cells are so easily and rapidly activated, but do not lead to outright autoimmune

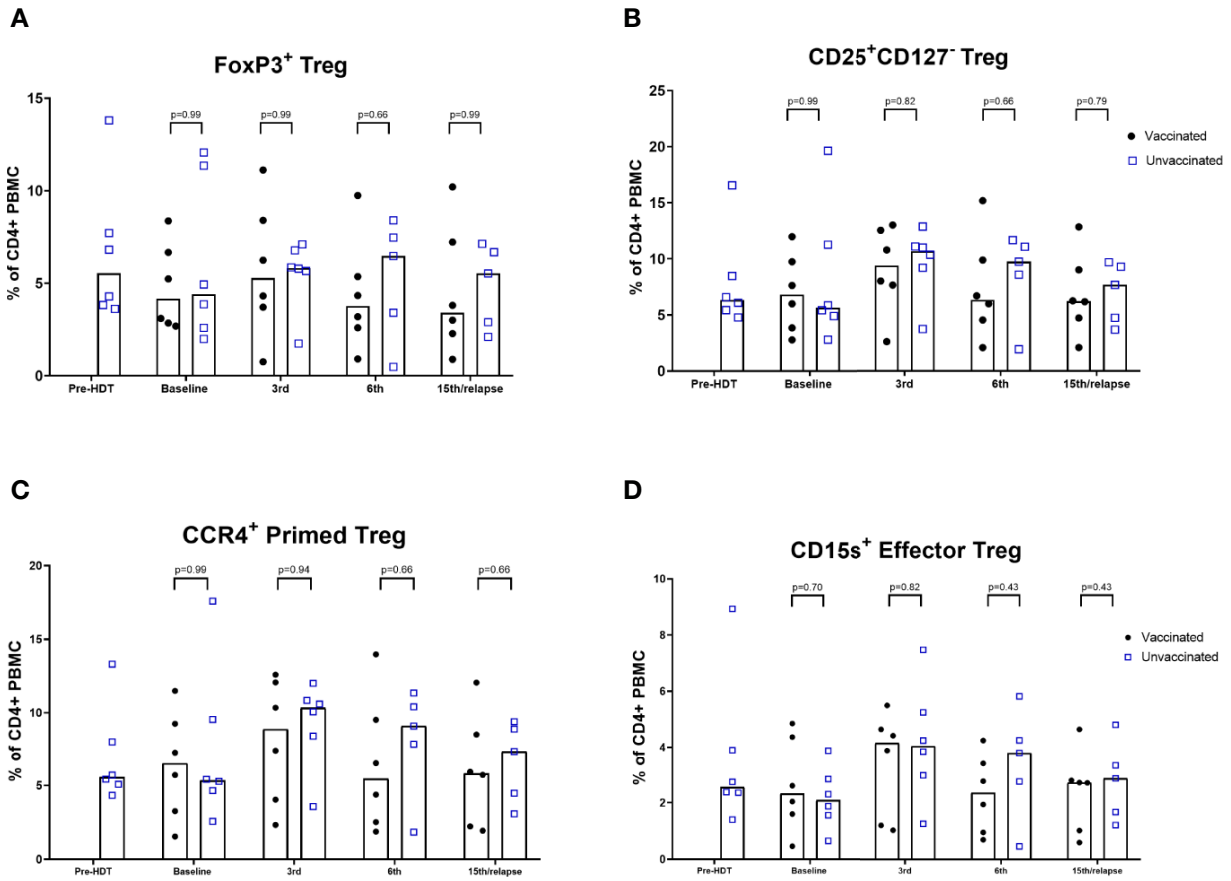

FIGURE 3 | Flow cytometric analyses of levels of Tregs. **(A)** FoxP3+ Treg. **(B)** CD25highCD127neg Treg; **(C)** CCR4 + Primed Tregs; **(D)** CD15s Effector Tregs. % of CD4+ PBMCs. Bars represent median (Mann-Whitney).

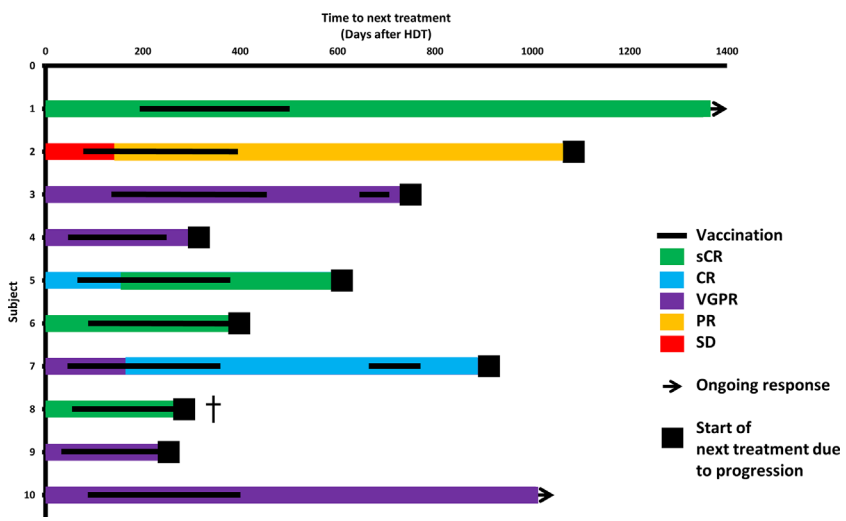

FIGURE 4 | Clinical course. Swimmer's plot. Colors of bars symbolize depth of response at start of vaccinations, after HDT and during the vaccination course. †patient 8 had a rapid relapse after having received 11 vaccinations and died shortly thereafter despite initiation of daratumumab-lenalidomide-dexamethasone.

reactions, implies that these cells are strictly regulated. Mouse studies of vaccination with murine PD-L1 peptides confirm the absence of signs of autoimmune events (in preparation). In this first-in-human study, we observed immune reactions to the vaccine in blood samples and skin tests from all patients. It is intriguing that stimulation of these self-reactive T cells strongly induced immune responses in all patients, with low toxicity.

In the months following lymphodepleting chemotherapy in HDT, $CD8^+$ T-cell repopulation is aided by homeostatic peripheral expansion more than the $CD4^+$ compartment, yielding a relatively low Treg/$CD8^+$ ratio, which gradually normalizes as levels return to baseline (25). An inverted ratio of $CD4^+$/$CD8^+$ T cells was found in both vaccinated patients and the unvaccinated reference cohort. In preclinical studies, activation of PD-L1–specific T-cells reduced Treg levels in autologous PBMCs (37). Vaccination against an indoleamine 2,3-dioxygenase (IDO) peptide in patients with lung cancer similarly induced a significant decrease in Tregs (38). IDO is another self-antigen expressed in regulatory immune cells, which is recognized by pro-inflammatory T cells (39, 40). In the present study, although the proportion of $CD4^+$ T cells was lower in vaccinated patients at the last time point, the levels of Tregs was not significantly lower among vaccinated patients at any time point. This study setting might not permit the assessment of the vaccine's effect on Treg levels, due to the recently been exposure to lymphodepleting chemotherapy.

Antigen presenting cells at the vaccination site may be PD-L1 positive. Thus, vaccination induced elimination of these cells could impact antigen presentation at the vaccination site. However, analysis of DC infiltration at the vaccination site was not been performed in this study but will be part of future investigations. Importantly, no signs of a major effect of vaccinations were seen on the frequencies of DC in peripheral blood.

One limitation of this study was our inability to thoroughly investigate immune responses in BM samples. Since MM is a disease of BM-residing cells, one would hope to see an immune response in the BM. However, the viability of BM samples precluded other functional assays of BM immune cells, and assessment of immune responses at the tumor site. These limitations led us to instead analyze the impact of vaccinations on T-cell-receptor (TCR) diversity in SKILs and BM samples, including PD-L1–specific TCRs. These studies are currently on-going.

The current study was valuable for examining the vaccine's safety. The minimal tumor burden post-HDT allowed us to vaccinate many times, over a prolonged period. Phase one studies are often performed in the relapsed or refractory setting, which would likely not leave sufficient time to test the vaccine's safety before disease progression. One downside of the post-HDT setting is that clinical efficacy was difficult to investigate. Nine patients were vaccinated post-HDT as part of primary treatment of newly diagnosed MM. In this patient population, median progression-free survival without maintenance treatment is 32 months, and 20% of patients will be in long-term remission (6 years post-HDT) (41). With a median follow-up of 29 months, the PFS data are not yet mature. In a Mayo Clinic study, response improvements after day +100 occurred in up to 39% of cases (42). However, among patients treated in Barcelona and Salamanca, only 1/74 patients had an upgraded response after day 100 without maintenance or consolidation (43). Response improvements beyond day 100 rarely occur at our institution (personal communication), and late improvements have been used as an argument regarding response to immunotherapy after HDT (12). The three late response improvements (over 100 days post-HDT), and one case of short-term stabilization coinciding with revaccination, may indicate the vaccine's efficacy.

The incidental findings of spontaneous BCC regression in patients 2 and 6 are interesting. After the initial spontaneous BCC clearance, patient 6 experienced clinical relapse of BCC coinciding with biochemical relapse of MM. This suggests that the vaccine induced a response toward the BCC, which lasted for months, and then experienced a loss of immune control affecting both malignancies once the vaccination was no longer effective. This cannot be tested with current methods but has prompted the initiation of a phase IIa study of vaccination with IO103 in BCC (NCT03714529).

Based on the present promising safety and immune data, several clinical trials have been initiated. It is hypothesized that therapeutic cancer vaccines, without chemotherapy or ICB, are likely to be most effective if administered in early disease stages (44, 45). Thus, a trial of IO103 in high-risk smoldering myeloma has been initiated (NCT03850522). Additionally, we are testing this vaccine combined with other peptide vaccines against PD-L2, IDO, and arginase, and with immune checkpoint-blocking antibodies (NCT03381768, NCT03939234, and NCT04051307).

In conclusion, the vaccination against PD-L1 was easily administered and was associated with few and low-grade and reversible side effects. Furthermore, the vaccine induced strong immune responses in all patients.

DATA AVAILABILITY STATEMENT

The raw data supporting the conclusions of this article will be made available by the authors, without undue reservation.

ETHICS STATEMENT

The studies involving human participants were reviewed and approved by De Videnskabsetiske Komiteer i Region Hovedstaden. The patients/participants provided their written informed consent to participate in this study.

AUTHOR CONTRIBUTIONS

NJ designed the study, obtained institutional approval, performed the research, analyzed data, and wrote the manuscript. UK, JG, CH, TA, and TD recruited and treated the patients and critically revised the manuscript. SA, MB, EM, and ÖM performed laboratory

research and critically revised the manuscript. LO, TK, and MH assisted in the data analysis and critically revised the manuscript. IS, LK, and MA conceptualized the study, designed the study, supervised the project, and critically revised the manuscript. All authors contributed to the article and approved the submitted version.

FUNDING

The work was funded by The Danish Cancer Society, The Copenhagen University Hospital Herlev and Gentofte, and through a research funding agreement between IO Biotech ApS and National Center for Cancer Immune Therapy (CCIT-DK).

ACKNOWLEDGMENTS

We greatly appreciate the tremendous technical support from Merete Jonassen, Sandra Ullitz Færch, Betina Saxild, Susanne Wendt, and Kirsten Nikolajsen. Ida Schjødt is thanked for very good advice on flowcytometric analyses. We would also like to thank Eva Ehrnrooth for her help and good discussions.

SUPPLEMENTARY MATERIAL

The Supplementary Material for this article can be found online at: https://www.frontiersin.org/articles/10.3389/fimmu.2020.595035/full#supplementary-material

REFERENCES

1. Bedognetti D, Ceccarelli M, Galluzzi L, Lu R, Palucka K, Samayoa J, et al. Toward a comprehensive view of cancer immune responsiveness: A synopsis from the SITC workshop. *J Immunother Cancer* (2019) 7:1–23. doi: 10.1186/s40425-019-0602-4
2. Naidoo J, Page DB, Li BT, Connell LC, Schindler K, Lacouture ME, et al. Toxicities of the Anti-PD-1 and Anti-PD-L1 Immune Checkpoint Antibodies. *Ann Oncol* (2015) 26:2375–91. doi: 10.1093/annonc/mdv383
3. Munir S, Andersen GH, Met Ö, Donia M, Frøsig TM, Larsen SK, et al. HLA-restricted CTL that are specific for the immune checkpoint ligand PD-L1 occur with high frequency in cancer patients. *Cancer Res* (2013) 73:1764–76. doi: 10.1158/0008-5472.CAN-12-3507
4. Munir S, Andersen GH, Woetmann A, Ødum N, Becker JC. Andersen MH.Cutaneous T cell lymphoma cells are targets for immune checkpoint ligand PD-L1-specific, cytotoxic T cells. *Leukemia* (2013) 27:2251–2253. doi: 10.1038/leu.2013.118
5. Ahmad SM, Larsen SK, Svane IM, Andersen MH. Harnessing PD-L1-specific cytotoxic T cells for anti-leukemia immunotherapy to defeat mechanisms of immune escape mediated by the PD-1 pathway. *Leukemia* (2013) 28:236–8. doi: 10.1038/leu.2013.261
6. Holmström MO, Riley CH, Skov V, Svane IM, Hasselbalch HC. Andersen MH.Spontaneous T-cell responses against the immune check point programmed-death-ligand 1 (PD-L1) in patients with chronic myeloproliferative neoplasms correlate with disease stage and clinical response. *Oncoimmunology* (2018) 7:1–6. doi: 10.1080/2162402X.2018.1433521
7. Munir S, Andersen GH, Svane IM, Andersen MH. The immune checkpoint regulator PD-L1 is a specific target for naturally occurring CD4(+) T cells. *Oncoimmunology* (2013) 2:e23991. doi: 10.4161/onci.23991
8. Munir Ahmad S, Martinenaite E, Hansen M, Junker N, Borch TH, Met Ö, et al. PD-L1 peptide co-stimulation increases immunogenicity of a dendritic cell-based cancer vaccine. *Oncoimmunology* (2016) 5:e1202391. doi: 10.1080/2162402X.2016.1202391
9. Benson DM, Bakan CE, Mishra A, Hofmeister CC, Efebera Y, Becknell B, et al. The PD-1 / PD-L1 axis modulates the natural killer cell versus multiple myeloma effect : a therapeutic target for CT-011, a novel monoclonal anti – PD-1 antibody. *Blood* (2010) 116:2286–94. doi: 10.1182/blood-2010-02-271874
10. Liu J, Hamrouni A, Wolowiec D, Coiteux V, Kuliczkowski K, Hetuin D, et al. Plasma cells from multiple myeloma patients express B7-H1 (PD-L1) and increase expression after stimulation with IFN-γ and TLR ligands via a MyD88-, TRAF6-, and MEK-dependent pathway. *Blood* (2007) 110:296–304. doi: 10.1182/blood-2006-10-051482
11. Hallett WHD, Jing W, Drobyski WR, Johnson BD. Immunosuppressive Effects of Multiple Myeloma Are Overcome by PD-L1 Blockade. *Biol Blood Marrow Transplant* (2011) 17:1133–45. doi: 10.1016/j.bbmt.2011.03.011
12. Rosenblatt J, Avivi I, Vasir B, Uhl L, Munshi NC, Katz T, et al. Vaccination with dendritic cell/tumor fusions following autologous stem cell transplant induces immunologic and clinical responses in multiple myeloma patients. *Clin Cancer Res* (2013) 19:3640–8. doi: 10.1158/1078-0432.CCR-13-0282
13. Ray A, Das DS, Song Y, Richardson P, Munshi NC, Chauhan D, et al. Targeting PD1–PDL1 immune checkpoint in plasmacytoid dendritic cell interactions with T cells, natural killer cells and multiple myeloma cells. *Leukemia* (2015) 29:1441–4. doi: 10.1038/leu.2015.11
14. Sponaas AM, Moharrami NN, Feyzi E, Standal T, Rustad EH, Waage A, et al. PDL1 expression on plasma and dendritic cells in myeloma bone marrow suggests benefit of targeted anti PD1-PDL1 therapy. *PloS One* (2015) 10:e0139867. doi: 10.1371/journal.pone.0139867
15. An G, Acharya C, Feng X, Wen K, Zhong M, Zhang L, et al. Osteoclasts promote immune suppressive microenvironment in multiple myeloma: therapeutic implication. *Blood* (2016) 128:1590–1603. doi: 10.1182/blood-2016-03-707547
16. Paiva B, Azpilikueta A, Puig N, Ocio EM, Sharma R, Oyajobi BO, et al. PD-L1/PD-1 presence in the tumor microenvironment and activity of PD-1 blockade in multiple myeloma. *Leukemia* (2015) 29:2110–3. doi: 10.1038/leu.2015.79
17. Ishibashi M, Tamura H, Sunakawa M, Kondo-Onodera A, Okuyama N, Hamada Y, et al. Myeloma Drug Resistance Induced by Binding of Myeloma B7-H1 (PD-L1) to PD-1. *Cancer Immunol Res* (2016) 4:779–88. doi: 10.1158/2326-6066.CIR-15-0296
18. Crescenzi A, Annibali O, Bianchi A, Pagano A, Donati M, Grifoni A, et al. PD-1/PD-L1 expression in extra-medullary lesions of multiple myeloma. *Leuk Res* (2016) 49:98–101. doi: 10.1016/j.leukres.2016.09.008
19. Gasmi B, Smith E, Dogan A, Hsu M, Devlin S, Pichardo J, et al. *Presence of PD-1 Expressing T Cells Predicts for Inferior Overall Survival in Newly Diagnosed Multiple Myeloma. ASH 2015 (abstract 1785)* (2015). Available at: https://ash.confex.com/ash/2015/webprogram/Paper84149.html (Accessed 10th December 2015).
20. Tamura H, Ishibashi M, Yamashita T, Tanosaki S, Okuyama N, Kondo A, et al. Marrow stromal cells induce B7-H1 expression on myeloma cells, generating aggressive characteristics in multiple myeloma. *Leukemia* (2013) 27:464–472. doi: 10.1038/leu.2012.213
21. Lesokhin AM, Ansell SM, Armand P, Scott EC, Halwani A, Gutierrez M, et al. Nivolumab in Patients with Relapsed or Refractory Lymphoid Malignancy: Preliminary Results of a Phase I Study. *J Clin Oncol* (2016) 34:2698–704. doi: 10.1200/JCO.2015.65.9789
22. Usmani SZ, Schjesvold F, Oriol A, Karlin L, Cavo M, Rifkin RM, et al. Pembrolizumab plus lenalidomide and dexamethasone for patients with treatment-naive multiple myeloma (KEYNOTE-185): a randomised, open-label, phase 3 trial. *Lancet Haematol* (2019) 6:e448–58. doi: 10.1016/s2352-3026(19)30109-7
23. Mateos M-V, Blacklock H, Schjesvold F, Oriol A, Simpson D, George A, et al. Pembrolizumab plus pomalidomide and dexamethasone for patients with relapsed or refractory multiple myeloma (KEYNOTE-183): a randomised, open-label, phase 3 trial. *Lancet Haematol* (2019) 6:e459–69. doi: 10.1016/s2352-3026(19)30110-3

24. van der Burg SH, Arens R, Ossendorp F, van Hall T, Melief CJM. Vaccines for established cancer: overcoming the challenges posed by immune evasion. *Nat Rev Cancer* (2016) 16:219–233. doi: 10.1038/nrc.2016.16
25. Chung DJ, Pronschinske KB, Shyer JA, Sharma S, Leung S, Curran SA, et al. T-cell Exhaustion in Multiple Myeloma Relapse after Autotransplant: Optimal Timing of Immunotherapy. *Cancer Immunol Res* (2016) 4:61–71. doi: 10.1158/2326-6066.CIR-15-0055
26. Svane IM, Nikolajsen K, Johnsen HE. Antigen-specific T-cell immunity in multiple myeloma patients is restored following high-dose therapy: implications for timing of vaccination. *Scand J Immunol* (2007) 66:465–75. doi: 10.1111/j.1365-3083.2007.01993.x
27. Williams KM, Hakim FT, Gress RE. T cell immune reconstitution following lymphodepletion. *Semin Immunol* (2007) 19:318–330. doi: 10.1016/j.smim.2007.10.004
28. Gökbuget N, Canaani J, Nagler A, Bishop M, Kröger N. Avigan D.Prevention and treatment of relapse after stem cell transplantation with immunotherapy. *Bone Marrow Transplant* (2018) 53:664–72. doi: 10.1038/s41409-018-0232-3
29. Melief CJM, van der Burg SH. Immunotherapy of established (pre)malignant disease by synthetic long peptide vaccines. *Nat Rev Cancer* (2008) 8:351–60. doi: 10.1038/nrc2373
30. Ascarateil S, Puget A, Koziol M-E. Safety data of Montanide ISA 51 VG and Montanide ISA 720 VG, two adjuvants dedicated to human therapeutic vaccines. *J Immunother Cancer* (2015) 3:2015. doi: 10.1186/2051-1426-3-S2-P428
31. Rajkumar SV, Harousseau JL, Durie B, Andersen KC, Dimopoulos M, Kyle R, et al. Consensus recommendations for the uniform reporting of clinical trials: report of the International Myeloma Workshop Consensus Panel 1. *Blood* (2011) 117:4691–5. doi: 10.1182/blood-2010-10-299487
32. de Vries IJM, Bernsen MR, Lesterhuis WJ, Scharenborg NM, Strijk SP, Gerritsen MJP, et al. Immunomonitoring tumor-specific T cells in delayed-type hypersensitivity skin biopsies after dendritic cell vaccination correlates with clinical outcome. *J Clin Oncol* (2005) 23:5779–87. doi: 10.1200/JCO.2005.06.478
33. McCutcheon M, Wehner N, Wensky A, Kushner M, Doan S, Hsiao L, et al. A sensitive ELISPOT assay to detect low-frequency human T lymphocytes. *J Immunol Methods* (1997) 210:149–66. doi: 10.1016/S0022-1759(97)00182-8
34. Moodie Z, Price L, Janetzki S, Britten CM. Response Determination Criteria for ELISPOT: Toward a Standard that Can Be Applied Across Laboratories. *Methods Mol Biol* (2012) 792:185–96. doi: 10.1007/978-1-61779-325-7_15
35. Yang B, Parsha K, Schaar K, Satani N, Xi X, Aronowski J, et al. Cryopreservation of Bone Marrow Mononuclear Cells Alters Their Viability and Subpopulation Composition but Not Their Treatment Effects in a Rodent Stroke Model. *Stem Cells Int* (2016) 2016:5876836. doi: 10.1155/2016/5876836
36. Garcia-Diaz A, Shin DS, Moreno BH, Saco J, Escuin-Ordinas H, Rodriguez GA, et al. Interferon Receptor Signaling Pathways Regulating PD-L1 and PD-L2 Expression. *Cell Rep* (2017) 19:1189–201. doi: 10.1016/j.celrep.2017.04.031
37. Munir S, Lundsager MT, Jørgensen MA, Hansen M, Petersen TH, Bonefeld CM, et al. Inflammation induced PD-L1-specific T cells. *Cell Stress* (2019) 3:319–327. doi: 10.15698/cst2019.10.201
38. Iversen TZ, Engell-Noerregaard L, Ellebaek E, Andersen R, Larsen SK, Bjoern J, et al. Long-lasting disease stabilization in the absence of toxicity in metastatic lung cancer patients vaccinated with an epitope derived from indoleamine 2,3 dioxygenase. *Clin Cancer Res* (2014) 20:221–32. doi: 10.1158/1078-0432.CCR-13-1560
39. Sørensen RB, Hadrup SR, Svane IM, Hjortsø MC, Straten PT. Andersen MH.Indoleamine 2,3-dioxygenase specific, cytotoxic T cells as immune regulators. *Blood* (2011) 117:2200–10. doi: 10.1182/blood-2010-06-288498
40. Andersen MH. The balance players of the adaptive immune system. *Cancer Res* (2018) 78:1379–1382. doi: 10.1158/0008-5472.CAN-17-3607
41. Danish Myeloma Study Group. *Danish Myeloma Database*. (2017). Available at www.myeloma.dk.
42. Gonsalves WI, Gertz MA, Dispenzieri A, Lacy MQ, Lin Y, Singh PP, et al. Implications of continued response after autologous stem cell transplantation for multiple myeloma. *Blood* (2013) 122:1746–49. doi: 10.1182/blood-2013-03-492678
43. Fernández De Larrea C, Dávila J, Isola I, Ocio EM, Rosinol L, García-Sanz R, et al. Absence of spontaneous response improvement beyond day +100 after autologous stem cell transplantation in multiple myeloma. *Bone Marrow Transplant* (2017) 52:567–9. doi: 10.1038/bmt.2016.299
44. Tran T, Blanc C, Granier C, Saldmann A, Tanchot C. Tartour E.Therapeutic cancer vaccine: building the future from lessons of the past. *Semin Immunopathol* (2018) 41:69–85. doi: 10.1007/s00281-018-0691-z
45. van der Burg SH. Correlates of immune and clinical activity of novel cancer vaccines. *Semin Immunol* (2018) 39:119–36. doi: 10.1016/j.smim.2018.04.001

Conflict of Interest: NJ: Research position is funded by The Danish Cancer Society; Copenhagen University Hospital, Herlev and Gentofte; and through a research funding agreement between IO Biotech ApS and National Center for Cancer Immune Therapy (CCIT-DK). MA: Author of a filed patent application based on the use of the PD-L1 peptide IO103 for vaccination. The patent rights have been transferred to Copenhagen University Hospital, Herlev, and Gentofte/The Capital Region of Denmark, in accordance with the Danish Law of Public Inventions at Public Research Institutions. Additionally, the author is a shareholder and board member of the company IO Biotech ApS, which has the purpose of developing commercial PD-L1 vaccines for cancer treatment. IS: Co-founder and shareholder in IOBiotech Aps.

The remaining authors declare that the research was conducted in the absence of any commercial or financial relationships that could be construed as a potential conflict of interest.

frontiers in Immunology

ORIGINAL RESEARCH
published: 12 November 2020
doi: 10.3389/fimmu.2020.584423

Tumor Infiltrating Effector Memory Antigen-Specific CD8$^+$ T Cells Predict Response to Immune Checkpoint Therapy

*Nicola Principe[1,2], Joel Kidman[1,2], Siting Goh[1], Caitlin M. Tilsed[1,2], Scott A. Fisher[1,2], Vanessa S. Fear[3], Catherine A. Forbes[3], Rachael M. Zemek[3], Abha Chopra[4], Mark Watson[4], Ian M. Dick[1,2], Louis Boon[5], Robert A. Holt[6], Richard A. Lake[1,2], Anna K. Nowak[1,7], Willem Joost Lesterhuis[1,2,3], Alison M. McDonnell[1,2,3] and Jonathan Chee[1,2]**

[1] National Centre for Asbestos Related Diseases, Institute for Respiratory Health, University of Western Australia, Nedlands, WA, Australia, [2] School of Biomedical Sciences, University of Western Australia, Crawley, WA, Australia, [3] Telethon Kids Institute, Perth, WA, Australia, [4] Institute of Immunology and Infectious Diseases, Murdoch University, Murdoch, WA, Australia, [5] Polpharma Biologics, Utrecht, Netherlands, [6] BC Cancer Agency, Vancouver, BC, Canada, [7] School of Medicine, University of Western Australia, Crawley, WA, Australia

Immune checkpoint therapy (ICT) results in durable responses in individuals with some cancers, but not all patients respond to treatment. ICT improves CD8$^+$ cytotoxic T lymphocyte (CTL) function, but changes in tumor antigen-specific CTLs post-ICT that correlate with successful responses have not been well characterized. Here, we studied murine tumor models with dichotomous responses to ICT. We tracked tumor antigen-specific CTL frequencies and phenotype before and after ICT in responding and non-responding animals. Tumor antigen-specific CTLs increased within tumor and draining lymph nodes after ICT, and exhibited an effector memory-like phenotype, expressing IL-7R (CD127), KLRG1, T-bet, and granzyme B. Responding tumors exhibited higher infiltration of effector memory tumor antigen-specific CTLs, but lower frequencies of regulatory T cells compared to non-responders. Tumor antigen-specific CTLs persisted in responding animals and formed memory responses against tumor antigens. Our results suggest that increased effector memory tumor antigen-specific CTLs, in the presence of reduced immunosuppression within tumors is part of a successful ICT response. Temporal and nuanced analysis of T cell subsets provides a potential new source of immune based biomarkers for response to ICT.

Keywords: immune checkpoint therapy, tumor-specific T cells, TCR repertoire, cytotoxic T lymphocytes, effector memory

OPEN ACCESS

Edited by:
Maysaloun Merhi, Hamad Medical Corporation, Qatar

Reviewed by:
Chunwan Lu, Augusta University, United States
Xiang-Yang Wang, Virginia Commonwealth University, United States

***Correspondence:**
Jonathan Chee
jonathan.chee@uwa.edu.au

Specialty section:
This article was submitted to Cancer Immunity and Immunotherapy, a section of the journal Frontiers in Immunology

Received: *17 July 2020*
Accepted: *15 October 2020*
Published: *12 November 2020*

Citation:
Principe N, Kidman J, Goh S, Tilsed CM, Fisher SA, Fear VS, Forbes CA, Zemek RM, Chopra A, Watson M, Dick IM, Boon L, Holt RA, Lake RA, Nowak AK, Lesterhuis WJ, McDonnell AM and Chee J (2020) Tumor Infiltrating Effector Memory Antigen-Specific CD8$^+$ T Cells Predict Response to Immune Checkpoint Therapy. Front. Immunol. 11:584423. doi: 10.3389/fimmu.2020.584423

INTRODUCTION

Cancer immunotherapies that block inhibitory checkpoint receptors on T cells, such as cytotoxic T-lymphocyte associated protein 4 (CTLA-4) and programmed death receptor 1 (PD-1), have resulted in remarkable, long-term tumor control in a subset of patients (1–3). However, the majority of ICT-treated patients do not benefit. ICT is very expensive and causes immune-related toxicities. Accordingly, there is an urgent need for sensitive and specific biomarkers of response. Current biomarkers include the expression of checkpoint inhibitory ligands such as PD-L1 (4), tumor mutation burden (5), gene expression profiles of the tumor microenvironment (6), and the extent of tumor infiltrating immune cells (7). Each biomarker has its own strengths and limitations, but there is currently no accurate predictor of responsiveness to ICT across multiple cancers. Developing novel, complementary biomarkers associated with successful response to ICT will guide clinical decisions and help understand the underlying immune mechanisms of a successful anti-tumor immune response (8).

Analysis of $CD8^+$ cytotoxic T lymphocytes (CTL) could offer a biomarker of response to ICT. Inhibitory checkpoint signaling that occurs through the PD-1/PD-L1 pathway suppresses activated CTLs within the tumor microenvironment, preventing tumor cell killing. ICT drives dynamic changes in CTL frequency (7, 9), phenotype (10–12), proliferation (13, 14), and cytotoxic function (6, 15). T cell receptor (TCR) sequencing studies further suggest that ICT causes clonal proliferation of CTLs within the tumor (7, 16, 17) and the periphery (16, 18, 19). As antigen-specificity is crucial for a successful anti-tumor response, we reasoned that dynamic changes in tumor antigen-specific CTLs could inform ICT responses. Indeed, ICT can increase tumor antigen-specific CTLs (20, 21), but there are limited studies on how ICT-driven phenotypic changes in tumor antigen-specific CTLs correlate with ICT outcomes.

The ability to study how tumor antigen-specific CTLs contribute to ICT outcomes in clinical studies is limited because of variability in host genetics (which includes TCR repertoire), clinical history, tumor mutations, and antigen expression. Furthermore, serial tumor biopsies are often not feasible, making it difficult to assess dynamic changes within the tumor microenvironment. Murine models are useful in this context because variation can be controlled. We used a model in which inbred mice bearing tumors derived from monoclonal cancer cell lines respond dichotomously to anti-CTLA-4 and anti-PD-L1 ICT, with some mice experiencing complete tumor regression within days, and the others not responding to therapy (22). We previously defined a pre-treatment ICT responsive gene signature in the tumor microenvironment using this model (23). In the present study, we characterized CTLs specific for a model tumor antigen using this established model, correlating dynamic changes in T cell frequencies, phenotype, and clonality to ICT outcomes. We identified effector memory CTL phenotypes that can be further tested as immune biomarkers of ICT response.

MATERIALS AND METHODS

Mice

BALB/c.Arc and BALB/c.AusBP mice were bred and maintained at the Animal Resource Centre (ARC; Murdoch, WA, Australia) or Harry Perkins Institute of Medical Research (Nedlands, WA, Australia). Clone 4 (CL4xThy1.1) TCR transgenic mice express a TCR that recognizes a MHC class I-restricted influenza A/PR/8 hemagglutinin ($HA_{533-541}$) epitope (24). As >97% of $CD8^+Thy1.1^+$ T cells expressed the transgenic TCR, Thy1.1 was used as a surrogate marker to track HA-specific $CD8^+$ T cells. CL4xThy1.1 mice were kindly provided by Prof Linda Sherman (The Scripps Research Institute, La Jolla, CA) and bred at the Animal Resource Centre (ARC). All mice used in these studies were between 8 and 10 weeks of age and were maintained under standard specific pathogen free housing conditions at the Harry Perkins Bioresources Facility (Nedlands, WA, Australia). All animal experiments were carried out in accordance with the Harry Perkins Institute of Medical Research Animal Ethics guidelines and protocols (AE140).

Transfer of TCR Transgenic Splenocytes

Spleens from CL4xThy1.1 mice were manually dissociated through 40 μm strainers with phosphate-buffered saline (PBS) supplemented with 2% Newborn Calf Serum (NCS; Life Technologies). Red blood cells were lysed with Pharm Lyse (BD Biosciences) and splenocytes were washed twice with PBS. Mice were intravenously injected with 1 x 10^6 splenocytes suspended in 100 μl of PBS 24 h prior to tumor inoculation.

Cell Lines

The murine malignant mesothelioma cell line AB1 (25) was transfected with influenza hemagglutinin (HA) from the Mt Sinai strain of PR8/24/H1N1 influenza virus to generate the AB1-HA cell line (26) (CBA, Cat# CBA-1374, RRID: CVCL_G361). AB1 and renal cell carcinoma (RENCA) cell lines were used for re-challenge and ex-vivo co-culture experiments. RENCA was obtained from ATCC (ATCC, Cat# CRL-2947, RRID: CVCL_2174) and AB1 was obtained from Cell Bank Australia (CBA, Cat# CBA-0144, RRID: CVCL_4403). Cell lines were maintained in R10; RPMI 1640 (Invitrogen) supplemented with 20 mM HEPES (Gibco), 0.05 mM 2-mercaptoethanol (Sigma Aldrich), 100 units/ml benzylpenicillin (CSL), 50 μg/ml gentamicin (David Bull Labs), 10% NCS (Life Technologies) and 50 mg/ml of geneticin for AB1-HA only (G418; Life Technologies). Cells were grown to 80% confluence before passage and passaged three to five times before inoculation.

Tumor Cell Inoculation

Cells were harvested when they reached 80% confluence. Mice were inoculated subcutaneously (s.c.) into the shaved, right-hand flank (for single inoculations) or both left- and right-hand flanks (for dual-tumor inoculations) with 5 x 10^5 tumor cells suspended in 100 μl of PBS using one 26-gauge needle per injection (22). Length and width tumor measurements were monitored using calipers to calculate tumor area (mm^2).

Immune Checkpoint Therapy

Immune checkpoint antibodies anti-CTLA4 (clone 9H10) and anti-PD-L1 (clone MIH5) were prepared and purified by Polpharma Biologics (Urecht, Netherlands) as previously described (23). Mice received an intraperitoneal injection (i.p.) of 100 μg of anti-CTLA4 and 100 μg of anti-PD-L1. 100 μg of anti-PD-L1 was subsequently administered 2 and 4 days after the initial dose, as previously optimized (22). Control mice received PBS at the equivalent volume, as previous work found no difference between control immunoglobulin G and PBS (27). Mice were randomized before treatment. The first dose of ICT was administered 7 to 10 days after tumor inoculation, when tumors were between 9 and 20 mm^2 in size. Mice were defined as responders when their tumor completely regressed and remained tumor-free for at least 4 weeks after treatment. Mice were designated as non-responders if their tumors grew to 100 mm^2 within 4 weeks after the start of therapy, similar to PBS controls. Mice that had a delay in tumor growth or partial regression were designated as intermediate responders and excluded from the analysis. We only used experiments in which mice displayed a dichotomous response, where there had to be at least one non-responder and one responder in each cage (22, 23).

Surgical Excision of Lymph Nodes and Complete Tumor Debulking

Complete tumor debulking and lymphadenectomy of the right-hand flank was performed either on the day of treatment (prior to ICT administration; day 0) or 7 days post-therapy (day 7), as previously described (22). Briefly, mice were dosed with 0.1 mg/kg of buprenorphine in 100 μl, 30 min before anaesthesia with isoflurane (4% in 100% oxygen at a flow rate of 2 liters/min). Whole tumors and draining inguinal lymph nodes (DLN) were surgically excised. Surgical wounds were closed using Reflex wound clips (CellPoint Scientific). Mice received subsequent doses of 0.1 mg/kg of buprenorphine in 100 μl 6 and 24 h after surgery for pain relief.

Preparation of Single Cell Suspensions

DLNs were manually dissociated through 40 μm strainers with PBS + 2% NCS. Tumors were dissected into smaller pieces with a scalpel blade and subjected to digestion with 1.5 mg/ml type IV collagenase (Worthington Biochemical) and 0.1 mg/ml type I DNAse (Sigma Aldrich) in PBS + 2% NCS for 45 min at 37°C on a Microtitre Plate Shaker Incubator (Thomas Scientific) (28). Tumors were washed twice in PBS + 2% NCS following digestion. Cell counts were performed using a hemocytometer with trypan blue exclusion.

T Cell: Tumor Co-Culture

Spleens from ICT responders were harvested 14 days post re-challenge with cell line AB1-HA. Splenocytes were seeded at a density of 1 x 10^6 cells/well in a 96-well plate and stimulated with cell lines; AB1-HA, AB1 or RENCA, or the HA peptide at a 10:1 effector:target ratio for 20 h at 37°C. Brefeldin A (Biolegend) was added into each well for the last 4 h of the culture. Cells were washed twice with PBS + 2% NCS before antibody staining.

Flow Cytometry

Four flow cytometry panels outlined in **Table S1** were performed. Samples were stained with Fixable Viability Dye (FVD) eFluor™ 506 (eBioscience) or Zombie UV™ (BioLegend) to exclude dead cells. Cells were incubated with Zombie UV™ suspended in PBS in the dark for 30 min at room temperature (RT) prior to staining with surface antibodies. Antibodies for surface staining (including FVD eFluor™ 506) were suspended in PBS + 2% NCS and incubated on cells for 30 min at 4°C. PBS + 2% NCS was used to wash cells between incubations. Samples were then fixed and permeabilised for 10 min at 4°C using the Foxp3/Transcription Factor Staining Buffer Set (eBioscience). Cells were washed with Permeabilization Buffer (eBioscience), subjected to intracellular staining and left overnight at 4°C. Single stain and fluorescence minus-one (FMO) controls were also used. Data were acquired using a BD LSRFortessa™ SORP or BD FACSCanto II™ (BD Biosciences) with 50,000 live events collected per sample where possible. All flow cytometry analyses were completed using FlowJo™ Software version 10 (BD Biosciences). Summary of antibodies concentrations and gating strategies is outlined (**Table S1**, **Figure S8**).

Fluorescence Activated Cell Sorting

Tumors were stained for fluorescence activated sorting using the BD FACSMelody™ cell sorter (BD Biosciences). All samples were stained with antibodies outlined in **Table S1** for 30 min at 4°C to sort for $CD8^+$ T cells for TCRβ sequencing or $CD8^+Thy1.1^+$ T cells for RNA sequencing. Sorted cells were collected in 500 μl of RNAprotect cell reagent (QIAGEN) and stored at −20°C. Sorts were run on greater than 85% efficiency. Sorting gates are described in **Figure S9**.

Bulk TCRβ Sequencing

TCRβ libraries were made using a 5'Rapid Amplification of cDNA Ends (5'RACE) technology optimised from R. Holt and colleagues (29). RNA was extracted from cell sorted samples using the RNeasy Plus Micro Kit (QIAGEN). Total RNA was transcribed to cDNA using a TCRβ constant region primer (Integrated DNA Technologies) and a modified SMARTerIIA primer (Integrated DNA Technologies), adding unique molecular identifiers (UMI) to individual TCRβ cDNA sequences for unbiased PCR amplification. The TCRβ locus was amplified by nested PCR with another TCRβ constant region primer (Integrated DNA Technologies), and a universal primer to SMARTerIIA, with the final PCR adding sequencing adaptors and barcodes to the TCRβ libraries. PCR products were purified using AMPure XP AgenCourt Beads (Beckman Coulter).

Paired-end (2 × 300 bp) high-throughput sequencing was performed using the Illumina MiSeq platform (Illumina, RRID: SCR_016379). Data processing, aggregation of UMIs and alignment of CDR3 sequences to the IMGT/V-QUEST reference genome (30) were performed using repertoire analysis software based on MIGEC (31) (RRID:SCR_016337) and MiXCR (32) (RRID:SCR_018725) pipelines. Only sequences with UMIs were aligned. In-house analysis tools used were

provided by AC and MW (Institute for Immunology and Infectious Diseases, Murdoch, Australia).

TCRβ Repertoire Analysis

TCRβ libraries were analyzed using functions in R (R Project for Statistical Computing, RRID: SCR_001905, v3.6.0). A TCRβ clone was defined by the CDR3 amino acid sequence. Clones that were less than 8 or greater than 20 amino acids in length, included a stop codon or a frameshift were defined as non-functional and were excluded from analysis. To measure TCRβ repertoire diversity, Renyi entropy was used given by $H_\alpha(X) = \frac{1}{1-\alpha}\log(\Sigma_{i=1}^{n} p_i^{\alpha})$ where α is a scale of values, ranging from 0 to infinity. The closer α gets to infinity, the more weight is given to more abundant TCRs. α = 0 corresponds to 'richness', the number of unique TCRβ sequences (TCRβ clones). α = 1 corresponds to Shannon's entropy. α = 2 corresponds to Simpson's diversity (33). Shannon's entropy was also calculated by; $H = 1 - \frac{(-\Sigma_{i=1}^{N} p_i ln p_i)}{n}$ where p_i is the proportion of sequence *i* relative to the total *N* sequences (34). This index ranges from 0 to 1; 0 being an entirely monoclonal sample, and 1 meaning each unique TCRβ clone only occurs once. Networks of the most abundant TCRβ clones were constructed using the *ggraph* extension (v2.0.2) of *ggplot2* package in R (RRID: SCR_014601, v3.2.1). Each node in the network represents a unique CDR3 TCRβ sequence. Each edge is defined as a single amino acid difference (levenshtein distance of 1) between the CDR3 TCRβ sequences (35). TCRβ CDR3 sequence for the CL4 clone (CASGETGTNERLFF) was determined by bulk TCRβ sequencing of sorted $CD8^+$ splenocytes from CL4xThy1.1 mice.

Bulk RNA Sequencing

RNA was extracted from $CD8^+Thy1.1^+$ cell sorted samples using the RNeasy Plus Micro Kit (QIAGEN). RNA quality was confirmed on the Bioanalyzer (Agilent Technologies). Library preparation and sequencing on the Novaseq 550 (75 base pair, paired-end, Illumina), quality assessment using FastQC and alignment to the GRCm38/mm10 mouse reference genome were performed by the Institute for Immunology and Infectious Diseases (Murdoch, Australia). The Broad Institute Inc. Gene Set Enrichment Analysis (GSEA) Software (RRID: SCR_003199, v4.0.2) was used to analyze 50 MSigDB hallmark gene sets on normalized gene expression data (36). Gene sets enriched at a nominal $P < 0.05$ and FDR < 0.25 were considered significant.

Statistical Analysis

Data are presented as mean ± SD. Mann-Whitney *U* tests were used for comparisons between the means of two variables. Ordinary Two-way ANOVA with Sidak's multi-comparisons was used to compare the interaction between two variables. Correlation was analyzed using Pearson correlation tests. Kaplan-Meier method was used for survival analysis with log-rank test (Mantel-Cox) to analyze significance. All statistics was performed using GraphPad Prism Software (Graph Pad Software Inc., RRD:SCR_002798, v8). Results were significant when $p < 0.05$ (*$p < 0.05$, **$p < 0.01$, ***$p < 0.001$, ****$p < 0.0001$).

RESULTS

The Frequency of Tumor Antigen-Specific $CD8^+$ TILs Is Highly Variable Irrespective of Response Phenotype

To track how ICT changes the frequency and phenotype of tumor antigen-specific $CD8^+$ T cells, we transferred T cells specific for a MHC-I restricted $HA_{533-541}$ antigen from CL4xThy1.1 mice (24) into BALB/c recipient mice prior to inoculation of a HA expressing tumor cell line (26). Mice were treated with anti-CTLA-4 and anti-PD-L1, and HA-specific ($CD8^+Thy1.1^+$) T cells in tumors (Tum) and draining lymph nodes (DLN) post therapy were analyzed (**Figures 1A, B**).

Overall, there was no significant difference in frequency of $CD8^+Thy1.1^+$ and $CD8^+Thy1.1^-$ T cells between ICT treated and control groups. However, $CD8^+Thy1.1^+$ T cells tended to increase in the tumors of ICT treated mice (**Figures 1C, D**). Recipient and donor $CD8^+$ T cells in DLNs expressed minimal granzyme B (GrB), regardless of treatment (**Figure 1E**). The number of $CD8^+Thy1.1^+GrB^+$ TILs were significantly higher in the ICT treated group ($P = 0.013$), but this difference was not found in endogenous $CD8^+$ T cell populations, suggesting that our ICT regime increased the cytotoxic function of HA-specific CTLs.

Interestingly, the number of HA-specific CTLs varied between ICT treated animals, making up greater than 20% of $CD8^+$ TIL populations in some tumors, and less than 5% in others. This suggests that although all tumors expressed HA (26), the frequencies of HA-specific CTLs did not increase in all animals after ICT.

A Unique Murine Bilateral Tumor Model to Track Tumor Antigen-Specific CTLs in ICT Outcomes

To have more certainty on the presence or absence of a correlation between the frequency of HA-specific CTLs and outcome to ICT, we utilized our established bilateral tumor model where inbred, age-matched mice harboring monoclonal tumors display dichotomous responses to ICT (22) (**Figure 2A**). Importantly, the addition of CL4xThy1.1 splenocytes did not alter ICT response rate or symmetry in the bilateral model (**Figures 2B**, **S1**). Symmetry in tumor growth and regression upon ICT allowed us to surgically remove one tumor and its corresponding DLN to track HA-specific CTLs, while tracking how this tumor would have responded to ICT, by monitoring the contralateral tumor.

Tumors and their corresponding DLNs were resected for analysis either prior to ICT administration (day 0) or 7 days after (day 7; **Figure 2A**). At day 0, excised tumors were indistinguishable by size, total cell count, and proportions of $CD45^+$ cells regardless of subsequent response outcomes (**Figure S2A**). At day 7, non-responding tumors were greater in size than responding tumors ($P = 0.003$), however total cell counts and proportions of $CD45^+$ cells were similar between groups (**Figure S2A**). Dichotomous responses to ICT were observed, with tumors reaching 100 mm^2 in non-responders (NR; red), or

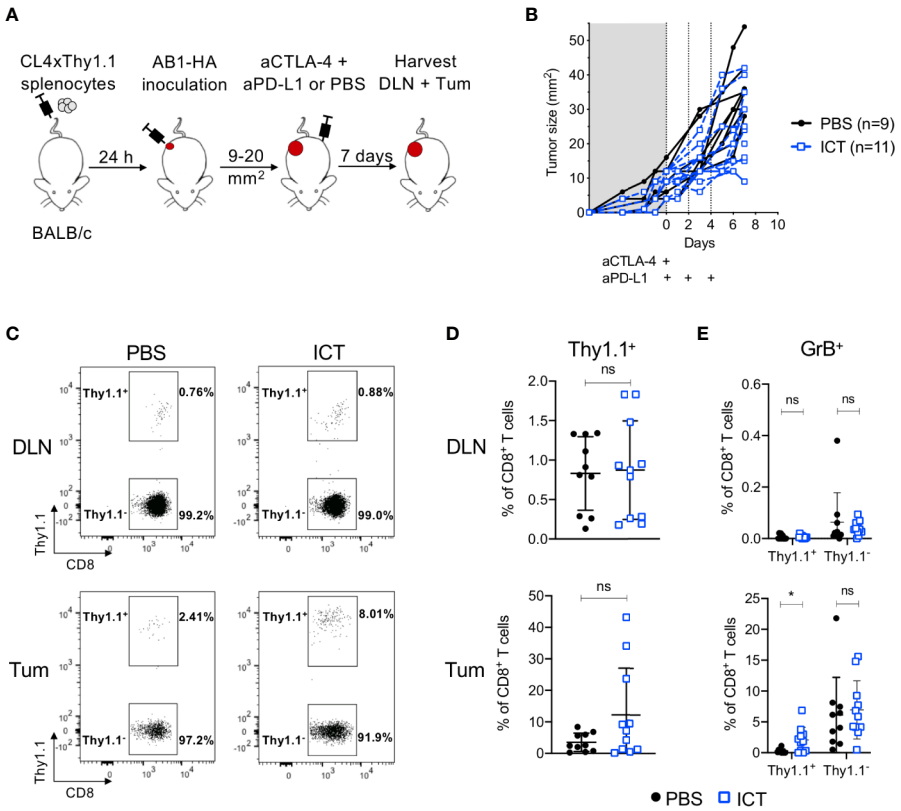

FIGURE 1 | ICT increases tumor infiltrating cytotoxic tumor antigen-specific CD8$^+$ T cells. **(A)** Experimental timeline. CL4xThy1.1 splenocytes were adoptively transferred into BALB/c mice one day prior to AB1-HA tumor inoculation. Mice were treated with ICT (aCTLA-4 and aPD-L1) or PBS when tumors reached 9 to 20 mm^2 in size. Tumors (Tum) and corresponding draining lymph nodes (DLN) were harvested 7 days post-treatment. **(B)** Tumor growth curves of mice treated with PBS (black) or ICT (blue). Each line represents an individual animal. Dotted lines indicate days of treatment. **(C)** Representative FACS plots, and **(D)** dot plots representing frequencies of CD8$^+$Thy1.1$^+$ (HA-specific) T cells in DLN and Tum of both treatment groups. **(E)** Frequency of granzyme B (GrB) expressing CD8$^+$Thy1.1$^+$ or Thy1.1$^-$ T cells. Data in dot plots represented as mean ± SD. Mann-Whitney *U* tests were used to compare groups; *P ≤ 0.05. Data represents two independent experiments.

completely regressing to 0 mm^2 in responders (R; blue) by 20 days post-treatment (**Figure 2C**).

ICT Responders Have More Tumor Antigen-Specific CTLs in Tumors and Draining Lymph Nodes, and Reduced Intra-Tumoral T_{regs} Compared to Non-Responders

In responding mice, the number of CD8$^+$ TILs were significantly higher after treatment (**Figure 2D**). In contrast, non-responding animals had a similar amount of CD8$^+$ TILs pre- and post-treatment (**Figure 2D**; R vs NR; DLN: P > 0.05; Tum: P = 0.0011). The number of HA-specific CD8$^+$Thy1.1$^+$ T cells in DLNs and tumors were significantly higher after treatment in responding, but not in non-responding mice (**Figure 2D**; R vs NR; DLN: P = 0.02; Tum: P = 0.004). Endogenous CD8$^+$Thy1.1$^-$ T cells significantly decreased after treatment in DLNs, but remained similar in tumors in both responders and non-responders (**Figure 2D**).

The number of total CD4$^+$ T cells, T_{regs} (CD4$^+$Foxp3$^+$) and helper T cells (CD4$^+$Foxp3$^-$) in the DLN increased after treatment in both responding and non-responding animals (**Figure 2E**). Intra-tumoral CD4$^+$ T cell frequencies decreased post-ICT in responders, which was largely attributed to a reduction in T_{regs}. This reduction was not observed in non-responders (**Figure 2E**, R vs NR; DLN: P > 0.05; Tum: P = 0.002). Intra-tumoral CD4$^+$Foxp3$^+$ frequencies inversely correlated to the proportion of CD8$^+$Thy1.1$^+$ T cells after treatment (**Figure S3**; r = −0.393; P = 0.03). Taken together, our data suggests that a post-treatment increase in HA-specific CD8$^+$ T cells in DLN and tumors, accompanied by a reduction in intra-tumoral T_{regs} is associated with ICT response.

Responding Tumors Have a More Clonal TCRβ Repertoire Compared to Non-Responders, but Each Animal Uses a Private CD8$^+$ TIL Repertoire

As responding animals had increased frequencies of CTLs specific against one tumor antigen, we next examined if there was oligoclonal expansion of other CTL specificities in the endogenuous population. To characterize TCR repertoires of

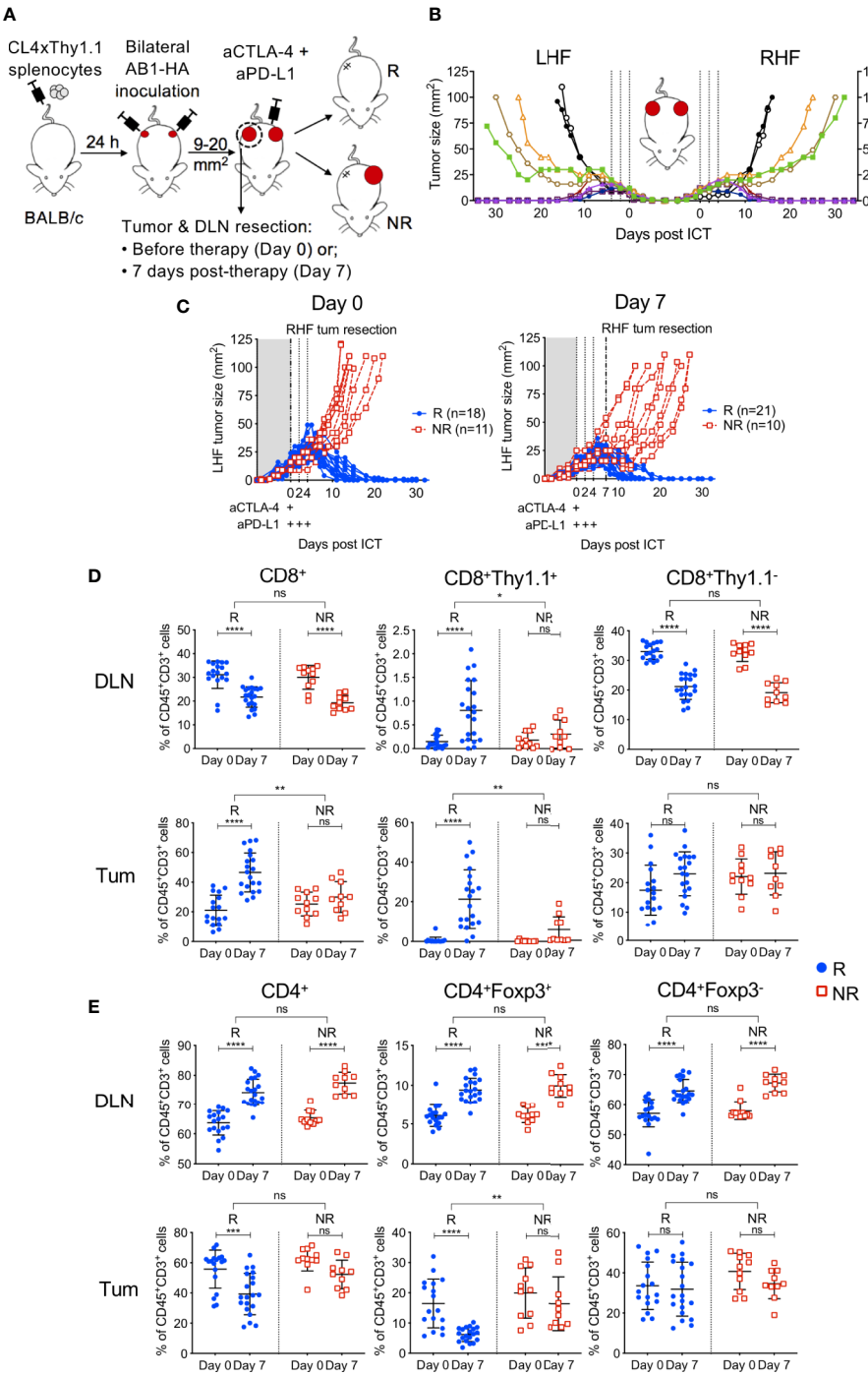

FIGURE 2 | Tumor antigen-specific CD8$^+$ T cells increase in ICT responding DLN and tumors. **(A)** Experimental timeline. CL4xThy1.1 splenocytes were adoptively transferred into BALB/c mice one day prior to bilateral AB1-HA tumor inoculation. Right-hand flank (RHF) tumor (Tum) and draining lymph node (DLN) were surgically resected either pre- (day 0) or post-ICT (day 7). Left-hand flank (LHF) tumor was followed for ICT response. **(B)** Growth curves representing symmetrical growth and regression of bilateral AB1-HA tumors treated with ICT (n = 8; color-coded per mouse) or PBS (n = 2; black), without surgery. Dotted lines indicate days of treatment. **(C)** Growth curves of LHF tumors for mice that had their RHF tumors and DLNs resected at day 0 (left) or day 7 (right). Mice were characterized as responders (R; blue) or non-responders (NR; red). Dotted lines indicate days of treatment. Pre (Day 0) and post (day 7) treatment frequencies of total CD8$^+$, CD8$^+$Thy1.1$^+$ and CD8$^+$Thy1.1$^-$ **(D);** total CD4$^+$, CD4$^+$Foxp3$^+$ and CD4$^+$Foxp3$^-$ T cells **(E)** in resected DLNs (top) and tumors (bottom) of responding and non-responders. Data represented as mean ± SD, summary of five independent experiments. Two-way ANOVAs were used to compare the magnitude of difference between responders and non-responders, with Tukey's multiple-comparisons to compare pre- and post-treatment frequencies within each group; *P ≤ 0.05, **P ≤ 0.01, ***P ≤ 0.001, ****P ≤ 0.0001.

post-treatment CD8$^+$ TILs, we performed bulk TCRβ sequencing on sorted CD8$^+$ TIL populations. The total number of sorted cells significantly correlated with the total number of TCRβ sequences returned (**Figure S4A**; r = 0.89, P < 0.0001), and the total number of sorted cells, unique and total TCRβ sequences were similar between responders and non-responders (**Figure S4B**). The frequency of HA-specific CD8$^+$ T cells identified by flow cytometry also significantly correlated with the number of CL4 TCRβ CDR3 sequences (CASGETGTNERLFF) in matched samples (**Figure 3A**; r = 0.87, P < 0.0001), highlighting that the most abundant TCR clones were being captured by our TCRseq assay.

Consistent with our previous experiments, the proportion of post-treatment CL4 TCRβ sequences was significantly greater in responders (80.5 ± 16.1%) than non-responders (26.9 ± 35.5%) (**Figure 3B**; P = 0.03). We estimated the diversity of TCRβ repertoires by their Renyi entropies (**Figure 3C**), and found that responders had significantly less diverse TCRβ repertoires than non-responders (**Figure S4C, D**; P = 0.019), suggesting that expansion of the CL4 clone correlated with response. The CL4 clone was the most frequent TCRβ clone for all responding animals (47.9–92.3%) and the majority of non-responding animals (11.6–87.9%). The subsequent most abundant TCR clonotypes (2nd to 10th) varied between animals, making up

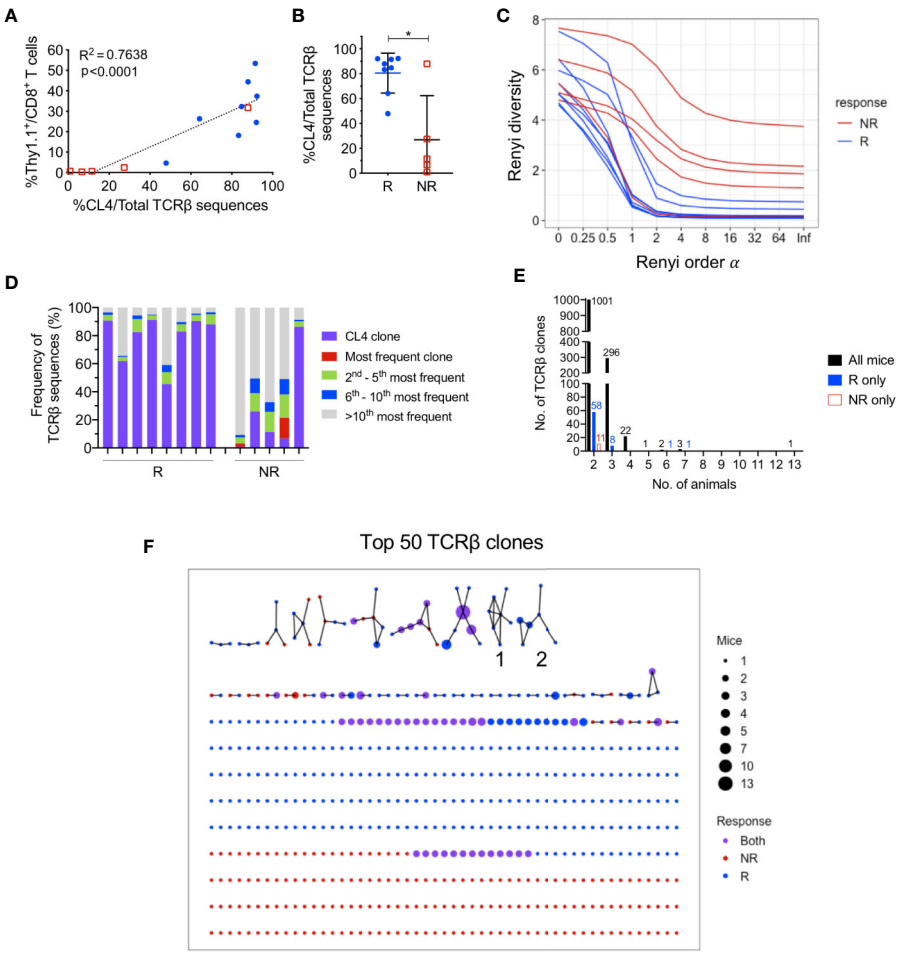

FIGURE 3 | CL4 transgenic TCRβ clone dominated post-treatment CD8$^+$ TIL TCRβ repertoire in responding animals. **(A)** Linear regression analysis between the CL4 TCRβ clone frequency in TCRβ sequencing and the frequency of CD8$^+$Thy1.1$^+$ T cells analyzed in flow cytometry. **(B)** Dot plot representing the CL4 TCRβ clone frequencies in responders (R; blue) and non-responders (NR; red). **(C)** Graph of Renyi diversity profiles for each TCRβ repertoire. The scale of Renyi order α corresponds to calculated diversity metrics. α = 0 indicates the richness of the repertoire (number of unique TCRβ clones). Shannon's diversity index corresponds to α = 1. Each line represents the Renyi entropy of one animal, and a steeper gradient between α = 0 and 1 represents a less diverse repertoire. **(D)** Bar graph displaying proportions of the 10 most frequent TCRβ clones in responders and non-responders. Each bar represents the TCRβ repertoire of one animal. CL4 clone (purple) is the most frequent clone in 11/13 animals. **(E)** Bar graphs representing the number of shared TCRβ clones between 2 or more animals. Shared clones are separated into overlap within only responders (blue), only non-responders (red), or all mice regardless of outcome (black). **(F)** Network analysis of the top 50 most abundant TCRβ clones for each animal. Each node represents a unique CDR3 TCRβ sequence (TCRβ clone) and each edge defines a single amino acid difference (levenshtein distance of 1). Size of each node represents the number of mice that have the TCRβ clone in their repertoire and nodes are colored by presence of TCRβ clone in only responders (blue), only non-responders (red) or both groups (purple). Data is shown as mean ± SD where appropriate; R (n = 8) and NR (n = 5) were sampled from three independent experiments; Mann-Whitney *U* tests; *P ≤ 0.05.

3.72% to 27.6% of each repertoire (**Figure 3D**), suggesting that expansion within responding tumors was mostly monoclonal.

As all mice harbored a tumor that expressed a common antigen (HA), we examined the overlap between tumor-infiltrating $CD8^+$ TCRβ clones between animals. Excluding the transferred CL4 clone, there was minimal sharing of TCRβ clones between all animals, regardless of response. The majority of overlapping clones were shared between two and three animals (**Figure 3E**). We next represented the top 50 most abundant TCRβ clones from each animal in a network based on their TCRβ CDR3 amino acid sequence similarities. 57 out of 560 TCRβ clones formed networks, but the majority of TCRβ clones were not related to any other clone, failing to form any networks (**Figure 3F**). Most TCRβ CDR3 sequences were randomly distributed throughout the networks regardless of response, with the exception of two groups of highly similar TCRβ CDR3 sequences that were exclusively found in responding tumors (Group 1, 2, **Figure 3F**). However, each clone from these groups was present in only one to three responding mice and comprised less than 0.6% of the TCRβ repertoire.

These data suggest that apart from the clone we introduced, each animal had a private and highly diverse tumor-infiltrating $CD8^+$ TCRβ repertoire. Importantly, responders had a less diverse $CD8^+$ TCR repertoire compared to non-responders, but this was largely attributed to the expansion of HA-specificity in this model.

ICT Responders Have Increased Post-Treatment Tumor Antigen-Specific Effector Memory CTLs Compared to Non-Responders

We next investigated $CD8^+$ T cell phenotype in ICT responders and non-responders. Endogenous ($Thy1.1^-$) and transferred ($Thy1.1^+$) $CD8^+$ T cells were analyzed for expression of differentiation and memory-associated markers. We focused on post-treatment (day 7) because pre-treatment DLN and tumors contained <1% of $CD8^+Thy1.1^+$ T cells (**Figure 2D**), making it difficult to accurately analyze their phenotype.

Post-treatment $CD8^+Thy1.1^+$ T cells were activated ($CD44^{hi}CD62L^{lo}$) and upregulated memory and differentiation markers IL-7Rα (CD127), killer cell lectin-like receptor subfamily G1 (KLRG1) and transcription factor T-box (T-bet), suggesting that the HA-specific CTLs acquired an effector memory (T_{EM}) like phenotype (**Figures 4A, B**, **Figures S5A–C**). More than 92% of $CD8^+Thy1.1^+$ T cells displayed a naive phenotype ($CD44^{lo}CD62L^{hi}CD127^{lo}KLRG1^{lo}$) prior to transfer, indicating that upregulation of these markers occurred *in vivo* within the tumor-bearing animal (**Figure S5D**). Importantly, ICT responders displayed increased frequencies of $CD44^{hi}CD62L^{lo}CD127^{hi}KLRG1^{hi}$ T_{EM} $CD8^+Thy1.1^+$ T cells compared to non-responders in both DLNs (**Figure 4C**; P = 0.0002) and tumors (**Figure 4D**; P < 0.0001). Endogenous $CD8^+Thy1.1^-$ T cells retained a naïve phenotype ($CD44^{lo}CD62L^{hi}$) in DLNs and an effector phenotype (T_{EFF}; $CD44^{hi}CD62L^{lo}CD127^{lo}KLRG1^{lo}$) in tumors (**Figures 4A, B**). Endogenous $CD8^+Thy1.1^-$ T cells were similar between responding and non-responding tumors and DLNs (**Figures 4C, D**), suggesting that differences in T_{EM} frequencies were mostly found in the HA-specific CTLs.

A small proportion of non-responding mice exhibited tumor infiltration of $CD8^+Thy1.1^+$ T cells (>10%). To determine whether HA-specific CTLs acquired a T_{EM} surface phenotype in these non-responding animals, we examined the expression profiles of CD127 and KLRG1 based on their median fluorescence intensity (MFI). Responders had a significantly higher CD127 MFI compared to non-responders in tumors, but not DLNs (**Figures 4E, F**; DLN: P = 0.05; Tum: P = 0.02). KLRG1 MFI was similar between responders and non-responders for both compartments (**Figures 4E, F**; DLN: P = 0.77; Tum: P = 0.08).

We questioned whether CTL function, as measured by the release of cytotoxic effector molecules and the expression of proliferation and activation markers, was associated with response to ICT. Although $CD8^+Thy1.1^+$ T cells had increased expression of Granzyme B, Ki67 and PD-1 compared to their endogenous $CD8^+Thy1.1^-$ counterparts, the frequencies for both endogenous and HA-specific $CD8^+$ T cells that expressed these markers were similar between responders and non-responders (**Figure S6**). Bulk RNAseq of $CD8^+Thy1.1^+$ TILs supported this, as we found minimal differences in immune-related gene sets between responders and non-responders, with the exception of genes associated with WNT/β-catenin signaling being upregulated in non-responders (**Figure S7**).

Together, these data suggest that HA-specific CTLs display an activated phenotype after ICT, and that animals with increased frequencies of T_{EM} HA-specific CTLs are more likely to respond to ICT. Although non-responding animals had significantly lower frequencies of tumor infiltrating HA-specific CTLs, they still exhibited a memory-like phenotype and retained cytotoxic function.

ICT Responders Maintain a Tumor-Specific Memory T Cell Response

To determine if ICT responders formed a memory T cell response against a broad range of tumor antigens, we re-challenged responding animals with AB1-HA or the parental AB1 tumor cell lines 30 days after the original tumor completely regressed. All ICT responders were protected from re-challenge of either tumor cell line (**Figure 5A**). $CD8^+Thy1.1^+$ T cells were detected in the spleen of these re-challenged animals, indicating that they persisted after tumors regressed (**Figure 5B**). $CD8^+$ T cells from splenocytes of ICT responders produced IFNγ and upregulated CD137 when co-cultured with AB1-HA tumor cells (P = 0.002) and HA peptide (P = 0.007), but minimally with AB1 or MHC-I matched control (RENCA) tumor cells (**Figures 5C–E**). These results suggest that ICT responders successfully formed a long-lasting memory $CD8^+$ T cell response against AB1-HA tumors.

DISCUSSION

Here, we studied tumor antigen (HA)-specific CTLs in ICT responders and non-responders using an established murine

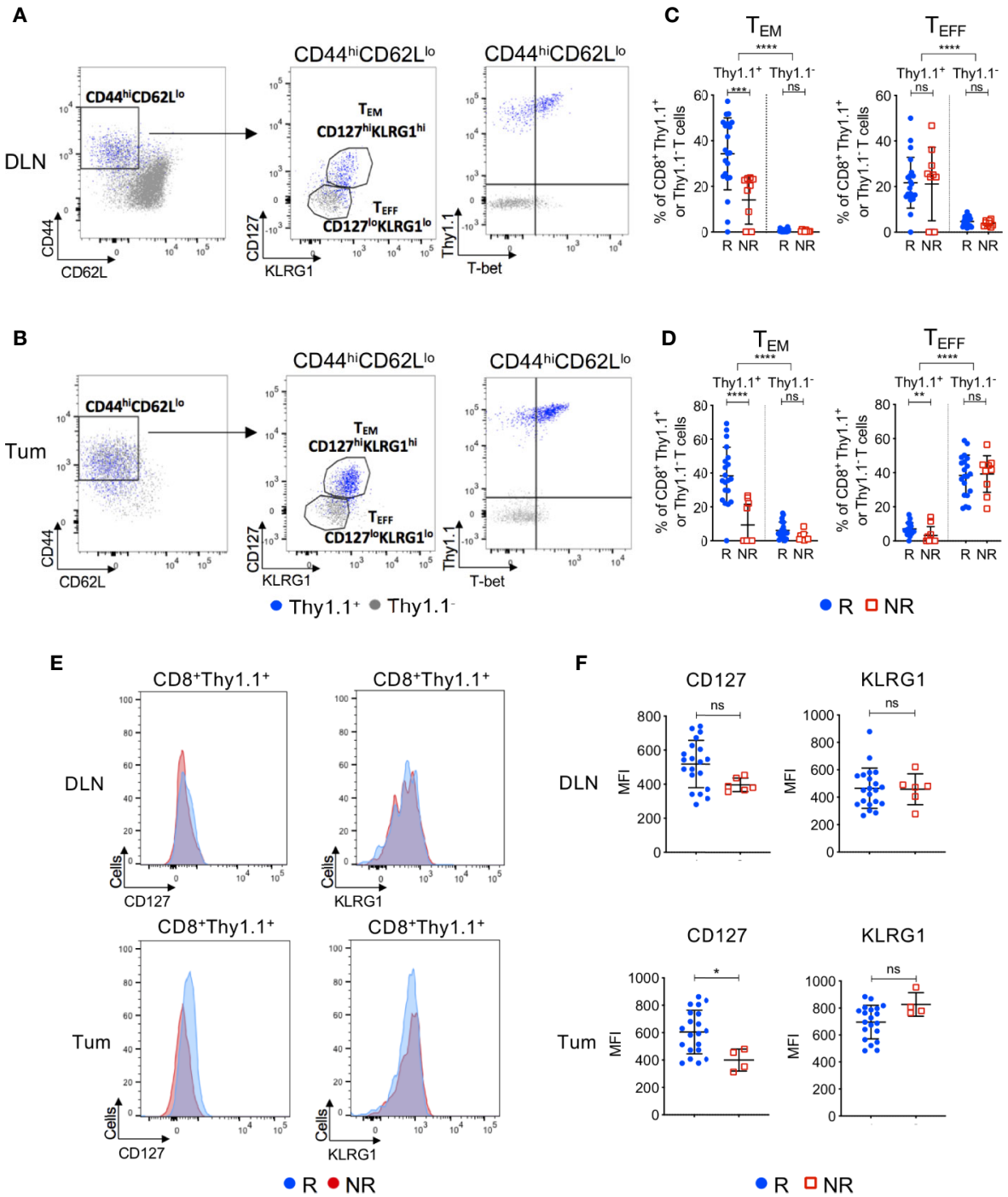

FIGURE 4 | Tumor infiltrating tumor antigen-specific CD8$^+$ T cells acquire an effector memory phenotype in ICT responding animals. Representative FACs plots comparing CD8$^+$Thy1.1$^+$ (blue) and CD8$^+$Thy1.1$^-$ (gray) T cell phenotype in post-treatment **(A)** DLNs and **(B)** tumors. Cells were analyzed for CD44, CD62L, CD127, KLRG1 and T-bet expression. Gates on the FACS plot represent effector memory (T_{EM}; CD44^{hi}CD62L^{lo}CD127^{hi}KLRG1^{hi}) and effector (T_{EFF}; CD44^{hi}CD62L^{lo}CD127^{lo}KLRG1^{lo}) T cell subsets. Graphs representing frequencies of tumor antigen-specific (CD8$^+$Thy1.1$^+$) and endogenous (CD8$^+$Thy1.1$^-$) T cells that exhibit T_{EM} or T_{EFF} phenotypes in **(C)** DLNs and **(D)** tumors, grouped by response/non-response to ICT. **(E)** Representative histograms comparing CD127 and KLRG1 expression on activated (CD44^{hi}CD62L^{lo}) CD8$^+$Thy1.1$^+$ T cells between responding and non-responding DLNs (top) and tumors (bottom). **(F)** Median fluorescence intensity (MFI) expression of CD127 and KLRG1 on CD8$^+$Thy1.1$^+$ T cells in DLNs (top) and tumors (bottom) represented as dot plots. Data shown as mean ± SD. Mann-Whitney *U* tests were used to compare between both responders and non-responders, and between Thy1.1$^+$ and Thy1.1$^-$ T cells for each T cell phenotype; *P ≤ 0.05, **P ≤ 0.01, ***P ≤ 0.001, ****P ≤ 0.0001.

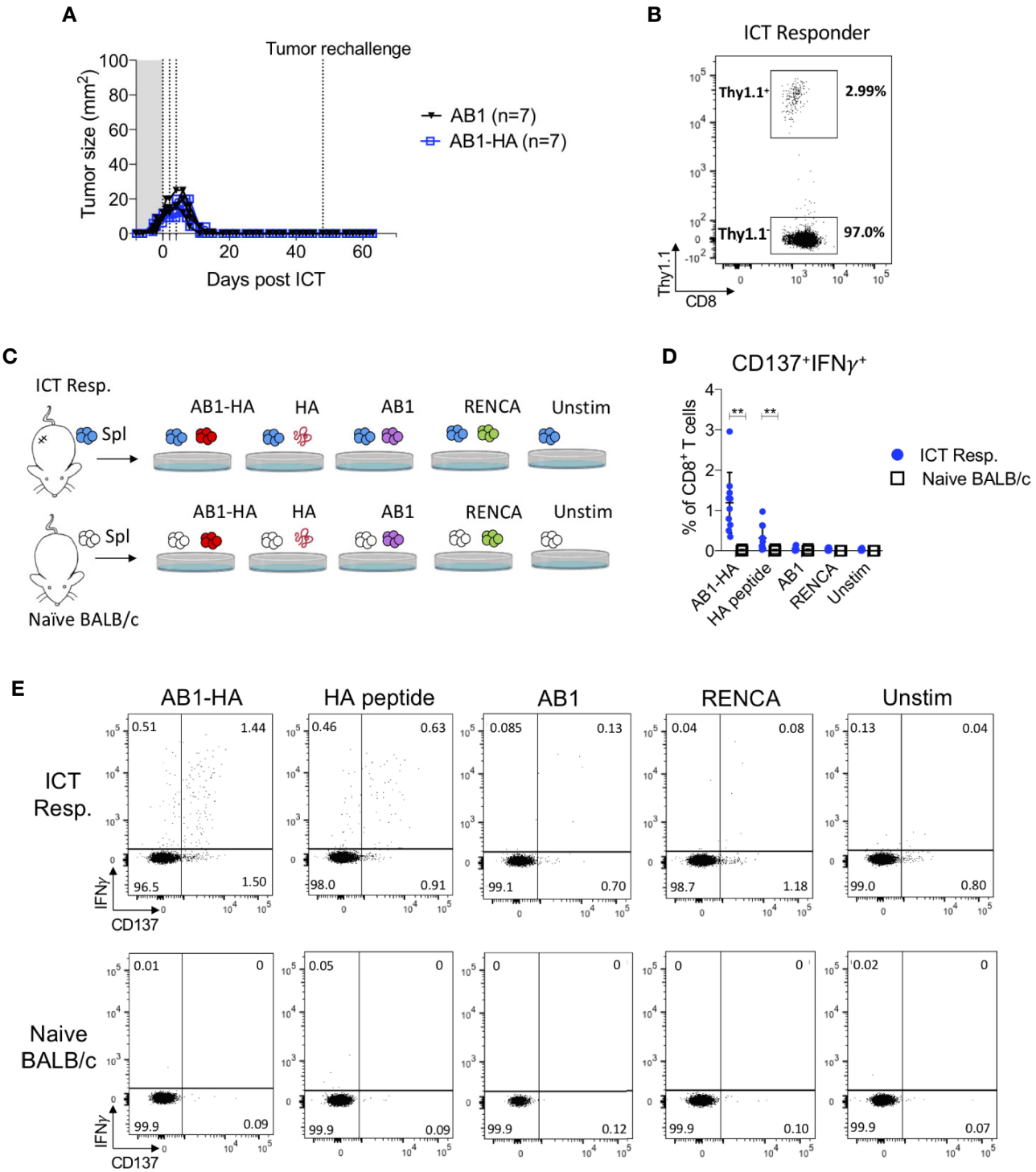

FIGURE 5 | ICT responders develop a tumor antigen-specific memory T cell response. **(A)** Representative tumor growth curves of ICT responders re-challenged with AB1-HA or AB1 tumor cells 30 days after the primary tumor regressed to 0 mm^2. **(B)** Representative FACs plot of $CD8^+Thy1.1^+$ T cells from splenocytes from an ICT responder, 15 days after AB1-HA tumor re-challenge. **(C)** *Ex vivo* co-culture setup to assess antigen-specific T cell responses. Splenocytes from ICT responders or naive BALB/c mice were co-cultured with AB1-HA, AB1, RENCA tumor cells, or HA peptide. **(D)** Dot plots and **(E)** representative flow cytometry plots, showing percentages of $CD8^+$ T cells that co-expressed IFNγ and CD137 for each culture condition. Data shown as mean ± SD, summary of two independent experiments; ICT responders: n = 10; Naïve BALB/c: n = 4. Mann-Whitney *U* tests; $^{**}P \leq 0.01$.

bilateral tumor model (22, 23, 37). We found that ICT increased tumor infiltration of HA-specific CTLs, but this increase varied between animals. Successful ICT responses were associated with increased post-treatment frequencies of effector memory (T_{EM}) HA-specific CTLs within tumors and draining lymph nodes, but not with pre-treatment frequencies. Previous murine studies demonstrated that some ICTs enhanced tumor antigen-specific CTL responses (21, 38, 39), and increased expression of activation and memory associated markers (20, 40). While these reports have added to our understanding of how ICT changes tumour antigen-specific CTLs, the majority are limited to comparisons between ICT-treated and untreated animals. Our study adds to this as we relate ICT induced changes in tumor antigen-specific CTLs to eventual outcomes in treated mice.

Our main finding is that increased frequencies of IL-7Rα expressing HA-specific T_{EM} CTLs correlated with ICT response. The T_{EM} phenotype reported in our study is similar to memory precursor effector T cells found in chronic viral infections (41–44). IL-7/IL-7Rα signalling pathway is crucial for memory CTL formation. The effects of ICT are IL-7 dependent (45), and combination IL-7 and ICT improved therapeutic benefit and long-term memory T cell responses in murine models (46–48). Increased frequencies of IL-7Rα expressing tumor antigen-specific CTLs found in the present study could indicate increased survival and persistence of memory CTLs in the tumor microenvironment and possibly providing long-term therapeutic benefit to ICT. A recent study by Sade-Feldman and colleagues similarly found an effector/memory CTL gene signature including the IL-7R gene, that was enriched in ICT responding tumors (12). IL-7R expressing memory T cells could be a T cell population of interest that defines ICT outcomes.

A challenge lies in identifying definitive CTL populations that correlate with ICT outcomes. Memory CTLs exist in heterogeneous differentiation states expressing different combinations of surface markers CCR7, CD69, CD44, Slamf7, PD-1, and T cell factor 1 (TCF1). However, the change in different memory CTL subsets during ICT vary between studies (12, 20, 40, 49, 50). In contrast to published studies, we did not observe any difference in post-ICT PD-1 expression or proliferation (Ki67) of HA-specific CTLs between responding and non-responding animals (9, 13, 51). This highlights the complexity in memory CTL differentiation and the need to understand how these populations change during ICT, especially in relation to treatment outcome.

HA-specific CTLs present in non-responding tumors were enriched for genes involved in WNT/β-catenin signaling, which could be a mechanism underlying the difference in HA-specific CTL frequencies between responders and non-responders. Our result is supported by studies which show that increased β-catenin *in vitro* reduces $CD8^+$ T cell proliferation, decreases tumor antigen-specific CTL function and promotes resistance to ICT *in vivo* (52–55). Neutralising WNT signaling *in vivo* expands tumor antigen–specific effector memory CTLs, which were phenotypically similar to our study (56). However, WNT signaling is also associated with the formation of stem-cell like memory T cells through the upregulation of TCF1, which mediate superior anti-tumor T cell responses (57). Increased proportions of $CD8^+PD\text{-}1^+TCF1^+$ T cells associated with improved survival for ICT treated melanoma patients (11). A caveat with our study is that non-responding mice with HA-specific CTLs present in tumors are rare, and we were unable to perform an in-depth phenotypic analysis to address this discrepancy. The role of WNT/β-catenin signaling in the development of anti-tumor $CD8^+$ T cell immunity requires further investigation.

In clinical studies, increased frequencies of tumor antigen-specific CTLs from pre- to post-ICT have been reported in ICT responders (5, 58). While most responding tumors generally exhibited high frequencies of HA-specific CTLs in the present study, there were some exceptions. A small proportion of animals had greater than 20% tumor infiltration of HA-specific CTLs however did not respond to ICT. This may be due to the presence of immune suppressive cells, such as myeloid derived suppressor cells and regulatory T cells, which suppressed tumor antigen-specific CTL function even if they were present (59, 60). Conversely, few animals had an absence of HA-specific CTLs but still displayed complete tumor regression following ICT. This suggested that while it is desirable to have large numbers of CTLs specific for one tumor antigen, it is not essential for response; CTLs specific for multiple tumor antigens may be required (61). The present study was limited to analysing the role of CTLs against one model tumor antigen. We did not analyse the tumor reactivity of endogenous CTLs which could have correlated to ICT response. Tracking one antigen specificity allowed us to study the effects of antigen-specific CTLs in ICT outcomes however the frequency and phenotype of multiple tumor antigen-specific CTLs in ICT should be investigated in future studies.

TCR sequencing is often used as a complementary approach to assess the breadth of antigen-specific T cell responses and is a potential biomarker of response to ICT. Successful ICT responses were associated with reduced tumor TCRβ diversity in our study, similar to other murine studies (38, 62, 63). Cancer patients with improved survival exhibit a greater expansion of TCRβ clones after ICT in their tumors and peripheral blood, compared to non-responders (16–19, 64), suggesting that effective therapy requires expansion of tumor antigen-specific CTLs. Although we were able to track the expansion of a single antigen-specific CTL clone, the dominance of this clone prevented us from studying the breadth of the anti-tumor T cell response or identifying expansion of other TCRβ clones in the endogenous $CD8^+$ T cell compartment in relation to ICT outcomes. The combination of the high affinity CL4 TCR transgenic, and robust cross presentation of the HA antigen in draining lymph nodes (65, 66) could have resulted in the dominant expansion of HA-specific CTLs over other specificities in responding animals.

Apart from the introduced CL4 clone, there was minimal sharing and similarities in tumor TCRβ clones between animals. Highly private tumor TCRβ repertoires have been described in pre-clinical studies by others (38, 67) and ourselves (unpublished data). Crosby and colleagues found that ICT expanded private

tumor TCRβ clones even in the presence of a fixed tumor antigen (38). This highlights the highly diverse nature of TCRβ repertoires in tumor models with limited variation. Each animal expands unique tumor TCRβ clones during ICT, and identifying cognate antigens of expanded TCR clones associated with successful ICT responses will inform personalized antigen-specific therapies.

In conclusion, post-treatment frequencies of effector memory tumor antigen-specific CTLs, and a clonal CTL repertoire correlate with response to ICT in our model. A potential dynamic biomarker of response could lie within the distribution of TCRβ clones within a memory T cell population (18). Further validation is required to investigate if this could predict ICT outcomes in cancer patients.

DATA AVAILABILITY STATEMENT

The original contributions presented in the study are included in the article/**Supplementary Material**, further inquiries can be directed to the corresponding author/s.

ETHICS STATEMENT

The animal study was reviewed and approved by Harry Perkins Institute of Medical Research Animal Ethics Committee.

AUTHOR CONTRIBUTIONS

NP performed mouse experiments, analyzed and interpreted all flow cytometry, TCRβ and RNA sequencing data, and wrote the manuscript. JK performed mouse experiments and TCRβ repertoire analysis. SG performed mouse experiments. CT assisted with murine surgery experiments and RNA sequencing analysis. SF assisted generating TCRβ libraries. VF and CF performed surgery experiments. RZ and WL designed and provided technical assistance with the bilateral tumor model. AC and MW performed TCRβ and RNA sequencing. ID assisted with statistical analysis. LB provided reagents. RH provided and optimized TCRβ sequencing. RL, AN, AM, and WL interpreted experiments and critically revised the manuscript. JC designed the study, supervised the project and edited the manuscript. All authors contributed to the article and approved the submitted version.

FUNDING

NP was supported by Cancer Council WA and UWA Richard Walter Gibbon Medical Research scholarships. JK was supported by an icare Dust Diseases Board scholarship. WL was supported by a Simon Lee Fellowship, an NHMRC Fellowship, and a Cancer Council WA fellowship. JC was supported by grants and fellowship from the UWA Raine Foundation, Cancer Council WA, WA Department of Health, and icare Dust Diseases Board. The National Centre for Asbestos Related Diseases receives funding through the National Health and Medical Research Council Centres of Research Excellence scheme.

ACKNOWLEDGMENTS

We acknowledge the facilities and the scientific and technical assistance of the Australian Microscopy and Microanalysis Research Facility at the Centre for Microscopy, Characterization and Analysis, The University of Western Australia, a facility funded by the University, State and Commonwealth Governments. We also thank Harry Perkins Institute of Medical Research Bioresources staff for their assistance with animal husbandry.

SUPPLEMENTARY MATERIAL

The Supplementary Material for this article can be found online at: https://www.frontiersin.org/articles/10.3389/fimmu.2020.584423/full#supplementary-material

REFERENCES

1. Garon EB, Rizvi NA, Hui R, Leighl N, Balmanoukian AS, Eder JP, et al. Pembrolizumab for the treatment of non-small-cell lung cancer. *N Engl J Med* (2015) 372(21):2018–28. doi: 10.1056/NEJMoa1501824
2. Hellmann MD, Paz-Ares L, Bernabe Caro R, Zurawski B, Kim S-W, Carcereny Costa E, et al. Nivolumab plus Ipilimumab in Advanced Non–Small-Cell Lung Cancer. *New Engl J Med* (2019) 381(21):2020–31. doi: 10.1056/NEJMoa1910231
3. Larkin J, Chiarion-Sileni V, Gonzalez R, Grob JJ, Rutkowski P, Lao CD, et al. Five-Year Survival with Combined Nivolumab and Ipilimumab in Advanced Melanoma. *N Engl J Med* (2019) 381(16):1535–46. doi: 10.1056/NEJMoa1910836
4. Herbst RS, Soria JC, Kowanetz M, Fine GD, Hamid O, Gordon MS, et al. Predictive correlates of response to the anti-PD-L1 antibody MPDL3280A in cancer patients. *Nature* (2014) 515(7528):563–7. doi: 10.1038/nature14011
5. Rizvi NA, Hellmann MD, Snyder A, Kvistborg P, Makarov V, Havel JJ, et al. Cancer immunology. Mutational landscape determines sensitivity to PD-1 blockade in non-small cell lung cancer. *Science* (2015) 348(6230):124–8. doi: 10.1126/science.aaa1348
6. Ayers M, Lunceford J, Nebozhyn M, Murphy E, Loboda A, Kaufman DR, et al. IFN-gamma-related mRNA profile predicts clinical response to PD-1 blockade. *J Clin Invest* (2017) 127(8):2930–40. doi: 10.1172/JCI91190
7. Tumeh PC, Harview CL, Yearley JH, Shintaku IP, Taylor EJ, Robert L, et al. PD-1 blockade induces responses by inhibiting adaptive immune resistance. *Nature* (2014) 515(7528):568–71. doi: 10.1038/nature13954
8. Lesterhuis WJ, Bosco A, Millward MJ, Small M, Nowak AK, Lake RA. Dynamic versus static biomarkers in cancer immune checkpoint blockade: unravelling complexity. *Nat Rev Drug Discovery* (2017) 16(4):264–72. doi: 10.1038/nrd.2016.233
9. Chen PL, Roh W, Reuben A, Cooper ZA, Spencer CN, Prieto PA, et al. Analysis of Immune Signatures in Longitudinal Tumor Samples Yields Insight into Biomarkers of Response and Mechanisms of Resistance to

Immune Checkpoint Blockade. *Cancer Discovery* (2016) 6(8):827–37. doi: 10.1158/2159-8290.CD-15-1545
10. Li H, van der Leun AM, Yofe I, Lubling Y, Gelbard-Solodkin D, van Akkooi ACJ, et al. Dysfunctional CD8 T Cells Form a Proliferative, Dynamically Regulated Compartment within Human Melanoma. *Cell* (2019) 176(4):775–89 e18. doi: 10.1016/j.cell.2018.11.043
11. Miller BC, Sen DR, Al Abosy R, Bi K, Virkud YV, LaFleur MW, et al. Subsets of exhausted CD8(+) T cells differentially mediate tumor control and respond to checkpoint blockade. *Nat Immunol* (2019) 20(3):326–36. doi: 10.1038/s41590-019-0312-6
12. Sade-Feldman M, Yizhak K, Bjorgaard SL, Ray JP, de Boer CG, Jenkins RW, et al. Defining T Cell States Associated with Response to Checkpoint Immunotherapy in Melanoma. *Cell* (2018) 175(4):998–1013.e20. doi: 10.1016/j.cell.2018.10.038
13. Huang AC, Postow MA, Orlowski RJ, Mick R, Bengsch B, Manne S, et al. T-cell invigoration to tumour burden ratio associated with anti-PD-1 response. *Nature* (2017) 545(7652):60–5. doi: 10.1038/nature22079
14. Agdashian D, ElGindi M, Xie C, Sandhu M, Pratt D, Kleiner DE, et al. The effect of anti-CTLA4 treatment on peripheral and intra-tumoral T cells in patients with hepatocellular carcinoma. Cancer Immunology. *Immunotherapy* (2019) 68(4):599–608. doi: 10.1007/s00262-019-02299-8
15. Prat A, Navarro A, Pare L, Reguart N, Galvan P, Pascual T, et al. Immune-Related Gene Expression Profiling After PD-1 Blockade in Non-Small Cell Lung Carcinoma, Head and Neck Squamous Cell Carcinoma, and Melanoma. *Cancer Res* (2017) 77(13):3540–50. doi: 10.1158/0008-5472.CAN-16-3556
16. Zhang J, Ji Z, Caushi JX, El Asmar M, Anagnostou V, Cottrell TR, et al. Compartmental Analysis of T-cell Clonal Dynamics as a Function of Pathologic Response to Neoadjuvant PD-1 Blockade in Resectable Non-Small Cell Lung Cancer. *Clin Cancer Res* (2020) 26(6):1327–37. doi: 10.1158/1078-0432.CCR-19-2931
17. Roh W, Chen P-L, Reuben A, Spencer CN, Prieto PA, Miller JP, et al. Integrated molecular analysis of tumor biopsies on sequential CTLA-4 and PD-1 blockade reveals markers of response and resistance. *Sci Trans Med* (2017) 9(379):eaah3560. doi: 10.1126/scitranslmed.aah3560
18. Fairfax BP, Taylor CA, Watson RA, Nassiri I, Danielli S, Fang H, et al. Peripheral CD8+ T cell characteristics associated with durable responses to immune checkpoint blockade in patients with metastatic melanoma. *Nat Med* (2020) 26(2):193–9. doi: 10.1038/s41591-019-0734-6
19. Valpione S, Galvani E, Tweedy J, Mundra PA, Banyard A, Middlehurst P, et al. Immune-awakening revealed by peripheral T cell dynamics after one cycle of immunotherapy. *Nat Cancer* (2020) 1(2):210–21. doi: 10.1038/s43018-019-0022-x
20. Fehlings M, Simoni Y, Penny HL, Becht E, Loh CY, Gubin MM, et al. Checkpoint blockade immunotherapy reshapes the high-dimensional phenotypic heterogeneity of murine intratumoural neoantigen-specific CD8+ T cells. *Nat Communications* (2017) 8(1):562. doi: 10.1038/s41467-017-00627-z
21. Ma S, Chee J, Fear VS, Forbes CA, Boon L, Dick IM, et al. Pre-treatment tumor neo-antigen responses in draining lymph nodes are infrequent but predict checkpoint blockade therapy outcome. *Oncoimmunology* (2020) 9 (1):1684714. doi: 10.1080/2162402X.2019.1684714
22. Zemek RM, Fear VS, Forbes C, de Jong E, Casey TH, Boon L, et al. Bilateral murine tumor models for characterizing the response to immune checkpoint blockade. *Nat Protoc* (2020) 15(5):1628–48. doi: 10.1038/s41596-020-0299-3
23. Zemek RM, De Jong E, Chin WL, Schuster IS, Fear VS, Casey TH, et al. Sensitization to immune checkpoint blockade through activation of a STAT1/NK axis in the tumor microenvironment. *Sci Transl Med* (2019) 11(501): eaav7816. doi: 10.1126/scitranslmed.aav7816
24. Morgan DJ, Liblau R, Scott B, Fleck S, McDevitt HO, Sarvetnick N, et al. CD8 (+) T cell-mediated spontaneous diabetes in neonatal mice. *J Immunol* (1996) 157(3):978–83.
25. Davis MR, Manning LS, Whitaker D, Garlepp MJ, Robinson BW. Establishment of a murine model of malignant mesothelioma. *Int J Cancer* (1992) 52(6):881–6. doi: 10.1002/ijc.2910520609
26. Marzo AL, Lake RA, Robinson BW, Scott B. T-cell receptor transgenic analysis of tumor-specific CD8 and CD4 responses in the eradication of solid tumors. *Cancer Res* (1999) 59(5):1071–9.
27. Lesterhuis WJ, Salmons J, Nowak AK, Rozali EN, Khong A, Dick IM, et al. Synergistic effect of CTLA-4 blockade and cancer chemotherapy in the induction of anti-tumor immunity. *PloS One* (2013) 8(4):e61895. doi: 10.1371/journal.pone.0061895
28. Fear VS, Tilsed C, Chee J, Forbes CA, Casey T, Solin JN, et al. Combination immune checkpoint blockade as an effective therapy for mesothelioma. *Oncoimmunology* (2018) 7(10):e1494111. doi: 10.1080/2162402X.2018.1494111
29. Freeman JD, Warren RL, Webb JR, Nelson BH, Holt RA. Profiling the T-cell receptor beta-chain repertoire by massively parallel sequencing. *Genome Res* (2009) 19(10):1817–24. doi: 10.1101/gr.092924.109
30. Giudicelli V, Brochet X, Lefranc MP. IMGT/V-QUEST: IMGT standardized analysis of the immunoglobulin (IG) and T cell receptor (TR) nucleotide sequences. *Cold Spring Harb Protoc* (2011) 2011(6):695–715. doi: 10.1101/pdb.prot5633
31. Turchaninova MA, Davydov A, Britanova OV, Shugay M, Bikos V, Egorov ES, et al. High-quality full-length immunoglobulin profiling with unique molecular barcoding. *Nat Protoc* (2016) 11(9):1599–616. doi: 10.1038/nprot.2016.093
32. Bolotin DA, Poslavsky S, Mitrophanov I, Shugay M, Mamedov IZ, Putintseva EV, et al. MiXCR: software for comprehensive adaptive immunity profiling. *Nat Methods* (2015) 12(5):380–1. doi: 10.1038/nmeth.3364
33. Joshi K, Robert de Massy M, Ismail M, Reading JL, Uddin I, Woolston A, et al. Spatial heterogeneity of the T cell receptor repertoire reflects the mutational landscape in lung cancer. *Nat Med* (2019) 25(10):1549–59. doi: 10.1038/s41591-019-0592-2
34. Venturi V, Kedzierska K, Turner SJ, Doherty PC, Davenport MP. Methods for comparing the diversity of samples of the T cell receptor repertoire. *J Immunol Methods* (2007) 321(1-2):182–95. doi: 10.1016/j.jim.2007.01.019
35. Madi A, Poran A, Shifrut E, Reich-Zeliger S, Greenstein E, Zaretsky I, et al. T cell receptor repertoires of mice and humans are clustered in similarity networks around conserved public CDR3 sequences. *Elife* (2017) 6:e22057. doi: 10.7554/eLife.22057
36. Subramanian A, Kuehn H, Gould J, Tamayo P. GSEA-P: a desktop application for Gene Set Enrichment Analysis. *Bioinformatics* (2007) 23(23):3251–3. doi: 10.1093/bioinformatics/btm369
37. Lesterhuis WJ, Rinaldi C, Jones A, Rozali EN, Dick IM, Khong A, et al. Network analysis of immunotherapy-induced regressing tumours identifies novel synergistic drug combinations. *Sci Rep* (2015) 5:12298. doi: 10.1038/srep12298
38. Crosby EJ, Wei J, Yang XY, Lei G, Wang T, Liu CX, et al. Complimentary mechanisms of dual checkpoint blockade expand unique T-cell repertoires and activate adaptive anti-tumor immunity in triple-negative breast tumors. *Oncoimmunology* (2018) 7(5):e1421891. doi: 10.1080/2162402X.2017.1421891
39. Gubin MM, Zhang X, Schuster H, Caron E, Ward JP, Noguchi T, et al. Checkpoint blockade cancer immunotherapy targets tumour-specific mutant antigens. *Nature* (2014) 515(7528):577–81. doi: 10.1038/nature13988
40. Kurtulus S, Madi A, Escobar G, Klapholz M, Nyman J, Christian E, et al. Checkpoint Blockade Immunotherapy Induces Dynamic Changes in PD-1(-) CD8(+) Tumor-Infiltrating T Cells. *Immunity* (2019) 50(1):181–94.e6. doi: 10.1016/j.immuni.2018.11.014
41. Kaech SM, Cui W. Transcriptional control of effector and memory CD8+ T cell differentiation. *Nat Rev Immunol* (2012) 12(11):749–61. doi: 10.1038/nri3307
42. Herndler-Brandstetter D, Ishigame H, Shinnakasu R, Plajer V, Stecher C, Zhao J, et al. KLRG1(+) Effector CD8(+) T Cells Lose KLRG1, Differentiate into All Memory T Cell Lineages, and Convey Enhanced Protective Immunity. *Immunity* (2018) 48(4):716–29.e8. doi: 10.1016/j.immuni.2018.03.015
43. Joshi NS, Cui W, Chandele A, Lee HK, Urso DR, Hagman J, et al. Inflammation Directs Memory Precursor and Short-Lived Effector CD8+ T Cell Fates via the Graded Expression of T-bet Transcription Factor. *Immunity* (2007) 27(2):281–95. doi: 10.1016/j.immuni.2007.07.010
44. Utzschneider DT, Charmoy M, Chennupati V, Pousse L, Ferreira DP, Calderon-Copete S, et al. T Cell Factor 1-Expressing Memory-like CD8+ T Cells Sustain the Immune Response to Chronic Viral Infections. *Immunity* (2016) 45(2):415–27. doi: 10.1016/j.immuni.2016.07.021

45. Shi LZ, Fu T, Guan B, Chen J, Blando JM, Allison JP, et al. Interdependent IL-7 and IFN-gamma signalling in T-cell controls tumour eradication by combined alpha-CTLA-4+alpha-PD-1 therapy. *Nat Commun* (2016) 7:12335. doi: 10.1038/ncomms12335
46. Nakao S, Arai Y, Tasaki M, Yamashita M, Murakami R, Kawase T, et al. Intratumoral expression of IL-7 and IL-12 using an oncolytic virus increases systemic sensitivity to immune checkpoint blockade. *Sci Transl Med* (2020) 12 (526):eaax7992. doi: 10.1126/scitranslmed.aax7992
47. Colombetti S, Levy F, Chapatte L. IL-7 adjuvant treatment enhances long-term tumor-antigen-specific CD8+ T-cell responses after immunization with recombinant lentivector. *Blood* (2009) 113(26):6629–37. doi: 10.1182/blood-2008-05-155309
48. Pfannenstiel LW, Diaz-Montero CM, Tian YF, Scharpf J, Ko JS, Gastman BR. Immune-Checkpoint Blockade Opposes CD8(+) T-cell Suppression in Human and Murine Cancer. *Cancer Immunol Res* (2019) 7(3):510–25. doi: 10.1158/2326-6066.CIR-18-0054
49. Gide TN, Quek C, Menzies AM, Tasker AT, Shang P, Holst J, et al. Distinct Immune Cell Populations Define Response to Anti-PD-1 Monotherapy and Anti-PD-1/Anti-CTLA-4 Combined Therapy. *Cancer Cell* (2019) 35(2):238–55.e6. doi: 10.1016/j.ccell.2019.01.003
50. Araujo B, Borch A, Hansen M, Draghi A, Spanggaard I, Rohrberg K, et al. Common phenotypic dynamics of tumor-infiltrating lymphocytes across different histologies upon checkpoint inhibition: impact on clinical outcome. *Cytotherapy* (2020) 22(4):204–13. doi: 10.1016/j.jcyt.2020.01.010
51. Thommen DS, Koelzer VH, Herzig P, Roller A, Trefny M, Dimeloe S, et al. A transcriptionally and functionally distinct PD-1(+) CD8(+) T cell pool with predictive potential in non-small-cell lung cancer treated with PD-1 blockade. *Nat Med* (2018) 24(7):994–1004. doi: 10.1038/s41591-018-0057-z
52. Chee J, Wilson C, Buzzai A, Wylie B, Forbes CA, Booth M, et al. Impaired T cell proliferation by ex vivo BET-inhibition impedes adoptive immunotherapy in a murine melanoma model. *Epigenetics* (2020) 15(1-2):134–44. doi: 10.1080/15592294.2019.1656156
53. Liang X, Fu C, Cui W, Ober-Blobaum JL, Zahner SP, Shrikant PA, et al. beta-catenin mediates tumor-induced immunosuppression by inhibiting cross-priming of CD8 (+) T cells. *J Leukoc Biol* (2014) 95(1):179–90. doi: 10.1189/jlb.0613330
54. Spranger S, Bao R, Gajewski TF. Melanoma-intrinsic beta-catenin signalling prevents anti-tumour immunity. *Nature* (2015) 523(7559):231–5. doi: 10.1038/nature14404
55. Pai SG, Carneiro BA, Mota JM, Costa R, Leite CA, Barroso-Sousa R, et al. Wnt/beta-catenin pathway: modulating anticancer immune response. *J Hematol Oncol* (2017) 10(1):101. doi: 10.1186/s13045-017-0471-6
56. Pacella I, Cammarata I, Focaccetti C, Miacci S, Gulino A, Tripodo C, et al. Wnt3a Neutralization Enhances T-cell Responses through Indirect Mechanisms and Restrains Tumor Growth. *Cancer Immunol Res* (2018) 6 (8):953–64. doi: 10.1158/2326-6066.CIR-17-0713
57. Gattinoni L, Zhong XS, Palmer DC, Ji Y, Hinrichs CS, Yu Z, et al. Wnt signaling arrests effector T cell differentiation and generates CD8+ memory stem cells. *Nat Med* (2009) 15(7):808–13. doi: 10.1038/nm.1982
58. Fehlings M, Jhunjhunwala S, Kowanetz M, O'Gorman WE, Hegde PS, Sumatoh H, et al. Late-differentiated effector neoantigen-specific CD8+ T cells are enriched in peripheral blood of non-small cell lung carcinoma patients responding to atezolizumab treatment. *J ImmunoTherapy Cancer* (2019) 7(1):249. doi: 10.1186/s40425-019-0695-9
59. Weide B, Martens A, Hassel JC, Berking C, Postow MA, Bisschop K, et al. Baseline Biomarkers for Outcome of Melanoma Patients Treated with Pembrolizumab. *Clin Cancer Res* (2016) 22(22):5487–96. doi: 10.1158/1078-0432.CCR-16-0127
60. Weide B, Martens A, Zelba H, Stutz C, Derhovanessian E, Di Giacomo AM, et al. Myeloid-derived suppressor cells predict survival of patients with advanced melanoma: comparison with regulatory T cells and NY-ESO-1- or melan-A-specific T cells. *Clin Cancer Res* (2014) 20(6):1601–9. doi: 10.1158/1078-0432.CCR-13-2508
61. Friedman J, Moore EC, Zolkind P, Robbins Y, Clavijo PE, Sun L, et al. Neoadjuvant PD-1 Immune Checkpoint Blockade Reverses Functional Immunodominance among Tumor Antigen-Specific T Cells. *Clin Cancer Res* (2020) 26(3):679–89. doi: 10.1158/1078-0432.CCR-19-2209
62. Zhigalova EA, Izosimova AI, Yuzhakova DV, Volchkova LN, Shagina IA, Turchaninova MA, et al. RNA-Seq-Based TCR Profiling Reveals Persistently Increased Intratumoral Clonality in Responders to Anti-PD-1 Therapy. *Front Oncol* (2020) 10:385. doi: 10.3389/fonc.2020.00385
63. Rudqvist NP, Pilones KA, Lhuillier C, Wennerberg E, Sidhom JW, Emerson RO, et al. Radiotherapy and CTLA-4 Blockade Shape the TCR Repertoire of Tumor-Infiltrating T Cells. *Cancer Immunol Res* (2018) 6(2):139–50. doi: 10.1158/2326-6066.CIR-17-0134
64. Riaz N, Havel JJ, Makarov V, Desrichard A, Urba WJ, Sims JS, et al. Tumor and Microenvironment Evolution during Immunotherapy with Nivolumab. *Cell* (2017) 171(4):934–49 e16. doi: 10.1016/j.cell.2017.09.028
65. Nowak AK, Lake RA, Marzo AL, Scott B, Heath WR, Collins EJ, et al. Induction of Tumor Cell Apoptosis In Vivo Increases Tumor Antigen Cross-Presentation, Cross-Priming Rather than Cross-Tolerizing Host Tumor-Specific CD8 T Cells. *J Immunol* (2003) 170(10):4905–13. doi: 10.4049/jimmunol.170.10.4905
66. McDonnell AM, Lesterhuis WJ, Khong A, Nowak AK, Lake RA, Currie AJ, et al. Tumor-infiltrating dendritic cells exhibit defective cross-presentation of tumor antigens, but is reversed by chemotherapy. *Eur J Immunol* (2015) 45 (1):49–59. doi: 10.1002/eji.201444722
67. Aoki H, Ueha S, Shichino S, Ogiwara H, Hashimoto SI, Kakimi K, et al. TCR Repertoire Analysis Reveals Mobilization of Novel CD8(+) T Cell Clones Into the Cancer-Immunity Cycle Following Anti-CD4 Antibody Administration. *Front Immunol* (2018) 9:3185. doi: 10.3389/fimmu.2018.03185

Conflict of Interest: LB was employed by the company Polpharma Biologics.

The remaining authors declare that the research was conducted in the absence of any commercial or financial relationships that could be construed as a potential conflict of interest.

frontiers in Oncology

ORIGINAL RESEARCH
published: 15 January 2021
doi: 10.3389/fonc.2020.570752

Incidence of Skin and Respiratory Immune-Related Adverse Events Correlates With Specific Tumor Types in Patients Treated With Checkpoint Inhibitors

Lynn M. Rose[1], Hannah A. DeBerg[2], Prakash Vishnu[3], Jason K. Frankel[4], Adarsh B. Manjunath[2], John Paul E. Flores[5] and David M. Aboulafia[5,6]*

[1] Scientific Administration, Benaroya Research Institute at Virginia Mason, Seattle, WA, United States, [2] Systems Immunology, Benaroya Research Institute at Virginia Mason, Seattle, WA, United States, [3] Division of Hematology, CHI Franciscan Medical Group, Seattle, WA, United States, [4] Section of Urology, Virginia Mason Medical Center, Seattle, WA, United States, [5] Department of Hematology and Oncology, Virginia Mason Medical Center, Seattle, WA, United States, [6] Division of Hematology, University of Washington, Seattle, WA, United States

OPEN ACCESS

Edited by:
Taha Merghoub,
Memorial Sloan Kettering Cancer Center, United States

Reviewed by:
Rodabe N. Amaria,
University of Texas MD Anderson Cancer Center, United States
Missak Haigentz,
Atlantic Health System, United States

***Correspondence:**
Lynn M. Rose
lrose@benaroyaresearch.org;
lmrose@uw.edu

Specialty section:
This article was submitted to Cancer Immunity and Immunotherapy, a section of the journal Frontiers in Oncology

Received: 08 June 2020
Accepted: 03 December 2020
Published: 15 January 2021

Citation:
Rose LM, DeBerg HA, Vishnu P, Frankel JK, Manjunath AB, Flores JPE and Aboulafia DM (2021) Incidence of Skin and Respiratory Immune-Related Adverse Events Correlates With Specific Tumor Types in Patients Treated With Checkpoint Inhibitors. Front. Oncol. 10:570752. doi: 10.3389/fonc.2020.570752

Checkpoint inhibitors (CPIs) increase antitumor activity by unblocking regulators of the immune response. This action can provoke a wide range of immunologic and inflammatory side effects, some of which can be fatal. Recent studies suggest that CPI-induced immune-related adverse events (irAEs) may predict survival and response. However, little is known about the mechanisms of this association. This study was undertaken to evaluate the influence of tumor diagnosis and preexisting clinical factors on the types of irAEs experienced by cancer patients treated with CPIs. The correlation between irAEs and overall survival (OS) was also assessed. All cancer patients treated with atezolizumab (ATEZO), ipilimumab (IPI), nivolumab (NIVO), or pembrolizumab (PEMBRO) at Virginia Mason Medical Center between 2011 and 2019 were evaluated. irAEs were graded according to the Common Terminology Criteria for Adverse Events (Version 5) and verified independently. Statistical analyses were performed to assess associations between irAEs, pre-treatment factors, and OS. Of the 288 patients evaluated, 59% developed irAEs of any grade, and 19% developed irAEs of grade 3 or 4. A time-dependent survival analysis demonstrated a clear association between the occurrence of irAEs and OS ($P < 0.001$). A 6-week landmark analysis adjusted for body mass index confirmed an association between irAEs and OS in non-Small Cell Lung Cancer (NSCLC) ($P < 0.03$). An association between melanoma and skin irAEs ($P < 0.01$) and between NSCLC and respiratory irAEs ($P = 0.03$) was observed, independent of CPI administered. Patients with preexisting autoimmune disease experienced a higher incidence of severe irAEs ($P = 0.01$), but not a higher overall incidence of irAEs ($P = 0.6$). A significant association between irAEs and OS was observed in this diverse patient population. No correlation was observed between preexisting comorbid conditions and the type of irAE observed. However, a correlation between skin-related irAEs and melanoma and between respiratory irAEs and NSCLC was observed, suggesting that many irAEs are driven by a specific response to the primary tumor. In patients with NSCLC, the respiratory irAEs were associated with a survival benefit.

Keywords: checkpoint inhibitors, immunotherapy, immune-related adverse events, biomarkers, survival benefits, preexisting conditions, autoimmune disease

INTRODUCTION

Immune checkpoint inhibitors (CPIs) that target the cytotoxic T-lymphocyte-associated antigen 4 (CTLA-4) and the programmed cell death protein-1 (PD-1)/programmed cell death ligand-1 (PD-L1) pathway have demonstrated remarkable efficacy across a wide variety of cancer types (1). In addition to inducing durable anti-tumor responses and improving survival of patients, treatment with CPIs is often better tolerated than conventional cytotoxic chemotherapeutic agents. However, CPIs can lead to immune-related adverse events (irAEs) that result in significant morbidity and discontinuation of therapy (2). Recent studies suggest that CPI-induced irAEs can predict survival and response, however little is known about the mechanisms of this association (3, 4).. We undertook this study to evaluate the relationship between tumor type, preexisting clinical factors, the occurrence and type of irAEs, and OS in a diverse set of cancer patients treated with CPIs. Accurately measuring the prognostic significance of preexisting clinical factors could help identify those patients at higher or lower risk for developing irAEs (5–8).

MATERIALS AND METHODS

Patients

This retrospective study included all cancer patients treated at the Virginia Mason Medical Center (Seattle, WA) between July 2011 and October 2019 with *atezolizumab* (ATEZO), *ipilimumab* (IPI), *nivolumab* (NIVO), or *pembrolizumab* (PEMBRO). No exclusions were based on preexisting conditions or other clinical factors that frequently preclude participation in clinical trials. Thus, these data represent "real world" patients and treatment responses (9). Patients were only excluded if they were on a blinded clinical trial where their CPI was unknown or if there was missing clinical data. Institutional review board approval was obtained prior to initiation of the study. All data were gathered retrospectively (by LR and AM) using diagnostic codes, search terms, and manual chart review.

Clinical Measures

Patients were separated into three groups: those treated with inhibitors of CTLA-4 (IPI) alone, CTLA-4 in combination with PD-1 (IPI and NIVO), or PD-1/PD-L1 inhibitors alone (ATEZO, NIVO, or PEMBRO). Data collection included patient demographics (e.g., gender, age, and body mass index [BMI]), primary diagnoses, dates of CPI administration and pre-infusion laboratory test results. All irAEs were graded 1–5 according to the Common Terminology Criteria for Adverse Events (Version 5) (10) and verified independently by the treating physicians. No grade 5 irAEs were recorded. Grade 4 irAEs were life-threatening, requiring urgent hospitalization and suspension of CPI treatment. Preexisting diseases were grouped as: cardiovascular (e.g., coronary artery disease), endocrine/metabolic (e.g., type 2 diabetes mellitus), allergy and/or asthma, autoimmune disease, gastrointestinal (e.g., GERD, colitis), and prior cancers unrelated to the CPI-treated diagnosis. Pre-treatment laboratory test results were categorized according to whether the reported result fell within, above, or below the normal ranges. Prior treatment with steroids (e.g., dexamethasone) within the six months prior to checkpoint inhibitor therapy was also assessed as a possible mitigator of irAEs and overall survival. For purposes of our study, we defined sustained steroid use to be the administration of a prednisone-equivalent dose of 20 mg or higher at least four times in the six months prior to CPI administration

Statistical Analysis

We calculated summary statistics for demographic and clinical variables and for subgroups categorized by CPI treatment regimen. A Chi-square or Fisher's exact test was used to evaluate relationships between categorical variables, including cancer diagnosis, preexisting disease, demographic variables, and the grade of the irAE. For patients who were treated with more than one CPI regimen, irAEs associated with the first CPI were used for analysis to avoid introducing bias from double-counting these individuals. Logistic regression was used to model the odds of experiencing an irAE within the first 6 weeks of treatment. Two statistical methods were used to assess the association between irAEs and OS. In the first, a time-dependent Cox proportional hazard regression was performed. In this analysis, irAE experience was modeled as a binary time-dependent covariate for the entire study population. In the second, a landmark approach to Cox proportional hazards regression with a landmark time of 6 weeks was employed to assess OS models (11). Patients with survival times of less than 6 weeks after first CPI treatment (n = 36) were excluded from the both the irAE development and landmark survival analyses. Patients with incomplete irAE records (n = 6) were also excluded. Patients who were treated in an adjuvant setting (n = 20) were excluded from the survival analysis. A heat map showing the incidence of irAEs according to cancer diagnosis was generated using a Fisher's exact test. A false discovery rate multiple testing correction was applied to the test.

RESULTS

Patient Demographics

A total of 321 CPI treatment courses were identified, corresponding to 288 individual patients (**Tables 1** and **2**). Patients were predominantly men (62%) with a median age of 69 years. Almost all patients had metastatic disease (94%). The most common diagnoses were non-Small Cell Lung Cancer (NSCLC-31%), melanoma (24%), urothelial cancer (13%), and renal cell carcinoma (9%) (**Table 1**). The distribution of treatments over time is provided in **Table 2**. Comorbid conditions were grouped as: cardiovascular (n=204); endocrine/metabolic (n = 99); allergy and/or asthma (n = 64), autoimmune disease (n = 58), gastrointestinal (n = 127) and prior cancers unrelated to the CPI-treated diagnosis (n = 96). The cases of preexisting autoimmune disease included: autoimmune thyroid disease (n = 17), rheumatoid arthritis (n = 9), Crohn's disease or

TABLE 1 | Patient cohort demographics.

	CTLA-4	CTLA-4/PD-1	PD-1/PD-L1	Overall
Number	37	18	233	288
Age, median (range)	68 (25-90)	68 (44–79)	70 (30–95)	69.5 (25–95)
Body mass index median (range)	29 (19–52)	28 (18–38)	25 (16–46)	25 (16–52)
Sex, n (%)				
Male	27 (73)	14 (78)	138 (59)	179 (62)
Female	10 (27)	4 (22)	95 (41)	109 (38)
Adjuvant therapy, n (%)	9 (24)	0 (0)	11 (5)	20 (7)
Metastatic disease, n (%)	37 (100)	17 (94)	216 (93)	270 (94)
Cancer diagnosis, n (%)				
Bladder	0 (0)	0 (0)	37 (16)	37 (13)
Melanoma	36 (97)	5 (28)	27 (12)	68 (24)
NSCLC	0 (0)	0 (0)	89 (38)	89 (31)
RCC	0 (0)	11 (61)	14 (6)	25 (9)
Other[a]	1 (3)	2 (11)	66 (28)	69 (24)
Preexisting conditions, n (%)				
Cardiovascular	22 (59)	14 (78)	168 (72)	204 (71)
Gastrointestinal	13 (35)	8 (44)	106 (45)	127 (44)
Endocrine or metabolic	7 (19)	4 (22)	88 (38)	99 (34)
Other cancer	10 (27)	3 (17)	83 (36)	96 (33)
Allergy or asthma	7 (19)	6 (33)	51 (22)	64 (22)
Allergy	6 (16)	3 (17)	38 (16)	47 (16)
Asthma	3 (8)	3 (17)	21 (9)	27 (9)
Autoimmune disease	6 (16)	4 (22)	48 (21)	58 (20)

[a]*Head and neck (n = 16), colorectal (n = 7), hepatocellular (n = 7), esophageal (n = 7), and other (n = 32).*

TABLE 2 | CPI use over time. Number of CPI treatment courses administered by year.

	2011	2012	2013	2014	2015	2016	2017	2018	2019[a]	Total
CTLA-4	5	7	8	9	7	2	0	1	0	39
CTLA-4/PD-1	0	0	0	0	2	3	4	8	6	23
PD-1/PD-L1	0	0	0	1	11	56	60	78	53	259
Total	5	7	8	10	20	61	64	87	59	321

[a]*Data collected from July 2011 through October 2019.*

ulcerative colitis (n = 9), systemic lupus erythematosus (n = 3), psoriasis (n = 5), polymyalgia rheumatica (n=3), multiple sclerosis (n = 2), Raynaud's syndrome (n = 2), chronic lichen planus (n = 2), and ankylosing spondylitis (n = 2). Five individuals had more than one autoimmune disease.

Overall Incidence of irAEs

Fifty-nine percent of patients treated with CPIs (**Table 3**) developed irAEs (n = 171). Severe irAEs (grade 3 or 4) occurred in 29% of patients (n = 55) (**Table 3**). The median time to first irAE was 4 weeks. The median time from initial CPI treatment to the most severe irAE was 10 weeks. Of the irAEs evaluated, 147 (41%) were grade 1, 137 (38%) grade 2, 63 (18%) grade 3, and 15 (4%) grade 4. Maculopapular skin rashes and pruritis were the most frequently reported irAEs with 34% of patients reporting at least one skin-related irAE. Other common irAEs were immune-mediated colitis and other gastrointestinal irAEs (23% of patients), endocrine or metabolic adverse events (14%), and respiratory irAEs (11%) (e.g., pneumonitis). Hepatobiliary, blood, eye, musculoskeletal, nervous system, and renal irAEs each affected less than 10% of patients. The grade 3 and 4 irAEs were predominantly respiratory, hepatobiliary, gastrointestinal, and endocrine. One patient developed chronic type 1 diabetes mellitus because of treatment with PEMBRO. **Figure 1** presents the distribution of irAEs by severity and type.

Factors Impacting irAE Development

Anti-PD-1/PD-L1-treated patients were less likely to experience an irAE than patients treated with anti-CTLA-4 (OR=0.33, 95% CI 0.15 to 0.70, $P = 0.004$). Odds ratios (OR) for the occurrence of irAEs are shown in **Figure 2**. **A** 6-week landmark analysis was applied to pre-treatment OR calculations to avoid potential bias from patients with very short survival times. No other factors were significantly associated with increased odds of irAE development (**Figure 2**). As previously reported, two factors decreased odds of irAE development, age > 70 and low pre-infusion lymphocyte counts ($P = 0.05$) (5, 6). In subjects who survived for at least 6 weeks, there was an association between preexisting autoimmune disease and the occurrence of a severe irAE (grade 3 or 4; $P = 0.01$, Chi-squared test).

Categories of irAEs

An increased incidence of skin-related irAEs was observed in melanoma patients receiving CPI treatment relative to other cancer diagnoses, with 51% of melanoma patients experiencing at least one skin-related irAE. An increased incidence of

TABLE 3 | irAE incidence. Numbers and percentages of patients who experienced at least one irAE of the specified type. Numbers inside of parentheses indicate percentages of patients relative to the CPI treatment group.

irAE Type	CTLA-4 (n = 37)			CTLA-4/PD-1 (n = 18)			PD-1/PD-L1 (n = 233)			Overall (n = 288)		
	All	Grades 1–2	Grades 3–4	All	Grades 1–2	Grades 3–4	All	Grades 1–2	Grades 3–4	All	Grades 1–2	Grades 3–4
Blood	0 (0)	0 (0)	0 (0)	1 (6)	1 (6)	0 (0)	1 (0)	0 (0)	1 (0)	2 (1)	1 (0)	1 (1)
Cardiac	0 (0)	0 (0)	0 (0)	0 (0)	0 (0)	0 (0)	1 (0)	0 (0)	1 (0)	1 (0)	0 (0)	1 (1)
Dermatological	18 (49)	16 (43)	2 (5)	12 (67)	12 (67)	0 (0)	62 (27)	59 (25)	3 (1)	102 (32)	97 (39)	5 (7)
Endocrine/ Metabolic	5 (14)	2 (5)	4 (11)	2 (11)	1 (6)	1 (6)	29 (12)	24 (10)	5 (2)	39 (12)	28 (11)	11 (16)
Eye	0 (0)	0 (0)	0 (0)	1 (6)	0 (0)	1 (6)	5 (2)	5 (2)	0 (0)	6 (2)	5 (2)	1 (1)
Gastrointestinal	14 (38)	10 (27)	4 (11)	9 (50)	7 (39)	3 (17)	40 (17)	36 (15)	4 (2)	66 (21)	55 (22)	11 (16)
Hepatobiliary	4 (11)	2 (5)	2 (5)	5 (28)	2 (11)	5 (28)	15 (6)	11 (5)	6 (3)	39 (12)	20 (8)	19 (27)
Musculo-skeletal	2 (5)	2 (5)	0 (0)	1 (6)	0 (0)	1 (6)	18 (8)	16 (7)	3 (1)	22 (7)	18 (7)	4 (6)
Nervous system	0 (0)	0 (0)	0 (0)	2 (11)	2 (11)	0 (0)	10 (4)	8 (3)	2 (1)	14 (4)	11 (4)	3 (4)
Renal	0 (0)	0 (0)	0 (0)	0 (0)	0 (0)	0 (0)	2 (1)	1 (0)	1 (0)	2 (1)	1 (0)	1 (1)
Respiratory	1 (3)	1 (3)	0 (0)	1 (6)	1 (6)	0 (0)	26 (11)	13 (6)	13 (6)	28 (9)	15 (6)	13 (19)

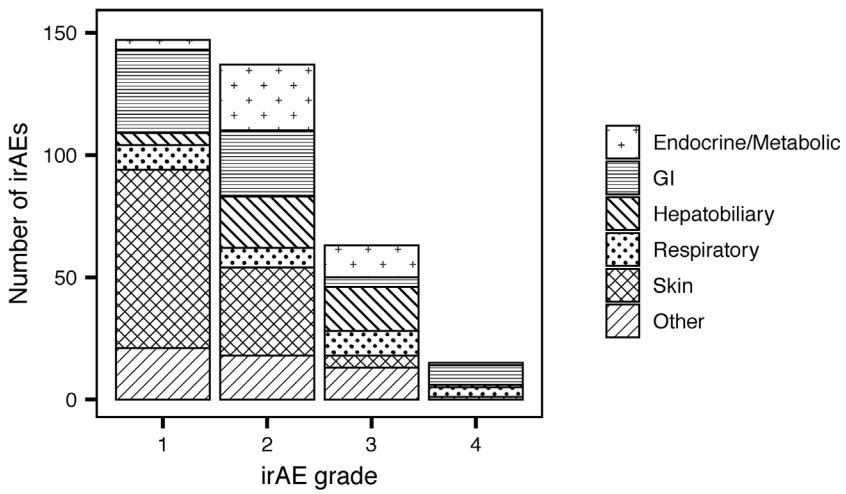

FIGURE 1 | Numbers of reported immune-related adverse events (irAEs) by severity and type.

respiratory irAEs was also observed in patients undergoing CPI therapy for NSCLC with at least one respiratory irAE reported in 17% of NSCLC patients (**Figure 3**). These differences were significant even with a multiple testing correction applied (**Figure 4**). To account for the possible confounding effect of *ipilimumab*, used predominantly in treatment of melanoma patients, we conducted a subgroup analysis of patients only treated with anti-PD-1/PD-L1 CPIs. Within this subset, significantly more respiratory irAEs were reported in NSCLC patients than in patients with other diagnoses (OR = 2.4, $P < 0.03$, Fisher's exact test) and significantly more skin-related irAEs were reported in melanoma patients than in patients with other diagnoses (OR = 2.9, $P = 0.01$, Fisher's exact test). No melanoma patients developed vitiligo, a skin irAE reported in the literature. A positive correlation ($P < 0.05$) between gastrointestinal irAEs was observed in patients with renal cell carcinoma (RCC).

Factors Impacting Survival

Using a time-dependent Cox proportional hazard regression analysis to model irAEs as a binary time-dependent covariate, we observed a clear relationship between irAE and improved survival (HR = 0.41, 95% CI 0.29 to 0.57, $P < 0.001$) (12–14). To account for potential bias due to variability in survival times, we also employed a landmark approach to assess the effects of irAEs and the impact on OS models (11). We employed a 6-week landmark based on the median time to first irAE and to be consistent with previous studies that have used landmark times between 6 and 12 weeks (3, 12–14). Using this approach, we observed a median survival of 57.1 weeks in patients without irAEs and 78.1 weeks in patients with irAEs. However, these differences were not statistically significant (HR = 0.78, 95% CI 0.54 to 1.13, $P = 0.19$, **Figure 5A**). We observed significantly worse OS in patients who experienced sustained steroid treatment prior to CPI treatment, which may have resulted in a less robust response to

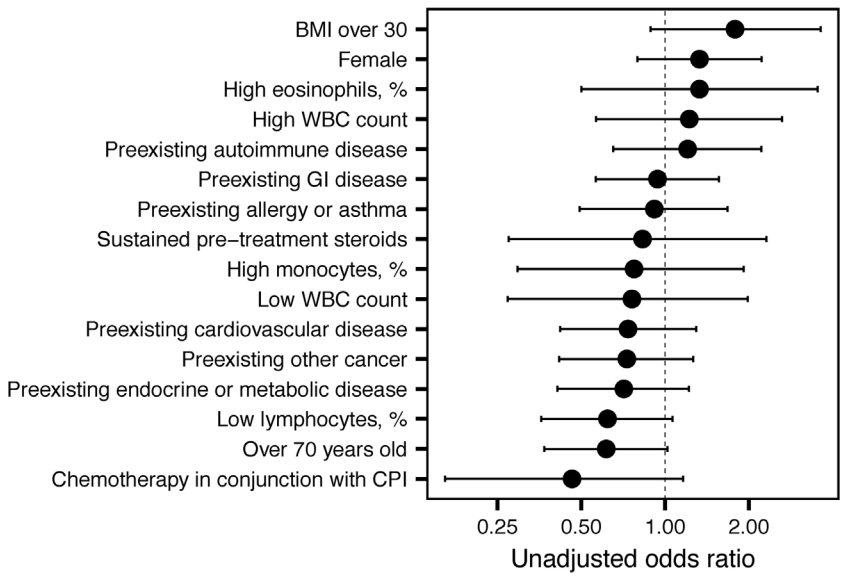

FIGURE 2 | Unadjusted odds ratios for immune-related adverse event (irAE) development. Unadjusted odds ratios and 95% confidence intervals are shown for the indicated variables.

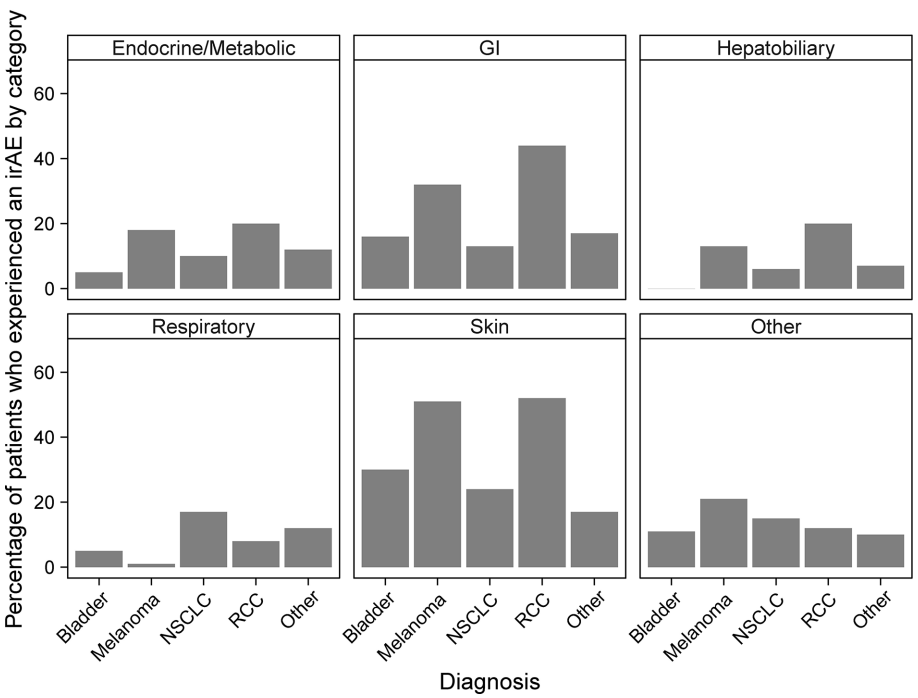

FIGURE 3 | Percentages of patients who experience immune-related adverse events (irAEs) by cancer diagnosis and irAE type. Bars report the percentage of patients with the indicated diagnosis who experienced at least one irAE of the type indicated by the panel title.

CPI. Among PD1/PDL1 treated patients, we identified 21 patients (9%) who received steroids with a prednisone-equivalent dose of 20 mg or higher at least four times in the six months prior to CPI administration. This sustained steroid treatment was associated with significantly worse OS in this patient population (HR = 2.16, 95% CI 1.39 to 3.61, P = 0.003, **Figure 5B**). No patients with sustained steroid treatment were identified in other CPI classes. We also identified 20 individuals who were administered a prednisone-equivalent dose of 20 mg or higher in the month following the first CPI infusion. The OS of this patient group did

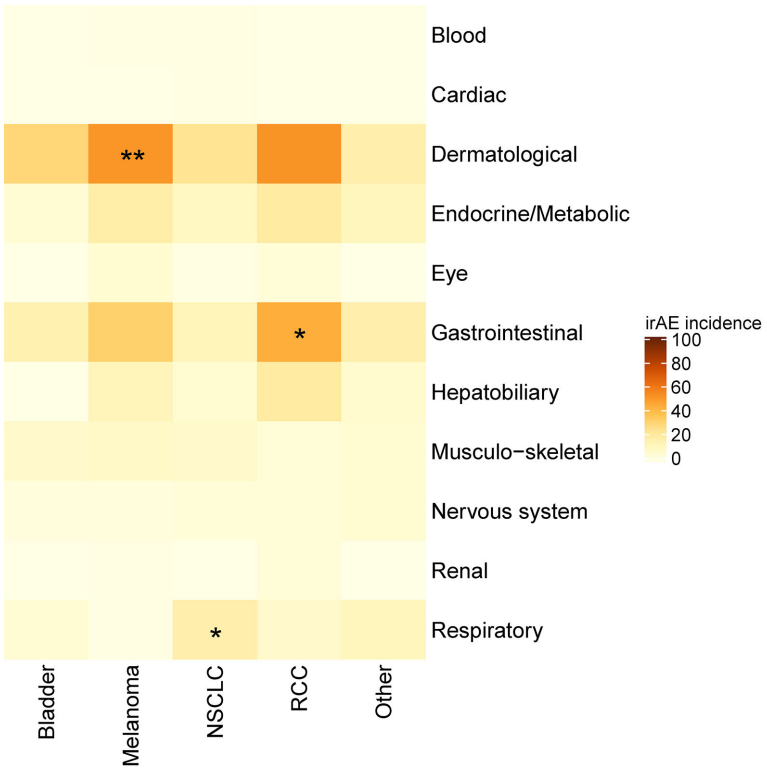

FIGURE 4 | Heatmap showing the incidence of immune-related adverse events (irAEs) according to cancer diagnosis. Color indicates the percent of individuals with a diagnosis (column) who experienced an irAE of the indicated class (row). Asterisks indicate a significance, *p < 0.05, **p < 0.01 (Fisher's exact test with a false discovery rate multiple testing correction applied).

not differ significantly from the group that did not receive steroids following CPI administration (HR = 1.38, 95% CI 0.33 to 1.56, P = 0.41). The only other factor that showed a significant association with OS was pre-treatment BMI > 30 kg/m^2 (p = 0.03). A subset analysis employing an adjustment for patient BMI of the two largest patient populations, NSCLC and melanoma, revealed a significant OS benefit in patients with NSCLC who experienced irAEs (adjusted HR = 0.43, 95% CI 0.21 to 0.93, P = 0.03, **Figure 5C**), but not in melanoma (adjusted HR = 1.35, 95% CI 0.58 to 3.14, P = 0.49, **Figure 5D**).

DISCUSSION

We undertook this study to assess the impact of tumor type and other preexisting factors on the development and type of irAEs, while also examining the effect of irAEs on OS. The study is based on a retrospective analysis of the irAEs observed across a diverse set of malignancies. In this study, no exclusions were imposed based on preexisting conditions or other comorbid conditions that frequently preclude participation in clinical trials, which represent the "real world" experience of the irAEs in cancer patients treated with CPIs and the outcomes.

We employed two methods to evaluate the OS benefit: a landmark survival analysis, which excluded patients who died in the first 6 weeks of treatment and a time-dependent covariate analysis which included all patients. Previous studies of NSCLC and melanoma have reported an association between improved survival and irAE experience using survival analyses with 6 to 12-week landmarks. Our 6-week landmark analysis confirmed an association between survival and irAEs in NSCLC patients but was inadequately powered in the "no-irAE" group to assess survival of melanoma patients on the basis of irAE. The result in NSCLC patients is consistent with previously reported results in which a 6-week landmark analysis of 134 NSCLC patients receiving NIVO demonstrated increased progression-free survival (PFS) and OS in patients who experienced an irAE (3).

The landmark analysis also revealed a trend towards an OS benefit in individuals experiencing an irAE in the first 6 weeks of treatment. For this reason, OS was also calculated as a time-dependent variable which included patients who experienced irAEs within the first 6 weeks of treatment (3, 12–14). This analysis identified a highly significant association between irAEs and OS. Sato and colleagues also noted an association between irAEs and PFS in the absence of a landmark or other accounting for the time-dependence of irAEs in 38 NSCLC patients treated with NIVO (15). Teroaka et al. reported an association between irAEs and survival in NIVO-treated NSCLC patients with a 2-week landmark time (16). Based on our comparison of the landmark and time-dependent analyses, we propose that a

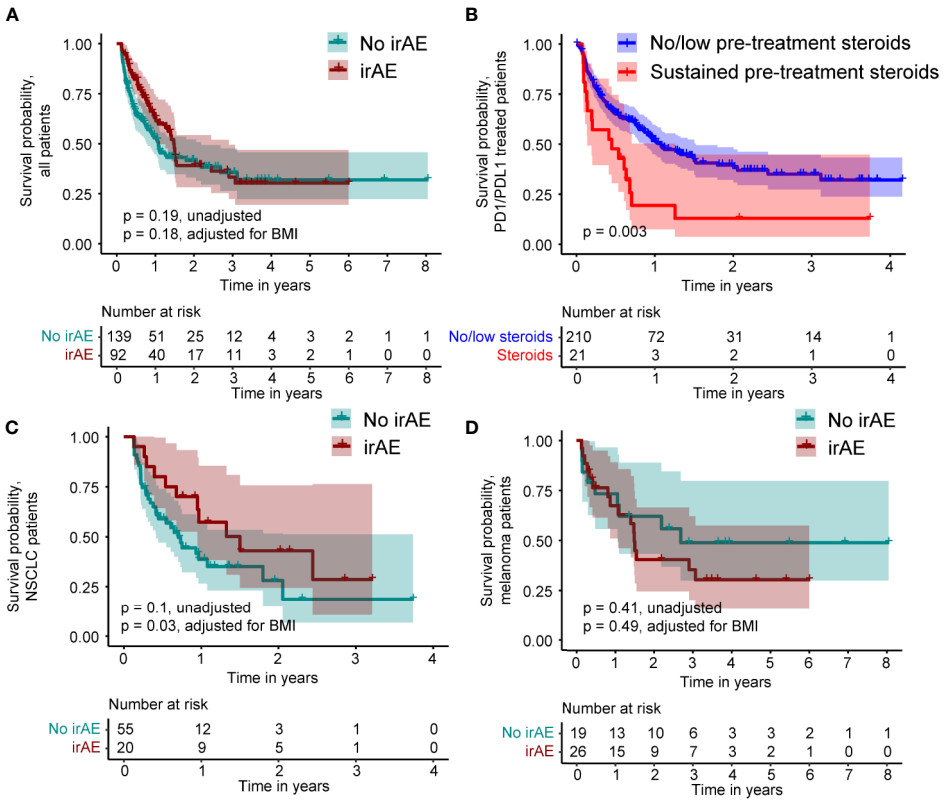

FIGURE 5 | Kaplan-Meier survival curves comparing patients who do and do not experience an immune-related adverse event (irAE) in the 6-week landmark analysis and survival relative to pre-treatment steroid administration. **(A)** Survival of all patients. **(B)** Survival relative to pre-treatment steroid administration in PD1/PDL1 treated patients. **(C)** Survival within the subset of non-Small Cell Lung Cancer (NSCLC) patients. **(D)** Survival within the subset of melanoma patients.

time-dependent treatment of irAEs may be a more relevant measure of survival benefit, since landmark analyses, by definition, do not account for early irAEs. Relative to time-dependent Cox regression, landmark analyses have been shown to attenuate the effect of a time-dependent covariate and our results are consistent with this observation (11).

None of the preexisting comorbid conditions which we evaluated (e.g., cardiovascular disease, autoimmune disease, etc.) altered the overall incidence or type of irAEs experienced by the various patient subgroups, but the higher incidence of grade 3 or 4 irAEs which we detected in patients with preexisting autoimmune disease did appear to be clinically relevant ($P = 0.01$). However, in this subset of 58 patients, there was no obvious link between the type of irAE experienced and the underlying autoimmune condition. Thus, although exacerbations of preexisting autoimmune disease are a predicted consequence of CPI treatment, this was not observed in our study (17). Our data do suggest that patients with preexisting autoimmune disease are more prone to developing serious irAEs of any type, thus emphasizing the need for careful monitoring of this patient population. Most irAEs were managed with corticosteroids and irAEs subsided without permanent discontinuation of CPI therapy. Recent studies do suggest that limiting the use of corticosteroids to the lowest dose possible to achieve clinical benefit may lead to better control of cancer for these patients (18). In one study, NSCLC patients treated with ≥ 10 mg of prednisone at the time of CPI initiation had worse outcomes than patients who received 0 to < 10 mg of prednisone. The authors suggest that this difference may be driven by a poor-prognosis subgroup of patients who receive corticosteroids for palliative reasons (19).

Our most significant finding is that the lung and skin irAEs correlate with the primary tumor sites for both NSCLC and melanoma. This suggests, that at least in these two diseases, the irAEs are an important biomarker of a specific tumor-directed response. Previous reports have suggested that the incidence of respiratory irAEs is similar between NSCLC and melanoma patients, however our data do not support this conclusion (20, 21). In our cohort of 68 melanoma patients, only one patient experienced pneumonitis, a significantly lower incidence than in NSCLC (p = 0.01, Fisher's exact test). In this study, the incidence of respiratory irAEs was higher than in other published reports (22). This difference may be due to the challenge in distinguishing pneumonia due to infection from pneumonitis due to CPI treatment. With respect to melanoma, we observed a strong association between the skin irAEs and melanoma, but no association with OS. We hypothesize that the skin rashes, which occur early in the treatment with CPIs, may predict later development of vitiligo, another skin-related irAE that is

associated with successful anti-melanoma responses (23). The pathogenesis of vitiligo is unknown, but one potential link may be epitope spreading, in which initial immune activity against one or more tumor-specific epitope extends to antigens shared by melanoma cells and melanocytes (24).

The main limitation of this study is its retrospective design and the inclusion of data generated by multiple treating physicians. Due to potential variability in practice patterns, there could be inconsistencies in the reporting of irAEs, patient follow-up, and administration of interventions to reduce or prevent irAEs. We sought to mitigate these variables by having the treating physicians review their medical records and confirm the irAE grade assignment. Certain irAEs, e.g., pneumonitis, were radiographically diagnosed and therefore not associated with the bias of oncologist's notation of the irAE. Furthermore, all oncologists involved in this study treated multiple cancer types, which mitigates the risk of reporting diagnosis specific effects being associated with an individual physician. Therefore, we believe that the timing of irAEs post-CPI treatment, was consistent across all treating physicians, suggesting no specific interference of effect.

Use of a broad study interval for CPI experience, in this case July 2011–October 2019, though inclusive for patients, is also a potential limitation given that clinical experience in managing irAEs has increased over time. In addition, the number of CPIs and their applicability across different tumor types have also increased over time. The newer CPIs are purported to have less side effects. A review of treatments by year indicated that the incidence of irAEs remained consistent, although the severity dropped as ipilimumab was replaced by less toxic PD1/PDL1 inhibitors for the treatment of metastatic melanoma. In recent years, the combination of CPIs with cytotoxic chemotherapy (e.g., pembrolizumab plus platinum-based agents), may have contributed to the heterogeneity of reported irAEs. Chemotherapy may have inherent immunosuppressive effects, albeit low and variable, and also some regimens (e.g., carboplatin/paclitaxel) may incorporate a single time low-dose of steroids. These factors may have led to a lower incidence of irAEs in this cohort. With respect to findings of interstitial pneumonia in this cohort, we note that interstitial pneumonitis is a rare complication of paclitaxel and does not increase the incidence of pneumonitis compared to patients treated with pembrolizumab as single therapy (25, 26). While we hope to establish a consistent grading system for future retrospective analyses of responses to therapy, we note that the frequencies of irAEs identified in this study are not dissimilar from those reported in the literature.

In conclusion, there is growing evidence that irAEs may be directly linked to improved survival in cancer patients treated with CPIs. We undertook this retrospective study to identify clinical factors that inhibit or contribute to an active irAE response. A time-dependent analysis confirmed a significant association between irAEs and OS. We observed a clear association between skin-related irAEs and melanoma as well as between respiratory irAEs and NSCLC, suggesting that these two types of irAEs may be driven by specific immune responses to the primary tumor. In patients with NSCLC, the respiratory irAEs were associated with a survival benefit.

DATA AVAILABILITY STATEMENT

The raw data supporting the conclusions of this article will be made available by the authors, without undue reservation.

ETHICS STATEMENT

The studies involving human participants were reviewed and approved by Benaroya Research Institute Institutional Review Board. Written informed consent for participation was not required for this study in accordance with the national legislation and the institutional requirements.

AUTHOR CONTRIBUTIONS

Conception and design: LR, JKF, JPF, PV, and DA. Development of methodology: LR and HD. Acquisition of data: LR and AM. Analysis and interpretation of data: HD and LR. Writing, review, and revision of the manuscript: LR, HD, JKF, JPF, PV, and DA. Administrative, technical, or material support: LR and HD. All authors contributed to the article and approved the submitted version.

FUNDING

This work was funded by Benaroya Research Institute, not by a grant.

ACKNOWLEDGMENTS

We thank Margaret T. Mandelson, PhD, for her guidance on retrospective analyses and Virginia M. Green, PhD, for editorial assistance.

REFERENCES

1. Keung EZ, Wargo JA. The current landscape of ommune checkpoint inhibition for solid malignancies. *Surg Oncol Clin N Am* (2019) 28:369–86. doi: 10.1016/j.soc.2019.02.008
2. Schadendorf D, Wolchok JD, Hodi FS, Chiarion-Sileni V, Gonzalez R, Rutkowski P, et al. Efficacy and Safety Outcomes in Patients With Advanced Melanoma Who Discontinued Treatment With Nivolumab and Ipilimumab Because of Adverse Events: A Pooled Analysis of Randomized Phase II and III Trials. *J Clin Oncol* (2017) 35:3807–14. doi: 10.1200/JCO.2017.73.2289
3. Haratani K, Hayashi H, Chiba Y, Kudo K, Yonesaka K, Kato R, et al. Association of immune-related adverse events with nivolumab efficacy in Non-Small-Cell Lung Cancer. *JAMA Oncol* (2018) 4:374–8. doi: 10.1001/jamaoncol.2017.2925
4. Rogado J, Sanchez-Torres JM, Romero-Laorden N, Ballesteros AI, Pacheco-Barcia V, Ramos-Levi A, et al. Immune-related adverse events predict the therapeutic efficacy of anti-PD-1 antibodies in cancer patients. *Eur J Cancer* (2019) 109:21–7. doi: 10.1016/j.ejca.2018.10.014
5. Conforti F, Pala L, Bagnardi V, De Pas T, Martinetti M, Viale G, et al. Cancer immunotherapy efficacy and patients' sex: a systematic review and meta-analysis. *Lancet Oncol* (2018) 19:737–46. doi: 10.1016/S1470-2045(18)30261-4

6. Kugel CH,3, Douglass SM, Webster MR, Kaur A, Liu Q, Yin X, et al. Age correlates with response to anti-PD1, reflecting age-related differences in intratumoral effector and regulatory T-cell populations. *Clin Cancer Res* (2018) 24:5347–56. doi: 10.1158/1078-0432.CCR-18-1116
7. McQuade JL, Daniel CR, Hess KR, Mak C, Wang DY, Rai RR, et al. Association of body-mass index and outcomes in patients with metastatic melanoma treated with targeted therapy, immunotherapy, or chemotherapy: a retrospective, multicohort analysis. *Lancet Oncol* (2018) 19:310–22. doi: 10.1016/S1470-2045(18)30078-0
8. Kennedy LC, Bhatia S, Thompson JA, Grivas P. Preexisting autoimmune disease: Implications for immune checkpoint inhibitor therapy in solid tumors. *J Natl Compr Canc Netw* (2019) 17:750–7. doi: 10.6004/jnccn.2019.7310
9. George S, Zheng Y, Kim R, Yu T, Dreyfus J, Gayle JA, et al. Real world outcomes of immune-related adverse events (irAEs) among patients receiving immune checkpoint inhibitors (ICIs) in hospital settings. *Ann Oncol* (2019) 30:v475–532. doi: 10.1093/annonc/mdz253.109
10. US Department of Health and Human Services. Common Terminology Criteria for Adverse Events (CTCAE) Version 5.0. November 27, 2017.
11. Putter H, van Houwelingen HC. Understanding Landmarking and Its Relation with Time-Dependent Cox Regression. *Stat Biosci* (2017) 9:489–503. doi: 10.1007/s12561-016-9157-9
12. Cortellini A, Chiari R, Ricciuti B, Metro G, Perrone F, Tiseo M, et al. Correlations between the immune-related adverse events spectrum and efficacy of anti-PD1 immunotherapy in NSCLC patients. *Clin Lung Cancer* (2019) 20:237–47 e1. doi: 10.1016/j.cllc.2019.02.006
13. Freeman-Keller M, Kim Y, Cronin H, Richards A, Gibney G, Weber JS. Nivolumab in resected and unresectable metastatic melanoma: Characteristics of immune-related adverse events and association with outcomes. *Clin Cancer Res* (2016) 22:886–94. doi: 10.1158/1078-0432.CCR-15-1136
14. Fukihara J, Sakamoto K, Koyama J, Ito T, Iwano S, Morise M, et al. Prognostic impact and risk factors of immune-related pneumonitis in patients with Non-Small-Cell Lung Cancer who received programmed death 1 inhibitors. *Clin Lung Cancer* (2019) 20(6):442–50. doi: 10.1016/j.cllc.2019.07.006
15. Sato K. Correlation between immune-related adverse events and efficacy in non-small cell lung cancer treated with nivolumab. *Lung Cancer* (2018) 115:71–4. doi: 10.1016/j.lungcan.2017.11.019
16. Teraoka S, Fujimoto D, Morimoto T, Kawachi H, Ito M, Sato Y, et al. Early Immune-Related Adverse Events and Association with Outcome in Advanced Non-Small Cell Lung Cancer Patients Treated with Nivolumab: A Prospective Cohort Study. *J Thorac Oncol* (2017) 12:1798–805. doi: 10.1016/j.jtho.2017.08.022
17. Menzies AM, Johnson DB, Ramanujam S, Atkinson VG, Wong ANM, Park JJ, et al. Anti-PD-1 therapy in patients with advanced melanoma and preexisting autoimmune disorders or major toxicity with ipilimumab. *Ann Oncol* (2017) 28:368–76. doi: 10.1093/annonc/mdw443
18. Danlos FX, Voisin AL, Dyevre V, Michot JM, Routier E, Taillade L, et al. Safety and efficacy of anti-programmed death 1 antibodies in patients with cancer and pre-existing autoimmune or inflammatory disease. *Eur J Cancer* (2018) 91:21–9. doi: 10.1016/j.ejca.2017.12.008
19. Ricciuti B, Dahlberg SE, Adeni A, Sholl LM, Nishino M, Awad MM. Immune Checkpoint Inhibitor outcomes for patients with Non-Small-Cell Lung Cancer Receiving Baselin Corticosteroids for Palliative versus Nonpaaliative Indications. *J Clin Oncol* (2019) 37(22):1927–34. doi: 10.1200/JCO.19.00189
20. Martins F, Sofiya L, Sykiotis GP, Lamine F, Maillard M, Fraga M, et al. Adverse effects of immune-checkpoint inhibitors: epidemiology, management and surveillance. *Nat Rev Clin Oncol* (2019) 16:563–80. doi: 10.1038/s41571-019-0218-0
21. Naidoo J, Wang X, Woo KM, Iyriboz T, Halpenny D, Cunningham J, et al. Pneumonitis in Patients Treated With Anti-Programmed Death-1/Programmed Death Ligand 1 Therapy. *J Clin Oncol* (2017) 35:709–17. doi: 10.1200/JCO.2016.68.2005
22. Cadranel J, Canellas A, Matton L, Darrason M, Parrot A, Naccache JM, et al. Pulmonary complications of immune checkpoint inhibitors in patients with nonsmall cell lung cancer. *Eur Respir Rev* (2019) 28:190058. doi: 10.1183/16000617.0058-2019
23. Lo JA, Fisher DE, Flaherty KT. Prognostic Significance of Cutaneous Adverse Events Associated With Pembrolizumab Therapy. *JAMA Oncol* (2015) 1:1340–1. doi: 10.1001/jamaoncol.2015.2274
24. Ma Y, Pitt JM, Li Q, Yang H. The renaissance of anti-neoplastic immunity from tumor cell demise. *Immunol Rev* (2017) 280:194–206. doi: 10.1111/imr.12586
25. Seliger B. Combinatorial Approaches With Checkpoint Inhibitors to Enhance Anti-Tumor Immunity. *Front Immunol* (2019) 10:999. doi: 10.3389/fimmu.2019.00999
26. FDA Keytruda Prescribing Information. (2014). Available at: https://www.accessdata.fda.gov/drugsatfda_docs/label/2018/125514s041lbl.pdf (Accessed November 2, 2020).

Conflict of Interest: The authors declare that the research was conducted in the absence of any commercial or financial relationships that could be construed as a potential conflict of interest.

frontiers in Oncology

MINI REVIEW
published: 11 February 2021
doi: 10.3389/fonc.2020.585311

Biomarkers of Checkpoint Inhibitor Induced Immune-Related Adverse Events—A Comprehensive Review

Josefien W. Hommes[1†], *Rik J. Verheijden*[2†], *Karijn P. M. Suijkerbuijk*[2‡] *and Dörte Hamann*[1,3*‡]

[1] Center for Translational Immunology, University Medical Center Utrecht, Utrecht, Netherlands, [2] Department of Medical Oncology, Cancer Center, University Medical Center Utrecht, Utrecht, Netherlands, [3] Central Diagnostic Laboratory, University Medical Center Utrecht, Utrecht, Netherlands

OPEN ACCESS

Edited by:
Maysaloun Merhi,
Hamad Medical Corporation, Qatar

Reviewed by:
Ekaterina Jordanova,
Center for Gynaecologic Oncology Amsterdam, Netherlands
Shaheen Khan,
University of Texas Southwestern Medical Center, United States

***Correspondence:**
Dörte Hamann
d.wenzlau@umcutrecht.nl

[†]These authors have contributed equally to this work

[‡]These authors have contributed equally to this work

Specialty section:
This article was submitted to Cancer Immunity and Immunotherapy, a section of the journal Frontiers in Oncology

Received: 20 July 2020
Accepted: 19 November 2020
Published: 11 February 2021

Citation:
Hommes JW, Verheijden RJ, Suijkerbuijk KPM and Hamann D (2021) Biomarkers of Checkpoint Inhibitor Induced Immune-Related Adverse Events—A Comprehensive Review. Front. Oncol. 10:585311. doi: 10.3389/fonc.2020.585311

Immune checkpoint inhibitors (ICIs) have substantially improved the prognosis of patients with different types of cancer. Through blockade of cytotoxic T-lymphocyte antigen 4 (CTLA-4) and programmed cell death protein 1 (PD-1), negative feedback mechanisms of the immune system are inhibited, potentially resulting in very durable anti-tumor responses. Despite their promise, ICIs can also elicit auto-immune toxicities. These immune-related adverse events (irAEs) can be severe and sometimes even fatal. Therefore, being able to predict severe irAEs in patients would be of added value in clinical decision making. A search was performed using "adverse events", "immune checkpoint inhibitor", "biomarker", and synonyms in PubMed, yielding 3580 search results. After screening title and abstract on the relevance to the review question, statistical significance of reported potential biomarkers, and evaluation of the remaining full papers, 35 articles were included. Five additional reports were obtained by means of citations and by using the similar article function on PubMed. The current knowledge is presented in comprehensive tables summarizing blood-based, immunogenetic and microbial biomarkers predicting irAEs prior to and during ICI therapy. Until now, no single biomarker has proven to be sufficiently predictive for irAE development. Recommendations for further research on this topic are presented.

Keywords: biomarker, immune checkpoint inhibition, immunotherapy, cytokines, blood cells, review (article), checkpoint inhibitor toxicity, immune-related adverse event

INTRODUCTION

Since the U.S. Food and Drug administration (FDA)'s approval of ipilimumab for metastatic melanoma patients in 2011, immune checkpoint inhibitors (ICIs) have become an important treatment for many cancer patients (1). Since then, ICIs have been approved for a wide range of cancer types, including melanoma, kidney cancer, lung cancer, lymphoma, and liver cancer (1). Immune checkpoints successfully targeted by ICIs are cytotoxic T lymphocyte antigen 4 (CTLA-4) and programmed cell death protein 1 (PD-1).

Immune checkpoints play an important role in immune homeostasis by controlling immune responses, maintaining self-tolerance and preventing autoimmunity. ICIs are monoclonal

antibodies that specifically target immune checkpoints and block their function. Upon initial response of a T cell to an antigen, CTLA-4 is upregulated on its membrane and competes with CD28 for binding B7-1 (CD80) and B7-2 (CD86) on antigen presenting cells (APCs) by binding with higher affinity (2). In contrast to CD28 which is a costimulatory factor on T cells, CTLA-4 inhibits further activation of effector T cells. Furthermore, CTLA-4 expression on regulatory T cells (Tregs) may result in trans-endocytosis of B7-1 and B7-2 on APCs, thereby leaving APCs without costimulatory factors. PD-1, upon binding its ligands (PD-L1 and to a lesser extend PD-L2), which are mainly present on non-lymphoid cells in peripheral tissues, generates local tolerance by dephosphorylating the T-cell receptor, leading to T-cell exhaustion (2). By blocking the above described tolerance mechanisms, ICIs enforce anti-tumor immunity, which has clinically proven to result in long-lasting responses even after stopping treatment.

As a consequence of their mechanism of action, ICIs can cause immune-related adverse events (irAEs). The onset of irAEs is highly unpredictable, as they may develop early after ICI treatment up to more than 18 months after treatment started (3, 4). Furthermore, patients do not necessarily develop a single irAE, but may develop multiple different irAEs, either simultaneously or subsequently (5). Severity of irAEs is graded according to the Common Terminology Criteria for Adverse Events (CTCAE) on a scale from 1 (mild) to 5 (death) (6). IrAE frequency differs per ICI treatment, with any irAE occurring in 60%–85% of anti-CTLA-4 treated patients, 57%–85% of anti-PD-1 treated patients, and 95% in patients receiving combined CTLA-4 and PD-1 blockade (7). Severe irAEs (≥grade 3) occur in approximately 10%–27% of anti-CTLA-4 treated patients, 7%–20% of anti-PD-1 treated patients, and 55% of patients receiving combined anti-CTLA-4 and anti-PD-1 (7). Patterns of irAEs differ per ICI type. As an example, colitis occurs more frequently in anti-CTLA-4 treated patients while thyroid disorders are more frequently seen during anti-PD-1 therapy (8). While CTLA-4 is thought to inhibit immune responses in an earlier phase, PD-1 inhibits T cells at a later stage in the peripheral tissue. Although it has not been fully understood why irAE profiles differ between anti-CTLA-4 and anti-PD-1 treated patients, some hypotheses have been proposed (4). As an example, the higher frequency of autoantibody-related irAEs such as thyroid disorders in PD-1 treated patients could be a result of the modulation of humoral immunity by PD-1-inhibitors, or of its effects on self-tolerance. Keeping this in mind, biomarkers could very well be ICI type-specific. This hypothesis is supported by data showing that anti-CTLA-4-induced and anti-PD-1-induced colitis are eminently different in their immune cell composition, suggesting a distinct underlying mechanism for these toxicities (9).

Frequently observed irAEs include dermatitis, colitis, and thyroiditis, while especially the more rare irAEs, such as myocarditis, myositis, and encephalitis have a high fatality rate (5). It has been suggested that irAE kinetics differ per organ type. Dermatological irAEs usually develop early, followed by gastrointestinal irAEs such as colitis (after 1 to 3 months), with hepatitis and endocrinopathies occurring later (10). Usually, irAEs are diagnosed once patients experience symptoms, and after alternative diagnoses are ruled out by additional testing, such as imaging, endoscopic evaluation, biopsies or blood tests (11, 12). Treatment depends on the severity of the irAE, and can include temporary or permanent ICI discontinuation, corticosteroids and second line immunosuppressants (3).

With more ICIs being approved and increasing indications, patients and healthcare professionals will progressively be confronted with irAEs. However, diagnosing irAEs is challenging due to their highly variable and often aspecific clinical presentation, which complicates distinguishing irAEs from alternative diagnoses such as infection or tumor progression. This often leads to delay in diagnosis and since early immunosuppressive treatments for irAEs can prevent morbidity and even mortality, biomarkers that can predict or signal irAEs in an early stage are urgently needed (13). A biomarker is defined as a characteristic measured as an indicator of pathogenic processes or responses to an exposure or intervention (14). While starting with proof that a biomarker is statistically associated with the clinical state of interest (i.e., irAEs), subsequent assessment of its diagnostic or predictive accuracy is essential to determine clinical utility. Two types of biomarkers can be distinguished: biomarkers assessed either at baseline or during treatment that predict irAEs, or biomarkers that can be used to signal/diagnose irAEs at the moment of signs or symptoms during treatment. Biomarkers determining the risk of irAE development prior to the start of therapy could be used to stratify patients offering alternative treatments, or monotherapy instead of combination ICIs to patients who are predicted to be at high-risk. However, sufficient discriminative power is a prerequisite for its use in clinical decision making. If, for example, a two times increased risk of severe irAEs is predicted, alternative treatment strategies could be considered (including refraining from ICIs in the adjuvant setting) as well as more intensive clinical monitoring of the patients by more frequent and lower ICI dosing. A biomarker during treatment, signaling upcoming toxicity, could serve as a warning upon which patients could be monitored more strictly, ICIs could be discontinued early or immunosuppressive therapy could be started more rapidly. However, a particularly strong correlation with both timing and severity of toxicity is required to take such far-reaching decisions. Finally, a biomarker that can help to adequately diagnose irAEs at the moment of signs or symptoms during ICI treatment could prevent delay in diagnosis and enable early immunosuppressive management.

In the last years, several studies have been performed searching for potential irAE biomarkers. Recently, two reviews on irAE biomarkers have been published (15, 16). However, these reviews did not include all studies reported. Particularly, studies describing biomarkers during ICI treatment were lacking. In this review we aim to provide an overview of primary articles on blood-based and microbial biomarkers described so far. We performed a search using "adverse events", "immune checkpoint inhibitor", "biomarker", and synonyms in PubMed, yielding 3580 search results (see Appendix 1 for complete search). After screening title and abstract on the relevance to the review

question and evaluation of the remaining full papers, 35 articles were included. Five additional reports were obtained by means of citations and by using the similar article function on PubMed. We excluded case reports and included only papers with statistically substantiated data. The majority of studies analyzed in this review, focused on predictive biomarkers.

BIOMARKERS

An overview of the studies on irAE biomarkers at baseline and during treatment is given in **Tables 1** and **2**, respectively. The studies are discussed in more detail below.

Immune Cells

High neutrophil-to-lymphocyte ratio (NLR) was shown to correlate with worse survival in multiple ICI treated malignancies (56), which might suggest that ICI-induced anti-tumor responses are less effective in these patients. In line with this hypothesis, patients with high NLR might also have a lower risk of immune-mediated toxicities. Indeed, among 391 anti-PD-1 treated patients with various types of malignancies, Eun et al. demonstrated that patients with an NLR ≥ 3 less often experienced irAEs than patients with a low NLR (17). However, the median follow-up time in this study was less than 7 weeks and irAEs were reported in only 17% of patients. In their study amongst 102 anti-PD-1 treated melanoma patients, Peng et al. reported that patients with NLR>5 experienced less irAEs (18). Additionally, they observed that a prognostic nutrition index (PNI), which is calculated from the serum albumin level and total lymphocyte count, of 45 or higher was correlated with increased risk of irAEs. In a third study consisting of 173 anti-PD-(L)1 treated NSCLC patients, Pavan et al. reported that patients with an NLR < 3 had an increased risk of irAEs in univariable analysis, as did patients with a platelet-to-lymphocyte ratio (PLR) < 180. In multivariable analysis however, only a low-PLR remained significant, which was confirmed in a competing risk analysis accounting for death (19). Altogether, these three studies support the hypothesis that high NLR may be associated with less irAEs. However, confirmational studies accounting for time at risk should be conducted to dissect the risk of irAEs from survival.

In a retrospective analysis of 167 anti-PD-1 treated patients, Diehl et al. observed that patients with an absolute lymphocyte count (ALC) > 2,000 at baseline and at one month into therapy significantly more often developed grade ≥ 2 irAEs (20). Additionally, a 10% increase of overall leukocyte count and relative lymphocyte count were associated with grade ≥ 3 irAEs in a univariable analysis of 101 anti-PD-1 treated melanoma patients. However, this association was not significant in adjusted analyses (45).

Since a pathogenic role of eosinophils has been proposed in various autoimmune diseases such as inflammatory bowel disease, primary biliary cirrhosis, bullous pemphigoid, and eosinophilic myocarditis (57), eosinophils might be an interesting biomarker of irAEs. Indeed, two studies reported increased peripheral blood eosinophil counts both at baseline and one month after start of anti-CTLA-4 or anti-PD-1 in patients with irAEs compared to those without (20, 21). While Diehl et al. aimed to study the relationship between lymphocyte counts and irAEs in 167 solid tumor patients treated with anti-PD-1 or anti-PD-1/CTLA-4 combination therapy, they also observed that absolute eosinophil counts correlated to ≥2 grade irAEs. However, the OR was just 1.34 for increments of 100, which may not be clinically relevant. In an analysis of 44 anti-PD-1 treated melanoma patients, Nakamura et al. showed that elevated baseline absolute eosinophil levels (>240/μl) and a relative eosinophil count after one month >3.2% correlated to endocrine irAEs specifically. A third study by Jaber et al. in nine anti-CTLA-4 treated melanoma patients showed increased blood eosinophil levels after onset of dermal irAEs compared to pre-treatment levels, which was not found in 8 patients without irAEs (46). In contrast to these studies, Eun et al. found no correlation of eosinophil counts with toxicity in 391 anti-PD-1 treated patients with various types of malignancies (17). Still, these results demonstrate that eosinophils might play a role in the development of irAEs and could pose as interesting biomarkers.

As key players in cancer immunology and main target cells of ICI therapy (58), T cells are of particular interest in the quest for biomarkers of irAEs. Only few studies reported on specific T-cell subsets. To analyze myeloid-derived suppressor cell (MDSC) and T-cell subsets, Damazzu et al. conducted multi-color flow cytometry on fresh whole blood samples of 44 anti-CTLA-4 treated melanoma patients at baseline and at 12 week time intervals after treatment initiation (22). Although they found no difference in $CD3^+$ count or $CD3^+/CD4^+$ ratio, they demonstrated lower percentages of PD-1-expressing $CD4^+$ and $CD8^+$ T cells at baseline in patients with grade ≥3 irAEs compared to those without. In addition, significant upregulation of PD-1 expression was observed on $CD4^+$ T cells in patients without irAEs. In patients with irAEs, PD-1 was also upregulated on $CD4^+$ T cells but this did not reach statistical significance. In $CD8^+$ T cells, PD-1 expression was significantly upregulated in both patients with irAEs and those without. There were no differences in MDSC subsets in patients with or without severe toxicities. Chaput et al. reported that patients with anti-CTLA-4-induced colitis had higher absolute $CD4^+$ T-cell numbers at baseline in peripheral blood compared to non-colitis patients according to flow-cytometry analysis. The difference did not reach statistical significance ($p = 0.053$) (23). Whereas Damazzu et al. did not report on regulatory T-cells (Tregs), Chaput et al. reported that the percentage of Tregs at baseline in patients with anti-CTLA-4-induced colitis was significantly lower compared to non-colitis patients, although absolute numbers were not significantly different. Taken together, although correlations of some T-lymphocyte subsets with irAEs have been reported, further research is needed to prove their predictive value.

Changes in T-cell receptor repertoire in peripheral blood early during treatment were linked to irAEs in two studies reporting on anti-CTLA-4 treatment combined with either androgen deprivation therapy (ADP) or granulocyte-macrophage colony-stimulating factor (GM-CSF) (47, 48). Both studies used

TABLE 1 | Potential biomarkers for irAE development measured prior to ICI treatment.

Potential biomarker	Determinant	Results	Significance	Accuracy	Cancer type	n	Treatment	Study design	References
Cellular									
Neutrophil to lymphocyte ratio (NLR)	Ratios calculated from peripheral neutrophil, eosinophils and lymphocyte count; and albumin	NLR ≥3 associated with less irAEs	OR_{adj} = 0.37; 95%CI 0.17–0.81; p = 0.012	–	Solid tumor	391	Anti-PD-1	Retrospective cohort	(17)
NLR; prognostic nutrition index (PNI)	Ratio calculated from neutrophil and lymphocyte counts; LDH and serum albumin	Low NLR (<5) and high PNI (≥45) independently associated with irAEs	p < 0.001 | p = 0.001	–	NSCLC	102	Anti-PD-1	Retrospective cohort	(18)
Platelet to lymphocyte ratio (PLR)	Ratios calculated from peripheral neutrophil, lymphocyte, and platelet counts	PLR <180 associated with irAEs	OR_{adj} = 2.3; 95%CI 1.1–4.8; p = 0.027	–	NSCLC	173	Anti-PD-(L)1	Retrospective cohort	(19)
Eosinophils	Peripheral blood cell counts	Eosinophil count associated with grade ≥2 irAEs	OR_{adj} = 1.003; 95%CI 1.000–1.006; p = 0.027	–	Solid tumor	167	Anti-PD-1, combination	Retrospective cohort	(20)
	Peripheral blood cell counts	Eosinophil count of >240/μl associated with endocrine (but not any) irAEs	OR = 7.0; 95%CI 1.50–32.72; p = 0.0134	Sens = 88% Spec = 50%	Advanced melanoma	44	Anti-PD-1	Retrospective cohort	(21)
Lymphocytes	Peripheral blood cell counts	Lymphocyte count >2,000 associated with risk of grade ≥2 irAEs	OR_{adj} = 1.996; 95% CI 1.16–3.49; p = 0.014	–	Solid tumor	167	Anti-PD-1, combination	Retrospective cohort	(20)
	Myeloid and T cell subsets by flow cytometry	Lower % PD-1 expression on CD4+ and CD8+ T cells associated with grade ≥3 irAEs	p = 0.025 | p = 0.022	–	Metastatic melanoma	44	Anti-CTLA-4	Retrospective cohort	(22)
	CD4+ T cells and Treg cells counts at baseline	Lower percentage of Tregs associated with colitis	p = 0.018	–	Metastatic melanoma	18	Anti-CTLA-4	Prospective cohort	(23)
Cytokines/Chemokines									
IL-6	5 cytokines and lymphocyte subsets	Lower IL-6 levels associated with grade ≥3 irAEs	OR = 2.84; 95%CI 1.34–6.03; p = 0.007	Sens = 70% Spec = 66%	Metastatic melanoma	140	Anti-CTLA-4	Prospective cohort	(24)
IL-6, IL-8, and sCD25	Baseline IL-6, IL-8 and sCD25 in serum	Lower levels of IL-6, IL-8, and sCD25 associated with colitis	p = 0.008 | p = 0.0031 | p = 0.0097	–	Melanoma	18	Anti-CTLA-4	Prospective cohort	(23)
IL-17	Multiplex serum testing for 36 different cytokines and chemokines	Higher IL-17 levels associated with grade ≥3 colitis and grade ≥3 irAEs	p = 0.02 | p = 0.03	–	Advanced melanoma	35	Anti-CTLA-4	Clinical trial	(25)
Various cytokines/ chemokines	65 cytokines/ chemokines profiles; validated in separate cohort	CYTOX score (G-CSF, GM-CSF, fractalkine, FGF-2, IFNα2, IL1a, IL1B, IL1RA, IL2, IL12p70 and IL13) associated with irAEs that required ICI discontinuation or immunosuppression	p = 0.0366	AUC = 0.68	Melanoma	49	Anti-PD-1 or combination	Prospective cohort	(26)
IL-1β, IL-2, GM-CSF	13 cytokines in serum	Increased levels of IL-1β, IL-2, and GM-CSF correlated with thyroid irAEs	p < 0.05	–	Advanced malignancies	26	Anti-PD-1, anti-CTLA-4, or combination	Prospective cohort	(27)
CXCL9, CXCL10, CXCL11, CCL19	40 cytokines in serum	Lower levels of CXCL9, CXCL10, CXCL11, and CCL19 associated with irAEs	p < 0.05	–	Solid tumor	42	Anti-PD-(L)1	Prospective cohort	(28)

(Continued)

TABLE 1 | Continued

Potential biomarker	Determinant	Results	Significance	Accuracy	Cancer type	n	Treatment	Study design	References
Autoantibodies									
Anti-thyroid antibodies	Thyroid peroxidase and thyroglobulin antibodies in serum	Anti-Tg and anti-TPO associated with thyroid dysfunction	$p < 0.001$ | $p = 0.002$	–	NSCLC	64	Anti-PD-1	Retrospective cohort	(29)
	Anti-thyroid antibodies in serum	Anti-Tg antibody, but not anti-TPO associated with thyroid dysfunction	$OR_{adj} = 26.5$; 95% CI 8.18–85.8; $p < 0.001$ | $p > 0.05$	–	Solid tumor	168	Anti-PD-1	Retrospective cohort	(30)
Anti-BP180 IgG	Serum IgG directed against BP180, BP230, and type VII collagen measured by ELISA	Anti-BP180 IgG levels associated with dermal irAE	$p = 0.04$	–	NSCLC	40	Anti-PD-(L)1	Prospective cohort	(31)
Anti-GNAL and anti-CD74	Identification of autoantibodies using recombinant cDNA expression libraries	Anti-GNAL presence associated with hypophysitis | anti-CD74 presence associated with pneumonitis	OR = 2.66; 95%CI 1.14–7.29; $p = 0.02$ OR = 1.25; 95%CI 1.03–1.52; $p = 0.03$	AUC = 1 for both	Solid tumor	20 32	Anti-CTLA-4, anti-PD-1, combination	Nested prospective cohort	(32)
Various autoantibodies	Autoantibodies tested with HuProt array covering >19,000 proteins	Enrichment of autoantibodies directed against targets in (auto) immunity pathways associated with grade ≥3 irAEs Classification model based on baseline antibody levels predicts risk of developing severe irAEs	$p < 0.05$	- Classification models: Sens≥0.89 Spec≥0.85 for each therapy	Melanoma	75	Anti-CTLA-4, anti-PD-1, combination	Prospective cohort	(33)
Immunogenetics									
Single-nucleotide polymorphisms (SNPs)	7 SNPs in the *PDCD1, PTPN11, ZAP70* and *IFNG* genes analyzed using whole blood DNA sequencing	PDCD1 804C>T associated with increased irAE risk in exploration cohort, but not in validation cohort	$p = 0.039$ | $p = 0.828$	–	NSCLC	161| 161	Anti-PD-1	Prospective cohort	(34)
	166 SNPs in 86 immune or cancer related genes analyzed using sequenom MassArray iPLEX assay	SNPs in *UNG*, *IFNW1*, *IFNL4*, *PD-L1*, and *CTLA-4* associated with grade ≥3 irAEs	$p < 0.05$	AUC = 0.89 Sens = 0.8 Spec = 0.85	Solid tumor	94	Anti-PD-(L)1	Retrospective cohort	(35)
	Polygenic risk scores for skin autoimmunity computed with whole-genome germline sequencing	Psoriasis-associated polygenic risk score associated with skin irAEs	$p < 0.05$	–	Bladder cancer	220	Anti-PD-L1	Retrospective analysis of clinical trial data	(36)
	miR-146a rs2910164 CC genotype	rs2910164 CC genotype associated with grade 3-4 irAEs	OR = 6.78; 95%CI 1.87–24.6; $p = 0.004$	–	Solid tumor	167	Anti-PD-(L)1	Prospective cohort	(37)
Human leukocyte antigen (HLA)	HLA-A*02:01 subtype	No association between HLA-A*0201 status and irAEs	Not reported	–	Melanoma	450	Anti-CTLA-4	Retrospective analysis of pooled clinical trial data	(38)

(Continued)

TABLE 1 | Continued

Potential biomarker	Determinant	Results	Significance	Accuracy	Cancer type	n	Treatment	Study design	References
	HLA loci with common variants associated with autoimmune disease	No association of HLA and risk of any irAE HLA-DRB1*11:01 associated with pruritis and HLA-DQB1*03:01 with colitis	Not reported OR = 4.53; p = 0.002 | OR = 3.94; p = 0.017	–	Melanoma, NSCLC	102	Anti-CTLA-4, anti-PD-1, combination	Prospective cohort	(39)
	HLA subtypes in patients with ICI-induced diabetes	Higher HLA-DR4 frequency compared to general population and spontaneous type I diabetes is associated with ICI-induced diabetes	p < 0.0001 | p = 0.002	–	Solid tumor	23	Anti-CTLA-4, anti-PD-1, combination	Case series	(40)
	HLA haplotypes in patients with ICI-induced adrenal insufficiency	HLA-DR15 associated with pituitary irAEs	p = 0.0014	–	Advanced cancer	11	Anti-PD-1 or anti-CTLA-4	Case-control study	(41)
Microbiome									
Bacteroidetes, Firmicutes	Microbiome composition in fecal samples using 16S rRNA and shotgun metagenomic sequencing	Enrichment of Bacteroidetes in patients without colitis. Lack of pathways involved in vitamin B synthesis associated with increased colitis risk	p < 0.05 | p < 0.05	Sens = 70% spec = 83%	Melanoma	34	Anti-CTLA-4	Prospective cohort	(42)
	Microbiome composition in fecal samples using16S rRNA sequencing	Enrichment of Bacteroidetes in patients without colitis. Enrichment of Firmicutes in patients with colitis	p = 0.011 | p = 0.009	–	Melanoma	26	Anti-CTLA-4	Prospective cohort	(23)
Other									
Thyroid stimulating hormone (TSH)	TSH, free T3 and free T4 in serum	TSH ≥5 µIU/ml associated with increased risk of thyroid dysfunction	OR_{adj} = 7.36; 95%CI 1.66–32.7; p = 0.01	–	Solid tumor	168	Anti-PD-1	Retrospective cohort	(30)
	Serum TSH	TSH >2.19 µIU/ml associated with increased risk of thyroid dysfunction	OR = 3.46; 95%CI 1.2–9.8	AUC = 0.66 Sens = 53% Spec = 76%	Melanoma	99	Anti-PD-1, combination	Retrospective cohort	(43)
Soluble CTLA-4	sCTLA-4 in serum by ELISA	>200 pg/ml sCTLA-4 associated with irAEs	OR_{adj} = 3.63; 95%CI 1.14–11.5; p = 0.029	–	Melanoma	113	Anti-CTLA-4	Prospective cohort	(44)

n, number of patients included in the reported analysis (irrespective of irAE presence); irAE, immune-related adverse event; OR, odds ratio; OR_{adj}, adjusted odds ratio; 95%CI, 95% confidence interval; Sens, sensitivity; Spec, specificity; AUC, area under the receiver operating curve; NSCLC, non-small cell lung cancer; Anti-PD-(L)1, anti-programmed cell death protein (ligand) 1; anti-CTLA-4, anti-cytotoxic T lymphocyte antigen 4; combination, combined anti-CTLA-4 plus anti-PD-1 therapy; ICI, immune checkpoint inhibitor; CD, cluster of differentiation; sCD, soluble CD; Tregs, regulatory T-cells; NLR, neutrophil to lymphocyte ratio; PNI, prognostic nutrition index; PLR, platelet to lymphocyte ratio; IL, interleukin; G-CSF, granulocyte colony-stimulating factor; GM-CSF, granulocyte-macrophage colony-stimulating factor; FGF, fibroblast growth factor; IFN, interferon; CXCL, chemokine C-X-C motif ligand; CCL, chemokine C-C motif; Tg, Thyroglobulin; TPO, Thyroid peroxidase; BP, bullous pemphigoid; IgG, immunoglobulin G; GNAL, guanine nucleotide-binding protein G subunit alpha; SNPs, single-nucleotide polymorphisms; HLA, human leukocyte antigen; TSH, thyroid stimulating hormone; T3, Triiodothyronine; T4, thyroxine; miR, micro-RNA; ELISA, enzyme-linked immunosorbent assay.

next-generation sequencing of CDR3 regions in rearranged T-cell receptor (TCR) β-chains and reported that a more diverse T-cell repertoire is observed in patients with irAEs. Subudhi et al. demonstrated in 16 anti-CTLA-4 + ADP treated patients, that the number of expended clonotypes of $CD8^+$ (but not $CD4^+$) T cells just before toxicity compared to baseline was significantly higher in 11 patients with grade ≥2 irAEs compared to five patients without. An expansion of ≥55 T-cell clones was reported to be 100% sensitive and 42% specific of grade ≥2 irAEs, which was confirmed in a validation cohort of 11 patients. Similarly, Oh et al. reported that an increase in frequency of preexisting clonotypes in the blood was associated with irAEs in a study with 35 anti-CTLA-4 + GM-CSF treated patients. In addition, irAE occurrence was also associated with an increase of newly detected TCR clones. Overall clonality declined in $CD4^+$ and $CD8^+$ T cells at week 2 after treatment initiation in all patients, which was significant in patients with irAEs but not in patients without. Taken together, these data show that anti-CTLA-4-induced increase in T-cell diversity preceded irAEs. This observation is not surprising considering that CTLA-4 suppresses T cells early after activation, thereby preventing T-cell reactions against self-antigens. Thus, blocking CTLA-4 might allow activation of

TABLE 2 | Potential biomarkers for irAE development during ICI treatment.

Potential biomarker	Determinant	Results	Significance	Accuracy	Cancer type	n	Treatment	Study design	References
Cellular									
Leukocytes	Peripheral blood cell counts after irAE onset**	Increase in leukocyte count and decrease in relative lymphocyte count associated with grade ≥3 irAEs in univariable, but not multivariable analysis	OR_{adj} = 1.13; 95%CI 0.99–1.29; p = 0.074 | OR_{adj} = 1.18; 95%CI 0.94–1.48; p = 0.15	–	Melanoma	101	Anti-PD-1	Retrospective cohort	(45)
Eosinophils	Leukocyte subsets at 1, 3 and 6 months*	Absolute eosinophil count after 1 month associated with grade ≥2 irAEs	OR_{adj} = 1.002; 95%CI 1.000–1.004; p = 0.027	–	Solid tumor	167	Anti-PD-1, combination	Retrospective cohort	(20)
	Absolute and relative eosinophil counts after 1, 3 and 6 months*	Relative eosinophil count at 1 month >3.2% associated with endocrine irAEs	OR = 5.11; 95%CI 1.23-21.3; p = 0.025	Sens = 67% Spec = 72%	Melanoma	44	Anti-PD-1	Retrospective cohort	(21)
	Relative eosinophil count after onset of dermal irAEs compared with baseline**	Relative eosinophil count increased during treatment in patients with dermal irAEs, but not in those without	p = 0.006 vs. p = 0.19	–	Melanoma	17	Anti-CTLA-4	Nested case control	(46)
Lymphocytes	Leukocyte subsets at 1, 3 and 6 months*	Lymphocyte count >2,000 at 1 month associated with risk of grade ≥2 irAEs, any irAEs and irAEs requiring treatment	OR_{adj} = 1.81; 95%CI 1.03–3.25; p = 0.039 | p < 0.05 | p < 0.01	–	Solid tumor	167	Anti-PD-1, combination	Retrospective cohort	(20)
	T-cell receptor β-chain sequencing in purified T cells from blood at baseline and before irAE occurrence (median 13 days; IQR 2-24)*	Clonal expansion of ≥55 CD8 T-cell clones associated with grade ≥2 irAEs	p < 0.0001	Sens = 100% Spec = 42% AUC = 0.87	Prostate cancer	27	Anti-CTLA-4 + androgen deprivation	Retrospective analysis of clinical trial data	(47)
	T-cell receptor β-chain sequencing in purified T cells from blood at baseline and week 2*	Clonal expansion of more T-cell clones and higher number of newly emerging T-cell clones are associated with irAEs; decline in T-cell clonality in patients with irAEs at week 2 versus baseline	p = 0.028 | p = 0.042; p = 0.023	–	Prostate cancer	21	Anti-CTLA-4 + GM-CSF	Retrospective analysis of clinical trial data	(48)
	Circulating B-cell changes after the first cycle of treatment compared to baseline*	≥30% decline in B cells and doubling of CD21lo cells or plasmablasts associated with grade ≥3 irAEs	p < 0.001	–	Melanoma	23	Combination of anti-CTLA-4 and anti-PD-1	Prospective cohort	(49)
Cytokines/Chemokines									
IL-6	Pre- and post-treatment serum samples tested for IL-6, TNF-α, IFN-γ, IL-8 and IL-17A analysis?	Increased IL-6 levels in irAE patients post-treatment compared to pre-treatment, not in patients without irAEs	p = 0.018	–	Melanoma	20	Anti-PD-1	Case series	(50)
Various cytokines/ chemokines	65 cytokines/ chemokines profile at week 1-6 validated in separate cohort*	CYTOX score (G-CSF, GM-CSF, fractalkine, FGF-2, IFNα2, IL1a, IL1B, IL1RA, IL2, IL12p70, and IL13) associated with irAEs that required ICI discontinuation or immunosuppression	p = 0.0168	AUC = 0.70	Melanoma	49	Anti-PD-1 or combination	Prospective cohort	(26)
CXCL9, CXCL10	40 cytokines in serum tested at baseline and after 2-3 and 6 weeks*	A greater increase of CXCL9 and CXCL10 at week 6 in irAE patients compared to non-irAE patients	p < 0.05	–	Solid tumor	42	Anti-PD-(L)1	Prospective cohort	(28)

(Continued)

TABLE 2 | Continued

Potential biomarker	Determinant	Results	Significance	Accuracy	Cancer type	n	Treatment	Study design	References
CCL5	75 serum proteins measured by Milliplex MAP assay at baseline and after 4 weeks*	CCL5 levels at 4 weeks in irAE patients increased compared to non-irAE patients	$p < 0.05$	–	NSCLC	32	Anti-PD-1	Prospective cohort	(51)
sCD163	Serum levels of sCD163 and CXCL5 measured at day 0 and day 42*	Change from baseline of sCD163 level at day 42 was higher in irAE patients compared to non-irAE patients	$p = 0.0018$	Sens = 73% Spec = 75%	Melanoma	46	Anti-PD-1	Retrospective cohort	(52)
Autoantibodies									
Anti-thyroid antibodies	Anti-Tg and anti-microsomal antibodies measured at baseline and every cycle during treatment*/**	Anti-Tg present in 80% of patients with thyroid dysfunction compared to 8% of patients without	$p < 0.0001$	–	NSCLC	48	Anti-PD-1	Prospective cohort	(53)
	Autoantibodies tested at baseline and after 4 weeks*	Increased levels of anti-Tg and anti-TPO at 4 weeks compared to baseline associated with thyroid irAEs	$p = 0.012$ | $p = 0.048$	–	Advanced cancer	26	Anti-PD-1, anti-CTLA-4, or combination	Prospective cohort	(27)
Anti-GNAL and anti-ITM2B antibodies	Pre-treatment and post-treatment before irAE analysis with recombinant cDNA libraries	Stronger increase of anti-GNAL and anti-ITM2B in patients with hypophysitis	$p < 0.001$ | $p < 0.001$	AUC = 1 | AUC = 1	Solid tumor	20	Anti-CTLA-4, anti-PD-1, combination	Nested prospective cohort	(32)
Other									
CRP	CRP levels measured at baseline and just before or at irAE onset*/**	CRP levels rose from mean 8.4 mg/L at baseline to 52.7 mg/L at irAE onset	$p < 0.0001$	–	Melanoma	37	Anti-CTLA-4, anti-PD-1, combination	Case series	(12)
	CRP levels at baseline, at irAE onset and after tocilizumab administration**	CRP levels increased from median 23 mg/L at baseline to 109 mg/L at onset of irAEs and decreased to 19 mg/L after irAE treatment	$p < 0.00001$	–	Advanced cancer	34	Anti-PD-1	Case series	(54)
CD177	Gene expression profiling of 9697 non-control probe sets on whole blood samples at baseline, week 3 and 11*	Increased CD177 gene expression at 3 weeks in patients with GI irAEs compared to non-irAE patients and compared to baseline	$p = 0.0076$	–	Melanoma	162	Anti-CTLA-4	Retrospective analysis of clinical trial data	(55)

**before onset of irAEs, either obtained through collection at regular time points or at last measurement before irAE onset; **at onset of irAEs; ?timing not clear from report*
n, number of patients included in the reported analysis (irrespective of irAE presence); irAE, immune-related adverse event; OR, odds ratio; OR_{adj}, adjusted odds ratio; 95%CI, 95% confidence interval; IQR, interquartile range; Sens, sensitivity; Spec, specificity; AUC, area under the receiver operating curve; NSCLC, non-small cell lung cancer; Anti-PD-(L)1, anti-programmed cell death protein (ligand) 1; anti-CTLA-4, anti-cytotoxic T lymphocyte antigen 4; combination, combined anti-CTLA-4 plus anti-PD-1 therapy; ICI, immune checkpoint inhibitor; GM-CSF, granulocyte-macrophage colony-stimulating factor; CD, cluster of differentiation; sCD, soluble CD; IL, interleukin; TNF, tumor necrosis factor; IFN, interferon; G-CSF, granulocyte colony-stimulating factor; FGF, fibroblast growth factor; CXCL, chemokine C-X-C motif ligand; CCL, chemokine C-C motif; Tg, Thyroglobulin; TPO, Thyroid peroxidase; GNAL, guanine nucleotide-binding protein G subunit alpha; ITM, integral membrane protein; CRP, c-reactive protein.

previously suppressed self-reactive T-cell clones and the degree of activation expressed as early diversification of T-cell repertoire after treatment might be associated with occurrence of irAEs. As PD-1 acts later after T-cell activation in the peripheral tissue, the results obtained by Subudhi and Oh et al. may not be translatable to anti-PD-1 therapies.

Three recent papers simultaneously identified B cells as major actors in ICI therapy by demonstrating that B-cell tumor infiltration and formation of tertiary lymphoid tissues was correlated with better prognosis (59–61). The role of B cells and their predictive value in irAEs has however been less well studied. Only one study on B-cell changes has been reported. By using flow cytometry on PBMCs of 23 anti-CTLA-4 + anti-PD-1 treated melanoma patients, at baseline and during follow-up, Das et al. demonstrated that an early decline in B-cell numbers of more than 30% together with a doubling of $CD21^{lo}$ B cells or plasmablasts preceded grade ≥3 irAEs (49). The severity of the decline in B cells was directly correlated with the time of onset of the irAEs.

Cytokines/Chemokines

Various cytokines, such as interleukin (IL)-6 and IL-17, are associated with inflammation and autoimmune diseases (62) and have therefore been proposed as predictors of irAEs.

IL-6, produced by almost all stromal and immune cells, has broad context-dependent pro-inflammatory effects on innate and adaptive immunity and is also important in epithelial homeostasis (62, 63). Two studies reported that lower baseline serum IL-6 was associated with irAEs in anti-CTLA-4 treated melanoma patients. In blood of 140 anti-CTLA-4 treated melanoma patients at baseline, Valpione et al. analyzed LDH, S-100, CRP, β-2-microglobulin, VEGF, IL-2, and IL-6 levels using various techniques including immune-enzymatic methods as well as lymphocyte subsets using flow cytometry (24). They observed that only low baseline IL-6 serum levels (<2.5ng/L) and female sex were correlated with increased risk of grade ≥3 irAEs after adjustment for follow-up time. Similarly, Chaput et al. observed lower levels of IL-6, IL-8, and sCD25 in patients with anti-CTLA-4-induced colitis using multiplex assays (23). Furthermore, Tanaka et al. reported that serum IL-6 levels increased during treatment in all six patients with anti-PD-1-induced psoriasis and all seven patients with other irAEs, while IL-6 levels declined in five out of seven control patients without irAEs according to a multiplex assay (50). In agreement with these findings, C-reactive protein (CRP), a general marker of inflammation, which is sometimes suggested as surrogate marker of IL-6 (64), was reported to rise in patients with irAEs just preceding or at onset of irAEs in two studies (presented under "other" section in **Table 2**). In 37 ICI-treated melanoma patients with 88 cases of irAEs, Abolhassani et al. observed a statistically significant increase of the mean CRP level from 8.4 mg/L at baseline to 52.7 mg/L just before or at onset of irAEs for all 88 cases (12). Similarly, Stroud et al. reported a statistically significant increase in CRP from a median of 23 mg/L at baseline to 109 mg/L at time of irAEs, which decreased to 19 mg/L after tocilizumab (anti-IL-6) in 87 anti-PD-1 treated patients (54). However, a remarkably high percentage of these patients (39%) required tocilizumab to treat the irAE, which suggests selection of patients. Furthermore, neither Abolhassani, nor Stroud et al. reported data on CRP alterations in patients without toxicity, so a rise in CRP during ICI treatment irrespective of irAE development could not be ruled out.

Five additional studies reported on the correlation between numerous cytokines/chemokines and irAEs using multiplex assays consisting of 18 to 65 variables in cohorts ranging from 26 to 49 patients, which yielded contradicting results (**Supplementary Table S1**). In contrast to the studies discussed above, none of these five studies reported a correlation between IL-6 and irAEs (25–28, 51). Nevertheless, IL-6 and CRP could be promising predictors of irAEs if validated in sufficiently powered cohorts.

In a study of 35 anti-CTLA-4 treated patients, Tarhini et al. observed higher baseline IL-17 levels to be associated with grade ≥3 irAEs and colitis, using a multiplex panel of 36 cytokines and chemokines (25). IL-17 is a pro-inflammatory cytokine mainly produced by T-helper 17 (Th17) cells, and contributes to the pathogenesis of several autoimmune diseases, such as psoriasis and rheumatoid arthritis (65). IL-17 seems to have both oncogenic and anti-tumor effects, as comprehensively reviewed by Qian et al. (66) and Th17 cells have been proposed as important actors in irAEs (67). In line with this, colonic mRNA expression of IL-17A was shown to be upregulated in nine anti-CTLA-4-induced colitis patients compared to eight healthy controls as well as interferon-γ, FoxP3, IL-10 and TNF-like molecule TL1A in a study of mRNA expression of 14 inflammatory mediators in colon tissue biopsies (68). In the studies on anti-PD-(L)1 or combination therapy treated patients however, no significant correlation of IL-17 with toxicity was observed.

In an analysis of 65 cytokines or chemokines in combination ICI-treated patients, an aggregated CYTOX score consisting of 12 cytokines/chemokines was associated with severe irAEs in exploratory (n = 58) and validation (n = 49) cohorts at baseline and 1-6 weeks after treatment initiation (26). Three of these 12 parameters (IL-1β, IL-2, and GM-CSF) were also observed to be associated with irAEs among a multiplex assay of 18 cytokines/chemokines in 26 anti-PD-1, anti-CTLA-4 or combined therapy-treated patients (27). Additionally, this study found an early decrease of IL-8, G-CSF, and MCP-1 during treatment to be associated with thyroid irAEs.

With their role in the migration of immune cells into tissues, chemo-attractants may play a crucial role in irAE development. In a 40-plex assay in 65 patients receiving ICIs, Khan et al. observed that CXCL9 (monokine induced by gamma interferon [MIG]), CXCL10 (IFN-γ induced protein -10 [IP-10]), CXCL11 (interferon-inducible T cell α chemoattractant [I-TAC]), and CCL19 (macrophage inflammatory protein 3β [MIP-3β]) were lower at baseline in patients with irAEs compared to those without (28). Furthermore, they reported a greater increase of CXCL9 and -10 in patients with irAEs at 2-3 and 6 weeks after treatment initiation. Interaction of the chemokines CXCL9, -10, and -11 with their receptor CXCR3 can elicit differentiation of naïve T cells into Th1 cells and plays a role in the recruitment of these Th1 cells, cytotoxic T cells and natural killer (NK) cells, as comprehensively reviewed by Tokunaga et al. (69). Another chemoattractant, RANTES (regulated on activation, normal T cell expressed and secreted/CCL5) was observed to be higher in 11 anti-PD-1 treated patients with irAEs compared to the 21 patients without 4 weeks after treatment initiation, but not at baseline (51).

Fujimura et al. reported a greater increase of soluble CD163 after 42 days of anti-PD-1 treatment in 22 patients with irAEs compared to the 24 without, using enzyme-linked immunoassays (ELISA) on serum (52). However, this seems to be mainly due to 3 patients with major increases, as sCD163 levels actually decreased in half of the patients with irAEs. In fact, the authors report a receiver operating characteristic (ROC) curve in which the cut-off level of 21.3% is based on both increase or decrease of sCD163 serum levels.

Autoantibodies

The observation that pre-existing autoantibodies are present in patients with several specific types of irAEs has led to the hypothesis that these play a role in modulation of irAE pathogenesis (4). For example, increased anti-thyroid antibody levels at baseline or during anti-PD-1 treatment were associated

with thyroid dysfunction in three studies (29, 30, 53). The study of Maekura et al. included 64 anti-PD-1 treated NSCLC patients of which serum thyroid peroxidase and thyroglobulin antibody levels were determined with an electrochemiluminescence immunoassay. Five patients developed hyperthyroidism, and this was significantly and positively correlated to the presence of thyroid peroxidase and thyroglobulin antibodies at baseline. A second study by Kimbara et al. in 168 anti-PD-1 treated solid tumor patients reported baseline thyroglobulin antibody levels to be significantly correlated to later thyroid dysfunction after multivariate analysis. However, no correlation of thyroid peroxidase antibodies with thyroid dysfunction was observed in this study. Anti-thyroid antibodies determined during treatment have also been shown to correlate to thyroid dysfunction occurrence. Osorio et al. studied 48 anti-PD-1 treated NSCLC patients and found that 80% of patients with thyroid dysfunction (8 out of 10 patients) displayed anti-thyroglobulin and/or anti-microsomal antibodies compared to 7.8% of patients who did not develop thyroid dysfunction (3 out of 38 patients). Not all patients with anti-thyroglobulin antibodies developed thyroid dysfunction during the study. The majority of patients, 7 out of 11, who were positive for anti-thyroglobulin antibodies developed these antibodies during anti-PD-1 treatment. For six out of these seven patients, antibody presence coincided with thyroid dysfunction onset. Furthermore, Kurimoto et al. studied thyroglobulin and thyroid peroxidase autoantibodies in 26 advanced malignancy patients. Autoantibody levels were determined using an electrochemiluminescence immunoassay. They observed that levels of both autoantibodies showed a more significant increase after four weeks of treatment in patients developing irAEs compared to patients who did not develop irAEs (27). Interestingly, these four studies identified predictive value of anti-thyroid antibodies for irAE development at various time points. Based on the presented data, the strongest predictive value for this biomarker seems to be at baseline.

Various other autoantibodies have been associated with irAE development. One study tested anti-BP-180 IgG (which is associated with bullous pemphigoid) levels by means of ELISA. The authors demonstrated that elevated baseline levels of these antibodies were associated with skin irAEs, but not with irAEs in general in 40 anti-PD-(L)1 treated patients included in the study (31). Using ELISA, baseline anti-GNAL and elevation of both anti-GNAL and anti-ITM2B antibodies during treatment were shown to be associated with hypophysitis in 20 patients and anti-CD74 antibodies with pneumonitis occurrence in 32 patients with solid tumors (32). Finally, one study used a human proteome array covering >19,000 human proteins to assess the presence of autoantibodies against these proteins in serum samples of 75 ICI-treated melanoma patients (33). This study demonstrated a differential expression of autoantibodies in patients with grade ≥3 irAEs compared to those with no or mild irAEs for 914 autoantibodies in 37 anti-CTLA-4 treated patients, for 723 autoantibodies in 27 anti-PD-1 treated patients, and for 1161 autoantibodies in 11 combined anti-CTLA-4 plus anti-PD-1 treated patients. Interestingly, there was only minor overlap in differential expression of autoantibodies in anti-CTLA-4 versus combined and anti-PD-1 versus combined therapy (99 and 54 autoantibodies respectively). Pathway analysis on the protein antigen targets revealed involvement of proteins associated with (auto)immunity. A support vector machine (SVM) classification model was developed to classify patients according to their risk of developing severe immunotherapy-related toxicity based on specific antibody levels in baseline sera. SVM model testing using "curated" antibody lists with lower numbers of antibodies ($n = 45$ for anti-CTLA-4, $n = 25$ for anti-PD-1, $n = 575$ for combination treatment) revealed a high sensitivity (>0.89) and specificity (>0.85) for all treatment groups.

Although autoantibodies have been found that correlate with irAE development, the results certainly warrant further investigation. Remarkably, the strongest correlation of specific autoantibodies with irAE development was seen at baseline. It is well known that organ-specific autoantibodies can be present before onset of clinical symptoms of autoimmune diseases (70). Therefore, patients who present with autoantibodies at baseline might already be prone to develop autoimmune disease irrespective of ICI treatment. Still, ICIs might accelerate the development of immunological disease in these patients. The study of Gowen et al. suggests that prediction models based on baseline random antibody signatures could be further developed as biomarkers to predict toxicity from immunotherapy.

Immunogenetics

Several single-nucleotide polymorphisms (SNPs) in immune-associated gene loci and human leukocyte antigen (HLA) profiles have been described to be associated with irAEs. Associations with anti-PD-(L)1 related irAEs were found for SNPs in UNG, IFNW1, IFNL4, PDCD1, PD-L-1 and CTLA-4, although this could not be confirmed in a validation cohort (34, 35). Both these studies used a different approach to find useful SNPs. The study of Bins et al. composed an exploration cohort and a validation cohort, both consisting of 161 NSCLC patients. They investigated seven specific SNPs in the PDCD1, PTPN11, ZAP70, and IFNG genes by means of DME Taqman allelic discrimination assays. Specifically, the 804C>T SNP in the PDCD1 gene was shown to correlate to increased risk of irAE development. The other study by Refae et al. selected genes that have been reported in literature to be of relevance for the immune and/or cancer response, which resulted in 166 SNPs in 86 genes. These were analyzed in 94 solid tumor patients with a sequenom MassArray iPLEX assay. This resulted in association of SNPs in UNG, IFNW1, IFNL4, PD-L1, and CTLA-4 with grade ≥3 irAE development. In addition to these two studies, Khan et al. recently published a retrospective analysis of clinical trial data of 220 bladder cancer patients (36). By means of whole genome sequencing they calculated polygenic risk scores for skin autoimmunity and found that psoriasis-associated polygenic risk scores were correlated to dermal irAE development ($p < 0.05$).

A recent study by Marschner et al. demonstrated microRNA-146a to be of importance for irAE development (37). Mouse models deficient for microRNA-146 showed a higher incidence

of severe irAEs compared to wild type mice. In addition, severity of irAEs in mice could be lowered by administering a microRNA-146a mimic *in vivo*. Based on this finding, SNP analysis was performed to identify the SNP rs2910164 (C>G), which is known to decrease microRNA-146a expression, in 167 patients with solid tumors, who had been treated with anti–PD-1 or anti–PD-L1 antibodies. Patients with an rs2910164 CC genotype and therefore decreased microRNA-146a expression had a significantly higher risk of grade ≥3 irAEs development compared to patients with a GC or GG genotype. Patients with rs2910164 CC genotype also showed progression-free survival and increased neutrophil counts both at baseline and during ICI therapy. The frequency of the rs2910164 CC genotype in the study population was low (7%), which was comparable to previously published data in the European population (5%–6%), whereas in Asians, the frequency might be higher (33%) (71). Although the rs2910164 CC genotype was significantly enriched in patients with grade 3–4 irAEs (17.9% versus 3.1% in grade 0–2 irAEs), the majority of patients developed severe irAEs without this genotype. Further studies have to be performed to evaluate the use of this SNP as a biomarker.

HLA profiles have been linked to several autoimmune diseases, such as ankylosing spondylitis (72). Four independent studies reported on HLA profile and irAE development (38–41). In a retrospective analysis of pooled clinical trial data of 450 anti-CTLA-4 treated melanoma patients, Wolchok et al. did not observe a significant association between HLA-A*02:01 profile and irAE occurrence (38). However, this study did notice a trend toward increased irAE frequency in HLA-A*02:01-positive patients, although this was only observed in the subgroup of patients treated with 3 mg/kg anti-CTLA-4. The second study looked at HLA haplotyping by means of next generation sequencing in a prospective cohort of 102 metastatic cancer patients. HLA profiles did not correlate to all developed irAEs, but specifically HLA-DRB1*11:01 was shown to be associated with ICI-induced pruritis and HLA-DQB1*01:01 was associated with colitis (39). Yano et al. performed a case-control study on 11 advanced cancer patients who developed ICI-induced adrenal insufficiency. HLA haplotyping showed a positive association between HLA-DR15 and pituitary irAE development compared to a healthy control group. The study of Stamatouli et al. used a reverse sequence-specific oligonucleotide HLA typing method in 23 patients with solid tumors who developed ICI-induced diabetes. They reported the presence of HLA-DR4 in 76% of these patients, which was significantly higher than in the general population (17%) and in a population with type-1 diabetes (42%). It is known that HLA-DR4 is associated with a higher risk to develop diabetes type 1 (73). It is therefore not surprising that patients expressing this HLA type have a higher risk to develop type 1 diabetes after ICI treatment. Taken together, the data show that certain HLA types might be predictive for a specific irAE type. Since HLA types are associated with different autoimmune phenomena and hence different irAEs, a single HLA type might not serve as a good predictive biomarker for development of irAEs.

Microbiome

It has been well accepted that the microbiome impacts immune homeostasis (74), and microbiome composition has been demonstrated to impact ICI-efficacy (75–77). Two small studies analyzed microbiome composition in relation to irAEs. Dubin et al. prospectively analyzed the baseline microbiome composition of 34 anti-CTLA-4 treated patients of whom 10 developed colitis using 16S rRNA and metagenomic shotgun sequencing. They reported significantly increased fecal abundance of Bacteroidetes phylum at baseline in patients without colitis (42). Furthermore, they found a relative lack of pathways involved in vitamin B synthesis in the patients who developed colitis. Looking at the predictive accuracy of a four-module analysis identified by machine learning, a 70% sensivity and 83% specificity was reported. In another prospective analysis of 26 anti-CTLA-4 treated patients using 16S rRNA sequencing, a significantly lower abundance of Bacteroidetes but higher abundance of Firmicutes at baseline was reported in the nine patients who developed ICI-associated colitis (23). Although the numbers of patients with irAEs in these studies were small, the identification of Bacteroidetes in both studies is remarkable and deserves further validation in larger cohorts.

Other

Two studies have reported that baseline thyroid stimulating hormone (TSH) was associated with thyroid dysfunction due to anti-PD-1 or combined therapy, although cut-off values used were different (30, 43). Among 168 anti-PD-1 treated patients, Kimbara et al. observed that a baseline TSH level ≥5 μIU/ml was significantly associated with thyroid dysfunction in a multivariable model. Similarly, in 99 melanoma patients treated with either anti-PD-1 monotherapy or combined with anti-CTLA-4, Pollack et al. reported higher TSH levels at baseline to be associated with thyroid dysfunction, although they used a cut-off of 2.19 μIU/ml. Together and in line with the autoantibody data, this suggests that some patients might have had subclinical thyroid disease before the start of ICIs.

Soluble CTLA-4 has been reported to be associated with irAE development at baseline (44). For this study, serum samples of 113 melanoma patients were collected at baseline and tested with a soluble CTLA-4 specific ELISA. They demonstrated that high baseline levels of soluble CTLA-4 of >200 pg/ml resulted in more than three-fold increased risk of any irAE occurrence.

Retrospective analysis of clinical trial data by Shahabi et al. in 162 melanoma patients identified CD177 mRNA expression as a potential biomarker (55). Gene expression profiling was performed on whole blood samples at baseline and three and six weeks after ICI treatment. They reported increased CD177 mRNA expression levels after three weeks of treatment to be correlated with gastro-intestinal irAEs, when compared to baseline and non-irAE patients. CD177 is a neutrophil marker, which is upregulated during inflammatory responses with neutrophil activation (55). However, only a minority of patients developing grade ≥2 gastro-intestinal irAEs showed an elevated mRNA expression of CD177. Therefore, CD177 has a

low sensitivity for prediction of gastro-intestinal irAE development that hampers its use as a biomarker.

DISCUSSION

This review presents an overview of suggested biomarkers in patients undergoing ICI therapy. We conclude that thus far, none of the proposed biomarkers has shown sufficient accuracy in predicting or signaling irAEs to be of value for clinical practice.

Despite the substantial number of studies on irAE biomarkers, some methodological issues in these studies thus far limit their translation to clinical practice. Generally, the number of patients at risk is low. With the minority of patients developing severe irAEs, this results in low statistical power. As a consequence, most studies focused on irAEs of any grade, including low-grade irAEs, which are less reliably graded. More importantly, the clinical significance of these biomarkers is limited, because low-grade irAEs have fewer clinical implications. Moreover, most analyses were performed retrospectively, and some data are based on case series with their inherent risk of selection bias. Measures indicating their predictive or diagnostic accuracy (such as sensitivity and specificity, ROC analysis) were often not reported. Furthermore, many studies regarding on-treatment irAE biomarkers even lack the comparison with non-irAE patients, making it impossible to analyze their accuracy. Lastly, validation cohorts are lacking in most studies. Future prospectively designed studies should be well powered and address these issues, in order to advance the field.

In our search, we focused on studies reporting potential blood-based, microbiome and immunogenetic biomarkers, but did not include the more pathogenesis focused studies reporting histopathological changes in irAE affected tissue, which could evolve into diagnostic biomarkers in the future. The fact that we only searched PubMed could be seen as a limitation. Although we did not search on other databases such as Embase and Cochrane, we do not expect to have missed articles, because we assume that these articles would have been published in journals which are included in the Medline database.

Reviewing the data, it is unlikely that one single biomarker will be specific or sensitive enough to predict irAE development accurately. Given the fact that there are several mechanisms involved in this process (4) and considering the difference in immunological set-up between patients, it is likely that a combination of multiple biomarkers is needed. Pre-treatment biomarkers should focus on risk stratification and the type of treatment most suited to prevent occurrence of irAEs. A combination of genetic markers (either DNA or RNA based), characteristics of the microbiome and pre-clinical signs of autoimmune disease like presence of autoantibodies or expression of cytokines could be of added value herein. During treatment, biomarkers are needed that distinguish between potential irAE, infection or tumor progression and ideally already indicate development of irAE before onset of clinical symptoms. In this setting, a combination of markers that show a high dynamic range like RNA or protein expression together with traditional inflammatory parameters, like CRP or blood cell counts, seems more suited.

Moreover, as mentioned, biomarkers for anti-PD-(L)1 related irAEs will probably differ from anti-CTLA-4 irAE biomarkers, requesting sufficiently powered studies in these separate populations. In analogy with the work of Bigot et al. who developed a score predicting overall survival for patients receiving ICIs in phase 1 trials (78), a risk score for irAE development could be established. Naturally, such a prediction model should be developed and subsequently validated in separate patient cohorts with sufficient power. The complexity of data generated with different methods, i.e., genomics, transcriptomics, proteomics, and microbiome analysis clearly requires new methods of data analysis. Machine learning techniques could be of added value in this setting as have been applied to predict cutaneous adverse events in patients receiving anti–PD-1 immunotherapy (79).

The development of irAEs has been associated with improved response to ICI treatment, as reviewed by Das & Johnson (80). In line with this, some of the irAE biomarkers in this review have also shown associations with ICI responses (18–22, 31, 37, 44). This is not surprising, in view of the common underlying mechanism of irAEs and anti-tumor responses (48). It is important to consider that the patients at increased risk of irAEs could also be the patients deriving the most benefit from ICIs and that aggressive or early irAE management could compromise ICI efficacy (81).

In conclusion, no single blood-based biomarker has been identified to date that has the potential to accurately predict risk of irAE development in patients undergoing ICI treatment. Future prospective studies using standardized sampling and analyses should be performed in well-powered cohorts and focus on combinations of potential biomarkers that are validated in separate cohorts. The overview of suggested biomarkers in this review could be a starting point for further research in order to develop a successful prediction method.

AUTHOR CONTRIBUTIONS

JH and DH designed the study. JH and RV performed the systematic literature search and selected studies to be included. DH and KS advised on search and selection strategy. JH and RV drafted the manuscript. DH and KS edited the manuscript. All authors contributed to the article and approved the submitted version.

SUPPLEMENTARY MATERIAL

The Supplementary Material for this article can be found online at: https://www.frontiersin.org/articles/10.3389/fonc.2020.585311/full#supplementary-material

REFERENCES

1. Hargadon KM, Johnson CE, Williams CJ. Immune checkpoint blockade therapy for cancer: An overview of FDA-approved immune checkpoint inhibitors. *Int Immunopharmacol* (2018) 62(July):29–39. doi: 10.1016/j.intimp.2018.06.001
2. Fritz JM, Lenardo MJ. Development of immune checkpoint therapy for cancer. *J Exp Med* (2019) 216(6):1244–54. doi: 10.1084/jem.20182395
3. Khan S, Gerber DE. Autoimmunity, checkpoint inhibitor therapy and immune-related adverse events: A review. *Semin Cancer Biol* (2019) 6 (12):93–101. doi: 10.1016/j.semcancer.2019.06.012
4. Postow MA, Sidlow R, Hellmann MD. Immune-related adverse events associated with immune checkpoint blockade. *N Engl J Med* (2018) 378 (2):158–68. doi: 10.1056/NEJMra1703481
5. Wang DY, Salem JE, Cohen JV, Chandra S, Menzer C, Ye F, et al. Fatal Toxic Effects Associated With Immune Checkpoint Inhibitors: A Systematic Review and Meta-analysis. *JAMA Oncol* (2018) 4(12):1721–8. doi: 10.1001/jamaoncol.2018.3923
6. National Cancer Institute. *Common Terminology Criteria for Adverse Events v4.0. NIH Publ [Internet]*. National Institutes of Health Publication (2009). pp. 0–71. Available at: http://ctep.cancer.gov/protocolDevelopment/electronic_applications/docs/ctcaev3.pdf.
7. Haanen J, Carbonnel F, Robert C, Kerr K, Peters S, Larkin J, et al. Management of toxicities from immunotherapy ESMO slide guidelines. *Ann Oncol* (2017) 28(Suppl_4):iv119–42. doi: 10.1093/annonc/mdx225
8. Khoja L, Day D, Wei-Wu Chen T, Siu LL, Hansen AR. Tumour- and class-specific patterns of immune-related adverse events of immune checkpoint inhibitors: A systematic review. *Ann Oncol* (2017) 28(10):2377–85. doi: 10.1093/annonc/mdx286
9. Coutzac C, Adam J, Soularue E, Collins M, Racine A, Mussini C, et al. Colon immune-related adverse events: Anti-CTLA-4 and anti-PD-1 blockade induce distinct immunopathological entities. *J Crohn's Colitis* (2017) 11 (10):1238–46. doi: 10.1093/ecco-jcc/jjx081
10. Weber JS, Kähler KC, Hauschild A. Management of immune-related adverse events and kinetics of response with ipilimumab. *J Clin Oncol* (2012) 30 (21):2691–7. doi: 10.1200/JCO.2012.41.6750
11. Teufel A, Zhan T, Härtel N, Bornschein J, Ebert MP, Schulte N. Management of immune related adverse events induced by immune checkpoint inhibition. *Cancer Lett* (2019) 456:80–7. doi: 10.1016/j.canlet.2019.04.018
12. Abolhassani A-R, Schuler G, Kirchberger MC, Heinzerling L. C-reactive protein as an early marker of immune-related adverse events. *J Cancer Res Clin Oncol* (2019) 145(10):2625–31. doi: 10.1007/s00432-019-03002-1
13. Mehnert JM, Monjazeb AM, Beerthuijzen JMT, Collyar D, Rubinstein L, Harris LN. The challenge for development of valuable immuno-oncology biomarkers. *Clin Cancer Res* (2017) 23(17):4970–9. doi: 10.1158/1078-0432.CCR-16-3063
14. Califf RM. Biomarker definitions and their applications. *Exp Biol Med* (2018) 243(3):213–21. doi: 10.1177/1535370217750088
15. Urwyler P, Earnshaw I, Bermudez M, Perucha E, Wu W, Ryan S, et al. Mechanisms of checkpoint inhibition-induced adverse events. *Clin Exp Immunol* (2020) 200(2):141–54. doi: 10.1111/cei.13421
16. von Itzstein MS, Khan S, Gerber DE. Investigational Biomarkers for Checkpoint Inhibitor Immune-Related Adverse Event Prediction and Diagnosis. *Clin Chem* (2020) 66(6):779–93. doi: 10.1093/clinchem/hvaa081
17. Eun Y, Kim IY, Sun JM, Lee J, Cha HS, Koh EM, et al. Risk factors for immune-related adverse events associated with anti-PD-1 pembrolizumab. *Sci Rep* (2019) 9(14039):1–8. doi: 10.1038/s41598-019-50574-6
18. Peng L, Wang Y, Liu F, Qiu X, Zhang X, Fang C, et al. Peripheral blood markers predictive of outcome and immune-related adverse events in advanced non-small cell lung cancer treated with PD-1 inhibitors. *Cancer Immunol Immunother* (2020) 69:1813–22. doi: 10.1007/s00262-020-02585-w
19. Pavan A, Calvetti L, Dal Maso A, Attili I, Del Bianco P, Pasello G, et al. Peripheral Blood Markers Identify Risk of Immune-Related Toxicity in Advanced Non-Small Cell Lung Cancer Treated with Immune-Checkpoint Inhibitors. *Oncologist* (2019) 24(8):1128–36. doi: 10.1634/theoncologist.2018-0563
20. Diehl A, Yarchoan M, Hopkins A, Jaffee E, Grossman SA. Relationships between lymphocyte counts and treatmentrelated toxicities and clinical responses in patients with solid tumors treated with PD-1 checkpoint inhibitors. *Oncotarget* (2017) 8(69):114268–80. doi: 10.18632/oncotarget.23217
21. Nakamura Y, Tanaka R, Maruyama H, Ishitsuka Y, Okiyama N, Watanabe R, et al. Correlation between blood cell count and outcome of melanoma patients treated with anti-PD-1 antibodies. *Jpn J Clin Oncol* (2019) 49(5):431–7. doi: 10.1093/jjco/hyy201
22. Damuzzo V, Solito S, Pinton L, Carrozzo E, Valpione S, Pigozzo J, et al. implication of tumor-associated and immunological parameters in melanoma patients treated with ipilimumab. *Clinical Oncoimmunol* (2016) 5(12). doi: 10.1080/2162402X.2016.1249559
23. Chaput N, Lepage P, Coutzac C, Soularue E, Le Roux K, Monot C, et al. Baseline gut microbiota predicts clinical response and colitis in metastatic melanoma patients treated with ipilimumab. *Ann Oncol* (2017) 28(6):1368–79. doi: 10.1093/annonc/mdx108
24. Valpione S, Pasquali S, Campana LG, Piccin L, Mocellin S, Pigozzo J, et al. Sex and interleukin-6 are prognostic factors for autoimmune toxicity following treatment with anti-CTLA4 blockade. *J Transl Med* (2018) 16(94). doi: 10.1186/s12967-018-1467-x
25. Tarhini AA, Zahoor H, Lin Y, Malhotra U, Sander C, Butterfield LH, et al. Baseline circulating IL-17 predicts toxicity while TGF-β1 and IL-10 are prognostic of relapse in ipilimumab neoadjuvant therapy of melanoma. *J Immunother Cancer* (2015) 3(39):15–20. doi: 10.1186/s40425-015-0081-1
26. Lim SY, Lee JH, Gide TN, Menzies AM, Guminski A, Carlino MS, et al. Circulating cytokines predict immune-related toxicity in melanoma patients receiving anti-PD-1–based immunotherapy. *Clin Cancer Res* (2019) 25 (5):1557–63. doi: 10.1158/1078-0432.CCR-18-2795
27. Kurimoto C, Inaba H, Ariyasu H, Iwakura H, Ueda Y, Uraki S, et al. Predictive and sensitive biomarkers for thyroid dysfunctions during treatment with immune-checkpoint inhibitors. *Cancer Sci* (2020) 111(5):1468–77. doi: 10.1111/cas.14363
28. Khan S, Khan SA, Luo X, Fattah FJ, Saltarski J, Gloria-McCutchen Y, et al. Immune dysregulation in cancer patients developing immune-related adverse events. *Br J Cancer* (2019) 120(1):63–8. doi: 10.1038/s41416-018-0155-1
29. Maekura T, Naito M, Tahara M, Ikegami N, Kimura Y, Sonobe S, et al. Predictive factors of nivolumab-induced hypothyroidism in patients with non-small cell lung cancer. *In Vivo (Brooklyn)* (2017) 31(5):1035–9. doi: 10.21873/invivo.11166
30. Kimbara S, Fujiwara Y, Iwama S, Ohashi K, Kuchiba A, Arima H, et al. Association of antithyroglobulin antibodies with the development of thyroid dysfunction induced by nivolumab. *Cancer Sci* (2018) 109(11):3583–90. doi: 10.1111/cas.13800
31. Hasan Ali O, Bomze D, Ring S, Berner F, Fässler M, Diem S, et al. BP180-specific IgG is associated with skin adverse events, therapy response and overall survival in non-small cell lung cancer patients treated with checkpoint inhibitors. *J Am Acad Dermatol* (2019) 82(4):854–61. doi: 10.1016/j.jaad.2019.08.045
32. Tahir SA, Gao J, Miura Y, Blando J, Tidwell RSS, Zhao H, et al. Autoimmune antibodies correlate with immune checkpoint therapy-induced toxicities. *PNAS* (2019) 116(44):22246–51. doi: 10.1073/pnas.1908079116
33. Gowen MF, Giles KM, Simpson D, Tchack J, Zhou H, Moran U, et al. Baseline antibody profiles predict toxicity in melanoma patients treated with immune checkpoint inhibitors. *J Transl Med* (2018) 16(82):1296–301. doi: 10.1186/s12967-018-1452-4
34. Bins S, Basak EA, El Bouazzaoui S, Koolen SLW, Oomen De Hoop E, Van Der Leest CH, et al. Association between single-nucleotide polymorphisms and adverse events in nivolumab-treated non-small cell lung cancer patients. *Br J Cancer* (2018) 118(10):1296–301. doi: 10.1038/s41416-018-0074-1
35. Refae S, Gal J, Ebran N, Otto J, Borchiellini D, Peyrade F, et al. Germinal Immunogenetics predict treatment outcome for PD-1/PD-L1 checkpoint inhibitors. *Invest New Drugs* (2020) 38(1):160–71. doi: 10.1007/s10637-019-00845-w
36. Khan Z, Di Nucci F, Kwan A, Hammer C, Mariathasan S, Rouilly V, et al. Polygenic risk for skin autoimmunity impacts immune checkpoint blockade in bladder cancer. *Proc Natl Acad Sci U S A* (2020) 117(22):12288–94. doi: 10.1073/pnas.1922867117
37. Marschner D, Falk M, Javorniczky NR, Hanke-Müller K, Rawluk J, Schmitt-Graeff A, et al. MicroRNA-146a regulates immune-related adverse events

caused by immune checkpoint inhibitors. *JCI Insight* (2020) 5(6):1–14. doi: 10.1172/jci.insight.132334
38. Wolchok JD, Weber JS, Hamid O, Lebbé C, Maio M, Schadendorf D, et al. Ipilimumab efficacy and safety in patients with advanced melanoma: A retrospective analysis of HLA subtype from four trials. *Cancer Immun* (2010) 10(9).
39. Hasan Ali O, Berner F, Bomze D, Fässler M, Diem S, Cozzio A, et al. Human leukocyte antigen variation is associated with adverse events of checkpoint inhibitors. *Eur J Cancer* (2019) 107:8–14. doi: 10.1016/j.ejca.2018.11.009
40. Stamatouli AM, Quandt Z, Perdigoto AL, Clark PL, Kluger H, Weiss SA, et al. Collateral damage: Insulin-dependent diabetes induced with checkpoint inhibitors. *Diabetes* (2018) 67(8):1471–80. doi: 10.2337/dbi18-0002
41. Yano S, Ashida K, Sakamoto R, Sakaguchi C, Ogata M, Maruyama K, et al. Human leucocyte antigen DR15, a possible predictive marker for immune checkpoint inhibitor–induced secondary adrenal insufficiency. *Eur J Cancer* (2020) 130:198–203. doi: 10.1016/j.ejca.2020.02.049
42. Dubin K, Callahan MK, Ren B, Khanin R, Viale A, Ling L, et al. Intestinal microbiome analyses identify melanoma patients at risk for checkpoint-blockade-induced colitis. *Nat Commun* (2016) 7(10391). doi: 10.1038/ncomms10391
43. Pollack RM, Kagan M, Lotem M, Dresner-Pollak R. Baseline TSH level is associated with risk of anti-PD-1-induced thyroid dysfunction. *Endocr Pract* (2019) 25(8):824–9. doi: 10.4158/EP-2018-0472
44. Pistillo MP, Fontana V, Morabito A, Dozin B, Laurent S, Carosio R, et al. Soluble CTLA-4 as a favorable predictive biomarker in metastatic melanoma patients treated with ipilimumab: an Italian melanoma intergroup study. *Cancer Immunol Immunother* (2019) 68:97–107. doi: 10.1007/s00262-018-2258-1
45. Fujisawa Y, Yoshino K, Otsuka A, Funakoshi T, Fujimura T, Yamamoto Y, et al. Fluctuations in routine blood count might signal severe immune-related adverse events in melanoma patients treated with nivolumab. *J Dermatol Sci* (2017) 88(2):225–31. doi: 10.1016/j.jdermsci.2017.07.007
46. Jaber SH, Cowen EW, Haworth LR, Booher SL, Berman DM, Rosenberg SA, et al. Skin reactions in a subset of patients with stage IV melanoma treated with anti-cytotoxic T-lymphocyte antigen 4 monoclonal antibody as a single agent. *Arch Dermatol* (2006) 142(2):166–72. doi: 10.1001/archderm.142.2.166
47. Subudhi SK, Aparicio A, Gao J, Zurita AJ, Araujo JC, Logothetis CJ, et al. Clonal expansion of CD8 T cells in the systemic circulation precedes development of ipilimumab-induced toxicities. *PNAS* (2016) 113 (42):11919–24. doi: 10.1073/pnas.1611421113
48. Oh DY, Cham J, Zhang L, Fong G, Kwek SS, Klinger M, et al. Immune toxicities elicted by CTLA-4 blockade in cancer patients are associated with early diversification of the T cell repertoire. *Cancer Res* (2017) 77(6):1322–30. doi: 10.1158/0008-5472.CAN-16-2324
49. Das R, Bar N, Ferreira M, Newman AM, Zhang L, Bailur JK, et al. Early b cell changes predict autoimmunity following combination immune checkpoint blockade. *J Clin Invest* (2018) 128(2):715–20. doi: 10.1172/JCI96798
50. Tanaka R, Okiyama N, Okune M, Ishitsuka Y, Watanabe R, Furuta J, et al. Serum level of interleukin-6 is increased in nivolumab-associated psoriasiform dermatitis and tumor necrosis factor-α is a biomarker of nivolumab recativity. *J Dermatol Sci* (2017) 86:71–8. doi: 10.1016/j.jdermsci.2016.12.019
51. Oyanagi J, Koh Y, Sato K, Mori K, Teraoka S, Akamatsu H, et al. Predictive value of serum protein levels in patients with advanced non-small cell lung cancer treated with nivolumab. *Lung Cancer* (2019) 132(January):107–13. doi: 10.1016/j.lungcan.2019.03.020
52. Fujimura T, Sato Y, Tanita K, Kambayashi Y, Otsuka A, Fujisawa Y, et al. Serum levels of soluble CD163 and CXCL5 may be predictive markers for immune-related adverse events in patients with advanced melanoma treated with nivolumab: A pilot study. *Oncotarget* (2018) 9(21):15542–51. doi: 10.18632/oncotarget.24509
53. Osorio JC, Ni A, Chaft JE, Pollina R, Kasler MK, Stephens D, et al. Antibody-mediated thyroid dysfunction during T-cell checkpoint blockade in patients with non-small-cell lung cancer. *Ann Oncol* (2017) 28(3):583–9. doi: 10.1093/annonc/mdw640
54. Stroud CRG, Hegde A, Cherry C, Naqash AR, Sharma N, Addepalli S, et al. Tocilizumab for the management of immune mediated adverse events secondary to PD-1 blockade. *J Oncol Pharm Pract* (2019) 25(3):551–7. doi: 10.1177/1078155217745144
55. Shahabi V, Berman D, Chasalow SD, Wang L, Tsuchihashi Z, Hu B, et al. Gene expression profiling of whole blood in ipilimumab-treated patients for identification of potential biomarkers of immune-related gastrointestinal adverse events. *J Transl Med* (2013) 11(75). doi: 10.1186/1479-5876-11-75
56. Sacdalan DB, Lucero JA, Sacdalan DL. Prognostic utility of baseline neutrophil-to-lymphocyte ratio in patients receiving immune checkpoint inhibitors: A review and meta-analysis. *Onco Targets Ther* (2018) 11:955–65. doi: 10.2147/OTT.S153290
57. Diny NL, Rose NR, Čiháková D. Eosinophils in autoimmune diseases. *Front Immunol* (2017) 8:484. doi: 10.3389/fimmu.2017.00484
58. Blank CU, Haanen JB, Ribas A, Schumacher TN. The "cancer immunogram." *Cancer Immunol* (2016) 352(6286):658–60. doi: 10.1126/science.aaf2834
59. Cabrita R, Lauss M, Sanna A, Donia M, Skaarup Larsen M, Mitra S, et al. Tertiary lymphoid structures improve immunotherapy and survival in melanoma. *Nature* (2020) 577(7791):561–5. doi: 10.1038/s41586-019-1914-8
60. Petitprez F, de Reyniès A, Keung EZ, Chen TWW, Sun CM, Calderaro J, et al. B cells are associated with survival and immunotherapy response in sarcoma. *Nature* (2020) 577(7791):556–60. doi: 10.1038/s41586-019-1906-8
61. Helmink BA, Reddy SM, Gao J, Zhang S, Basar R, Thakur R, et al. B cells and tertiary lymphoid structures promote immunotherapy response. *Nature* (2020) 577(7791):549–55. doi: 10.1038/s41586-019-1922-8
62. Schett G, Elewaut D, McInnes IB, Dayer J-M, Neurath MF. How Cytokine Networks Fuel Inflammation: Toward a cytokine-based disease taxonomy. *Nat Med* (2013) 19(7):822–4. doi: 10.1038/nm.3260
63. Hunter CA, Jones SA. IL-6 as a keystone cytokine in health and disease. *Nat Immunol* (2015) 16(5):448–57. doi: 10.1038/ni.3153
64. Lee DW, Gardner R, Porter DL, Louis CU, Ahmed N, Jensen M, et al. Current concepts in the diagnosis and management of cytokine release syndrome. *Blood* (2014) 124(2):188–96. doi: 10.1182/blood-2014-05-552729
65. Miossec P, Kolls JK. Targeting IL-17 and T H 17 cells in chronic inflammation. *Nat Rev Drug Discov* (2012) 11(10):763–76. doi: 10.1038/nrd3794
66. Qian X, Chen H, Wu X, Hu L, Huang Q, Jin Y. Interleukin-17 acts as double-edged sword in anti-tumor immunity and tumorigenesis. *Cytokine* (2017) 89:34–44. doi: 10.1016/j.cyto.2015.09.011
67. Anderson R, Rapoport BL. Immune dysregulation in cancer patients undergoing immune checkpoint inhibitor treatment and potential predictive strategies for future clinical practice. *Front Oncol* (2018) 8 (MAR):1–13. doi: 10.3389/fonc.2018.00080
68. Bamias G, Delladetsima I, Perdiki M, Siakavellas SI, Goukos D, Papatheodoridis GV, et al. Immunological Characteristics of Colitis Associated with Anti-CTLA-4 Antibody Therapy. *Cancer Invest* (2017) 35 (7):443–55. doi: 10.1080/07357907.2017.1324032
69. Tokunaga R, Zhang W, Naseem M, Puccini A, Berger MD, Soni S, et al. Target for Novel Cancer Therapy. *Cancer Treat Rev* (2018) 63:40–7. doi: 10.1016/j.ctrv.2017.11.007
70. Sarzi-Puttini P, Doria A. Organ specific-autoantibodies: Their role as markers and predictors of disease. *Autoimmunity* (2008) 41(1):1–10. doi: 10.1080/08916930701619136
71. Lian H, Wang L, Zhang J. Increased risk of breast cancer associated with CC genotype of has-miR-146a Rs2910164 polymorphism in Europeans. *PLoS One* (2012) 7(2):1–7. doi: 10.1371/journal.pone.0031615
72. Sieper J, Poddubnyy D. Axial spondyloarthritis. *Lancet* (2017) 390(10089):73–84. doi: 10.1016/S0140-6736(16)31591-4
73. Baxter AG, Jordan MA. From markers to molecular mechanisms: Type 1 diabetes in the post-GWAS era. *Rev Diabetes Stud* (2012) 9(4):201–23. doi: 10.1900/RDS.2012.9.201
74. Li B, Selmi C, Tang R, Gershwin ME, Ma X. The microbiome and autoimmunity: a paradigm from the gut–liver axis. *Cell Mol Immunol* (2018) 15(6):595–609. doi: 10.1038/cmi.2018.7
75. Routy B, Le Chatelier E, Derosa L, Duong CPM, Alou MT, Daillère R, et al. Gut microbiome influences efficacy of PD-1-based immunotherapy against epithelial tumors. *Science (80-)* (2018) 359(6371):91–7. doi: 10.1126/science.aan3706
76. Gopalakrishnan V, Spencer CN, Nezi L, Reuben A, Andrews MC, Karpinets TV, et al. Gut microbiome modulates response to anti-PD-1 immunotherapy in melanoma patients. *Science (80-)* (2018) 359(6371):97–103. doi: 10.1016/j.ccell.2018.03.015

77. Matson V, Fessler J, Bao R, Chongsuwat T, Zha Y, Alegre ML, et al. The commensal microbiome is associated with anti-PD-1 efficacy in metastatic melanoma patients. *Science (80-)* (2018) 359(6371):104–8. doi: 10.1126/science.aao3290
78. Bigot F, Castanon E, Baldini C, Hollebecque A, Carmona A, Postel-Vinay S, et al. Prospective validation of a prognostic score for patients in immunotherapy phase I trials: The Gustave Roussy Immune Score (GRIm-Score). *Eur J Cancer* (2017) 84:212–8. doi: 10.1016/j.ejca.2017.07.027
79. Lewinson RT, Meyers DE, Vallerand IA, Suo A, Dean ML, Cheng T, et al. Machine learning for prediction of cutaneous adverse events in patients receiving anti-PD-1 immunotherapy. *J Am Acad Dermatol* (2020) 84 (1):183–5. doi: 10.1016/j.jaad.2020.04.069
80. Das S, Johnson DB. Immune-related adverse events and anti-tumor efficacy of immune checkpoint inhibitors. *J Immunother Cancer* (2019) 7(306). doi: 10.1186/s40425-019-0805-8
81. Verheijden RJ, May AM, Blank CU, Aarts MJB, van den Berkmortel FWPJ, van den Eertwegh AJM, et al. Association of Anti-TNF with Decreased Survival in Steroid Refractory Ipilimumab and Anti-PD1-Treated Patients in the Dutch Melanoma Treatment Registry. *Clin Cancer Res* (2020) May26 (9):2268–74. doi: 10.1158/1078-0432.CCR-19-3322

Conflict of Interest: KS reports advisory relationships with Novartis, Pierre Fabre, MSD, Abbvie and Bristol Myers Squibb and received honoraria from Novartis and Roche; all outside the submitted work and paid to institution.

The remaining authors declare that the research was conducted in the absence of any commercial or financial relationships that could be construed as a potential conflict of interest.

APPENDIX 1: SEARCH STRATEGY

A search was conducted using PubMed with search terms for immune checkpoint inhibitor therapy, immune-related adverse events and biomarker (full search question below). The search on PubMed yielded 3580 results on the 1st of July 2020, of which 35 were included in this review. Five other articles were obtained by means of citation and by using the similar article function on PubMed.

((toxicit*[Title/Abstract] OR (adverse[Title/Abstract] AND (event [Title/Abstract] OR events[Title/Abstract])) OR irAE [Title/Abstract])

AND

(PD-1[Title/Abstract] OR PD1[Title/Abstract] OR anti-PD1 [Title/Abstract] OR anti-PD 1[Title/Abstract] OR pembrolizumab[Title/Abstract] OR nivolumab[Title/Abstract]

OR

PD-L1[Title/Abstract] OR anti-PD-L1[Title/Abstract] OR anti-PDL1[Title/Abstract] OR durvalumab[Title/Abstract] OR avelumab[Title/Abstract] OR atezolizumab[Title/Abstract]

OR

CTLA-4[Title/Abstract] OR CTLA4[Title/Abstract] OR ipilimumab[Title/Abstract] OR tremelimumab[Title/Abstract] OR cemiplimab[Title/Abstract] OR anti-CTLA-4[Title/Abstract] OR anti-CTLA4[Title/Abstract] OR

Anti cytotoxic T-lymphocyte-associated protein 4[Title/Abstract] OR anti-CD152[Title/Abstract]

OR

checkpoint inhibit*[Title/Abstract] OR immune checkpoint [Title/Abstract])

AND

(predict*[Title/Abstract] OR associate*[Title/Abstract] OR biomarker*[Title/Abstract] OR signal*[Title/Abstract] OR increase*[Title/Abstract] OR decrease*[Title/Abstract]))

frontiers in Immunology

ORIGINAL RESEARCH
published: 24 February 2021
doi: 10.3389/fimmu.2021.561793

Triple-Negative Breast Cancer: Intact Mismatch Repair and Partial Co-Expression of PD-L1 and LAG-3

*Shafei Wu[1], Xiaohua Shi[1], Jing Wang[1], Xuefei Wang[2], Yuanyuan Liu[1], Yufeng Luo[1], Feng Mao[2] and Xuan Zeng[1]**

[1] Department of Pathology, Peking Union Medical College Hospital, Molecular Pathology Research Center, Chinese Academy of Medical Sciences, Beijing, China, [2] Department of Breast Surgery, Peking Union Medical College Hospital, Chinese Academy of Medical Sciences, Beijing, China

OPEN ACCESS

Edited by:
Taha Merghoub, Memorial Sloan Kettering Cancer Center, United States

Reviewed by:
Zong Sheng Guo, University of Pittsburgh, United States
Meenakshi Anurag, Baylor College of Medicine, United States

***Correspondence:**
Xuan Zeng
zengxuan88@yahoo.com

Specialty section:
This article was submitted to Cancer Immunity and Immunotherapy, a section of the journal Frontiers in Immunology

Received: *13 May 2020*
Accepted: *11 January 2021*
Published: *24 February 2021*

Citation:
Wu S, Shi X, Wang J, Wang X, Liu Y, Luo Y, Mao F and Zeng X (2021) Triple-Negative Breast Cancer: Intact Mismatch Repair and Partial Co-Expression of PD-L1 and LAG-3. Front. Immunol. 12:561793. doi: 10.3389/fimmu.2021.561793

Background and Aim: Poor response to immune checkpoint inhibitors (ICIs) has been observed in most triple-negative breast cancer (TNBC) cases (around 80%). Our aim was to investigate the status of mismatch repair (MMR), microsatellite instability (MSI), programmed death-ligand 1 (PD-L1), and lymphocyte-activation gene 3 (LAG-3) in TNBC.

Methods: A total of 74 TNBC samples were retrospectively analyzed. MMR and MSI were evaluated by immunohistochemistry (IHC) and polymerase chain reaction (PCR) using Promega 1.2 and NCI panels, respectively. PD-L1, LAG-3, and CD8 expression was assessed by IHC.

Results: None of the cases demonstrated deficient MMR (dMMR) or MSI. In total, 43/74 cases (58.1%) were PD-L1+, including 1 tumor PD-L1+, 25 tumor-infiltrating lymphocytes (TILs) PD-L1+, and 17 cases involving concurrence of tumor and TIL PD-L1+. The rate of TIL PD-L1+ was remarkably higher than that of tumor PD-L1+ ($P<0.001$). We identified 20 LAG-3+ cases (27.0%, 20/74), all of which were PD-L1+. Co-expression of PD-L1 and LAG-3 was noted in 46.5% (20/43) of the PD-L1+ population. In the LAG-3+ subtype (co-expression of PD-L1 and LAG-3), high correlation between TILs PD-L1+ and LAG-3+ was observed ($P<0.01$). A high frequency of CD8+ (98.6%, 73/74) was observed.

Conclusion: dMMR/MSI characteristics may not be a practical predictive marker for ICIs in TNBC. PD-L1+ is more common in TILs than in tumors. In the PD-L1+ population, approximately half of the cases showed LAG-3 co-expression. For patients with a poor response to PD-1(L1) mono ICI, dual blockade of PD-1(L1) and LAG-3 may be a viable option for the management of TNBC.

Keywords: CD8, LAG-3, PD-L1, microsatellite instability, triple-negative breast cancer

INTRODUCTION

Breast cancer (BC) is a heterogeneous disease. Molecular types, essentially including luminal, human epidermal growth factor receptor 2 positive (HER2+), and triple-negative, for which clinical outcomes are closely tied to the corresponding treatment, are categorized based on the status of estrogen receptor (ER), progesterone receptor (PR), and human epidermal growth factor receptor 2 (HER2). Unlike luminal (hormone receptor-positive) and HER2+ (HER2-rich) patients, who benefit from endocrine therapy and HER2-targeted therapy, respectively, cytotoxic chemotherapy is the standard strategy for the advanced triple-negative (HER2-, ER-, and PR-) cases, which account for 15%–20% of invasive BCs. The exception is a small number of TNBC cases with *BRCA* gene mutation (approximated 11-25%) that respond well to poly (ADP-ribose) polymerase (PARP) inhibitors. In general, the prognosis of triple-negative breast cancer (TNBC) is relatively poor, and the tumors recur rapidly (1–3).

Programmed death-ligand 1 (PD-L1), which is a negative regulator of T-cell activation, is expressed in many cancers. The interaction of programmed cell death 1 (PD-1) and its ligand, PD-L1, is known to act as a critical blockade pathway in malignant tumors for regulating immune escape. Therefore, exploring the mechanism of immune regulation involving the PD-1/PD-L1 axis, innovating blocking drugs, and implementing the related clinical practice has attracted a lot of attention among researchers. Naturally, inhibitors of PD-1(L1) are expected to be promising options for the treatment of TNBC (4, 5).

In the last two years, promising findings about the therapeutic effects of anti-PD-1(L1) agents in TNBC have been published. For example, the efficacy in patients who received atezolizumab (a monoclonal antibody targeting PD-L1) plus chemotherapy was significantly better than in those treated with chemotherapy alone. Moreover, PD-L1+ patients had prolonged median overall survival in advanced TNBC (6). Therefore, PD-L1 expression detected by immunohistochemistry (IHC) was considered as one of the most essential predictors for identifying potential beneficiaries of PD-1(L1) checkpoint inhibitors, and these inhibitors were approved by the US Food and Drug Administration (FDA) (https://www.fda.gov/medical-devices/vitro-diagnostics/list-cleared-or-approved-companion-diagnostic-devices-vitro-and-imaging-tools/).

However, clinical response to PD-1(L1) blockers as a single-drug therapy was quite limited, and sufficient benefit has not yet been achieved in the majority of TNBC patients based on the published data.

For example, in a phase I study of 116 patients with metastatic TNBC (mTNBC) to whom atezolizumab was administered, the objective response rates (ORRs) were 24% and 6% in first-line and second-line or greater for patients, respectively, and the ORRs were 12% and 0% for the PD-L1≥1% and <1% subgroups, respectively (7). Likewise, in a phase II study, KEYNOTE-086, 84 cases of PD-L1+ mTNBC were enrolled in first-line therapy with pembrolizumab (a PD-1 inhibitor). The ORR was 21.4% (8). Most TNBC cases had no benefit from anti-PD-1(L1) agents. Therefore, besides PD-L1 expression, it is important to investigate additional biomarker(s) to evaluate the efficacy of immune checkpoint inhibitors (ICIs) such as anti-PD-1(L1) and to determine which biomarker(s) may serve as indicator(s) for the combination regimens (e.g. ICI plus ICI) other than ICI plus chemotherapy.

Solid tumors with impaired DNA mismatch repair (MMR) system {mainly including MLH1, PMS2, MSH2, and MSH6 molecules from which phenotype microsatellite instability (MSI) was determined} responded well to ICI therapy (e.g. pembrolizumab) due to the existence of mutation-related neoantigens presumably derived from high tumor mutation burden, which was recognized by the immune system and triggered T-cell function upregulation. High concordance between high-frequency microsatellite instability (MSI-H) and deficient mismatch repair (dMMR) was revealed in colorectal cancer in many investigations (9–11). Nevertheless, the available results about MMR (conventionally detected by IHC) or MSI {usually detected by polymerase chain reaction (PCR)} status in TNBC are still limited and contradictory to the data compared to colorectal and endometrial carcinoma (started with Lynch syndrome research) for which there were relevant guidelines for MMR and MSI detection. Although the frequency of dMMR and/or MSI tumors in TNBC is very rare (0.04-1.8%), according to some investigators, as much as 20.5% of homogeneous dMMR and 9.1% of heterogeneous dMMR, 90% of which were microsatellite stable (MSS) and showed highly discordant results between IHC and PCR, have also been reported (12–14). Faced with the current situation in which tumors with dMMR/MSI-H obtained durable immune responses from ICIs which were approved by FDA but had insufficient and contrary findings about the molecular features, it is necessary to conduct more studies on this pathway for searching other biomarkers that can help identify patients who may potentially benefit from these treatments (15).

With respect to investigating the biomarker(s) to assess the efficacy of ICI *via* PD-1 (L1) blockade, a new checkpoint, lymphocyte-activation gene 3 (LAG-3), which is an inhibitory receptor expressed on activated T lymphocytes and down-regulates T cell-mediated immune response *via* LAG-3/MHC class II (ligand of LAG-3) interaction, has been the focus of recent research. Upregulated LAG-3 expression has been observed in some malignant diseases. Effector T lymphocytes were energized by blocking LAG-3 based on previous investigations. In addition, co-expression of PD-L1 and LAG-3 was identified in approximately 50% of PD-L1+ cases that were estrogen receptor-negative (16). Therefore, LAG-3-mediated immunosuppression was exhibited depending on the biological behavior of LAG-3 exposure. It is inferred to be a potential prospect for interdicting LAG-3 and exploring the combination of anti-PD-1(L1) and anti-LAG-3 strategies. From the available data, the responsiveness to PD-1(L1) inhibitor was improved when the dual inhibition immunotherapeutic strategy, anti-PD-1 (L1) plus anti-LAG-3, was applied (17, 18). Furthermore, trials focusing on the evaluation of clinical response to LAG-3 suppressor (IMP321, a recombinant soluble LAG-3Ig fusion protein) plus chemotherapy (paclitaxel) in BCs (e.g.,

NCT00349934) as well as IMP321 plus pembrolizumab in advanced solid tumors (e.g., NCT2676869), were carried out, respectively (19). Based on the findings described, examination of the LAG-3 expression and co-expression of PD-L1 as well as elucidation of the tumor microenvironment referring to immunotherapeutic resistance to anti-PD-1(L1) were all extremely valuable for adopting suitable immunologic treatment and improving the clinical effect of anti-PD-1(L1) therapy in TNBC.

Additionally, presence of cytotoxic CD8+ T cells has been found to indicate a favorable prognosis. High-frequency expressions of PD-L1 and tumor infiltrating lymphocytes (TILs) were distinguished, and CD8+ TILs attracted further attention in TNBC, although very few related studies have been conducted (12, 20). Consequently, the meaningful association between CD8+ TILs and the predictive markers of response to ICIs need to be assessed in combination and stratified precisely.

Our purpose was to evaluate the status of MMR/MSI, PD-L1, LAG-3+ TILs, and CD8+TILs and to survey the relationship between these markers in TNBC.

TABLE 1 | The clinicopathologic characteristics of 74 patients with TNBC.

Characteristics	Number of patients	Percent (%)
Gender		
Female	74	100.0
Male	0	0.0
Age		
<50	30	40.5
≥50,<60	21	28.4
≥60,<70	15	20.3
≥70	8	10.8
Degree of tumor differentiation		
High	3	4.1
Middle	32	43.2
low	39	52.7
Distant metastases		
0	52	70.3
1	22	29.7
Tumor size		
≤2cm	43	58.1
≤5cm,>2cm	25	33.8
>5cm	6	8.1

MATERIALS AND METHODS

Patients and Specimens

A total of 74 formalin-fixed paraffin-embedded specimens from primary and metastatic triple-negative invasive breast cancers, including 62 invasive breast cancers of no specific type cases and 12 invasive lobular carcinoma, archived in Peking Union Medical College Hospital between December 2015 and December 2018 were enrolled in the study. The ER, PR, and HER2 status were identified using protein expression and gene amplification by IHC (ER, PR, and HER2) and fluorescent *in situ* hybridization (FISH, reflex HER2 testing for IHC equivocal samples) assays along with the conventional histopathological diagnosis. The clinicopathological characteristics of the patients are listed in **Table 1**. This retrospective study was approved by the Institutional Review Board of Peking Union Medical College Hospital and was performed in accordance with the Declaration of Helsinki and the ethical standards for medical research involving human participants.

MMR Protein Expression Detection by IHC

IHC staining was conducted to assess the expression of four MMR proteins, MLH1, MSH2, MSH6, and PMS2 on 4 μm formalin-fixed paraffin-embedded slides. According to the manufacturer's protocols, primary monoclonal antibodies against MLH1 (clone M1), MSH2 (clone G219-1129), MSH6 (clone SP93), and PMS2 (clone A16-4) were used based on Ventana BenchMark autostainer (Ventana Medical System, Inc., Tucson, AZ, USA). dMMR was considered when any of the four MMR proteins were completely absent in the nuclear staining of tumor tissue, while concurrent positive benign cells were found in adjacent tissues, and intact IHC staining of these four antibodies was classified as proficient MMR (pMMR) according to the interpretation criteria described previously (21). For the pMMR subtype, MLH1, PMS2, MSH2, or MSH6 protein was scored as high if IHC staining was found in more than 50% of tumor cells according to a previous study (22).

Intrinsic Subtype Stratification by IHC and FISH

The expression of ER, PR, and HER2 proteins was evaluated on 4μm thick tissue sections by IHC using Ventana BenchMark automated immune stainer with antibodies of SP1, IE2, and 4B5 clones (Ventana Medical System, Inc., Tucson, AZ, USA), respectively, according to the manufacturer' s instructions. The tumors were classified as positive for ER or PR if immunoreactivity was found in ≥1% of tumor cell nuclei, according to ASCO/CAP recommendations for immunohistochemical testing of ER and PR in BC (23). HER2 status was detected by IHC in the initial examination, followed by FISH testing for IHC equivocal cases. FISH was performed on 4 μm sections using the Thermo-Brite Elite automated FISH slide prep system (Leica, Richmond, CA, USA) with a PathVysion HER2 DNA probe kit (Vysis/Abbott, Abbott Park, Illinois) as the standard protocol. HER2 IHC and FISH slides were scored according to the ASCO/CAP HER2 testing guidelines: IHC 0, 1+, 2+, and 3+ were determined. IHC 0 and IHC 1+ were classified as HER2-negative, and IHC 3+ was classified as HER2-positive. IHC 2+ was considered as HER2 equivocal and was further confirmed by FISH assay. HER2 FISH positivity was determined when the ratio of HER2/CEP17 ≥2.0 or the average HER2 signal/tumor cell ≥6.0, with a ratio of HER2/CEP17 <2.0; FISH negative was identified when the ratio of HER2/CEP17<2.0 (24). TNBC was defined as ER-, PR-, and HER2- (25).

MSI Detection by PCR With Two MSI Panels

MSI was measured using a Veriti DX 96-well PCR thermal cycler (Applied Biosystems, Foster City, CA, USA) for PCR assay with two panels of microsatellite markers {Promega 1.2: BAT-25, BAT-26, NR-21, NR-24, and MONO-27; National Cancer Institute (NCI): BAT25, BAT26, D2S123, D5S346, and D17S250}, respectively, and a 3500 Dx Genetic Analyzer

(Applied Biosystems, Foster City, CA, USA) for PCR product detection after DNA extraction from formalin-fixed paraffin-embedded tumor tissue and paired peritumoral benign tissue. The sample was considered to be microsatellite unstable if there was a shift of three base pairs in the tumor allele compared with normal tissue. MSI-H, MSI-L (low-frequency microsatellite instability), and MSS were distinguished when two or more, one, and no unstable markers were observed, respectively (26).

PD-L1, LAG-3, and CD8 Protein Expression Testing by IHC

IHC staining of three antibodies, including PD-L1 (clone E1L3N, dilution 1:200; Cell Signaling Technology, MA, USA), LAG-3 (clone D2G40, dilution 1:150; Cell Signaling Technology, MA, USA), and CD8 (clone 4B11, Leica, Newcastle upon Tyne, UK) were carried out using the DAKO EnVision method on 4 μm sections according to the manufacturers' protocols, respectively. Positive PD-L1 expression was interpreted when there was membranous staining with or without cytoplasmic staining of any intensity in ≥1% of tumor cells or immune cells as described previously (12). LAG-3 and CD8 were respectively defined as positive when there were intra tumoral and peri-tumor stromal lymphocytes with any immunoreactivity in ≥1% or in ≥10% of the entire tumoral area according to published studies and the recommendations of the International TILs Working Group (12, 27).

Statistical Analysis

The data were analyzed using SAS version 9.4 software. Significance was considered at a P-value < 0.05.

RESULTS

MMR and MSI Status

Four MMR proteins, MLH1, MSH2, MSH6, and PMS2, were homogenously expressed in all samples; all were pMMR. No heterogeneous expression was observed in our cohort. Except for one sample with low-expressed MLH1 and two samples with low-expressed PMS2, high expression of MMR proteins in all other cases was determined (**Table 2**). MMR protein expression is listed in **Figure 1**. Tumors with dMMR were not found in the series. All samples showed MSS detected by Promega 1.2 and NCI panels (**Figure 2**). There were no cases of MSI-H or MSI-L (**Table 3**).

TABLE 2 | MMR protein expression levels in the study cohort.

	MMR protein expression by IHC		
	Average (range)		n
MLH1	88.1%(30-90)	High	73
		Low	1
PMS2	83.4%(30-90)	High	72
		Low	2
MSH2	88.8%(70-90)	High	74
		Low	0
MSH6	89.9%(80-90)	High	74
		Low	0

PD-L1, LAG-3, and CD8 Expression

In 43 of the 74 cases (58.1%) PD-L1 expression was identified, including 1 case (1.4%, 1/74) with tumor PD-L1+, 25 cases (33.8%, 25/74) with TIL PD-L1+, and 17 cases (23.0%, 17/74) with tumor and TIL co-expression of PD-L1, respectively. The rate of PD-L1+ TILs was remarkably higher than that of PD-L1+ tumors (P<0.001).

From the perspective of expression level, 18 cases (24.3%, 18/74) with tumor PD-L1+ (the proportion of positive cells was 1%–80%) were observed, including 16 cases (88.9%, 16/18) of low-level expression (≥1% and <50%) and two cases (11.1%, 2/18) of high-level expression (≥50%). In another subtype, 42 cases (56.8%, 42/74) with TIL PD-L1+ were determined (the proportion of positive cells was also 1%–80%), including four cases (9.5%, 4/42) of low-level expression (1%) and 18 cases (42.9%, 18/42) of high-level expression (≥50%). In summary, PD-L1 was predominantly expressed in immune cells, most of which showed high-level expression.

We recognized 20 cases with LAG-3 expression (27.0%, 20/74) with a 1%–30% proportion of positive lymphocytes, including seven cases (35.0%, 7/20) of high-level expression (≥10%). The LAG-3 positive samples were PD-L1+ (the frequency of PD-L1 and LAG-3 co-expression was 27.0%, 20/74), which accounted for 46.5% (20/43) of all PD-L1+ cases. In the LAG-3+ subtype, 10 cases (50%, 10/20) had TIL PD-L1+, nine cases (45%, 9/20) showed concurrence in tumor and immune cells for PD-L1 expression, and 1 case (5.0%, 1/20) showed tumor PD-L1+ only. In the LAG-3+ subgroup, TIL PD-L1 expression was also dramatically higher than tumor PD-L1 expression. The high correlation between TIL PD-L1 expression and LAG-3 expression was explored (P<0.01). In brief, all LAG-3+ cases expressed PD-L1 simultaneously. Most samples with concurrence of PD-L1+ and LAG-3+ were of TILs PD-L1+ or concurrence of TILs and tumor PD-L1+.

Apart from one CD8- case (also PD-L1- and LAG-3-), high-frequency CD8 + was exhibited (98.6%, 73/74) with 20-90% positive cell proportion, including 64 cases (86.5%, 64/74) moderate or more level (≥50%) of expression, and 14 cases (18.9%, 14/74) of high-level expression (≥90%). CD8+ with high-level expression was a common feature in our patients (**Figure 3**).

In addition, these samples possessed 5%–90% Ki67 index, including 50 (67.6%, 50/74) cases with high proliferation index (Ki67≥30%). The proportion of high Ki67 index in the PD-L1+ and PD-L1- subgroups was 88.4% (38/43) and 38.7% (12/31), respectively. In the subgroup of concurrent PD-L1+ and LAG-3+, 18 cases had high Ki67 index (90.0%, 18/20), except for two cases with low expression of Ki67 (5% and 25%) (**Figure 4**).

DISCUSSION

With the increasing application of immune components in solid tumors, the detection of potential TNBC patients who could benefit by receiving ICIs warrants further research. Therefore, it is important to explore the incidence of TNBC with dMMR/MSI-H features, which is a predictive marker approved by the

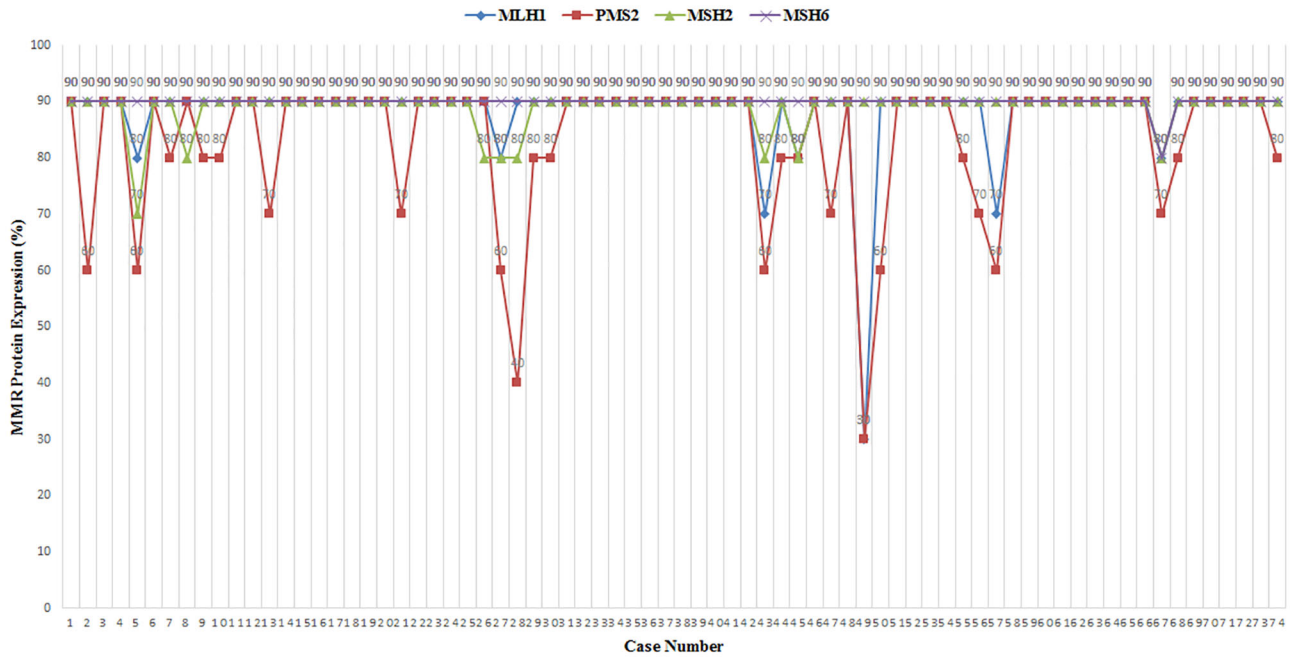

FIGURE 1 | MLH1, PMS2, MSH2, and MSH6 protein expression in 74 triple-negative breast cancer (TNBC) samples.

FDA for solid tumors treated with ICIs (pembrolizumab), and it is also vital to identify TNBC with dMMR/MSI-H or for drafting some recommendations of immune biomarkers in the future, although this indication of ICIs is not used in China to date.

In our series, all cases were pMMR, and no dMMR samples were found. The IHC results were confirmed by both Promega 1.2 and NCI panels, and MSS status were disclosed for all samples. IHC and PCR showed high consistency. Our findings corroborated the reports that dMMR and/or MSI were rare events (<1.0%) in TNBC (13, 28). Recently, MMR gene variation in 963 cases of invasive breast cancer in TCGA (The Cancer Genome Atlas) was evaluated by a research team. They confirmed a low incidence of MMR deficiency, reporting that 2.9% of specimens harbored any mutation in at least one of the MMR genes (MLH1, PMS2, MSH2, and MSH6) as well as a low frequency of driver mutation as compared to colorectal cancer (29). In our pMMR subgroup, majority of cases with highly expressed MMR proteins were found. Only one case with low-expressed MLH1 and two cases with low-expressed PMS2 were exposed. In a previous study, dMMR was observed in 0.4% (1/285) of breast cancer cases, which were TNBC cases with loss of MLH1 and PMS2 proteins (29). In another recent study including 63 TIL-high TNBC cases from Japan, MSS was identified in all samples, and only one dMMR case with loss of MLH1 and PMS2 was reported (22). Low or loss of MLH1 and PMS2 protein expression might often occur in TNBC patients based on our results and the published data available. Low-expressed PMS2 protein was also observed in one out of 10 cases of colorectal cancer in our previous study cohort, and other MMR proteins were all highly expressed in all samples (data not shown) (26). The potential biological implications of this process remain to be explored further. We used the IHC detection system approved by the FDA for Lynch syndrome test (https://www.fda.gov/medical-devices/vitro-diagnostics/nucleic-acid-based-tests) and two accepted conventional MSI panels (Promega 1.2 and NCI) to reduce approach bias. Similar to the findings from the literature mentioned above, we did not find a high discordance between MMR protein expression by IHC and MSI status by DNA testing (NCI panel), which has been reported previously (14). Although, a study declared that the hormone receptor-positive BC possessed a similar rate of dMMR as TNBC patients (17% vs. 20%), which was also noted, response rates from PD-1 inhibitors (e.g., avelumab, an anti-PD-L1 antibody) was obviously lower than that of TNBC (14, 30). Hence, screening of TNBC patients who benefit from ICIs has been brought into focus relatively so far.

Our data showed homogeneous pMMR staining and consistent results between IHC and PCR for MMR and MSI measurement, respectively, suggesting that the two methods could be used interchangeably in TNBC notwithstanding no infrequent dMMR/MSI-H or MSI-L cases in our cohort for conclusively verifying our view. Our results of IHC (whole slide staining) were different from a tissue microarray (TMA) cohort study in which 6.9% of TNBC cases with complete MMR loss were presented (12). These differences between the two studies were probably caused by different IHC antibody clones and sample types. Two out of 228 cases (0.9%) were found to harbor MSI-H in TNBC *via* the same analysis system (Promega

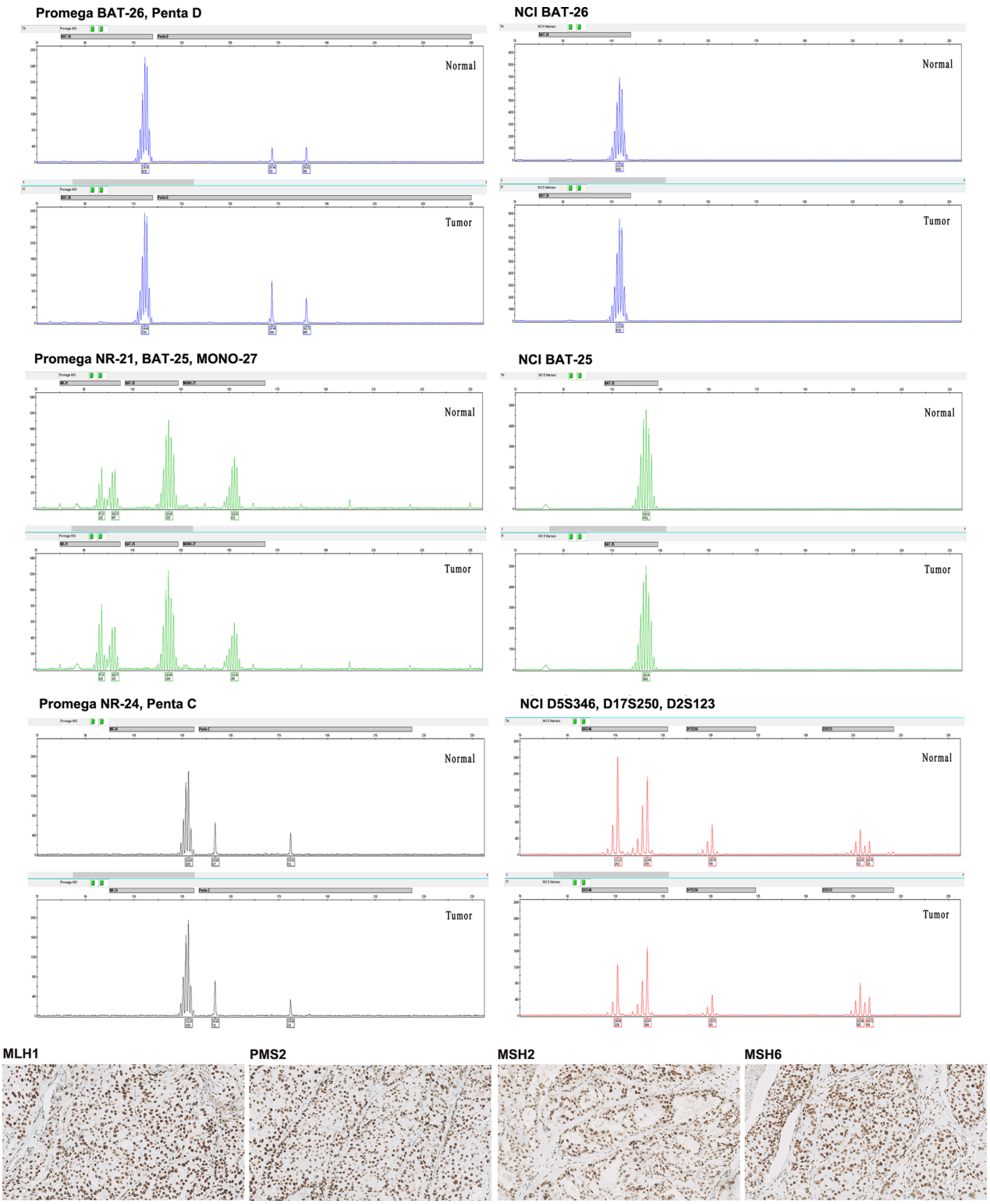

FIGURE 2 | Representative images from pMMR/MSS triple-negative breast cancer (TNBC) in our cohort. The four MMR proteins (MLH1, PMS2, MSH2, and MSH6) (X200) all showed intact immunohistochemistry (IHC) staining. The microsatellite markers presented MSS both by Promega 1.2 and NCI panels. Promega 1.2 panel: BAT-25, BAT-26, NR-21, NR-24, and MONO-27; NCI panel: BAT25, BAT26, D2S123, D5S346, and D17S250.

TABLE 3 | MSI status detected by Promega 1.2 and NCI panels.

		MSI status by Promega 1.2		
		MSI-H	**MSI-L**	**MSS**
MSI status by NCI	MSI-H	0	0	0
	MSI-L	0	0	0
	MSS	0	0	74

1.2) as ours, which was reported by another research team. IHC was supported for MMR assessment by some researchers despite being unchecked by MSI assay (28, 31). Consequently, adequate experience of detecting MMR/MSI in TNBC is still required. Despite PD-1(L1) ICIs (such as pembrolizumab) targeting dMMR/MSI-H tumors, the beneficiary was not preselected using this immune biomarker because of the rare event in TNBC. The exploration should be focused on other effective-related biomarkers of ICIs.

Currently, PD-L1 expression is considered to be one of the most important markers for predicting ICI effect. The data from clinical settings remain limited because ICIs (such as atezolizumab) are not currently used as first-line therapy for TNBC in China. A study involving 228 cases mentioned above showed that 39.5% of Japanese TNBC expressed tumor PD-L1 (same E1L3N and cutoff values as in our study), but immune cell PD-L1 status was not evaluated (28). Moreover, a Chinese team demonstrated that PD-L1+ (using E1L3N with 5% cutoff) accounted for 25.74% and 30.79% in tumor cells and lymphocytes, respectively, in primary TNBC (32). We identified 58.1% of cases with PD-L1+, including only 1 tumor PD-L1 expression (1.4%, 1/74), which was much lower than the positive rate in lymphocytes (33.8%, 25/74). This tendency was similar to another study on 119 cases of TNBC that reported 64.4% of TILs and 0% of tumor cell PD-L1+. Accordingly, they revealed that TNBC had a higher PD-L1 expression rate than

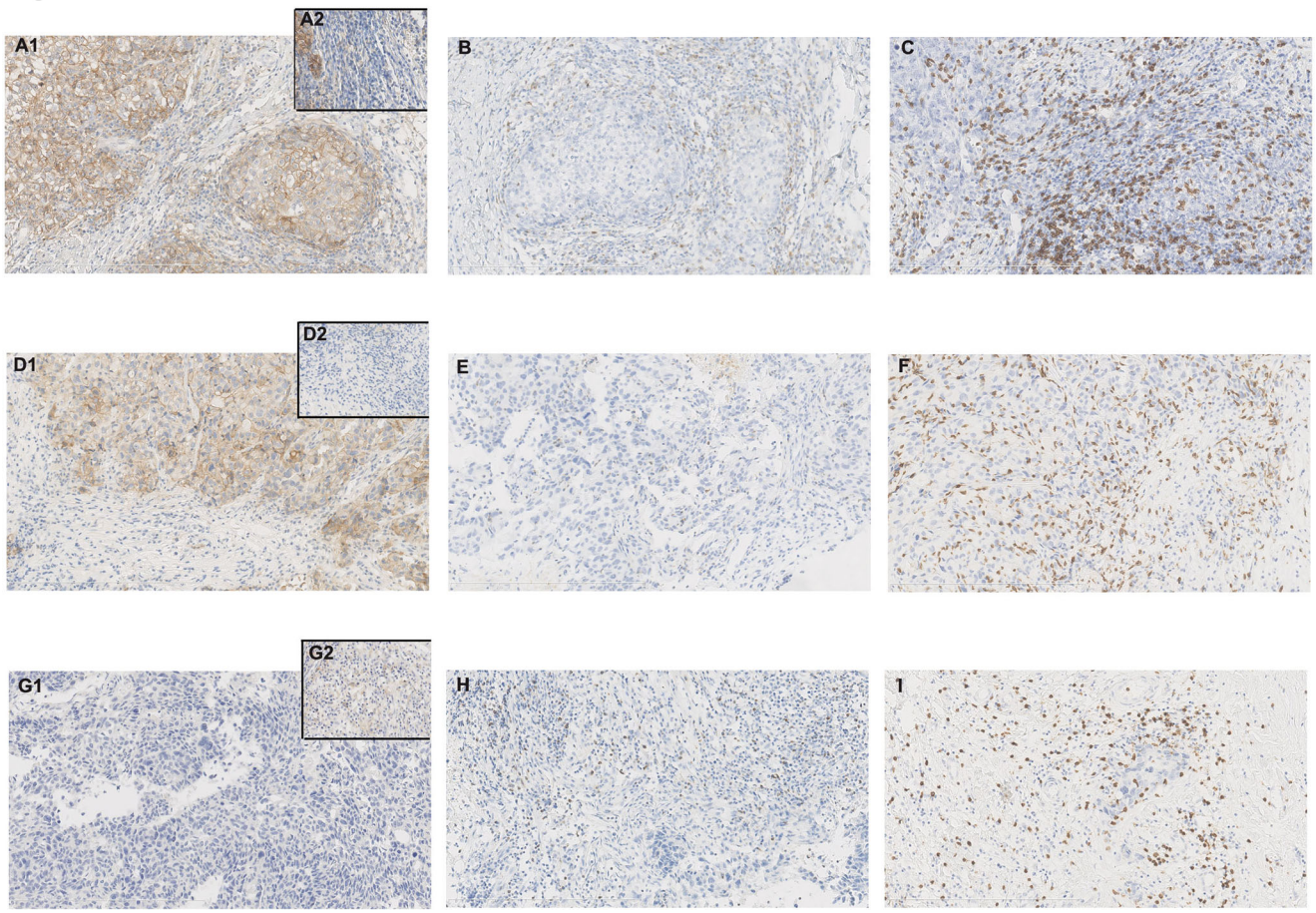

FIGURE 3 | Case no. 74 **(A–C)** showed tumor programmed death-ligand 1 (PD-L1)+, tumor-infiltrating lymphocytes (TILs) PD-L1+, lymphocyte-activation gene 3 (LAG-3)+, and CD8+ with 80%, 10%, 30%, and 70% positive cells, respectively (X200). **(A)** PD-L1 staining with clone E1L3N (A1. tumor PD-L1+/partial TILs PD-L1+; A2. TILs PD-L1+); **(B)** LAG-3 staining with clone D2G40; **(C)** CD8 staining with clone 4B11; Case no. 46 **(D–F)** showed tumor PD-L1+, TILs PD-L1-, LAG-3+, and CD8+ with 80%, 0%, 1%, and 90% positive cells respectively (X200). **(D)** PD-L1 staining with clone E1L3N (D1. tumor PD-L1+/TILs PD-L1-; D2. TILs PD-L1-); **(E)** LAG-3 staining with clone D2G40; **(F)** CD8 staining with clone 4B11; Case no. 34 **(G–I)** showed tumor PD-L1-, TILs PD-L1+, LAG-3+, and CD8+ with 0%, 10%, 10%, and 70% positive cells respectively (X200). **(G)** PD-L1 staining with clone E1L3N (G1. tumor PD-L1-; G2. TILs PD-L1+); **(H)** LAG-3 staining with clone D2G40; **(I)** CD8 staining with clone 4B11.

FIGURE 4 | The status of programmed death-ligand 1 (PD-L1), lymphocyte-activation gene 3 (LAG-3), CD8 and Ki67 index in our series.

HER2+ BC (75.2% vs16.8%), which validated the findings published previously (12, 33). In addition to PD-L1 commonly expressed on immune cells, in which PD-L1 expression (≥ 1%, with any intensity) was determined as a sensitive marker for evaluating TNBC response to ICI (Impassion 130 study) (34). Our data supported TNBC patients as a potential population who benefited from ICIs and indicated the need to focus on PD-L1 status in immune cells.

Available evidence indicates that the level of TILs, which are also important biomarkers for immunotherapy in TNBC, was much higher than in other subtypes, among which cytotoxic CD8+ lymphocytes were considered as independent markers of favorable prognosis in TNBC (35, 36). Vihervuori et al. reported that when the cutoff was ≥10%, ≥50%, and ≥90%, the CD8+ rates in the tumor center and invasive front of the tumors were 54% vs. 53.5%, 8.2% vs. 8.8%, and 0 vs. 0, respectively (37). A meta-analysis demonstrated that a high number of TILs would predict prolonged overall survival (OS) regardless of TIL location (intratumoral or stromal), total TILs, or CD8+ TILs (38). Thus, in the current study, we scored fashionable CD8+ immune cells, including intratumoral and

stromal infiltrating lymphocytes. The frequency of CD8+ (≥10%) T cells was up to 98.7%, among which the samples with CD8+ cells ≥50% and ≥90% were 87.8% and 18.9%, respectively. The different findings between our study and previous studies need to be further analyzed.

However, the response rates from ICIs (especially monotherapy) are usually lower because the tumor microenvironment is quite heterogeneous and have complicated interactions with biological factors that are less known. Several inhibitory checkpoints have been recognized and are being tested as promising new targets for cancer immunotherapy in addition to PD-1 (L1) blockade, including LAG-3, TIM-3 (T cell immunoglobulin and mucin domain-containing molecule-3), and TIGIT (T cell immunoreceptor with immunoglobulin and immunoreceptor tyrosine-based inhibitory motif domain) are highly anticipated (39). LAG-3 is considered the paramount target next to PD-1. At least 13 anti-LAG-3 reagents have been developed to date (40).

LAG-3 was found to be upregulated in some epithelial cancers. In addition, LAG-3 and PD-L1 showed synergism in T-cell action regulation causing immune resistance (17, 41). Inhibition of LAG-3/MHCII interaction with targeted reagents (such as IMP321) was found to activate tumor-related CD8 expression and produce cytokines (42–44). Furthermore, overexpression of LAG-3 was inferred to be one of the causes of poor response to PD-1(L1) ICIs in cancers. According to the reports, the clinical benefit of combining anti-LAG-3 (relatlimab) and anti-PD-1 (nivolumab) was observed for melanoma patients with progressive disease during prior nivolumab monotherapy, and the objective response rate (ORR) was 3 fold higher in patients with LAG-3 positive than in LAG-3 negative patients (45, 46). Semblance of LAG-3+ TILs may be a predictor of existing cancer–immune interaction and present an inflamed tumor, which indicates a better prognosis. In a phase I/II study (NCT02460224), LAG525 (an anti-LAG-3 reagent) plus spartalizumab (an anti-PD-1 reagent) showed a durable response in solid tumors including TNBC (47). In a BC study with TMA samples, 53% of PD-L1+ cases expressed LAG-3, and the proportion of concurrent LAG-3+ and CD8+, and PD-L1+ and CD8+, were 26% and 18%, respectively (data on TNBC were not available). In addition, compared with other subtypes, basal-like BC possessed more LAG-3+ cases (33%). They suggested that this may be significant for evaluating ICI anti-tumor activity in relevant clinical trials *via* stratification of PD-L1 + and double-positive PD-L1 and LAG-3 (16). In our specimens, we recognized 27.0% of LAG-3+ cases in TNBC, meaning that 46.5% of cases had concurrent PD-L1 and LAG-3 expression and high Ki67 index for most cases in the PD-L1+ subgroup. Our findings were consistent with those reported previously for BC. In summary, studies on the biological and clinical significance of LAG-3 in TNBC are extremely limited.

As mentioned above, like LAG-3, upregulation of TIM-3 or TIGIT is also associated with an immune resistance mechanism (39). Relevant data from a large cohort study strongly supported TIM-3 as a prospective target for BC immunotherapy based on their finding that 28% basal-like breast cancers and 18% non-basal TNBC possessed TIM-3 expression in intra-epithelial TILs (iTILs), respectively, and TIM-3 + iTILs significantly correlated with PD-1, LAG-3, and PD-L1 expression in BC (48). Several anti-TIM-3 agents are currently being used in clinical trials. The preliminary data showed 20% tumor regression from a phase 1 study of LY3321367 (an anti-TIM-3 antibody) monotherapy or in combination with LY3300054 (an anti-PD-L1 antibody) (49). TIGIT is another promising immune therapeutic target. Blocking TIGIT or its ligand poliovirus receptor leading to enhanced anti-tumor effects was observed in HER2 positive BC and TNBC cell lines (50). In a study of 10 fresh tumor samples from untreated TNBC patients, TIGIT overexpression was found in CD8+ and CD4+ TILs, and highly expressed TIGIT and its ligands (CD155 and CD112) were discovered in tumor cells and antigen-presenting cells (51). These data indicate that anti-TIGIT is a potentially valuable therapeutic approach for BC treatment. In a first-line therapy for non-small cell lung cancer, atezolizumab plus tiragolumab (an anti-TIGIT antibody) showed superior clinical efficacy as compared with anti-PD-L1 therapy alone recently (52). Therefore, dual PD-1(L1) and TIGIT blockade might be a promising option. However, TIM-3 and TIGIT targeting are still early in clinical research, and few reports of the therapeutic efficacy of anti-TIGIT or anti-TIM-3 including combinatorial therapies (TIGIT ICI or TIM-3 ICI plus PD-1(L1) ICI) are available in breast cancer to date. Furthermore, detailed mechanisms of anti-tumor immunotherapy, including blocking PD-1(L1), LAG-3, TIM-3, and TIGIT, are still unclear and require further research.

In conclusion, we retrospectively analyzed MMR, MSI, PD-L1, and LAG-3 status in TNBC. None of the cases demonstrated dMMR or MSI, as detected by authentic IHC assay and MSI panels, respectively. This indicates that potential beneficiaries of PD-1(L1) ICIs may not be preselected by these markers. All cases enrolled in the current study exhibited a high frequency of PD-L1+ and CD8+. Compared to tumors, PD-L1 expression in lymphocytes was more common and more attractive to investigators. Furthermore, in the PD-L1+ population, approximately half of the samples had PD-L1+ and LAG-3 co-expression, which symbolized the synergism of PD-L1 and LAG-3 in TNBC. For patients with poor responsiveness to PD-1(L1) mono immunotherapy, the possibility of benefiting from dual-blockading PD-1 and LAG-3 may not be neglected. It is worthwhile to further understand the significance of LAG-3 in TNBC.

DATA AVAILABILITY STATEMENT

The original contributions presented in the study are included in the article/supplementary materials. Further inquiries can be directed to the corresponding author.

ETHICS STATEMENT

The studies involving human participants were reviewed and approved by The Institutional Review Board (IRB) of Peking

Union Medical College Hospital (PUMCH). The ethics committee waived the requirement of written informed consent for participation.

AUTHOR CONTRIBUTIONS

SW, YYL, and YFL performed the experiments. SW, YYL, XW, and FM collected the clinicalpathological information. XS, JW, and SW scored the slides and analyzed the data. SW and XZ designed the study and wrote the manuscript. All authors contributed to the article and approved the submitted version.

FUNDING

This study was supported by the foundation from the National Key Research and Development Program of China (No.2017YFC1309004) and Chinese Academy of Medical Sciences (CAMS) Initiative for Innovative Medicine (No.2017-I2M-1-005).

REFERENCES

1. Gadi VK, Davidson NE. Practical Approach to Triple-Negative Breast Cancer. *J Oncol Pract* (2017) 13(5):293–300. doi: 10.1200/JOP.2017.022632
2. Winter C, Nilsson MP, Olsson E, George AM, Chen Y, Kvist A, et al. Targeted Sequencing of BRCA1 and BRCA2 Across a Large Unselected Breast Cancer Cohort Suggests That One-Third of Mutations Are Somatic. *Ann Oncol* (2016) 27(8):1532–8. doi: 10.1093/annonc/mdw209
3. Li YT, Ni D, Yang L, Zhao Q, Ou JH. The prevalence of BRCA1/2 mutations of triple-negative breast cancer patients in Xin jiang multiple ethnic region of China. *Eur J Med Res* (2014) 19:35. doi: 10.1186/2047-783X-19-35
4. Bastaki S, Irandoust M, Ahmadi A, Hojjat-Farsangi M, Ambrose P, Hallaj S, et al. PD-L1/PD-1 axis as a potent therapeutic target in breast cancer. *Life Sci* (2020) 15:117437. doi: 10.1016/j.lfs.2020.117437
5. Katz H, Alsharedi M. Mohamed Alsharedi. Immunotherapy in Triple-Negative Breast Cancer. *Med Oncol* (2017) 35(1):13. doi: 10.1007/s12032-017-1071-6
6. Schmid P, Adams S, Rugo HS, Schneeweiss A, Barrios CH, Iwata H, et al. Atezolizumab and Nab-Paclitaxel in Advanced Triple-Negative Breast Cancer. *N Engl J Med* (2018) 379(22):2108–21. doi: 10.1056/NEJMoa1809615
7. Emens LA, Cruz C, Eder JP, Braiteh F, Chung C, Tolaney SM, et al. Long-term Clinical Outcomes and Biomarker Analyses of Atezolizumab Therapy for Patients With Metastatic Triple-Negative Breast Cancer: A Phase 1 Study. *JAMA Oncol* (2019) 5(1):74–82. doi: 10.1001/jamaoncol.2018.4224
8. Adams S, Loi S, Toppmeyer D, Cescon DW, De Laurentiis M, Nanda R, et al. Pembrolizumab monotherapy for previously untreated, PD-L1-positive, metastatic triple-negative breast cancer: cohort B of the phase II KEYNOTE-086 study. *Ann Oncol* (2019) 30(3):405–11. doi: 10.1093/annonc/mdy518
9. Schwitalle Y, Kloor M, Eiermann S, Linnebacher M, Kienle P, Knaebel HP, et al. Immune response against frameshift-induced neopeptides in HNPCC patients and healthy HNPCC mutation carriers. *Gastroenterology* (2008) 134:988–97. doi: 10.1053/j.gastro.2008.01.015
10. Le DT, Durham JN, Smith KN, Wang H, Bartlett BR, Aulakh LK, et al. Mismatch repair deficiency predicts response of solid tumors to PD-1 blockade. *Science* (2017) 357(6349):409–13. doi: 10.1126/science.aan6733
11. Llosa NJ, Cruise M, Tam A, Wicks EC, Hechenbleikner EM, Taube JM, et al. The vigorous immune microenvironment of microsatellite instable colon cancer is balanced by multiple counter-inhibitory checkpoints. *Cancer Discov* (2015) 5:43–51. doi: 10.1158/2159-8290.CD-14-0863
12. Hou Y, Nitta H, Parwani AV, Li Z. PD-L1 and CD8 are associated with deficient mismatch repair status in triple-negative and HER2-positive breast cancers. *Hum Pathol* (2019) 86:108–14. doi: 10.1016/j.humpath.2018.12.007
13. Wen YH, Brogi E, Zeng Z, Akram M, Catalano J, Paty PB, et al. DNA Mismatch Repair Deficiency in Breast Carcinoma: A Pilot Study of Triple-negative and Non–Triple-negative Tumors. *Am J Surg Pathol* (2012) 36 (11):1700–8. doi: 10.1097/PAS.0b013e3182627787
14. Fusco N, Lopez G, Corti C, Pesenti C, Colapietro P, Ercoli G, et al. Mismatch Repair Protein Loss as a Prognostic and Predictive Biomarker in Breast Cancers Regardless of Microsatellite Instability. *JNCI Cancer Spectr* (2018) 2 (4):pky056. doi: 10.1093/jncics/pky056
15. Prasad V, Kaestner V, Mailankody S. Cancer drugs approved based on biomarkers and not tumor type-FDA approval of pembrolizumab for mismatch repair-deficient solid cancers. *JAMA Oncol* (2018) 4:157–8. doi: 10.1001/jamaoncol.2017.4182
16. Burugu S, Gao D, Leung S, Chia SK, Nielsen TO. LAG-3+ tumor infiltrating lymphocytes in breast cancer: clinical correlates and association with PD-1/PD-L1+ tumors. *Ann Oncol* (2017) 28(12):2977–84. doi: 10.1093/annonc/mdx557
17. Woo SR, Turnis ME, Goldberg MV, Bankoti J, Selby M, Nirschl CJ, et al. Immune inhibitory molecules LAG-3 and PD-1 synergistically regulate T-cell function to promote tumoral immune escape. *Cancer Res* (2012) 72(4):917–27. doi: 10.1158/0008-5472.CAN-11-1620
18. Su M, Huang CX, Dai AP. Immune Checkpoint Inhibitors: Therapeutic Tools for Breast Cancer. *Asian Pac J Cancer Prev* (2016) 17(3):905–10. doi: 10.7314/apjcp.2016.17.3.905
19. Andrews LP, Marciscano AE, Drake CG, Vignali DA. LAG-3 (CD223) as a cancer immunotherapy target. *Immunol Rev* (2017) 276(1):80–96. doi: 10.1111/imr.12519
20. Stanton SE, Adams S, Disis ML. Variation in the incidence and magnitude of tumor-infiltrating lymphocytes in breast cancer subtypes: a systematic review. *JAMA Oncol* (2016) 2:1354–60. doi: 10.1001/jamaoncol.2016.1061
21. Kheirelseid EA, Miller N, Chang KH, Curran C, Hennessey E, Sheehan M, et al. Mismatch repair protein expression in colorectal cancer. *J Gastrointest Oncol* (2013) 4:397–408. doi: 10.3978/j.issn.2078-6891.2013.021
22. Horimoto Y, Thinzar Hlaing M, Saeki H, Kitano S, Nakai K, Sasaki R, et al. Microsatellite instability and mismatch repair protein expressions in lymphocyte-predominant breast cancer. *Cancer Sci* (2020) 111(7):2647–54. doi: 10.1111/cas.14500
23. Hammond ME, Hayes DF, Wolff AC, Mangu PB, Temin S. American society of clinical oncology/college of american pathologists guideline recommendations for immunohistochemical testing of estrogen and progesterone receptors in breast cancer. *J Oncol Pract* (2010) 6(4):195–7. doi: 10.1200/JOP.777003
24. Wolff AC, Hammond ME, Hicks DG, Dowsett M, McShane LM, Allison KH, et al. Recommendations for human epidermal growth factor receptor 2 testing in breast cancer: American Society of Clinical Oncology/College of American Pathologists clinical practice guideline update. *J Clin Oncol (2013)* (2013) 31 (31):3997–4013. doi: 10.1200/JCO.2013.50.9984
25. Goldhirsch A, Winer EP, Coates AS, Gelber RD, Piccart-Gebhart M, Thürlimann B, et al. Panel members: personalizing the treatment of women with early breast cancer: highlights of the St Gallen International Expert Consensus on the Primary Therapy of Early Breast Cancer. *Ann Oncol* (2013) 24:2206–23. doi: 10.1093/annonc/mdt303
26. Wu S, Liu X, Wang J, Zhou W, Guan M, Liu Y, et al. DNA Mismatch Repair Deficiency Detection in Colorectal Cancer by a New Microsatellite Instability Analysis System. *Interdiscip Sci* (2020) 12(2):145–54. doi: 10.1007/s12539-020-00358-8
27. Salgado R, Denkert C, Demaria S, Sirtaine N, Klauschen F, Pruneri G, et al. The evaluation of tumor-infiltrating lymphocytes (TILs) in breast cancer: recommendations by an International TILs Working Group 2014. *Ann Oncol* (2015) 26(2):259–71. doi: 10.1093/annonc/mdu450
28. Kurata K, Kubo M, Kai M, Mori H, Kawaji H, Kaneshiro K, et al. Microsatellite instability in Japanese female patients with triple-negative

breast cancer. *Breast Cancer* (2020) 27(3):490–8. doi: 10.1007/s12282-019-01043-5
29. Mills AM, Dill EA, Moskaluk CA, Dziegielewski J, Bullock TN, Dillon PM. The Relationship Between Mismatch Repair Deficiency and PD-L1 Expression in Breast Carcinoma. *Am J Surg Pathol* (2018) 42(2):183–91. doi: 10.1097/PAS.0000000000000949
30. Dirix LY, Takacs I, Jerusalem G, Nikolinakos P, Arkenau HT, Forero-Torres A, et al. Avelumab, an anti-PD-L1 antibody, in patients with locally advanced or metastatic breast cancer: a phase 1b JAVELIN Solid Tumor study. *Breast Cancer Res Treat* (2018) 167(3):671–86. doi: 10.1007/s10549-017-4537-5
31. Cheng AS, Leung SCY, Gao D, Burugu S, Anurag M, Ellis MJ, et al. Mismatch repair protein loss in breast cancer: clinicopathological associations in a large British Columbia cohort. *Breast Cancer Res Treat* (2020) 179(1):3–10. doi: 10.1007/s10549-019-05438-y
32. Li M, Li A, Zhou S, Xu Y, Xiao Y, Bi R, et al. Heterogeneity of PD-L1 expression in primary tumors and paired lymph node metastases of triple negative breast cancer. *BMC Cancer* (2018) 18(1):4. doi: 10.1186/s12885-017-3916-y
33. Altan M, Kidwell KM, Pelekanou V, Carvajal-Hausdorf DE, Schalper KA, Toki MI, et al. Association of B7-H4, PD-L1, and tumor infiltrating lymphocytes with outcomes in breast cancer. *NPJ Breast Cancer* (2018) 4:40. doi: 10.1038/s41523-018-0095-1
34. Schmid P, Rugo HS, Adams S, Schneeweiss A, Barrios CH, Iwata H, et al. Atezolizumab plus nab-paclitaxel as first-line treatment for unresectable, locally advanced or metastatic triple-negative breast cancer (IMpassion130): updated efficacy results from a randomised, double-blind, placebo-controlled, phase 3 trial. *Lancet Oncol* (2020) 21(1):44–59. doi: 10.1016/S1470-2045(19)30689-8
35. Denkert C, von Minckwitz G, Darb-Esfahani S, Lederer B, Heppner BI, Weber KE, et al. Tumour-infiltrating lymphocytes and prognosis in different subtypes of breast cancer: a pooled analysis of 3771 patients treated with neoadjuvant therapy. *Lancet Oncol* (2018) 19(1):40–50. doi: 10.1016/S1470-2045(17)30904-X
36. Althobiti M, Aleskandarany MA, Joseph C, Toss M, Mongan N, Diez-Rodriguez M, et al. Heterogeneity of tumour-infiltrating lymphocytes in breast cancer and its prognostic significance. *Histopathology* (2018) 73(6):887–96. doi: 10.1111/his.13695
37. Vihervuori H, Autere TA, Repo H, Kurki S, Kallio L, Lintunen MM, et al. Tumor-infiltrating lymphocytes and CD8+ T cells predict survival of triple-negative breast cancer. *J Cancer Res Clin Oncol* (2019) 145(12):3105–14. doi: 10.1007/s00432-019-03036-5
38. Ibrahim EM, Al-Foheidi ME, Al-Mansour MM, Kazkaz GA. The prognostic value of tumor-infiltrating lymphocytes in triple-negative breast cancer: a meta-analysis. *Breast Cancer Res Treat* (2014) 148(3):467–76. doi: 10.1007/s10549-014-3185-2
39. Anderson AC, Joller N, Kuchroo VK. Lag-3, Tim-3, and TIGIT: Co-inhibitory Receptors with Specialized Functions in Immune Regulation. *Immunity* (2016) 44(5):989–1004. doi: 10.1016/j.immuni.2016.05.001
40. Maruhashi T, Sugiura D, Okazaki IM, Okazaki T. LAG-3: from molecular functions to clinical applications. *J Immunother Cancer* (2020) 8(2):e001014. doi: 10.1136/jitc-2020-001014
41. Pardoll DM. The blockade of immune checkpoints in cancer immunotherapy. *Nat Rev Cancer* (2012) 12(4):252–264.doi: 10.1038/nrc3239
42. Demeure CE, Wolfers J, Martin-Garcia N, Gaulard P, Triebel F. T Lymphocytes infiltrating various tumour types express the MHC class II ligand lymphocyte activation gene-3 (LAG-3): role of LAG-3/MHC class II interactions in cell–cell contacts. *Eur J Cancer* (2001) 37:1709–18. doi: 10.1016/S0959-8049(01)00184-8
43. Goldberg MV, Drake CG. LAG-3 in Cancer Immunotherapy. *Curr Top Microbiol Immunol* (2011) 344:269–78. doi: 10.1007/82_2010_114
44. Brignone C, Gutierrez M, Mefti F, Brain E, Jarcau R, Cvitkovic F, et al. Firstline chemoimmunotherapy in metastatic breast carcinoma: combination of paclitaxel and IMP321 (LAG-3Ig) enhances immune responses and antitumor activity. *J Transl Med* (2010) 8:71. doi: 10.1186/1479-5876-8-71
45. Chen DS, Mellman I. Elements of cancer immunity and the cancer immune set point. *Nature* (2017) 541(7637):321–30. doi: 10.1038/nature21349
46. Ascierto PA, Bono P, Bhatia S, Melero I, Nyakas MS, Svane I-M, et al. Efficacy of BMS-986016, a monoclonal antibody that targets lymphocyte activation gene-3 (LAG-3), in combination with nivolumab in pts with melanoma who progressed during prior anti-PD-1/PD-L1 therapy (mel prior IO) in all-comer and biomarker-enriched populations. *Ann Oncol* (2017) 28:403–40. doi: 10.1093/annonc/mdx440.011
47. Hong DS, Schoffski P, Calvo A, Sarantopoulos J, Ochoa de Olza M, Carvajal RD, et al. Phase I/II study of LAG525 ± spartalizumab (PDR001) in patients (PTS) with advanced malignancies. *J Clin Oncol* (2018) 36suppl; abstr 3012). doi: 10.1200/jco.2018.36.15_suppl.3012
48. Burugu S, Gao D, Leung S, Chia SK, Nielsen TO. TIM-3 expression in breast cancer. *Oncoimmunology* (2018) 7(11):e1502128. doi: 10.1080/2162402X.2018.1502128
49. Harding J, Patnaik A, Moreno V, Stein M, Jankowska AM, Velez de Mendizabal N, et al. A phase Ia/Ib study of an anti-TIM-3 antibody (LY3321367) monotherapy or in combination with an anti-PD-L1 antibody (LY3300054): interim safety, efficacy, and pharmacokinetic findings in advanced cancers. *J Clin Oncol* (2019) 37(8, 12). doi: 10.1182/blood-2019-128178
50. Stamm H, Oliveira-Ferrer L, Grossjohann EM, Muschhammer J, Thaden V, Brauneck F, et al. Targeting the TIGIT-PVR immune checkpoint axis as novel therapeutic option in breast cancer. *Oncoimmunology* (2019) 8(12):e1674605. doi: 10.1080/2162402X.2019.1674605
51. Pandey AK, Chauvin JM, Brufsky A, Pagliano O, Ka M, Menna C, et al. (2020). Targeting TIGIT and PD-1 in triple negative breast cancer, in: *Proceedings of the 2019 San Antonio Breast Cancer Symposium*, San Antonio, TX. Philadelphia PA, Cancer Res 2019 Dec 10-14, Vol. 80. AACR.
52. Rodriguez-Abreu D, Johnson ML, Hussein MA, Cobo M, Patel AJ, Secen NM, et al. Primary analysis of a randomized, double-blind, phase II study of the anti-TIGIT antibody tiragolumab (tira) plus atezolizumab (atezo) versus placebo plus atezo as first-line (1L) treatment in patients with PD-L1-selected NSCLC (CITYSCAPE). *J Clin Oncol* (2020) 38. doi: 10.1200/JCO.2020.38.15_suppl.9503

Conflict of Interest: The authors declare that the research was conducted in the absence of any commercial or financial relationships that could be construed as a potential conflict of interest.

frontiers in Oncology

SYSTEMATIC REVIEW
published: 19 March 2021
doi: 10.3389/fonc.2021.538174

Efficacy of Anti-PD-1/PD-L1 Monotherapy or Combinational Therapy in Patients Aged 75 Years or Older: A Study-Level Meta-Analysis

Run-Cong Nie[1†], Guo-Ming Chen[1†], Yun Wang[2†], Jie Zhou[3†], Jin-Ling Duan[3†], Zhi-Wei Zhou[1‡] and Shu-Qiang Yuan[1*‡]*

[1] Department of Gastric Surgery, Sun Yat-sen University Cancer Center, State Key Laboratory of Oncology in South China, Collaborative Innovation Center for Cancer Medicine, Guangzhou, China, [2] Department of Hematologic Oncology, Sun Yat-sen University Cancer Center, State Key Laboratory of Oncology in South China, Collaborative Innovation Center for Cancer Medicine, Guangzhou, China, [3] Department of Experimental Research, Cancer Institute, Sun Yat-sen University Cancer Center, State Key Laboratory of Oncology in South China, Collaborative Innovation Center for Cancer Medicine, Guangzhou, China

Recent trials have shown a promising anti-tumor activity for advanced cancer patients treated with PD-1/PD-L1 inhibitors; however, little is known on the use of PD-1/PD-L1 inhibitors in adults over 75 years of age. Here, we performed a study-level meta-analysis to compare the efficacy of anti-PD-1/PD-L1 agents between elderly (≥ 75 years) and non-elderly (< 75 years) patients. In the present study, we systematically reviewed phase 2/3 trials of PD-1/PD-L1 inhibitors of advanced solid tumors that reported treatment effect (hazard ratio [HR]) in patients based on age (≥ 75 years vs. < 75 years) and set anti-PD-1/PD-L1 monotherapy or combinational therapy as experimental arm. The HRs of OS and progression-free survival (PFS) are based on random-effect models. Overall, a total of eight qualifying trials comprising 5,393 subjects were included for meta-analysis, and 472 patients (8.8%) were aged 75 years or older. The overall estimated HR for OS was 0.70 (0.62–0.79) in patients < 75 years vs. 0.94 (0.67–1.30) in patients ≥ 75 years. Anti-PD-1/PD-L1 agents improved OS of melanoma patients in both elderly (HR 0.25 [0.10-0.60]) and non-elderly (HR 0.49 [0.33–0.71]) group. The OS difference in the efficacy of PD-1/PD-L1 inhibitors between elderly and non-elderly patients was significant (P = 0.043 for interaction). The overall estimated HR for PFS was 0.77 (0.60–1.00) in patients < 75 years vs. 0.97 (0.60–1.58) in patients ≥ 75 years. Therefore, with the exception of melanoma, elderly patients (≥ 75 years) could not benefit from the anti-PD-1/PD-L1 agents in survival, and toxicity profile of anti-PD-1/PD-L1 drugs should be explored in this population.

Keywords: programmed cell death 1 (PD-1), PD-L1, age, efficacy, overall survival

OPEN ACCESS

Edited by:
Taha Merghoub, Memorial Sloan Kettering Cancer Center, United States

Reviewed by:
Marie-Andree Forget, University of Texas MD Anderson Cancer Center, United States
Diego Salas Benito, University Clinic of Navarra, Spain

***Correspondence:**
Shu-Qiang Yuan
yuanshq@sysucc.org.cn
Zhi-Wei Zhou
zhouzhw@sysucc.org.cn

†These authors have contributed equally to this work

‡These authors share senior authorship

Specialty section:
This article was submitted to Cancer Immunity and Immunotherapy, a section of the journal Frontiers in Oncology

Received: *02 March 2020*
Accepted: *01 February 2021*
Published: *19 March 2021*

Citation:
Nie R-C, Chen G-M, Wang Y, Zhou J, Duan J-L, Zhou Z-W and Yuan S-Q (2021) Efficacy of Anti-PD-1/PD-L1 Monotherapy or Combinational Therapy in Patients Aged 75 Years or Older: A Study-Level Meta-Analysis. Front. Oncol. 11:538174. doi: 10.3389/fonc.2021.538174

INTRODUCTION

Recently, the advent of immune checkpoint inhibitors (ICIs) has tremendously revolutionized the landscape of cancer treatment. Monoclonal antibodies targeting the programmed cell death 1 (PD-1) or its ligand, programmed death ligand 1 (PD-L1), have been demonstrated to induce remarkable survival outcomes in a wide range of advanced malignancies (1–10). So far, the FDA has approved anti-PD-1/PD-L1 agents and their combinations for treatment of more than 13 cancer types and mismatch repair deficiency or microsatellite instable-high solid tumors (11). However, although cancer predominantly affects older adults (12), there is a lack of consensus on the efficacy of anti-PD-1/PD-L1 immunotherapy in this geriatric population (13).

It had been reported that aging is accompanied by decreased or dysregulation of immunity (14–16), which can theoretically blunt the efficacy of the PD-1/PD-L1 inhibitors. There have no prospective clinical trials focused specifically on the use of PD-1/PD-L1 inhibitors in elderly patients, which was mainly due to concerns about the safety profile. Elias et al. (17) also reported that PD-1/PD-L1 inhibitors had similar therapeutic effect in younger and older patients, with an age cutoff of 65 years. With the aging of society, average human lifespan has dramatically increased across the globe (12), with life expectancy higher than 75 years, and the therapeutic effect of PD-1/PD-L1 inhibitors in patients aged 75 years or older was still unknown. Therefore, we conducted a study-level meta-analysis to compare the efficacy of anti-PD-1/PD-L1 agents between elderly (≥ 75 years) and non-elderly (< 75 years) patients.

METHODS

Search Strategy and Study Selection

This study was conducted in compliance with Cochrane Handbook for Systematic Reviews of Interventions recommendations and was reported based on Preferred Reporting Items for Systematic Reviews and Meta-Analyses (PRISMA) statement guidelines (18).

We conducted a comprehensive systematic search of Medline (PubMed), Embase, ClinicalTrials.gov and Cochrane Library databases from inception to November 2019 using the following key words: "pembrolizumab", "nivolumab", "avelumab", "atezolizumab", "durvalumab", and "immune checkpoint inhibitor", limiting to phase 2 trials and phase 3 trials. The 2019 ASCO meeting and 2019 ESMO congress were also searched for the additional studies. The terms of the search strategy were shown in **Doc S1** (**Supplementary Materials**). The clinical trials should meet the following criteria: (1) phase 2 and phase 3 randomized controlled trials (RCTs) of advanced solid tumors; (2) studies that assigned participants to PD-1/PD-L1 inhibitors or non-PD-1/PD-L1 inhibitors, and set anti-PD-1/PD-L1 monotherapy or combinational therapy as experimental arms; (3) subgroup comparisons of overall survival (OS) using a hazard ratio (HR) based on the age (≥ 75 years versus < 75 years). Two independent authors (RCN and YFL) screened the titles and abstracts of the reports to identify the potential articles, and then assessed the eligibility of the full texts of these relevant articles. The references of the relevant trials were also reviewed through hand-searching strategy.

Data Extraction

Two reviewers (RCN and YFL) extracted the following data: first author's name, study number, accrual period, phase of study, included population, line of therapy, treatment strategy, number of patients by age, median follow-up duration, HR for OS and for progression-free survival (PFS) based on the age. The discrepancies in the literature search and data extraction were resolved by consensus.

We also used the MSKCC immunotherapy cohort (19) to further explore the tumor mutation burden (TMB) and survival outcomes according to the age through cBioPortal website (https://www.cbioportal.org/). We extracted the data of anti-PD1 monotherapy or combination therapy of the specified cancer types that were included in the meta-analysis.

Data Synthesis and Analysis

In our study, the primary outcome was to evaluate OS between elderly and non-elderly patients treated with PD-1/PD-L1 inhibitors. The secondary outcome was to compare the PFS between elderly and non-elderly patients. The measures of OS and PFS were quantified by the HR with the corresponding 95% confidence intervals (CI). The heterogeneity among trials was examined using Cochran Q statistic, and quantified by I^2 index. The heterogeneity was considered significant for $P < 0.1$ and $I^2 < 50\%$. All the pooled HR of this meta-analysis was calculated through random effects model because of the potential heterogeneity among the included trials. For studies that reported the HR estimates for < 65 and 65–75 years separately, we combined the estimate (< 75 years) using a random effects model. An interaction test was used to evaluate the heterogeneity of efficacy between subgroups, which was expressed as P for interaction to quantify the potential publication bias. Regarding the MSKCC immunotherapy cohort, TMB and OS based on the age were compared by t-test and log-rank test, respectively. All the statistical analyses were performed using Stata version 13.0 (StataCorp, College Station, TX) and R version 3.6.2 (https://www.r-project.org/). Statistical significance was considered as $P < 0.05$.

RESULTS

Search Results and Patient Characteristics

Initially, a total of 763 relevant publications matched our basic search strategy. After screening the titles and abstracts of these publications, 75 studies were reviewed the full-text for eligibility. Sixty-seven of those 75 articles were excluded since they did not report the OS subgroup by age with the cutoff 75 years (**Figure 1**). Finally, a total of eight phase 3 trials (1, 8, 20–25) were included for meta-analysis, among which four investigated nivolumab, two

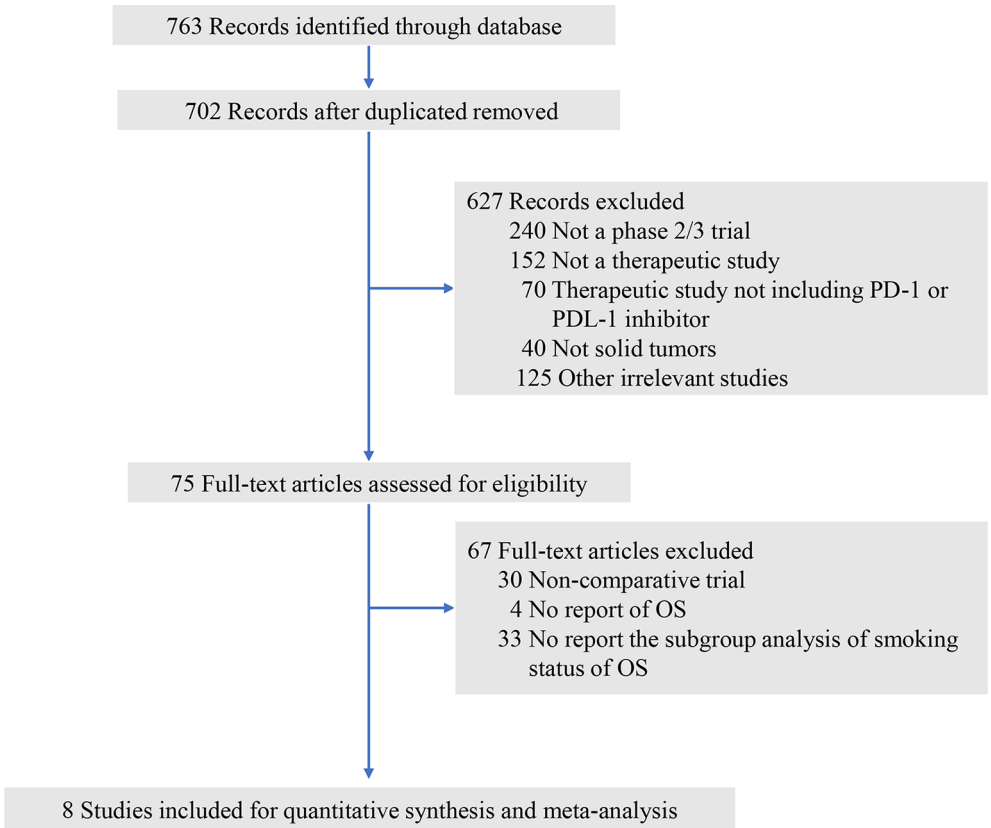

FIGURE 1 | Study flow diagram. OS, overall survival; PD-1, programmed death 1; PD-L1, programmed death-ligand 1.

investigated the combination of nivolumab plus ipilimumab, one investigated pembrolizumab, and one investigated avelumab. The underlying malignancies comprised were non-small-cell lung cancer (four trials), renal-cell carcinoma (two trials), melanoma (one trial), and head and neck cancer (one trial). There were six trials of anti-PD-1/PD-L1 monotherapy and two trials of anti-PD-1/PD-L1 plus anti-CTLA therapy as the experimental arms. A total of 5,393 patients (intervention: 2,698; control: 2,695) were included, and 472 patients (8.8%) were aged 75 years or older. The baseline characteristics of each trial are presented in **Table 1**. A funnel plot was performed to assess the publication bias, which showed a symmetric distribution of studies on either side of the funnel. The Begg and Egger test also indicated no obvious publication bias (P = 0.071; **Figure S1**).

Primary Outcome: Overall Survival

The primary outcome is OS in trials comparing PD-1/PD-L1 inhibitors with control agents. The HR of each trial and the pooled result based on the random effects model are shown in **Figure 2**. Overall, the estimated HR is 0.73 (95% CI: 0.65 to 0.81) (P < 0.001), suggesting that PD-1/PD-L1 inhibitors reduced the risk of death by 27% compared with control treatments. Patients were then dichotomized into elderly and non-elderly groups with the cutoff of 75 years. For non-elderly patients, the estimated HR for OS showed significant difference between PD-1/PD-L1 inhibitors and control agents (HR, 0.70; 95% CI: 0.62 to 0.79; P < 0.001; **Figure 3A**). For this subgroup, no significant heterogeneity was observed among individual trials (I^2 = 38.7%, chi-squared P = 0.122). For elderly patients, no significant heterogeneity was observed (I^2 = 41.1%, chi-squared P = 0.104), and all studies reported no OS benefit for PD-1/PD-L1 inhibitors except for the CheckMate 066, which explored the efficacy of nivolumab in melanoma (22); the overall estimated HR was 0.94 (95% CI: 0.67 to 1.30; P = 0.696; **Figure 3B**). Furthermore, we observed a significant heterogeneity of efficacy between elderly and non-elderly patients concerning the pooled HRs for OS (P = 0.043 for interaction), which indicated that the effects of the anti-PD-1/PD-L1 therapy on OS varied for the elderly and non-elderly adults (**Table 2**). Subgroup stratified by anti-PD-1/PD-L1 monotherapy and anti-PD-1/PD-L1 combinational therapy showed the similar results (Table S1). Moreover, we found that the estimated HR for OS was 0.68 (95% CI: 0.59 to 0.77; P < 0.001; **Figure S2**) in patients aged 65-75 years.

Secondary Outcome: Progression-Free Survival

The secondary outcome is PFS in trials comparing PD-1/PD-L1 inhibitors with control agents. Of the eight included trials, eight reported HR for overall PFS, and four reported HR for PFS based

TABLE 1 | Characteristics of the included trials.

Studies	Study number	Trial period	Population	Line of therapy	Experimental arm	Control arm	Patients number	N (%) < 75 years	N (%) ≥ 75 years	Follow-up (months)
Borghaei et al. (1)	CheckMate 057	2013–2013	Nonsquamous NSCLC	1–3	Nivolumab	Docetaxel	582	539 (92.6)	43 (7.4)	13.2
Brahmer et al. (20)	CheckMate 017	2012–2013	Squamous NSCLC	2	Nivolumab	Docetaxel	272	243 (89.3)	29 (10.7)	11.0
Motzer et al. (21)	CheckMate 025	2012–2014	Renal-Cell Carcinoma	2-3	Nivolumab	Everolimus	821	747 (91.0)	74 (9.0)	14.0
Robert et al. (22)	CheckMate 066	2013–2014	Melanoma	2	Nivolumab	Dacarbazine	481	414 (86.1)	67 (13.9)	16.7
Barlesi et al. (23)	JAVELIN Lung 200	2015–2017	NSCLC	1–3	Avelumab	Docetaxel	529	479 (90.5)	50 (9.5)	18.3
Motzer et al. (24)	CheckMate 214	2014–2016	Renal-Cell Carcinoma	1	Nivolumab +ipilimumab	Sunitinib	847	782 (92.3)	65 (7.7)	25.2
Cohen et al. (8)	KEYNOTE-040	2014–2016	Head and neck cancer	> 2	Pembrolizumab	ICC	495	464 (93.7)	31 (6.3)	7.5
Hellmann et al. (25)	CheckMate 227	2015–2016	NSCLC	1	Nivolumab +ipilimumab	Chemotherapy	1,166	1,053 (90.3)	113 (9.7)	29.3

NSCLC, non-small-cell lung cancer; ICC, investigator's choice-chemotherapy.

on the age group. Overall, the estimated HR for PFS is 0.76 (95% CI: 0.63 to 0.92; P = 0.005; **Figure 4**), indicating of 24% reduction of the risk of progression treated with anti-PD-1/PD-L1 agents. Using the random effects model, the measures of PFS of the non-elderly patients favored anti-PD-1/PD-L1 therapy for a HR of 0.77 (95% CI: 0.60 to 1.00; P = 0.054; **Figure 5A**). There was significant heterogeneity among individual trials (I^2 = 74.9%, chi-squared P = 0.008). However, for elderly patients, the PFS was not different between PD-1/PD-L1 inhibitors and controls (HR, 0.97; 95% CI: 0.60 to 1.58; P = 0.898; **Figure 5B**). No difference between elderly and non-elderly subsets was observed regarding the estimated HR for PFS (P = 0.433 for interaction) (**Table 2**).

Tumor Mutation Burden

Finally, we extracted the patients with non-small-cell lung cancer, renal-cell carcinoma, head and neck cancer and melanoma to explore the TMB differences between elderly and non-elderly patients in the MSKCC immunotherapy cohort (19). A total of 845 patients treated with PD-1/PD-L1 inhibitors were included. For non-melanoma cohort, the TMB between elderly and non-elderly patients was not significant (median TMB: 6.89 [0–33.45] vs 5.27 [0–100.37]; P = 0.230; **Figure 6A**), and elderly patients were associated with shorted OS (HR, 1.35; 95% CI: 1.02 to 1.78; P = 0.038; **Figure 6B**). Interesting, for melanoma cohort, elderly patients had higher TMB than non-elderly patients (median TMB: 15.74 [0–33.45] vs 7.87 [0–100.37]; P = 0.012; **Figure 6C**), and comparable OS with non-elderly patients (HR, 1.39; 95% CI: 0.87 to 2.22; P = 0.171; **Figure 6D**).

DISCUSSION

The aging phenomenon is one of the most significant global challenges today, which would accompany with age-related disease, such as increasing incidence of cancer. Aging is associated with the immune dysfunction that may affect the efficacy of PD-1/PD-L1 inhibitors (14, 15, 26, 27). Consequently, we performed this first meta-analysis of eight RCTs that comprised 5393 patients to explore the efficacy of PD-1/PD-L1 inhibitors in patients ≥ 75 years with metastatic cancer compared to those < 75 years. Overall, our finding suggested that the impact of PD-1/PD-L1 inhibitors significantly improved the OS (HR 0.70 [0.62–0.79] vs. 0.94 [0.67–1.30]) and PFS (HR 0.77 [0.60–1.00] vs. 0.97 [0.60–1.58]) in the non-elderly patients rather than elderly patients. Parallel results were confirmed in both monotherapy and combinational therapy. Melanoma patients aged 75 years or older can still benefit from PD-1/PD-L1 inhibitors.

Only two previous literatures attempt to review the topic of geriatric population in PD-1/PD-L1 inhibitors (17, 28). Nishijima et al. (28) compared the efficacy of ICIs between younger and older patients. However, only four of their included trials (eight trials) were anti-PD-1 trials. They concluded that a benefit in OS with ICIs was observed in both younger (HR, 0.75; 95% CI, 0.68–0.82) and older (HR, 0.73; 95% CI, 0.62–0.87) patients, but it should be noted that the age cutoff

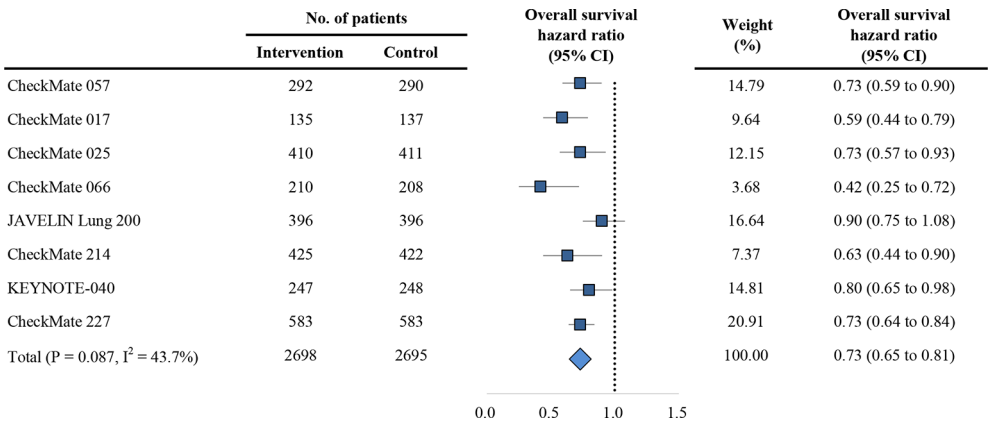

FIGURE 2 | Forest plot of hazard ratio for overall survival. CI, confidence interval; PD-1, programmed death 1; PD-L1, programmed death-ligand 1.

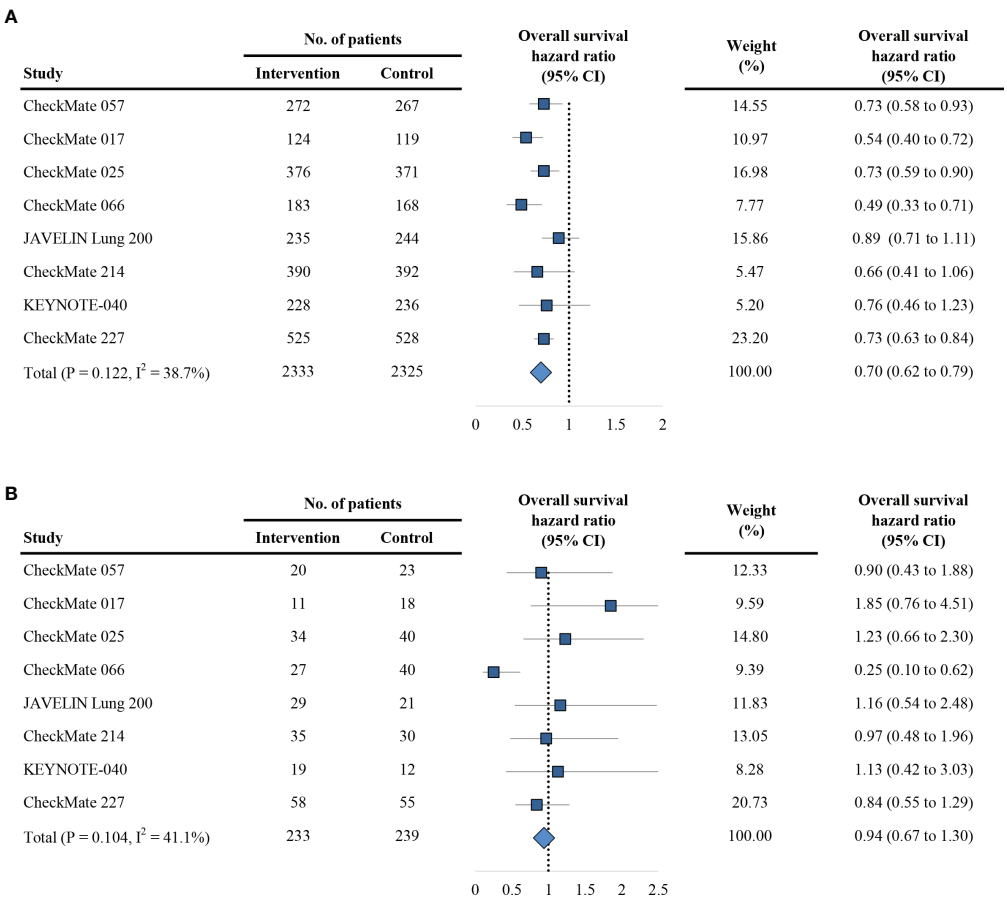

FIGURE 3 | Forest plot of hazard ratio for overall survival in patients < 75 years **(A)** and ≥ 75 years **(B)**. CI, confidence interval; PD-1, programmed death 1; PD-L1, programmed death-ligand 1.

TABLE 2 | Summary of HR for PFS and OS by age.

Age	OS		PFS	
	HR (95% CI)	P for interaction*	HR (95% CI)	P for interaction*
<75 years	0.70 (0.62 to 0.79)	0.043	0.77 (0.60 to 1.00)	0.433
≥75 years	0.94 (0.67 to 1.30)		0.97 (0.60 to 1.58)	

HR, hazard ratio; PFS, progression-free survival; OS, overall survival; CI, confidence interval.

**P for interaction was expressed as the heterogeneity of efficacy between elderly and non-elderly patients.*

of this study was non-uniform (65–70 years). Elias et al. (17) also reported that anti-PD-1/PD-L1 agents had similar therapeutic effect in younger and older patients. Nonetheless, this analysis dichotomized patients into younger and older with an age cutoff of 65 years. Initially, we also found that patients aged 65–75 years could still benefit from PD-1/PD-L1 inhibitors. With the aging of society, adults over 75 years of age contribute more than 25% of the new cancer cases annually (12). Therefore, it is critical to clarify the efficacy of PD-1/PD-L1 inhibitors specific to patients aged 75 years or older. In contrary to the previous meta-analysis, we observed the better survival outcomes only in patients < 75 years, but not in patients ≥ 75 years. It had been reported that aging is associated with immune dysregulation, such as the decreased TCR diversity in CD4+ T cells (14) and CD8+ T cells (15), but not the T-cell immunosenescence (29). In addition, aging-associated adipocyte accumulation in the bone marrow also contributes to reduced hematopoiesis with age (30), and hematopoiesis becomes skewed toward myeloid and away from lymphoid lineages with age (16). Moreover, aging is associated with increased M2 polarization (26). Thus, the hypothesis of immunosenescence, the age-related decline in host immunity, may explain the invalid efficacy of PD-1/PD-L1 inhibitors in patients ≥ 75 years.

Among the eight included trials, the CheckMate 066 (22) study reported the OS outcomes of melanoma for the age groups of 75 years. Notably, we found that a significant improvement in OS was still observed in melanoma patients aged 75 years or older (HR, 0.25; 95% CI, 0.10–0.62; **Figure 3B**). Betof et al. (31) reported the survival outcomes of 254 patients with metastatic melanoma treated with anti-PD-1/PD-L1 agents, and found that the OS and PFS of patients ≥ 75 years were comparable to those with age < 75 years. Additionally, the safety profiles were also similar. In the present study, we also used the MSKCC immunotherapy cohort (19) to further explore the underlying mechanism of age based efficacy difference in term of TMB (**Figure 6**). Interestingly, an increased TMB was observed in the elderly patient with melanoma; this increased TMB may restore the age-related immune dysfunction of melanoma, thus leading to the comparable immunity between patients younger and older than 75 years.

Our study has several potential limitations. First, we observed heterogeneity among the included trials, which was mainly due to the multiple cancer types among the included trials. Thus, we minimized its influence through the random effects model for quantitative synthesis. However, the conclusion of this study still cannot be expanded to all solid tumor types. Second, although our work contributes the best level of evidence showing an age-based (≥ 75 years vs. < 75 years) efficacy difference for anti-PD-1/PD-L1 agents, this is a meta-analysis at study-level in essence. A meta-analysis at individual level should be performed to further validate the impact of age on the efficacy of anti-PD-1/PD-L1 agents. Third, the toxicities difference between elderly and non-elderly patient could not be analyzed because of lack of report. The toxicity profile might influence the therapeutic choice between anti-PD-1/PD-L1 agents or standard chemotherapy in elderly patients. Finally, elderly patients enrolled in clinical trials were a selected population with good performance status at academic hospitals. These selected elderly patients do not represent the real medical conditions of the elderly adults. Therefore, whether our findings applicable to patients treated in the community remains further validation.

In conclusion, our study suggested that the use of anti-PD-1/PD-L1 significantly improved the survival of patients aged < 75

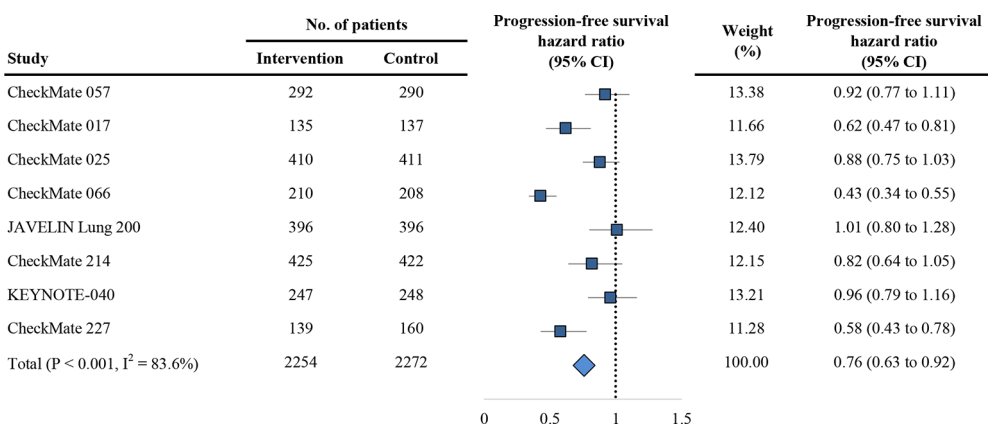

FIGURE 4 | Forest plot of hazard ratio for progression-free survival. CI, confidence interval; PD-1, programmed death 1; PD-L1, programmed death-ligand 1.

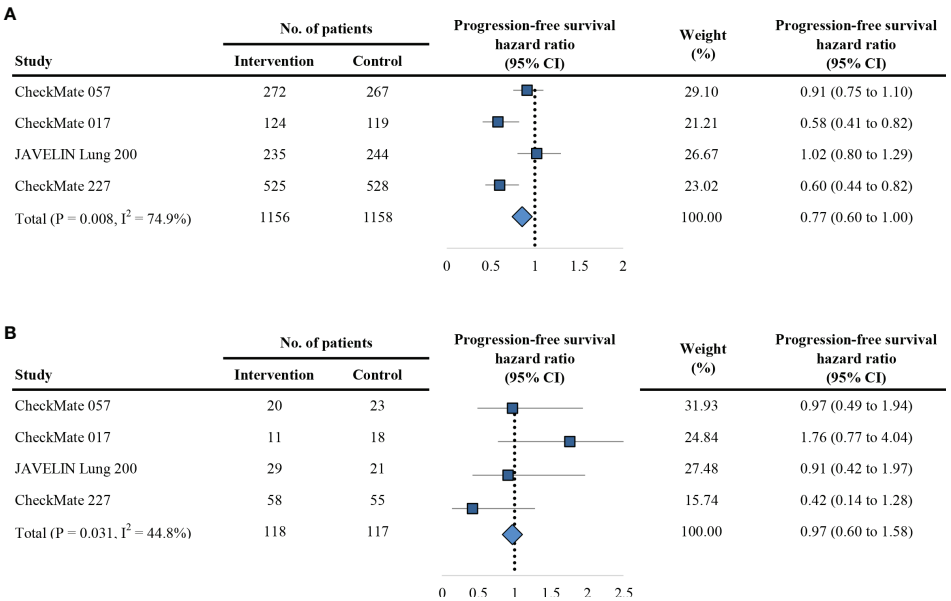

FIGURE 5 | Forest plot of hazard ratio for progression-free survival in patients < 75 years **(A)** and ≥ 75 years **(B)**. CI, confidence interval; PD-1, programmed death 1; PD-L1, programmed death-ligand 1.

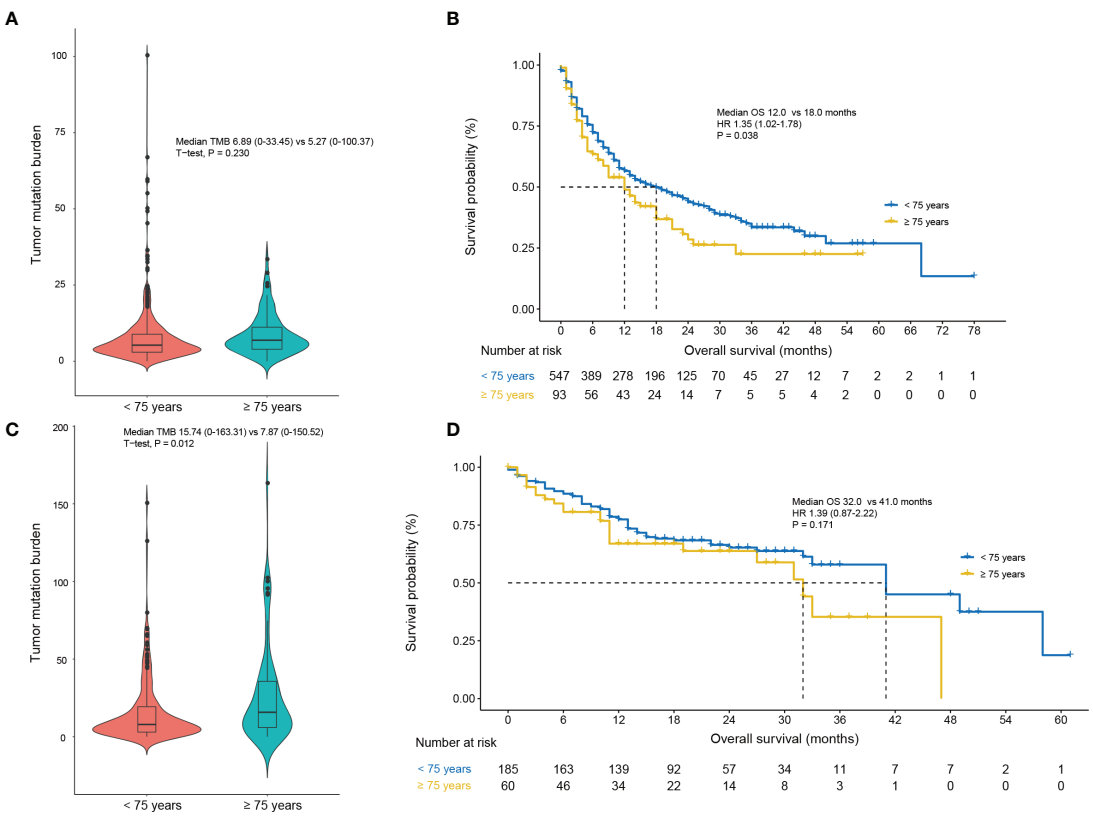

FIGURE 6 | Comparisons of the tumor mutation burden and OS based on the age (< 75 years vs. ≥ 75 years) in non-melanoma **(A, B)** and melanoma patients **(C, D)** of the MSKCC immunotherapy cohort (19). CI, confidence interval; HR, hazard ratio.

years, but not those aged ≥ 75 years. This is mainly due to a potential interaction of immunosenescence and efficacy of anti-PD-1/PD-L1 drugs. An improved OS was still observed in melanoma patients aged ≥ 75 years, owing to the increased TMB in the elderly melanoma patients. Overall, our study indicated that, with the exception of melanoma, elderly patients (≥ 75 years) could not benefit from the anti-PD-1/PD-L1 agents in survival, and toxicity profile of anti-PD-1/PD-L1 drugs should be explored in this population.

DATA AVAILABILITY STATEMENT

The datasets generated for this study are available on request to the corresponding authors.

AUTHOR CONTRIBUTIONS

All authors contributed to the study concept and design. R-CN and G-MC extracted the data and performed the quality assessment. R-CN, YW and JZ participated in analysis of the data. R-CN, YW, J-LD and JZ contributed to drafting of the manuscript. S-QY and Z-WZ revised the manuscript. All authors contributed to the article and approved the submitted version.

SUPPLEMENTARY MATERIAL

The Supplementary Material for this article can be found online at: https://www.frontiersin.org/articles/10.3389/fonc.2021.538174/full#supplementary-material

REFERENCES

1. Borghaei H, Paz-Ares L, Horn L, Spigel DR, Steins M, Ready NE, et al. Nivolumab versus Docetaxel in Advanced Nonsquamous Non-Small-Cell Lung Cancer. *N Engl J Med* (2015) 373:1627–39. doi: 10.1056/NEJMoa1507643
2. Ribas A, Puzanov I, Dummer R, Schadendorf D, Hamid O, Robert C, et al. Pembrolizumab versus investigator-choice chemotherapy for ipilimumab-refractory melanoma (KEYNOTE-002): a randomised, controlled, phase 2 trial. *Lancet Oncol* (2015) 16:908–18 doi: 10.1016/S1470-2045(15)00083-2.
3. Wolchok JD, Chiarion-Sileni V, Gonzalez R, Rutkowski P, Grob JJ, Cowey CL, et al. Overall Survival with Combined Nivolumab and Ipilimumab in Advanced Melanoma. *N Engl J Med* (2017) 377:1345–56 doi: 10.1056/NEJMoa1709684.
4. Antonia SJ, Villegas A, Daniel D, Vicente D, Murakami S, Hui R, et al. Overall Survival with Durvalumab after Chemoradiotherapy in Stage III NSCLC. *N Engl J Med* (2018) 379:2342–50 doi: 10.1056/NEJMoa1809697.
5. Larkin J, Minor D, D'Angelo S, Neyns B, Smylie M, Miller WH Jr, et al. Overall Survival in Patients With Advanced Melanoma Who Received Nivolumab Versus Investigator's Choice Chemotherapy in CheckMate 037: A Randomized, Controlled, Open-Label Phase III Trial. *J Clin Oncol* (2018) 36:383–90. doi: 10.1200/JCO.2016.71.8023
6. Paz-Ares L, Luft A, Vicente D, Tafreshi A, Gümüş M, Mazières J, et al. Pembrolizumab plus Chemotherapy for Squamous Non-Small-Cell Lung Cancer. *N Engl J Med* (2018) 379:2040–51. doi: 10.1056/NEJMoa1810865
7. Schmid P, Adams S, Rugo HS, Schneeweiss A, Barrios CH, Iwata H, et al. Atezolizumab and Nab-Paclitaxel in Advanced Triple-Negative Breast Cancer. *N Engl J Med* (2018) 379:2108–21. doi: 10.1056/NEJMoa1809615
8. Cohen EEW, Soulières D, Le Tourneau C, Dinis J, Licitra L, Ahn MJ, et al. Pembrolizumab versus methotrexate, docetaxel, or cetuximab for recurrent or metastatic head-and-neck squamous cell carcinoma (KEYNOTE-040): a randomised, open-label, phase 3 study. *Lancet* (2019) 393:156–67 doi: 10.1016/S0140-6736(18)31999-8.
9. Motzer RJ, Penkov K, Haanen J, Rini B, Albiges L, Campbell MT, et al. Avelumab plus Axitinib versus Sunitinib for Advanced Renal-Cell Carcinoma. *N Engl J Med* (2019) 380:1103–15. doi: 10.1056/NEJMoa1816047
10. Reck M, Rodriguez-Abreu D, Robinson AG, Hui R, Csőszi T, Fülöp A, et al. Updated Analysis of KEYNOTE-024: Pembrolizumab Versus Platinum-Based Chemotherapy for Advanced Non-Small-Cell Lung Cancer With PD-L1 Tumor Proportion Score of 50% or Greater. *J Clin Oncol* (2019) 37:537–46. doi: 10.1200/JCO.18.00149
11. Ribas A, Wolchok JD. Cancer immunotherapy using checkpoint blockade. *Science* (2018) 359:1350–5. doi: 10.1126/science.aar4060
12. Huang J, Mo H, Zhang W, Chen X, Qu D, Wang X, et al. Promising efficacy of SHR-1210, a novel anti-programmed cell death 1 antibody, in patients with advanced gastric and gastroesophageal junction cancer in China. *Cancer* (2019) 125:742–9. doi: 10.1002/cncr.31855
13. Elias R, Karantanos T, Sira E, Hartshorn KL. Immunotherapy comes of age: Immune aging & checkpoint inhibitors. *J Geriatr Oncol* (2017) 8:229–35. doi: 10.1016/j.jgo.2017.02.001
14. Naylor K, Li G, Vallejo AN, Lee WW, Koetz K, Bryl E, et al. The influence of age on T cell generation and TCR diversity. *J Immunol* (2005) 174:7446–52. doi: 10.4049/jimmunol.174.11.7446
15. Pfister G, Weiskopf D, Lazuardi L, Kovaiou RD, Cioca DP, Keller M, et al. Naive T cells in the elderly: are they still there? *Ann N Y Acad Sci* (2006) 1067:152–7. doi: 10.1196/annals.1354.018
16. Beerman I, Bhattacharya D, Zandi S, Sigvardsson M, Weissman IL, Bryder D, et al. Functionally distinct hematopoietic stem cells modulate hematopoietic lineage potential during aging by a mechanism of clonal expansion. *Proc Natl Acad Sci U S A* (2010) 107:5465–70. doi: 10.1073/pnas.1000834107
17. Elias R, Giobbie-Hurder A, McCleary NJ, Ott P, Hodi FS, Rahma O. Efficacy of PD-1 & PD-L1 inhibitors in older adults: a meta-analysis. *J Immunother Cancer* (2018) 6:26. doi: 10.1186/s40425-018-0336-8
18. Liberati A, Altman DG, Tetzlaff J, Mulrow C, Gøtzsche PC, Ioannidis JP, et al. The PRISMA statement for reporting systematic reviews and meta-analyses of studies that evaluate healthcare interventions: explanation and elaboration. *BMJ* (2009) 339:b2700. doi: 10.1136/bmj.b2700
19. Samstein RM, Lee CH, Shoushtari AN, Hellmann MD, Shen R, Janjigian YY, et al. Tumor mutational load predicts survival after immunotherapy across multiple cancer types. *Nat Genet* (2019) 51:202–6 doi: 10.1038/s41588-018-0312-8.
20. Brahmer J, Reckamp KL, Baas P, Crinò L, Eberhardt WE, Poddubskaya E, et al. Nivolumab versus Docetaxel in Advanced Squamous-Cell Non-Small-Cell Lung Cancer. *N Engl J Med* (2015) 373:123–35. doi: 10.1056/NEJMoa1504627
21. Motzer RJ, Escudier B, McDermott DF, George S, Hammers HJ, Srinivas S, et al. Nivolumab versus Everolimus in Advanced Renal-Cell Carcinoma. *N Engl J Med* (2015) 373:1803–13. doi: 10.1056/NEJMoa1510665
22. Robert C, Long GV, Brady B, Dutriaux C, Maio M, Mortier L, et al. Nivolumab in previously untreated melanoma without BRAF mutation. *N Engl J Med* (2015) 372:320–30 doi: 10.1056/NEJMoa1412082.
23. Barlesi F, Vansteenkiste J, Spigel D, Ishii H, Garassino M, de Marinis F, et al. Avelumab versus docetaxel in patients with platinum-treated advanced non-small-cell lung cancer (JAVELIN Lung 200): an open-label, randomised, phase 3 study. *Lancet Oncol* (2018) 19:1468–79 doi: 10.1016/S1470-2045(18)30673-9.
24. Motzer RJ, Tannir NM, McDermott DF, Arén Frontera O, Melichar B, Choueiri TK, et al. Nivolumab plus Ipilimumab versus Sunitinib in Advanced Renal-Cell Carcinoma. *N Engl J Med* (2018) 378:1277–90 doi: 10.1056/NEJMoa1712126.
25. Hellmann MD, Paz-Ares L, Bernabe Caro R, Zurawski B, Kim SW, Carcereny Costa E, et al. Nivolumab plus Ipilimumab in Advanced Non-Small-Cell Lung Cancer. *N Engl J Med* (2019) 381:2020–31 doi: 10.1056/NEJMoa1910231.

26. Mahbub S, Deburghgraeve CR, Kovacs EJ. Advanced age impairs macrophage polarization. *J Interferon Cytokine Res* (2012) 32:18–26. doi: 10.1089/jir.2011.0058
27. Kugel CH 3rd, Douglass SM, Webster MR, Kaur A, Liu Q, Yin X, et al. Age Correlates with Response to Anti-PD1, Reflecting Age-Related Differences in Intratumoral Effector and Regulatory T-Cell Populations. *Clin Cancer Res* (2018) 24:5347–56. doi: 10.1158/1078-0432.CCR-18-1116
28. Nishijima TF, Muss HB, Shachar SS, Moschos SJ. Comparison of efficacy of immune checkpoint inhibitors (ICIs) between younger and older patients: A systematic review and meta-analysis. *Cancer Treat Rev* (2016) 45:30–7. doi: 10.1016/j.ctrv.2016.02.006
29. Ferrara R, Naigeon M, Auclin E, Duchemann B, Cassard L, Jouniaux JM, et al. Circulating T-cell Immunosenescence in Patients with Advanced Non-small Cell Lung Cancer Treated with Single-agent PD-1/PD-L1 Inhibitors or Platinum-based Chemotherapy. *Clin Cancer Res* (2021) 27:492–503. doi: 10.1158/1078-0432.CCR-20-1420
30. Ambrosi TH, Scialdone A, Graja A, Gohlke S, Jank AM, Bocian C, et al. Adipocyte Accumulation in the Bone Marrow during Obesity and Aging Impairs Stem Cell-Based Hematopoietic and Bone Regeneration. *Cell Stem Cell* (2017) 20:771–84.e776. doi: 10.1016/j.stem.2017.02.009
31. Betof AS, Nipp RD, Giobbie-Hurder A, Johnpulle RAN, Rubin K, Rubinstein SM, et al. Impact of Age on Outcomes with Immunotherapy for Patients with Melanoma. *Oncologist* (2017) 22:963–71. doi: 10.1634/theoncologist.2016-0450

Conflict of Interest: The authors declare that the research was conducted in the absence of any commercial or financial relationships that could be construed as a potential conflict of interest.

frontiers in Oncology

ORIGINAL RESEARCH
published: 25 March 2021
doi: 10.3389/fonc.2021.558248

OPEN ACCESS

Edited by:
Taha Merghoub, Memorial Sloan Kettering Cancer Center, United States

Reviewed by:
Krithika Kodumudi, Moffitt Cancer Center, United States
Sangeeta Goswami, University of Texas MD Anderson Cancer Center, United States

***Correspondence:**
Vinicius Araujo B. de Lima vinicius.araujo.barbosa.de.lima@regionh.dk

Specialty section:
This article was submitted to Cancer Immunity and Immunotherapy, a section of the journal Frontiers in Oncology

Received: *01 May 2020*
Accepted: *04 March 2021*
Published: *25 March 2021*

Citation:
Araujo B. de Lima V, Hansen M, Spanggaard I, Rohrberg K, Reker Hadrup S, Lassen U and Svane IM (2021) Immune Cell Profiling of Peripheral Blood as Signature for Response During Checkpoint Inhibition Across Cancer Types. Front. Oncol. 11:558248. doi: 10.3389/fonc.2021.558248

Immune Cell Profiling of Peripheral Blood as Signature for Response During Checkpoint Inhibition Across Cancer Types

***Vinicius Araujo B. de Lima*[1]*, *Morten Hansen*[2], *Iben Spanggaard*[1], *Kristoffer Rohrberg*[1], *Sine Reker Hadrup*[3], *Ulrik Lassen*[1] *and Inge Marie Svane*[2]**

[1] Department of Oncology, Phase 1 Unit, Rigshospitalet, Copenhagen, Denmark, [2] National Center for Cancer Immune Therapy, Department of Oncology, Copenhagen University Hospital Herlev, Herlev, Denmark, [3] Department of Health Technology, Technical University of Denmark, Lyngby, Denmark

Despite encouraging results with immune checkpoint inhibition (ICI), a large fraction of cancer patients still does not achieve clinical benefit. Finding predictive markers in the complexity of the tumor microenvironment is a challenging task and often requires invasive procedures. In our study, we looked for putative variables related to treatment benefit among immune cells in peripheral blood across different tumor types treated with ICIs. For that, we included 33 patients with different solid tumors referred to our clinical unit for ICI. Peripheral blood mononuclear cells were isolated at baseline, 6 and 20 weeks after treatment start. Characterization of immune cells was carried out by multi-color flow cytometry. Response to treatment was assessed radiologically by RECIST 1.1. Clinical outcome correlated with a shift towards an effector-like T cell phenotype, PD-1 expression by CD8+T cells, low levels of myeloid-derived suppressor cells and classical monocytes. Dendritic cells seemed also to play a role in terms of survival. From these findings, we hypothesized that patients responding to ICI had already at baseline an immune profile, here called 'favorable immune periphery', providing a higher chance of benefitting from ICI. We elaborated an index comprising cell types mentioned above. This signature correlated positively with the likelihood of benefiting from the treatment and ultimately with longer survival. Our study illustrates that patients responding to ICI seem to have a pre-existing immune profile in peripheral blood that favors good

outcome. Exploring this signature can help to identify patients likely to achieve benefit from ICI.

Keywords: immune checkpoint inhibition, PBMCs, immune signature, prediction, clinical outcome

INTRODUCTION

The advent of immune checkpoint inhibitors (ICI) as an effective therapeutic modality in oncology has come under spotlight during the last decades, mainly after the first clinical trial showing positive impact of ipilimumab for treatment of patients with metastatic melanoma (1).

Despite encouraging results (2–4), a considerable fraction of patients undergoing ICI still do not benefit from the treatment (5) and primary or acquired ICI resistance is a significant problem that patients and clinicians face on a daily basis. In this context, the field of biomarkers has gained a lot of attention as tool to guide treatment indications and to promote understanding of the biological events taking place in the tumor.

Efforts trying to predict patients likely to respond to ICI are numerous and comprise a myriad of variables spanning from isolated genetic features (e.g. tumor mutational burden, neoepitope load, transcriptomic signatures) (6–9) to multiparametric approaches looking into the tumor microenvironment (TME)'s cellular composition (e.g. immunoscore (10)). Common ground for these methods is the fact that they are tumor tissue-centered, which is reasonable since tumor site harbors the 'battlefield' where interactions between cancer and immune system unfold. However, these approaches are limited by the fact that they offer a glimpse of a very dynamic cell milieu and do not take into consideration the effect of non-cellular (11, 12) and extrinsic features (13) that equally can affect T cell function. Another disadvantage is that invasive procedures are required to keep track of changes happening during ICI, which is not always feasible.

Analyses of peripheral blood offer, on the other hand, a non-invasive and simpler alternative to monitor not only biochemical changes (e.g. lactate dehydrogenase, cytokines) but also variations along the treatment in frequencies of immune cells (peripheral blood mononuclear cells - PBMCs) that ultimately can infiltrate the TME and therefore add valuable information in the context of ICI. In this regard, there is evidence supporting that counts of lymphocytes and myeloid subsets in the peripheral blood (14–16), and phenotypical features of circulating T cells [e.g. regulatory T cells (17), CD8+effector-like (18)] seem to correlate with clinical outcome. These analyses, however, have focused on the impact of isolated cell populations on reactivity against neoantigens and/or clinical outcome upon treatment with ICI. Efforts to obtain a more comprehensive knowledge of how different cell types interact with each other during ICI and ultimately affect response patterns is still an ongoing task.

Since most studies addressing the use of PBMCs as predictive tools are restricted to specific tumor types (mainly melanoma) or assess few cell subpopulations at a time, the use of PBMCs requires further investigation prior to implementation in a clinical setting (19–22). Furthermore, predictive power can potentially be increased by involving multiple variables, bearing in mind the multitude of factors preceding and perpetuating immune responses.

In this study, we took a different approach and investigated the immune cell repertoire from peripheral blood (including the influence of both lymphoid and myeloid subsets) of patients with different metastatic solid tumors, in order to gain insight into the impact of differences in distribution of T cells and myeloid cells prior to treatment start and whether changes in these subsets during ICI can shed light on the clinical outcome. We present data indicating that despite possible differences in the PBMC's composition across patients with different tumor types, there is an underlying preexisting immune signature (here called 'favorable immune periphery') among patients likely to benefit from ICI.

As novelty, our study takes into consideration the simultaneous effect of lymphoid and myeloid cells showing that information regarding how peripheral blood is populated may provide patients undergoing ICI with a better starting point.

MATERIALS AND METHODS

Study Design

In order to investigate common immunological features across different tumor types, we designed a basket study.

The protocol was approved by The Danish National Committee on Health Research Ethics (H-16046968) and the Danish Data Protection Agency (RH-2018-44). Informed consent was obtained from all individual participants included in the study prior to collection of biological material. This study was conducted in accordance to 1964 Declaration of Helsinki and its later amendments.

Cohort

Patients with histologically confirmed metastatic solid tumors referred to our department for ICI treatment were considered as potential candidates for inclusion. Other inclusion criteria were ECOG performance status 0 to 1, age above 18 years, at least one measurable lesion according to response evaluation criteria in solid tumors version 1.1 (RECIST 1.1).

Response Assessment

Response to the treatment was assessed both clinically and radiologically. Computed Tomography (CT) scan was performed during treatment and assessed with RECIST 1.1. Patients were pooled in two groups referred as 'benefit' and 'no benefit'. The first group comprised individuals who achieved, as best response, either complete response (CR), partial response (PR) or stable disease (SD) with progression free survival (PFS) larger than the median value for the whole cohort (i.e. above than 3 months as described in the result section).

Blood Samples PBMCs

Immune monitoring was carried out by collection of heparinized blood up to three times over treatment period, i.e. baseline, 6 weeks after treatment start (called 'T1') and approximately 20 weeks after treatment initiation('T2'). Blood samples were transported in room temperature from ambulatory to our laboratory (elapsed time approximately 2 hours), where they were diluted with phosphate-buffered saline (PBS) (Lonza, Basel, Switzerland), facilitating PBMCs' by means of centrifugation. Cell count was carried out automatically by Sysmex-XP 300 (Kobe, Japan). Aliquots containing between $2.5x10^6$ to 15x106 cells were cryopreserved in 90% Human AB serum and 10% DMSO. To control the freezing process during the first 24 hours at -80˚C, alcohol-free freezing containers (Cool cell, Biocision) were used. Samples were stored at -140˚C until further use. Overview of biological material is displayed on **Supplementary Table 1**.

TABLE 1 | Cohort characteristics.

Patient no.	General features					Treatment characteristics		Response pattern			
	Gender	Diagnosis	No. of previous treatment lines	PS	Age	Checkpoint inhibition target	No. of immunotherapy cycles	Best achieved RECIST response	OS (months)	PFS (months)	Clinical Benefit
PB2	M	CRC[a]	2	1	71	PD-1	4	PD	3.3	1.8	No benefit
PB6	F	Pancreas adenocarcinoma	3	0	75	PD-L1	1	PD	3.1	1.4	No benefit
PB10	M	HCC[b]	2	0	43	PD-1+LAG-3	2	SD	4.7	4.0	Benefit
PB12	M	CRC[a]	5	1	72	PD-1	7	PD	16.9	6.3	No benefit
PB16	F	Upper GI adenocarcinoma[c]	2	1	68	PD-1+LAG-3	4	PD	12.5	1.9	No benefit
PB18	M	Upper GI adenocarcinoma[c]	3	1	53	PD-1+LAG-3	1	PD	1.4	0.9	No benefit
PB20	M	HCC[b]	2	0	75	PD-1+LAG-3	13	CR	10.8	10.8	Benefit
PB22	M	Urothelial Carcinoma	1	0	62	PD-1	20	PR	15.5	15.5	Benefit
PB24	M	Urothelial Carcinoma	1	0	56	PD-1	22	PR	14.8	14.8	Benefit
PB26	M	CRC[a]	3	0	73	PD-L1	6	PD	7.5	4.2	No benefit
PB28	M	NEC[d]+NSCLC[e]	0	1	68	PD-1	1	PD	6.1	0.7	No benefit
PB30	F	Ovarian cancer	6	0	64	PD-L1	4	SD	7.1	2.1	No benefit
PB32	F	IDC[f]	3	0	40	PD-1	11	PR	12.5	12.2	Benefit
PB34	F	IDC[f]	1	0	42	PD-1	6	PR	8.6	2.7	Benefit
PB36	F	CRC[a]	2	1	57	PD-L1	2	PD	6.3	3.1	No benefit
PB38	F	Ovarian cancer	3	1	49	PD-L1	8	SD	8.7	5.6	Benefit
PB40	F	Head and Neck	0	1	64	PD-1	4	PD	6.3	4.5	No benefit
PB42	M	CRC[a]	4	1	66	PD-L1	4	PD	4.0	2.9	No benefit
PB44	F	HCC[b]	4	0	58	PD-1+LAG-3	16	CR	24.9	24.9	Benefit
PB46	F	Urothelial Carcinoma	2	1	43	PD-1	1	PD	2.4	0.7	No benefit
PB48	M	Upper GI adenocarcinoma[c]	2	0	70	PD-L1	4	PD	6.8	0.6	No benefit
PB50	M	UPT[g]	1	1	59	PD-L1	12	SD	9.6	9.6	Benefit
PB54	F	IDC[f]	2	0	36	PD-L1	3	PD	4.7	1.5	No benefit
PB56	F	UPT[g]	2	1	50	PD-1	1	PD	0.7	0.4	No benefit
PB58	F	Ovarian cancer	3	0	52	PD-L1	3	SD	5.5	4.5	Benefit
PB60	F	MPM[h]	3	0	58	PD-1	1	PD	3.3	2.1	No benefit
PB62	F	NSCLC[e]	2	1	72	PD-1	4	PD	0.5	2.7	No benefit
PB64	F	Ovarian cancer	7	0	65	PD-L1	1	PD	14.5	1.2	No benefit
PB66	M	NSCLC[e]	0	0	60	PD-1	3	PD	4.8	1.8	No benefit
PB68	M	MPM[h]	3	0	56	PD-L1	7	SD	4.0	4.0	Benefit
PB70	F	NSCLC[e]	2	1	62	PD-1	2	PD	3.3	1.9	No benefit
PB72	F	NSCLC[e]	4	0	53	PD-1+CTLA-4	6	PD	2.6	3.7	No benefit
PB74	F	NSCLC[e]	5	1	68	PD-1+CTLA-4	4	PD	4.2	1.9	No benefit

[a]*Colorectal adenocarcinoma.*
[b]*Hepatocellular carcinoma.*
[c]*Upper gastrointestinal adenocarcinoma.*
[d]*Neuroendocrine carcinoma.*
[e]*Non-small cell lung cancer-adenocarcinoma.*
[f]*Invasive ductal carcinoma.*
[g]*Unknown primary tumor.*
[h]*Malignant peritoneal mesothelioma.*

In this paper, we focused our flowcytometry analyses on the characterization of subsets of T cells (i.e. CD4+ and CD8+), since they are known to be the final target of checkpoint inhibition. We investigated also the impact of myeloid cell populations known to affect antigen presentation (dendritic cells) and modulate T cell response such as monocytic populations such as classic/non-classic and myeloid derived suppressor cells (MDSCs).

Phenotyping of PBMCs by Flowcytometry

Cryopreserved PBMCs were thawed in wash buffer (0.5% BSA, 2mM EDTA in PBS) at 37˚C and Fc-receptors blocked by incubation with human IgG (20 μg/mL).

PBMCs were stained in three panels with pre-titrated amounts of premixed reagents: CD3 FITC, CD56 PE, CD11c PE, CD8 PerCP, HLA-DR PerCP, CD27 BV421, CD25 BV421, CD4 BV510, CD28 PE-Cy7, CD3 PE-Cy7, CD19 PE-Cy7, CD127 PE-Cy7, CD45RA APC, CD56 BV510 (all from BD Bioscience, New Jersey, United States), CCR7 PE, PD-1 APC, CD14 BV421 (all from Biolegend, California, United States), CD16 FITC (Dako, Glostrup, Denmark) and NiR live-dead reagent for APC-Cy7 channel (Invitrogen- Thermo Fischer, United States).

Samples were incubated 20 minutes in the dark at 4˚C and then washed prior to acquiring on a FACS Canto II flow cytometer (BD). Data was analyzed on FACSDiva Software version 8.0.1 (BD).

Characterization of CD3+ T cells in both CD4 and CD8 compartments was done by looking at the live singlet events in the PBMC (lymphocyte and monocyte) gate in the forward and side scatter plot. Naïve T cells were further characterized as CCR7+ CD45RA+, central memory (CM) as CCR7+CD45RA-, effector memory as CCR7-CD45RA-, and effector memory RA+ (EMRA) as CCR7-CD45RA+. Exhaustion marker programmed cell death-1 (PD-1) was gated on live CD3+CD8+ cells. Gating strategy for lymphoid cells are displayed on **Supplementary Figure 1**. Myeloid populations were defined as fraction of live singlet cells in the PBMC gate (forward and side scatter plot). Representative gating strategy is displayed on **Supplementary Figure 2**.

Statistical Analysis

Due to non-normality in flow cytometric data, Mann-Whitney test was used for assessing differences in distributions of cell subpopulations among group of patients according to response pattern. For paired sample analysis, stepwise Wilcoxon test was chosen in order to find whether significant changes occurred and at which timepoint they took place (i.e. from baseline to T1, from T1 to T2 and from baseline to T2). Survival analysis and Cox regression models were done using median value of cell population of interest as threshold for stratification of patients.

All analyses are done using IBM SPSS version 25. Tests were two-sided and p values ≤ 0.05 were considered as significant.

RESULTS

Cohort Characteristics

From February 2017 to September 2018, 37 patients with metastatic solid tumors referred to treatment with ICI, either as standard treatment or in a protocol, were screened for inclusion in this study. Four patients were excluded due to withdrawal of informed consent or worsening of performance status (PS) prior to treatment initiation. All patients received ICIs targeting either PD-1 or PD-L1, some in combination with novel therapies targeting potential synergistic targets (**Table 1**). Thirteen different diagnosis were included. The median age at inclusion was 60 years (range 36 to 75) with all patients having PS 0 or 1 by the time of treatment initiation. Prior to inclusion, patients had on average undergone three previous treatment lines. Two patients (no. PB72 and PB74) had previously failed to other ICIs with an interval between failure and inclusion in this study of 12 and 9 months, respectively.

Response to the Treatment

Median follow-up period was 7.4 months. The overall median PFS was 81 days (95%CI 46-116) and the median OS was 188 days (95%CI 148-227). We did not observe any statistically significant correlation between the number of treatments received prior to initiation of ICI and clinical outcome (Mann-Whitney test, p= 0.15; Fisher exact test assuming cut-off of three treatments with p=0.69). Neither did we observe any difference in benefit between the group receiving combination therapy and the group receiving monotherapy (Fischer exact test p=0.29). Best tumor size variation during therapy for each patient can be seen on waterfall plot - **Supplementary Figure 3**.

Exploring the T Cell Phenotype in Peripheral Blood

In order to get insight into how treatment impacted the functional repertoire of T cells, we performed phenotyping of cryopreserved PBMCs collected at 3 time points, i.e. baseline, T1 and T2. Differences in distribution of several subsets of T cells were investigated at each time point. Stepwise changes from baseline to T1, from T1 to T2 and baseline to T2 were based on paired samples available for 26 patients (9 presenting treatment benefit), 12 patients (7 with benefit) and 11 patients (6 with benefit), respectively.

In the current study, we hypothesized that patients likely to respond to ICI have a peripheral lymphoid and myeloid cell signature characterized by high cytotoxic activity, presence of treatment target on T cells (i.e. expression of PD-1), high antigen presentation, and low counts of immunosuppressive cells.

To address the first premise of our hypothesis, we investigated the functional subsets of circulating $CD4^+$ and $CD8^+$ T cells by looking into expression of CD45RA, CCR7, CD25 and expression of PD-1.

In the CD4 compartment, T cells were mainly represented by naïve and central memory (CM) phenotypes at all time points, regardless of response pattern. We also observed that percentages of different $CD4^+$ subsets at each time point were similar between patients that benefited from the treatment and those that did not (p>0.05 - **Supplementary Figure 4A**). Paired samples analysis revealed among the patients benefiting from ICI a statistically significant decrease of $CD4^+$ effector memory (EM) from baseline to T1(median 21.7% vs 19.6%,

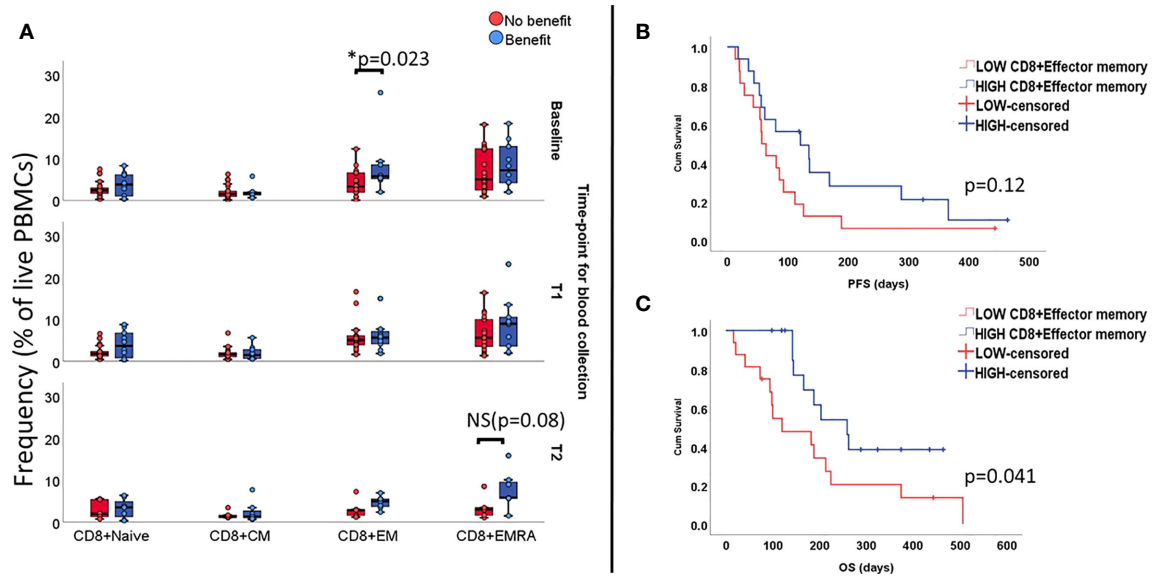

FIGURE 1 | Levels of functional subsets of CD8+T cells as fraction of live PBMCs at all three time-points (unpaired samples). Baseline analysis are carried out on 32 samples (10 deriving from patients benefiting from treatment), T1 comprises 27 samples (10 presenting benefit) and T2 comprises 12 samples (7 with treatment benefit). Section **(A)** shows an association with benefit during ICI treatment and levels of CD8+EM T cells at baseline and increased levels of EMRA in the group benefiting from treatment at late follow-up, with marginal p value. Effect of CD8+EM T cells on survival is displayed on **(B)** for PFS and **(C)** for OS.

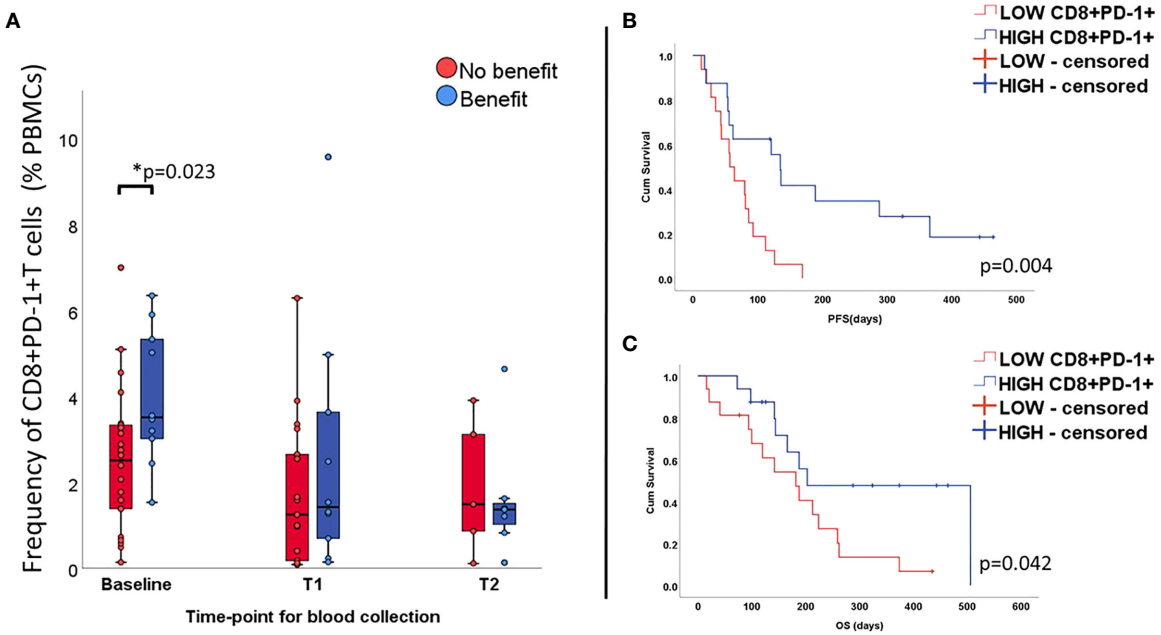

FIGURE 2 | Percentage of CD8+T cells expressing PD-1 at all time-points (unpaired samples) and correlation with outcome. Levels of CD8+PD-1+ T cells are higher at baseline in the group benefiting from the treatment **(A)** and correlates positively with longer PFS **(B)** and OS **(C)**.

p=0.008) whereas $CD4^+$ effector memory RA^+ (EMRA) increase from baseline to T1, and overall from baseline to T2 (Wilcoxon test p=0.024 and p=0.043, respectively-**Supplementary Figure 4B**).

Unlike CD4 compartment, $CD8^+$ T cells had a predominant effector/cytotoxic phenotype (i.e. EM and EMRA) at all time points (**Supplementary Figure 5A**). Paired analysis comprising baseline and T1 samples revealed a slight but non-significant

increase of the effector subset (i.e. sum of EM and EMRA) from 70.4% to 72.6% during treatment (p=0.052). Variations in levels of EMRA CD8+ T cells in the benefit and no benefit group were not statistically significant - **Supplementary Figure 5B**.

Next, we proceeded to investigate to which extent lymphocyte subsets as a fraction of the PBMC gate are associated with clinical outcome. Patients with clinical benefit presented higher percentage of $CD8^+$ EM T cells at baseline (5.7% vs 3.3%, p=0.023). In the same group of patients, we found that, over time, the phenotype became more effector-like with increasing numbers of circulating $CD8^+$EMRA at T1 which, despite a decrease at T2, still seemed to be higher when compared to patients not benefiting from ICI (5.8% vs. 2.9%; p=0.08, **Figure 1A**).

In terms of survival, patients with high numbers of circulating $CD8^+$EM T cells at baseline(i.e. above median value), did not have longer median PFS (121days vs. 57 days, Log rank p=0.12 **Figure 1B**), but the observed median OS was longer (259 days vs.120 days, Log Rank p= 0.04, **Figure 1C**).

Since all patients in our cohort received treatment blocking the PD-1/PD-L1 axis, we then proceeded to investigate whether the expression of PD-1 by circulating $CD8^+$T cells correlated with outcome. Results for baseline samples demonstrated that patients with relatively high values of $CD8^+PD\text{-}1^+$T cells in the peripheral blood (i.e. above median value) benefited most from the treatment (p=0.023, **Figure 2A**) presenting extended PFS (135 days vs. 57 days; LogRank p=0.004, **Figure 2B**) and OS (203 days vs 188 days; Log Rank p=0.042, **Figure 2C**). In univariate Cox regression, baseline high counts of $CD8^+PD\text{-}1^+$T cells correlated significantly to longer PFS (HR=0.31, p=0.006; 95% CI 0.12-0.71) but no solid trend regarding longer OS was verified (HR 0.4, p=0.051; 95%CI 0.16-1.0). No difference in $CD8^+PD\text{-}1^+$ T cell levels was observed for follow-up samples.

It has also been reported that expression of PD-1 and effects deriving from blockade of this axis are tightly related to expression of CD28 by $CD8^+$ T cells. In our data, we observed that the number of $CD8^+$ T cells expressing this molecule increased significantly upon treatment initiation, regardless of clinical outcome (**Supplementary Figure 6**).

Further, we investigated the impact of regulatory T cells ($CD3^+CD4^+CD25^+CD127$low). Even though, this cell subset is known for damping immune responses, levels of Tregs have not served as a unifying marker for response to therapy. In our study, we found that, at all timepoints, T regs were elevated among patients benefiting from treatment, reaching statistical significance level at T2 (p=0.045; **Supplementary Figure 7**). Longitudinal measurements showed in benefiting patients a gradual and statistically significant increase in the levels of the T reg population, especially from baseline to T2 (median 7.7% to 11.6%, p= 0.046; **Supplementary Figure 7**).

Role of Myeloid Cells

The association of myeloid cell levels and clinical outcome and survival was addressed by investigating dendritic cells (DC), monocytic MDSC (mMDSCs) and monocyte subpopulations. DCs were chosen due to the important role they play in terms of antigen presentation. This cell subset was gated as the fraction of PBMCs co-expressing CD11c and HLA-DR, and lacking CD14, CD16 and CD56. We found a trend between treatment benefit and abundance of DCs at baseline, however not statistically significant (1.15% vs. 0.8%, p=0.074, **Figure 3A**). Over time,

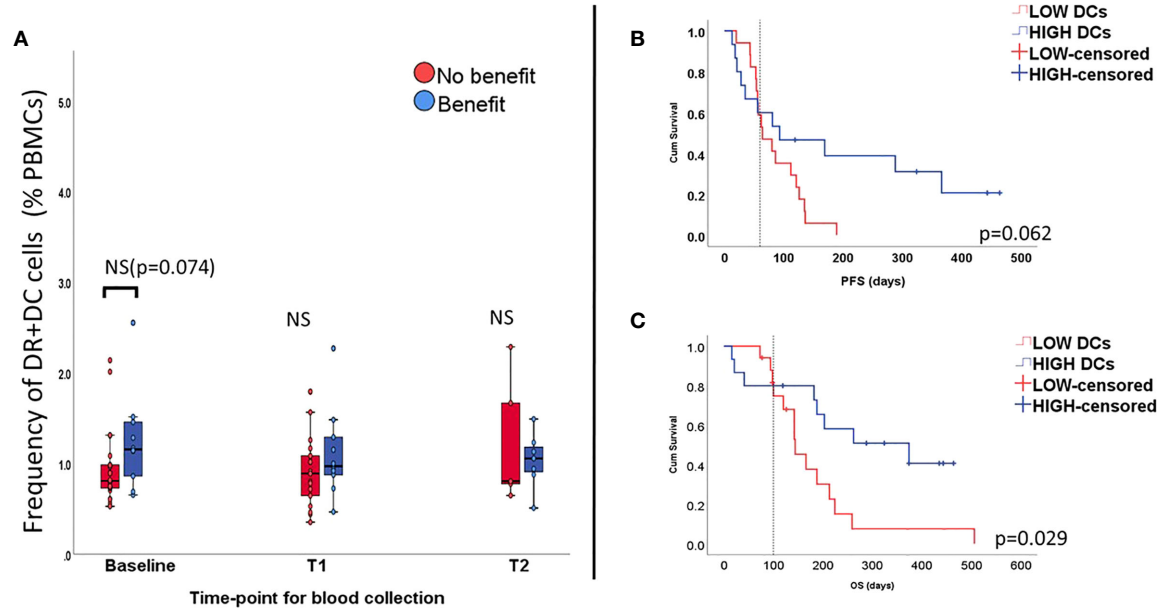

FIGURE 3 | Percentage of dendritic cells (DCs) all time-points (unpaired samples) and correlation with outcome. Levels of DCs seem to be elevated at baseline in the group benefiting from the treatment, but not at longitudinal measurements **(A)**. High levels of DCs seem to affect PFS **(B)** and OS **(C)**.

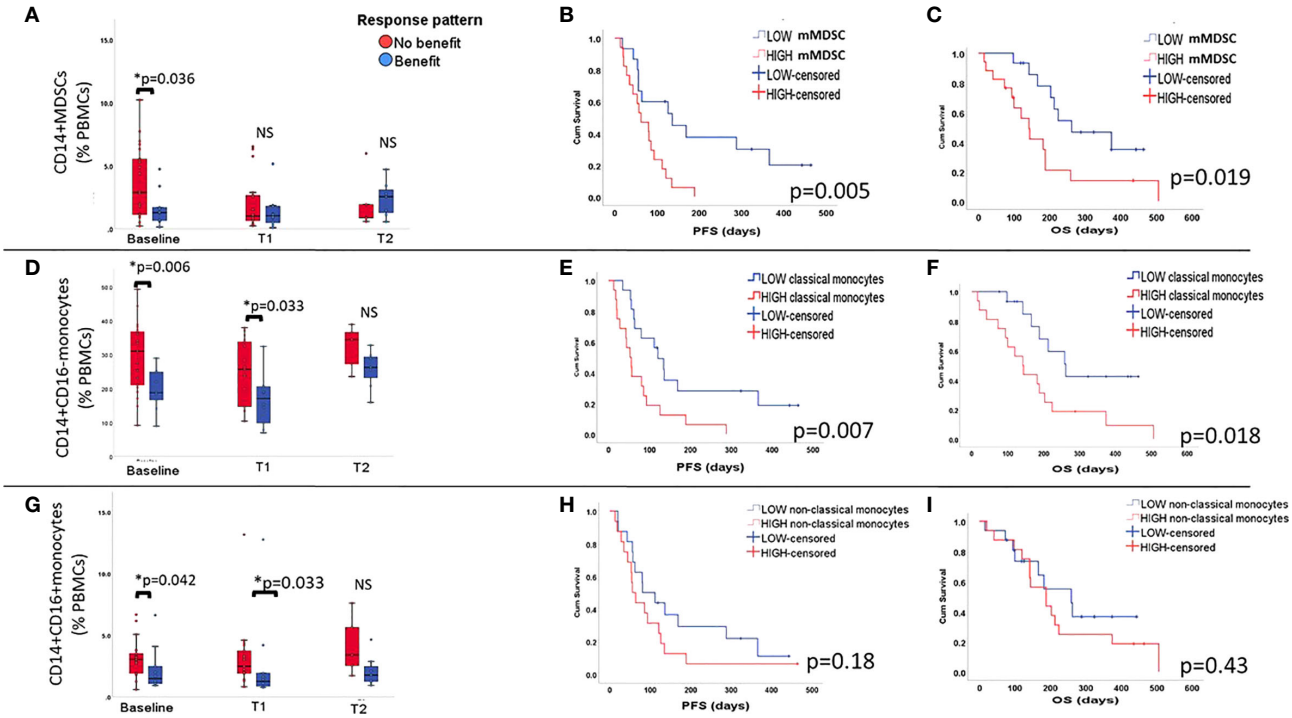

FIGURE 4 | Frequency of CD14$^+$ myeloid populations is inversely associated with benefit and survival. Percentages of mMDSCs **(A)**, classical monocytes **(D)** and non-classical monocytes **(G)** out of alive PBMCs (y-axis) are, already at baseline, elevated in the group of patients that did not achieve benefit during ICI treatment. Effects on survival for the respective myeloid subsets are displayed on **(B, E, H)** for PFS and **(C, F, I)** for OS. Overall, classical monocytes and mMDSCs affected negatively survival times. No effect on PFS nor OS was observed for non-classical monocytes.

variations in percentage of this cell type were small and not significant. Yet, survival analysis appeared to show impact of DC levels at baseline on PFS (Log Rank p= 0.062, **Figure 3B**) and OS (p=0.029, **Figure 3C**). High counts of DCs (i.e. above median value) also correlated with longer PFS (HR=0.14, p=0.03 95%CI 0.026-0.83) but not OS (HR=0.18, p=0.087 95%CI 0.026-1.28).

Other cell types of myeloid lineage have been reported as immune suppressive elements in TME. To investigate whether this applies for the periphery we explored the impact of mMDSC and monocyte populations. In this regard, we found that high baseline levels (i.e. superior to the median value) of mMDSCs (CD14$^+$ CD3$^-$ CD19$^-$ HLA-DR^{low}, CD56$^-$), classical (CD14$^+$CD16$^-$HLA-DR$^+$), and non-classical (CD14$^+$CD16$^+$ HLA-DR$^+$) monocytes were associated with poorer outcome (p= 0.036, 0.006, 0.042, respectively - **Figures 4A, D** and **G**). Changes of these populations during therapy did not reach statistically significant levels (Wilcoxon test p>0.05).

Longer PFS and OS were associated with low baseline levels of mMDSC (LogRank p=0.005 and 0.019, **Figures 4B, C**) and classical monocytes (Log Rank p=0.007 and 0.018, **Figures 4E, F**). Non-classical monocytes did not seem to have any impact on survival (**Figures 4H, I**).

Univariate Cox regression models were then used to investigate the effects of mMDSC and classical monocytes on survival. We found that high baseline counts of circulating mMDSC were associated with shorter PFS (p= 0.008, HR= 3.15, 95%CI 1.35-7.35) and OS (p=0.025, HR=2.78, 95%CI 1.13-6.8). For classical monocytes, we also found a similar trend both in terms of PFS (p=0.01, HR= 2.7, 95%CI 1.2-6.0) and OS (p=0.024, HR= 2.85, 95%CI 1.14-7.1).

The 'Favorable Immune Periphery' Concept

The previous analysis showed that several immune cell types in peripheral blood have the potential to affect how patients undergoing ICI benefit from the treatment in terms of clinical response and survival.

Overall, we noted that baseline counts of CD8$^+$ T cells with effector memory phenotype, CD8$^+$T cells expressing PD-1 and DC cells as a fraction of total live PBMCs seemed to correlate positively to response and survival, whereas mMDSCs and classical monocytes as a fraction of total live PBMCs seemed to be associated with poor clinical outcome. Based on these results, we hypothesized that patients benefitting from checkpoint inhibition have already at baseline a favorable immune signature that upon ICI could lead to improved clinical outcome. Bearing this in mind, we elaborated a numerical index where relative counts (i.e. percentage of live PBMCs) of CD8$^+$PD1$^+$, CD8+effector memory cells and DCs were entered as numerator and mMDSCs and classical monocytes were entered as denominator (Equation 1 - **Supplementary Material**). The geometric

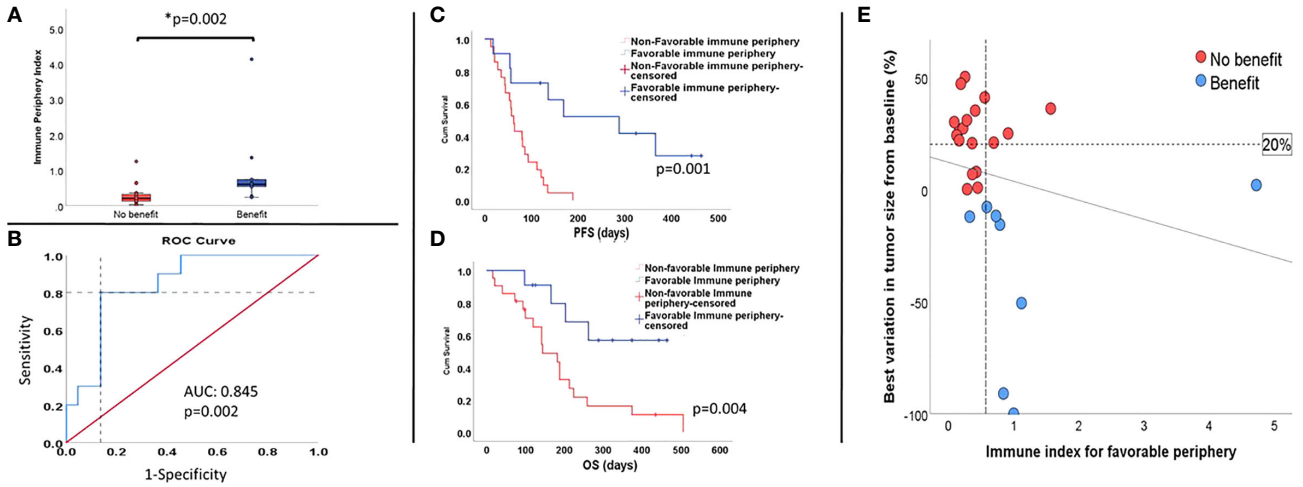

FIGURE 5 | The favorable immune periphery index and its impact on clinical outcome. Patients benefiting from ICI treatment presented a higher index **(A)**. Threshold for favorable immune periphery index was determined by ROC, assuming the highest sensitivity and specificity as possible **(B)** represented by the point where dashed lines cross each other. Patients with a favorable immune periphery had longer PFS **(C)** and OS **(D)**. On **(E)**, the scatter plot depicts correlation between best tumor variation and immune index based on baseline samples. Two parameters are inversely correlated (Spearman's ρ= -0.40; p=0.043). Vertical dashed line represents the threshold for immune index determined by ROC. Horizontal dashed line represents 20% limit for tumor growth and distinguishes patients who progressed (zone above 20%) from those that did not (area bellow below 20%). Patients that did not benefit from the treatment tend to cluster below the threshold for favorable periphery index.

mean values for both parts of the fraction where used to minimize the effect of outliers. Patients achieving clinical benefit had a significantly higher index, suggesting a prevalence of factors promoting immune antitumor activity, p=0.002 (**Figure 5A**). Reiterating this, we noted that our index significantly correlated with treatment related change in tumor size (Spearman's rho: -0.40, p=0.043, **Figure 5E**).

Sensitivity and specificity of the index were tested by looking at receiver operational characteristic curve (ROC). A cut off for the index was determined where sensitivity and specificity were equally as high as possible (dashed lines on **Figure 5B**).

Patients were subsequently pooled in two groups, namely high (i.e. favorable immune periphery; n=11) and low 'favorable immune periphery'-index (i.e. non-favorable immune periphery, n=21). The high favorable-index patients presented longer PFS (288 days vs 62 days; p= 0.001, **Figure 5C**) and OS (p=0.013, median survival not reached, **Figure 5D**), and equally exhibited reduced risk of progression (HR=0.18, p=0.002, 95%CI 0.065-0.52) and death (HR=0.27, p=0.021, 95%CI 0.09-0.82).

DISCUSSION

Immunotherapy with checkpoint blockade is a fast-growing field in the landscape of cancer treatment. However, despite documented benefit in terms of survival, the effect is only seen in a smaller fraction of patients which most likely reflects the multiple features that directly and indirectly affect T cell reactivity (23). Studies trying to find predictive biomarkers for response have broadly focused on variables spanning from genetic determinants, cell composition in the tumor microenvironment to markers in the peripheral blood and microbiome (22, 24). Majority of these approaches have focused on specific tumor types and have taken into consideration few factors at a time. With the increasing number of basket trials trying to find best therapeutic options and which patients are likely to benefit from ICI, there is an imperative need of multiparametric biomarker models capable of assessing broader and more heterogenous cohort of patients. Studies conducted so far using circulating immune cells have mainly investigated role played by T cells upon ICI, despite the growing evidence that other cell types might equally influence how patients respond to immunotherapy.

Bearing this in mind, we investigated by means of conventional flow cytometry and across tumor types, the peripheral immune cell repertoire (both lymphoid and myeloid subsets) of patients undergoing ICI, how the treatment affects this immune profile and whether these changes can possibly impact clinical outcome.

Our results suggest that patients benefiting from ICI seem to have a pre-treatment immunological profile (here called 'favorable immune periphery') entailing: high levels of T cells carrying treatment target (i.e. PD-1) and with cytotoxic potential; moreover, a periphery where cells involved in antigen processing/presentation (DCs) were present and where immunosuppressive effects (mMDSC, $CD14^{+}CD16^{-}$monocytes) were not prominent. Such changes were not observed to be reliant of tumor type. By pooling patients according to the two possible scenarios (favorable versus non-favorable immune periphery), we could distinguish patients with high chance of achieving benefit from those where treatment did not improve outcome.

In the lymphoid lineage, we focused our analysis on T cells, since they are the ultimate target of ICI. For the $CD4^{+}$ compartment we observed that, T cells mainly expressed a naïve

or central memory phenotype. Percentages of these functional subsets remained stable over time, while a decrease in EM and an increase in EMRA$^+$ CD4$^+$ was seen in patients responding to the treatment. CD4$^+$T cells play a role not well-explored in checkpoint inhibition as cellular cytotoxic activity usually is attributed to CD8$^+$ T cells. However, there is growing evidence supporting the role played by CD4$^+$T cells in cancer immunology. Active circulating CD4$^+$Th cells (i.e. expressing PD-1 and TIM-3 or CD62L^{low}) have, for instance, been shown to correlate with a better outcome in cohorts of breast (25) and lung cancer (26).

Intriguingly, we found an increased level of T regs in patients benefiting from ICI at late follow-up as well as expansion of T regs during treatment, possibly as an attempt to keep homeostasis upon the successful activation of T cells during ICI among patients responding to the treatment Proliferation of CD4$^+$CD25$^+$T regs following treatment with checkpoint inhibition has been previously observed mainly in patients treated with anti-CTLA-4 (27–29), with some data showing that T regs expanded upon ICI targeting CTLA-4 expressed FoxP3 but did not release IL-2, inferring that they were in fact 'bona fide'-T regs (30). On the other hand, studies assessing T regs under PD-1/PD-L1 blockade show a distinct downregulation of FoxP3 for melanoma (31) while in gliomas exhausted T regs with high expression of PD-1 failing to suppress effector T cell proliferation accumulated (32). These diverse results demonstrate the heterogeneity of T regs and that further studies are needed to get a clearer picture of their role in immune activation during ICI.

Contrarily to the observations for CD4$^+$T cells, a large fraction of CD8$^+$ T cells exhibited a more effector-like phenotype and clinical benefit was associated with higher baseline levels of EM and, at late follow-up, with increased levels of CD8$^+$EMRA, a functional subset known to produce granzymes, perforin and INF-gamma (33). The correlation between a shift towards a more effector-like phenotype and positive outcome has also been demonstrated by Kamphorst et al (18). in a NSCLC cohort undergoing PD-1 targeted therapy where efficacy was associated with an increase in CD8$^+$ effector T cells in peripheral blood within the first 4 weeks. Positive effects of CD8+EM T cells on survival during treatment with ICI have also been shown in patients with metastatic melanoma (34).

Although outcome seemed to be linked to a more cytotoxic CD8 phenotype, we did not note any significant correlation to progression-free survival. A possible explanation is that, even though, phenotypically, these T cells have cytolytic activity, that does not necessarily imply that the circulating CD8$^+$T cells in question are indeed only tumor specific. As a matter of fact, Kamphorst et al (18). highlights that the tumor reactive CD8$^+$T cells expanding in peripheral blood expressed Ki67 and were positive for PD-1$^+$. Also, Gros et al. find that expression of PD-1 could be used to determinate tumor specific reactive CD8$^+$T cells in the tumor (35) as well as in peripheral blood in melanoma patients (36). In line with these findings our results suggest that patients benefiting from ICI have high counts of CD8$^+$T cells expressing PD-1 at baseline. Thus, expression of PD-1 indicates tumor reactive T cells and by blocking PD-1/PD-L1, specific antitumor activity is unleashed initially at periphery and later in the tumor as CTLs move from blood stream into the TME. As a matter of fact, a recent work by Yost and colleagues has shown that T cells responses arising upon PD-1 blockade are mainly due to new T cell clones entering the tumor rather than the already existing T cells in TME (37).

Follow-up measurements indicated a reduction of the PD-1 positive CD8 population during therapy which could be explained by the fact that PD-1 staining was affected by the therapeutic antibody given during ICI treatment, as previously demonstrated by Zelba et al. (38). Another reason could also be that our second blood collection (approximately 6 weeks after treatment start) does not time with the moment when expansion in relative numbers of this cell population took place or due to migration of these tumor specific T cells to TME.

Reactivity of T cells is also reliant on the crosstalk between lymphoid and non-lymphoid cell types. An important part of cytotoxicity lies on antigen presentation and activation provided by APCs, which in the peripheral blood, are represented by a broader class of myeloid cells. We covered the role of antigen presentation by looking into myeloid DCs as they are capable of antigen uptake/processing/presentation and thereby promote priming of naïve T cells (39). In line with other studies (40, 41), DCs were scarcely represented at the periphery. Circulating myeloid DCs tended already at baseline to be slightly more abundant among patients experiencing treatment benefit, however, not reaching statistical significance. The lack of impact on response, when employing DCs as a single parameter, could likely be attributed to their paucity in peripheral blood

The relevance of the myeloid lineage in the context of ICI is still noteworthy. Several studies have provided strong evidence that these cells, although not directly involved in the immunological synapse, can still influence processes triggered upon antigen recognition (20, 42, 43). Sun et al. has recently demonstrated that abrogation of mMDSCs' trafficking into the TME using chemokine receptor inhibitors led to improved T cell infiltration and subsequent tumor cell killing (44). In our study, high counts of mMDSCs prior to treatment culminated with shortened PFS and OS. Our analyses corroborate the immunosuppression associated with this myeloid fraction (20, 44, 45) and similar trend for classical monocytes. Several studies have shown that the presence of macrophages in the tumor is, in general, associated with a poor prognosis (46). A recent work by Krieg et al. showed, however, that the circulating counterpart of classical monocytes (CD14$^+$CD16$^-$HLA-DR+) actually seem to be associated with better response in melanoma patients undergoing anti-PD-1 therapy (16), which is in contrast to our findings. Reasons for these divergent results could be difference in patient cohort composition (several histologies versus one single immunogenic tumor type) and the method used of characterizing cell phenotype (conventional Flow cytometry versus Mass Cytometry - CyTOF).

Overall, we did not find any statistically significant increase of specific myeloid and lymphoid subsets (except for T regs, as previously discussed) from baseline to later time-points. Even though, we could not see clear expansion of certain cell subsets among patients benefitting ICI, we did find that the effect on clinical outcome of the cells populations we looked into was also

quite similar to what has been previously described, which is noteworthy considering the heterogeneous cohort composition. Moreover, we found a persistent pattern showing that patients who benefitted from the treatment seem to have at baseline a preexisting immune signature in peripheral blood which makes the basis for our predictive index.

Even though our study has the clear limitation of sample size, the exploratory character, cohort's heterogenicity and need of validation in bigger cohorts it brings as novelty the fact that compiling the activity of lymphoid and myeloid subsets suggests that, also across tumor types, patients benefiting from ICI seem to have a pre-existing favorable immune signature in peripheral blood that provides a better biological starting point and ultimately better outcome. Furthermore, different cell types taken as explanatory variables cannot stand alone when predicting response to ICI, which underscores the complexity of mechanisms preceding and sustaining T cell activation. Therefore, designing multiparametric peripheral immunity models like ours and validating them in a bigger scale of patients is important to enable more precise predictive tools for clinical decision making.

DATA AVAILABILITY STATEMENT

The original contributions presented in the study are included in the article/**Supplementary Material**. Further inquiries can be directed to the corresponding authors.

AUTHORS CONTRIBUTIONS

VL: study design, idea development, inclusion of patients, collection of biological material and clinical data, flow cytometry panel design(secondary), statistical analysis and data visualization, manuscript writing. MH: Primarily flow cytometry panel design, gating and export of flow cytometry data. Review of manuscript. IS: facilitating patient recruitment, review of manuscript. KR: facilitating patient recruitment, review of manuscript. SH: study design, review of manuscript. UL: study design, patient recruitment and logistics related to transport of biological material, review of manuscript I-MS: study design, laboratory facilities, review of manuscript. All authors contributed to the article and approved the submitted version.

ETHICS STATEMENT

The protocol was approved by The Danish National Committee on Health Research Ethics (H-16046968) and the Danish Data Protection Agency (RH-2018-44). Informed consent was obtained from all individual participants included in the study prior to collection of biological material. This study was conducted in accordance to 1964 Declaration of Helsinki and its later amendments.

FUNDING

This study was only possible due to financial support granted by The Danish Cancer Society (R149-A10123) and Preben & Anna Simonsens Fond (Grant number 021892-0009).

ACKNOWLEDGMENTS

We thank biotechnicians Susanne Wendt, Sandra Ullitz and Bettina Johansen for great laboratory assistance, and Kirsten Nikolajsen for staining and acquiring PBMC samples by flow cytometer.

SUPPLEMENTARY MATERIAL

The Supplementary Material for this article can be found online at: https://www.frontiersin.org/articles/10.3389/fonc.2021.558248/full#supplementary-material

REFERENCES

1. Hodi FS, O'Day SJ, McDermott DF, Weber RW, Sosman JA, Haanen JB, et al. Improved survival with ipilimumab in patients with metastatic melanoma. *N Engl J Med* (2010) 363(8):711–23. doi: 10.1056/NEJMoa1003466
2. Schadendorf D, Hodi FS, Robert C, Weber JS, Margolin K, Hamid O, et al. Pooled Analysis of Long-Term Survival Data From Phase II and Phase III Trials of Ipilimumab in Unresectable or Metastatic Melanoma. *J Clin Oncol* (2015) 33(17):1889–94. doi: 10.1200/JCO.2014.56.2736
3. Rizvi NA, Mazieres J, Planchard D, Stinchcombe TE, Dy GK, Antonia SJ, et al. Activity and safety of nivolumab, an anti-PD-1 immune checkpoint inhibitor, for patients with advanced, refractory squamous non-small-cell lung cancer (CheckMate 063): a phase 2, single-arm trial. *Lancet Oncol* (2015) 16(3):257–65. doi: 10.1016/S1470-2045(15)70054-9
4. Hodi FS, Chesney J, Pavlick AC, Robert C, Grossmann KF, McDermott DF, et al. Combined nivolumab and ipilimumab versus ipilimumab alone in patients with advanced melanoma: 2-year overall survival outcomes in a multicentre, randomised, controlled, phase 2 trial. *Lancet Oncol* (2016) 17 (11):1558–68. doi: 10.1016/S1470-2045(16)30366-7
5. Yarchoan M, Hopkins A, Jaffee EM. Tumor Mutational Burden and Response Rate to PD-1 Inhibition. *N Engl J Med* (2017) 377(25):2500–1. doi: 10.1056/NEJMc1713444
6. Van Allen EM, Miao D, Schilling B, Shukla SA, Blank C, Zimmer L, et al. Genomic correlates of response to CTLA-4 blockade in metastatic melanoma. *Science* (2015) 350(6257):207–11. doi: 10.1126/science.aad0095
7. Rooney MS, Shukla SA, Wu CJ, Getz G, Hacohen N. Molecular and genetic properties of tumors associated with local immune cytolytic activity. *Cell* (2015) 160(1-2):48–61. doi: 10.1016/j.cell.2014.12.033
8. Rizvi NA, Hellmann MD, Snyder A, Kvistborg P, Makarov V, Havel JJ, et al. Cancer immunology. Mutational landscape determines sensitivity to PD-1 blockade in non-small cell lung cancer. *Science* (2015) 348(6230):124–8. doi: 10.1126/science.aaa1348
9. Riaz N, Havel JJ, Makarov V, Desrichard A, Urba WJ, Sims JS, et al. Tumor and Microenvironment Evolution during Immunotherapy with Nivolumab. *Cell* (2017) 171(4):934–49 e16. doi: 10.1016/j.cell.2017.09.028
10. Galon J, Pagès F, Marincola FM, Angell HK, Thurin M, Lugli A, et al. Cancer classification using the Immunoscore: a worldwide task force. *J Trans Med* (2012) 10:205–. doi: 10.1186/1479-5876-10-205

11. Eil RL, Roychoudhuri R, Clever D, Patel S, Sukumar M, Pan JH, et al. Elevated potassium levels suppress T cell activation within tumors. *J Immunother Cancer* (2015) 3(Suppl 2):P403–P. doi: 10.1186/2051-1426-3-S2-P403
12. Chouaib S, Messai Y, Couve S, Escudier B, Hasmim M, Noman MZ. Hypoxia promotes tumor growth in linking angiogenesis to immune escape. *Front Immunol* (2012) 3:21. doi: 10.3389/fimmu.2012.00021
13. Yi M, Qin S, Chu Q, Wu K. The role of gut microbiota in immune checkpoint inhibitor therapy. *Hepatobiliary Surg Nutr* (2018) 7(6):481–3. doi: 10.21037/hbsn.2018.11.12
14. Pages F, Berger A, Camus M, Sanchez-Cabo F, Costes A, Molidor R, et al. Effector memory T cells, early metastasis, and survival in colorectal cancer. *N Engl J Med* (2005) 353(25):2654–66. doi: 10.1056/NEJMoa051424
15. De Angulo G, Yuen C, Palla SL, Anderson PM, Zweidler-McKay PA. Absolute lymphocyte count is a novel prognostic indicator in ALL and AML. *Cancer* (2008) 112(2):407–15. doi: 10.1002/cncr.23168
16. Krieg C, Nowicka M, Guglietta S, Schindler S, Hartmann FJ, Weber LM, et al. High-dimensional single-cell analysis predicts response to anti-PD-1 immunotherapy. *Nat Med* (2018) 24(2):144–53. doi: 10.1038/nm.4466
17. Saleh R, Elkord E. Treg-mediated acquired resistance to immune checkpoint inhibitors. *Cancer Lett* (2019) 457:168–79. doi: 10.1016/j.canlet.2019.05.003
18. Kamphorst AO, Pillai RN, Yang S, Nasti TH, Akondy RS, Wieland A, et al. Proliferation of PD-1+ CD8 T cells in peripheral blood after PD-1-targeted therapy in lung cancer patients. *Proc Natl Acad Sci USA* (2017) 114(19):4993–8. doi: 10.1073/pnas.1705327114
19. Retseck J, VanderWeele R, Lin HM, Lin Y, Butterfield LH, Tarhini AA. Phenotypic and functional testing of circulating regulatory T cells in advanced melanoma patients treated with neoadjuvant ipilimumab. *J Immunother Cancer.* (2016) 4:38. doi: 10.1186/s40425-016-0141-1
20. Meyer C, Cagnon L, Costa-Nunes CM, Baumgaertner P, Montandon N, Leyvraz L, et al. Frequencies of circulating MDSC correlate with clinical outcome of melanoma patients treated with ipilimumab. *Cancer Immunol Immunother* (2014) 63(3):247–57. doi: 10.1007/s00262-013-1508-5
21. Takeuchi Y, Tanemura A, Tada Y, Katayama I, Kumanogoh A, Nishikawa H. Clinical response to PD-1 blockade correlates with a sub-fraction of peripheral central memory CD4+ T cells in patients with malignant melanoma. *Int Immunol* (2018) 30(1):13–22. doi: 10.1093/intimm/dxx073
22. Kitano S, Nakayama T, Yamashita M. Biomarkers for Immune Checkpoint Inhibitors in Melanoma. *Front Oncol* (2018) 8:270. doi: 10.3389/fonc.2018.00270
23. Blank CU, Haanen JB, Ribas A, Schumacher TN. CANCER IMMUNOLOGY. The "cancer immunogram". *Science* (2016) 352(6286):658–60. doi: 10.1126/science.aaf2834
24. Gibney GT, Weiner LM, Atkins MB. Predictive biomarkers for checkpoint inhibitor-based immunotherapy. *Lancet Oncol* (2016) 17(12):e542–e51. doi: 10.1016/S1470-2045(16)30406-5
25. Yuan Y, Hou W, Padam S, Frankel P, Sedrak MS, Portnow J, et al. 297PPeripheral blood mononuclear cell biomarkers predict response to immune checkpoint inhibitor therapy in metastatic breast cancer. *Ann Oncol* (2018) 29(suppl_8). doi: 10.1093/annonc/mdy272.287
26. Kagamu H, Yamaguchi O, Shiono A, Mouri A, Miyauchi S, Utsugi H, et al. CD4+ T cells in PBMC to predict the outcome of anti-PD-1 therapy. *J Clin Oncol* (2017) 35(15_suppl):11525–. doi: 10.1200/JCO.2017.35.15_suppl.11525
27. Maker AV, Attia P, Rosenberg SA. Analysis of the cellular mechanism of antitumor responses and autoimmunity in patients treated with CTLA-4 blockade. *J Immunol* (2005) 175(11):7746–54. doi: 10.4049/jimmunol.175.11.7746
28. Menard C, Ghiringhelli F, Roux S, Chaput N, Mateus C, Grohmann U, et al. Ctla-4 blockade confers lymphocyte resistance to regulatory T-cells in advanced melanoma: surrogate marker of efficacy of tremelimumab? *Clin Cancer Res* (2008) 14(16):5242–9. doi: 10.1158/1078-0432.CCR-07-4797
29. Tarhini AA, Butterfield LH, Shuai Y, Gooding WE, Kalinski P, Kirkwood JM. Differing patterns of circulating regulatory T cells and myeloid-derived suppressor cells in metastatic melanoma patients receiving anti-CTLA4 antibody and interferon-alpha or TLR-9 agonist and GM-CSF with peptide vaccination. *J Immunother.* (2012) 35(9):702–10. doi: 10.1097/CJI.0b013e318272569b
30. Khan S, Burt DJ, Ralph C, Thistlethwaite FC, Hawkins RE, Elkord E. Tremelimumab (anti-CTLA4) mediates immune responses mainly by direct activation of T effector cells rather than by affecting T regulatory cells. *Clin Immunol* (2011) 138(1):85–96. doi: 10.1016/j.clim.2010.09.011
31. Wang W, Lau R, Yu D, Zhu W, Korman A, Weber J. PD1 blockade reverses the suppression of melanoma antigen-specific CTL by CD4+ CD25(Hi) regulatory T cells. *Int Immunol* (2009) 21(9):1065–77. doi: 10.1093/intimm/dxp072
32. Lowther DE, Goods BA, Lucca LE, Lerner BA, Raddassi K, van Dijk D, et al. PD-1 marks dysfunctional regulatory T cells in malignant gliomas. *JCI Insight* (2016) 1(5):1–15. doi: 10.1172/jci.insight.85935
33. Hamann D, Baars PA, Rep MH, Hooibrink B, Kerkhof-Garde SR, Klein MR, et al. Phenotypic and functional separation of memory and effector human CD8+ T cells. *J Exp Med* (1997) 186(9):1407–18. doi: 10.1084/jem.186.9.1407
34. Wistuba-Hamprecht K, Martens A, Heubach F, Romano E, Geukes Foppen M, Yuan J, et al. Peripheral CD8 effector-memory type 1 T-cells correlate with outcome in ipilimumab-treated stage IV melanoma patients. *Eur J Cancer* (2017) 73:61–70. doi: 10.1016/j.ejca.2016.12.011
35. Gros A, Robbins PF, Yao X, Li YF, Turcotte S, Tran E, et al. PD-1 identifies the patient-specific CD8(+) tumor-reactive repertoire infiltrating human tumors. *J Clin Invest* (2014) 124(5):2246–59. doi: 10.1172/JCI73639
36. Gros A, Parkhurst MR, Tran E, Pasetto A, Robbins PF, Ilyas S, et al. Prospective identification of neoantigen-specific lymphocytes in the peripheral blood of melanoma patients. *Nat Med* (2016) 22(4):433–8. doi: 10.1038/nm.4051
37. Yost KE, Satpathy AT, Wells DK, Qi Y, Wang C, Kageyama R, et al. Clonal replacement of tumor-specific T cells following PD-1 blockade. *Nat Med* (2019) 25(8):1251–9. doi: 10.1038/s41591-019-0522-3
38. Zelba H, Bochem J, Pawelec G, Garbe C, Wistuba-Hamprecht K, Weide B. Accurate quantification of T-cells expressing PD-1 in patients on anti-PD-1 immunotherapy. *Cancer Immunol Immunother* (2018) 67(12):1845–51. doi: 10.1007/s00262-018-2244-7
39. Robinson SP, Patterson S, English N, Davies D, Knight SC, Reid CDL. Human peripheral blood contains two distinct lineages of dendritic cells. *Eur J Immunol* (1999) 29(9):2769–78. doi: 10.1002/(SICI)1521-4141(199909)29:09<2769::AID-IMMU2769>3.0.CO;2-2
40. Ho CS, Lopez JA, Vuckovic S, Pyke CM, Hockey RL, Hart DN. Surgical and physical stress increases circulating blood dendritic cell counts independently of monocyte counts. *Blood* (2001) 98(1):140–5. doi: 10.1182/blood.V98.1.140.h8000140_140_145
41. Knight SC, Farrant J, Bryant A, Edwards AJ, Burman S, Lever A, et al. Non-adherent, low-density cells from human peripheral blood contain dendritic cells and monocytes, both with veiled morphology. *Immunology* (1986) 57(4):595–603.
42. Gebhardt C, Sevko A, Jiang H, Lichtenberger R, Reith M, Tarnanidis K, et al. Myeloid Cells and Related Chronic Inflammatory Factors as Novel Predictive Markers in Melanoma Treatment with Ipilimumab. *Clin Cancer Res* (2015) 21(24):5453–9. doi: 10.1158/1078-0432.CCR-15-0676
43. Kitano S, Postow MA, Ziegler CG, Kuk D, Panageas KS, Cortez C, et al. Computational algorithm-driven evaluation of monocytic myeloid-derived suppressor cell frequency for prediction of clinical outcomes. *Cancer Immunol Res* (2014) 2(8):812–21. doi: 10.1158/2326-6066.CIR-14-0013
44. Sun L, Clavijo PE, Robbins Y, Patel P, Friedman J, Greene S, et al. Inhibiting myeloid-derived suppressor cell trafficking enhances T cell immunotherapy. *JCI Insight* (2019) 4(7):1–12. doi: 10.1172/jci.insight.126853
45. Parker KH, Beury DW, Ostrand-Rosenberg S. Myeloid-Derived Suppressor Cells: Critical Cells Driving Immune Suppression in the Tumor Microenvironment. *Adv Cancer Res* (2015) 128:95–139. doi: 10.1016/bs.acr.2015.04.002
46. Gentles AJ, Newman AM, Liu CL, Bratman SV, Feng W, Kim D, et al. The prognostic landscape of genes and infiltrating immune cells across human cancers. *Nat Med* (2015) 21(8):938–45. doi: 10.1038/nm.3909

Conflict of Interest: The authors declare that the research was conducted in the absence of any commercial or financial relationships that could be construed as a potential conflict of interest.

frontiers in Immunology

REVIEW
published: 31 March 2021
doi: 10.3389/fimmu.2021.590742

High Throughput Multi-Omics Approaches for Clinical Trial Evaluation and Drug Discovery

Jessica M. Zielinski[1], *Jason J. Luke*[2], *Silvia Guglietta*[1†] *and Carsten Krieg*[1*†]

[1] Hollings Cancer Center, Medical University of South Carolina (MUSC), Charleston, SC, United States, [2] Hillman Cancer Center, Department of Medicine, Division of Hematology/Oncology, University of Pittsburgh Medical Center, Pittsburgh, PA, United States

High throughput single cell multi-omics platforms, such as mass cytometry (cytometry by time-of-flight; CyTOF), high dimensional imaging (>6 marker; Hyperion, MIBIscope, CODEX, MACSima) and the recently evolved genomic cytometry (Citeseq or REAPseq) have enabled unprecedented insights into many biological and clinical questions, such as hematopoiesis, transplantation, cancer, and autoimmunity. In synergy with constantly adapting new single-cell analysis approaches and subsequent accumulating big data collections from these platforms, whole atlases of cell types and cellular and sub-cellular interaction networks are created. These atlases build an ideal scientific discovery environment for reference and data mining approaches, which often times reveals new cellular disease networks. In this review we will discuss how combinations and fusions of different -omic workflows on a single cell level can be used to examine cellular phenotypes, immune effector functions, and even dynamic changes, such as metabolomic state of different cells in a sample or even in a defined tissue location. We will touch on how pre-print platforms help in optimization and reproducibility of workflows, as well as community outreach. We will also shortly discuss how leveraging single cell multi-omic approaches can be used to accelerate cellular biomarker discovery during clinical trials to predict response to therapy, follow responsive cell types, and define novel druggable target pathways. Single cell proteome approaches already have changed how we explore cellular mechanism in disease and during therapy. Current challenges in the field are how we share these disruptive technologies to the scientific communities while still including new approaches, such as genomic cytometry and single cell metabolomics.

Keywords: CyTOF/mass cytometry, Cite/REAP-seq, high-dimensional analysis, bioinformatics, machine learning, biomarker

OPEN ACCESS

Edited by:
Said Dermime,
National Center for Cancer Care and Research, Qatar

Reviewed by:
Nahum Puebla-Osorio,
University of Texas MD Anderson Cancer Center, United States
Alaaeldin Shablak,
Hamad Medical Corporation, Qatar

****Correspondence:***
Carsten Krieg
kriegc@musc.edu

†ORCID:
Carsten Krieg
orcid.org/0000-0002-5145-7591
Silvia Guglietta
orcid.org/0000-0001-9998-5716

Specialty section:
This article was submitted to Cancer Immunity and Immunotherapy, a section of the journal Frontiers in Immunology

Received: *02 August 2020*
Accepted: *01 March 2021*
Published: *31 March 2021*

Citation:
Zielinski JM, Luke JJ, Guglietta S and Krieg C (2021) High Throughput Multi-Omics Approaches for Clinical Trial Evaluation and Drug Discovery. Front. Immunol. 12:590742. doi: 10.3389/fimmu.2021.590742

INTRODUCTION

Since the early days of cell biology scientists have been using optical instruments to identify cell types in homeostatic conditions and diseases. With the wide introduction of flow cytometry in the early 70-ies markers and subsequent cell types have evolved but it was only in the last decade that the introduction of single cell transcriptome sequencing, high dimensional cytometry and imaging cytometry started revolutionizing the way we interrogate biological samples.

Isolation of multiple types of molecules (DNA, RNA, or protein) from a single cell simultaneously, stands at the beginning of each approach and having standardized and validated protocols for single cell solutions is surely the foundation of all the herein described approaches. Utilizing single cell genome, methylome, chromatin accessibility, while RNA or protein from the same cell can be used to profile the transcriptome, and proteome, different single cell omics profiles alone or in combination can serve as building blocks to construct a multi-omics profile for the same cell.

In this review article we will recapitulate the highlights of each of these technologies, analysis pipelines and discuss their potential to revolutionize future sample analysis, clinical trial design and ultimately redefine clinical research.

A NEW ERA OF SINGLE CELL DATA GENERATION

Pioneering Flow Cytometry

The first particle separator using the flow cytometry technology was employed in 1965 at Los Alamos National Laboratory (1) for sorting particles with different volumes to meet the needs of Mack Fulwyler. Meanwhile, Len Herzenberg, who was interested in a machine that could sort living cells based on their fluorescence, applied the design of the Fulwyler particle separator to build the first fluorescence activated cell sorting (FACS) instrument at Stanford University in the late 1960s (see the video Inventing the Cell Sorter, Herzenberg Lab, https://www.youtube.com/watch?v=Ro8P3w9BPhg).

The HIV/AIDS pandemic in the 1980s then gave a dramatic impulse to the technology of counting specific cells, since it became clear that the quantification of peripheral blood CD4+ T cells was crucial to follow the course of the infection, and eventually for monitoring response to therapy (2). As a consequence, the development of flow cytometers that had to be easy-to-use in all clinical laboratories, mainly focused on the proteome, and helped to widely disseminate this technology. Nowadays, flow cytometry is a commonly used tool in the field of immunology to finely dissect the diverse phenotypic and functional properties of immune cells.

Decades of development have created very robust flow cytometers aimed to deliver data from thousands to millions of individual cells from tubes or multi-well plates at acquisition rates of tens of thousands of cells per minute and expanding from the proteome, over genes to reporters of transcription. In order to have a wide dynamic range, the systems are designed for optimal signal to noise ratios. Typically, fluorescence tagged antibodies as well as molecular sensors (such as Ca2+-flux), and genetically encoded reporters (GFP, tdTomatoe, RFP, etc.) can be detected. The main limitation of this technology lies in the amount of available dyes, lasers and comparable detectors. Currently, up to seven lasers with emission wavelengths from 325nm to 650nm are used and tunable lasers are becoming increasingly common. Nevertheless, the overlap in the emission spectra limits the number of detectable markers.

Flow cytometers use either photomultipliers or avalanche diodes to convert fluorochrome-emitted light into electrical impulse. The advent of advanced detectors, such as spectral flow analyzers, first introduced in 1979 (3), allows the acquisition of biological information over multiple channels/probes. Modern high parameter flow cytometers, like the BD Symphony, the Beckham Coulter CytoFLEX, or the Sony Spectral Cell Analyzer easily allow the measurement of 20+ parameters in a single sample at high throughput.

Prior to expert guided or automated analysis, data from flow cytometers needs rigorous pre-processing, which includes compensation and data normalization. To compensate the spectral overlap automated approaches using fluorescence beads and software solutions can be used. Normalization represents a more complex issue. Traditionally, standardization of flow cytometry data is difficult as flow cytometry settings change over time also in the same instrument, therefore creating batch effects when samples are analyzed days or even months apart. This issue is also caused by the fact that in flow cytometry samples cannot be acquired using a truly multiplexing approach, rather they can only be acquired sequentially over days or weeks if a plate reader is available. Therefore, curative naming and metadata are necessary to identify sources of batch effects. To date, several software solutions are available to normalize fluorescence values between data sets (4, 5). Magnetic gates on sub-population landmarks (6) are one of these solutions and consist in expert-identification of cell sub-populations with subsequent use of a software tool that automatically adjusts the gate on the identified populations. However, while this and all other available solutions are effective when minor shifts occur during acquisition, they might not be suitable in case of more substantial shifts occurring during time intensive acquisitions or when multiple instruments or data from multiple sites are used.

Mass Cytometry: A Truly Multiplexing Single Cell Technology

Mass cytometry is a new hybrid technology employing principles of flow cytometry and mass spectrometry. Introduced in 2009 (7), mass cytometry (or Cytometry by Time-Of-Flight, CyTOF) has pioneered a new era of high-dimensional single-cell analysis, surpassing the limitations imposed by the spectral overlap in conventional flow cytometry (8, 9). The new concept of mass cytometry is the use of high purity, stable, rare earth metal isotopes coupled to a target-specific probe for single cell labeling. These probes are detected based on the metals' mass/charge ratios by inductively-coupled plasma time of flight mass spectrometry (10). Among the advantages of this technology are the absence of spectral overlap, which allows to realistically measure over 40 markers on a single cell; absence of tissue auto-fluorescence; true multi-plexing capacity using barcoding matrices, which allow to run up to 100 samples in parallel without compromising dimensionality. To date, mass cytometry has not only been performed on leukocytes by using antibody-labeled probes but also on cell lines, bacteria, nanoparticles and beads (11–15). The core technology is rapidly developing along with bioinformatics and reagent

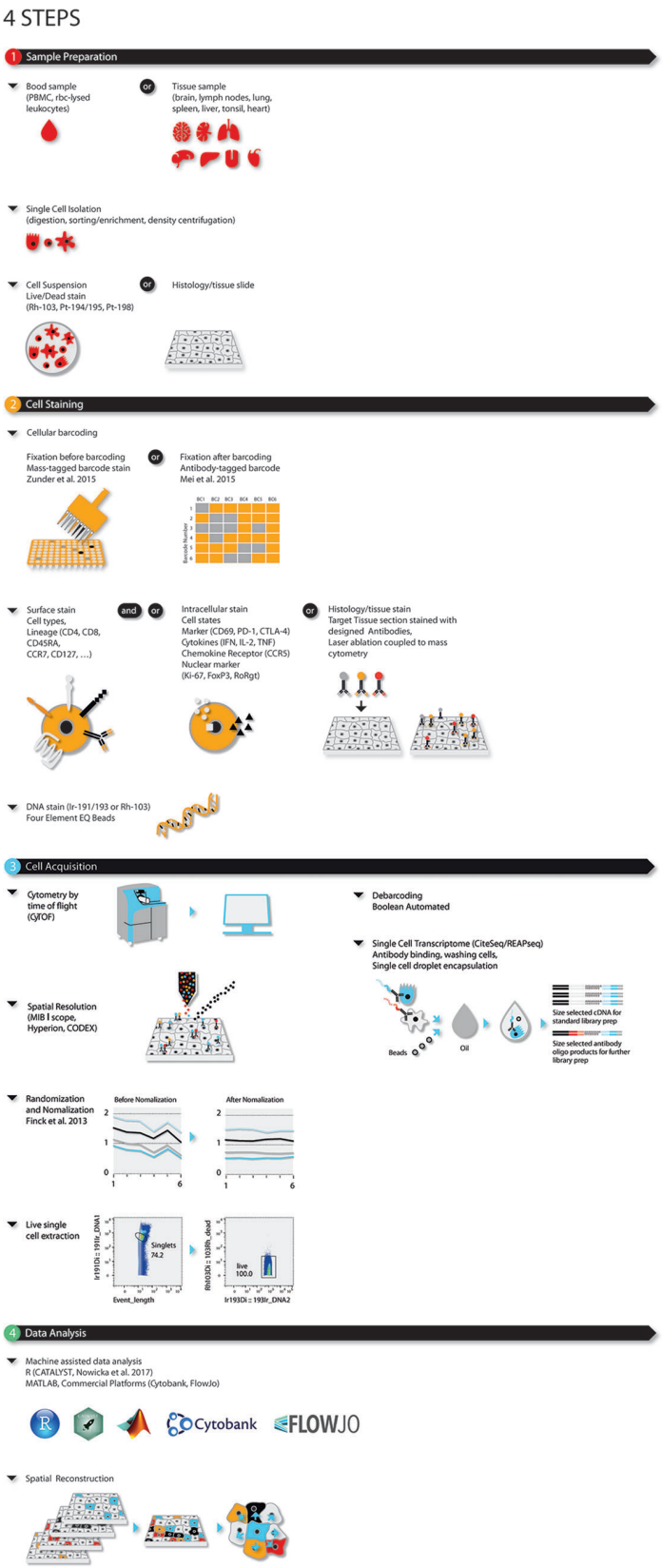

FIGURE 1 | Continued

FIGURE 1 | Four-step modular approach for high dimensional OMICS analysis for immune profiling during disease and (immuno)-therapy. Steps consist of (1) sample preparation, (2) cell barcoding and staining, (3) sample acquisition, and (4) data analysis. Briefly, single cells or histologic slides are prepared from blood, or fixed tissue samples. Single cells from blood or dissociated fresh tissues are barcoded, stained for live/dead, surface and/or intracellular markers and acquired using single cell solution mass cytometry. As an alternative CiteSeq can be utilized. Tissues on histologic slides are stained and acquired using imaging mass cytometry. For mass cytometry, data is bead-normalized and randomized. After de-barcoding data can be loaded in the bioinformatic analysis platform of choice.

chemistry, thereby creating a largely universal and extendable next generation platform for multiplexing high-dimensional single-cell cytometry applied to translational research, systems biology, and biomarker discovery.

Mass cytometry is ideally applied to research requiring high parametrization at single-cell resolution such as: (i) resolving cellular heterogeneity in complex mixtures of cells (e.g. bone marrow, blood or tissue); (ii) delineating complex phenotypes of isolated cell types, such as T-cell or myeloid subsets (16–19); or (iii) extracting maximum information out of limited (clinical) samples, such as tissue biopsies, blood samples from cancer patients and children (20–22). This latter makes mass cytometry ideal for large-scale immune monitoring and drug screening studies in clinical/translational research and systems immunology (**Figure 1**). The type of probes (antibodies) used by mass cytometry are the same as the ones used in flow cytometry with the caveat that mass cytometry is less sensitive than flow cytometry.

Multiparametric Tissue Imaging

More recently, multiparametric (>6 markers) imaging using immunofluorescent or metal-labeled probes has been translated to tissues. Currently there are four commercially available systems: the Hyperion technology (Fluidigm), the MIBIscope system (Ionpath), the CO-Detection by indEXing (CODEX, Akoya) instrument platform and the MACSima (Miltenyi). The concept behind all of these technologies arose from Stanford University with the idea to extend high dimensional studies from solution mass cytometry to tissues, thus allowing efficient spatial resolution.

Mass spectrometry-based instruments like the Hyperion and MIBIScope vaporize histologic samples previously tagged with rare metals conjugated-antibodies and analyze their content in a mass spectrometer. The Hyperion system is an appendix to the Helios solution mass cytometer and can be operated using the same instrument with the addition of a laser ablation table to vaporize histologic samples (23). The MIBIScope is a stand-alone instrument, which uses an Ion beam for ablating rare metal stained tissues and needs special gold-coated slides for sample preparation (24, 25). The administered energy and speed of the ion beam can be regulated thus enabling different ablation speeds and tissue resolutions. Most importantly, the ion beam can reach sub-cellular resolution, therefore allowing the study of intracellular organelles and structures. The CODEX as well as the MACSima technologies use antibodies conjugated to unique oligonucleotide sequence barcodes. Target-specific barcodes with a dye-labeled reporter allow for highly specific detection.

All data generated on imaging platforms are displayed as data spots per area revealing the amount of probe that was bound to that spot when the tissue section was stained and ablated/screened. By plotting the data so that the single-spot data points are next to each other in the order they were originally sampled, highly multiplexed images of the tissue sections can be reconstructed. Together with the spatial information, whole tissues are electronically reassembled by using bioinformatics. By employing tissue microarrays and standardized staining panels, these technologies can be high throughput. Sensitivity for some probes on Hyperion is low. Due to a higher amount of energy transferred to the probe, the MIBIscope may offer higher sensitivity. As for the CODEX platform, this technology has just become commercially available and evaluation of performance in terms of sensitivity is still premature. Of note, the MIBIscope and CODEX systems are less tissue destructive, therefore allowing downstream use of the tissue for microdissection and further analyses. All technologies are relatively new to the broad scientific community and time and user preferences will clarify which technology is best to address each individual scientific question.

Genomic Cytometry

Due to its long history and multiple validated analysis workflows, single cell (sc) RNA sequencing (scRNASeq) in combination with unsupervised machine-learning bioinformatics is nowadays the preferred approach to in-depth reveal the complexity of the cellular landscape in multiple diseases. In 2011 a pioneering study from Wigler and colleagues using scRNASeq showed that the metastatic dissemination is the consequence of a single clonal expansion (26). Increasing scRNASeq throughput (27) (28), has enabled the identification and characterization of novel or rare cell types (29), in addition to providing insights into the underlying mechanisms of cellular development (30) and response to therapeutic interventions (31).

However, proteins, not mRNAs, are the primary targets of drugs and protein abundance cannot necessarily be inferred directly from mRNA abundance (32–35). An unbiased view of proteins is thus necessary to model cellular dynamics and response to environmental and therapeutic perturbations. To address this need, recently, new cross over technologies using specific protein-targeted tags and untargeted transcriptomic or targeted genomic approaches have been developed. Cellular Indexing of Transcriptomes and Epitopes by Sequencing (CITE-seq) (36) and its sister technology RNA Expression and Protein Sequencing assay (REAP-seq) (37) use DNA-barcoded antibodies to convert detection of proteins into a quantitative, sequenceable readout. CITE-seq uses biotin-conjugated barcodes, while in the REAP-seq technology barcodes are directly bound to the probes. These antibody-bound oligos act as synthetic transcripts that are captured during most large-scale

oligodT-based scRNA-seq library preparation protocols (e.g. 10x Genomics, Drop-seq, ddSeq).

BIOMARKER DISCOVERY AND NOVEL TARGET IDENTIFICATION

scRNA-Seq in Biomarker Discovery

According to the DNA-RNA dogma, DNA provides the code for RNA, which in turn is translated into protein (38). The majority of cell populations studies from complex heterogenous tissues such as cancer has been conducted on bulk samples, which read the average signal within a population thus preventing measurements of the single cell variation. The widespread knowledge of transcriptomic analysis fueled the study of single cell genes, transcriptomes and proteomes in several different diseases and cell types.

Non-invasive single cell-based sequencing of liquid biopsy has been proposed to screen circulating clonal population of cancer cells (39). For these reason, sophisticated methods to capture, enrich and sequence circulating tumor cells (CTCs) have been optimized. In metastatic breast cancer, scRNA analysis of CTCs has been performed using Hydro-Seq: high-efficiency-cell-capture-contamination free scRNA-seq. Using this powerful method, the authors revealed clinically relevant markers to identify CTCs and, interestingly, inter- and intra-patient transcriptome heterogeneity (40). In addition, the use of single cells sequencing enabled the identification of disease-associated cellular profile and interactome, which have been subsequently validated across 13 different diseases such as asthma, atherosclerosis, breast cancer, chronic lymphocytic leukemia (CLL), Crohn's disease, eczema, obesity, influenza, psoriasis, seasonal allergic rhinitis, type 1 diabetes, tonsillitis and ulcerative colitis. This further supports the universality and the power of scRNA-seq for biomarkers detection and identification of therapeutic targets (41). The breakdown of immune cells activation and interaction have been analyzed by single cells studies during bacterial infection: over 7000 human PBMC *ex-vivo* infected with *Salmonella* have been sequenced using 10X Genomics with the aim to generate a detailed picture of infection-induced cell states (42).

A similar dynamic of the immune cells can be investigated in the tumor microenvironment. In hepatocellular carcinoma the combination of two scRNASeq technologies, SMART-Seq2 and drop-based platform, revealed six different macrophage clusters and a novel class of LAMP3+ mature dendritic cells, which dampens T cell antitumor functions. Additionally, the analysis of cell populations in multiple organs and body sites has revealed both the migration paths of immune cells and their origins (43). Single cell studies of lymphoid cells in cancer are also leading to the discovery of stronger predictors for disease and treatment outcomes. TCGA multi-omic data was collected across several cancers to identify novel markers from tumor infiltrating lymphocytes as key indicators for prognosis. Protein and mRNA expression profiles were correlated with survival curves leading to the discovery of *GPR18* as a better prognostic indicator over the previously established CD20+ (44). The interaction between immune cells and cancer can also be useful to identify novel therapeutic strategies. In this context, using scRNA-seq, lymphoid cells generated in the gut mucosa have been proposed as modulators in colorectal cancer. Various differentiation states can also play significant roles in the tumor microenvironment and be potentially relevant for novel immunotherapy strategies (45). In addition to the interaction among different immune cell subsets, scRNA-seq has proved valid to investigate the interaction between immune cells and non-immune cells such as tumor cells and stroma (46). The power of scRNA-seq in exploring cell heterogeneity within the same population has been also applied to the analysis of HIV permissiveness in CD4+ T cells. In this study CD298, CD63 and CD317 have been identified as a biomarker signature of cell permissiveness to the viral infection (47).

Besides study focusing on CTC and immune cells in the context of cancer, scRNA-seq has recently been used to unearth a range of clinically relevant non-immune markers from tumor samples. Recent work has defined cell populations within malignant osteosarcoma using scRNA-seq and Monocle 2 for pseudo-time analysis. Markers identified with this method were accurate in predicting metastases and disease recurrence (48). Similar techniques were applied to existing data to define novel biomarkers for hepatocellular carcinoma (49). Zhao et al. exposed glioblastoma samples to different chemotherapeutics and used scRNA-seq expression profiles to predict drug response in individual patients (50). A different study focused on glioma used existing multi-omic data, including scRNA-seq, to identify novel biomarkers in cerebrospinal fluid that can be used to assess diagnosis, prognosis, and directions for therapy (51). In patients with lung adenocarcinoma, scRNAseq on samples collected at different time points during disease, including at the time of metastases formation, enabled the identification of markers of cellular reprogramming and immunosuppression (52).

Lately, single cell methods have been employed to characterize SARS-CoV-2. Using scRNA-seq on COVID-19 positive patient bronchoalveolar lavage fluids (BAL), key immune cell populations were found to predict disease severity (53). In another study, peripheral blood mononuclear cells (PBMC) were collected from patients in the early recovery phase and using scRNA-sequencing Wen et al. showed a pro-inflammatory state following the primary infection, therefore suggesting that patients should be monitored for up to one week after the primary infection wanes (54). Using previously collected scRNA-seq data, one study developed a pipeline for identifying drug targets for COVID-19 and another combined this data with viral receptor interaction information to identify mechanisms of COVID entry across multiple organs (54, 55).

Single Cell Proteomics in Biomarker Discovery

The Nolan laboratory has conducted pioneer work to adapt analysis of single cell proteomes to immunology using CyTOF. The more abundant proteomic information from each single cell

enabled by mass cytometry provides a much broader landscape for different types of biological questions such as the frequency of immune cells in response to a stimulus (56) and the correlation between tumor pathology and phosphoproteins signaling (57). Relevant clinical information such as immune response during diseases (58, 59), assessment of clinical recovery after surgery (60), and guidance to effective therapy (22, 59) has also been obtained using this method. Over time, several research groups have combined this technology with clinical samples, clinical data and novel functional assays to assist easier disease diagnosis (61). Mass cytometry has been crucial in deciphering dendritic cell ontogeny (19, 62), B cell development (63) and in characterizing the human mucosal immune system in gastrointestinal pathologies (64). Krieg et al. used high-dimensional single-cell mass cytometry to characterize subsets of immune cells in the peripheral blood of metastatic melanoma patients before and during anti-PD-1 immunotherapy (20). Thirty surface markers were first assayed in the leukocytes and a set of T cell subsets at the different stages of differentiation and activation. Then, functional phenotypes of T cells and myeloid cells were extensively characterized with single-cell proteomic profiling to discover the difference between responders and non-responders to anti-PD-1 immunotherapy. This study showed for the first time that the frequency of CD14+ CD16− HLA-DR^{hi} monocytes may serve as a prognostic biomarker of progression-free and overall survival before immunotherapy (20). Wei et al. characterized single tumor-infiltrating T cells (TILs) with mass cytometry by assessing 33 surface and 10 intracellular markers, including non-T cell lineage markers, T cell differentiation and activation markers, and T cell lineage transcription factors. This study showed that both anti-CTLA-4 and anti-PD-1 antibodies expand exhausted-like CD8 T cells, and that anti-CTLA-4 antibody modulates an ICOS+ Th1-like CD4 effector subset for engaging exhausted-like CD8 T cells. Wei et al. discovered the distinct cellular mechanisms of antitumor immune responses induced by CTLA-4 and PD-1 blockade in the preclinical and clinical analysis (65). Recently, Spitzer et al. proposed that effective cancer immunotherapy depends on systemic immunity. To validate this hypothesis, they assessed antitumor immune response in lymph node, spleen, blood, and bone marrow in mouse models of breast cancer using 39 immune markers for surface and intracellular proteins. This study provided evidence that a population of CD4+ T cells in peripheral blood could predict systemic active immunity required for tumor rejection (66). In addition, Becher et al. showed circulating auto-reactive T cells in patients suffering from narcolepsy and multiple sclerosis (21, 67).

Compared to scRNAseq and fluid phase mass cytometry, imaging mass cytometry (IMC) is still in its infancy mainly because of the still limited distribution of the technology and expert laboratories across the world. To date, the most exhaustive results obtained using IMC have been produced by the Bodenmiller laboratory using the Hyperion system and focused on the characterization of immune contexture and tumor microenvironment in breast cancer (23, 68). We envisage a widespread dissemination of high dimensional imaging using the Hyperion and previously mentioned sister technologies. This in turn will contribute to the generation of very comprehensive atlases, which will be of great value for a deeper understanding of cellular interactions during health and disease.

INTEGRATION USING BIOINFORMATCS

Pre-print Platforms

One of the biggest challenges posed by single-cell-omic approaches is the simplification of data processing and analysis, so that workflows can become readily available not only for research purposes but also for clinical application. Several solutions for data storage and processing are nowadays free or commercially available *via* subscription or licensing.

Free platforms are FlowRepository (www.flowrepository.org), ImmPort (import.niaid.nih.gov), and ImmuneSpace (www.immunespace.org). One commercial service, **CytoBank**, offers a cloud-based network that allows easy accessibility to data and code in a user-friendly format. Online support for analysis or workflow problem solving is also available. CytoBank includes analysis packages for FlowSOM and CITE-seq, which are used for proteomic and transcriptomic data sets, respectively.

FlowJo and **SeqGe** are two additional large platforms from BD, which offer user-friendly workflows. Each of these applications uses extension plugins that can provide quality control, data analysis, and visualization tools. Because of the user-friendly data analysis, there are far more limitations on how the user controls the data meaning that the preprocessing of single cell data files requires higher refinement prior to using such a service and often may still require some expertise to ensure the analysis is robust and significant. Much of the preprocessing and detailed aspects of data organization are not controllable within such platforms, which means there is still room for mistakes.

VDJViewer was specifically developed with the intention to provide single cell data processing for users that do not have advanced bioinformatic expertise, therefore making immunologic single cell data more accessible (69). In addition to modeling antigen markers, scRNA seq, and meta data, this application can also perform pseudo-time analysis and dimensionality reduction (69). As more data and platforms like VDJViewer become available, there is also a need to improve the models that operate within a given platform.

While these platforms are undoubtedly allowing wet laboratories to successfully analyze complex -omic data sets with minimal assistance of trained bioinformaticians, they are often limited in their application especially when dealing with complex datasets.

An alternative approach to commercially available solutions is the use of preprint platforms, which rely on community feedback for rapid development of data processing solutions. Because there is no "universal standard method" to process single cell data from different experiments and combining these large data sets requires creative and strategic methodology, actively seeking user feedback can streamline

solutions. The use of these platforms is free and only requires updated software and operation systems. Further, it ensures reproducibility, which is essential when the aim is the generation of a data cloud containing standardized cell and diseases atlases as references.

There are several leaders in preprint workflows, including **Bioconductor** and **F1000**. F1000 is a life sciences publisher with four primary divisions. F1000Research is the branch that focuses on data sharing. Bioconductor is a ready to download software package available within F1000Research, written in R and used as a bioinformatics community platform. Bioconductor offers free download of user-friendly workflows, sample data sets, and data analysis software packages. Additionally, an updated package is released every six months. Some of the common workflows within Bioconductor include scRNAseq and proteomic differential analysis. One example is Catalyst, a software program within Bioconductor developed by Mark Robinson laboratory. This program was specifically developed to offer a simplified way to analyze single cell mass cytometry data. One recent application of Catalyst allowed the identification of immunologic phenotypes pertinent to lung cancer prognosis (70). Other software programs within Bioconductor optimize single cell RNA-seq and epigenomic data. Among these softwares, the ChAMP software program recently allowed the identification of novel epigenomic biomarkers in colorectal cancer (71).

Another preprint leader, the **10X genomics** platform, is an organization focused on the development of single cell technologies and analysis pipelines. Although CellRanger is best used by commercially available kits, the free available software is gauged at the analysis of single cell data. Recent technologies within the 10X genomic project include the Visium Spatial Gene Expression Solution, which was developed for spatial resolution of transcriptomic data. In this assay, total mRNA samples are collected and processed by linking the transcriptomic barcode to a defined region of interest on the slide, thus providing spatially relevant information. In addition to technology development, 10X has led efforts to expand the power of single cell analysis. In 2017, 10X initiated a project in partnership with the Human Cell Atlas to create a single-cell based atlas available as a reference, which would initially include scRNA-seq data.

CHALLENGES

The field of high dimensional data poses several challenges, which in our view limit the accessibility of high dimensional technologies to clinical trial evaluation and drug discovery. The challenges are mostly related to three major areas: 1) data quality, 2) computational tools, and 3) training of the end user and generating the infrastructure.

Challenge One—Data Quality

Examples of high dimensional data include genomic, transcriptomic, proteomic, and microbiome data, which are derived from different sources and are collected in a variety of distinct formats and often over several sites. This data is complemented by patient data/medical records. Errors occurring during measurement or during processing can compromise the reproducibility and the use of the generated data. To overcome this hurdle, details about data collection and generation must be transparently reported and each processing step must be documented to avoid or minimize data alteration. Additionally, wet laboratories must follow strict standards during sample collection, storage, processing and acquisition. It is also important that data collection, processing and management follow pre-defined national or international standards. The national FAIR (findable, accessible, interoperable, reusable) initiative is one attempt to imply such a standard (72). Notably, attempts in ensuring procedural standards must be supported by the application of ethical standards to protect the privacy of the participating patients (73). Furthermore, throughout processing and management data must remain reliable and therefore be complete, of high quality, diverse, relevant to the question asked, timeless and accurate (74). Furthermore, data quality must be maintained upon data compression, storage, transfer and analysis and the entire process must be reproducible.

Challenge Two—Computational Tools

A desirable goal in the clinics is the creation of a FDA-approved software that can support clinical decisions (75). A prerequisite to this is the development of well tested wet lab protocols and computational tools, which can be easily used by users with a diverse knowledge level encompassing computational scientists, wet lab scientist and medical personnel (76). Open shared resources and code transparency as well as snapshots of program development can vastly enhance computational tool development and make the field more attractive to a wide group of users. Most importantly, wet lab protocols must be developed and pre-tested over several sites. Docker engines, which allow running software in a container, therefore making its installation independent on the environment, resulted in the use of software by a larger community (77). In this context, it will be of utmost importance having accessible, large and free data sets to allow for the testing and validation of software tools on real world data (78). Approaches such as the moonshot atlas initiative and the whole genome sequencing project are some of the examples.

Challenge Three—Training of the End User and Generating the Infrastructure

With the continuous growth of the big data field, the training of wet lab and clinical scientists in computational sciences becomes essential (76). Ideally the training should be multi-disciplinary and cover a broad array of concepts such as molecular diagnosis, cellular immunology, computer programming, system biology and patient care. This broad rather than specialized knowledge will empower the next generation of students to use new software tools with ease. This can be done in specialized PhD programs or in the form of on job training degrees. Most importantly, to optimally achieve these objectives, hospitals and universities should provide the infrastructure, such as cloud computing,

high speed internet connections in central as well as rural areas, easy access to the necessary software and sufficient support staff.

CONCLUSION

There are endless challenges facing multi-omic data processing, as it is critical to consistently assess analysis methods and avoid over fitting. Part of this challenge is interpreting how the individual cell features and their interaction with other cell types contributes to specific outcomes and therefore designing appropriate algorithms. Such theory is relevant in economics and consumer behavior and many of these models have operated as examples for single cell analysis. For instance, economic game theory models weigh the net effects of individual decisions and small subgroups to understand what drives certain economic trends and this type of strategy has been used to create novel analysis methods for single cell data (79).

Furthermore, when dealing with multi-omic approaches layers of single cell data need to be stacked. Therefore, another challenge is the creation of robust systems to process individual data sets as well as effective strategies to combine multiple data sets and produce meaningful outcomes. Novel technologies like single cell proteomics, single cell sequencing, and single cell spatial resolution are rapidly developing. As more and more laboratories world-wide get access to these technologies, network like the Immuno-Oncology Translational Network (IOTN) develop reference atlases of tissues and lay the basis to analytical tools. With these atlases as reference we are witnessing the beginning of tremendous insight into immune and disease mechanisms during (immuno)therapy.

AUTHOR CONTRIBUTIONS

JZ and CK drafted the review. SG and JL gave feedback and performed editing. CK and SG finalized the review. All authors contributed to the article and approved the submitted version.

FUNDING

Supported by Hollings Cancer Center startup funds (#87455) for CK; the Abney Foundation MD/PhD scholarship to JZ; ACS-IRG grant to SG.

ACKNOWLEDGMENTS

We thank Drs. Gari Hardiman, Mark Rubinstein, and Shikhar Mehrotra for valuable discussions and Mirja Loth for the graphical abstract. Supported in part by the Cell Evaluation & Therapy Shared Resource, Hollings Cancer Center, Medical University of South Carolina (P30 CA138313).

REFERENCES

1. Fulwyler MJ, Glascock RB, Hiebert RD. Device which separates minute particles according to electronically sensed volume. *Rev Sci Instrum* (1969) 40:42–8. doi: 10.1063/1.1683746
2. Ohno T, Kanoh T, Suzuki T, Masuda T, Kuribayashi K, Araya S, et al. Comparative analysis of lymphocyte phenotypes between carriers of human immunodeficiency virus (HIV) and adult patients with primary immunodeficiency using two-color immunofluorescence flow cytometry. *Tohoku J Exp Med* (1988) 154:157–72. doi: 10.1620/tjem.154.157
3. Wade CG, Rhyne RHJr., Woodruff WH, Bloch DP, Bartholomew JC. Spectra of cells in flow cytometry using a vidicon detector. *J Histochem Cytochem* (1979) 27:1049–52. doi: 10.1177/27.6.110874
4. Mosmann TR, Naim I, Rebhahn J, Datta S, Cavenaugh JS, Weaver JM, et al. SWIFT-scalable clustering for automated identification of rare cell populations in large, high-dimensional flow cytometry datasets, part 2: biological evaluation. *Cytometry A* (2014) 85:422–33. doi: 10.1002/cyto.a.22445
5. Finak G, Perez JM, Weng A, Gottardo R. Optimizing transformations for automated, high throughput analysis of flow cytometry data. *BMC Bioinf* (2010) 11:546. doi: 10.1186/1471-2105-11-546
6. Finak G, Jiang W, Krouse K, Wei C, Sanz I, Phippard D, et al. High-throughput flow cytometry data normalization for clinical trials. *Cytometry A* (2014) 85:277–86. doi: 10.1002/cyto.a.22433
7. Bandura DR, Baranov VI, Ornatsky OI, Antonov A, Kinach R, Lou X, et al. Mass cytometry: technique for real time single cell multitarget immunoassay based on inductively coupled plasma time-of-flight mass spectrometry. *Anal Chem* (2009) 81:6813–22. doi: 10.1021/ac901049w
8. Bendall SC, Simonds EF, Qiu P, Amir E-AD, Krutzik PO, Finck R, et al. Single-cell mass cytometry of differential immune and drug responses across a human hematopoietic continuum. *Science Am Assoc Advancement Sci* (2011) 322:687–96. doi: 10.1126/science.1198704
9. Bendall SC, Nolan GP, Roederer M, Chattopadhyay PK. A deep profiler's guide to cytometry. *Trends Immunol* (2012) 33:323–32. doi: 10.1016/j.it.2012.02.010
10. Tanner SD, Baranov VI, Ornatsky OI, Bandura DR, George TC. An introduction to mass cytometry: fundamentals and applications. *Cancer Immunol Immunother* (2013) 62:955–65. doi: 10.1007/s00262-013-1416-8
11. Pejoski D, Tchitchek N, Rodriguez Pozo A, Elhmouzi-Younes J, Yousfi-Bogniaho R, Rogez-Kreuz C, et al. Identification of Vaccine-Altered Circulating B Cell Phenotypes Using Mass Cytometry and a Two-Step Clustering Analysis. *J Immunol* (2016) 196:4814–31. doi: 10.4049/jimmunol.1502005
12. Leipold MD, Ornatsky O, Baranov V, Whitfield C, Nitz M. Development of mass cytometry methods for bacterial discrimination. *Anal Biochem* (2011) 419:1–8. doi: 10.1016/j.ab.2011.07.035
13. Guo Y, Baumgart S, Stark HJ, Harms H, Muller S. Mass Cytometry for Detection of Silver at the Bacterial Single Cell Level. *Front Microbiol* (2017) 8:1326. doi: 10.3389/fmicb.2017.01326
14. Yang YS, Atukorale PU, Moynihan KD, Bekdemir A, Rakhra K, Tang L, et al. High-throughput quantitation of inorganic nanoparticle biodistribution at the single-cell level using mass cytometry. *Nat Commun* (2017) 8:14069. doi: 10.1038/ncomms15343
15. Abdelrahman AI, Ornatsky O, Bandura D, Baranov V, Kinach R, Dai S, et al. Metal-Containing Polystyrene Beads as Standards for Mass Cytometry. *J Anal At Spectrom* (2010) 25:260–8. doi: 10.1039/b921770c
16. Newell EW, Sigal N, Bendall SC, Nolan GP, Davis MM. Cytometry by time-of-flight shows combinatorial cytokine expression and virus-specific cell niches within a continuum of CD8+ T cell phenotypes. *Immunity* (2012) 36:142–52. doi: 10.1016/j.immuni.2012.01.002
17. Newell EW, Sigal N, Nair N, Kidd BA, Greenberg HB, Davis MM. Combinatorial tetramer staining and mass cytometry analysis facilitate T-cell epitope mapping and characterization. *Nat Biotechnol* (2013) 31:623–9. doi: 10.1038/nbt.2593

18. Wong MT, Ong DE, Lim FS, Teng KW, McGovern N, Narayanan S, et al. A High-Dimensional Atlas of Human T Cell Diversity Reveals Tissue-Specific Trafficking and Cytokine Signatures. *Immunity* (2016) 45:442–56. doi: 10.1016/j.immuni.2016.07.007
19. Schlitzer A, Sivakamasundari V, Chen J, Sumatoh HR, Schreuder J, Lum J, et al. Identification of cDC1- and cDC2-committed DC progenitors reveals early lineage priming at the common DC progenitor stage in the bone marrow. *Nat Immunol* (2015) 16:718–28. doi: 10.1038/ni.3200
20. Krieg C, Nowicka M, Guglietta S, Schindler S, Hartmann FJ, Weber LM, et al. High-dimensional single-cell analysis predicts response to anti-PD-1 immunotherapy. *Nat Med* (2018) 24:144–53. doi: 10.1038/nm.4466
21. Hartmann FJ, Bernard-Valnet R, Queriault C, Mrdjen D, Weber LM, Galli E, et al. High-dimensional single-cell analysis reveals the immune signature of narcolepsy. *J Exp Med* (2016) 213:2621–33. doi: 10.1084/jem.20160897
22. Nair N, Mei HE, Chen SY, Hale M, Nolan GP, Maecker HT, et al. Mass cytometry as a platform for the discovery of cellular biomarkers to guide effective rheumatic disease therapy. *Arthritis Res Ther* (2015) 17:127. doi: 10.1186/s13075-015-0644-z
23. Giesen C, Wang HA, Schapiro D, Zivanovic N, Jacobs A, Hattendorf B, et al. Highly multiplexed imaging of tumor tissues with subcellular resolution by mass cytometry. *Nat Methods* (2014) 11:417–22. doi: 10.1038/nmeth.2869
24. Angelo M, Bendall SC, Finck R, Hale MB, Hitzman C, Borowsky AD, et al. Multiplexed ion beam imaging of human breast tumors. *Nat Med* (2014) 20:436–42. doi: 10.1038/nm.3488
25. Keren L, Bosse M, Thompson S, Risom T, Vijayaragavan K, McCaffrey E, et al. MIBI-TOF: A multiplexed imaging platform relates cellular phenotypes and tissue structure. *Sci Adv* (2019) 5:eaax5851. doi: 10.1126/sciadv.aax5851
26. Navin N, Kendall J, Troge J, Andrews P, Rodgers L, McIndoo J, et al. Tumour evolution inferred by single-cell sequencing. *Nature* (2011) 472:90–4. doi: 10.1038/nature09807
27. Macosko EZ, Basu A, Satija R, Nemesh J, Shekhar K, Goldman M, et al. Highly Parallel Genome-wide Expression Profiling of Individual Cells Using Nanoliter Droplets. *Cell* (2015) 161:1202–14. doi: 10.1016/j.cell.2015.05.002
28. Zheng GX, Terry JM, Belgrader P, Ryvkin P, Bent ZW, Wilson R, et al. Massively parallel digital transcriptional profiling of single cells. *Nat Commun* (2017) 8:14049. doi: 10.1038/ncomms14049
29. Villani AC, Satija R, Reynolds G, Sarkizova S, Shekhar K, Fletcher J, et al. Single-cell RNA-seq reveals new types of human blood dendritic cells, monocytes, and progenitors. *Science* (2017) 356:1–12. doi: 10.1126/science.aah4573
30. Rizvi AH, Camara PG, Kandror EK, Roberts TJ, Schieren I, Maniatis T, et al. Single-cell topological RNA-seq analysis reveals insights into cellular differentiation and development. *Nat Biotechnol* (2017) 35:551–60. doi: 10.1038/nbt.3854
31. Tirosh I, Izar B, Prakadan SM, Wadsworth MH2nd2nd, Treacy D, Trombetta JJ, et al. Dissecting the multicellular ecosystem of metastatic melanoma by single-cell RNA-seq. *Science* (2016) 352:189–96. doi: 10.1126/science.aad0501
32. Liu Y, Beyer A, Aebersold R. On the Dependency of Cellular Protein Levels on mRNA Abundance. *Cell* (2016) 165:535–50. doi: 10.1016/j.cell.2016.03.014
33. Darmanis S, Gallant CJ, Marinescu VD, Niklasson M, Segerman A, Flamourakis G, et al. Simultaneous Multiplexed Measurement of RNA and Proteins in Single Cells. *Cell Rep* (2016) 14:380–9. doi: 10.1016/j.celrep.2015.12.021
34. Battle A, Khan Z, Wang SH, Mitrano A, Ford MJ, Pritchard JK, et al. Genomic variation. Impact of regulatory variation from RNA to protein. *Science* (2015) 347:664–7. doi: 10.1126/science.1260793
35. Schwanhausser B, Busse D, Li N, Dittmar G, Schuchhardt J, Wolf J, et al. Global quantification of mammalian gene expression control. *Nature* (2011) 473:337–42. doi: 10.1038/nature10098
36. Stoeckius M, Hafemeister C, Stephenson W, Houck-Loomis B, Chattopadhyay PK, Swerdlow H, et al. Simultaneous epitope and transcriptome measurement in single cells. *Nat Methods* (2017) 14:865–8. doi: 10.1038/nmeth.4380
37. Peterson VM, Zhang KX, Kumar N, Wong J, Li L, Wilson DC, et al. Multiplexed quantification of proteins and transcripts in single cells. *Nat Biotechnol* (2017) 35:936–9. doi: 10.1038/nbt.3973
38. Crick F. Central dogma of molecular biology. *Nature* (1970) 227:561–3. doi: 10.1038/227561a0
39. Krasnitz A, Kendall J, Alexander J, Levy D, Wigler M. Early Detection of Cancer in Blood Using Single-Cell Analysis: A Proposal. *Trends Mol Med* (2017) 23:594–603. doi: 10.1016/j.molmed.2017.05.005
40. Cheng YH, Chen YC, Lin E, Brien R, Jung S, Chen YT, et al. Hydro-Seq enables contamination-free high-throughput single-cell RNA-sequencing for circulating tumor cells. *Nat Commun* (2019) 10:2163. doi: 10.1038/s41467-019-10122-2
41. Gawel DR, Serra-Musach J, Lilja S, Aagesen J, Arenas A, Asking B, et al. A validated single-cell-based strategy to identify diagnostic and therapeutic targets in complex diseases. *Genome Med* (2019) 11:47. doi: 10.1186/s13073-019-0657-3
42. Bossel Ben-Moshe N, Hen-Avivi S, Levitin N, Yehezkel D, Oosting M, Joosten LAB, et al. Predicting bacterial infection outcomes using single cell RNA-sequencing analysis of human immune cells. *Nat Commun* (2019) 10:3266. doi: 10.1038/s41467-019-11257-y
43. Zhang Q, He Y, Luo N, Patel SJ, Han Y, Gao R, et al. Landscape and Dynamics of Single Immune Cells in Hepatocellular Carcinoma. *Cell* (2019) 179:829–845 e20. doi: 10.1016/j.cell.2019.10.003
44. Liu Y, Wang L, Lo KW, Lui VWY. Omics-wide quantitative B-cell infiltration analyses identify GPR18 for human cancer prognosis with superiority over CD20. *Commun Biol* (2020) 3:234. doi: 10.1038/s42003-020-0964-7
45. Wang C, Yang J, Luo H, Wang K, Wang Y, Xiao Z-X, et al. CancerTracer: a curated database for intrapatient tumor heterogeneity. *Nucleic Acids Res* (2019) 48(D1):D797-806 doi: 10.1093/nar/gkz1061
46. Kumar MP, Du J, Lagoudas G, Jiao Y, Sawyer A, Drummond DC, et al. Analysis of Single-Cell RNA-Seq Identifies Cell-Cell Communication Associated with Tumor Characteristics. *Cell Rep* (2018) 25:1458–1468 e4. doi: 10.1016/j.celrep.2018.10.047
47. Rato S, Rausell A, Munoz M, Telenti A, Ciuffi A. Single-cell analysis identifies cellular markers of the HIV permissive cell. *PloS Pathog* (2017) 13:e1006678. doi: 10.1371/journal.ppat.1006678
48. Zhou Y, Yang D, Yang Q, Lv X, Huang W, Zhou Z, et al. Single-cell RNA landscape of intratumoral heterogeneity and immunosuppressive microenvironment in advanced osteosarcoma. *Nat Commun* (2020) 11:6322. doi: 10.1038/s41467-020-20059-6
49. Kaur H, Dhall A, Kumar R, Raghava GPS. Identification of Platform-Independent Diagnostic Biomarker Panel for Hepatocellular Carcinoma Using Large-Scale Transcriptomics Data. *Front Genet* (2019) 10:1306. doi: 10.3389/fgene.2019.01306
50. Zhao W, Li J, Chen MM, Luo Y, Ju Z, Nesser NK, et al. Large-Scale Characterization of Drug Responses of Clinically Relevant Proteins in Cancer Cell Lines. *Cancer Cell* (2020) 38:829–843 e4. doi: 10.1016/j.ccell.2020.10.008
51. Liu L, Wang G, Wang L, Yu C, Li M, Song S, et al. Computational identification and characterization of glioma candidate biomarkers through multi-omics integrative profiling. *Biol Direct* (2020) 15:10. doi: 10.1186/s13062-020-00264-5
52. Kim N, Kim HK, Lee K, Hong Y, Cho JH, Choi JW, et al. Single-cell RNA sequencing demonstrates the molecular and cellular reprogramming of metastatic lung adenocarcinoma. *Nat Commun* (2020) 11:2285. doi: 10.1038/s41467-020-16164-1
53. Liao M, Liu Y, Yuan J, Wen Y, Xu G, Zhao J, et al. Single-cell landscape of bronchoalveolar immune cells in patients with COVID-19. *Nat Med* (2020) 26:842–4. doi: 10.1038/s41591-020-0901-9
54. Wen W, Su W, Tang H, Le W, Zhang X, Zheng Y, et al. Erratum: Author Correction: Immune cell profiling of COVID-19 patients in the recovery stage by single-cell sequencing. *Cell Discovery* (2020) 6:41. doi: 10.1038/s41421-020-00187-5
55. Qi F, Qian S, Zhang S, Zhang Z. Single cell RNA sequencing of 13 human tissues identify cell types and receptors of human coronaviruses. *Biochem Biophys Res Commun* (2020) 526:135–40. doi: 10.1016/j.bbrc.2020.03.044
56. Fisher DAC, Malkova O, Engle EK, Miner CA, Fulbright MC, Behbehani GK, et al. Mass cytometry analysis reveals hyperactive NF Kappa B signaling in myelofibrosis and secondary acute myeloid leukemia. *Leukemia* (2017) 31:1962–74. doi: 10.1038/leu.2016.377
57. Spitzer MH, Nolan GP. Mass Cytometry: Single Cells, Many Features. *Cell* (2016) 165:780–91. doi: 10.1016/j.cell.2016.04.019

58. Kaiser Y, Lakshmikanth T, Chen Y, Mikes J, Eklund A, Brodin P, et al. Mass Cytometry Identifies Distinct Lung CD4(+) T Cell Patterns in Lofgren's Syndrome and Non-Lofgren's Syndrome Sarcoidosis. *Front Immunol* (2017) 8:1130. doi: 10.3389/fimmu.2017.01130
59. O'Gorman WE, Kong DS, Balboni IM, Rudra P, Bolen CR, Ghosh D, et al. Mass cytometry identifies a distinct monocyte cytokine signature shared by clinically heterogeneous pediatric SLE patients. *J Autoimmun* (2017) 16. doi: 10.1016/j.jaut.2017.03.010
60. Gaudilliere B, Fragiadakis GK, Bruggner RV, Nicolau M, Finck R, Tingle M, et al. Clinical recovery from surgery correlates with single-cell immune signatures. *Sci Transl Med* (2014) 6:255ra131. doi: 10.1126/scitranslmed.3009701
61. Tsai AG, Glass DR, Juntilla M, Hartmann FJ, Oak JS, Fernandez-Pol S, et al. Multiplexed single-cell morphometry for hematopathology diagnostics. *Nat Med* (2020) 26:408–17. doi: 10.1038/s41591-020-0783-x
62. See P, Dutertre CA, Chen J, Gunther P, McGovern N, Irac SE, et al. Mapping the human DC lineage through the integration of high-dimensional techniques. *Science* (2017) 356:1-13. doi: 10.1126/science.aag3009
63. Bendall SC, Davis KL, Amir el AD, Tadmor MD, Simonds EF, Chen TJ, et al. Single-cell trajectory detection uncovers progression and regulatory coordination in human B cell development. *Cell* (2014) 157:714–25. doi: 10.1016/j.cell.2014.04.005
64. van Unen V, Li N, Molendijk I, Temurhan M, Hollt T, van der Meulen-de Jong AE, et al. Mass Cytometry of the Human Mucosal Immune System Identifies Tissue- and Disease-Associated Immune Subsets. *Immunity* (2016) 44:1227–39. doi: 10.1016/j.immuni.2016.04.014
65. Wei SC, Levine JH, Cogdill AP, Zhao Y, Anang NAS, Andrews MC, et al. Distinct Cellular Mechanisms Underlie Anti-CTLA-4 and Anti-PD-1 Checkpoint Blockade. *Cell* (2017) 170:1120–1133 e17. doi: 10.1016/j.cell.2017.07.024
66. Spitzer MH, Carmi Y, Reticker-Flynn NE, Kwek SS, Madhireddy D, Martins MM, et al. Systemic Immunity Is Required for Effective Cancer Immunotherapy. *Cell* (2017) 168:487–502 e15. doi: 10.1016/j.cell.2016.12.022
67. Galli E, Hartmann FJ, Schreiner B, Ingelfinger F, Arvaniti E, Diebold M, et al. GM-CSF and CXCR4 define a T helper cell signature in multiple sclerosis. *Nat Med* (2019) 25:1290–300. doi: 10.1038/s41591-019-0521-4
68. Jackson HW, Fischer JR, Zanotelli VRT, Ali HR, Mechera R, Soysal SD, et al. The single-cell pathology landscape of breast cancer. *Nature* (2020) 578:615–20. doi: 10.1038/s41586-019-1876-x
69. Samir J, Rizzetto S, Gupta M, Luciani F. Exploring and analysing single cell multi-omics data with VDJView. *BMC Med Genomics* (2020) 13:29. doi: 10.1186/s12920-020-0696-z
70. Shaul ME, Eyal O, Guglietta S, Aloni P, Zlotnik A, Forkosh E, et al. Circulating neutrophil subsets in advanced lung cancer patients exhibit unique immune signature and relate to prognosis. *FASEB J* (2020) 34:4204–18. doi: 10.1096/fj.201902467R
71. Ishak M, Baharudin R, Rose IM, Sagap I, Mazlan L, Azman ZAM, et al. Genome-Wide Open Chromatin Methylome Profiles in Colorectal Cancer. *Biomolecules* (2020) 10:719. doi: 10.3390/biom10050719
72. Wilkinson MD, Dumontier M, Aalbersberg IJ, Appleton G, Axton M, Baak A, et al. The FAIR Guiding Principles for scientific data management and stewardship. *Sci Data* (2016) 3:160018. doi: 10.1038/sdata.2016.18
73. SJ Nass, LA Levit, LO Gostin eds. *Beyond the HIPAA Privacy Rule: Enhancing Privacy, Improving Health Through Research*. Washington (DC): National Academic Press (US) (2009).
74. Goodman SN, Fanelli D, Ioannidis JP. What does research reproducibility mean? *Sci Transl Med* (2016) 8:341ps12. doi: 10.1126/scitranslmed.aaf5027
75. Parikh RB, Obermeyer Z, Navathe AS. Regulation of predictive analytics in medicine. *Science* (2019) 363:810–2. doi: 10.1126/science.aaw0029
76. Rozman D, Acimovic J, Schmeck B. Training in Systems Approaches for the Next Generation of Life Scientists and Medical Doctors. *Methods Mol Biol* (2016) 1386:73–86. doi: 10.1007/978-1-4939-3283-2_5
77. Benson M. Clinical implications of omics and systems medicine: focus on predictive and individualized treatment. *J Intern Med* (2016) 279:229–40. doi: 10.1111/joim.12412
78. Van Steen K, Moore JH. How to increase our belief in discovered statistical interactions *via* large-scale association studies? *Hum Genet* (2019) 138:293–305. doi: 10.1007/s00439-019-01987-w
79. Razi A, Afghah F, Singh S, Varadan V. Network-Based Enriched Gene Subnetwork Identification: A Game-Theoretic Approach. *BioMed Eng Comput Biol* (2016) 7:1–14. doi: 10.4137/BECB.S38244

Conflict of Interest: The authors declare that the research was conducted in the absence of any commercial or financial relationships that could be construed as a potential conflict of interest.

Advantages of publishing in Frontiers

OPEN ACCESS
Articles are free to read for greatest visibility and readership

FAST PUBLICATION
Around 90 days from submission to decision

HIGH QUALITY PEER-REVIEW
Rigorous, collaborative, and constructive peer-review

TRANSPARENT PEER-REVIEW
Editors and reviewers acknowledged by name on published articles

Frontiers
Avenue du Tribunal-Fédéral 34
1005 Lausanne | Switzerland

Visit us: www.frontiersin.org
Contact us: frontiersin.org/about/contact

REPRODUCIBILITY OF RESEARCH
Support open data and methods to enhance research reproducibility

DIGITAL PUBLISHING
Articles designed for optimal readership across devices

FOLLOW US
@frontiersin

IMPACT METRICS
Advanced article metrics track visibility across digital media

EXTENSIVE PROMOTION
Marketing and promotion of impactful research

LOOP RESEARCH NETWORK
Our network increases your article's readership